

DIVERSITY, TAXONOMY, AND CHEMICAL EVALUATION OF TRUFFLES (*TUBER*) AND FALSE TRUFFLES (*CHOIROMYCES* AND *MELANOGASTER*) AND COMMERCIAL BOLETES IN SOUTHWEST CHINA

TIANJUN YUAN

DOCTOR OF PHILOSOPHY
IN
BIOLOGICAL SCIENCE

SCHOOL OF SCIENCE
MAE FAH LUANG UNIVERSITY
2024
©COPYRIGHT BY MAE FAH LUANG UNIVERSITY

DIVERSITY, TAXONOMY, AND CHEMICAL EVALUATION OF TRUFFLES (*TUBER*) AND FALSE TRUFFLES (*CHOIROMYCES* AND *MELANOGASTER*) AND COMMERCIAL BOLETES IN SOUTHWEST CHINA

TIANJUN YUAN

THIS DISSERTATION IS A PARTIAL FULFILLMENT OF
THE REQUIREMENTS FOR THE DEGREE OF
DOCTOR OF PHILOSOPHY
IN
BIOLOGICAL SCIENCE

SCHOOL OF SCIENCE
MAE FAH LUANG UNIVERSITY
2024
©COPYRIGHT BY MAE FAH LUANG UNIVERSITY

DIVERSITY, TAXONOMY, AND CHEMICAL EVALUATION OF TRUFFLES (*TUBER*) AND FALSE TRUFFLES (*CHOIROMYCES* AND *MELANOGASTER*) AND COMMERCIAL BOLETES IN SOUTHWEST CHINA

TIANJUN YUAN

THIS DISSERTATION HAS BEEN APPROVED
TO BE A PARTIAL FULFILLMENT OF THE REQUIREMENTS
FOR THE DEGREE OF DOCTOR OF PHILOSOPHY
IN
BIOLOGICAL SCIENCE
2024

EXAMINATION COMMITTEE

.....CHAIRPERSON
(Santhiti Vadthanarat, Ph. D.)

.....ADVISOR
(Olivier Jean-Mari Raspé, Ph. D.)

.....EXAMINER
(Asst. Prof. Sunita Chamyuang, Ph. D.)

.....EXAMINER
(Asst. Prof. Putarak Chomnunti, Ph. D.)

.....EXTERNAL EXAMINER
(Komsit Wisitrassameewong, Ph. D.)

©COPYRIGHT BY MAE FAH LUANG UNIVERSITY

ACKNOWLEDGEMENTS

When I enter this phase, it signifies the near end of my doctoral journey. Throughout this long and enriching voyage, many selfless individuals have assisted and encouraged me, for whom I am profoundly thankful.

First of all, I extend my sincere gratitude to my academic advisor, Honorary Professor Olivier Raspé, whose rigorous academic style and tireless teaching noble ethics have given me a fresh understanding of the world of fungi. He offered me the study opportunity in one of the finest fungal research laboratories at the Mae Fah Luang University, where his pursuit of excellence in research profoundly influenced me. Without his invaluable guidance, encouragement, and unwavering assistance, this dissertation would not be accomplished. Additionally, I deeply appreciate the guidance from my mentor in China, Prof. Shuhong Li from the Biotechnology and Germplasm Resources Institute of the Yunnan Academy of Agricultural Sciences, who provided me with the opportunity to study under Professor Olivier and offered me a research platform for my doctoral studies, providing significant assistance in both life and learning. Furthermore, I would like to thank the Medicinal Plant Research Institute of the Yunnan Academy of Agricultural Sciences for their assistance in sample collection.

I extend special thanks to Prof. Ying Hou from the School of Chemistry and Chemical Engineering at Southwest Forestry University for providing me with extensive experimental assistance, and to Prof. Yun Wang from the New Zealand Institute for Plant and Food Research Limited (Plant & Food Research), Prof. Xianghua Wang from the Kunming Institute of Botany, Chinese Academy of Sciences and Dr. Shanping Wan from Yunnan Agricultural University for their assistance in data analysis. Without their advice and guidance, I would be confronted with great challenge to complete my doctoral research.

Much of my doctoral work was conducted at the Key Laboratory of Biotechnology and Germplasm Resources and the Medicinal Plant Research Institute of the Yunnan Academy of Agricultural Sciences. Therefore, I take this opportunity to express my heartfelt gratitude to all the staff who taught me basic molecular and chemical experimental skills.

I am very grateful for the support of Researcher Shuhong Li's National Natural Science Foundation of China (No. 31560009), Researcher Xianghua Wang's Biodiversity Survey and Assessment Project of the Ministry of Ecology and Environment (2019HJ2096001006), the Key Projects of Joint Research on Basic Research of Yunnan Province (202101BD070001-012), the Talent Project for Young and Middle-aged Academic and Technical Leaders in Yunnan Province (202305AC160025), Yunnan Province Science and Technology Plan Project (Approval No. 202202AE090001), and the Thesis Writing Assistance Fund from the Mae Fah Luang University, Thailand.

I extend my gratitude to all the staff working at the Center of Excellence for Fungal Research at the Mae Fah Luang University, Thailand, for their assistance in my studies and life. I also thank my fellow Dr. Zonglong Luo, Dr. Xiangyu Zeng, Dr. Jinfeng Zhang, Dr. Chuangen Lin, Dr. Yuanshuai Liu, Dr. Songming Tang, as well as Dr. Qingfeng Meng, Dr. Raghoonundon Bhavesh, Dr. Jian Ma, Dr. Hongwei Shen, Dr. Jingyi Zhang, and others friends for their care and assistance.

I am deeply thankful to my family, who have encouraged and supported me at every stage of my personal and academic life. Born in a rural area, my parents always admonished me to "study hard and change my destiny with knowledge." With their encouragement and support, I continuously sought new knowledge and broadened my horizons. Finally, I want to thank my beloved wife and our daughter. It is your selfless love and understanding during my most difficult and helpless times that have enabled me to complete my studies. Thank you very much!

Tianjun Yuan

Dissertation Title	Diversity, Taxonomy, and Chemical Evaluation of Truffles (*Tuber*) and False Truffles (*Choiromyces* and *Melanogaster*) and Commercial Boletes in Southwest China
Author	Tianjun Yuan
Degree	Doctor of Philosophy (Biological Science)
Advisor	Olivier Jean-Mari Raspé, Ph. D.

ABSTRACT

China, especially the southwestern region, boasts astonishing diversity of mushrooms. These mushrooms exhibit various nutrition modes, including saprotrophic, ectomycorrhizal (EcM), or parasitic. Particularly, ectomycorrhizal fungi play crucial roles in ecosystems and provide valuable resources for contemporary medicine and daily diet. This thesis focuses on hypogeous fungi and boletes in southwestern China, conducting research on the taxonomy and phylogeny of hypogeous fungi, the relationship between chemical information of boletes and species, and the exploration of chemical markers as the basis for species identification.

Hypogeous fungi are difficult to discover because their sporophores grow underground. This thesis identifies and describes the following new species through morphological and phylogenetic analysis. Two new species, *Tuber maroonense* nom. prov. and *T. conditum* nom. prov., belong to the Latisporum group, are described from Yunnan province of southwest China. Phylogenetic placements and morphological characteristic of these novel *Tuber* species in the Latisporum group are discussed. *T. maroonense* is phylogenetically closely related to *T. caoi*. Morphologically, *T. caoi* has gray and pubecens ascomata while *T. maroonense* has whitish and glabrous ascomata. *Tuber* conditum differs from *T. qujingense* and *T. songlu* by its thinner peridium (120–200 µm) and larger ascospores

(49–66.5 × 34.5–60 μm in one-spored asci). *Tuber qujingense* has a greyish white ascomata, brown snowflake-shaped gleba, prosenchymatous peridium, fusiform and *T. songlu* has dense spine-like dermatocystidia, which is completely different from each other. In addition, DNA sequence analysis revealed the similarity between two species is less than 67 % (*T. qujingense*) and 93 % (*T. songlu*) in ITS sequences, strongly supporting the separation of *T. conditum* from the Chinese species of *T. qujingense* and *T. songlu*.

Choiromyces cerebriformis sp. nov. is described and illustrated from Yunnan province, China. Both morphological evidence and sequence analyses of the internal transcribed spacer region (ITS1-5.8S-ITS2) support the species as new to science. *C. cerebriformis* differs from other *Choiromyces* species in having ascomata with larger lobes and light orange-brown gleba, and globose ascospores with short stick-like sparse spines ornamentation. Morphological differences and genetic distances with the similar species *C. helanshanensis* and *C. alveolatus* are discussed. A phenotypic key including related species is provided.

Three newly discovered *Melanogaster* species, namely *M. cyaneus* sp. nov., *M. diqingensis* sp. nov., and *M. truncatisporus* sp. nov., are introduced and illustrated based on both morphological and molecular data from Sichuan and Yunnan provinces in China. A multigene phylogenetic analysis (nrITS, nrLSU, and rpb2) was performed mainly to verify the placement of the new species in *Melanogaster*. A second, nrITS-only phylogenetic analysis comprising more *Melanogaster* species for which only ITS sequences were available, was used to infer the relationship between the new species and as many known Melanogaster species as possible. Specimens of *M. cyaneus*, *M. diqingensis*, and *M. truncatisporus* formed three independent clades in a phylogenetic tree inferred from the ITS data set. The robust support from ITS for these clades and genetic similarity with other species being lower than 93.2% suggest that these three species are indeed distinct from the other Melanogaster species in the phylogeny. Morphologically, *M. cyaneus* is characterized by its blue or bluish gleba, light brown to yellowish brown peridium,

and subglobose to globose basidiospores, 6.2–15 × 4.6–9.0 μm. *Melanogaster diqingensis* is distinguished from other *Melanogaster* species by its pale yellow to brown-yellow peridium and obovate to subglobose basidiospores, 3.0–5.1 × 2.0–4.0 μm. *Melanogaster truncatisporus* is diagnosed by its subglobose to globose or irregularly elongate-pyriform basidiomata, pale yellow to deeply orange-yellow peridium, and subglobose to globose or pyriform, truncate basidiospores.

The Agaricomycetidae (Agaricomycetes) are the most morphologically diverse Basidiomycota and they comprise two well-known orders, Agaricales and Boletales. As one of the most diverse representative species, over 500 species of boletes have been reported in China in recent years. Some of these boletes are widely consumed as delicacies, but there are still some species that are highly toxic, causing poisoning or even death (e.g. *Rubroboletus satanas* (Lenz) Kuan Zhao & Zhu L. Yang and *Heimioporus retisporus* [Pat. & C. F. Baker]) if ingested accidentally. The diversity of chemical components within boletes forms the material basis for studying their nutrition and toxicity. Currently, although species classification studies of common boletes are relatively mature, there is limited research on classifying species based on chemical information, whether there is a certain correlation between chemical information and species phylogeny and growth environment, and how the intrinsic chemical characteristics of species change. According to market research, this paper focuses on 11 common edible boletes conducts the following studies:

Here we collected 509 individuals of boletes samples on the field (belonging to 11 species identified by molecular analyses) from different geographic regions in Yunnan and Sichuan provinces of Southwest China. Those 11 species include *Boletus bainiugan* (BoB, 32 samples), *Butyriboletus pseudospeciosus* (BuP, 30 samples), *Butyriboletus roseoflavus* (BuR, 55 samples), *Lanmaoa asiatica* (LA, 56 samples), *Neoboletus obscureumbrinus* (NO, 21 samples), *Rugiboletus extremiorientalis* (RugE, 55 samples), *Rubroboletus sinicus* (RubS, 26 samples), *Retiboletus fuscus* (RetF, 60 samples), *Phlebopus portentosus* (PP, 35 samples), *Neoboletus hainanensis* (NH, 25 samples), *Neoboletus magnificus* (NM, 55 samples).

Chemical information, was gathered using near infrared spectroscopy (NIR), common peaks of high–performance liquid chromatography (HPLC) and volatile constituents. The degree of phylogenetic signal of chemical information and its relationship with ecological factors were analyzed by bioinformatics and chemometrics. We found the following: (1) The chemodiversity of boletes is widely correlated with phylogenetic signals and ecological and environmental factors. Thus, evolutionary history and ecological and environmental factors may play key roles in driving the formation of chemodiversity. (2) Phylogenetic relatedness is the best predictor of all chemical characteristics, and vice versa. Chemical information of phylogenetic conservatism is a powerful tool to identify species (addition to methods of molecular and morphological identification). (3) Chemical characteristic information strongly correlated with ecological and environmental factors could be used to identify the geographical regions of species. This study provides multiple lines of evidence that the chemodiversity of boletes is driven by both phylogeny and ecological and environmental factors. The chemical characteristic information could be used to identify species and geographical regions, which provided strong evidence for evolutionary species and ecological change in the future to explore the origin by chemical traits.

In addition, we explored the heterogeneity of volatile components (VOCs) in eleven bolete species by multivariate statistical analyses. A total of 97 VOCs were detected in 445 samples of 11 boletes species by gas chromatography-mass spectrometry, among which alkanes and esters were dominant. Principal component analysis and one-way analysis of variance revealed potential differences among the 11 boletes species. Partial least squares discriminant analysis (PLS-DA) combined with variable importance in projection results (22, VIP >1) and relative odor activity values (21, ROAV >0.1) revealed that 38 VOCs (5 common compounds) contributed to the classification of species, and identify models were effectively validated. Next, based on the analysis of the correlated heatmap combined with volcanic maps, 9 VOCs were selected as the key VOCs of 11 species. Furthermore, Fisher's linear discriminant function analysis combined with literature reports showed that 5 VOCs including methyl (9E)-9-octadecenoate, 2,6-dimethylpyrazine, 1-decen-3-one, furfural, and

methional could be used as signature compounds to identify the 11 bolete species. Ultimately, Fourier transform near infrared spectroscopy (FT-NIR) combined with partial least squares regression (PLSR) provides a fast and reliable quantitative technique for predicting the contents of the five characteristic VOCs in boletes. This study provides a strategy for effective species identification and rapid prediction of characteristic aroma substances of wild edible boletes based on qualitative and quantitative analysis of VOCs and FT-NIR spectra.

Keywords: Ectomycorrhizal Fungi, Edible Mushrooms, Chemodiversity, Pattern Recognition Research, Phylogenetics

TABLE OF CONTENTS

	Page
ACKNOLEDGEMENTS	**(3)**
ABSTRACT	**(5)**
LIST OF TABLES	**(15)**
LIST OF FIGURES	**(17)**
ABBREVIATIONS AND SYMBOLS	**(21)**
CHAPTER	
1 INTRODUCTION	**1**
1.1 Introduction of Ectomycorrhizal Fungi	1
1.2 Hypogeous Fungi	2
1.3 Order Boletales	9
1.4 Chemotaxonomy to Improve Fungal Classification	20
1.5 Chemotaxonomy and Chemical Diversity	23
1.6 Evaluation of Commercial Boletes	27
1.7 Research Objectives	30
1.8 Research Outlines	31
2 RESEARCH METHODOLOGY	**32**
2.1 Taxonomy and Phylogeny Study	32
2.2 Identification of Wild Edible Boletes	39
2.3 The Evolutionary History of Boletes	43
2.4 Analytical Fingerprint Information and Chemical Diversity of Wild Edible Boletes	44

TABLE OF CONTENTS (continued)

	Page
CHAPTER	
2.5 Construction of Chemical Classification Models of Wild Edible Boletes	52
2.6 Construction of Chemical Evaluation Models of Wild Edible Boletes	55
2.7 Chemometric Methods	57
2.8 Statistical Analysis	61
3 RESEARCH RESULTS	**62**
3.1 Taxonomy and Phylogeny of *Tuber* (True Truffles)	62
3.2 Taxonomy and Phylogeny of *Choiromyces*	79
3.3 Taxonomy and Phylogeny of *Melanogaster*	88
3.4 Identification of Wild Edible Boletes	106
3.5 Construction of Chemical Evaluation Models of Wild Edible Boletes	156
4 DISCUSSION	**175**
4.1 Taxonomy and Phylogeny of *Tuber* (True Truffles)	175
4.2 Taxonomy and Phylogeny of *Choiromyces*	176
4.3 Taxonomy and Phylogeny of *Melanogaster*	177
4.4 The Chemodiversity of Boletes Driven by Both Phylogeny and Ecological and Environmental Factors	180
4.5 A Qualitative and Quantitative Analysis of Wild Boletes Based on Multivariate Statistics of Volatile Components and FT-NIR Spectra	183

TABLE OF CONTENTS (continued)

	Page
CHAPTER	
5 OVERALL CONCLUSIONS	**184**
5.1 Taxonomy and Phylogeny of Hypogeous Fungi	184
5.2 Chemodiversity and Chemotaxonomy Analyses of Wild Boletes	185
5.3 Volatile Components and Key Aroma Components Predicted of Wild Boletes	187
5.4 Research Advantages	188
5.5 Future Work	189
5.6 Publications	190
REFFERENCES	**192**
APPENDICES	**247**
APPENDIX A THE DETAILED INFORMATION OF SPECIES	248
APPENDIX B THE DETAILED INFORMATION OF PHYLOGENETIC ANALYSES	264
APPENDIX C THE DETAILED INFORMATION OF AGARICOMYCOTINA	292
APPENDIX D THE DETAILED INFORMATION OF AGARICOMYCOTIN	330
APPENDIX E THE AVERAGE COMPONENTS OF 11 SPECIES OF BOLETES	331

TABLE OF CONTENTS (continued)

		Page
APPENDIX F	DISTANCE MATRIX BETWEEN PHYLOGENETIC SIGNALS AND CHEMICAL CHARACTERISTIC INFORMATION OF SPECIES	384
APPENDIX G	DISTANCE MATRIX OF ECOLOGICAL ENVIRONMENTAL FACTORS AND CHARACTERISTIC CHEMICAL INFORMATION OF DIFFERENT PRODUCING AREAS	386
APPENDIX H	DETECTION RESULTS OF DIFFERENT CHEMICAL INFORMATION PHYLOGENETIC SIGNALS	388
APPENDIX I	THE TWO-DIMENSIONAL CORRELATION SPECTRA AND HPLC-FINGERPRINT	420
APPENDIX J	THE CHEMICAL STRUCTURAL FORMULA OF VOCs BY GC-MS	423
APPENDIX K	THE CHEMICAL STRUCTURAL FORMULA OF VOCs BY GC-MS	428
APPENDIX L	THE VIP SCREEN OF THE CHEMICAL INFORMATION SIGNIFICANTLY CORRELATED WITH REFION CLASSIFICATION	431
APPENDIX M	CORRELATION COEFFICIENT BETWEEN ECOLOGICAL ENVIROMENTAL FACTORS AND PRODUCING AREAS	436

TABLE OF CONTENTS (continued)

		Page
APPENDIX N	THE CONTRIBUTION DIAGRAM OF ECOLOGICAL ENVIRONMENTAL FACTORS TO DIFFERENT REGIONS ANALYZED BY CONSENSUS CLUSTER PLUS	437
APPENDIX O	THE SPECIMENS AND RESULTS OF VOLATILE COMPONENTS	438
APPENDIX P	THE RESULTS OF CROSS VALIDATION	451
APPENDIX Q	THE PUBLISHED PARPERS	452
CURRICULUM VITAE		**454**

LIST OF TABLES

Table		Page
2.1	The TEF1 and RPB2 sequences of specimens	43
2.2	Results of optimization	50
3.1	Details of *Tuber* sequences used in phylogenetic analysis	63
3.2	GenBank numbers of *Choiromyces* specimens used for phylogeny analysis	80
3.3	Intraspecific and interspecific genetic distances of *Choiromyces* species	81
3.4	GenBank numbers of *Melanogaster* specimens used for phylogeny analysis	90
3.5	The main morphological characterization of *Melanogaster* species	103
3.6	Estimation of divergence time of Basidiomycota	110
3.7	The OPLS-DA model of species established by characteristic near-infrared information	134
3.8	External validation of the OPLS-DA model of species established by characteristic near-infrared information	135
3.9	The OPLS-DA model of boletes species established by characteristic chromatographic information	136
3.10	External validation of the OPLS-DA model of species established by characteristic chromatographic information	137
3.11	The OPLS-DA model of boletes species established by characteristic volatile constituent information	138
3.12	External validation of the OPLS-DA model of species established by characteristic volatile constitute information	139

LIST OF TABLES (continued)

Table		Page
3.13	The OPLS-DA model of regions established by characteristic near-infrared information	148
3.14	External validation of the OPLS-DA model of regions established by characteristic near-infrared information	148
3.15	The OPLS-DA model of regions established by characteristic chromatographic information	149
3.16	External validation of the OPLS-DA model of regions established by characteristic chromatographic information	149
3.17	The OPLS-DA model of regions established by characteristic volatile constituent information	150
3.18	External validation of the OPLS-DA model of regions established by characteristic volatile constituent information	150
3.19	The ROAV of 44 volatile compounds in 11 species of boletes	158
3.20	The training results of the VIP-PLS-DA model	163
3.21	The validation results of VIP-PLS-DA model	165
3.22	The training results of the ROAV-PLS-DA model	168
3.23	The validation results of the ROAV-PLS-DA model	168

LIST OF FIGURES

Figure		Page
1.1	Beneficial effects of ECM fungi	2
1.2	Phylogram showing the distribution of truffle-forming fungi throughout the fungal tree of life	4
1.3	The culinarily famous *Tuber melanosporum* (black truffle) and *Tuber magnatum* (white truffle)	6
1.4	The type of *Choiromyces*	7
1.5	The type of *Melanogaster*	8
1.6	The species of *Boletus edulis* and *B. bainiugan*	11
1.7	The species of *Butyriboletus roseoflavus* and *B. pseudospeciosus*	12
1.8	The species of *Rubroboletus sinicus*	13
1.9	The species of *Retiboletus fuscus*	14
1.10	The species of *Lanmaoa asiatica*	16
1.11	The species of *Neoboletus obscureumbrinus*, *N. magnificus* and *N. hainanensis*	17
1.12	The species of *Rugiboletus extremiorientalis*	18
1.13	The species of *Phlebopus portentosus*	20
1.14	Boletes from Mu Shui Hua wild fungus trading market in Kunming city, Yunnan province, southwestern China	29
2.1	HPLC precision experiment	47
2.2	HPLC repeatability experiment	48
2.3	HPLC stability experiment	48

LIST OF FIGURES (continued)

Figure	Page
3.1 Phylogenetic tree of the genus *Tuber* constructed by ITS-LUS-TEF1-RPB2 rDNA sequences	69
3.2 Phylogenetic tree of the genus *Tuber* constructed by ITS1-5.8S-ITS2 sequences	70
3.3 Photographs of *Tuber* maroonense (YAAS L3694, holotype)	73
3.4 Photographs of *Tuber* conditum (YAAS L3385, holotype)	76
3.5 Phylogenetic tree of the genus *Choiromyces*	83
3.6 The habitat and morphological characteristics of *Choiromyces cerebriformis*	87
3.7 Phylogenetic tree of the genera *Melanogaster* and *Alpova*	89
3.8 Phylogenetic tree of the genus *Melanogaster*	95
3.9 Photographs of *Melanogaster* species	102
3.10 The discrimination result of three sections of Chinese species based on its main characteristic by OPLS-DA	104
3.11 The 110 collection sites of 11 species of boletes	106
3.12 Maximum likelihood phylogenetic trees of 11 species of boletes	107
3.13 Maximum clade credibility tree of Agaricomycotina and 11 species based on ITS, LSU, RPB1, RPB2 and TEF1 genes	109
3.14 Original NIR and chromatographic fingerprints of different species and regions of boletes	122
3.15 STDEV and diversity analysis of different species and regions of boletes by spectral, chromatographic and mass spectrometry	123

LIST OF FIGURES (continued)

Figure		Page
3.16	Pearson correlation analysis of phylogenetic signals of species, regions and chemical information of boletes	127
3.17	Phylogenetic signal analysis and Mantel test of chemical characteristic information of boletes species	129
3.18	Pattern recognition model of boletes species based on characteristic spectral information	131
3.19	Pattern recognition model of boletes species based on characteristic chromatographical information	132
3.20	Pattern recognition model of boletes species based on characteristic volatile constituent information	133
3.21	The correlation between different collection sites and their ecological environmental factors and the division of producing areas of boletes	141
3.22	The correlation analysis between chemical characteristic information and ecological environmental factors of producing areas of boletes	143
3.23	The PLS-DA model of characteristic spectral information of six different regions of boletes established by different methods	144
3.24	The PLS-DA model of characteristic chromatographic information of six different regions of boletes established by different methods	145
3.25	The PLS-DA model of characteristic volatile constituents of six different regions of boletes established by different methods	146

LIST OF FIGURES (continued)

Figure		Page
3.26	RLQ analysis of species, chemical characteristic information, ecological environmental factors and producing areas	147
3.27	Species richness in different producing areas and heterogeneity analysis of chemical characteristic information	152
3.28	Phylogenetic tree of selected Boletaceae using maximum likelihood inferred from the two-gene dataset (*tef1* and *rpb2*)	156
3.29	The original spectrum and second derivative spectrum of the Fourier Near-Infrared spectrum of boletes	157
3.30	PCA loading plot of the correlation between the species of boletes and volatile compounds	162
3.31	Classification and prediction models of boletes established by PLS-DA	164
3.32	Classification and prediction models of boletes established by ROAV-PLS-DA	167
3.33	Classification effects of volatile compounds on different species of boletes	171
3.34	Calibration and validation models of the characteristic markers of volatile compounds of boletes built by NIR combined with PLSR	174

ABBREVIATIONS AND SYMBOLS

100%	Percentage
≥	Greater than or equal to
≤	Less than or equal to
2DCOS	Two dimensional correlation spectrum
ANOVA	One-way analysis of variance
AUC	Area under the curve
BI	Bayesian inference
℃	Degree Celsius temperature
CCS	Cluster consensus score
cm	Centimeter
com.	Combination
DFA	Fisher's linear discriminant function analysis
diam.	Diameter
e.g.	For example
et al.	And others
FT-NIR	Fourier transform near-infrared spectroscopy
g/l	Gram per liter
GC/MS	Gas chromatography-mass spectrometer
gen.	Genus (singular) and genera (plural)
GPS	Global positioning system
HCA	Hierarchical clustering analysis
HPLC	High-performance liquid chromatography

ABBREVIATIONS AND SYMBOLS (continued)

i.e.	That is
Blomberg's *K*	A relatively recent measure of phylogenetic signal
mg	Milligram
ml	Milliliter
ML	Maximum likelihood
mm	Millimeter
nov.	Novum (Latin for new thing)
OPLS-DA	Orthogonal partial least square discriminant analysis
P value	Probability value
PCA	Principal component analysis
PCAC	Principal component clustering
PLS	Partial least squares
PLS-DA	Partial least square discriminant analysis
PLSR	Partial Least Squares Regression
Q	Length-to-width ratio
Q^2	Goodness of prediction ability of the model
r	Correlation coefficient
R^2	Coefficient of determination
RMSECV	Root mean square error of cross-validation
RMSEP	Root mean square error of prediction
ROAV	Relative odor activity value
RPD	Residual predictive deviation

ABBREVIATIONS AND SYMBOLS (continued)

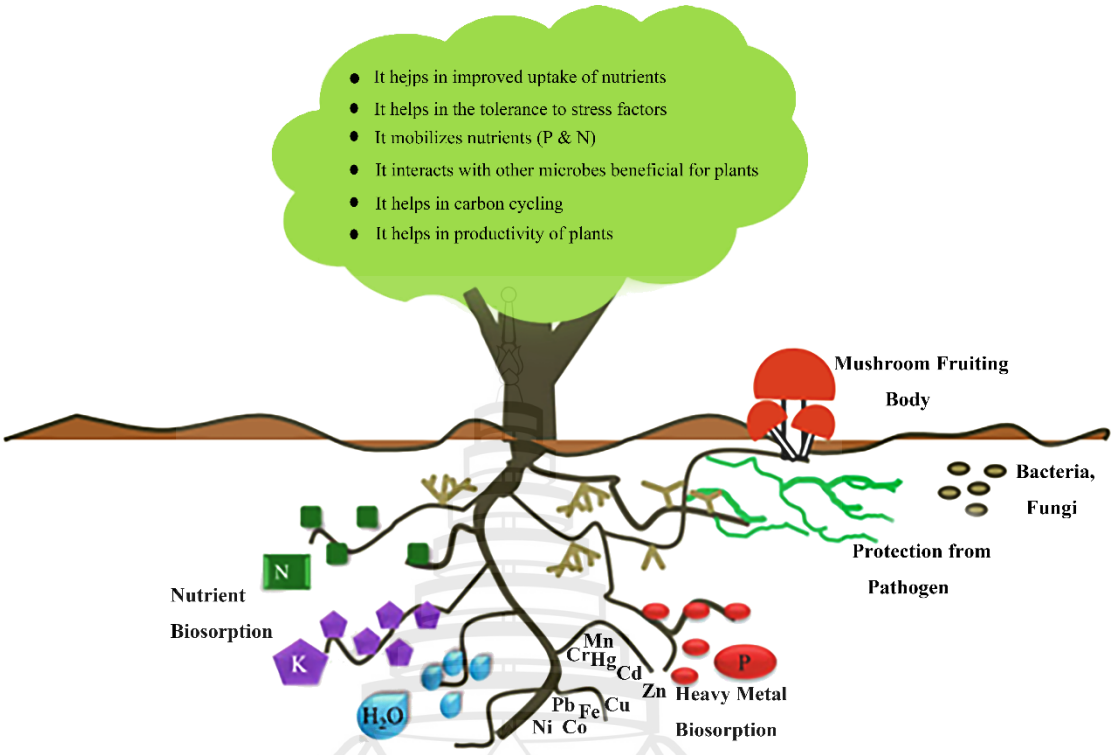
rpm	Revolutions per minute
SDE	Simultaneous distillation extraction
sp.	Species
spp.	Species (plural)
STDEV	Standard deviation
VIP	Variable importance in projection
VOCs	Volatile compounds
vs.	Versus
$\bar{X}$	Average
µg/ml	Microgram per milliliter
µl	Microliter
µm	Micrometer

CHAPTER 1

INTRODUCTION

1.1 Introduction of Ectomycorrhizal Fungi

There are several groups of mycorrhizal fungi, of which the main types are the endomycorrhizal (such as the arbuscular and orchid mycorrhizae) and ectomycorrhizal (ECM) (Smith & Read, 2008). Ectomycorrhizal symbiosis is an association of fungal mycelia and root tips of plants, mostly woody trees. Ectomycorrhizae are formed by fungi like *Russula*, *Boletus*, *Choiromyces*, *Melanogaster*, *Tuber*, *Cantharellus,* etc., most of which are common edible mushrooms (Moreno et al., 2012; Wan et al., 2016; Zambonelli et al., 2016; Sharma, 2017; Xu, Yan et al., 2022). It has been estimated that over 20,000 species of ECM fungi exist worldwide (Rinaldi et al., 2008). The presence of ECM fungi significantly contributes to biodiversity and various ecosystem processes, thereby maintaining the equilibrium of Earth's ecological system. Of particular importance, ECM fungi enhance the efficiency of nutrient absorption by plants, ultimately benefiting both the fungi and the plants (Figure 1.1) (Sharma, 2017; Wu et al., 2022). also, many ECM fungi are highly valued for their edibility (e.g. *Tuber*, some *Boletes* species) and medicinal properties (e.g. Some *Russula* species), bringing economic benefits to remote mountainous areas and gaining favor among medical experts and culinary enthusiasts (Chen, Jiang et al., 2016; Panda et al., 2020; Tian et al., 2022; Wa & Daba, 2022).



Source Adapted from Sharma (2017)

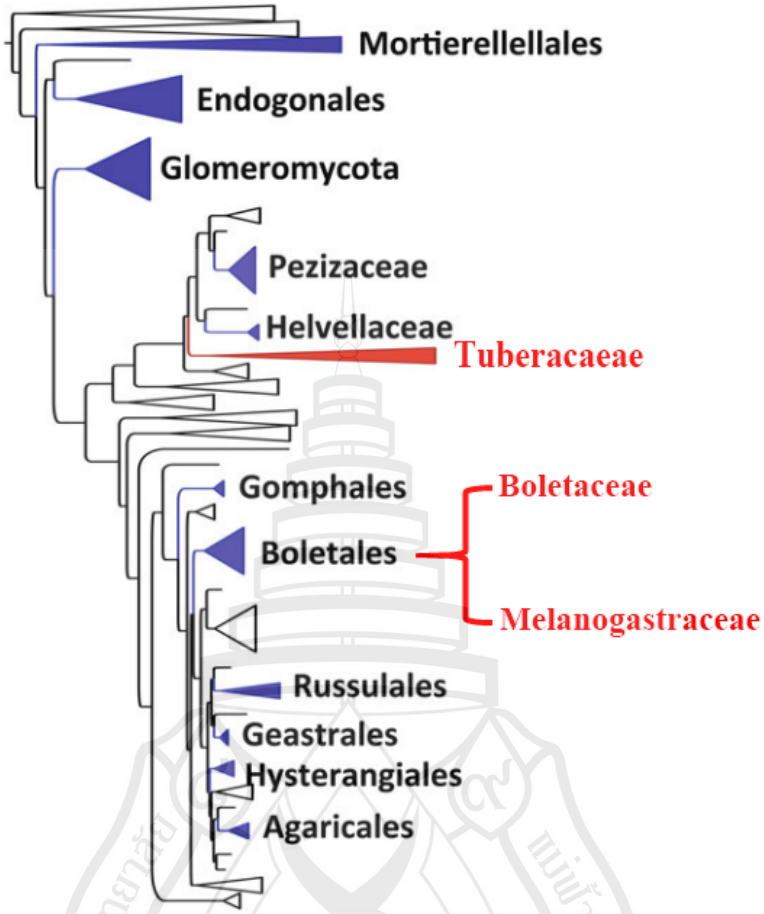
Figure 1.1 Beneficial effects of ECM fungi

1.2 Hypogeous Fungi

Hypogeous fungi comprise species belonging to several genera of Ascomycota (including the true truffles), Basidiomycota and Muromycotina (false truffles) (Piattoni et al., 2012; Bonito et al., 2013). Hypogeous fungi are soil fungi that produce macroscopic fruiting bodies partially or completely embedded in soil, which have evolved several morphological changes, such as the loss of the ability to discharge spores actively (Trappe & Claridge, 2005). This leads to the development of several survival strategies, such as the development of a strong aroma, a trait commonly found in various truffle species (Gioacchini et al., 2005). This aromatic trait attract wild animals that feed on the sporophores, particularly rodents and

mammals. As these animals consume the sporophores, the spores within them are subsequently dispersed through their feces (Piattoni et al., 2012). The aroma of hypogeous fungi possesses an quality that makes it appealing even to humans, who find it delectable and consider it a culinary delicacy.

Fungi that form truffle-like sporophores have evolved independently in at least 13 orders in phylum that represent phylogenetically distant fungal lineages (Figure 1.2). Hypogeous fungi include two kinds, true truffles and false truffles. *Tuber* P. Micheli ex F.H. Wigg. is the commonly named "true truffles", which form ectomycorrhizae with different host tree species in Fagaceae, Pinaceae, Betulaceae, etc. (Zambonelli et al., 2016). False truffles refer to hypogeous fungi other than *Tuber*, which include *Choiromyces* Vittad (Tuberaceae, Pezizales, Ascomycota) and *Melanogaster* Quercus L. (Paxillaceae, Boletales). *Choiromyces*, commonly known as "pig truffles", form ectomycorrhizae with different host tree species of *Picea*, *Abies*, *Pinus,* etc. (Chen, Sun et al., 2016; Csorbainé et al., 2008). *Melanogaster,* commonly known as "like truffles", form symbiotic relationships with different host trees of Betulaceae, Cistaceae, Fagaceae, Pinaceae, Salicaceae, etc. (Perič & Moreau, 2010; Lacheva, 2015; Comandini et al., 2006).



Source Adapted from Smith and Bonito (2013), Zambonelli et al. (2016)

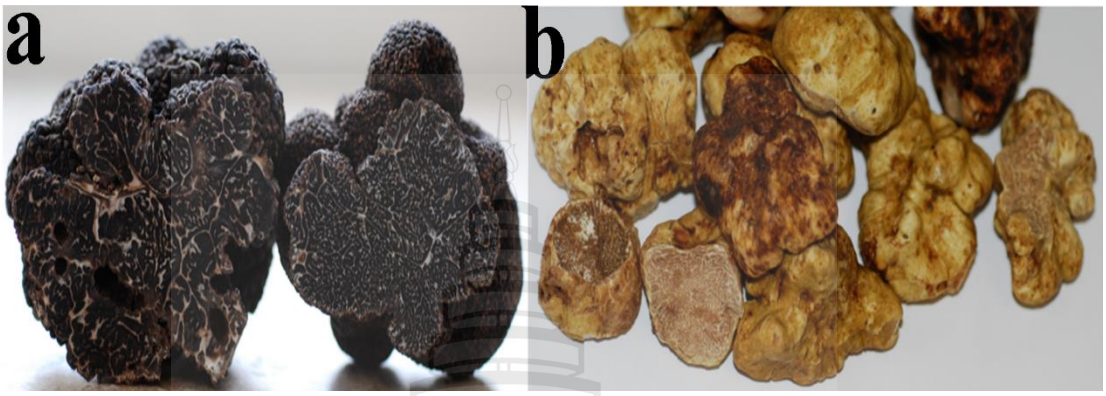
Figure 1.2 Phylogram showing the distribution of truffle-forming fungi throughout the fungal tree of life

1.2.1 True Truffles

Truffles are a group of fungi that produce hypogeous ascomata and belong to the genus *Tuber* (Tuberaceae, Pezizales, Ascomycota) (Trappe, 1975b). All *Tuber* species are ectomycorrhizal with a wide range of host plants (Fan et al., 2022). They enhance the resilience of plants and their ability to absorb water and nutrients (Zambonelli et al., 2016; Albornoz et al., 2020; Guerin-Laguette, 2021). *Tuber* is widely distributed in Europe, Asia,

and America (Bonito et al., 2013; Zambonelli et al., 2016;). The main morphological characteristics of the *Tuber* are as follows: the ascocarps (fruiting bodies) develop underground, with a smooth or warty surface; the spore-bearing tissue is solid, featuring white, marble-like veining; each ascus contains 1 to 8 spores, which are randomly arranged within the spore-bearing tissue; the surface of the ascospores is adorned with spiny or reticulate (honeycomb-like) ornamentation (Bonito et al., 2013; Fan et al., 2022). As edible fungi, some *Tuber* species, such as *Tuber. melanosporum* (the Perigord black truffle, see the Figure 1.3 a), *T. magnatum* (the Italian white truffle, see the Figure 1.3 b), *T. aestivum* (the Burgundy truffle), have been widely used as edible mushrooms in Europe for a long time owing to their unique fragrance and flavor (Trappe, 1975a). Besides their economic and culinary importance, many truffle species play a key role in the forest ecosystem, including disturbed forests, where they are often generally ectomycorrhizal symbionts (Zambonelli et al., 2016). The scientific classification of *Tuber* species plays an important role in perceiving their characteristic and serves as the foundation for subsequent research, such as functional development of chemistry, medicine and cultivation. However, the traditional classification and identification of fungi primarily rely on the macroscopic features of their peridium, the composition of their gleba, the size, shape, and surface ornamentation of their spores. However, sometimes these features overlap in different species, making their identification challenging. For example, *T. aestivum* and *T. uncinatum* Chatin, two species with different aromas and variations in the depth of spore surface reticulation, have long been considered distinct species. Molecular analyses, relying on DNA sequence data, offer robust tools for the precise identification of *Tuber* species (Wang et al., 2006, 2007; Bonito et al., 2010; Kinoshita et al., 2011). These methods not only enhance our ability to distinguish *Tuber* species, but also enable the examination of *Tuber* species using environmental DNA sequences, thus expanding our understanding of their ecology and diversity. Recently, Bonito et al. (2013) reassessed the diversity, ecology, and historical biogeography of the genus *Tuber* using polygenetic loci for inferences (ITS, 28S, RPB2 and TEF1 rDNA). They distinguished 11 major clades within *Tuber* and estimated

the number of species to be between 180 and 220, while more than 80 *Tuber* species have been recorded from China (Fan et al., 2022).



Source Adapted from Wilkinson et al. (2014)

Figure 1.3 The culinarily famous *Tuber melanosporum* (black truffle) and *Tuber magnatum* (white truffle)

1.2.2 False Truffles

False truffles are any of various fungi that produce underground sporophores that resemble truffles. False truffles, such as genus *Choiromyces* Vittad (Tuberaceae, Pezizales, Ascomycota), *Hydnotrya* Berk. & Broome (Pezizomycetes, Pezizales, Ascomycota), *Hydnobolites* Tul. & C. Tul. (Pezizaceae, Peziales, Ascomycota), *Melanogaster* Quercus L. (Paxillaceae, Boletales, Basidiomycota), and *Aplova* C. W. Dodge (Paxillaceae, Boletales, Basidiomycota), etc., which are distributed worldwide.

Choiromyces, with *C. meandriformis* Vittad. as the type species (Figure 1.4), was first described in 1831 (Vittadini, 1831). The genus, subglobose, or irregular, whitish to pale yellow in color, has a fragrant ascomata, and is solid gleba, which is often mistaken for a species of the genus *Tuber*, is widely distributed in Europe, North America, and Asia, but the species diversity is low, with only nine species confirmed, namely *C. alveolatus* (Harkn.)

Trappe, *C. cooei* Gilkey, *C. ellipsosporus* Gilkey, *C. helanshanensis* Juan Chen & P.G. Liu, *C. magnusii* (Mattir.) Paol., *C. meandriformis* Vittad., *C. tetrasporus* Velen., *C. venosus* (Fr.) Th. Fr. and *C. sichuanensis* S.P. Wan, Ran Wang & F.Q. Yu (Pegler et al., 1993; Moreno et al., 2012; Chen, Sun et al., 2016; Wang et al., 2022). Among them, the species of *C. helanshanensis* and *C. sichuanensis* are sporadically reported from China.



Source Adapted from Bîrsan et al. (2019)

Figure 1.4 The type of *Choiromyces meandriformis*

Melanogaster, with *M. tuberiformis* Corda as a type species (Figure 1.5), was established in 1831 (Corda, 1831). *Melanogaster* species commonly form estctomycorrhizae with both conifer and broadleaved trees, and are wildly distributed in Europe, North America, and Asia in the northern hemisphere (Wang et al., 2005; Rinaldi et al., 2008; Trappe et al., 2009; Tedersoo et al., 2010; Moreau et al., 2011; Moreno et al., 2012; Türkoğlu & Castellano, 2013; De la Fuente et al., 2021; Xu, Yan et al., 2022). This genus is characterized by gasteroid hypogeous to semi-hypogeous basidiomata, sometimes with mycelial strands at the surface or base, prosenchymatic peridium, gleba with gelatinous small chambers separated by sterile

veins scattered when mature, yellow to dark brown, globose, ellipsoid, pyriform or fusiform basidiospores (Trappe et al., 2009; Moreau et al., 2011; Alvarado et al., 2021; De la Fuente et al., 2021; Xu, Yan et al., 2022). It is estimated that there are about 26 species in the world (He et al., 2019), and about 19 species in north temperate forests (Trappe et al., 2009). In China, the first species was collected from Jinshajiang Valley in Yunnan province, southwestern China in 1915. It was originally identified as *M. variegatus* (Vittad.) Tul. & Tul. (Keissler & Lohwag, 1937), but re-described as a new species *M. ovoidisporus* Y. Wang by Wang et al. (1995). More and more novel species have been described from China?, namely *M. spinisporus* Y. Wang, *M. tomentellus* L. Fan, X.Y. Yan & Y.Y. Xu, *M. broomeanus* Berk., M. *subglobisporus* K. Tao, Ming C. Chang & B. Liu, *M. panzhihuaensis* L. Fan, X.Y. Yan & Y.Y. Xu, *M. shanxiensis* B. Liu, K. Tao & Ming C. Chang, *M. minobovatus* L. Fan, X.Y. Yan & Y.Y. Xu and *M. natsii* Y. Wang, K. Tao & B. Liu (Yan et al., 2020; Xu,Yan et al., 2022).



Source Adapted from Melanogaster (fungus), (2024, April 3)

Figure 1.5 The type of *Melanogaster tuberiformis*

1.3 Order Boletales

Classification

Kingdom Fungi

Phylum Basidiomycatota

Class Agaricomycetes

Subclass Agaricomycetidae

Order Boletales

Family Boletaceae

Genus *Boletus*

Genus *Butyriboletus*

Genus *Rubroboletus*

Genus *Retiboletus*

Genus *Lanmaoa*

Genus *Neoboletus*

Genus *Rugiboletus*

Family Boletinellaceae

Genus *Phlebopus*

The order Boletales (Gilbert, 1931) is one of the largest groups of Basidiomycota and most of them are ectomycorrhizal and edible (Zhou et al., 2023). They are economically and ecologically important (Wu, Li et al., 2016). They can form mycorrhizal relationships with some families of plants, including Dipterocarpaceae, Pinaceae, Betulaceae and Salicaceae, which play vital roles in vegetation restoration, water and soil protection, maintaining forest ecosystems, and contributing to the diversification of both fungi and their host plants (Li & Yang, 2021). Typically, basidiomes of Boletales are pileate-stipitate with a tubular hymenophore, though some exhibit lamellate hymenophores or intermediates that show transitions between these two types (e.g., *Boletus*, *Lamaoa*, *Rugiboletus*, *Butyriboletus*, *Retiboletus, Suillus*), but secotioid (*Neoboletus*) or gasteroid

forms (e.g., *Astraeus*, *Melanogaster*) also occur. In addition, resupinate forms with smooth or warted (*Coniophora*), merulioid (*Serpula*, *Leucogyrohana*), and toothed (*Gyrodontium*) hymenophore also exist. Those various forms of basidiomes are used as an important basis for classification of Boletales. With the rapid development of molecular technology, molecular methods have been applied to the taxonomy, systematics, phylogeny and biogeography of macrofungi, and the classification of boletes has made unprecedented progress (Zhou et al., 2023). Up to now, over 500 species of Boletales, including nearly 100 species, have been reported from China (Zeng et al., 2012; Cui et al., 2016; Wu et al., 2014, Wu, Zhao et al., 2016, Wu, Li et al., 2016). The discovery of these species provides the foundation for research on China's Boletales species diversity, chemical diversity, ecosystem protection, cultivation and domestication, the development of potential medicinal and edible species, and the understanding of species origin and evolution.

1.3.1 *Boletus*

Boletus L. (Linnaeus, 1753) was established for the porcini mushrooms (*Boletus edulis* and its allies), which is one of the most important fungal groups due to their ecological and economic value (Arora, 2008; Sitta & Floriani, 2008). More and more species have been found around the world by mycologists. The status of the taxonomy of the Boletaceae has long been controversial, either suggesting to keep *Boletus* in a broad sense that would represent the currently accepted whole family Boletaceae or split it into different genera (Singer, 1986; Zang, 2006; Horak, 2005, 2011; Cui et al., 2016). However, several molecular phylogenetic studies have indicated that the genus *Boletus* in the broad sense is polyphyletic (Binder & Hibbett, 2006; Dentinger et al., 2010; Feng et al., 2012; Li, Wei et al., 2014; Nuhn et al., 2013; Wu et al., 2014; Cui et al., 2016). Boletus sect. *Boletus*, as the porcini group, typified by *B. edulis* Bull., is monophyletic (Dentinger et al., 2010; Feng et al., 2012; Nuhn et al., 2013; Wu et al., 2014; Cui et al., 2016). This genus shares the following common features: the surface of immature poroid hymenophore is covered with a layer of tangled white hyphae, the stipe is more or less reticulated, and the whitish

to white flesh is without color change when cut, bruised, or exposed to air (Singer, 1986; Wu et al., 2014; Cui et al., 2016). They are gourmet mushrooms, highly prized in many parts of the world (Feng et al., 2012). To date, more than 50 species have been reported in this genus in the world (http://www.speciesfungorum.org/Names/Names.asp). Recent molecular phylogenetic analyses indicated that there are more than 20 species of porcini mushrooms in China (Yang, Xu et al., 2022).



Source Adapted from Cui et al. (2016), Reilly (2011)

Figure 1.6 The species of *Boletus edulis* and *B. bainiugan*

1.3.2 *Butyriboletus*

Butyriboletus Arora & J. L. Frank (Boletaceae, Boletales), typified by *Butyriboletus appendiculatus* (Schaeff.) D. Arora & J. L. Frank, was erected in 2014 to accommodate the "butter boletes" (Arora & Frank, 2014). Until now, more than 30 taxa of *Butyriboletus* have been described in the world, and most of them are from temperate and tropical regions (Takahashi et al., 2013; Arora & Frank, 2014; Zhao et al., 2015; Liang et al., 2016). The genus *Butyriboletus* differs from all other genera of Boletaceae in its brown to reddish pileal surface, yellowish to yellow hymenophore and context staining bluish to blue when hurt, concolorous

reticulations on the stipe surface and mild taste. The basidiospores are smooth, subfusiform, and brownish-yellow. The pileipellis is an interwoven trichodermium (Arora & Frank, 2014).



Source Adapted from Wu, Zhao et al. (2016)

Figure 1.7 The species of *Butyriboletus roseoflavus* and *B. pseudospeciosus*

1.3.3 *Rubroboletus*

Rubroboletus Kuan Zhao & Zhu L. Yang was erected to accommodate *Boletus* sinicus W. F. Chiu and its allied species (Zhao et al., 2014). *Ruroboletus* can be distinguished from other genera in the Boletaceae by several distinctive features: a reddish pileal surface, red hymenophore surface, yellow tubes, pink to red reticulum or spots on the stipe, a bluish color change when injured, smooth, olive-brown spores, and an interwoven

trichodermal pileipellis (Zhao et al., 2014; Zhao & Shao, 2017). This genus was widely accepted around the world, more than 20 species were recorded in the Index Fungorum, of which 7 species were described from China, including *R. esculentus* Kuan Zhao, H. M. Shao & Zhu L. Yang, *R. flavus* G. Wu & Zhu L. Yang, *R. latisporus* Kuan Zhao & Zhu L. Yang, *R. reticulatus* L. Fan, N. Mao & T.Y. Zhao, *R. satanas* (Lenz) Kuan Zhao & Zhu L. Yang, *R. serpentiformis* G. Wu, Hai J. Li & Zhu L. Yang, *R. sinicus* (W. F. Chiu) Kuan Zhao & Zhu L. Yang, (Zhao et al., 2014; Zhao & Shao, 2017; Zhang et al., 2022; Mao et al., 2023; Wu et al., 2023).



Source Adapted from Zhao et al. (2014)

Figure 1.8 The species of *Rubroboletus sinicus*

1.3.4 *Retiboletus*

Retiboletus Manfr. Binder & Bresinsky, was established based on the presence of retipolides (unusual spiromacrolactones) in the Boletaceae with the type species *R. ornatipes* (Peck) Manfr. Binder & Bresinsky (Binder & Bresinsky, 2002). *Retiboletus* differs from other Boletaceae genera by its reticulate stipe with a base usually darker than the apical region. The

part of basidiomata stains yellow-orange to rusty brown after bruising, which is not like many other boletes. Moreover, the mushrooms easy stain the fingers yellow on handling or picking. This yellow staining is due to retipolides that is a unique kind of metabolite so far only found in the genus Retiboletus (Justus et al., 2007). Based on the DNA phylogenetic analyses and their characteristic retipolides, *Retiboletus* was erected as a new genus of Boletaceae by Binder and Bresinsky (Binder & Bresinsky, 2002). To date, seventeen *Retiboletus* species have been reported from temperate or tropical (http://www.indexfungorum.org/Names/Names.asp), of which ten species have been found in China, including *R. atrofuscus* Yan C. Li & T. Bau, *R. brunneolus* Yan C. Li & Zhu L. Yang, *R. cyanescens* Yan C. Li & Zhu L. Yang, *R. fuscus* N.K. Zeng & Zhu L. Yang, *R. kauffmanii* N.K. Zeng & Zhu L. Yang, *R. nigrogriseus* N. K. Zeng, S. Jiang & Zhi Q. Liang, *R. pseudogriseus* N. K. Zeng & Zhu L. Yang, *R. sinensis* N. K. Zeng & Zhu L. Yang, *R. sinogriseus* Yan C. Li & T. Bau and *R. zhangfeii* N. K. Zeng & Zhu L. Yang (Wu, Zhao et al., 2016; Zeng et al., 2016; Zeng et al., 2018; Liu et al., 2020; Zhou et al., 2022).



Source Adapted from Zeng et al. (2016)

Figure 1.9 The species of *Retiboletus fuscus*

1.3.5 *Lanmaoa*

Lanmaoa G. Wu & Zhu L. Yang (Boletaceae, Boletales), typified by *L. asiatica* G. Wu & Zhu L. Yang, was erected recently to accommodate several species formerly classified in genus *Boletus* L. (Wu, Zhao et al., 2016). *B. carminipes* A. H. Sm. & Thiers (1971), *B. flavoruber* Halling & M. Mata (2004) and *B. pseudosensibilis* A. H. Sm. & Thiers (1971) were transferred into the genus *Lanmaoa* by Wu et al (Wu, Zhao et al., 2016). In addition, the species *B. fragrans* Vittad. (1835) was transferred into this genus by Vizzini (2015). Three species were also described as new to science, *L. angustispora* G. Wu & Zhu L. Yang, *L. asiatica* G. Wu & Zhu L. Yang (Wu, Zhao et al., 2016) and *L. roseocrispans* Bessette, A. R. Bessette, Nuhn & Halling (Bessett, 2015). Up to now, eleven species of *Lanmaoa* have been reported on the IndexFungorum (http://www.indexfungorum.org/Names/Names.asp). However, except for *L. flavorubra* (Halling & M. Mata) G. Wu, Halling & Zhu L. Yang (Wu, Zhao et al., 2016) described from Central America, *Lanmaoa* species were described from temperate, subtropical and tropical regions of Asia and America (Wu, Zhao et al., 2016; Chai et al., 2018; Garey, 2021). This genus differs from all other genera of Boletaceae by its thin hymenophore, and stains blue when bruised, a light-yellow context which stains pale blue slowly when cut, and an interwoven trichodermium to a subcutis pileipellis (Wu, Zhao et al., 2016).



Source Adapted from Wu, Zhao et al. (2016)

Figure 1.10 The species of *Lanmaoa asiatica*

1.3.6 *Neoboletus*

Neoboletus Gelardi, Simonini & Vizzini were newly segregated from *Boletus* L. and typified by *N. luridiformis* (Rostk.) Gelardi, Simonini & Vizzini (Vizzini, 2014). The genus is characterized by its stipitate-pileate or sequestrate basidiomata, and basidiomata stipitate-pileate, with pores brown, dark brown to reddish brown when young, after becoming yellow when old, tubes always yellow, context and hymenophore staining blue, the stipe commonly covered with punctuations (Vizzini, 2014; Wu, Zhao et al., 2016; Chai et al., 2019; Jiang et al., 2021). In the past decade, more than twenty species have accommodated in the genus based on Index Fungorum (http://www.indexfungorum.org/Names/Names.asp), of which 11 were described from China, including *Neoboletus brunneorubrocarpus* G. Wu, Hai J. Li & Zhu L. Yang, *N. ferrugineus* (G. Wu, Fang Li & Zhu L. Yang) N.K. Zeng, H. Chai & Zhi Q. Liang, *N. flavidus* (G. Wu & Zhu L. Yang) N.K. Zeng, H. Chai & Zhi Q. Liang, *N. hainanensis* (T.H. Li & M. Zang) N.K. Zeng, H. Chai & Zhi Q. Liang, *N. infuscatus* N.K. Zeng, S. Jiang & Zhi Q. Liang, *N. multipunctatus* N.K. Zeng,

H. Chai & S. Jiang, *N. obscureumbrinus* (Hongo) N.K. Zeng, H. Chai & Zhi Q. Liang, *N. rubriporus* (G. Wu & Zhu L. Yang) N.K. Zeng, H. Chai & Zhi Q. Liang, *N. sanguineoides* (G. Wu & Zhu L. Yang) N.K. Zeng, H. Chai & Zhi Q. Liang, *N. sanguineus* (G. Wu & Zhu L. Yang) N.K. Zeng, H. Chai & Zhi Q. Liang, and *N. tomentulosus* (M. Zang, W.P. Liu & M.R. Hu) N.K. Zeng, H. Chai & Zhi Q. Liang (Wu, Zhao et al., 2016, Wu, Li et al., 2016; Chai et al., 2019; Jiang et al., 2021).



Source Adapted from Wu, Zhao et al. (2016), Chai et al. (2019)

Figure 1.11 The species of *Neoboletus obscureumbrinus*, *N. magnificus* and *N. hainanensis*

1.3.7 *Rugiboletus*

Rugiboletus G. Wu & Zhu L. Yang, typified by *R. extremiorientalis* (Lar. N. Vassiljeva) G. Wu & Zhu L. Yang (Wu, Zhao et al., 2016), which is characterized by wrinkled or convoluted and glutinous surface of pileus, always yellow tubes, dot-like squamules or scabers on stipe surface and an ixotrichodermis pileipellis (Chakraborty, 2015; Wu, Zhao et al., 2016). Up to now, only three species of this genus have been reported worldwide. In addition to the type species are *Rug. andinus* (Halling) Halling & B. Ortiz and *Rug. brunneiporus* G. Wu & Zhu L. Yang. Both *Rug. extremiorientalis* and *Rug. brunneiporus* were described from China.



Source Adapted from Wu, Zhao et al. (2016)

Figure 1.12 The species of *Rugiboletus extremiorientalis*

1.3.8 *Phlebopus*

Phlebopus was proposed as a subgenus of *Boletus* to accommodate *Boletus colossus* R. Heim by Heim (1936). Later, *Phlebopus* was reclassified as a separate genus, with *P. colossus* (R. Heim) Singer being designated as the typified species by the mycologist Singer (1936). Subsequently, Heinemann and Rammeloo (1982), Singer et al. (1983), and Singer (1986) further emended the limits of the genus to encompass all taxa of

Phaeogyroporus (Singer, 1945). Recently, Binder and Bresinsky (2002) have classified *Phlebopus* in the Boletinellaceae (Boletales). *Phlebopus* is a genus primarily found in tropical or subtropical regions. It is characterized by its solenoid basidiomata, which are fruiting bodies that resemble those of boletes. These basidiomata produce spores with an olivaceous brown spore print. Under a light microscope, the basidiospores of *Phlebopus* are ellipsoidal and have smooth surfaces. Additionally, the hyphae of *Phlebopus* fungi are notable for having clamp connections, which are specialized structures that aid in the transfer of nuclei during cell division in the fungal mycelium. To date, there are 18 species have been reported in the database (Index Fungorum, http://www.indexfungorum.org/Names/Names.asp). Them of eight species (including *P. braunii* (Bres.) Heinem., *P. bruchii* (Speg.) Heinem. & Rammeloo, *P. colossus* (R. Heim) Singer, *P. cystidiosus* Heinem. & Rammeloo, *P. harleyi* Heinem. & Rammeloo, *P. latiporus* Heinem. & Rammeloo, *P. silvaticus* Heinem., *P. sulfureus* (Quél.) Singer) are found to be from Africa; four species of Phlebopus (*P. marginatus* Watling & N.M. Greg., *P. spongiosus* Pham & Har. Takah., *P. viperinus* Singer, and *P. xanthopus* T.H. Li & Watling) are reported to be from Asia and Australasia, respectively. Three species (*P. brasiliensis* Singer, *P. mexicanus* Cifuentes, Cappello, T.J. Baroni & B. Ortiz, *P. tropicus* (Rick) Heinem. & Rammeloo) are known to be from the neotropics. Two species (*P. beniensis* (Singer & Digilio) Heinem. & Rammeloo and *P. roseus* Mei Yang, C.Y. Liu & Yun Wang) are usually found in Africa and the neotropics. *P. poretentosus* (Berk. & Broome) Boedijn is known to be from Asia, Africa and neotropics (Heinemann, 1982; Halling & Mueller, 2002; Ji et al., 2010; Pham et al., 2012; Kumla et al., 2015; Callac & Chen, 2018; Mei et al., 2021).



Source Adapted from Zhang et al. (2017)

Figure 1.13 The species of *Phlebopus portentosus*

1.4 Chemotaxonomy to Improve Fungal Classification

Chemotaxonomy, also known as chemosystematics, is the classification and identification of organisms, originally focusing on plants, based on verifiable differences and similarities in their biochemical compositions (Steiner & Leistner, 2012). Chemotaxonomy lies at the intersection of natural product chemistry and taxonomy. It is grounded in the frequent observation that identical or closely related natural products indicate the shared evolutionary history among different yet related organisms (Bhargava et al., 2013; Umoh, 2020). All living organisms (including fungi) produce secondary metabolites, which are derived from primary metabolites. The chemical structures of these secondary metabolites and their biosynthetic pathways are often specific to taxonomically related groups, making them valuable for classification. This method is considered superior to traditional classification techniques due to its straightforward methodology. In chemotaxonomy,

materials for analysis can be either dried or crushed; fresh or whole samples are not mandatory (Ankanna et al., 2012; Singh, 2016). So far as to the fungi develop and thrive in a wide variety of environments, containing within them a multitude of useful, harmful, and inert chemical components. These compounds provide the foundational basis for the chemical classification of fungi. (Singh, 2016). The four significant and widely studied groups of compounds used in chemotaxonomic classification are phenolics, alkaloids, terpenoids, and non-protein amino acids (Smith, 1976; Singh, 2016). These compounds demonstrate a considerable diversity in their chemical properties, distribution, and functions (Hegnauer, 1986; Singh, 2016). Chemotaxonomic classification is based on the chemical similarities among taxa (Rasool et al., 2010; Singh, 2016). The compounds employed in chemotaxonomy can be broadly categorized into two groups: primary metabolites and secondary metabolites. For example, Hyde et al. (2023) reported that from 2010 to 2022, there were 845 publications and 26,288 citations on the Web of Science website using the keywords ‘fungi’, ‘natural product’, and ‘classification’. Additionally, there were 259 publications with 4,662 citations using the keywords ‘fungi’ and ‘chemotaxonomy’. Numerous publications emphasize the benefits of incorporating chemical profiles in fungal classifications (Frisvad et al., 2008; Raja et al., 2017; Reich & Labes, 2017; Guo et al., 2021, Mahaarachchikumbura et al., 2021). In speciose groups, morphological characteristics can be misleading due to cryptic speciation, hybridization, and convergent evolution (Raja et al., 2017; Sun et al., 2019; Boekhout et al., 2022). Consequently, chemotaxonomy has often been applied to improve the efficiency of identifying, exploring, and exploiting fungi (Frisvad, 2015). Furthermore, studies suggest that secondary metabolites, also known as specialized metabolite profiles in fungi, can be strain-specific, species-specific, or common to multiple species. This variation may arise because fungal extracts contain both secondary and primary metabolites (Hyde et al., 2023). Chemotaxonomy is frequently employed to classify and identify filamentous fungi based on their chemical diversity for taxonomic purposes. However, not all compounds are suitable for chemotaxonomy, as the profiles are based solely on compounds with distinguishing features (Frisvad et al., 2008). Most fungi are fast-growing

and have high reproductive capacities, leading to generally unique metabolite profiles within individual groups (Walker & White, 2017). Nonetheless, different fungal species may produce one or more common secondary metabolites. For instance, cytochalasin D has been reported in several fungal species across phylogenetically diverse groups, such as Basidiomycota (Coriolus vernicipes (Berk.) Murrill) and Ascomycota (Hypoxylon terricola J.H. Mill., Metarhizium anisopliae (Metschn.) Sorokīn and Zygosporium masonii S. Hughes) (Cole et al., 2003; Vicente et al., 2003). Chemotaxonomy is highly valuable for delineating species, particularly in resolving species complexes that cannot be distinguished using classical morphological methods. It can also serve as a tool for identifying chemotaxonomic markers in comparative studies (Lauri et al., 2009; Surup et al., 2014; Kuhnert et al., 2017; Rinkel et al., 2018; Lambert et al., 2019; Ekman & Tønsberg, 2002).

A functional identification system is the core of fungal taxonomy, providing sufficient diagnostic characteristics for species delimitation. Phenotype-based identification systems have significant drawbacks, such as being laborious and time-consuming. Therefore, molecular-based identification systems (e.g., rDNA, DNA fingerprinting) are proposed for fungi that lack reliable morphological characteristics. High-throughput sequencing also greatly contributes to fungal taxonomy. However, formally naming nonculturable fungi from environmental sequencing remains a significant challenge. Biochemical profile-based identification systems hold outstanding value in fungal taxonomy and can occasionally be indispensable. This method utilizes biomarker metabolites and proteins that are expected to be unequivocal and stable (Lin et al., 2023). Particularly, earlier monographs were exclusively based on morphological data. However, Stadler et al. (2014) employed a polyphasic approach for *Daldinia*, incorporating molecular and chemotaxonomic data to delimit species and define infrageneric relationships. This polyphasic approach has been applied to characterize small genera such as *Rhopalostroma*, *Ruwenzoria*, and *Thamnomyces*, as well as to introduce new species of *Hypoxylon* and Annulohypoxylon (Stadler et al., 2010; Kuhnert et al., 2015; Daranagama et al., 2015; Sir et al., 2016; Kuhnert et al., 2017).

1.5 Chemotaxonomy and Chemical Diversity

Fungi are diverse in terms of their morphology, ecology, and chemical profiles (Naranjo-Ortiz & Gabaldón, 2019). Within the environment, all living entities produce secondary metabolites derived from primary metabolites. These secondary metabolites often possess unique and limited chemical structures specific to taxonomically related organisms. The categorization of fungi according to particular classes of secondary metabolites and their respective biosynthetic pathways forms the foundation of chemotaxonomy. The study of chemotaxonomy serves as a valuable tool for taxonomists, mycologist, and pharmacologists in addressing specific taxonomical challenges.

In the present study, morphology combined with molecular analyses are the main methods to study the taxonomy of fungi. Especially, with the increasing maturity of second and third-generation sequencing technologies for molecular sequencing and the continuous innovation in genome sequencing, the classification and identification of fungal species have become even more efficient, which coupled with the continuous development of computer technology, provides a fundamental guarantee for the accurate identification of fungal species. Above methods maybe easier for mycologists than chemists, pharmacologists, agronomists, and excellent agricultural workers. In addition, many species of fungiare difficult to differentiate from related species of the same genus or sometimes even family based only on their morphological characteristics. The confusion of species can easily bring inconvenience to the subsequent applications. In wild edible mushrooms, the confusion caused by the similarity of species morphology, is one of the most serious food safety issues in the world, such as edible king bolete (*Boletus edulis* complex) and the toxic *Boletus huronensis* and *Sutorius eximius*, edible Bicolor Bolete (*Boletus bicolor*) and the toxic sensitive bolete (*Boletus sensibilis*), *Calvatia* spp. and *Lycoperdon* spp. and the toxic *pigskin puffballs* (*Scleroderma* spp.) (Gonmori et al., 2011; Chen et al., 2013; Beug, 2021; Li, Chen et al., 2021; Li, Pires et al., 2021; Li, Zhang et al., 2022; Li, Zhang et al., 2023; Li, Hu et al., 2023; Ma et al., 2023). Among these confusing

species, although their morphological characteristics are similar, there are certain differences in their molecular features and chemical categories, which is also the main reason for poisoning after mistaken consumption. However, for special samples, such as dried or powdered samples, it is often difficult to obtain their DNA, making molecular analysis inadequate for species identification. In such cases, using chemical taxonomy to explore differences in their intrinsic chemical compositions to assist in species identification is not only more efficient but also highly effective. This technique has been widely applied in various fields for species identification, such as traditional Chinese medicinal materials, gemstones, drugs, and even the detection of food alteration.

Mushrooms have been an indispensable element of human culture since antiquity and are appreciated all over the globe for their nutritive and therapeutic benefits. Their nutritional value is due to their high protein, fiber, vitamin, and mineral contents, low-fat levels and flavor and texture (Mattila et al., 2001; Karine et al., 2006; Xu et al., 2011; Nakalembe & Kabasa, 2013; Jedidi et al., 2017; Ugbogu et al., 2018; Zhang, Pu et al., 2018; Zhang, Hu et al., 2018). In addition, the medicinal mushrooms mainly contain many different bioactive compounds including polysaccharides, steroids, phenols, terpenoids, and nucleosides, et al. (Wasser, 2002; Ghahremani-Majd & Dashti, 2015; Friedman, 2016; Meng et al., 2016; Singdevsachan et al., 2016; Roncero-Ramos & Delgado-Andrade, 2017; Wang et al., 2017; Xu, Xu et al., 2022). The category of chemical components plays an important role in effectively identifying species and tracing their source of mushrooms. Meanwhile, these chemical components are also the substance basis of chemotaxonomy. Although the significance of chemical compounds as markers for fungal taxonomy is still unclear, enough information is available to justify investigations in this field (Petrini et al., 2009). A large of literatures show that biochemical methods have been introduced in mycology to further characterize genera and species. For example, *Isaria cicadae* and *I. tenuipes*, belong to the anamorph of *Cordyceps* genus, the second metabolites in them are different. *I. cicadae* mainly includes nucleoside, amino acids, beauvericins, myriocin, and oosporein. In contrast, trichothecene derivatives, isariotins, cyclopenta benzopyrans

and PKs were found in *I. tenuipes* (Zhang et al., 2018). Malheiro et al. (2013) identified that volatile compounds were capable to distinguish six wild mushroom species (*Clitocybe odora*, *C. fragrans*, *Hebeloma crustuliniforme*, *Lepista nuda*, *Tricholoma fracticum* and *T. terreum*) for taxonomic and authentication purposes. The results showed that 11 volatile compounds (3-octanol, 3-octanone, linalool, 1-octanol, 1-pentanol, (E)-2-octen-1-ol, hexanol, hexanal, (E)-2-octenal, ρ-anisaldehyde and sesquiterpene-like compound) in common with an important discriminating power, which can play a crucial biomarker role in the characterization of those six wild species of mushrooms. Li, Wu et al. (2021) performed ultra-performance liquid chromatography-electrospray ionization-tandem mass spectrometry (UPLC-ESI-MS/MS) based on widely targeted metabolomics analysis to identify key compounds for wild edible boletus mushrooms. A total of 194 metabolites, including 49 lipids, 34 amino acids and derivatives, 30 organic acids, 18 phenolic acids, 16 nucleotides and derivatives, 13 alkaloids, 6 flavonoids, 3 lignans and coumarins, 3 tannins, 2 terpenoids, and 20 others were significantly differed between *Boletus bainiugan* and *B. subsplendidus*. Those metabolites have provided new insights for the identification of two wild edible boletus mushrooms. Nakalembe and Kabasa (2013) analyzed the fatty and amino acids composition of five wild edible mushrooms *Termitomyces microcarpus*, *Termitomyces sp.* (Bunyanaka), *T. globulus*, *T. eurrhizus* and *Polyporus tenuiculus* in Bunyoro sub-region, Uganda, African. The essential amino acids ranged from 23.6% in *P. tenuiculus* to 59.0% in *T. microcarpus* of the total amino acids. *Termitomyces sp*. (Bunyanaka) and *T. globulus* were the most nutritious species based on essential amino acid indices. These fatty and amino acid compositions as a basis for the identification of the mushrooms of local communities. The diversity of the intrinsic chemical components or primary and second metabolites of these fungi provides the foundation for fungal chemical taxonomy.

Furthermore, study on the types and structures of fungal chemical components can not only effectively assess the quality of edible fungi, but also provide a basis for further exploration of the potential medicinal, material, and functional value of fungi. For chemical

diversity, many literatures have reported and shown some chemical compounds possess a range of nutritive values and beneficial biological activities. Such as *Boletus* mushrooms are rich in polysaccharides, proteins, amino acids, vitamins and mineral elements, while polysaccharides have been revealed to have biological activities of anti-inflammatory, hepatoprotective, antibacterial and antiviral (Tan et al., 2022; Tian et al., 2022; Chen et al., 2023; Su et al., 2023). Phenolic compounds and phytosterols of *Boletus* mushrooms have been verified with pharmacological properties of antioxidant, antineoplastic and anti-inflammatory (Tan et al., 2022). Eight wild edible Boletaceae mushrooms were analyzed and compared for their basic chemical compositions and the antioxidant properties of their phenols. The mushrooms included *Boletus bicolor*, *Boletus craspedius*, *Butyriboletus brunneus*, *Rubroboletus sinicus*, *Retiboletus ornatipes*, *Suillus placidus*, *Xerocomus* sp., and *Tylopilus* sp., all collected from Yunnan province, China. The nutrient contents analyzed included crude protein, total soluble amino acids, amino acid profiles, crude fat, fatty acid compositions, total carbohydrates, total soluble sugars, total dietary fiber, monosaccharide compositions, crude ash, metal profiles, total phenols, and their antioxidant activities. The results showed a rich chemical diversity among different species, and these chemical compounds have potential medicinal value (Ahmed et al. 2015). Lin et al. (2022) determined the chemical composition of *Pleurotus* species, and investigated their chemical diversity and to compare the differences between them. *Pleurotus* species were rich in sugars, amino acids, polar lipids, mycolic acids, quinones, and fatty acids, and chemical information would promote the efficient identification of the genus *Pleurotus*. Manikandan (2011) reported that different mushroom species were rich in ash (7–17%), fiber (16–20%), protein (30–48%), fat (1–4%), and carbohydrate (125– 40%). Chuankid et al. (2020) revealed seven known secondary metabolites including methyl atromentate, methyl isoxerocomate, atromentic acid, xerocomic acid, variegatic acid, methyl variegatate and variegatorubin and isolated two new compounds, namely 9′-hydroxyphenyl pulvinone and phlebopyrone from the edible species *Phlebopus portentosus* and *P. spongiosus* from northern Thailand.

1.6 Evaluation of Commercial Boletes

Boletes are one of the most widely collected edible mushrooms in the world (Boa, 2004; Kirk et al., 2008; Sitta & Floriani, 2008; Simmonds et al., 2020; Pérez-Moreno et al., 2021). It was estimated about 50 genera and 800 species of Boletaceaea in the world according to Wu et al. (2014), while 1343 species of Boletaceae were recorded in the Index Fungorum (http://www.indexfungorum.org/Names/Names.asp). Boletes is the biggest group under the Agaricomycetes.

Studies show that the species (e.g. *Boletus aereus, Suillus bovinus, Suillellus luridus, Bo. edulis, Bo. violaceofuscus,* and so on) of Boletaceae have abundant chemical compounds including moisture, ash, crude protein, crude fat, total carbohydrates, amino acids, minerals and heavy metals, etc. (Liu et al., 2016). Meanwhile, some unexpected compounds were reported from mushroom boletes. For example, analyses of the structure characteristics of the crude polysaccharides revealed that *Butyriboletus pseudospeciosus* was mainly composed of mannose, glucose and galactose, possessing the pyranose ring and β/α-glycosidic linkages. Based on the experimental modulation effects on gut microbiota, the abundance of beneficial microbiota in *B. pseudospeciosus* treated group was significantly increased, while the abundance of harmful microbiota was significantly decreased. The results suggest that *B. pseudospeciosus* could serve as potential functional food or medicine (Tian et al., 2023). Li, Hu et al. (2023) performed metabolomics profiling to determine changes of flavor quality and bioactive components of *Phlebopus portentosus* under low-temperature storage by LC/MS and GC/MS. The metabolites results showed that they were different at the same period and significantly different after 7 days of storage in caps and stipes. A total of 583 and 500 different metabolites were detected in caps and stipes, respectively, and were mainly lipids and lipid-like molecules, organic acids and derivatives, organic oxygen compounds and others.

Moreover, Yang, Che et al. (2022) evaluated the delicious taste characteristics of *Butyriboletus roseoflavus*, the aqueous extract was separated and combined with sensory

analysis. The results found that four novel umami peptides, GSAQA, ISKEK, LPKERLYV, and VENQQLAL were isolated and identified by Gel chromatography, RP-HPLC, and Nano-LC-MS/MS, and sensory evaluation revealed that these umami peptides could elicit umami and umami enhancement, among them VENQQLAL performing best. Yang et al. (2021) found that lipid molecules and their concentrations in *Boletus speciosus*, *Bo. bainiugan*, and *Tricholoma matsutake* exhibited significantly different behaviors compared with the remaining mushrooms. Hierarchical cluster analysis (HCA) revealed that lipid profiles of *Bo. bainiugan* were most similar to *B. speciosus* followed by *T. matsutake*, *Canthar-ellus cibarius*, *Sarcodon aspratus*, *Termitomyces eurrhizus*, *Laccaria laccata*, and *Thelephora ganbajun*. Su et al. (2020) revealed a rearranged ergostane-steroid from the fruiting bodies of *Butyriboletus roseoflavus*, which is Spiroseoflosterol, a 7(8→9)-abeo-ergostane steroid with a unique spiro [4.5] decan-6-one system. Sun et al. (2018) obtained seven pyrrole alkaloids, three of which were novel and isolated from the fruiting bodies of the edible mushroom *Phlebopus portentosus*. In addition, with the continuous development of computer science, chemometrics combined with chemical fingerprint or spectroscopic fingerprint (such as near-infrared spectroscopy, mid-infrared spectroscopy, and ultraviolet spectroscopy, etc.) has been applied in quality assessment, species identification, and geographical origin tracing of edible boletus mushrooms. This non-destructive technology has achieved some success as a fast and effective method (Barreira et al., 2012; Wang et al., 2021; Chen et al., 2022; Yan et al., 2022; Liu et al., 2023; Yan et al., 2023).

With the continuous improvement of molecular systematics and morphological analysis techniques, an increasing number of species of boletes can be accurately identified. Boletes encompass a wide variety of species, and besides mycologists and scholars specialized in fungal taxonomy, the majority of fungal collectors, consumers, and even chemical classification experts find it difficult to effectively identify bolete species based on morphological characteristics alone. Edible boletes are highly favored by consumers due to their rich nutritional content and enticing aroma. However, in recent years, incidents of poisoning from mistakenly consumed boletes have become increasingly common both

domestically and internationally. Some of these incidents are attributed to the mixing and sale of morphologically similar boletes, particularly five toxic species that are prone to confusion, including *Chiua virens* (W. F. Chiu) Y. C. Li & Z. L. Yang, *Heimioporus retisporus* (Pat. & C. F. Baker) E.Horak, *Pulveroboletus ravenelii* (Berk. & M. A. Curtis) Murrill, *Sutorius eximius* (Peck) Singer, and *Tylopilus microsporus* S. Z. Fu, Q. B. Wang & Y. J. Yao (Li et al., 2011). Dry samples, in particular, are susceptible to confusion (Figure 1.3). This situation severely undermines food safety risk control efforts.

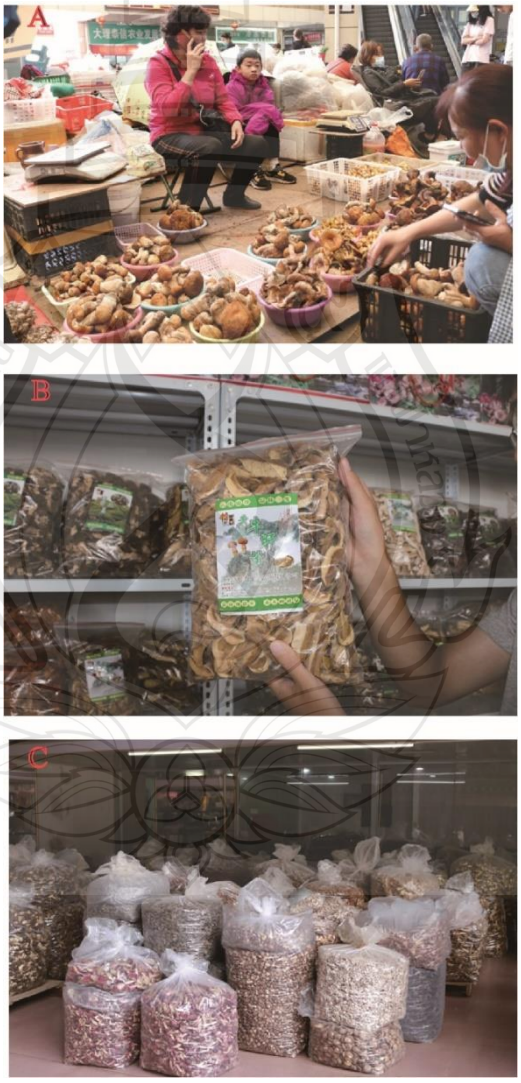


Figure 1.14 Boletes from Mu Shui Hua wild fungus trading market in Kunming city, Yunnan province, southwestern China

Herein, 11 species of commercial boletes from different producing areas including *Boletus bainiugan*, *Butyriboletus roseoflavus*, *Butyriboletus pseudospeciosus*, *Lanmaoa asiatica*, *Neoboletus hainanensis*, *Neoboletus magnificus, Neoboletus obscureumbrinus*, *Phlebopus portentosus*, *Rugiboletus extremiorientalis*, *Retiboletus fuscus*, and *Rubroboletus sinicus* were selected as objects, based on the analysis of molecular phylogeny and morphological characteristics, the chemical classification analysis were conducted, and the contents of characteristic aroma substance were predicted and analyzed, which could provide a new method for effective identification of boletus.

1.7 Research Objectives

1.7.1 The Diversity and Taxonomy of Truffles, False Truffles and Commercial Boletes

To study the diversity and taxonomy of truffles and false truffles (*Tuber*, *Choiromyces* and *Melanogaster*), including the description of new species, and identification of some commercial boletes from southwest China.

1.7.2 Establishment of the Geographical Pattern Recognition Model of Commercial Boletes

To establish the geographical pattern recognition model of the commercial boletes based on phylogenetic analyses combined with rich biochemical information.

1.7.3 Rapid Identification of Commercial Boletes

Evaluation of chemical profiling as amethod for rapid identification of the commercial boletes.

1.8 Research Outline

This thesis is comprised of seven chapters devoted to the study of hypogeous fungi including genus *Tuber*, *Choiromyces* and *Melanogaster* and 11 species of boletes including *Boletus bainiugan*, *Butyriboletus roseoflavus*, *Butyriboletus pseudospeciosus*, *Lanmaoa asiatica*, *Neoboletus hainanensis*, *Neoboletus magnificus, Neoboletus obscureumbrinus*, *Phlebopus portentosus*, *Rugiboletus extremiorientalis*, *Retiboletus fuscus*, and *Rubroboletus sinicus* collected from Yunnan and Sichuan provinces in southwestern China. The thesis covers two main topics: the identification of hypogeous fungi and the classification of boletes species based on chemical diversity.

Chapter 1 – An introduction of the importance of the study of taxonomy, phylogeny, and chemistry of edible ectomycorrhizal (ECM) fungi, true truffle, false truffle and Boletales from China. An overview of the genera *Boletus*, *Butyriboletus*, *Lanmaoa*, *Neoboletus*, *Phlebopus*, *Rugiboletus*, *Retiboletus* and *Rubroboletus*, including the progress and importance of research on chemotaxonomy, quality evaluation, and chemical diversity.

Chapter 2 – Research methodology

Chapter 3 – Research results

Chapter 4 – Discussion

Chapter 5 – Overall conclusions and perspectives

CHAPTER 2

RESEARCH METHODOLOGY

2.1 Taxonomy and Phylogeny Study

2.1.1 Morphological Study of *Tuber* (True Truffle)

Fresh samples were collected from forests of *Pinus yunnanensis* Franch. in Yunnan, China. Microscopic and macroscopic characteristics are described based on the specimen materials (L3694 and L3385) following the methods of Yang and Zhang (2003). Sections were made with a razor blade by hand, mounted in a 5 % (w/v) KOH solution, then lactophenol cotton blue, and examined under an OLYMPUS BH-2 microscope. For scanning electron microscopy (SEM), spores were scraped from the dried gleba onto double-sided tape and mounted directly on an SEM stub. They were then coated with gold-palladium, examined and photographed with a JEOL, JMS-5600LV SEM. For evaluation of range of spore-size, at least 40 ascospores each from one specimen of each collection site were measured. For spores, *Q*, the length-to-width ratio is given in the same format as spore dimensions and ***Q*** is the average *Q* of the all speciemens ± standard deviation. The specimens were deposited in the herbarium of Biotechnology and Germplasm Resources Institute, Yunnan Academy of Agricultural Science, and the Herbarium of Cryptogams, Kunming Institute of Botany, Chinese Academy of Sciences.

2.1.2 PCR Amplification and Sequencing of *Tuber* (True Truffle)

Total DNA was extracted from pieces of dried ascomata with a modified CTAB methodology (Hofstetter et al., 2002; Li et al., 2011). PCR were performed using the primer combination ITS4/ITS5 (Hofstetter et al., 2002; Larsson & Sundberg, 2011) and

LROR/LR5 (Vilgaly & Hester, 1990), respectively. In 25 µL of PCR reaction solution contained 1 µL DNA, 1 µL 5 µm of each primer pair, 2.5 µL 10 × buffer (Mg^{2+} plus), 1 µL Dntp (1 mM), 0.5 µL BSA (0.1 %), 0.5 µL $MgCl_2$, 1 U of Taq DNA polymerase (Takara Tag, Takara Biotechnology, Dalian, China). PCR reactions were run as follows: for the ITS gene, 94 ℃ for 5min, followed by 35 cycles of 94 ℃ for 30 s, 54 ℃ for 1 min and 72 ℃ for 1 min. The final reaction was followed by an extension at 72 ℃ for 10 min. For the LSU gene, 94 ℃ for 5 min, followed by 35 cycles of 94 ℃ for 1min, 60 ℃ for 50 s, 72 ℃ for 1min, and a final extension at 72 ℃ for 10 min. The PCR products were sent to Sangon Biotech Corporation (Shanghai, China) for purifying and sequencing by using ITS4/ITS5 and LROR/LR5, respectively.

2.1.3 Sequence Data Analyses of *Tuber* (True Truffle)

A total of 210 sequences of *Tuber* were used for phylogenetic analysis, of which 8 sequences were obtained in this study and 202 were derived from GenBank database as shown in Table 3.1, and also 5 sequences derived from two species of *Choiromyces helanshanensis* and *C. meandriformis* were selected and used as outgroups. Sequences were edited and assembled using SeqMan pro (DNAStar, Inc.). Alignment was performed using the online version of the multiple sequence alignment program MAFFT v7 (Katoh & Standley, 2013), appling the G-INS-I strategy, and the alignments were manually adjusted in BioEdit. Poorly aligned sites were identified and ambiguous sites were excluded by Gblocks v. 0.91b (Castresana, 2000) using default options except “Allowed Gap Postions” =half with default parameters. The multiple sequence alignments of both ITS1 + ITS2 based on the sequence of *Tuber glabrum* NR_153217 and ITS-LSU were carried out establishing the phylogenetic trees, respectively. A ML phylogenetic tree was constructed using RAxML v7.0.3 on the online server accessed at https://mafft.cbrc.jp/alignment/server/, applying the rapid boots-trapping algorithm for 1000 replications using the GTRGAMMA model. Clades with bootstrap values (BS) ≥ 75 % were considered as significantly supported (Hillis & Bull, 1993). BI were performed using the Metropolis-coupled Markov

chain Monte Carlo (MCMCMC) method in MrBayes version 3.2.7a (Ronquist et al., 2012) and the GTR+I+G model was selected as the best model under the Akaike Information Criterion (AIC) implemented by MrModeltest v.2.3 (Nylander, 2004). Two independent runs chains were conducted for 1,000,000 (ITS1+ITS2) and 2,000,000 (ITS-nrLSU). The average standard deviations of split frequencies (ASDSF) were less than 0.01 at end of the run and effective sampling size (ESS) values were more than 200. Tree sampling occurred every 100 generations post burn-in, well beyond convergence, and 50% majority-rule consensus trees were then constructed and visualized using TreeView32. Bayesian posterior probabilities (PP) ≥ 0.90 were deemed to indicate significant support, following the criteria established by Alfaro et al. (2003).

2.1.4 Morphological Study of *Choiromyces*

The *Choiromyces* samples were collected from Shangri-La County, Diqing Autonomous Prefecture, and Yongren County, Chuxiong Autonomous Prefecture, Yunnan Province, China. Macroscopic and microscopic descriptions were based on fresh ascomata following the methods of Wan (2016). Hand-cut sections were mounted in 5% (w/v) aqueous KOH solution, Cotton blue or Congo red solutions and examined with a compound microscope OLYMPUS BH-2. For scanning electron microscopy (SEM), spores were scraped from the gleba of dried specimens onto double-sided tape, which was mounted directly on a SEM stub, coated with gold-palladium, examined and photographed with a SEM JSM-5600LV (JEOL, Tokyo, Japan). Spore dimensions were measured on about 50 ascospores, and are presented in the following format: (*a*–) *b*–*c*–*d* (–*e*), with *a* and *e* representing the extreme values, *c* representing the average, *b*= *c* - 1.96 * S.D. and *d*= *c* + 1.96 * S.D. *Q*, the length to width ratio is given in the same format as spore dimensions. The specimens were deposited at the Herbarium of Biotechnology and Germplasm Resources Institute, Yunnan Academy of Agricultural Sciences, and the Herbarium of Cryptogams, Kunming Institute of Botany, Chinese Academy of Sciences, Yunnan, China.

2.1.5 Polymerase Chain Reaction (PCR) Amplification and Sequencing of *Choiromyces*

Total DNA was extracted from pieces of fresh ascomata with a modified CTAB procedure (Hofstetter et al., 2002). The internal transcribed spacer (ITS) region was amplified by PCR, using the primer combination ITS4/ITS5 (White et al., 1990), and the following cycling conditions: 94 ℃ for 5 min, followed by 35 cycles of 94 ℃ for 30 s, 55 ℃ for 40 s and 72 ℃ for 30 s, and a final extension step at 72 ℃ for 5 min. The PCR products were sent to Beijing Genomics Institute (Beijing, China) for purification and sequencing with ITS4 and ITS5.

2.1.6 Sequence Data Analyses of *Choiromyces*

The newly generated sequences were assembled and edited using SeqMan II (SeqMan Pro, DNAStar). A total of forty-one ITS sequences were used for phylogenetic analysis, among which five were generated in this study (3 sequences of known species and 2 sequences of *C. cerebriformis*) and thirty-six were downloaded from GenBank. Four sequences of *Dingleya* spp. and *Labyrinthomyces* spp. were selected as the outgroup.

The sequences were aligned using MAFFT ver. 7 (Katoh & Standley, 2013) on the online server accessed at https://mafft.cbrc.jp/alignment/server/, with the G-INS-I algorithm. The resulting alignment was manually adjusted by BioEdit. Identical sequences were removed from the dataset, but included the labels when editing the tree. ITS1 and ITS2 were delimited by comparison with the sequence HM485331 (*C. meandriformis*, isolate GB285), which is fully annotated in GenBank. The phylogenetic relationships of the taxa were inferred using maximum likelihood (ML) and Bayesian inference (BI). Partitioned ML phylogenetic inference was performed with RAxML v.7.2.6 (Stamatakis et al., 2005; Stamatakis, 2006, 2014, 2015) on the Cipres web server (Miller et al., 2009). The partition consisted of two blocks, with ITS1 and ITS2 in the first block, and 5.8S in the second block. Two species of *Dingleya* spp. and two species of *Labyrinthomyces* spp. were used as outgroup taxa. Clade support was estimated by rapid bootstrapping, using 1,000

replicates and the GTRCAT model with 25 categories.

Partitioned Bayesian analysis was carried out in MrBayes v.3.1.2 (Ronquist & Huelsenbeck, 2003), following the same partition as in ML analysis. The best-fit model of sequence evolution was estimated for each partition block separately with jModeltest 2.3 on Cipres, using the Bayesian information criterion. GTR+I+G was selected for ITS1 and ITS2, and K80+I was selected for 5.8S. Two runs with four chains each were run for 1,000,000 generations and sampled every 500 generations. At the end of the run, the average standard deviations of split frequencies were less than 0.01 and effective sampling size values were larger than 200 for all parameters. A majority-rule consensus tree was built and posterior probabilities (PP) were calculated after discarding the first 25 % of sampled trees as burn-in, using the sumt command of MrBayes.

To provide further evidence that *Choiromyces cerebriformis* is a new species distinct from the phylogenetically closest species, pairwise genetic distances (proportion of variable sites) within and among *C. cerebriformis* and other *Choiromyces* species were computed using MEGA ver. 4 (Tamura et al., 2007), with pairwise deletion of gaps and missing data.

2.1.7 Morphological Study of *Melanogaster*

The *Melanogaster* specimens were collected from Yunnan and Sichuan Provinces in China. They were photographed in the field, placed in sterilized plastic tubes or boxes, returned to the laboratory, and stored at 4 °C. Macroscopic and microscopic descriptions were based on fresh ascomata following the methods of Wan (2016). Hand-cut sections were mounted in 5% (w/v) aqueous KOH solution, Cotton blue, or Congo red solutions and examined with a compound microscope OLYMPUS BH-2. At least 50 basidiospores were measured of selected specimens, and the measurements are presented in the following format: L, W, Q, representing the extreme values of length, width, length to width ratio, $L_m = L \pm S.D.$, $W_m = W \pm S.D.$ and $Q_m = Q \pm S.D.$ For scanning electron microscopy (SEM), spores were scraped from the gleba of dried specimens onto double-sided tape, which was

mounted directly on an SEM stub, coated with gold-palladium, examined and photographed with an SEM JSM-5600LV (JEOL, Tokyo, Japan).

The dried specimens were deposited in the Herbarium of Biotechnology and Germplasm Resources Institute, Yunnan Academy of Agricultural Sciences, and the Herbarium of Cryptogams, Kunming Institute of Botany, Chinese Academy of Sciences, Yunnan, China.

2.1.8 PCR Amplification and Sequencing of *Melanogaster*

About 10–20 mg of dried gleba were placed in a 1.5 mL tube together with one 3 mm in diameter tungsten carbide bead, and crushed by shaking two to four times for 50 s at 30Hz with a Mixer Mill MM301 (Haan, Germany) Total DNA was extracted using the CTAB method described by Hofstetter et al. (2002). The following primer pairs were used for PCR amplification. The primer pair ITS4/ITS5 was used to amplify the nuclear ribosomal internal transcribed spacer region (White et al., 1990), the primers bRPB2-5F/bRPB2-7.1R for the second largest subunit of RNA polymerase II gene (rpb2) (Matheny, 2005; Matheny et al., 2007), and the LR0R/LR5 primers (Vilgalys & Hester, 1990; Cubeta et al., 1991) for the 28S nrDNA region (nrLSU). Amplifications were carried out in 25 μL reaction containing 0.2 μL of GoTaq polymerase of 5 U/μL (Promega), 5 μL of Buffer 5X (Promega), 0.2 μL of 1 μM primer, 5 μL of dNTPs 5mM, 2 μL of template DNA and 15.8 μL of nuclease-free water. Standard cycles of denaturation at 94 ℃ for 45 seconds, annealing for 45 seconds at different temperatures depending on the primer set (50 ℃ for RPB2, 54 ℃ for nrLSU, and 55 ℃ for ITS), and elongation at 72 ℃ for 1.5 min, followed by a final elongation step at 72 ℃ for 10 min. Then, samples were held at 4 ℃. PCR products were sent to Shanghai Sangon Biotechnology (Shanghai, China) for purifying and sequencing.

2.1.9 Sequence Data Analyses of *Melanogaster*

The newly generated sequences were assembled and edited using SeqMan II (SeqMan Pro, DNAStar) with generic-level identifies for sequences confirmed via BLAST

queries of GenBank. A total of 89 sequences (including ITS1-2, 5.8S, nrLSU, and RPB2) were used in the molecular phylogenetic analyses, including 7 sequences newly generated in this study and 82 downloaded from GenBank. Six sequences including *Paragyrodon sphaerosporus*, *Paxillus involutus*, *Alpova alpestris*, *Alpova conclor*, and *Alpova cinnamomeus* were selected as the outgroup. A sequence (AJ555527) of *M. tuberiformis* was served as the reference for delineating 5.8S, ITS1, and ITS2. The ITS, 5.8S, nrLSU and RPB2 sequences were separately aligned using MAFFT ver. 7 (Katoh & Standley, 2013) on the online server accessed at https://mafft.cbrc.jp/alignment/server/, with the G-INS-I algorithm. The obtained alignment was manually refined in BioEdit, and ambiguously aligned sites were pinpointed using Gblocks 0.91b (Castresana, 2000; using default options, except "Allowed Gap Positions" = half). This process involved identifying positions at 90%, 99%, 99.5%, and 99% for ITS1-2, 5.8S, nrLSU, and RPB2. The ITS1-2, 5.8S, nrLSU, and RPB2 alignments including gaps were 537, 157, 886, 715 bp, respectively. All sequences, including sequences from GenBank, were aligned using MAFFT (Katoh & Standley, 2013), and alignment were deposited in Figshare (doi: 10.6084/m9.figshare.25440544). Phylogenetic analyses were performed using ML and BI to validate the affiliation of our specimens with *Melanogaster*, relying on multi-gene sequences, which included *Alpova*, *Paralpova*, and *Neoalpova*. Additionally, an ITS dataset (including 159 bp 5.8S, and 527 bp ITS1+ITS2) was compiled to infer the phylogenetic relationships between *Melanogaster* species. The ML analyses were performed with RAxML 8.0.14 (Stamatakis et al., 2005; Stamatakis, 2006, 2014, 2015) with all parameters at default settings, except a mixed-model partitioning (with the same character sets as in the BI analyses), GTRGAMMA+I for all character sets, and 1,000 bootstrap pseudoreplicates. Partitioned BI analyses were performed with MrBayes v.3.1.2 (Ronquist & Huelsenbeck, 2003) based on the following best-fit substitution models estimated by jModelTest2 on Cipres XSEDE (2.1.6, https://www.phylo.org; Miller et al., 2010). For the multi-gene dataset, 5.8S: K80+G; ITS1-2: HKY+I+G; nrLSU and RPB2: GTR+I+G). For the ITS-only dataset, 5.8S: HKY+I+G; and ITS1-2: GTR+I+G. Two independent runs of four chains were conducted for 2.5×10^{6}

generations (ITS dataset) and 5×10^6 generations (multiple-gene dataset), with trees were sampled every 100 generations. The average standard deviation of split frequency (ASDSF) values at the conclusion of the runs were 0.009248 for the multi-gene tree and 0.001889 for the ITS tree. After discarding the samples from the burn-in phase (first 25% of trees), a 70% majority-rule consensus tree was constructed and posterior probabilities computed.

The trees were visualized with TreeView32 (Page, 2001), exported in PDF format, and edited in Adobe Illustrator CS6. Clades with bootstrap support (BS) ≥ 70% and Bayesian posterior probabilities (PP) ≥ 0.90 were considered significantly supported (Alfaro et al., 2003).

2.1.10 Subdivision of the Genus Melanogaster based on Morphological Characteristics

In order to explore the correlation among the morphological features of the subdivision of *Melanogaster* from China (including the three new species described herein), Japan and Mexico (non-European regions), the main morphological features including the number of peridium layers, average thickness of peridium, average length, and width of basidiospores were selected for statistical analysis. Using the three sections *Melanogaster*, *Rivulares*, and *Variegati* as the dependent variable (*Y*), and the morphological features of the species as independent variables (*X*), we conducted a visual analysis of subdivision of different species through Orthogonal partial least squares discriminant analysis (OPLS-DA) by SIMCA 14.0.

2.2 Identification of Wild Edible Boletes

2.2.1 Collection and Pretreatment of Wild Edible Boletes Samples

The samples were collected from the Yunnan-Guizhou plateau in southwest China, where is one of the most sensitive areas to climate change in China. A total of 509 individuals of boletes belonging to 11 species from 110 sites were collected from 15th June

to 20th August during 2019-2020. The fresh specimens were taken to the laboratory as soon as possible after wrapped in tin foil. A part of tissues was used to extracted DNA and the remained parts were washed and dried at 50 ℃. The dried samples were crushed into powder and passed through a 100-mesh stainless sieve to obtain same-sized particles. The powder after sieving were set in vacuum ziplock bags and stored at 4 ℃ in an independent refrigerator for chemical analyses.

The datasets were integrated, and duplicate data within 1 km were removed. The final species distribution data of 110 populations were obtained by ArcGIS 10.0 (Esri, Redlands, California USA) analysis, and the dataset was stored in CSV format to build the MaxEnt model (Naranjo-Ortiz et al., 2019; Rathor et al., 2019). According to the reported ecological factors that impact the occurrence of macrofungi (Hu et al., 2022; Jiang, Pettitt et al., 2022; Romero et al., 2022), 19 climate data of collection sites were origined from the World Climate Database, soil power of hydrogen (pH) values were derived from World Soil Database (http://webarchive.iiasa.ac.at/Research/LUC/External-World-soil-database/HTML/), longitude, latitude and elevation data were recorded by global position system (GPS). The ecological factors extracted by ArcGIS were as following: The environmental variables including spatial resolution of 30 s and raster data of approximately 1.0×1.0 km^2 were downloaded from WorldClim (https://www.worldclim.org/) based on the grid data generated by interpolating observations from the global climate from 1970 to 2000. Twenty-three ecological environmental variables potentially affected the geographical distribution of wild boletes were preliminarily selected, including elevation, longitude, latitude, pH, and 19 bioclimatic variables of precipitation and average temperature from June to September as shown in Table appendix A1 and A2). We also explored the use of Spearman correlation analysis to test multicollinearity among these variables.

2.2.2 Analysis of Molecular Phylogenetic

A total of 509 fruiting bodies of 11 frequently consumed boletes including *Boletus bainiugan* (BoB), *Butyriboletus pseudospeciosus* (BuP), *Butyriboletus roseoflavus* (BuR),

Lanmaoa asiatica (LA), *Neoboletus obscureumbrinus* (NO), *Rugiboletus extremiorientalis* (RugE), *Rubroboletus sinicus* (RubS), *Retiboletus fuscus* (RetF), *Phlebopus portentosus* (PP), *Neoboletus hainanensis* (NH), *Neoboletus magnificus* (NM) were collected from 2020-2021 in different microhabitats of Yunnan Province and Sichuan Province, China (Table 2.1 and appendix Table B). All of the bolete samples were identified based on their macroscopic features according to detailed field notes and photographs. The macroscopic identification of those specimens was performed based on taxonomic characteristics (Ruiz-Mirazo et al., 2014; Wu, Zhao et al., 2016; Wu, Li et al.,2016; Sun et al., 2017; Feng et al., 2018; Salazar et al., 2018; Rokas et al., 2020; Zhang, Huang et al., 2020; Allgeier et al., 2021). Additionally, the genomic DNA was extracted from fresh tissue or dried specimens using the CTAB isolation method adapted from Doyle et al. (1990) and Münkemüller et al. (2012). The tailed primer pairs EF1-983F/EF1-1567R (Rehner & Buckley, 2005) and bRPB2-6F/bRPB2-7.1R (Matheny, 2005; Matheny et al., 2007) were used to amplify translation elongation factor 1-α gene (*tef1*) and RNA polymerase Π largest (*rpb2*), respectively. The PCR amplification procedure was performed according to the method reported by Wu et al. (2014). Sequencing was performed with the Ezup column Fungi Genomic DNA Purification Kit (Sangon Biotech, Shanghai, China) on a representative sample of each species. The sequences were assembled in GENEIOUS Pro v. 6.0.6 (Biomatters) and introns were removed prior to alignment, based on the amino acid sequences of previously published. 509 sequences obtained from this study and 1073 sequences acquired from GenBank were aligned using MAFFT ver. 7 (Katoh & Standley, 2013) online server https://mafft.cbrc.jp/alignment/server/ with the G-INS-I algorithm. The resulting alignment was manually adjusted in BioEdit and poorly aligned sites were identified by Gblocks 0.91b using default options, except "Allowed Gap Positions" = half with default parameters (Castresana, 2000). Then, all identified ambiguous sites were excluded before the phylogenetic analysis, but the labels were included when editing the trees. The two gene sequences, *tef1* and *rpb2*, have alignments of 432 and 383 bp including gaps, respectively. The phylogenetic relationships of the taxa were inferred using ML and BI. We used

MrModeltest 2.3 (Nylander, 2004) under the Akaike information criterion to choose the best substitution model for multigene *tef1* and *rpb2* phylogenies. ML analyses were constructed with RAxML 8.0.14 (Stamatakis et al., 2005; Stamatakis, 2014) based on the GTRGAMMI substitution model with unlinked parameters. ML bootstrap support based on 1000 replicates were assessed in RAxML with a rapid bootstrap analysis and search for the best-scoring ML tree. The ML trees were viewed with TreeView32 (Page, 2001). Clades with bootstrap values (BS) ≥ 70% were considered significantly supported (Hillis & Bull, 1993). Bayesian analyses were performed using Mr. Mayes v.3.1.2 (Ronquist & Huelsenbeck 2003; Ronquist et al., 2012) software following the same partition as in the ML analysis. The best-fit model of sequence evolution was estimated for each partition block separately with jModeltest 2.3 on Cipres using the Bayesian information criterion. After the best substitution model was determined by SMS (GTR+G+I), it was chosen for *tef1* and *rpb2* sequences analyses. we ran two independent Mettropolis coupled Markov chain Monte Carlo (MCMC) chains each for 50,000,000, sampling every 500 generations until the standard deviation of the split frequency (ASDSF) became < 0.01, and effective sampling size values were larger than 200 for all parameters. A majority-rule consensus tree was established and Bayesian posterior probabilities (PP) ≥0.95 were considered significantly supported (Alfaro et al., 2003), after discarding the first 25% of sampled trees as burn-in using the sumt command of MrBayes. The phylogenetic tree was inferred from a four-partition combined dataset using the GTRCAT model with 25 categories. Statistical support of clades was obtained with 1,000 rapid bootstrap replicates. Finally, the comparison results showed that similarity was greater than 99.5% for each species.

Table 2.1 The TEF1 and RPB2 sequences of specimens

Species	TEF1	RPB2
Boletus bainiugan	PP036902–PP036940	PP037411–PP037449
Butyriboletus pseudospeciosus	PP036941–PP036978	PP037450–PP037487
Butyriboletus roseoflavus	PP036979–PP037044	PP037488–PP037553
Lanmaoa asiatica	PP037045–PP037101	PP037554–PP037610
Neoboletus hainanensis	PP037102–PP037121	PP037611–PP037630
Neoboletus magnificus	PP037122–PP037182	PP037631–PP037691
Neoboletus obscureumbrinus	PP037183–PP037209	PP037692–PP037718
Phlebopus portentosus	PP037210–PP037244	PP037719–PP037753
Retiboletus fuscus	PP037245–PP037308	PP037754–PP037817
Rubroboletus sinicus	PP037309–PP037340	PP037818–PP037849
Rugiboletus extremiorientalis	PP037341–PP037410	PP037850–PP037919

Note "–" connecting rod for indication.

2.3 The Evolutionary History of Boletes

Sequences focused on five genes, namely ITS, LSU, *tef1*, *rpb1*, and *rpb2* were retrieved from GenBank (Zhao, Li et al., 2017; He et al., 2019). Only species with two or more gene sequences available were included in the phylogenetic analyses, and the sequence details are listed in Supplementary Table appendix C. Initial sequence validation was conducted using BioEdit V.7.0.4 (Hall, 1999). Alignments were individually performed for each gene region using Muscle 3.8.31 (Edgar, 2004) and manually adjusted. To prevent substitutional saturation in the third codon position, translated amino acid sequences were employed for *tef1, rpb1, and rpb2* (Matheny et al., 2007). Subsequently, these amino acid sequences were combined with DNA sequences from rDNA genes. Divergence times were estimated by BEAST 1.10.4 (Drummond et al., 2012; Bouckaert & Drummond, 2017; Tedersoo et al., 2018; Zeng et al., 2019) combined with the stability phylogenetic tree (ML tree and Bayesian tree) and the TimeTree of boletaceae

(http://www.timetree.org/) (Kumar et al., 2022). An XML file was generated with BEAUTI v1. 10.4., and per-gene alignments were incorporated as distinct partitions. Clock and substitution models were unlinked, independently estimated for each gene partition. Nucleotide substitution models were determined using jModelTest v2: GTR+I+G for ITS and LSU, and WAG for *tef1*, *rpb1*, and *rpb2* in the Agaricomycotina tree; We adopted a Yule speciation model as a prior, which assumes a constant speciation rate per lineage. For the analysis, we employed the uncorrelated lognormal relaxed clock model, specifying a gamma distribution for the ulcd.mean parameter (shape = 1.0, scale = 0.001, offset = 0). Calibration values were derived from a prior study. (Zhao, Li et al., 2017) with normal distribution priors (SD = 1): mean age 406 Mya for Agaricomycotina. Four independent Monte Carlo Markov Chains were run for 30 million generations each, with states logged every 10,000 generations. Log files were scrutinized for convergence and mixing using Tracer v1.6 (Rambaut & Drummond, 2013; http://tree.bio.ed.ac.uk/software/tracer/). A Maximum Clade Credibility (MCC) tree was summarized using TreeAnnotator 1.10.4, discarding 10% of states as burn-in and annotating clades with a posterior probability (PP) cutoff of 0.9.

2.4 Analytical Fingerprint Information and Chemical Diversity of Wild Edible Boletes

2.4.1 Acquisition of NIR Spectra

NIR spectra were acquired by an Antaris Π spectrometer (Thermo Fisher Scientific, America) conFigured with a diffuse reflectance module and Results in 2.1 software. The NIR spectra were collected in the region of 10000-4000 cm^{-1} with the resolution of 8 cm^{-1}, and the signal accumulation of 64 scans. Each sample was scanned three times, and the average spectrum was calculated and used for the following analysis to reduce errors.

The synchronous two-dimensional correlation spectrum (2DCOS) images were calculated through the perturbation-based generalized 2DCOS algorithm proposed by Noda (1993). The spectral information on the diagonal was extracted based on the average spectrum of each species (Figure appendix I1). The dynamic spectral intensity **S** at variable ϑ is expressed as follows:

$$S(\vartheta) = \begin{bmatrix} y(\vartheta, t_1) \\ y(\vartheta, t_2) \\ y(\vartheta, t_3) \\ \cdot \\ \cdot \\ \cdot \\ y(\vartheta, t_{n-1}) \\ y(\vartheta, t_n) \end{bmatrix} \quad \text{..... (1)}$$

$$\varphi(\vartheta_1, \vartheta_2) = \frac{1}{n-1} \acute{y}(\vartheta_1)^T \times \acute{y}(\vartheta_2) \quad \text{..... (2)}$$

As reported by the theory of 2DCOS images, the synchronous correlation intensities between variables ϑ_1 and ϑ_2 were calculated as $\varphi(\vartheta_1, \vartheta_2)$. The relevant equation was shown as the above formula (2). In this study, the average spectrum of each species was independently set as a variable ϑ (Yang et al., 2014; Yang et al., 2015; Chen et al., 2018).

The rich information areas (7500-4000 cm^{-1}) including characteristic peaks were selected for subsequent analysis. The 2DCOS images were automatically generated using Matlab 2017b and saved as JPEG form Dong et al. (2022). Meanwhile, the data sets were put in matrix form and saved as csv form. The information on the diagonal of the matrix were extracted as new data and represented for each sample.

2.4.2 Acquisition of HPLC Fingerprints

Each sample powder (0.500 g) was accurately weighed and put into a 50 mL centrifugal tube. The sample was extracted by ultrasonication for 40 min with 20 mL ethyl alcohol. The tube was subsequently placed in a 60°C water bath for 1 hour and then centrifuged at 5000 rpm for 5 minutes. Following centrifugation, the supernatant was

filtered through a 0.45 μm filter membrane to obtain the sample solution. Three standard solutions containing uridine, guanosine, and adenosine were prepared by precisely weighing 1.0 mg of each compound and dissolving it in methanol in 10 mL volumetric flasks. All solutions were stored at 4°C for subsequent analysis.

The HPLC analysis was performed using an Agilent 1260 Infinity HPLC system equipped with a G1311C quaternary pump, an Agilent Intersil-C18 column (150 × 4.6 mm, 5 μm). The mobile phase consisted of water (A) and acetonitrile (B) at a flow rate of 1.0 mL/min, and the injection volume was 10 μL. The gradient elution program was as follows: (1) 0-5 min, 5–10% B; (2) 5–10 min, 10–20% B; (3) 10–20 min, 20–40% B; (4) 20–30 min, 40–60% B; (5) 30–45 min, 60-90% B; (6) 45-55 min, 90-95% B. The column temperature was maintained at 40 °C. The detection wavelength was set at 254 nm for fingerprint establishment (Wang et al., 2021). The standard solutions were used to optimize methodology and calibration of HPLC chromatograms. The standard curves of three standard solutions uridine (P8), guanosine (P9) and adenosine (P10) were $Y_{(rrT=0.802)}$=12.83X-13.008 with coefficient of determination (R^2)=1.0, $Y_{(rrT=9.355)}$=12.226X+9.5297 (R^2=0.9994), and $Y_{(rrT=10.156)}$=10.774X-8.3695 (R^2=1.0), respectively.

2.4.2.1 Standard recovery experiment. The average recovery rates of three compounds (uridine, guanosine and adenosine) were calculated as follows: (1) one randomly selected sample was prepared and divided into seven, and (2) one sample was detected by the methods of optimization (control). (3) The other sample solutions were added in a mixed standard solution (low: 0.5 mg/mL; medium: 1.0 mg/mL; high: 2.0 mg/mL). (4) All of the sample solutions were detected based on the methods of optimization, and the difference value between the results of the six measures and the control was calculated. The average recovery rates were between 80% and 120%, which suggested that the standard recovery rates agreed with the requirements of detection.

2.4.2.2 Precision experiment. One randomly selected sample was prepared and detected eight times in a row based on the methods of optimization. The RSD of all peak areas was calculated less than 3.5%, which indicated that the precision of the instrument and methods agreed with the requirements of detection (Figure 2.1).

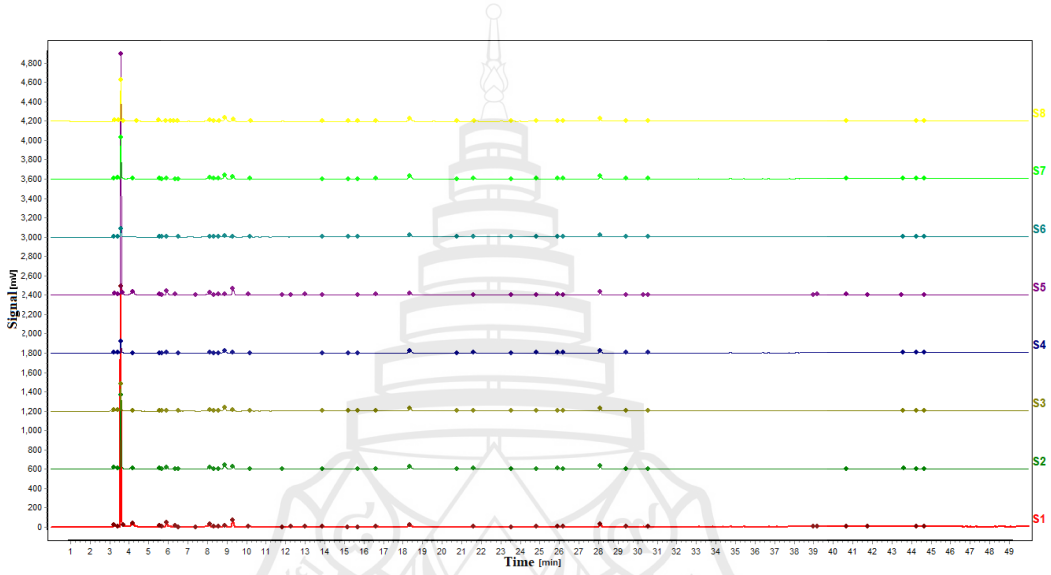


Figure 2.1 HPLC precision experiment

2.4.2.3 Repeatability experiment. One sample was prepared seven times based on the same methods and detected based on the methods of optimization. The RSD of all peak areas was calculated less than 5.0%, which indicated that the repeatability of the methods agreed with the requirements of detection (Figure 2.2).

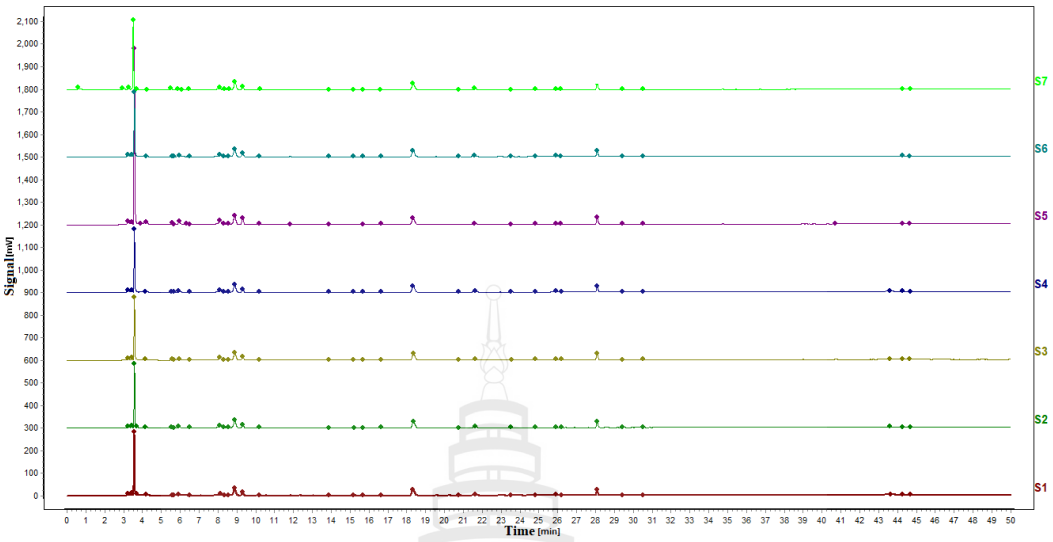


Figure 2.2 HPLC repeatability experiment

2.4.2.4 Stability experiment. One randomly selected sample was prepared and detected eight times at 0, 1, 3, 5, 7, 10, 15, and 24 h based on the methods of optimization. The RSD of all peak areas was calculated less than 5.0%, which indicated that the stability within 24 h agreed with the requirements of detection (Figure 2.3).

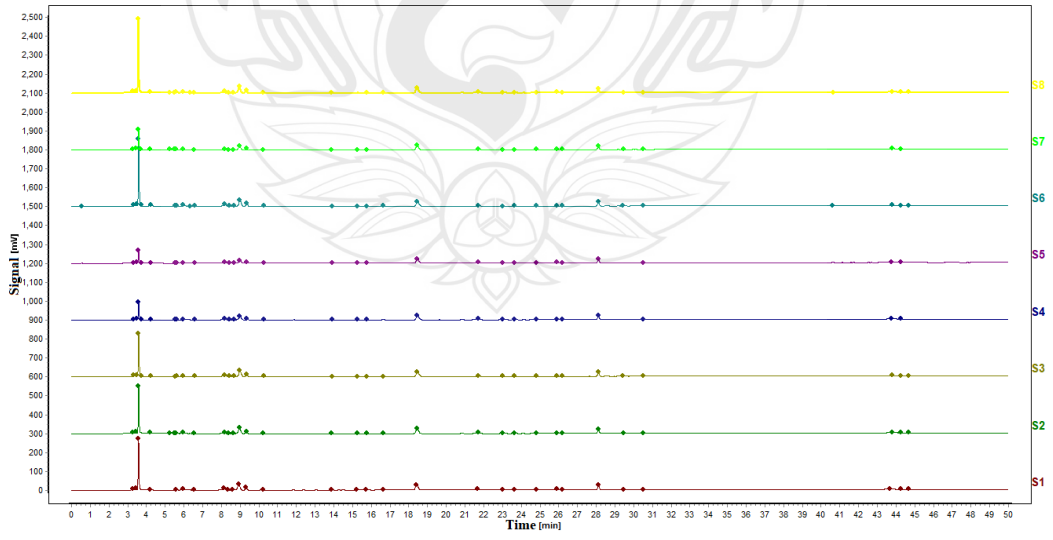


Figure 2.3 HPLC stability experiment

The chromatographic data were processed by the Similarity Evaluation System for Chromatographic Fingerprint of Traditional Chinese Medicine (Version 2012, The Chinese State Food and Drug Administration) and the two-dimensional correlation chromatography (2DCC, the method was the same as the 2DCOS above) (Gong et al., 2003; Rees et al., 2018). The similarity of different chromatograms as a new data of each species was used to visualized analyze by 2DCC and extract the correlation coefficient data on the diagonal matrix (appendix Fig. I2). Additionally, common peaks in the chromatograms were selected based on the following four principles: (1) the selected peaks should be presented in 80% of samples; (2) the sum of peak areas of common peaks should account for 90% of the peak areas; (3) the selected peaks should be well-separated from adjacent peaks; (4) the selected peaks should include the chromatographic peaks of standard constituents (uridine, guanosine and adenosine) (García-Palacios et al., 2018).

2.4.3 Detection of Volatile Constitutes by GC-MS Method

The sample powder 3.000 g was accurately weighed into a 1000 mL flask with 350 mL distilled water and 30 mL dichloromethane was added to the other 100 mL flask as the extractant. The two flasks were connected to both ends of the equipment of simultaneous distillation and extraction, and were heated by an adjust table electric stove at 100 °C (aqueous phase) and water bath at 60 °C (organic phase) for 1.5 h. After cooling down to room temperature, 3.000 g sodium sulphate anhydrous was added into the organic phase (100 mL flask) to dry, then the organic phase was concentrated to 1 mL using rotary evaporation, and transferred to a well-sealed 1.5 mL injection bottle. All solutions were stored at 4 °C for subsequent analysis.

The GC-MS analysis was performed using an equipment of 6890N/5973N Gas chromatography combine with mass spectrometer that equipped with a HP-5MS capillary column (30 m × 0.25 mm × 0.25μm), detector of FID and the library of Wiley 275. The conditions of gas chromatography were as follows: the carrier gas was helium, the flow rate was set at 1.0 mL/min, the temperature of sample inlet was 280 °C, and the temperature

programming were: firstly maintained at 60 °C for 2 min, secondly the temperature rose to 135 °C at a rate of 4 °C/min, thirdly the temperature rose to 175 °C at a rate of 2 °C/min, lastly the temperature reached at 250 °C at a rate of 5 °C/min and maintained for 2 min. The conditions of Mass were: delay time of solvent was performed for 5 min, the line temperature of transmission was 250 °C, the ion trap temperature was 220 °C, and the cavity temperature was 40 °C, the quality of scanning was ranged from 50 to 350 amu and naphthalene was used as the internal standard.

2.4.3.1 Optimization of the experiment. For optimization of the experiment, the extraction conditions of simultaneous distillation-extraction were optimized by an orthogonal experimental design. The results of optimization included the weight of the sample powder, the volume of the extraction solvent (appendix Fig. J), and the time of extraction. The details are as follows:

Table 2.2 Results of optimization

NO	Weight	Volume of solvent	Time of extraction	Peaks numbers Matching rate≥70%)	Responsivity
1#	2.5 g	20 mL	1 h	62	$0.70*10^7$
2#	2.5 g	25 mL	1.5 h	85	$0.95*10^7$
3#	2.5 g	30 mL	2 h	89	$1.2*10^7$
4#	3 g	20 mL	1.5 h	79	$1.0*10^7$
5#	3 g	25 mL	2 h	84	$1.3*10^7$
6#	3 g	30 mL	1 h	73	$0.6*10^7$
7#	5 g	20 mL	2 h	97	$1.1*10^7$
8#	5 g	25 mL	1 h	91	$1.1*10^7$
9#	5 g	30 mL	1.5 h	96	$1.2*10^7$
10#	3 g	30 mL	2 h	91	$2.0*10^7$
11#	3 g	30 mL	2 h	77	$1.6*10^7$
12#	3 g	30 mL	2 h	79	$1.6*10^7$
13#	3 g	25 mL	1.5 h	72	$1.4*10^7$
14#	3 g	25 mL	1.5 h	72	$1.1*10^7$
15#	3 g	25 mL	1.5 h	69	$1.2*10^7$

The results showed that the most optimized experimental parameters were a weight of 5.0 g, volume of solvent of 30 mL, and time of extraction of 1.5 h based on the peak numbers and responsivity, respectively.

2.4.3.2 Precision experiment. One sample was prepared based on the extraction conditions and detected six times in a row based on the optimization methods. The RSD of all peak areas was calculated and showed was between 1.2 to 4.8%, which indicated that the precision of the instrument and methods agreed with the requirements of detection.

2.4.3.3 Repeatability experiment. One of the samples was prepared six times based on the extraction conditions and detected based on the optimized methods. The RSD values of all peak areas were calculated from 3.1 to 5.0%, which indicated that the repeatability of the methods agreed with the detection requirements.

2.4.3.4 Stability experiment. One randomly selected sample was prepared and measured eight times at 0, 2, 4, 6, 8, 10, 12 h based on the optimized methods. The RSD values of all peak areas were calculated from 3.2 to 5.6%, which indicated that the stability within 12 h agreed with the detection requirements.

The volatile constituents were searched and extracted by library Wiley 275. The threshold value of integral area of mass spectra was set to 14.0. The substances with matching degree greater than 70% were extracted and confirmed based on the #CAS. The percentage of mass of compounds were calculated according to the formula:

$$m_i = \frac{f_i \times V}{l_0 \times m} \times 100 \quad \text{..... (3)}$$

Where m_i is the percentage of mass of compound i, f_i is the peak area of compound i, v is the volume of the interior label, l_0 is the peak area of the compound of interior label, and the m is the mass of weight (Yang, Zhu et al., 2022).

2.5 Construction of Chemical Classification Models of Wild Edible Boletes

2.5.1 Analysis of Relationship between Chemical Characteristic Variables of Species and Phylogenetic Signal

To determine whether chemical information is diverse among species and show non-random phylogenetic patterns, (1) The STDEV of chemical information including NIR spectra, common peaks of HPLC fingerprints, and volatile constituents of species were calculated to represent the variance of species (Jin et al., 2009). (2) The Bray-Curtis chemical similarity distance between each species was calculated by R package Vegan (Kembel et al., 2010) to assess the distribution trend of chemical information in different species. (3) The phylogenetic tree was re-established based on holotype of species. The STDEV of chemical information of different species and phylogenetic distance were analyzed by correlation of Pearson in the Performance Analytics R package (Peterson & Carl, 2018; Maranna et al., 2021). (4) The average chemical information including NIR spectra, HPLC fingerprints and volatile constituents of each species of boletes were calculated. Blomberg's K in the Picante R package (Blomberg et al., 2003; Dixon et al., 2003; Thuiller et al., 2011; Münkemüller et al., 2012;) was applied to assess the phylogenetic signal of chemical information for overall 11 species. For NIR spectra, HPLC fingerprints and volatile constituents, Blombergs' *K* values larger than 0.75, 0.90 and 0.90 were extracted as characteristic variables respectively to assess the diversity of chemical information among different species. Mantel test (Ade 4 package, 10,000 iterations) was used to validate the correlation of chemical similarity of species and phylogenetic distance (Dray & Dufour, 2007; Sunagawa et al., 2015; Salazar et al., 2018). (5) Randomly 80% samples were selected as training set and 20% as test set for different species of boletes samples by an algorithm of Kennard-Stone (K-S). Chemical characteristic variables of species were used to establish identification model by both ropls package (Trygg & Wold, 2002; Thévenot et al., 2015) and SIMCA-P+ version14.1 (Umetrics company from Sweden) (Trivedi & Iles, 2012). (6) To assess whether chemical characteristic variable can precise

identification of different species, four parameters of validation including accuracy, precision, efficiency and specificity were used based on external validation of test set and 200-fold cross-validation. (7) The consistency of chemical characteristic variable and phylogentic signal was assessed by mSD (tidyr package) (Villéger et al., 2017; Jarzyna et al., 2021; Magneville et al., 2022). The functions are as follows:

$$y_{ij}^{st} = \frac{y_{ij}}{\max_{i,j}(y_{ij})} \times \max_{i,j}(x_{ij}) \quad \text{..... (4)}$$

$$\text{mSD} = \frac{\sum_{i-1}^{S-1}\sum_{j=i+1}^{S}\left(x_{ij}-y_{ij}^{st}\right)^2}{\frac{S\times(S-1)}{2}} \quad \text{..... (5)}$$

where *S* is the number of species, x_{ij} represents the phylogenetic distance between i and j and y_{ij}^{st} represents the Euclidean distance of characteristic variable in the informational space for the same pair of species. The mSD is minimal and equals 0 when the characterstic informational space perfectly represents the phylogentic distance ($x_{ij} = y_{ij}^{st}$ for all pair of species) and it increase when some pair of species are poorly represented in the informational space, i.e. when species with similar trait values are far in the informational space or alternatively when species with different trait values are close in the informational space (Maire et al. 2015; Zhao et al. 2020).

2.5.2 Analysis of Relationship between Chemical Characteristic Variables of Regions and Ecological Environmental Factors

To determine whether chemical characteristic variables were influenced by ecological and environmental factors, (1) mahalanobis distance of 23 ecological environmental factors of 110 collection sites were calculated by the method of unsupervised pattern recognition of principal component clustering (SIMCA-P+) and consensus clustering (ConsensusClusterPlus package, 1,000 repetitions). According to the report by Wikerson and Hayes (2010), the collection sites were divided to 6 regions. (2) The STDEV of chemical information of different regions and mahalanobis distance of

ecological environmental factors were analyzed by the correlation of pearson in the PerformanceAnalytics R package (Peterson & Carl, 2018; Maranna et al., 2021). Then, the distribution trend of chemical information in different regions were assessed. (3) The correlation between the average chemical information including NIR spectra, HPLC fingerprints and volatile constituents of each region and ecological environmental factors were analyzed according to the Euclidean distance of vegdist function by Vegan package (Philip, 2003), and were validated by Mantel test (Ade 4 package, 10,000 iterations) (Blomberg et al., 2003; Thuiller et al., 2011). (4) The average chemical information of each region of the *p* value less than 0.05 based on Mantel test and the variable importance in the projection (VIP) value larger than 1.0 using ropls package (Trygg & Wold, 2002; Thévenot et al., 2015) were selected as chemical characteristic variables of regions. Mantel test (Ade 4 package, 10,000 iterations) was used to validate the correlation of chemical similarity of regions and ecological environmental factors (Dray & Dufour, 2007; Sunagawa et al., 2015; Salazar et al., 2018). (5) The pattern recognition model based on the chemical characteristic variables of regions was built by both ropls package (Trygg & Wold, 2002; Thévenot et al., 2015) and SIMCA-P+ version14.1 (Umetrics company from Sweden) (Trivedi et al., 2012). (6) To assess whether chemical characteristic variable of regions can precise identification of different regions, four parameters of validation including accuracy, precision, efficiency and specificity were used based on external validation of test set and 100-fold cross-validation.

2.5.3 Analysis of the Effects of Ecological Environmental Factors (Regions) and Phylogentic Signal (Species) on Chemical Variable Diversity

To analyze the effects of ecological environmental factors (regions) and phylogentic signal (species) on chemical variable diversity, (1) species richness of per regions were calculated by Circos (http://circos.ca) (Krzywinski et al., 2009)**.** (2) The correlation of chemical characteristic variables of species and regions, ecological environmental factors and species were analyzed by the methods of RLQ (ade4 pacage)

(Dray et al., 2014; Gámez-Virués et al., 2015). (3) The relationships between chemical characteristic variables of species and regions were analyzed by the method of Venn diagram (https://bioinformatics.psb.ugent.be/webtools/Venn/) (Jakobs et al., 2018).

2.6 Construction of Chemical Evaluation Models of Wild Edible Boletes

2.6.1 Chemicals

Dichloromethane (analytical grade) was used as the extraction solvent for SDE. Naphthalene (HPLC grade) was used as an internal standard (IS). Anhydrous sodium sulfate and sodium chloride (analytical grade), were used for the SDE experiment. All the chemicals were purchased from Beijing Chemical Reagents Company, Beijing, China.

2.6.2 Sample Collection and Identification

A total of 445 fruiting bodies of 11 frequently consumed boletes, including *Boletus bainiugan* (BoB), *Butyriboletus pseudospeciosus* (BuP), *Butyriboletus roseoflavus* (BR), *Lanmaoa asiatica* (LA), *Neoboletus obscureumbrinus* (NO), *Rugiboletus extremiorientalis* (RugE), *Rubroboletus sinicus* (RubS), *Retiboletus fuscus* (RetF), *Phlebopus portentosus* (PP), *Neoboletus hainanensis* (NH), and *Neoboletus magnificus* (NM), were collected from 2019–2020 in different microhabitats of Yunnan and Sichuan Provinces, China.

2.6.3 Simultaneous Distillation Extraction (SDE)

Each powder sample (3.000 g) was accurately weighed into a 1000 mL flask with 350 mL of distilled water and 30 mL of dichloromethane was added to another 100 mL flask as the extractant. Before heating, the whole apparatus was purged for 3 min with nitrogen to remove oxygen. The two flasks were connected to either end of the equipment for simultaneous distillation and extraction and were heated by an adjusTable electric stove at 100 °C (aqueous phase) and a water bath at 60 °C (organic phase) for 1.5 h. After cooling to room temperature, 3.000 g of sodium sulfate anhydrous was added to the organic phase

(100 mL flask) for drying, and the organic phase was then concentrated to 1 mL using rotary evaporation (RE-52AA Rotary Evaporator, Shanghai Yarong Biochemistry Instrument Factory) and transferred to a well-sealed 1.5 mL injection bottle. All solutions were stored at -18 °C for subsequent analysis. The SDE extraction and subsequent analyses were performed in duplicate.

2.6.4 GC–MS Analysis

GC-MS analysis was performed on an Agilent 6890 N gas chromatograph, equipped with an Agilent 5973 N mass spectrometer (Agilent Technologies, Inc., Palo Alto, CA, USA). Helium was used as a carrier gas at a constant flow rate of 1.0 mL / min. SDE samples were loaded in splitless mode and analyzed on an Agilent HP-5MS capillary column (30 m × 0.25 mm × 0.25 μm). The temperature of the sample inlet was 280 °C, and oven temperature programming was started at 60 °C and maintained for 2 min, raised to 135 °C at 4 °C/min, raised to 175 °C at 2 °C / min, and finally ramped to 250 °C at 5 °C / min and maintained for 2 min. The MS system operated in electron ionization (EI) mode at 70 eV, with the ion source, transmission line, and quadrupole temperatures set at 220 °C, 250 °C, and 150 °C, respectively. The mass scan range ranged from 30 to 450 m/z. Identification of volatiles was conducted by comparing their mass spectra with MS spectra libraries (Wiley 275 library and NIST08) and naphthalene was used as the internal standard. All analyses were performed in duplicate. The substances with matching degrees greater than 70 % were extracted and confirmed based on the #CAS. The mass percentages of compounds were calculated according to the formula 3.

2.6.5 Odor Thresholds and ROAV Calculation

The odor activity value (OAV) is the ratio of the concentration of odor compounds to the odor threshold detected in the water. The thresholds of aroma compounds referred to the results of previous studies shown in Table 3.13. The relative odor activity value (ROAV), which ranges from 0 to 100, was used to evaluate the contribution of individual compounds to the overall aroma. The ROAV used to identify key odor compounds of mushrooms was

calculated according to the formula:

$$ROAV_i \approx 100 \times \frac{C_i}{T_i} \times \frac{T_{stan}}{C_{stan}} = 100 \times \frac{OAV_i}{OAV_{max}} \quad (6)$$

where OAV_{max} is the highest OAV among the VOCs, and OAV_i is the OAV of each specific volatile compound. OAV is generally calculated via the equation $OAV_i = C_i/T_i$; where C_i is the concentration of the volatile compound in the sample and T_i is the odor threshold in water expressed in ppb, among which the odor thresholds of compounds in the water were taken from the literature in this study.

2.7 Chemometric Methods

2.7.1 Spectral Data Preprocessing

The original FT-NIR data encompass ample sample information, yet they may encounter interference from baseline drift and noise simultaneously (Mishra et al., 2020). Consequently, extracting precise information from the spectral signals becomes paramount. Preprocessing of the spectrum is typically imperative to alleviate interference effects and enhance the contribution of chemical constituents prior to model construction. Multiplicative signal correction (MSC) is an effective method for eliminating spectral differences based on different scattering levels and can enhance the correlation between spectra and data (He et al., 2007). The baseline drift and noise can be effectively eliminated and removed by derivation and Norris derivative filter (Chen et al., 2008; Yang et al., 2019). The pretreatment combination of 2SD + MSC + NDF were used in subsequent qualitative and quantitative analyses in this study. Additionally, in multivariate analyses and modeling of complex data, all data and samples were divided into calibration (training) and validation (testing) sets according to the ratio 7: 3 of each species by the K-S (Kennard-stone) algorithm.

2.7.2 *t* tests and one-way Analysis of Variance (ANOVA)

The *t*-test is a direct method to evaluate the significance level of difference between two independent data sets, while one-way ANOVA is an effective method to explore the significance level of difference among multigroup data sets (Liu & Wang, 2021). In this paper, the *t*-test is used to examine significant differences between predicted and true test values according to the results of the calibration model. One-way ANOVA was used to analyze the differences among the contents of VOCs of 11 bolete species.

2.7.3 Variable Selection

A robust prediction model isn't always achieved by utilizing the entire spectral region or all datasets. To optimize the performance of the model and improve model accuracy, the characteristic bands of the FT-NIR spectrum and characteristic variables of VOCs were extracted using the spectrum standard deviation (SDD) method and VIP, respectively. Finally, the bands of the spectrum (7500-4050 cm^{-1}) were selected for the established calibration model based on the second derivative. In addition, to optimize the discriminant model, Venn diagram analysis (VDA) and cluster heatmap analysis (CHMA) were used to extract the characteristic VOCs.

2.7.4 Principal Component Analysis (PCA)

PCA is a multivariate statistical analysis technique for evaluating the regularity and differences among samples by determining a few principal component factors to represent many complex and difficult-to-find variables in the original samples (Li et al., 2019). It aids in determining the most important variables in the dataset and is one of the pattern recognition methods used for analyzing the differences in a series of datasets. In this study, Principal Component Analysis (PCA) was conducted on all samples to investigate sample clustering.

2.7.5 Partial Least Squares Discriminant Analysis (PLS-DA)

PLS-DA applies the extended PLS algorithm for classification, which is similar to PCA in theory. Both methods can reduce the dimensions of high-dimensional data space. PCA is a commonly used unsupervised pattern recognition method based on transformed orthogonal rotation of variables so that extracted comprehensive variables can interpret the original data, enabling the qualitative analysis of data (Anowar et al., 2021). PLS-DA is a generally used supervised pattern recognition algorithm, where the X variable is the spectral data and the Y variable is a vector containing class information. By using PLS-DA dimension reduction, not only can the characteristic variable (X matrix) be effectively extracted and the information of the original variable be summarized, but it also has a strong ability to explain the dependent variable (Y matrix), so that Y=XB+E, where B is a matrix of regression coefficients and E is a matrix of residuals (Marchand et al., 2000). In PLS models, scores and loadings delineate how samples and variables are projected along the factors. Specifically, PLS scores are calculated to capture the predictive structure in X relative to Y. Meanwhile, PLS loadings indicate the extent to which each X-variable contributes to a specific model component (Lasalvia et al., 2022). The scatter plots of scores and loadings can clearly describe the relationships among the samples. In this study, samples were assigned to eleven categories (1 to 11) according to the predicted value of the virtual Y variable. Therefore, these samples will be assigned to specific groups when the Y value belongs to one category.

The identification model for the bolete species was established using the VOCs. For the PLS-DA model, the accuracy of the model was evaluated based on the root mean square error of cross-validation (RMSECV) and root mean square error of prediction (RMSEP). Additionally, R^2 and Q^2 served as metrics to assess the alignment between the dataset and the model. R^2 elucidates the extent to which the data can be accommodated by the model, with values nearing 1 indicating robustness. Q^2, on the other hand, gauges the model's predictive capability for unfamiliar data. Typically, a Q^2 value exceeding 0.5 signifies favorable predictive performance of the model. (Qin et al., 2022). To evaluate the

performance of the model and reduce the risk of overfitting, 5-fold cross-validation of the model was performed. Additionally, 200 iterations of permutation tests on the model were performed to test the overfitting of the PLS-DA model in this study.

To evaluate the performance of the PLS-DA model, sensitivity (*Sen*), specificity (*Spe*), efficiency (*Eff*) and accuracy (*Acc*) values were used to evaluate the results of the training set and test set in the model. The larger the values of these parameters are, the better the performance of the model. The evaluation indices of these three parameters were calculated by using true positives (TP), false positives (FP), true negatives (TN) and false negatives (FN). The calculation formulas for these three parameters are as follows:

$$Sen = {TP}/{(TP + FN)} \tag{7}$$

$$Spe = {TN}/{(TN + FN)} \tag{8}$$

$$Eff = \sqrt{\mathrm{Sen} \times \mathrm{Spe}} \tag{9}$$

$$Acc = (TP + TN)/(TP + FP + FN + TN) \tag{10}$$

2.7.6 Fisher's Linear Discriminant Function Analysis

Fisher's linear discriminant function analysis (DFA) is one potential tool that could be used in the assessment of interspecific differences by establishing the function of a few characteristic compounds. Discriminant function analysis is a multivariable statistical technique that is used to discriminate predictor variables of different groups and classify new observations into previously identified groups (Hou & Riley, 2015; Liberda et al., 2020). The number of discriminant functions is equal to the number of groups recognized a priori minus one. Thus, it takes at least two groups to obtain a discriminant function. The discriminant function equation (*DFE*) is as follows:

$$DFE = V_1X_1 + V_2X_2 + \cdots + V_iX_i + C \tag{11}$$

Here, *DFE* denotes the discriminant function equation, with V representing the weight of the variable (i.e., the canonical discriminant function coefficient, unstandardized),

X denoting the discriminating variable value for the participant, *i* indicating the number of predictor variables, and *C* representing the constant (Liu & Wang, 2021). In this study, we established the discriminant function equations of 11 bolete species using Fisher's linear discriminant function analysis according to the optimized results for VOCs. The suitability evaluation of discriminant function equations was assessed by back substitution analyses.

2.7.7 Partial Least Squares Regression (PLSR)

PLSR is a multivariate regression modeling method, that is based on a model for calculating the covariance between X and Y and finding the linear mathematical relationship for two data sets (Moros et al., 2010). Typically, the Partial Least Squares Regression (PLSR) model is developed using two independent datasets: the calibration set and the validation set. In this approach, the calibration set samples are employed to construct and assess the model, while the remaining validation samples serve as an external prediction set. In this study, to evaluate the PLSR model, the correlation coefficient (R^2), RMSECV (for the calibration set), RMSEP (for the validation set) and residual predictive deviation (RPD) were preliminarily used to evaluate the performance of the model. Then, the *t*-test was used to examine the significant difference between predicted and true values by the test set. Finally, the performance of the model was comprehensively evaluated based on the above characteristic VOCs.

2.8 Statistical Analysis

All experiments were carried out at least in duplicate. Figures were plotted using Microsoft Excel 2018, Origin 2018, and GraphPad Prism 8. PCA and PLS-DA were conducted via SIMCA 13.0 (Umitrics, Sweden). Statistical analysis and the calibration model were run using SPSS 21 software (SPSS Inc.; Chicago, USA), MATLAB software (version R2017a, MathWorks, USA), and TQ Analyst 9.1 (Thermo Scientific).

CHAPTER 3

RESEARCH RESULTS

3.1 Taxonomy and Phylogeny of *Tuber* (True Truffles)

3.1.1 DNA Sequence Analyses

A total of 210 sequences including 202 sequences by collections of *Tuber* and 8 sequences by sequencing in this study, and 5 sequences derived from two species of *Choiromyces helanshanensis* and *C. meandriformis* were selected and used as outgroups (Table 3.1). The phylograms of ITS1 + ITS2 (426 bp) and ITS-nrLUS (1219 bp) sequences are shown in Figure 3.1 and 3.2. ML and BI analyses produced similar tree topologies, and only the tree generated from the ML analysis is shown. Both phylograms indicated that specimens of *T. maroonense* and *T. conditum* form a monophyletic clade, which was distinct from other *Tuber* species with high BS and PP support. Based on the ITS1 + ITS2 analysis (Figure 3.2), *T. maroonense* and *T. conditum* stand with the Latisporum clade together with *Tuber* sp. 10, *Tuber* sp. *Wang*, *T. songlu*, *T. thailandicum*, *T. pseudosphaerosporum*, *T. polymorphosporum*, *T. panzhihuanense*, *T. lastisporum*, *T. baoshanense*, *T. parvomurphium*, *T. alboumbilicum*, *T. griseolivaceum*, and *T. caoi*, and the phylogenetic tree showed their strong bootstrap support values (BS= 100 % and PP=1.0).

Table 3.1 Details of *Tuber* sequences used in phylogenetic analysis

Name	Isolated / strain	ITS	LSU	RPB2	TEF1
Choiromyces meandriformis	RH691	HM485330	FJ809794	JQ954471	JX022550
C. helanshanensis	HKAS_80630	KU531603	/	/	/
C. helanshanensis	HKAS_80633	KU531604	/	/	/
C. helanshanensis	HKAS_80634	NR_153899	/	/	/
C. meandriformis	GB285	HM485331	/	/	/
Tuber alboumbilicum	YAAS_L2324	NR_155904	/	/	/
T. anniae	JT13209	HM485338	JQ925680	/	JX022567
T. anniae	BJTC_FAN640	OM286868	OM366215	OM584274	OM649620
T. badium	BJTC FAN371	OM256747	OM366192	OM584255	OM649597
T. badium	BJTC FAN381	OM256748	OM366193	OM584256	OM649598
T. baoshanense	HKAS_88788	NR_178114	/	/	/
T. baoshanense	BJTC_FAN400	OM256791	OM366197	OM584260	OM649602
T. borchii	IFS Y. Wang 89556	DQ478624	/	/	/
T. borchii	IFS Y. Wang 89377	DQ478656	/	/	/
T. borchii	BJTC_FAN217	KT067681	KT067706	OM584229	KT067717
T. borchii	Tbo1	MZ452886	/	MZ541897	MZ570608
T. brumale	Tbru-eu02	DQ329359	/	/	/
T. brumale	T.bru-eu03	DQ329360	/	/	/
T. brumale	GB53	FJ748900	/	/	/
T. brunneum	JT33836	KT897475	/	/	/
T. brunneum	JT33837	KT897479	/	/	/
T. buendiae	MUB_Fung-0974	NR_171295	/	/	/
T. buendiae	MUB_Fung-0976	MT006097	/	/	/
T. buendiae	MUB_Fung-0977	MT006098	/	/	/
T. californicum	JT28058	HM485346	JQ925685	JQ954496	JX022574
T. californicum	JT22590	HM485351	/	/	/
T. calosporum	HKAS_88791	KT444597	/	/	/
T. calosporum	HKAS_88790	KT444598	/	/	/
T. calosporum	**YAAS_L3648**	**ON454666**	**ON428902**	**OQ305201**	**OQ305198**
T. calosporum	**YAAS_L3684**	**OQ297679**	/	/	/
T. calosporum	BJTC_FAN301	/	OM366182	OM584242	OM649586
T. calosporum	BJTC_FAN418	/	OM366202	OM584265	OM649607
T. canaliculatum	OSC59072	HM485347	/	JQ954498	JX022576
T. canaliculatum	JT28215	JQ925643	/	JQ954497	JX022575
T. candidum	JT21856	HM485348	/	/	/
T. candidum	JT1844	HM485349	/	/	/
T. caoi	BJTC_FAN321	KP276180	/	/	/

Table 3.1 (continued)

Name	Isolated / strain	ITS	LSU	RPB2	TEF1
T. caoi	BJTC_FAN309	KP276181	/	/	/
T. caoi	BJTC_FAN293	KP276182	KP276198	OM584240	KP276217
T. caoi	BJTC_FAN271	KP276183	NG_059984	OM584237	KP276216
T. conditum	**YAAS_L3385**	**ON454665**	**ON428901**	**/**	**/**
T. conditum	**YAAS_L3682**	**ON454667**	/	/	/
T. crassitunicatum	BJTC_FAN465	MH115295	NG_088329	OM584268	OM649610
T. crassitunicatum	HMAS_88577	MH115297	/	/	/
T. dryophilum	GB37	HM485354	JQ925688	JQ954501	JX022578
T. dryophilum	GB35	JQ925644	JQ925687	/	JX022577
T. ferrugineum	JST22014	KX354297	/	/	/
T. ferrugineum	MUBFung-0972	MN962719	/	/	/
T. foetidum	ZB2452	JQ288905	/	/	/
T. foetidum	ZB2489	JQ288906	/	/	/
T. formosanum	BJTC_FAN107	MF621549	OM366159	OM584210	OM649564
T. formosanum	BJTC_FAN356	MF627986	OM366189	OM584252	OM649594
T. furfuraceum	HKAS_48272	GU979034	/	/	/
T. furfuraceum	HKAS_49707	GU979049	/	/	/
T. glabrum	BJTCFan232	KF002727	OM366179	OM584236	/
T. glabrum	BJTC_Fan228	NR_153217	NG_088326	OM584234	OM649581
T. griseolivaceum	BJTC_FAN469	KY428921	NG_088330	/	OM649612
T. griseolivaceum	BJTC_FAN470	KY428923	/	/	/
T. himalayense	CB20001	MW393547	/	/	/
T. himalayense	JJ22045	OQ054615	/	/	/
T. himalayense	JJ22046	OQ054619	/	/	/
T. hubeiense	HMAS_60233	KT067688	/	/	/
T. huidongense	BJTC_FAN103	MH115294	/	/	/
T. huidongense	BJTC_FAN101	/	OM366156	OM584208	OM649562
T. huidongense	BJTC_FAN104	/	OM366158	OM584209	OM649563
T. huidongense	885-1	MW201514	/	/	/
T. huizeanum	BJTC_FAN186	JQ910651	NG_059991	/	OM649575
T. huizeanum	BJTC_FAN314	KT067685	KT067692	OM584246	KT067712
T. indicum	T47	JQ639005	/	/	/
T. indicum	T49	JQ639007	/	/	/
T. jinshajiangense	BJTC_FAN124	KP276177	/	/	/
T. jinshajiangense	BJTC_FAN406	KX575841	OM366199	OM584262	OM649604
T. jinshajiangense	BJTC_FAN407	KX575842	OM366200	OM584263	OM649605
T. latisporum	BJTC_FAN126	KP276189	KP276204	OM584215	KP276205

Table 3.1 (continued)

Name	Isolated / strain	ITS	LSU	RPB2	TEF1
T. latisporum	BJTC_FAN125	KT067676	KT067695	OM584214	KT067725
T. liaotongense	OSC87602	HM485369	FJ809813	/	JX022589
T. liaotongense	BJTC_FAN550	MH115302	OM366213	OM584272	OM649618
T. lijiangense	BJTC_FAN307	KP276188	KP276203	OM584244	KP276206
T. lishanense	BJTC_FAN683	MH115305	MH115306	OM584275	OM649621
T. lishanense	BJTC_FAN718	NR_160619	NG_064527	OM584276	OM649622
T. liui	HXZE_984	DQ478636	/	/	/
T. liui	HKAS_48269	DQ898182	/	/	/
T. liyuanum	FAN162	JQ771191.2	KT067698	OM584218	KT067710
T. liyuanum	BJTC_FAN187	JQ771193	KT067704	/	KT067719
T. longispinosum	FFPRI_460530	LC508589	/	/	/
T. longispinosum	FFPRI_460528	LC508587	/	/	/
T. longispinosum	FFPRI_460529	LC508588	/	/	/
T. lyonii	FLASMES-614	MT156453	/	/	/
T. lyonii	FLASMES-615	MT156454	/	/	/
T. macrosporum	JT19458	HM485372	/	/	/
T. macrosporum	JT13362	HM485373	FJ809838	/	JX022590
T. maculatum	BJTC_FAN868	OM265274	OM366227	OM584283	OM649634
T. maculatum	BJTC_FAN876	OM265278	OM366228	OM584284	OM649635
T. malacodermum	JT32319	FJ809889	JQ925702	JQ954514	JX022593
T. maroonense	**YAAS_L3694**	**ON454668**	**ON428904**	**OQ305202**	**OQ305199**
T. maroonense	**YAAS_L3695**	**OQ297680**	/	/	/
T. melanosporum	MEL437_clone_25A	EU555389	/	/	/
T. melanosporum	MEL437_clone_26A	EU555390	/	/	/
T. microsphaerosporum	BJTC_Fan152	KF805726	/	/	/
T. microsphaerosporum	BJTC_FAN152	KP276187	/	/	KP276207
T. microspiculatum	BJTC_FAN220	MH115315	/	/	/
T. microspiculatum	BJTC_FAN138	MH115317	/	/	/
T. nitidum	BM105	FJ809885	FJ809807	JQ954517	JX022597
T. nitidum	MUB:Fung-0934	MN962721	/	/	/
T. nitidum	MUB:Fung-0935	MN962722	/	/	/
T. oligospermum	AH39338	JN392266	/	/	/
T. oligospermum	AH39336	JN392267	/	/	/
T. oligospermum	AH39337	JN392268	/	/	/
T. panzhihuanense	DXJ277	JQ978651	/	/	/
T. panzhihuanense	DXJ278	JQ978652	/	/	/
T. panzhihuanense	HKAS_72015	NR_120126	/	/	/

Table 3.1 (continued)

Name	Isolated / strain	ITS	LSU	RPB2	TEF1
T. parvomurphium	BJTC_FAN323	KP276185	KP276191	/	KP276215
T. parvomurphium	BJTC_FAN298	KP276186	NG_059981	OM584241	KP276214
T. piceatum	HMAS_97125	NR_160620	/	/	/
T. piceatum	HMAS_97124	MH115320	/	/	/
T. polymorphosporum	HKAS_88793	NR_178113	/	/	/
T. polymorphosporum	BJTC_FAN413	OM256794	/	/	/
T. polymorphosporum	BJTC_FAN544	OM256802	/	/	/
T. pseudobrumale	YAAS_L3181	KJ742703	/	/	/
T. pseudobrumale	BJTC_FAN306	OM287838	/	/	/
T. pseudobrumale	BJTC_FAN322	OM287839	/	/	/
T. pseudoexcavatum	T14_HKAS_44325b	GU979039	/	/	/
T. pseudoexcavatum	T29_HKAS_44324b	GU979040	/	/	/
T. pseudoexcavatum	HKAS_44346	GU979041	/	/	/
T. pseudoexcavatum	T18_HKAS_49851	GU979043	/	/	/
T. pseudoexcavatum	T31_HKAS_47617	GU979045	/	/	/
T. pseudoexcavatum	T80_HKAS_49747	GU979046	/	/	/
T. pseudoexcavatum	CJ408	HM485381	/	/	/
T. pseudoexcavatum	HKAS 86489	MG871289	/	/	/
T. pseudoexcavatum	**YAAS_L3932**	**ON454670**	/	/	**OQ305200**
T. pseudoexcavatum	**YAAS_L3933**	**OQ297681**	/	/	/
T. pseudohimalayense	BJTC_FAN122	MF627983	/	/	/
T. pseudohimalayense	BJTC_FAN297	OM287837	/	/	/
T. pseudohimalayense	BJTC_FAN328	OM287840	/	/	/
T. pseudohimalayense	BJTC_FAN354	OM287844	/	/	/
T. pseudohimalayense	BJTC_FAN541	OM287847	/	/	/
T. pseudohimalayense	mhll-10	MT446223	/	/	/
T. pseudohimalayense	mhll-11	MT446224	/	/	/
T. pseudomagnatum	BJTC_FAN163	JQ771192	KP276192	OM584219	KP276208
T. pseudomagnatum	BJTC_FAN299	KP276184	/	/	/
T. pseudomagnatum	BJTC_FAN391	OM265244	OM366195	OM584258	OM649600
T. pseudosphaerosporum	BJTC_FAN250	NR_153229	NG_059982	/	OM649584
T. pseudosphaerosporum	BJTC_FAN394	OM256789	/	/	/
T. puberulum	ZB1341	JF261381	/	/	/
T. puberulum	ZB1433	JF261382	/	/	/
T. pustulatum	AQUI_9725	MK211278	/	/	/
T. pustulatum	AQUI_9726	MK211279	/	/	/
T. qujingense	HKAS 95823	KX904885	/	/	/

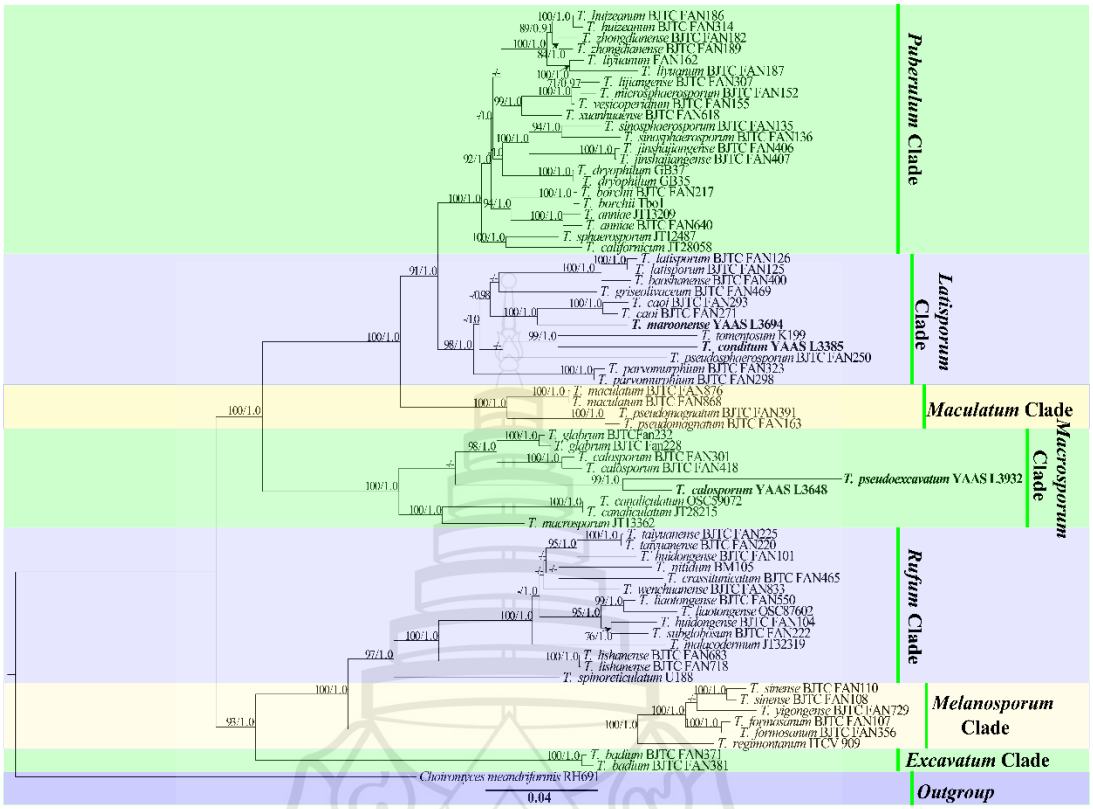
Table 3.1 (continued)

Name	Isolated / strain	ITS	LSU	RPB2	TEF1
T. rapaeodorum	IFS Y. Wang 89719	DQ478651	/	/	/
T. rapaeodorum	IFS Y. Wang 870202	DQ478654	/	/	/
T. rapaeodorum	ZB452	JF261396	/	/	/
T. rapaeodorum	ZB466	JF261397	/	/	/
T. regimontanum	ITCV_909	EU375838	NG_059920	JQ954520	JX022600
T. rufum	FLAS-F-65583	MT374049	/	/	/
T. rufum	FLAS-F-65584	MT374050	/	/	/
T. shidianense	HKAS_88770	KT444595	/	/	/
T. shidianense	HKAS_88771	KT444596	/	/	/
T. sinense	BJTC_FAN108	MF627968	OM366160	OM584211	OM649565
T. sinense	BJTC_FAN110	MF627970	OM366161	OM584212	OM649566
T. sinoalbidum	BJTC_FAN105	MH115298	/	/	/
T. sinomonosporum	BJTC_Fan150	KF002729	/	/	/
T. sinosphaerosporum	BJTC:FAN135	JX092086	NG_059983	OM584217	OM649569
T. sinosphaerosporum	BJTC_FAN136	JX092087	KP276196	/	KP276211
T. songlu	HKAS_95771	KX904883	/	/	/
T. songlu	HKAS_95777	KX904884	/	/	/
T. songlu	HKAS_95851	KX904886	/	/	/
T. sphaerosporum	JT12487	FJ809853	FJ809805	/	JX022609
T. sphaerosporum	JT19772	FJ809854	/	/	/
T. spinoreticulatum	U188	FJ809884	FJ809815	JQ954527	JX022608
T. spinoreticulatum	RH158	GQ221454	/	/	/
T. subglobosum	BJTC_FAN222	KF002728	OM366175	OM584232	OM649579
T. subglobosum	BJTC_FAN432	MH115323	/	/	/
T. taiyuanense	T42_HM75888	GU979033	/	/	/
T. taiyuanense	BJTC_FAN210	OM311199	/	/	/
T. Taiyuanense	BJTC_FAN220	/	OM366174	OM584231	OM649578
T. Taiyuanense	BJTC_FAN225	/	OM366176	OM584233	OM649580
T. texense	JT15162	HM485391	/	/	/
T. thailandicum	CMU-B31	MW470964	/	/	/
T. thailandicum	CMU-B33	MW470967	/	/	/
T. theleascum	AQUI_9729	MK211283	/	/	/
T. theleascum	AQUI_9730	MK211284	/	/	/
T. theleascum	ITCV_908	NR_164592	/	/	/
T. tomentosum	K126	AB553447	/	/	/
T. tomentosum	K199	AB553448	AB553521	AB553561	AB553541
T. tomentosum	K200	AB553449	/	/	/

Table 3.1 (continued)

Name	Isolated / strain	ITS	LSU	RPB2	TEF1
T. tomentosum	K409	AB553450	/	/	/
T. tomentosum	K410	AB553451	/	/	/
T. tomentosum	K412	AB553452	/	/	/
T. tomentosum	K413	AB553453	/	/	/
T. tomentosum	K414	AB553454	/	/	/
T. tomentosum	K415	AB553455	/	/	/
T. umbilicatum	T2_HKAS_44316	GU979031	/	/	/
T. umbilicatum	T30_HKAS_48267	GU979032	/	/	/
T. umbilicatum	BJTC_FAN225	MH115325	/	/	/
T. variabilisporum	BJTC_FAN330	OM287841	/	/	/
T. vesicoperidium	BJTC_FAN155	JQ690071	JQ690068	/	KP276212
T. vesicoperidium	L156	JQ690072	/	/	/
T. wanglangense	IFS Y.Wang_610	DQ478637	/	/	/
T. wenchuanense	HMAS_60239	JX267044	/	/	/
T. wenchuanense	BJTC_FAN833	OM311256	/	/	/
T. wenchuanense	BJTC_FAN833	/	OM366222	OM584280	OM649629
T. xuanhuaense	BJTC_FAN618	MK045627	OM366214	OM584273	OM649619
T. xuanhuaense	BJTC_FAN887	MK045644	/	/	/
T. xuanhuaense	BJTC_FAN886	MK045645	/	/	/
T. xuanhuaense	HMAS_60213	NR_147436	/	/	/
T. yigongense	BJTC_FAN729	MF663716	/	OM584277	OM649623
T. yigongense	BJTC_FAN731	MF663714	/	/	/
T. zambonelliae	MUB_Fung-1006	MW632954	/	/	/
T. zambonelliae	MUB_Fung-1007	MW632955	/	/	/
T. zambonelliae	MUB_Fung-0995	NR_174649	/	/	/
T. zhongdianense	BJTC_FAN176	KP276178	/	/	/
T. zhongdianense	BJTC_FAN178	KT067679	/	/	/
T. zhongdianense	BJTC_FAN182	KT067680	KT067702	/	KT067721
T. zhongdianense	BJTC_FAN189	KT067689	KT067705	/	KT067718
Tuber sp. 2 *KA-2010*	K22	AB553345	/	/	/
Tuber sp. 2 *KA-2010*	K108	AB553349	/	/	/
Tuber sp. 2 *KA-2010*	K205	AB553353	/	/	/
Tuber sp. 2 *KA-2010*	K445	AB553366	/	/	/
Tuber sp. 2 *KA-2010*	K446	AB553367	/	/	/

Note sequences newly generated in this study are shown in bold.



Note Phylogeny generated from maximum likelihood and Bayesian inference analysis of the ITS-LUS-TEF1-RPB2 rDNA sequences from *Tuber maroonense* and *T. conditum* related species. *Choiromyces meandriformis* served as outgroups. ML bootstrap values (>75%) and Posterior Probabilities (PPs) values (>0.90) are shown above or beneath the branches at nodes. Novel sequences are printed in bold

Figure 3.1 Phylogenetic tree of the genus *Tuber* constructed by ITS-LUS-TEF1-RPB2 rDNA sequences

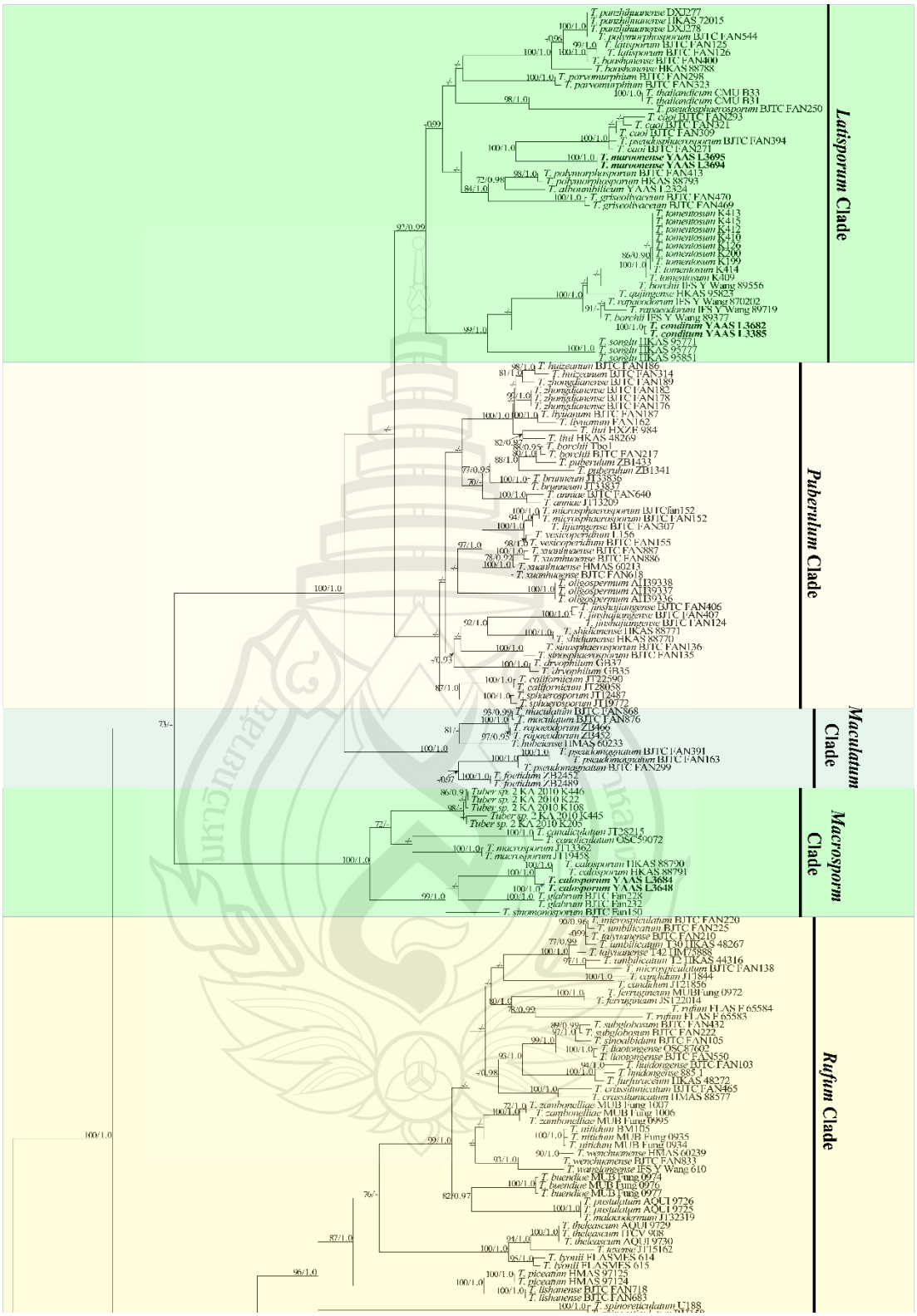
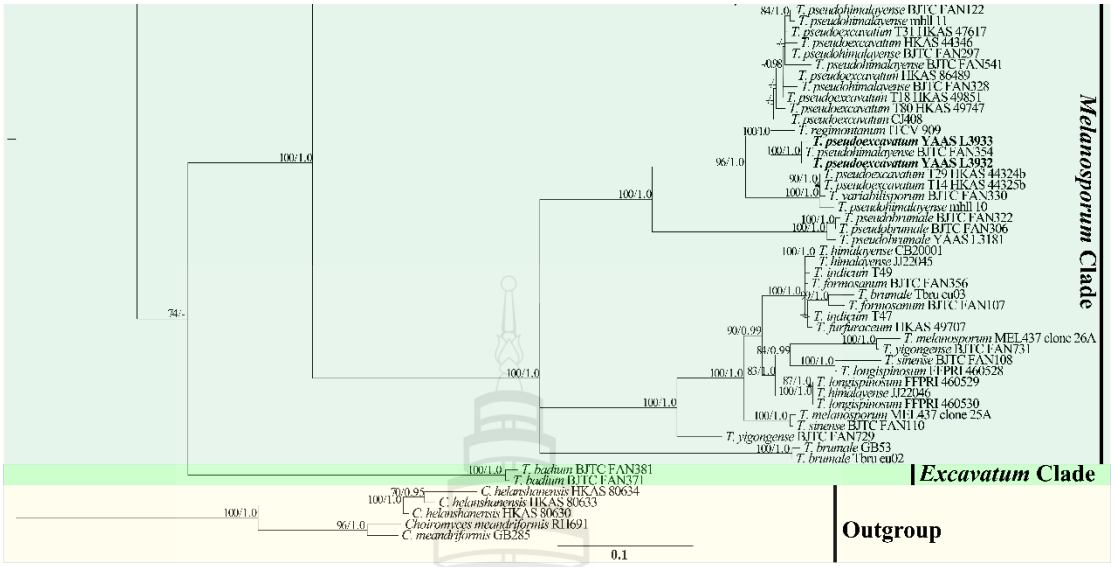


Figure 3.2 Phylogenetic tree of the genus *Tuber* constructed by ITS1-5.8S-ITS2 sequences



Note Phylogeny generated from maximum likelihood and Bayesian inference analysis of the ITS1-5.8S-ITS2 sequences from *Tuber maroonense* and *T. conditum* related species. *Choiromyces helanshanensis* and *C. meandriformis* served as outgroups. ML bootstrap values (>75%) and Posterior Probabilities (PPs) values (>0.90) are shown above or beneath the branches at nodes. Novel sequences are printed in bold

Figure 3.2 (continued)

3.1.2 Taxonomy

Tuber maroonense T. J. Yuan, Shu H. Li & X. H. Wang, sp. nov. Figure 3.3

MycoBank: MB901881

Typification: CHINA. YUNNAN PROVINCE: Xiangyun County (25º 20’768”E, 100º 43’34”N), in soil under mixed forest, with *Pinus yunnanensis* dominated, 20 Sep 2020, S. H. Li L3694 (holotype YAAS L3694, paratype YAAS L3695).

Gene sequences ex holotype: ON454668 (ITS); ON428904 (LSU); ex paratype: OQ297680 (ITS).

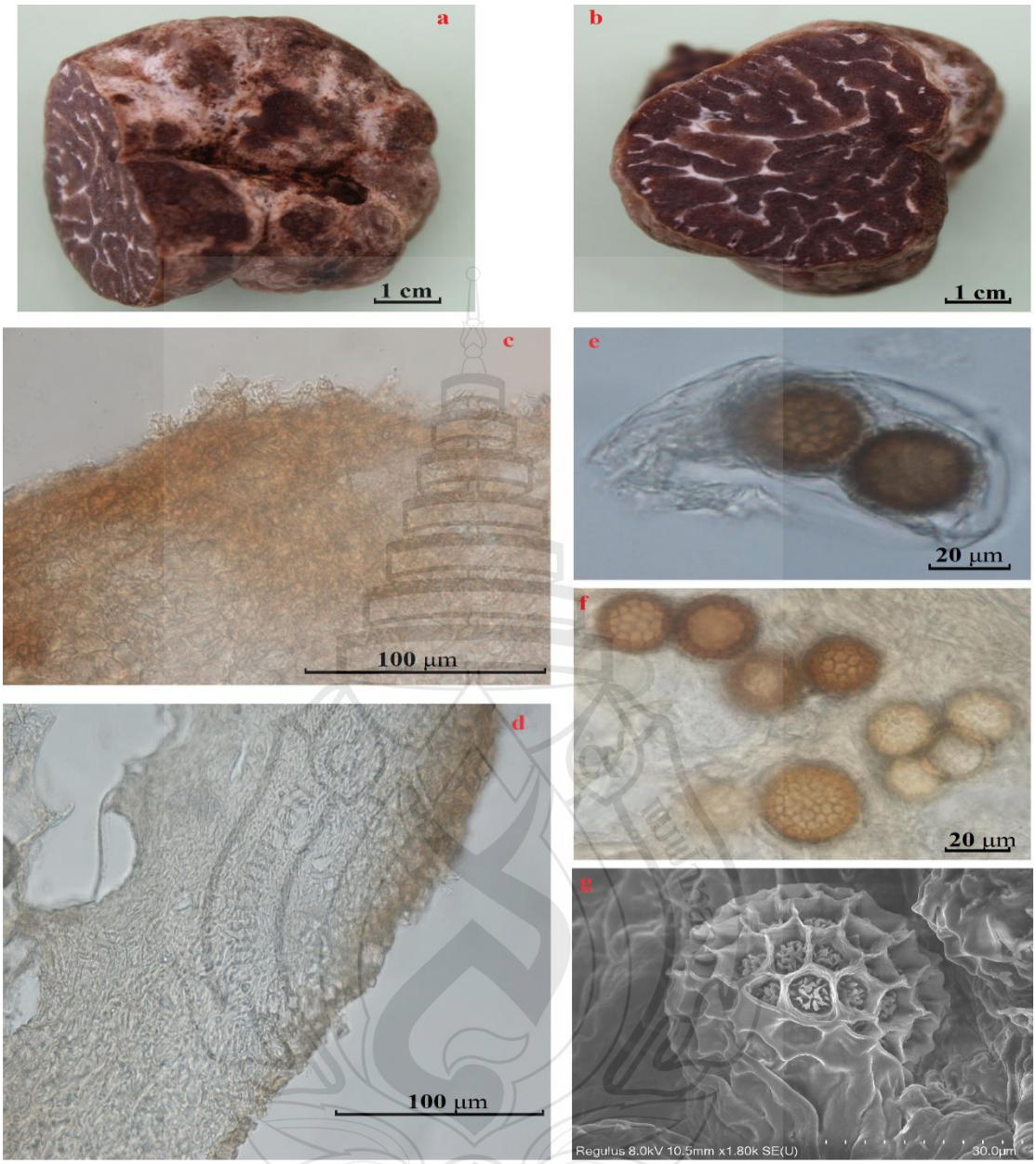
Etymology: maroonense, refers to the maroon color of the ascoma.

Ascomata (Figure 3.3 a and b) 3–5 cm diam, subglobose, hypogeous, whitish becoming brown when bruised, surface smooth, with white furrows; odor mild, taste not

recorded. *Peridium* (Figure 3.3 c and d) two-layer, 150–200 µm thick, outer layer 40–60 µm thick, pseudoparenchymatous, composed of subglobose or irregularly shaped cells of 7.5–16.8 (24.5) µm broad with thick walls, inner layer composed of thin-walled hyaline interwoven hyphae, 2.5–4 (5.5) µm diam, large cells of 20 × 10 µm diam. Sometimes, intermixed. *Gleba* (Figure 3.3 b) solid, firm, brown to dark brown at maturity, marbled with whitish narrow veins. *Asci* (Figure 3.3 e and g) subglobose, or inregular, 1-4 spored, with a short stalk, 50–75 (100) × 40–55 (80) µm (n = 50). *Ascospores* (Figure 3.3 e and g) subglobose to globose, pale yellow when young, becoming brown at maturity, excluding their spiny-reticulate ornamentation, 41.5–52 × 41–50 µm, *Q* =1.00–1.14 (n = 55), in one-spored asci, 33–41 × 32–40 µm (n = 50), *Q* = 1.00–1.15, in two-spored asci, 21–37 × 20–35.5 µm, *Q* = 1.01–1.12 (n=60), in three-spored asci, 20–35.5 × 18.5–30.5 µm, *Q* = 1.02–1.15 (n = 60), in four-spored asci, ***Q*** = 1.14 ± 0.07, ornamented with a reticulated, meshes 5–8 across the ascospore width, 1.5–3 µm tall.

Distribution and habitat: China: Yunnan province, Xiangyun county, hypogeous, in the soil in mixed woods dominated by *P. yunnanensis.*

Diagnosis: *Tuber maroonense* is phylogenetically closely related to *T. caoi* (Fan et al., 2016). In morphology, *T. caoi* has gray and pubescent ascomata but *T. maroonense* has whitish and glabrous ascomata. Both trees of ML and BI (Figure 3.1 and 3.2) also have strong bootstraps supporting the new species.



Note (a) Fresh ascomata showing cut section. (b) The gleba. (c) Vertical section of peridium. (d) The gleba and asci. (e) and (f) Ascospores. (g) Scanning electron micrograph of ascospore

Figure 3.3 Photographs of *Tuber* maroonense (YAAS L3694, holotype)

Tuber conditum T. J. Yuan, S. H. Li & X. H. Wang, sp. nov. Figure 3.4

MycoBank: MB901882

Typification: CHINA, YUNNAN PROVINCE: Changning County (38.3903º E, 102.3535º N), in soil under mixed forest, with *Pinus yunnanensis* dominanted, 20 Sep 2020, S. H. Li L3385 (holotype YAAS L3385, paratype YAAS L3682).

Gene sequences ex holotype: ON454665 (ITS); ON428901 (LSU); ex paratype: ON454667 (ITS).

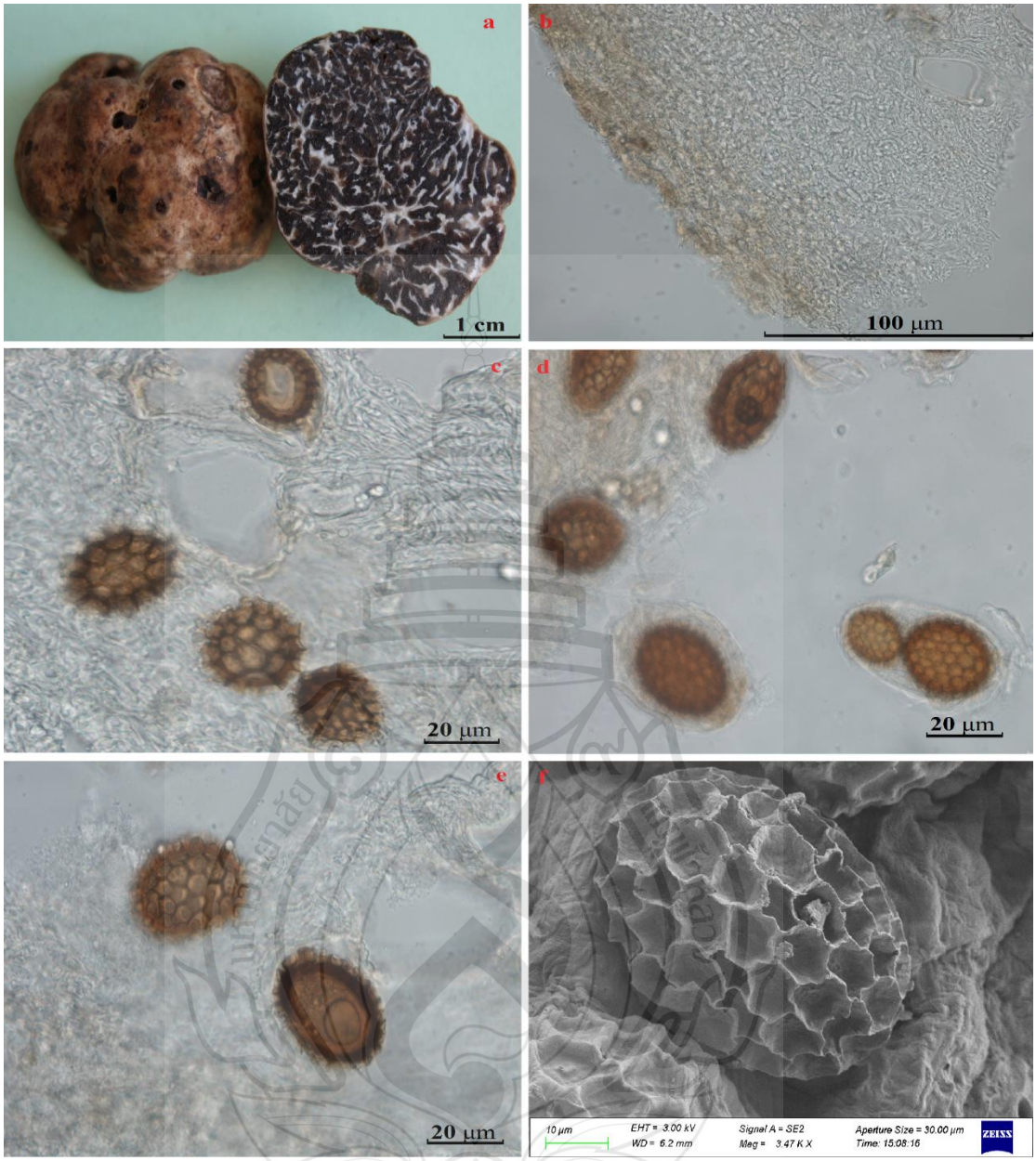
Etymology: conditum, Latin refers to the acrid smell of ascocarp.

Ascomata (Figure 3.4 a) 3–4 cm diam, subglobose, hypogeous, grey-white to grey-brown, surface smooth, with a few pinholes; odor acrid smell, taste not recorded. *Peridium* (Figure 3.4 b) one-layered, 120–200 µm thick, prosenchymatous, composed of interwoven hyphae 1.5–2.5 µm broad with thin-walled, and lumens 1.5–2.5 (3.5) µm diam, with ellipsoid or irregularity cells of 15 × 10 µm diam. Sometimes intermixed, wall thickness 1–2 µm. *Gleba* (Figure 3.4 a and c) solid, firm, brown to black at maturity, marbled with whitish narrow veins. *Asci* (Figure 3.4 d and e) subglobose, or irregularity, 1–4 spored, hyaline, thin-walled or occasionally with walls as thick as 2 µm, sessile stalk, 55–100 × 45–75 µm (n = 30). *Ascospores* (Figure 3.4 d, e and f) subglobose or ellipsoide, pale yellow, yellow-brown at maturity, excluding ornamentation, 49–66.5 × 34.5–60 µm, *Q*= 1.02–1.58 (n = 54), in one-spored asci, 33–54.5 × 30–47 µm, *Q* = 1.06–1.35 (n=50), in two-spored asci, 21.5–44 × 21–37 µm, *Q* = 1.00–1.26 (n = 60), in three-spored asci, 20.5–40.0 × 20–35.5 µm, *Q* = 1.01–1.30 (n = 40), in four-spored asci, ***Q***= 1.15 ± 0.23, reticulate ornamentation 2–5 µm in height, composed of irregular hexagonal meshes, 6–8 along the spore length and 3-6 along the breadth.

Distribution and habitat: China: Yunnan province, Changning county, hypogeous, in the soil in woods dominated by *Pinus yunnanensis*.

Diagnosis: *Tuber conditum* is phylogenetically closely related *Tuber* sp. 10 (Kinoshita et al., 2011), *T. qujingense* and *T. songlu* (Wan et al., 2021). However, *T. conditum* has no cystidia on the surface of ascomaya and larger ellipsoid ascospores

differing from *Tuber* sp. 10 (Sasaki et al., 2016; Kinoshita et al., 2011). *Tuber conditum* differs from *T. qujingense* and *T. songlu* by its thinner peridium (120–200 µm) and larger ascospores (49–66.5 × 34.5–60 µm in one-spored asci). *Tuber qujingense* has a greyish-white ascoma, brown snowflake-shaped gleba, prosenchymatous peridium, and fusiform and *T. songlu* has dense spine-like dermatocystidia, which are completely different from each other. In addition, DNA sequence analysis revealed the similarity between the two species is less than 82.73 % (*T. qujingense*) and 93 % (*T. songlu*) in ITS sequences, strongly supporting the separation of *T. conditum* from the Chinese species of *T. qujingense* and *T. songlu.* Phylogenetic analysis (Figure 3.7 and 3.8) also suggested that *T. conditum* is a distinct species because all sequences of this new species clustered within a strong bootstrap (BS ≥ 99% and PP=1.0). The truffle has the acrid smell which might be a good identifying feature for the fungus.



Note (a) Fresh ascomata showing cut section. (b) Vertical section of peridium. (c) and (d) The gleba and asci. (e) Ascospores. (f) Scanning electron micrograph of ascospore

Figure 3.4 Photographs of *Tuber* conditum (YAAS L3385, holotype)

Tuber pseudoexcavatum Y. Wang et al., Cryptogamie Mycologie, 1998, 19 (1-2): 113-120.

Notes: The description of *Tuber pseudoexcavatum* Y. Wang et al. was originally based on two specimens collected in China and published by Wang et al. in 1998. Subsequently, additional collections (AH18387, AH18331) from China were successfully used to generate DNA data, which were deposited in the Herbarium of the Institute of Forestry & Soil Sciences. This study reports two new collections that suggest the presence of this species may not be uncommon in the southwestern region of China. Morphologically, *T. pseudoexcavatum* is characterized by subglobose ascocarps with a deeply excavated appearance, ranging in color from brown to brown-orange. The surface exhibits a coarsely warted texture, while the asci contain 1-8 ascospores with spinoreticulate ornamentation, which may serve as diagnostic features based on the current collections. The known distribution of this species is limited to China.

Material Examined: Location: Yunnan Province, Changning County (37.1212º E, 101.7307º N) Habitat: Hypogeous, found in soil beneath a pure *Pinus armandii* forest Altitude: Approximately 2500 m Collection Date: 20 Sep. 2020 Specimens: YAAS L3932, YAAS L3933 Collector: S. H. Li Repository: Herbarium of Institute of Forestry & Soil Sciences (YAAS).

Tuber calosporum S. P. Wan et al. Mycoscience, doi.org/10.1016/j.myc.2016.06.007

Note: *Tuber calosporum* S. P. Wan et al. was originally described based on four specimens collected from Huize County in Yunnan province, as detailed by Wan et al. in 2016. The specimens (wsp352, wsp145, wsp186, and wsp382) provided successful DNA data. This study introduces two additional collections, suggesting a broader distribution of the species in the southwest region of China. Morphologically, *T. calosporum* is recognized by its brownish-yellow ascocarps with a verrucose surface, featuring superficial yellow furrows. The ascospores are characterized by their large, ellipsoid shape and shallow alveolar ornamentation, which can serve as diagnostic traits based on the present collections. The species is known to occur exclusively in China.

Material Examined: Location: Yunnan Province, Xiangyun County (25º 39’43”E, 100º 52’27” N) Habitat: Found in soil beneath a mixed forest dominated by *Pinus yunnanensis* Collection Date: 20 Sep 2020 Specimens: YAAS L3648, YAAS L3684 Collector: S. H. Li Repository: Herbarium of Institute of Forestry & Soil Sciences (YAAS).

3.1.3 Key to the Species of the Latisporum Group

1. One-layer peridium……2

1. Two-layer peridium……4

2. Peridium prosenchymatous……3

2. Perdium pseudoparenchymatous……5

3. Irregular and lobed……*T. panzhihuanense* (Deng et al., 2012)

3. Surface smooth and with a few pinholes……***T. conditum***

4. Peridium smooth and glabrous……6

4. Peridium puberulent……7

5. Ascomata white umbilicate……*T. alboumbilicum* (Li et al., 2014)

5. Ascomata whitish becoming brown when bruised with white furrow……
……***T. maroonense***

6. Ascomata whitish-yellow and mostly much lobed with deep furrows……
……*T. pseudosphaerosporum* (Fan & Yue, 2013)

6. Ascomata pale yellow to desert yellow with distinctively hygrophanous patch around or near the base……*T. parvomurphium* (Fan et al., 2016)

7. Ascospores mainly globose……8

7. Ascospores mainly broadly ellipsoid……9

8. Ascospores globose only……*T. caoi* (Fan et al., 2016)

8. Ascospores fusiform, globose or sometimes subglobose……
……*T. polymorphosporum* (Wan et al., 2017)

9. Ascomata olive gray or gray with green……*T. griseolivaceum* (Huang et al., 2017)

9. Ascomata pale yellowish brown or reddish brown……10

10. Ascospores broad ellipsoid…… ……11

10. Ascospores ellipsoid, subglobose……12

11. Asci 2–3 spored, ascospores smaller (25 – 40 × 14 – 25 µm) ……

……*Tuber* sp. 10 (Kinoshita et al., 2011)

11. Asci 1–4 spored, ascospores larger (30 – 60 × 25– 50 µm) ……

……*Tuber* sp. 12 (Kinoshita et al., 2011)

12. Ascomata ocher-yellow…… ……13

12. Ascomata whitish……14

13. Asci 2–3 spored, ascospores smaller (30 – 35 × 20 – 30 µm) ……

……..*Tuber* sp. 11 (Kinoshita et al., 2011)

13. Asci 2–3 spored, ascospores largerer (30 – 55 × 30 – 40 µm) ……

……*Tuber* sp. 13 (Kinoshita et al., 2011)

14. Ascospores reddish-brown, with five-spored in asci, and alveolar walls up to 2-6 µm tall……*T. baoshanense* (Wan et al., 2017)

14. Ascospores yellowish brown to brown, with four-spored in asci and alveolate reticulum 3-5 µm tall……*T. thailandicum* (Suwannarch et al., 2015)

14. Ascospores yellowish brown to reddish brown, with four-spored in asci and alveolar walls up to 3-5 µm deep……*T. latisporum* (Chen & Liu, 2007)

3.2 Taxonomy and Phylogeny of *Choiromyces*

3.2.1 DNA Sequence Analyses

A total of forty-one ITS sequences were used for phylogenetic analysis, among which five were generated in this study (3 sequences of known species and 2 sequences of *C. cerebriformis*) and thirty-six were downloaded from GenBank (Table 3.2). Four sequences of *Dingleya* spp. and *Labyrinthomyces* spp. were selected as the outgroup. The ITS data matrix consisted of 41 accessions and 696 characters, of which 350 characters were constant,

328 were parsimony-uninformative, and 240 were parsimony-informative. The ML analysis resulted in a tree with a log-likelihood of -4079. ML and Bayesian analyses yielded phylogenies with congruent topologies.

C. cerebriformis appeared distinct from other *Choiromyces* species and closely related to *C. helanshanensis* with high support (PP = 1.0, ML bootstrap support value = 100 %; Figure 3.5). Genetic distances between *C. cerebriformis* and the two most closely related species *C. helanshanensis* and *C. alveolatus* were greater than 3 % (Table 3.3), providing further evidence that they can be considered as different species.

Table 3.2 GenBank numbers of *Choiromyces* specimens used for phylogeny analysis

Species name	Voucher	Origin	ITS	References
C. alveolatus	22830	Israel	AF501258	Ferdman et al. (2005)
C. alveolatus	Trappe 17497	USA	EU669384	Unpublished
C. alveolatus	OSC 70417	USA	EU697268	Unpublished
C. alveolatus	HS2886	USA	HM485333	Bonito et al. (2010)
C. alveolatus	MES97	USA	HM485332	Bonito et al. (2010)
C. helanshanensis	80636	China	KP019343	Chen et al. (2016)
C. helanshanensis	80638	China	KP019344	Chen et al. (2016)
C. helanshanensis	80645	China	KP019345	Chen et al. (2016)
C. helanshanensis	80634	China	KP019346	Chen et al. (2016)
C. helanshanensis	80644	China	KP019347	Chen et al. (2016)
C. helanshanensis	80642	China	KP019348	Chen et al. (2016)
C. helanshanensis	80631	China	KP019349	Chen et al. (2016)
C. helanshanensis	80647	China	KP019350	Chen et al. (2016)
C. helanshanensis	80639	China	KP019351	Chen et al. (2016)
C. helanshanensis	YAAS L3051	China	MT672010	This study
C. helanshanensis	YAAS L3062	China	MT672011	This study
C. helanshanensis	YAAS L3063	China	MT672012	This study
C. magnusii	AH19770	Spain	JF300143	Moreno et al. (2012)
C. magnusii	AH11894	Spain	JF300144	Moreno et al. (2012)
C. meandriformis	Urbino/Stocchi	Italy	AF003910	Unpublished
C. meandriformis	K(M)135393	England	EU784184	Brock et al. (2009)
C. meandriformis	K(M)53644	England	EU784185	Brock et al. (2009)
C. meandriformis	RH691	USA	HM485330	Bonito et al. (2010)

Table 3.2 (continued)

Species name	Voucher	Origin	ITS	References
C. meandriformis	ZB2060	Romania	JQ288899	Unpubished
C. venosus	AH38935	UK	JF300145	Moreno et al. (2012)
C. venosus	AH38915	Italy	JF300146	Moreno et al. (2012)
C. venosus	AH38904	Romania	JF300147	Moreno et al. (2012)
C. cerebriformis	**YAAS TJ16-1**	**China**	**MT672013**	**This study**
C. cerebriformis	**YAAS TJ16-2**	**China**	**MT672014**	**This study**
C. cerebriformis	**YAAS 8890**	**China**	**MW209701**	**This study**
Choiromyces sp.	FB_D3_1_184a_4	USA	JX630489	Timling et al. (2012)
Choiromyces sp.	FB_D3_5_188_1	USA	JX630491	Timling et al. (2012)
Choiromyces sp.	PP_S3_3_287_1	Canada	JX630610	Timling et al. (2012)
Choiromyces sp.	HV_D3_8	USA	JX630713	Timling et al. (2012)
Choiromyces sp.	AR1647	Canada	JX630948	Timling et al. (2012)
Choiromyces sp.	AR1293	Canada	JX630960	Timling et al. (2012)
Choiromyces sp.	AR1291	Canada	JX630965	Timling et al. (2012)
Dingleya sp.	JT20122	Australia	JQ925626	Bonito et al. (2013)
Dingleya sp.	JT31036	Australia	JQ925628	Bonito et al. (2013)
Labyrinthomyces sp.	JT27750	Australia	JF300130	Moreno et al. (2012)
Labyrinthomyces sp.	JT25359	Australia	JQ925633	Bonito et al. (2013)

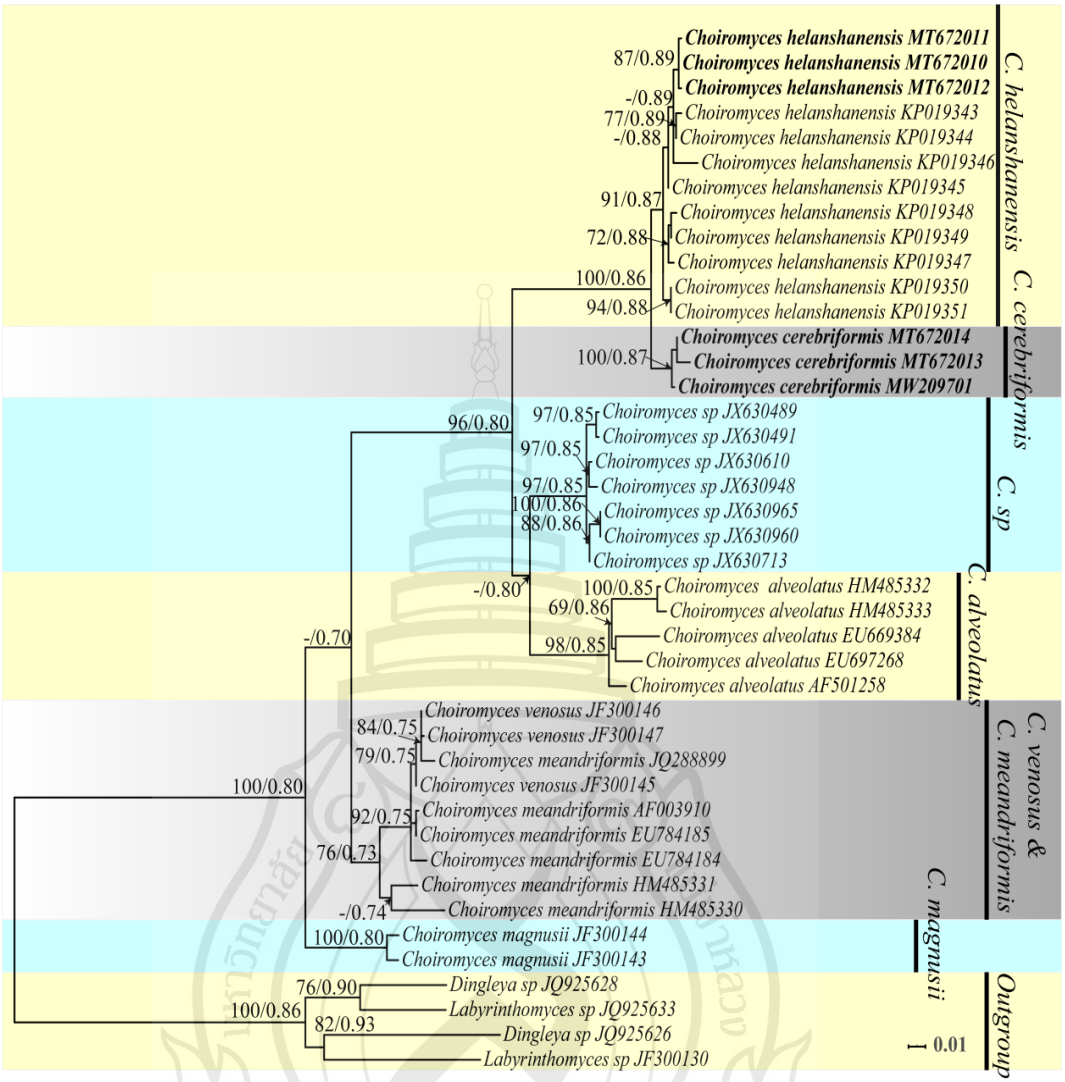
Table 3.3 Intraspecific and interspecific genetic distances of *Choiromyces* species

	1 (*N*=3)	2 (*N*=12)	3 (*N*=6)	4 (*N*=3)	5 (*N*=2)	6 (*N*=5)	7 (*N*=7)
1	0.000-**0.006**-0.007						
2	0.033-**0.037**-0.044	0.000-**0.011**-0.027					
3	0.181-**0.184**-0.189	0.172-**0.178**-0.186	0.000-**0.037**-0.073				
4	0.181-**0.184**-0.185	0.172-**0.175**-0.177	0.000-**0.025**-0.037	0			
5	0.185-**0.187**-0.207	0.185-**0.190**-0.193	0.106-**0.114**-0.126	0.114-**0.116**-0.118	0.02		
6	0.132-**0.136**-0.141	0.121-**0.128**-0.133	0.152-**0.162**-0.178	0.153-**0.160**-0.165	0.156-**0.172**-0.182	0.000-**0.027**-0.037	

Table 3.3 (continued)

	1 (*N*=3)	**2 (*N*=12)**	**3 (*N*=6)**	**4 (*N*=3)**	**5 (*N*=2)**	**6 (*N*=5)**	**7 (*N*=7)**
7	0.121-**0.128**-0.133	0.105-**0.118**-0.129	0.129-**0.138**-0.145	0.129-**0.137**-0.141	0.153-**0.167**-0.178	0.076-**0.086**-0.095	0.000-**0.012**-0.020

Note 1 = *C. cerebriformis*; 2 = *C. helanshanensis*; 3 = *C. meandriformis*; 4 = *C. venosus*; 5 = *C. magnusii*; 6 = *C. alveolatus*; 7 = *Choiromyces* sp. When more than 2 sequences are available, genetic distances are given as minimum-*mean*-maximum.



Note Phylogeny derived from ML analysis of the nrDNA-ITS sequences from the *Choiromyces* species, using *Dingleya* sp. and *Labyrinthomyces* sp. as the outgroup. Values next to nodes are ML bootstrap support values (BS, left) and Bayesian posterior probabilities (PP, right). Names of novel species and samples with newly generated sequences are shown in bold

Figure 3.5 Phylogenetic tree of the genus *Choiromyces*

3.2.2 Taxonomy

Choiromyces cerebriformis T. J. Yuan, S. H. Li & Y. Wang, sp. nov. Figure 3.6

MycoBank: MB837904.

Diagnosis: *Choiromyces cerebriformis* differs from similar species in having ascomata up to 10 cm in diameter, with larger and deeper lobes and light orange-brown gleba.

Holotype: CHINA, Yunnan Province, Diqing Autonomous Prefecture, Shangri-La County, Three dam township, Haba village, 27°21'6.3647"N, 100°06' 34.6895"E, elevation 4005 m, under *Abies delavayi* Franch. and *Rhododendron simsii Planch.* in mixed evergreen hill forest, with soil types mainly red and brown soils, 24 Sep. 2020, collected by X. H. Wang (KUN-HKAS107566, holotype; YAAS 8890, isotype).

Etymology: *cerebriformis* refers to the aspect of ascomata which looks like a brain.

Ascomata hypogeous, up to 10 cm in diam, knobby, with deep lobes; surface glabrous, whitish when young, then pale yellow to reddish-brown with dark spots at maturity (Figure 3.6 b and c). *Peridium* 210–280 µm thick, plectenchymatous, with two layers, the outer layer 60–80 µm thick, reddish-brown, the inner layer 150–200 µm thick, hyaline with larger cells (25–40 µm diam, wall 0.5–2.0 µm thick; Figure 3.6 d). *Gleba* (Figure 3.6 d and e) solid, labyrinthoid, light orange-brown, marbled with greyish white veins. *Odor* strong, pleasant. *Asci* hyaline, clavate to sac-like, 8-spored, (75–)75–85.5–96 (–96) × (42–)43–54–65(–66) µm (N = 20). *Ascospores* (N = 60) (17.5–)17.8–21.3–24.8 (–25.0) × (17.5–)17.6–21.0–24.4(–24.5) µm, Q = (1.00–)0.97–1.02–1.06(–1.12), globose to subglobose, pale yellow-brown, ornamented with straight or slightly curved stick-like sparse spines, 2–3 µm tall, with truncate or rounded tips (Figure 3.6 e–g).

Habitat, phenology, and distribution: Growing under *Abies delavayi* Franch., *Rhododendron simsii Planch.* and *Pinus yunnanensis* in mixed evergreen hill forest, in late autumn. So far found in Diqing and Yongren counties, Yunnan, China.

Other material examined: CHINA, Yunnan Province, Chuxiong Autonomous Prefecture, Yongren County, 26.0810°N 101.6632°E, elevation 1,834 m, under *Pinus yunnanensis* in mixed evergreen hill forest, with soil types mainly red and brown soils, 01 Nov. 2019, collected by H. K. Xiong. (YAAS TJ16-1 and YAAS TJ16-2).

Remarks: *Choiromyces cerebriformis* is characterized by hypogeous, glabrous, pale yellow or white, irregularly knobby, much lobed ascomata, and globose spores ornamented with conspicuous, straight or slightly curved spines with truncate or rounded tips when observed with SEM. This species resembles white *Tuber* truffles with white ascomata and sinuous veins in gleba. However, it is different from those *Tuber* species and other *Choiromyces* species by its globose spores ornamented with conspicuous spines and small pits. *C. cerebriformis* can be further distinguished from *C. meandriformis*, which has paler gleba, and spores with much taller spines (Csorbainé et al., 2008; Moreno et al., 2012). *C. echinulatus* Trappe & Marasas (Ferdman et al., 2005), differs from *C. cerebriformis* by spores with straight, obtuse spines < 2 µm high (spines are 2–3 µm high in *C. cerebriformis*). Moreover, *C. echinulatus* has tissues with greatly inflated cells, which is characteristic of all desert truffles. *C. cerebriformis* differs from *C. alveolatus* (Liu et al., 1990) in having larger asci (75–96 × 42–66) µm, mostly with 8 spores, compared to 40–85 × 30–55 µm asci, with (2–) 4–6 spores in the latter species. *C. magnusii* (Moreno et al., 2012) spore ornamentation is verrucose-reticulated with a minutely-meshed reticulum, which is different from *C. cerebriformis*. *C. helanshanensis* (Chen et al., 2016) differs from *C. cerebriformis* by its coarsely knobby ascomata 2–8 cm diam (ascomata up to 10 cm and with larger, deeper lobes in *C. cerebriformis*) and ascosporal ornamentation as conspicuous dense spines (as short stick-like sparse spines in *C. cerebriformis*).

3.2.3 Key to Choiromyces Species

1a. Ascospores broadly ellipsoid ..... ***C. ellipsosporus****

1b. Ascospores globose or subglobose **2**

2a. Ascospores ornamentation as a reticulum with small rounded meshes **3**

2b. Ascospores ornamentation as spines or rods and small pits..... **4**

3a. Distributed in North America..... ***C. alveolatus***

3b. Distributed in Europe..... ***C. magnusii***

4a. Asci 4-spored..... ***C. tetrasporus***

4b. Asci 8-spored..... **5**

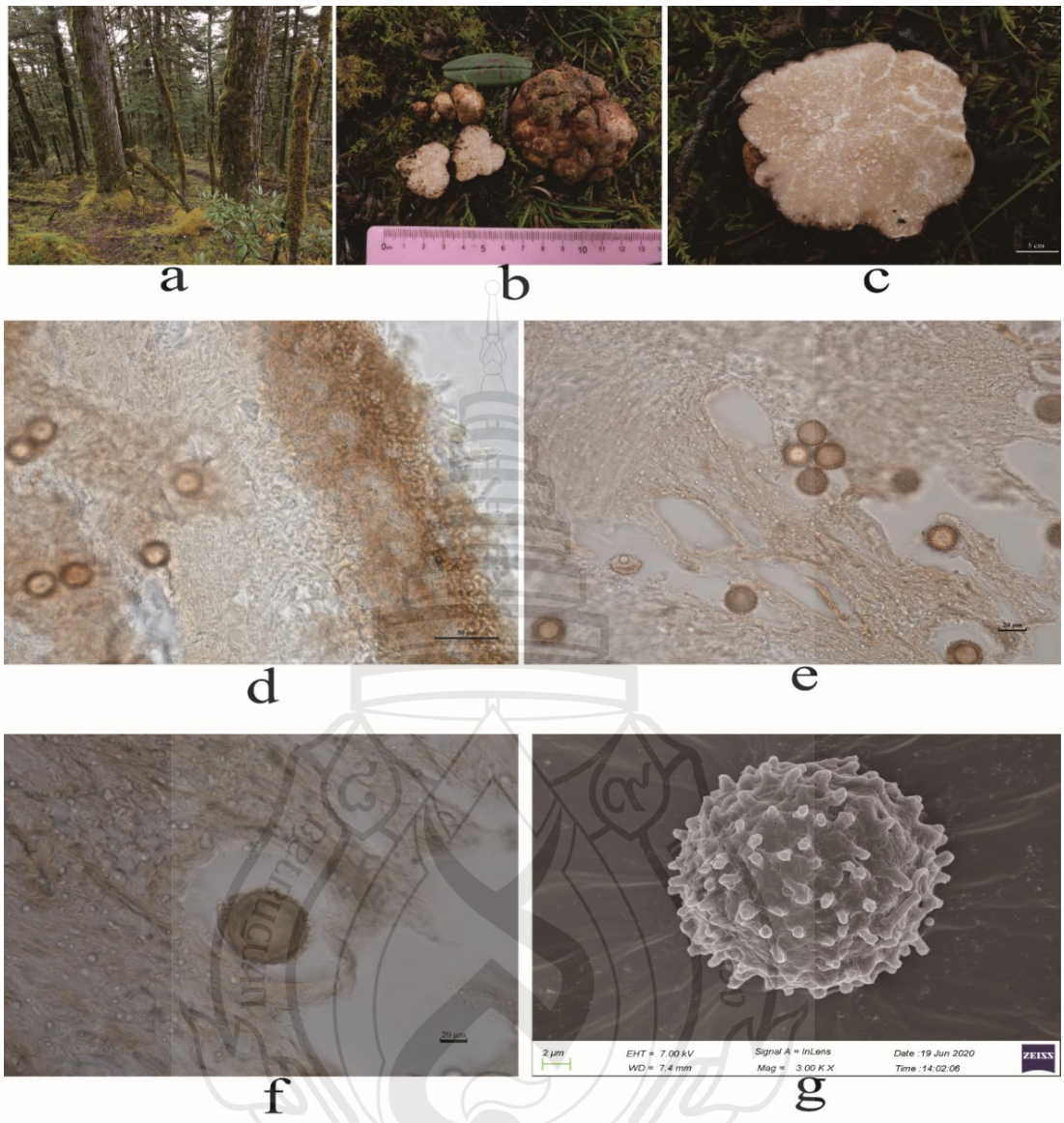
5a Ascospores ornamentation as spines that are often curved and with hollow tips ..... ***C. meandriformis = C. venosus***

5b. Ascospores ornamentation as spines with solid tips **6**

6a Ascomata coarsely knobby; ascospores ornamentation densely spiny ..... ***C. helanshanensis***

6b Ascomata knobby with deep lobes; ascospores ornamentation more sparsely spiny ... ***C. cerebriformis***

* The generic placement of *C. ellipsosporus* has not been re-evaluated since its publication, and might belong in other genera. It may be conspecific with *Hydnotryopsis setchellii* (Gilkey, 1939).



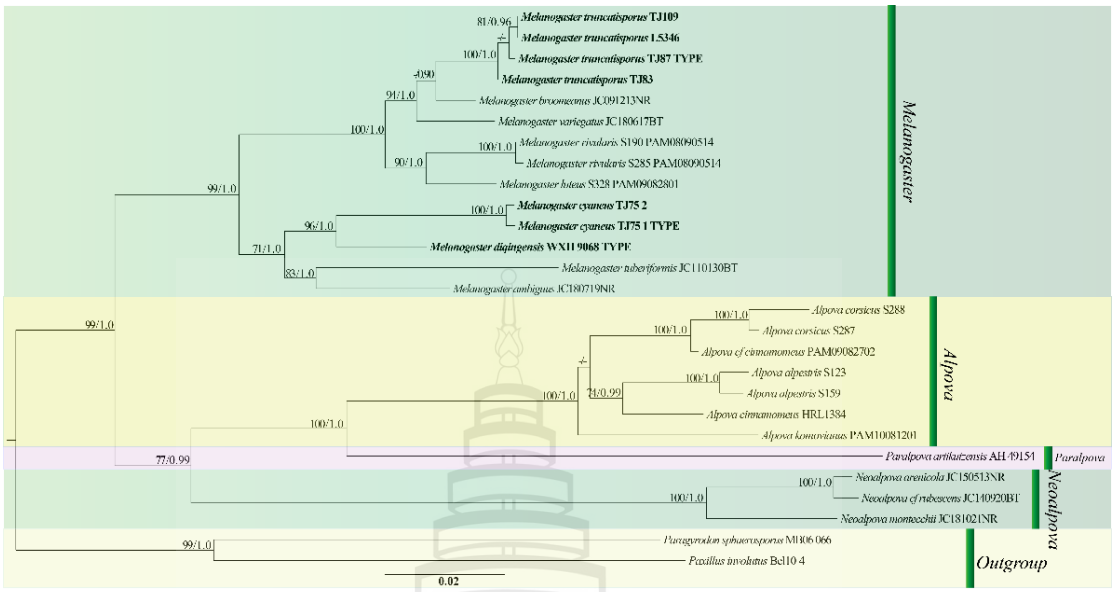
Note (a) The habitat of *Choiromyces cerebriformis*. (b) Fresh ascomata. (c) A sectioned ascoma showing the gleba. (d) Peridium with two differentiated pseudoparenchymatous layers. (e) and (f) Ascospores. (g) SEM photos of ascospores. Scale bars c = 5 cm; d = 50 µm; e, f = 20 µm; g = 2 µm

Figure 3.6 The habitat and morphological characteristics of *Choiromyces cerebriformis*

3.3 Taxonomy and Phylogeny of *Melanogaster*

3.3.1 Molecular Data Analyses

The multi-gene dataset (ITS, 5.8S, nrLSU and RPB2) contained 27 specimens (7 novel specimens from our collections) and had an aligned length of 2,295 characters. ML and BI yielded identical tree topologies and only the tree inferred from the ML analysis is shown (Table 3.4 and Figure 3.7). The ITS dataset contained 79 specimens, of which 7 were newly sequenced, and had an aligned length of 683 characters. ML and BI analyses produced identical tree topologies and only the tree derived from the ML analysis is shown (Figure 3.8). The four-gene datasets and ITS (ITS1-2 and 5.8S) resulted in ML trees with a log-likelihood of -9919.6 and -5052.3, respectively. The general topology of the trees (Figure 3.7 and 3.8) is congruent with those already published by Moreau et al. (2011, 2013). The ML phylogenetic tree, derived from the four-gene dataset (Figure 3.7), serves as a validation tool for confirming the association of our specimens with *Melanogaster*. The species of *Melanogaster* formed a monophyletic clade with support values (BS = 100%, PP = 1.00) by the phylogenetic tree of ITS (Figure 3.7). Our 7 specimens were resolved as 3 strongly supported species-level clades or branch, different from all known species included in the analysis. This suggests that these specimens represent three new species. Furthermore, two sequences (MT366708 and KY462394) from Chile, a sequence (MN594288) from Spain, two sequences (MN984333 from France, MN984335 from the USA), and two sequences (OP548647, OP548648) from Turkey formed three distinct, independent clades within *M*. sp1 to *M*. sp4. These clades exhibited less than 98.4% similarity (*M*. sp1=98.3%, *M*. sp2=93.47%, *M*. sp3=94.06%, and *M*. sp4=96.63%) in their ITS sequences compared to other species of *Melanogaster*. This observation suggests the likely presence of three additional undescribed species.



Note The consensus phylogram of *Melanogaster* and its closely related genera obtained with MrBayes (including ITS1, ITS2, 5.8S, nrLSU and RPB2). Two species *(Paragyrodon sphaerosporus* and Paxillus involutus) were included in the outgroup. Nodes were annotated with ML BS > 70 % and Bayesian PP > 0.90, "-" in case of non-significant support value. New species are shown in bold font

Figure 3.7 Phylogenetic tree of the genera *Melanogaster* and *Alpova*

Table 3.4 GenBank numbers of *Melanogaster* specimens used for phylogeny analysis

Species	Isolate/ Strain/ Clone/Voucher	Country	Genbank accession numbers			Reference
			ITS	nrLSU	*RPB2*	
Alpova alpestris	S123	France	HQ714711	/	HQ714846	Moreau et al. 2013
Alpova alpestris	S159	France	HQ714721	/	HQ714853	Moreau et al. 2013
Alpova cf. cinnamomeus	PAM09082702	France	HQ714779	/	HQ714901	Moreau et al. 2013
Alpova cinnamomeus	BROWN FP73	USA	KF835996	/	/	Hayward et al. 2014
Alpova cinnamomeus	HRL1384	Canada	MN594282	MN594298	MN594770	Unpublished
Alpova concolor	UBC F14673	USA	KF835997	/	/	Hayward et al. 2014
Alpova concolor	OSC 65696	USA	NR_154686	/	/	Unpublished
Alpova corsicus	S287	France	HQ714769	/	HQ714893	Hayward et al. 2014
Alpova corsicus	S288	France	HQ714770	/	HQ714894	Moreau et al. 2011
Alpova komovianus	PAM10081201	Montenegro	JQ436850	/	JQ436862	Moreau et al. 2013
Neoalpova arenicola	JC150513NR	Spain	MN594292	MN594304	MN594775	Unpublished
Neoalpova cf. rubescens	JC140920BT	Spain	MN594294	MN594305	MN594776	Unpublished
Neoalpova montecchii	JC181021NR	Spain	MN594296	MN594306	MN594777	Alvarado et al. 2021
Paralpova artikutzensis	AH 49154	Spain	NR_173892	MN594307	MN594778	Alvarado et al. 2021
Melanogaster ambiguus	B-2220	Hungary	AJ555510	/	/	Unpublished
Melanogaster ambiguus	51745	Hungary	AJ555511	/	/	Unpublished
Melanogaster ambiguus	B-1599	Hungary	AJ555512	/	/	Unpublished
Melanogaster ambiguus	B-1613	Hungary	AJ555513	/	/	Unpublished
Melanogaster ambiguus	B-2409	Hungary	AJ555514	/	/	Unpublished

Table 3.4 (continued)

Species	Isolate/ Strain/ Clone/Voucher	Country	Genbank accession numbers			Reference
			ITS	nrLSU	*RPB2*	
Melanogaster ambiguus	Ch12	Poland	KX438335	/	/	Unpublished
Melanogaster ambiguus	JC180719NR	Spain	MN594286	MN594299	MN594771	Unpublished
Melanogaster ambiguus	OSC158337 MES304	Poland	MN984308	/	/	Unpublished
Melanogaster ambiguus	MTH1	Germany	MN994353	/	/	Unpublished
Melanogaster broomeanus	JC091213NR	Spain	MN594287	MN594300	MN594772	Unpublished
Melanogaster broomeanus	OTU_718s	United Kingdom	MT095837	/	/	Arraiano-Castilho et al. 2021
Melanogaster broomeanus	OTU_719s	United Kingdom	MT095838	/	/	Arraiano-Castilho et al. 2021
Melanogaster cyaneus	TJ75_1 (TYPE)	China	ON427476	ON427489	ON533869	In this study
Melanogaster cyaneus	TJ75_2	China	ON427477	ON427490	ON533870	In this study
Melanogaster diqingensis	WXH_9068 (TYPE)	China	ON427482	ON427495	ON533874	In this study
Melanogaster euryspermus	OSC158352 DS1257	USA	MN984309	/	/	Unpublished
Melanogaster euryspermus	OSC158364 DS1555	USA	MN984310	/	/	Unpublished
Melanogaster euryspermus	OSC158339 JLF1044	USA	MN984311	/	/	Unpublished
Melanogaster euryspermus	OSC158325 JLF1129	USA	MN984312	/	/	Unpublished
Melanogaster euryspermus	OSC158351 JLF1456	USA	MN984313	/	/	Unpublished
Melanogaster euryspermus	OSC158317 JMT22778	USA	MN984314	/	/	Unpublished
Melanogaster euryspermus	OSC158333 MES110	USA	MN984315	/	/	Unpublished

Table 3.4 (continued)

Species	Isolate/ Strain/ Clone/Voucher	Country	Genbank accession numbers			Reference
			ITS	nrLSU	*RPB2*	
Melanogaster intermedius	B-1770	Hungary	AJ555515	/	/	Unpublished
Melanogaster intermedius	RBG Kew K(M)130202	England	EU784372	/	/	Brock et al. 2009
Melanogaster intermedius	MT48	Germany	KX168661	/	/	Unpublished
Melanogaster luteus	S328/PAM09082801	France	HQ714780	/	HQ714902	Moreau et al. 2011
Melanogaster luteus	S407/Mon06	Montenegro	HQ714794	/	/	Moreau et al. 2011
Melanogaster Macrosporus	cI-94	USA	AJ555526	/	/	Unpublished
Melanogaster Macrosporus	B-2254	USA	AJ555528	/	/	Unpublished
Melanogaster minobovat	BJTC FAN911	China	NR_186967	/	/	Xu et al. 2022
Melanogaster natsii	OSC82168 JMT7491	USA	MN984331	/	/	Unpublished
Melanogaster natsii	OSC158336 MES297	USA	MN984332	/	/	Unpublished
Melanogaster panzhihuaensis	HMAS 81915	China	NR_186968	/	/	Xu et al. 2022
Melanogaster rivularis	S190/PAM08090514	France	HQ714731	/	HQ714862	Moreau et al. 2011
Melanogaster rivularis	S285/PAM08090514	France	HQ714767	/	HQ714891	Moreau et al. 2011
Melanogaster rivularis	LIP PAM08090514 (TYPE)	France	NR_132848	/	/	Moreau et al. 2011
Melanogaster sp.	Melanog002FRA	France	KU924526	/	/	Unpublished
Melanogaster sp.	Melanog006FRA	France	KU924529	/	/	Unpublished
Melanogaster sp.	Melanog007FRA	France	KU924530	/	/	Unpublished
Melanogaster sp.	Melanog008FRA	France	KU924531	/	/	Unpublished
Melanogaster sp.	Melanog011FRA	France	KU924533	/	/	Unpublished
Melanogaster sp.	Melanog012FRA	France	KU924534	/	/	Unpublished
Melanogaster sp.	Melanog018FRA	France	KU924535	/	/	Unpublished

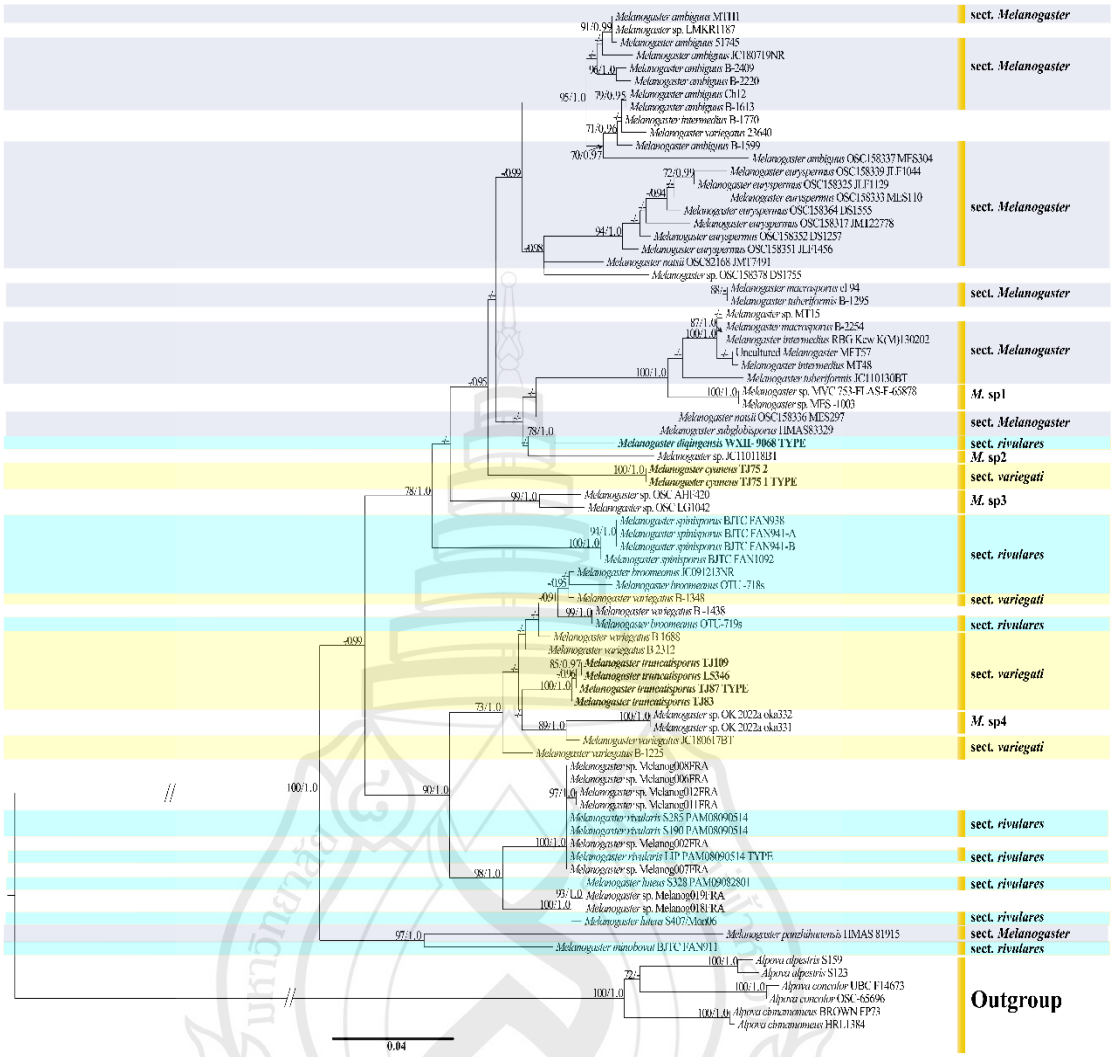
Table 3.4 (continued)

Species	Isolate/ Strain/ Clone/Voucher	Country	Genbank accession numbers			Reference
			ITS	nrLSU	*RPB2*	
Melanogaster sp.	Melanog019FRA	France	KU924536	/	/	Unpublished
Melanogaster sp.	MT15	Germany	KX168646	/	/	Unpublished
Melanogaster sp.	MES-1003	Chile	KY462394	/	/	Brock et al. 2009
Melanogaster sp.	LMKR1187	United Kingdom	MF352733	/	/	Suz et al. 2017
Melanogaster sp.	JC110118BT	Spain	MN594288	/	/	Unpublished
Melanogaster sp.	OSC AHF420	France	MN984333	/	/	Unpublished
Melanogaster sp.	OSC158378 DS1755	USA	MN984334	/	/	Unpublished
Melanogaster sp.	OSC LG1042	USA	MN984335	/	/	Unpublished
Melanogaster sp.	MVC 753_FLAS-F-65878	Chile	MT366708	/	/	Unpublished
Melanogaster sp. OK-2022a	oka331	Turkey	OP548647	/	/	Unpublished
Melanogaster sp. OK-2022a	oka332	Turkey	OP548648	/	/	Unpublished
Melanogaster spinisporus	BJTC FAN1092	China	MW598537	/	/	Xu et al. 2022
Melanogaster spinisporus	BJTC FAN938	China	MW598546	/	/	Xu et al. 2022
Melanogaster spinisporus	BJTC FAN941-A	China	MW598548	/	/	Xu et al. 2022
Melanogaster spinisporus	BJTC FAN941-B	China	MW598549	/	/	Xu et al. 2022
Melanogaster subglobisporus	HMAS83329	China	MW598534	/	/	Xu et al. 2022
Melanogaster truncatisporus	TJ83	China	ON427478	ON427491	ON533871	In this study
Melanogaster truncatisporus	TJ87 (TYPE)	China	ON427479	ON427492	ON533872	In this study
Melanogaster truncatisporus	TJ109	China	ON427480	ON427493	ON533873	In this study
Melanogaster truncatisporus	L5346	China	ON427481	ON427494	/	In this study

Table 3.4 (continued)

Species	Isolate/ Strain/ Clone/Voucher	Country	Genbank accession numbers			Reference
			ITS	nrLSU	*RPB2*	
Melanogaster tuberiformis	B-1295	Romania	AJ555527	/	/	Unpublished
Melanogaster tuberiformis	JC110130BT	Spain	MN594289	MN594302	MN594773	Unpublished
Melanogaster variegatus	23640	Hungary	AJ555522	/	/	Unpublished
Melanogaster variegatus	B-1438	Hungary	AJ555523	/	/	Unpublished
Melanogaster variegatus	B-1688	Hungary	AJ555524	/	/	Unpublished
Melanogaster variegatus	B-1225	Hungary	AJ555533	/	/	Unpublished
Melanogaster variegatus	B-1348	Hungary	AJ555534	/	/	Unpublished
Melanogaster variegatus	B-2312	Hungary	AJ555535	/	/	Unpublished
Melanogaster variegatus	JC180617BT	Spain	MN594290	MN594303	MN594774	Unpublished
Uncultured Melanogaster	MFT57	Germany	FJ403505	/	/	Pena et al. 2010
Paragyrodon sphaerosporus	MB06-066	USA	GU187540	GU187593	GU187803	Binder et al. 2010
Paxillus involutus	Bel10.4	France	KF261366	/	JQ436854	Jargeat et al. 2014

Note The symbol "/" means that the sequence was not available, and sequences newly generated for this study are shown in bold.



Note The consensus ITS phylogram of *Melanogaster* obtained with MrBayes (including ITS1, ITS2, and 5.8S). Six *Alpova* species were included in the outgroup. Nodes were annotated with ML BS > 70 % and Bayesian PP > 0.90, "-" in case of non-significant support value. New species are in bold font. New species are in bold font. The sections (abbreviation "sect.") were divided by the long of basidiospores of Moreau et al. (2011)

Figure 3.8 Phylogenetic tree of the genus *Melanogaster*

3.3.2 Taxonomy

Melanogaster cyaneus T. J. Yuan, Shu H. Li, & Raspé, sp. nov. (Figure 3.9 a-d)

MycoBank: MB901868

Diagnosis: *Melanogaster cyaneus* is characterized by its distinctive blue or bluish gleba and light brown to yellowish-brown basidiomata. The peridium consists of two layers: an outer layer (epipellis), 20–75 μm thick, with deeply orange-yellow to reddish hyphae, and an inner layer (subpellis), 145–335 μm thick, with bright white to pale-yellow hyphae. The basidiospores are globose to subglobose, measuring 6.2–15 × 4.6–9.0 μm ($L_m \times W_m$= 9.5 ± 3.0 × 7.0 ± 2.0, Q= 1.0–2.0, Q_m =1.4 ± 0.6, n = 75), with hyaline when immature, becoming yellow to reddish in 5% KOH.

Etymology: *M. cyaneus* refers to the blue or bluish gleba.

Holotype: China. Sichuan Province: Panzhihua City, Yanbian County, Shuanglong village, 26°49’12” N, 101°33’7.1028” E, elevation 1970 m, in mainly reddish brown soils under *Castanea mollissima* Bl., 16 Aug. 2020, collected by Yang, M. (KUN- HKAS129200, holotype; YAAS-Tj75-1, isotype).

Description: *Basidiomata*, 2.5–4.0 × 1.5–2.5 cm, hypogeous or semi hypogeous, subglobose to ellipsoidal, occasionally elongate; light brown to yellowish brown, with mycelial strands attached in the base (Figure 3.9 a). *Peridium* two-layered, out layer 20–75 μm thick, composed of interwoven hyphae, orange-yellow to reddish, 0.8–1.5 μm in diam, thick-walled, clamp connections present; inner layer 145–335 μm thick, composed of interwoven hyphae of strongly gelatinized, 0.5–1.0 μm in diam, pale-yellow, intermixed with massive inflated cells, 1.5–3 μm broad, with clamp connections present. Trama plates of gelatinized hyphae (Figure 3.9 b). *Gleba* solid, gelatinous, milk-white when immature, blue or bluish at mature, with small chambers separated by sterile pale-yellow veins scattered throughout, filled with black spores (Figure 3.9 c). *Basidia* exhibit limited revival, appearing clavate, hyaline, 4-spores, randomly distributed, gelatinized at maturity. *Basidiospores* subglobose to globose, 6.2–15 × 4.6–9.0 μm ($L_m \times W_m$= 9.5 ± 3.0 × 7.0 ± 2.0, Q= 1.0–2.0, Q_m =1.4 ± 0.6, n = 75), smooth, hyaline when immature, light yellow to

reddish at maturity, surfaces display distinctive spots, and optical microscopy reveals a notable hilar appendage, 0.5–1.0 μm in diam (Figure 3.9 d).

Other material examined: China, Sichuan province, Panzhihua City, Yanbian County, Shuanglong village, 26°49’12” N, 101°33’7.1029” E, elevation 2000 m, under *Castanea mollissima* Bl. in evergreen hill forest, with soil types mainly reddish-brown soils, 16 Aug. 2020, collected by Yang, M. (YAAS TJ75-2).

Notes: *Melanogaster cyaneus* was diagnosed by its characteristic of rhizomorphs on the base, thinner peridium (100–400 μm), blue or bluish gleba and longer and wider basidiospores (6.2–15 × 4.6–9.0 μm). The three Melanogaster species, *M. broomeanus* Berk (Uzun et al., 2014; Türkoğlu & Castellano, 2013), *M. shanxiensis and M. obovatisporus* (Liu & Tao, 1989), are similar and related to *M. cyaneus* in morphology. *M. cyaneus* (light brown to yellowish brown), *M. broomeanus* (yellow-brown to deep brown), *M. shanxiensis* (brown to rust-brown) and *M. obovatisporus* (brown to brownish-black), but the specimens of *M. cyaneus* clustered in an independent clade with strong support (BS = 100%, PP = 1.0) (figure 3.8), supporting it was a distinct species. Additionally, DNA analysis revealed *M. cyaneus* shared less than 92% ITS similarity with other *Melanogaster* species. It was classified into the *Melanogaster* section primarily based on morphological characteristics using Orthogonal Partial Least Squares Discriminant Analysis (OPLS-DA).

Melanogaster diqingensis. T. J. Yuan, Shu H. Li, & Raspé, sp. nov. (Figure 3.9 e-h)

MycoBank: MB901869

Diagnosis. Melanogaster diqingensis can be distinguished by its pale-yellow to brown-yellow basidiomata, scaled, lobed or concave in the surface. The peridium is 100–320 μm thick, comprising an outer layer of 40–80 μm and an inner layer of 150–260 μm. The peridium exhibits orange to bright pale hyphae. Additionally, the basidiospores are obovate to subglobose, smooth, with dimensions of 3.0–5.1 × 2.0–4.0 μm in diameter, Q= 1.0–1.8 μm.

Etymology: *M. diqingensis* refers to the only region of collected basidiomata.

Holotype: China. Yunnan Province: Diqing Autonomous Prefecture, Shangri-La County, Baishuitai village, 27°30’14.2236” N, 100°2’50.5716” E, elevation 2380 m, in brown soil under *Quercus aquifolioides* Rehd. et Wils., 25 Sep. 2020, collected by X. H. Wang (KUN- HKAS121212, holotype; YAAS-WXH_9068, isotype).

Description: *Basidiomata*, 0.5–2.5 × 0.2–2.2 cm, hypogeous, globose, subglobose or ellipsoidal, pale-yellow to orange or brown-yellow, scaled, lobed or concave in the surface, without visible rhizomorphs. *Odor* faint scent (Figure 9 e). *Peridium* two-layered, out layer 40–80 µm thick, composed of interwoven hyphae, 1.5–3 µm, with fusoid to cylindrical terminal cells, deeply orange-yellow walls toward surface, with clamp connections; inner layer 150–260 µm thick, composed of interwoven hyphae, 0.5–2.5 µm, with inflated cells, 3–8 µm in diam, bright pale-yellow, with abundant clamp connections. Trama plates of hyaline or yellowish gelatinized hyphae (Figure 3.9 f). *Gleba* solid, milk-white when immature, pale yellow at mature, hard dried, the locules (2–3 mm in diam). (Figure 3.9 g). *Basidia* exhibit limited reviving, appearing clavate, hyaline, 4–spores. *Basidiospores* obovate to subglobose, smooth, 3.0–5.1 × 2.0–4.0 µm ($L_m \times W_m = 3.8 \pm 1.0 \times 3.2 \pm 0.8$, $Q = 1.0–1.8$, $Q_m = 1.2 \pm 0.6$, n = 75), hyaline (immature) to light-yellow, dark brown (mature) in KOH 5%, with truncate-cupped base and very short hilar appendage in optical microscopy, 0.5–1.5 µm in diam (Figure 3.9 h).

Notes: *Melanogaster diqingensis* was diagnosed by the combination of middle sized pale-yellow to orange or brown-yellow basidiomata, scaled, lobed or concave in the surface, pale yellow gleba, and obovate to subglobose, smooth basidiospores. The six *Melanogaster* species, *M. subglobosporus, M. natsii, M. spinisporus* (Wang et al., 1995), *M. rivularis, M. luteus=M. microsporus* (Moreau et al. 2011) *and M. minisporus* (Cázares et al., 2008), are similar and related to *M. diqingensis* in morphology and phylogeny. Their color of basidiomata are similar, such as *M. subglobosporus* (rust brown to deep brown basidiomata), *M. natsii* (yellow-brown basidiomata), *M. spinisporus* (grayish brown to light brown basidiomata) and *M. minisporus* (bright gold-yellow basidiomata), but all of them without scaled, lobed or concave basidiomata, by which they were easily

differentiated from *M. diqingensis*. *M. rivularis* (anthracite-black gleba), and *M. luteus* (club-shaped or cylindro-elliptical to cylindrical basidiospores) were easily differentiation from *M. diqingensis.* It appears that the thickness of the peridium (within the scope of 300 μm) is similar among *M. subglobosporus*, *M. ovoidisporus*, and *M. coccoloba*, However, the sizes of basidiospores provide a clear distinction between these species (*M. subglobosporus* 8–11 × 7–9 μm, *M. ovoidisporus* 5–7 × 3.5–5.8 μm and *M. coccoloba* 6.2–12 ×5.2–10 μm). Phylogenetically, *M. diqingensis* and *M. subglobosporus* occupied an independent and strongly supported clade (BS = 78%, PP = 1.0) (figure 3.8), but *M. diqingensis* shared less than 93.2 % ITS similarity with *M. subglobisporus*, supporting *M. diqingensis* was a distinct species. It was classified into the *Rivulares* section primarily based on morphological characteristics using OPLS-DA.

Melanogaster truncatisporus T. J. Yuan, Shu H. Li, & Raspé, sp. nov. (Figure 3.9 i-l)

MycoBank: MB901870

Diagnosis: *Melanogaster truncatisporus* is characterized by its distinctive pale yellow to deeply orange-yellow peridium. The basidiomata are sized 1.5–3.0 × 0.4–2.3 cm and exhibit a subglobose to ellipsoidal shape. The basidiospores are subglobose to globose or irregularly elongate-pyriform, 3.5–9.5 × 3.0–7.0 μm, with a truncate morphology.

Etymology: "*truncatisporus*" refers to the truncate basidiospores.

Holotype: CHINA. Yunnan Province: Nujiang Autonomous Prefecture, Lanping County, Zhongpai township, Xinchangping village, 26°54'15" N, 99°10'32" E, elevation 1990 m, in mainly brown soils under *Castanea mollissima* Bl. and *Pinus yunnanensis* Franch., 26 Oct. 2020, collected by T. J. Yuan KUN-HKAS129199, holotype; YAAS-TJ87, isotype).

Description: *Basidiomata*, 1.5–3.0 × 0.4–2.3 cm, hypogeous or semi-hypogeous, subglobose to oval, occasionally irregular-elongated, yellowish when young, reddish-brown to dark brown at maturity, smooth or slightly velvety surface of the basidiomata, lobed or indented at the base, attached mycelial strands, occasionally extending to the surface, dark brown, rhizomorphs not distinct (Figure 3.9 i). *Peridium* two-layered, outer

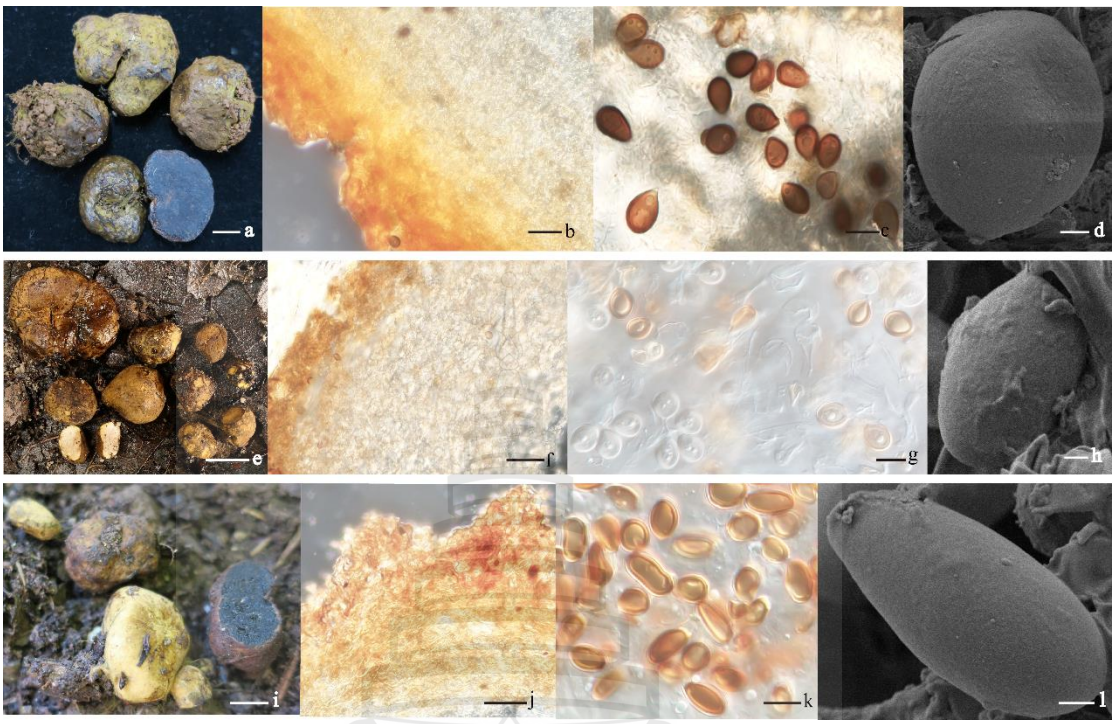
layer 50–100 μm thick, composed of interwoven hyphae, orange-yellow, with clamp connections, and fusoid to cylindrical terminal cells, 4–5 μm broad. Inner layer 150–350 μm thick, composed of interwoven hyphae, 3–5 μm broad, pale yellow, intermixed with massive inflated cells, ellipsoidal or irregular, 3–20 μm in diam. Trama plates of hyaline or yellowish gelatinized hyphae (Figure 3.9 j). *Gleba* solid, pale brown when young, blackish brown to black at maturity, separated by white or pale yellow trama when young, which becomes deep brown at maturity, hard when dried; locules 2–4 mm in diameter, polygonal to irregular (Figure 3.9 k). *Basidia* poorly recovered, hyaline, 4–spored, occurring randomly in the locules (Figure 3.9 k). *Basidiospores* subglobose to globose or irregularly elongate-pyriform, 3.5–9.5 × 3.0–7.0 μm ($L_m \times W_m = 7.0 \pm 2.5 \times 4.5 \pm 2.0$, $Q = 1.0–2.5$, $Q_m = 1.5 \pm 1.0$, n = 65), hyaline when immature, becoming dark brown at maturity, smooth, with truncate-cupped base and short hilar appendage,1–2 μm in diam in optical microscopy (Figure 3.9 l).

Habitat, phenology, and distribution: hypogeous to semi-hypogeous under *Castanea mollissima* Bl. and *Pinus yunnanensis* Franch., in mixed forest, in late autumn. So far found in Lanping and Gongshan counties, Yunnan Province, China.

Other material examined: China. Yunnan Province: Nujiang autonomous Prefecture, Lanping County, 26°54’17”N, 99°10’31”E, elevation 2,029.32 m, in mainly brown soils under *Castanea mollissima* Bl. and *Pinus yunnanensis* Franch., 26 Oct. 2020, collected by T. J. Yuan (YAAS TJ83 and YAAS TJ109); China. Yunnan Province: Nujiang Autonomous Prefecture, Gongshan County, 28°1’19”N, 98°37’2”E, elevation 1800 m, in mainly brown soils under *Castanea mollissima* Bl. and *Pinus yunnanensis* Franch., 25 Sep. 2020, collected by Li, S. H. (YAAS L5346).

Notes: *Melanogaster truncatisporus* was diagnosed by the combination of middle sized reddish-brown to dark brown basidiomata, orange-yellow peridium, and size of basidiospores. The four *Melanogaster* species, *M. minisporus* (Cázares et al., 2008), *M. broomeanus* Berk (Uzun et al., 2014; Türkoğlu and Castellano, 2013), *M. obovatisporus* (Liu and Tao, 1989), and *M. variegatus* (Halász, 2008), are similar and related to *M.*

truncatisporus in morphology and phylogeny. *M. truncatisporus* can be easily differentiated by its peridium thickness (*M. truncatisporus*, 200–450 μm vs *M. minisporus*, 160–240 μm) and its size of basidiospores (*M. truncatisporus*, 3.5–9.5 × 3.0–7.0 μm vs *M. minisporus*, 5–6.5 × 3–5 μm). Notable distinctions exist between the peridium layers of *M. truncatisporus* by two layers, and *M. broomeanus* (single layer). The disparity in basidiospore size is evident, with *M. truncatisporus* ranging (3.5–9.5 × 3.0–7.0 μm), while *M. broomeanus* exhibits spores measuring 7–9 × 4 μm. A distinctive contrast is evident in the spore count within the basidia, with *M. truncatisporus* typically presenting 4 spores, whereas *M. obovatisporus* consistently exhibits 8 spores. A significant difference arises in the size of basidiospores, with *M. variegatus* measuring 7.5–10 × 5.5–8 μm. Phylogenetically, the specimens of *M. truncatisporus* clustered in an independent clade with strong support (BS = 100%, PP = 1.0) (Figure 3.8), supporting it was a new species. Additionally, DNA analysis revealed *M. truncatisporus* (holotype: ON427479) shared less than 93.2 % ITS similarity with other *Melanogaster* species. It was classified into the *Variegati* section primarily based on morphological characteristics using OPLS-DA.



Note a. *Melanogaster cyaneus* (YAAS-Tj75-1, holotype). Basidioma. b. LM of Peridium. c. LM of basidiospores. d. SEM of basidiospore. Melanogaster diqingensis (YAAS-WXH_9068, holotype). e. Basidiomata. f. LM of Peridium. g. LM of basidiospores. h. SEM of basidiospore. *Melanogaster truncatisporus* (YAAS-TJ87, holotype). i. Basidioma. j. LM of peridium. k. LM of basidiospores. l. SEM of ascospore. Scale bars: a, e, i= 2 cm; b, f, g = 20 μm; c, g, k = 10 μm; d, h, l = 1 μm

Figure 3.9 Photographs of *Melanogaster* species

3.3.3 Subdivision of the Genus Melanogaster in Sections based on Morphology

The main characters to identify *Melanogaster* species are the number of layers of the peridium and thickness of the peridium, average length and width of basidiospores (Table 3.5). A discriminant analysis based on five variables, namely the number of layers of the peridium, the minimum and maximum thickness of the peridium, and the length and width of basidiospores, was performed by OPLS-DA (Figure 3.10). In this analysis, the three sections, *Melanogaster*, *Variegati*, and *Rivulares*, were separated in the 3D principal

component space by the average length and average width of basidiospores, and the minimum thickness of the peridium. The cumulative contribution of the first three principal components exceeded 80.5%. The primary factors determining the distribution of species in the 3-dimensional space are the average length and width of spores. The three new species (*M. cyaneus, M. diqingensis,* and *M. truncatisporus*) were placed into the section *Melanogaster*, *Rivulares*, and *Variegati* by OPLS-DA, respectively.

Table 3.5 The main morphological characterization of *Melanogaster* species

Species	Peridium			Basidiospores		Country
	layers	Min. (µm)	Max. (µm)	L_m (µm)	W_m (µm)	
M. quercicola	2	450	600	13.1	6.5	China
M. utriculatus	2	300	400	13	9	Japan
M. fusisporus	2	250	420	12.3	5.2	China
M. shanxiensis	2	180	420	12.2	6.1	China
M. obovatus	2	350	600	12.2	6	China
M. macrosporus	1	85	315	11.5	5.7	Hungary
M. panzhihuaensis	1	150	220	10.4	6.1	China
M. natsii	2	200	250	10	6	China
M. coccolobae	2	170	230	9.9	7.5	Mexico
M. subglobisorus	2	130	300	9.8	7	China
M. spinisporus	1	360	750	9.6	7.3	China
M. cyaneus	2	100	400	9.5	7	China
M. tomentellus	1	250	350	9.4	4.5	China
M. ovoidisporus	2	250	450	7.1	4.3	China
M. truncatisporus	2	200	450	7	4.5	China
M. minobovatus	2	350	500	6.1	4.7	China
M. broomeanus	1	150	400	6	3.9	China
M. luteus	2	100	250	6	2.75	France, Montenegro
M. minysporus	1	160	240	5.5	4	Mexico
M. rivularis	2	100	135	5.5	2.9	France
M. diqingensis	2	100	320	3.8	3.2	China

Notes The new species introduced in this study are presented in bold.

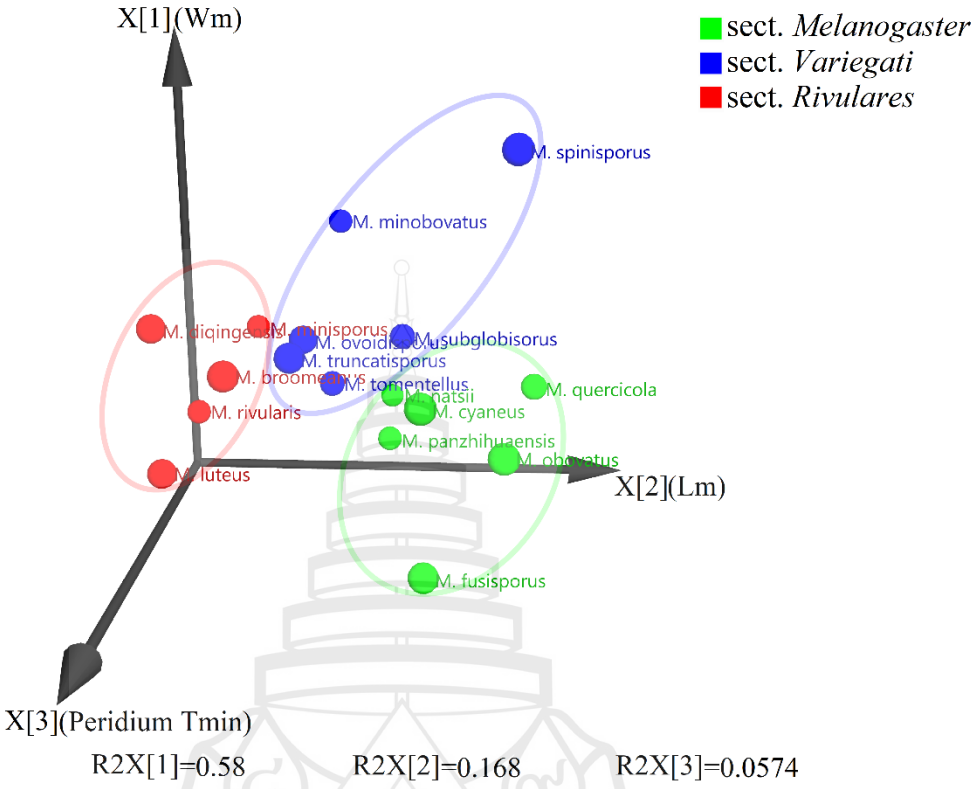


Figure 3.10 The discrimination result of three sections of Chinese species based on Its main characteristic by OPLS-DA

3.3.4 Key to the Melanogaster Species from China

1a. Basidiospores verrucose……2

1b. Basidiospores smooth……3

2a. Basidiomata brown to deep brown, peridium 250–350 µm thick, surface minutely green tomentose; basidiospores elongate fusiform……*M. tomentellus*

2b. Basidiomata light brown with some red-brown or brick red when fresh, peridium 360–750 µm thick, basidiospores ellipsoid to obovoid, subglobose……*M. spinisporus*

3a. Basidiospores light yellow or yellow……4

3b. Basidiospores brown to dark brown or reddish brown……5

4a. Basidiomata brick red with black green or dark green gleba at maturity……
……*M. obovatus*

4b. Basidiomata red brown to brown with yellow green gleba at maturity……...
……...……*M. quercicola*

5a. Basidiospores mostly longer than 10 µm……6

5b. Basidiospores mostly shorter than 10 µm……7

6a. Basidiomata yellow-brown to brown, gleba brown, basidiospores fusiform……
……*M. fusisporus*

6b. Basidiomata brown to rust-brown, gleba brownish, basidiospores long obovoid……
……*M. shanxiensis*

6c. Basidiomata light brown to yellowish-brown, gleba bluish, basidiospores subglobose to globose……***M. cyaneus***

6d. Basidiomata yellow-brown, gleba brown to dark, basidiospores limoniform or ellipsoid……*M. natsii*

7a. Basidiospores oblong to cylindrical……*M. broomeanus*

7b. Basidiospores obovate or obovate to subglobose……8

7c. Basidiospores subglobose to globose……9

8a. Basidiospores red brown, 8.7–12.4 × 5.2-7.6 µm……*M. panzhihuaensis*

8b. Basidiospores dark brown to brownish, 6.5–8 × 3.8–4.7 µm……*M. obovatisporus*

8c. Basidiospores yellowish-brown to brown, 8.7–10.6 × 6.6–8.0 µm……
……*M. subglobisporus*

8d. Basidiospores dark brown, 5.1–6.9 × 4.2–5.1 µm……*M. minobovatus*

9a. Basidiomata reddish brown to dark brown, gleba brownish-black or black, basidiospore 3.5–9.5 × 3.0–7.0 µm……..……***M. truncatisporus***

9b. Basidiomata pale yellow to orange, gleba pale yellow, basidiospore 3.0–5.1 × 2.0–4.0 µm
……***M. diqingensis***

3.4 Identification of Wild Edible Boletes

3.4.1 Identification of Species and Extraction of Ecological Environmental Factors

A total of 509 individuals of boletes with high economic and nutritional value were collected from Yunnan and Sichuan provinces in Southwest China (Figure 3.11). According to traditional methods, 11 species belonging to 9 genera were identified by their morphological characteristics and phylogenetic relationships after sample collection (Figure 3.12 and appendix Table A1 and A2). The results of the topologies of phylogenetic analyses including the ML tree and BI tree are consistent with the report by Wu et al. (2016). The collection sites showed conspicuous ecological diversity including typical subtropical, temperate and plateau climatic zones, with elevations ranging from 553 to 3283 m, which are hot spot regions of biodiversity (appendix Table B). There is much interest in studying fungi in these regions and revealing the relationships between chemical information, their phylogenetic signals and ecological environmental factors (Feng & Yang, 2018).

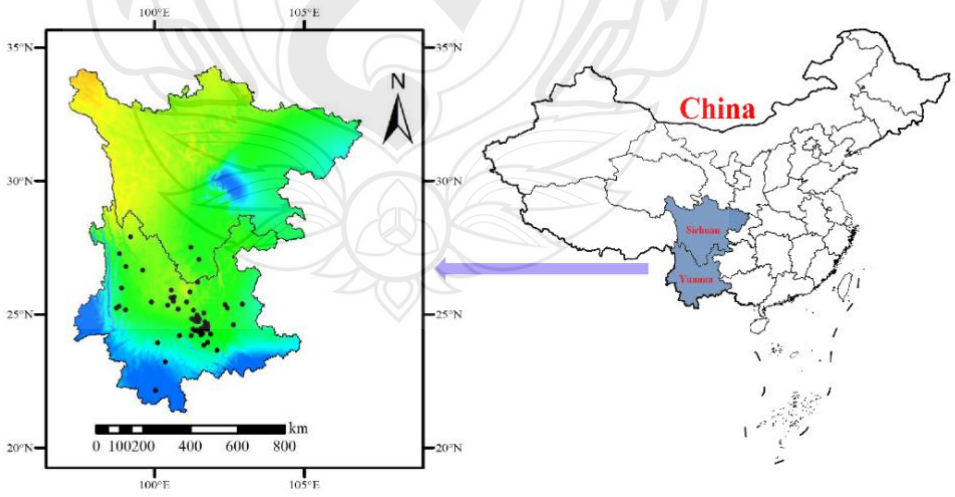
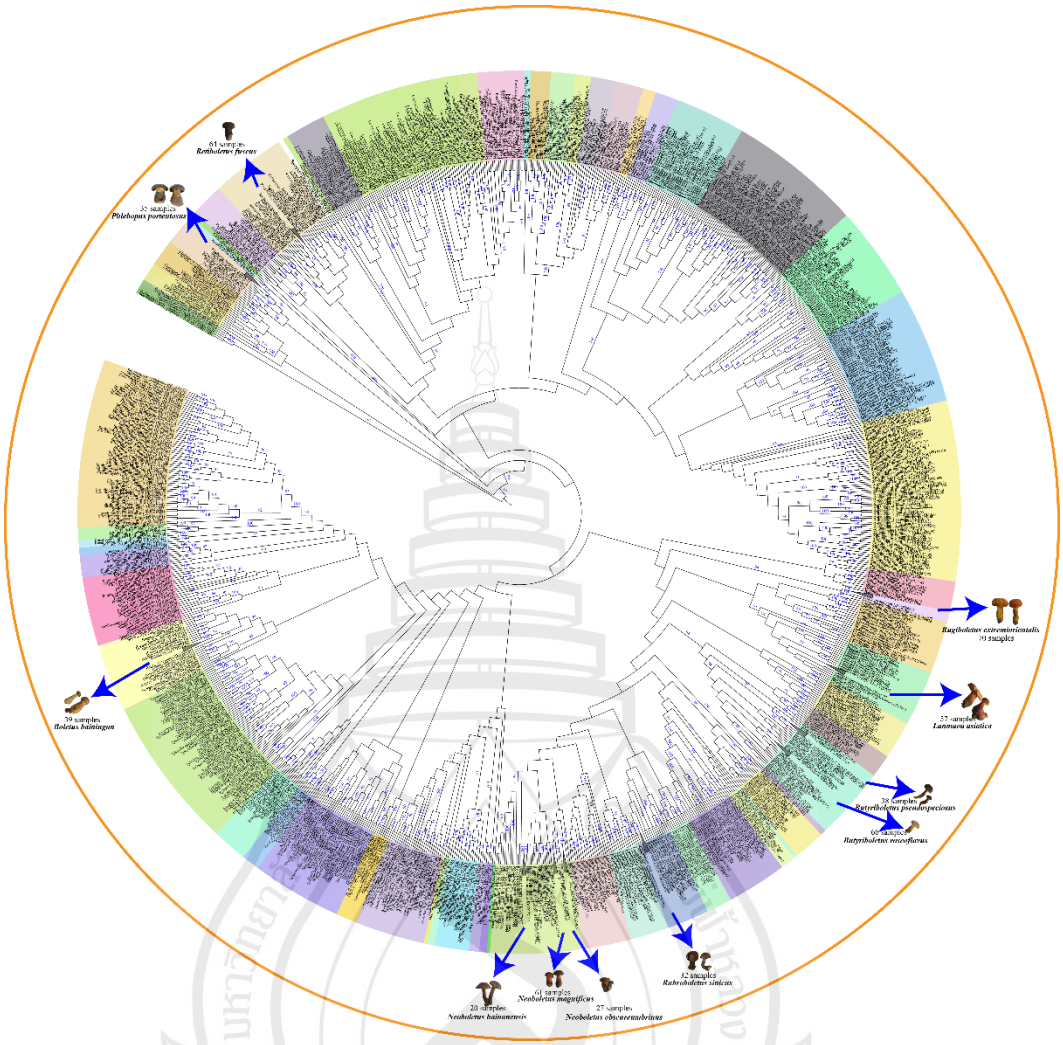


Figure 3.11 The 110 collection sites of 11 species of boletes



Note Marked in red are samples with an ML bootstrap support value greater than 95%

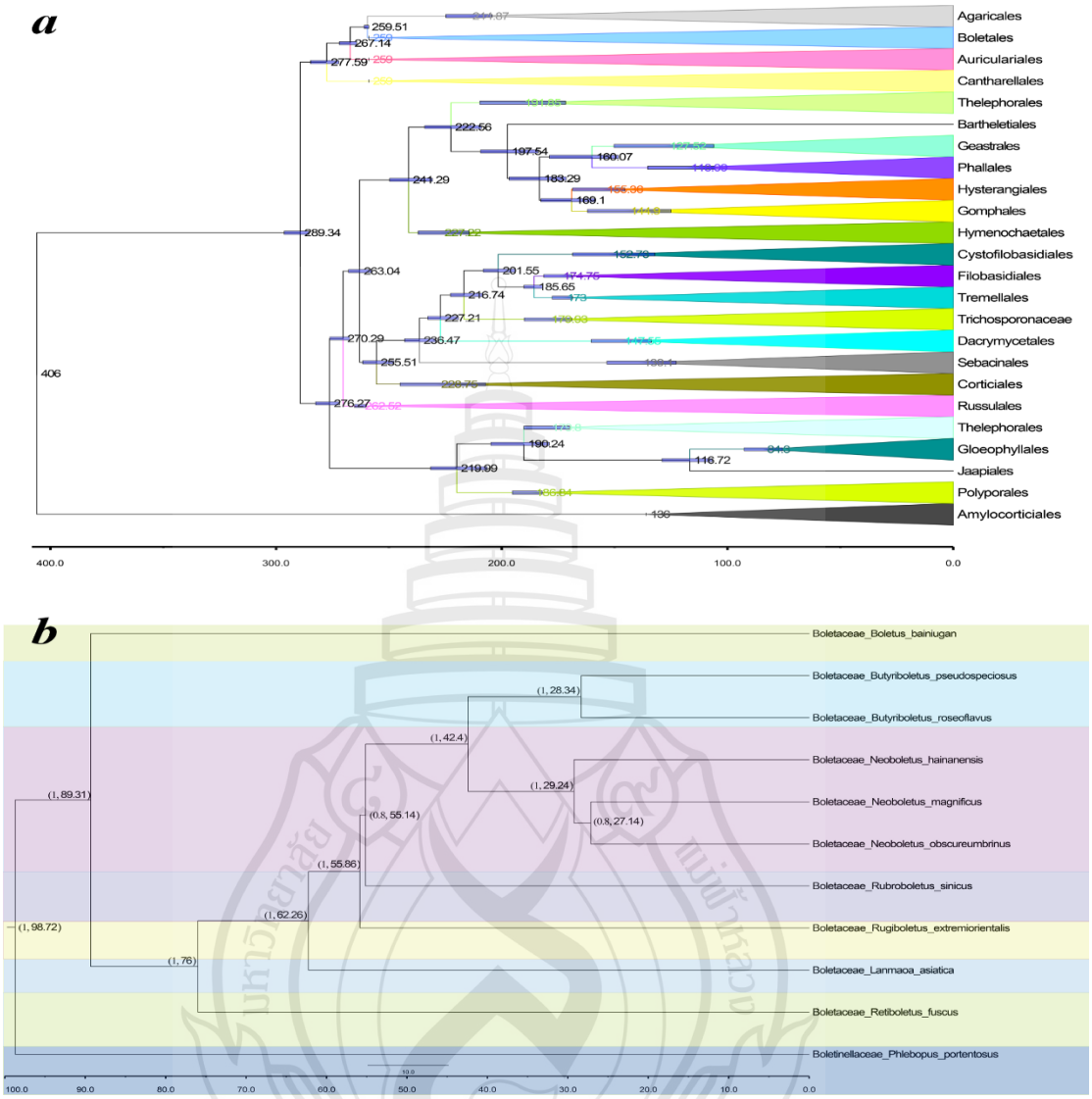
Figure 3.12 Maximum likelihood phylogenetic trees of 11 species of boletes

3.4.2 The Phylogeny and Divergence Time Analyses of Agaricomycotina

In the phylogenetic analyses of Agaricomycotina, a comprehensive dataset of 497 species from Agaricomycotina, along with six outgroup species from Pucciniomycotina, was utilized. These species were classified into three classes, 12 orders, 62 families, and 246 genera. Figure 3.13a illustrates the backbone-constrained tree at the order level, while appendix Figure D provides a more detailed view of the family and genus levels. Generally, orders and higher taxa, including Agaricomycetes, received strong support (appendix

Figure D). However, the suborders Auriculariales, Geastrales, and Atheliales did not attain statistical support. The phylogenetic relationships within the main clades of Boletales are in accordance with the findings of Binder & Hibbett (2006) and He (2019), who established these relationships based on a five-genes dataset. In Boletaceae, the subfamily Zangiodeae, represented by Zangia and Harrya, is identified and statistically supported, aligning with the observations reported by Wu, Zheng et al. (2014). Well-supported taxa were dated and indicated an estimated divergence time for Agaricomycotina at 419 million years ago (Mya), which was consistent with He (2019). The divergence times for individual orders ranged from 168 to 342 Mya (Table 3.6).

Further analyses involving 11 specific species, including *Boletus bainiugan* (BoB), *Butyriboletus pseudospeciosus* (BuP), *Butyriboletus roseoflavus* (BuR), *Lanmaoa asiatica* (LA), *Neoboletus obscureumbrinus* (NO), *Rugiboletus extremiorientalis* (RugE), *Rubroboletus sinicus* (RubS), *Retiboletus fuscus* (RetF), *Phlebopus portentosus* (PP), *Neoboletus hainanensis* (NH), and *Neoboletus magnificus* (NM), focused on phylogeny and divergence time. The estimated divergence time for these 11 species ranged from 53.43 to 121.2 Mya (Figure 3.13 b).



Note (a) Maximum clade credibility tree showing the relationships among orders of Agaricomycotina based on ITS, LSU, RPB1, RPB2 and TEF1. (b) the phylogeny and divergence time of 11 specific species

Figure 3.13 Maximum clade credibility tree of Agaricomycotina and 11 species based on ITS, LSU, RPB1, RPB2 and TEF1 genes

Table 3.6 Estimation of divergence time of Basidiomycota

Oder	Families recognized in this study	Genus recognized in this study	Mean of stem age in MCC tree (Mya)	Oder	Families recognized in this study	Genus recognized in this study	Mean of stem age in MCC tree (Mya)
		Stephanospora	81.57		Meruliaceae		114.27
	Tricholomataceae		114.86			Aurantiporus	22.8
		Corneriella	43.3			Ceriporiopsis	22.8
		Dennisiomyces	43.3			Climacodon	86.49
		Hemimycena	101.36			Crustodontia	48.43
		Leucopaxillus	101.36			Hydnophlebia	99.32
		Omphalina	62.14			Phlebia	85.97
		Porpoloma	43.3			Sarcodontia	48.43
		Pseudobaeospora	67.88			Scopuloides	86.49
		Resupinatus	114.86		Panaceae		108.14
		Tricholoma	68.77			Cymatoderma	61.5
	Tubariaceae		73.79			Panus	61.5
		Flammulaster	53.97		Phaeolaceae		123.97
		Pachylepyrium	42.46			Wolfiporia	123.97
		Tubaria	53.97		Phanerochaetaceae		112.61
Amylocorticiales	Amylocorticiaceae		406			Bjerkandera	112.61
		Podoserpula	136			Crepatura	42.97
		Serpulomyces	136			Donkia	64.94

Table 3.6 (continued)

Oder	Families recognized in this study	Genus recognized in this study	Mean of stem age in MCC tree (Mya)	Oder	Families recognized in this study	Genus recognized in this study	Mean of stem age in MCC tree (Mya)
Atheliales	Aporpiaceae		191.85			Hapalopilus	85.43
		Aporpium	191.85			Hyphodermella	42.97
	Atheliaceae		179.8			Phanerochaete	53.81
		Amphinema	179.8			Phanerodontia	53.81
		Piloderma	136.14			Rhizochaete	85.43
Auriculariales	Auriculariaceae		259			Roseograndinia	55.86
		Auricularia	83.33		Piptoporellaceae		116.36
		Tremellochaete	57.37			Piptoporellus	116.36
	Exidiaceae		83.33		podoscyphaceae		99.24
		Adustochaete	25.88			Abortiporus	55.63
		Eichleriella	25.88			Podoscypha	55.63
		Exidia	33.89		Polyporaceae		158.86
		Exidiopsis	45.14			Abundisporus	64.49
Bartheletiales	Bartheletiaceae		127.78			Amauroderma	66.21
		Bartheletia	127.78			Cerioporus	60.99

Table 3.6 (continued)

Oder	Families recognized in this study	Genus recognized in this study	Mean of stem age in MCC tree (Mya)	Oder	Families recognized in this study	Genus recognized in this study	Mean of stem age in MCC tree (Mya)
Boletales	Astraeaceae		80.8			Coriolopsis	94.1
		Astraeus	80.8			Crassisporus	86.57
	Boletaceae		131.41			Cryptoporus	75.38
		Austroboletus	88.47			Daedaleopsis	60.16
		Afroboletus	73.76			Datroniella	79.98
		Boletus	89.1			Dentocorticium	95.6
		Retiboletus	76.68			Earliella	83.9
		Butyriboletus	38.64			Favolus	87.18
		Rubroboletus	56.9			Fomes	98.03
		Strobilomyces	73.76			Fomitella	21.93
		Tylopilus	75.47			Funalia	21.93
		Xerocomellus	30.03			Ganoderma	66.82
		Buchwaldoboletus	67.09			Grammothele	81.93
		Chalciporus	67.09			Grammothelopsis	66.21
		Lanmaoa	62.78			Haploporus	75.38
		Leccinellum	37.37			Hexagonia	73.04
		Leccinum	37.37			Jorgewrightia	66.82
		Retiboletus	76.68			Lenzites	146.7
		Spongiforma	75.47			Lignosus	60.16
		Aureoboletus	63.81			Lopharia	95.6

Table 3.6 (continued)

Oder	Families recognized in this study	Genus recognized in this study	Mean of stem age in MCC tree (Mya)	Oder	Families recognized in this study	Genus recognized in this study	Mean of stem age in MCC tree (Mya)
		Boletellus	67.74			Mariorajchenbergia	62.62
		Corneroboletus	66.6			Megasporoporia	64.49
		Phylloporus	30.03			Megasporoporiella	87.18
		Pulchroboletus	44.7			Melanoderma	105.36
		Veloboletus	74.53			Microporus	68.28
		Xerocomus	88.47			Neodatronia	60.99
		Harrya	38.46			Neofavolus	126.48
		Zangia	38.46			Neofomitella	68.67
		Bothia	96.17			Perenniporia	54.36
		Hongoboletus	58.92			Perenniporiella	81.95
		Neoboletus	44.64			Picipes	102.11
		Rugiboletus	53.63			Polyporus	72.66
	Boletinellaceae		98.55			Porogramme	88.87
		Phlebopus	77.47			Pseudofavolus	72.66
		Boletinellus	77.47			Pycnoporus	129.31
	Calostomataceae		113.42			Sanguinoderma	56.93
		Calostoma	113.42			Sparsitubus	56.93
	Coniophoraceae		172.17			Tomophagus	54.36
		Coniophora	172.17			Trametes	68.67
		Gyrodontium	133.83			Vanderbylia	70.83

Table 3.6 (continued)

Oder	Families recognized in this study	Genus recognized in this study	Mean of stem age in MCC tree (Mya)	Oder	Families recognized in this study	Genus recognized in this study	Mean of stem age in MCC tree (Mya)
		Penttilamyces	139.58		Postiaceae		96.32
	Diplocystaceae		80.08			Amaropostia	77.56
		Diplocystis	20.99			Aurantipostia	60.73
	Gomphidiaceae		111.87			Austropostia	60.73
		Chroogomphus	74.48			Cyanosporus	74.85
		Gomphidius	74.48			Oligoporus	70.75
	Gyroporaceae		113.42			Osteina	96.62
		Gyroporus	113.42			Postia	74.85
	Hygrophoropsidaceae		126.77		Sparassidaceae		88.71
		Hygrophoropsis	126.77			Sparassis	88.71
	Melanogastraceae		75.12		Steccherinaceae		97.96
		Alpova	45.22			Antrodiella	49.27
		Corditubera	75.12			Cabalodontia	2.49
		Melanogaster	45.22			Loweomyces	74.48
	Paxillaceae		77.47			Steccherinum	2.49
		Gyrodon	49.6		Taiwanofungaceae		96.89
		Paragyrodon	49.6			Taiwanofungus	44.31
		Hydnomerulius	77.47			Taiwanofungus	44.31
		Paxillus	45.22	Russulales	Albatrellaceae		91.76
	Pisolithaceae		101.55			Albatrellopsis	91.76

Table 3.6 (continued)

Oder	Families recognized in this study	Genus recognized in this study	Mean of stem age in MCC tree (Mya)	Oder	Families recognized in this study	Genus recognized in this study	Mean of stem age in MCC tree (Mya)
		Pisolithus	101.55		Auriscalpiaceae		143.49
	Sclerodermataceae		80.8			Artomyces	143.49
		Scleroderma	75.12			Auriscalpium	143.49
		Tremellogaster	20.99		Bondarzewiaceae		133.81
	Serpulaceae		126.77			Bondarzewia	123.62
		Austropaxillus	126.77			Heterobasidion	123.62
		Serpula	126.77			Lauriliella	35.73
	Suillaceae		90.23		Echinodontiaceae		109.99
		Psiloboletinus	69.86			Echinodontiellum	35.91
		Suillus	90.23			Echinodontium	35.91
	Tapinellineae		106.4		Hericiaceae		109.99
		Bondarcevomyces	83.35			Hericium	109.99
		Pseudomerulius	106.4			Pseudowrightoporia	81.39
		Tapinella	83.35			Wrightoporiopsis	81.39
	Truncocolumellaceae		69.86		Lachnocladiaceae		225.18
		Truncocolumella	69.86			Lachnocladium	225.18
Cantharellales	Botryobasidiaceae		127.78		Russulaceae		132.55
		Botryobasidium	127.78			Lactarius	114.15
	Cantharellaceae		174.54			Lactifluus	117.2
		Cantharellus	69.54			Multifurca	114.15

Table 3.6 (continued)

Oder	Families recognized in this study	Genus recognized in this study	Mean of stem age in MCC tree (Mya)	Oder	Families recognized in this study	Genus recognized in this study	Mean of stem age in MCC tree (Mya)
		Craterellus	69.54			Russula	117.2
		Neoburgoa	59.07		Stereaceae		96.32
	Ceratobasidiaceae		215.46			Acanthobasidium	80.01
		Rhizoctonia	215.46			Acanthophysium	43.25
	Hydnaceae		80.81			Conferticium	43.25
		Clavulina	46.07			Neoaleurodiscus	96.32
		Hydnum	59.07			Stereodiscus	65.76
		Minimedusa	80.81		Terrestriporiaceae		91.76
	Tulasnellaceae		234.29			Terrestriporia	91.76
		Tulasnella	234.29		Wrightoporiaceae		225.18
Corticiales	Corticiaceae		262.59			Amylosporus	225.18
		Acanthophysellum	262.59	Sebacinales	Sebacinaceae		139.1
		Laetisaria	161.79			Ditangium	29.38
		Marchandiomyces	161.79			Paulisebacina	139.1
	Dendrominiaceae		228.75			Tremelloscypha	7.73
		Dendrominia	228.75		Serendipitaceae		65.75
	Punctulariaceae		95.52			Serendipita	65.75
		Dendrocorticiopsis	42.89	Thelephorales	Bankeraceae		93.91
		Punctularia	75.66			Bankera	26.78
		Punctulariopsis	42.89			Boletopsis	93.91

Table 3.6 (continued)

Oder	Families recognized in this study	Genus recognized in this study	Mean of stem age in MCC tree (Mya)	Oder	Families recognized in this study	Genus recognized in this study	Mean of stem age in MCC tree (Mya)
	Vuilleminiaceae		95.52			Phellodon	47.68
		Cytidia	63.53		Thelephoraceae		151.16
		Vuilleminia	63.53			Amaurodon	72.1
Cystofilobasidiales	Mrakiaceae		119.47			Hydnellum	66
		Itersonilia	100.53			Lenzitopsis	41.99
		Mrakia	70.68			Polyozellus	41.99
		Tausonia	70.68			Thelephora	28.32
		Udeniomyces	92.94			Tomentella	28.32
	Cystofilobasidiaceae		119.47		Hydnodontaceae		227.22
		Cystofilobasidium	119.47			Dextrinocystis	118.88
Dacrymycetales	Cerinomycetaceae		84.99			Litschauerella	227.22
		Cerinomyces	84.99			Porpomyces	84.27
	Dacrymycetaceae		147.55			Scytinopogon	84.27
		Calocera	84.51	Tremellales	Bulleraceae		148.4
		Dacrymyces	30.68			Bullera	66.53
		Dacryopinax	68.53			Fonsecazyma	98.99
		Ditiola	61.74			Genolevuria	46.21
		Guepiniopsis	51.84			Pseudotremella	94.12
		Dacryonaema	38.65		Bulleribasidiaceae		132.92
		Dendrodacrys	60.03			Bulleribasidium	46.73

Table 3.6 (continued)

Oder	Families recognized in this study	Genus recognized in this study	Mean of stem age in MCC tree (Mya)	Oder	Families recognized in this study	Genus recognized in this study	Mean of stem age in MCC tree (Mya)
		Femsjonia	61.74			Derxomyces	46.73
		Unilacryma	98.14			Dioszegia	46.21
Filobasidiales	Piskurozymaceae		115.34			Hannaella	132.92
		Piskurozyma	47.51			Vishniacozyma	78.91
		Solicoccozyma	115.34		Carcinomycetaceae		93.79
	Filobasidiaceae		135.55			Carcinomyces	93.79
		Filobasidium	108.19		Cryptococcaceae		148.4
		Goffeauzyma	80.32			Cryptococcus	49.73
		Heterocephalacria	56.98			Kwoniella	66.53
		Zyzygomyces	94.42			Teunia	77.73
Hymenochaetales	Hirschioporaceae		129.67		Naemateliaceae		93.79
		Pallidohirschioporus	109.96			Dimennazyma	42.42
		Perennihirschioporus	109.96			Naematelia	42.42
	Hymenochaetaceae		176.32		Phaeotremellaceae		78.91
		Arambarria	86.19			Gelidatrema	48.2
		Cyclomyces	44.16			Phaeotremella	48.2
		Fomitiporella	126.11		Rhynchogastremaceae		98.99
		Fomitiporia	86.19			Bandoniozyma	89.47
		Fulvifomes	97.59			Papiliotrema	62.76
		Fuscoporia	127.81			Rhynchogastrema	62.76

Table 3.6 (continued)

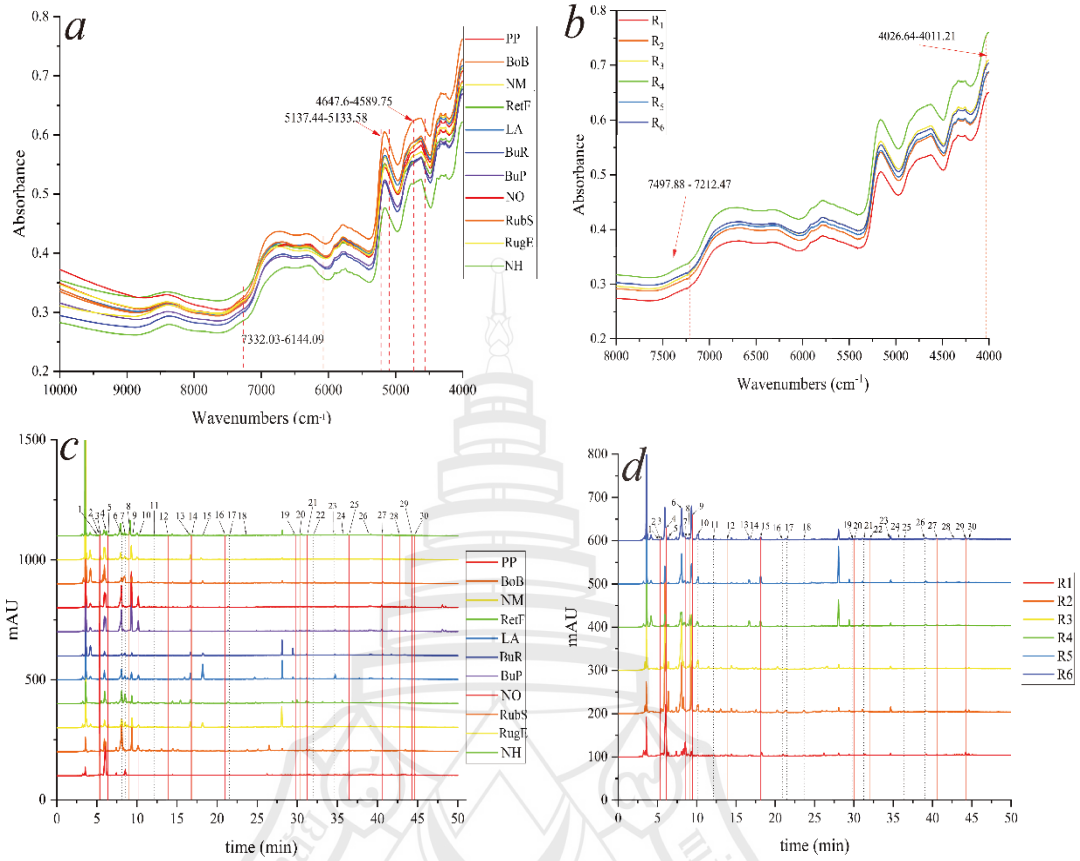
Oder	Families recognized in this study	Genus recognized in this study	Mean of stem age in MCC tree (Mya)	Oder	Families recognized in this study	Genus recognized in this study	Mean of stem age in MCC tree (Mya)
		Hydnochaete	44.16		Sirobasidiaceae		94.12
		Inocutis	81.24			Fibulobasidium	50.95
		Inonotus	25.98			Sirobasidium	50.95
		Neomensularia	97.59		Syzygosporaceae		94.42
		Nothophellinus	127.81			Syzygospora	94.42
		Onnia	76.09		Tetragoniomycetaceae		124.55
		Phellinopsis	104.64			Bandonia	124.55
		Phellinotus	81.24			Cryptotrichosporon	36.2
		Phellinus	154.7			Takashimella	64.98
		Phylloporia	87.27			Tetragoniomyces	36.2
		Porodaedalea	76.09		Tremellaceae		142.81
		Pseudoinonotus	147.46			Biatoropsis	77.73
		Sanghuangporus	60.76			Tremella	142.81
		Tropicoporus	25.98	Trichosporonales	Trichosporonaceae		75.89
	Rickenellaceae		116.06			Aegeritella	10.87
		Cantharellopsis	116.06			Apiotrichum	48.19
		Rickenella	116.06			Cutaneotrichosporon	48.19
	Schizoporaceae		162.89			Haglerozyma	49.27
		Hyphodontia	65.2			Pascua	10.87
		Kneiffiella	144.74			Prillingera	49.73

Table 3.6 (continued)

Oder	Families recognized in this study	Genus recognized in this study	Mean of stem age in MCC tree (Mya)	Oder	Families recognized in this study	Genus recognized in this study	Mean of stem age in MCC tree (Mya)
		Oxyporus	162.89	Erythrobasidiales	Erythrobasidiaceae		127.37
		Schizopora	63.28			Cyrenella	127.37
		Xylodon	63.28			Bannoa	97.46
	Trichaptaceae		162.89			Erythrobasidium	112.65
		Trichaptum	162.89	Cystobasidiales	Microsporomycetaceae		179.93
Gloeophyllales	Gloeophyllaceae		116.72			Microsporomyces	179.93
		Gloeophyllum	84.3	Sakaguchia	Sakaguchiaceae		97.46
		Neolentinus	84.3			Sakaguchia	97.46

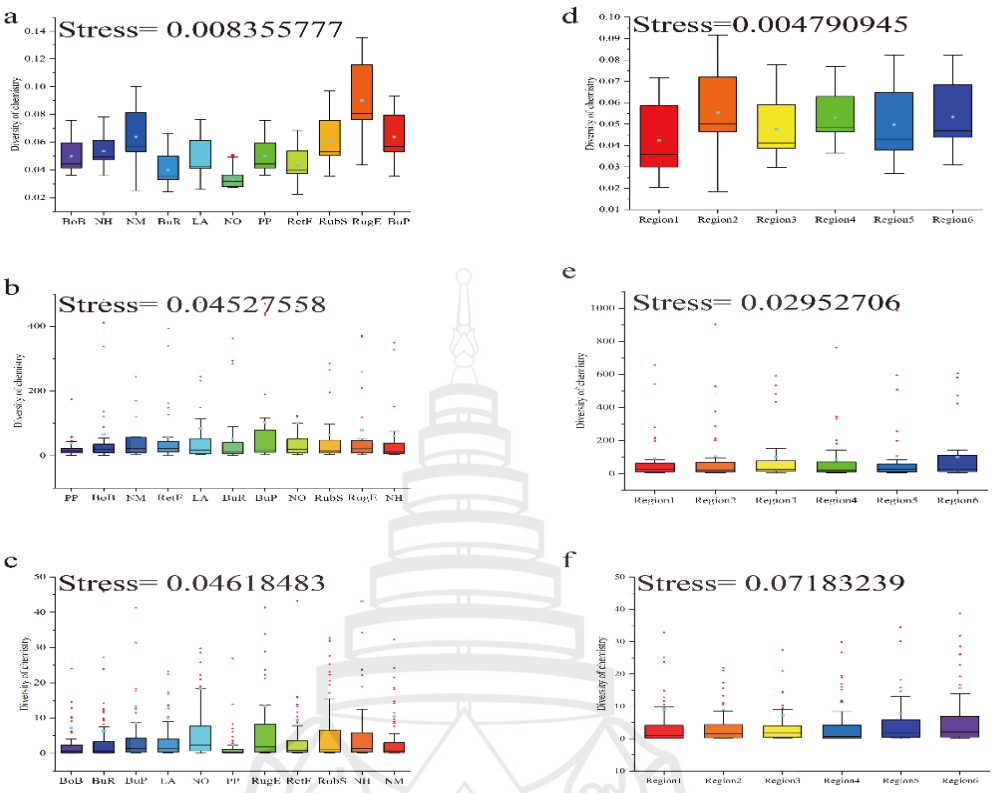
3.4.3 Ubiquitous Chemodiversity Related to Both Species and Ecological Environmental Factors

The chemical information diversity including NIR spectra, HPLC fingerprints and volatile constituents was analyzed by the standard deviation (STDEV) of species and regions, of which the different regions were identified by unsupervised pattern recognition of their ecological environmental factors (Figure 3.14a-d and appendix Tables E1, 2 and 3). Additionally, chemodiversity was calculated by using the Bray–Curtis chemical similarity distance of species and regions (Figure 3.15, appendix Table F1, 2 and 3 and appendix Table G1, 2 and 3). The chemical information demonstrated the distribution of heterogeneity not only in species (Figure 3.15a-c), but also in different regions (Figure 3.15d-f). The mean distances of the species were 0.3076 for spectra, 0.3561 for HPLC fingerprints, and 0.3259 for volatile constituents. The average distances of different regions were 0.0485 for the spectra, 0.1715 for the HPLC fingerprint, and 0.2026 for volatile constituents (appendix Table G1, 2 and 3**)**. The indices of chemical information diversity showed that the diversity of the spectrum (stress < 0.0084) was more reliable than fingerprints of HPLC (stress < 0.0453) and GC–MS volatile constituents (stress < 0.0462) in the species and for the regions. The results were consistent with previous reports that chemodiversity is a ubiquitous phenomenon that exists not only between plant families but also within one genus or species or even within one individual specimen (Feng and Yang, 2018; Salazar et al., 2018).



Note (a) The average spectra of 11 species and the bands selected are related to phylogeny. (b) The average spectra of the 6 producing areas and the bands screened were related to ecological environmental factors. (c) Chromatographic fingerprints of 11 species, with solid lines indicating common peaks that were significantly related to phylogeny. (d) Average chromatographic fingerprints of 6 producing areas, with solid lines indicating common peaks that were significantly related to phylogeny

Figure 3.14 Original NIR and chromatographic fingerprints of different species and regions of boletes



Note (a) Analysis of the difference and diversity of NIR spectral information among 11 species. (b) Analysis of the difference and diversity of chromatographic fingerprints among 11 species. (c) Variability and diversity of volatile components in 11 species. (d) Analysis of the difference and diversity of near-infrared spectral information among 6 producing areas. (e) Analysis of the difference and diversity of chromatographic fingerprint information among 6 producing areas. (f) Analysis of the difference and diversity of volatile components among 6 producing areas

Figure 3.15 STDEV and diversity analysis of different species and regions of boletes by spectral, chromatographic and mass spectrometry

3.4.4 Species Diversity Better Explains Chemical Trait Heterogeneity Than Ecological Environmental Factors

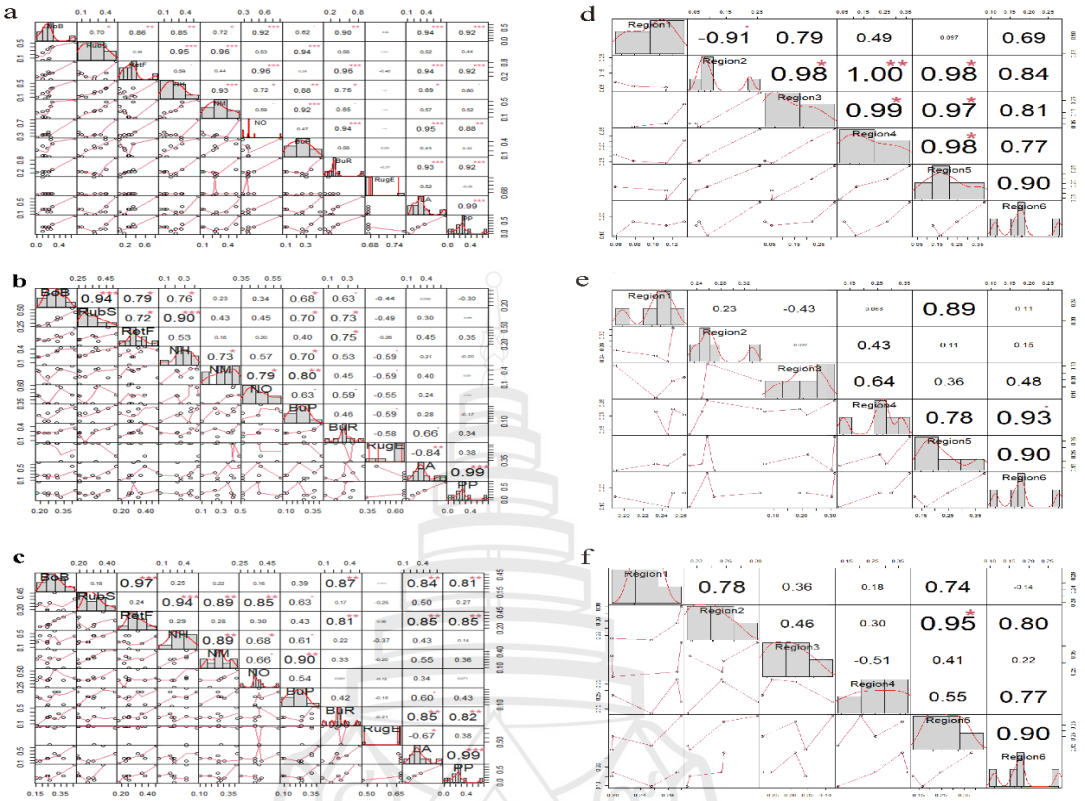
The correlation between the matrix of Euclidean distance of chemical information and the matrix of the distance of phylogenetic signal (evolutionary distance of species) was analyzed. Between the Euclidean distance of NIR spectra and the evolutionary distance of species, significant correlations were observed as follows: BoB and NO (r=0.92, p<0.001), BoB and LA (r=0.94, p<0.001), BoB and PP (r=0.92, p<0.001), BoB and RetF (r=0.86, p<0.01), BoB and NH (r=0.85, p<0.01), BoB and BuR (r=0.90, p<0.01), BoB and RubS (r=0.70, p<0.05), BoB and NM (r=0.72, p<0.01) were significantly positively correlated. RubS and NH (r=0.95, p<0.001), RubS and NM (r=0.96, p<0.001), RubS and BuP (r=0.94, p<0.001) were extremely significantly positively correlated. RetF and NO (r=0.96, p<0.001), RetF and BuR (r=0.96, p<0.001), RetF and LA (r=0.94, p<0.001), RetF and PP (r=0.92, p<0.001) were significantly positively correlated. NH and NM (r=0.93, p<0.001), NH and BuP (r=0.88, p<0.01), NH and NO (r=0.72, p<0.05), NH and BuR (r=0.75, p<0.05), NH and LA (r=0.69, p<0.05) were significantly positively correlated. NM and BuR (r=0.92, p<0.001) were significantly positively correlated. NO and BuR (r=0.94, p<0.001), NO and LA (r=0.95, p<0.001), NO and PP (r=0.88, p<0.01) were significantly positively correlated. BuR and LA (r=0.93, p<0.001), BuR and PP (r=0.92, p<0.001) were significantly positively correlated. LA and PP (r=0.99, p<0.001) were significantly positively correlated (Figure 3.16a). Between the Euclidean distance of the HPLC fingerprint and the evolutionary distance of species, general correlations were presented between species: BoB and RuS (r=0.94, p<0.001), BoB and RetF (r=0.79, p<0.05), BoB and NH (r=0.76, p<0.05), BoB and BuP (r=0.68, p<0.05) were extremely significantly positively correlated. RubS and NH (r=0.90, p<0.001), RubS and RetF (r=0.72, p<0.05), RubS and BuP (r=0.70, p<0.05), RubS and BuR (r=0.73, p<0.05) were extremely significantly positively correlated. RetF and BuR (r=0.75, p<0.05) were extremely significantly positively correlated. NH and NM (r=0.73, p<0.05), NH and BuP (r=0.70, p<0.05) were extremely significantly positively correlated. NM and BuP (r=0.80, p<0.01),

NM and NO (r=0.79, p<0.05) were extremely significantly positively correlated. RugE and LA (r=-0.84, p<0.01) were extremely significantly negatively correlated. LA and PP (r=0.99, p<0.001) were significantly positively correlated (Figure 3.16b). Between Euclidean distance of GC–MS volatile constituents and the evolutionary distance of species, as mentioned above, universally significant correlations were presented between species: BoB and RetF (r=0.97, p<0.001), BoB and BuR (r=0.87, p<0.01), BoB and LA (r=0.84, p<0.01), BoB and PP (r=0.81, p<0.01) were extremely significantly positively correlated. RubS and NH (r=0.94, p<0.001), RubS and NM (r=0.89, p<0.01), RubS and NO (r=0.85, p<0.01) were extremely significantly positively correlated. RetF and BuR (r=0.81, p<0.01), RetF and LA (r=0.85, p<0.01), RetF and PP (r=0.85, p<0.01) were extremely significantly positively correlated. NH and NM (r=0.89, p<0.01), NH and NO (r=0.68, p<0.05) were extremely significantly positively correlated. NM and BuP (r=0.90, p<0.01) were extremely significantly positively correlated. BuR and LA (r=0.85, p<0.01), BuR and LA (r=0.82, p<0.01) were extremely significantly positively correlated. LA and PP (r=0.99, p<0.001) were significantly positively correlated (Figure 3.16c). The above results showed a general significant correlation between the chemical information matrix and the signal phylogenetic signal matrix among species, which indicated that the chemical information had the potential to identify species.

Next, the correlation between the matrix of Euclidean distance of chemical information and the matrix of the distance of ecological environmental factors of different regions was analyzed. Between the Euclidean distance of NIR spectra and the distance of ecological environmental factors of different regions, significant correlations were observed as follows: Region 2 and Region 4 (r=1.00, p<0.001) were extremely significantly positively correlated, and Region 3 and Region 4 (r=0.99, p<0.05), Region 2 and Region 3 (r=0.98, p<0.05), Region 2 and Region 5 (r=0.98, p<0.05), Region 4 and Region 5 (r=0.98, p<0.05), and Region 3 and Region 5 (r=0.97, p<0.05) were significantly positively correlated (figure 3.16d). However, there was no significant correlation between the Euclidean distance of HPLC fingerprint and the distance of ecological environmental

factors of different regions, while Region 2 and Region 5 (r=0.95, p<0.05) were significantly positively correlated in the correlation between the matrix of Euclidean distance of volatile constituents and the matrix of distance of ecological environmental factors of different regions (Figure 3.16 e and f). The results showed a general correlation between the chemical information matrix and the ecological environmental factors of different regions matrix, which indicated that the chemical information had the potential to identify regions.

Comparing the correlations, we can observe that the influence of phylogenetic signals on chemical information is significantly stronger than that of ecological environmental factors in different regions, which suggests that chemical trait heterogeneity may depend on the evolution of species. This result is consistent with the chemical trait variation of coral reef fishes and plants, which is shaped more by evolutionary history than by ecological and environmental factors (Allgeier et al., 2021; Zhang, Lu et al., 2020).



Note (a–c) Correlation analysis between phylogenetic signals of species and the standard deviation matrix of NIR spectra, HPLC fingerprints, and volatile constituents of corresponding species, respectively. (d–f) Correlation analysis between regions and the standard deviation matrix of NIR spectra, HPLC fingerprints, and volatile constituents of corresponding regions, respectively. *Significant level (■ $p < 0.1$; *$p < 0.05$; **$p < 0.01$; ***$p < 0.001$). R package, chart. The correlation function of PerformanceAnalytics (https://cran.r-project.org/web/packages/PerformanceAnalytics/index.html) was used to analyze and visualize the plot

Figure 3.16 Pearson correlation analysis of phylogenetic signals of species, regions and chemical information of boletes

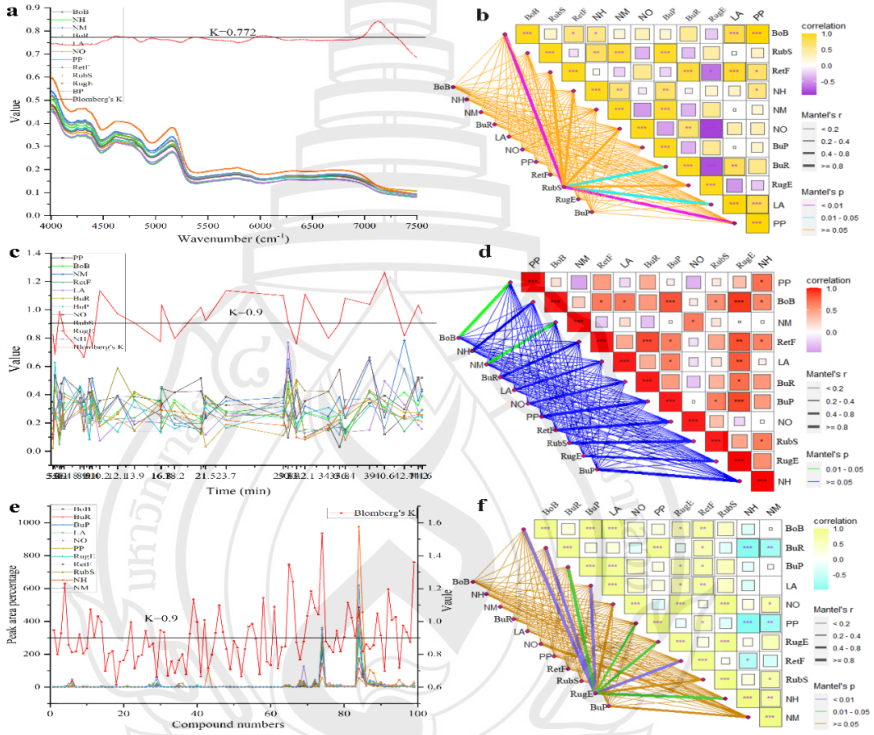
3.4.5 Identification of Species by Phylogenetic Conserved Chemical Information

Blomberg's *K* represents the strength of the phylogenetic signal, where a value close to zero indicates phylogenetic independence, and a value close to one indicates that species'

traits are distributed as expected under Brownian motion (Münkemüller et al., 2012). In this study, the ranges of *K* values of chemical information were 0.685–0.842, 0.663–1.265 and 0.617–1.535 for NIR spectra, HPLC fingerprint, and volatile constituents, respectively (Figure 3.17a, c and e and appendix Table H1, 2 and 3). Next, *K* values larger than the average 0.77 for NIR spectra, larger than 0.90 for HPLC fingerprints, and larger than 0.90 for volatile constituents were selected as characteristic chemical information and assumed to be phylogenetically conserved (Figure 3.17a, c and e and appendix Table H1, 2 and 3).

The correlation between the matrix of the Euclidean distance of characteristic chemical information and the matrix of the distance of the phylogenetic signal (evolutionary distance of species) was examined using the Mantel test. The greater the correlation coefficient of the Mantel test and the smaller the *p*-value, the greater the influence of phylogenetic signals on the characteristic chemical information. The results showed that, in general, the phylogenetic signal had a significant effect on the characteristic NIR spectrum of species (r=0.6854, $P<0.05$). In addition to the correlation between the phylogenetic signal of intraspecific species and its NIR characteristic spectrum, interspecies signals, such as the phylogenetic signal of BoB on the characteristic spectrum of RubS ($P<0.01$), and the phylogenetic signal of PP on the characteristic spectrum of RubS ($P<0.01$), the phylogenetic signal of BuR on the characteristic spectrum of RubS ($0.01<P<0.05$), and the phylogenetic signal of LA on the characteristic spectrum of RubS ($0.01<P<0.05$), also had significant effects (Figure 3.17b). Similarly, the phylogenetic signal had a significant effect on the characteristic information of the HPLC fingerprint of species (r=0.657, $P<0.05$). In addition to the correlation between the phylogenetic signal of intraspecific species and the characteristic information of the HPLC fingerprint, interspecies such as the phylogenetic signal of PP on the characteristic chromatography of BoB ($0.01<P<0.05$), and the phylogenetic signal of NM on the characteristic chromatography of NM ($0.01<P<0.05$), also had significant effects (Figure 3.17d). Likewise, the phylogenetic signal had a significant effect on the characteristic information of GC–MS volatile constitutes of species (r=0.809, $P<0.05$). In addition to the correlation between the phylogenetic signal of intraspecific species and its characteristic

information of volatile constitutes, interspecies such as the phylogenetic signal of BoB, BuR, LA and RetF and the characteristic information of GC–MS volatile constituents of RugE ($P<0.01$), the phylogenetic signal of BuP, PP, RugE and NH and the characteristic information of GC–MS volatile constituents of RugE ($0.01<P<0.05$) were extremely significantly correlated (Figure 3.17f). Given the above, the phylogenetic signals of species have a certain influence on the characteristic chemical signals both intraspecies and interspecies.



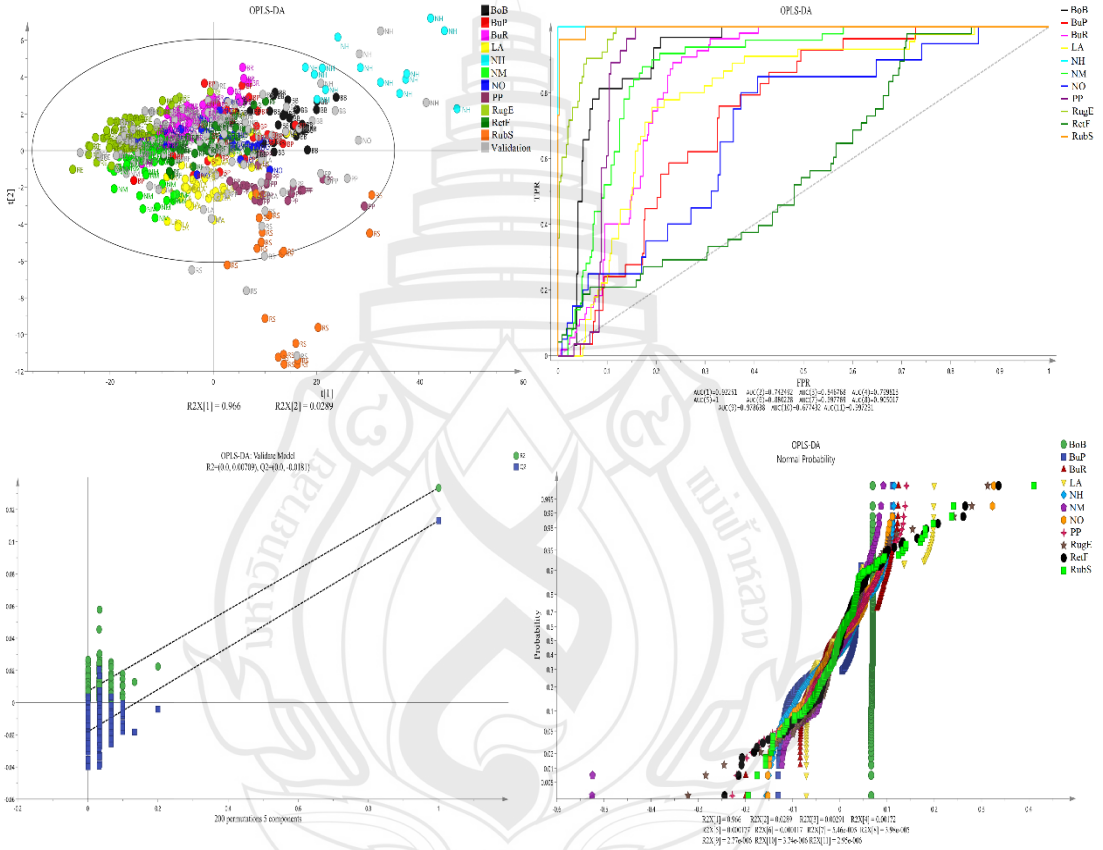
Note (a–c) Blomberg's *K* values of NIR spectra, HPLC fingerprints and volatile constituents obtained through phylogenetic signal analysis, respectively. (d–f) Mantel test of Blomberg's *K* values of NIR spectra, HPLC fingerprint and volatile constituents, respectively. The trigonometric matrix represents the correlation between characteristic chemical information (spectra, chromatography and volatile components), and the line represents the correlation between the species phylogenetic signal matrix and the chemical characteristic information matrix

Figure 3.17 Phylogenetic signal analysis and Mantel test of chemical characteristic information of boletes species

Furthermore, mSD was used to assess the matrix of Euclidean distance of characteristic chemical information and the matrix of distance of the phylogenetic signal. When the value of mSD is 0, it indicates that the two matrices fit perfectly. The larger the value is, the greater the difference between the two matrices. The results showed that the mSD was 0.077 for the NIR spectra, 0.0105 for the HPLC fingerprint and 0.067 for the GC–MS volatile constituents, which indicated that the compatibility between the two matrices was high and suggested that there was a strong correlation between the phylogenetic signal and the chemical characteristic information of the species.

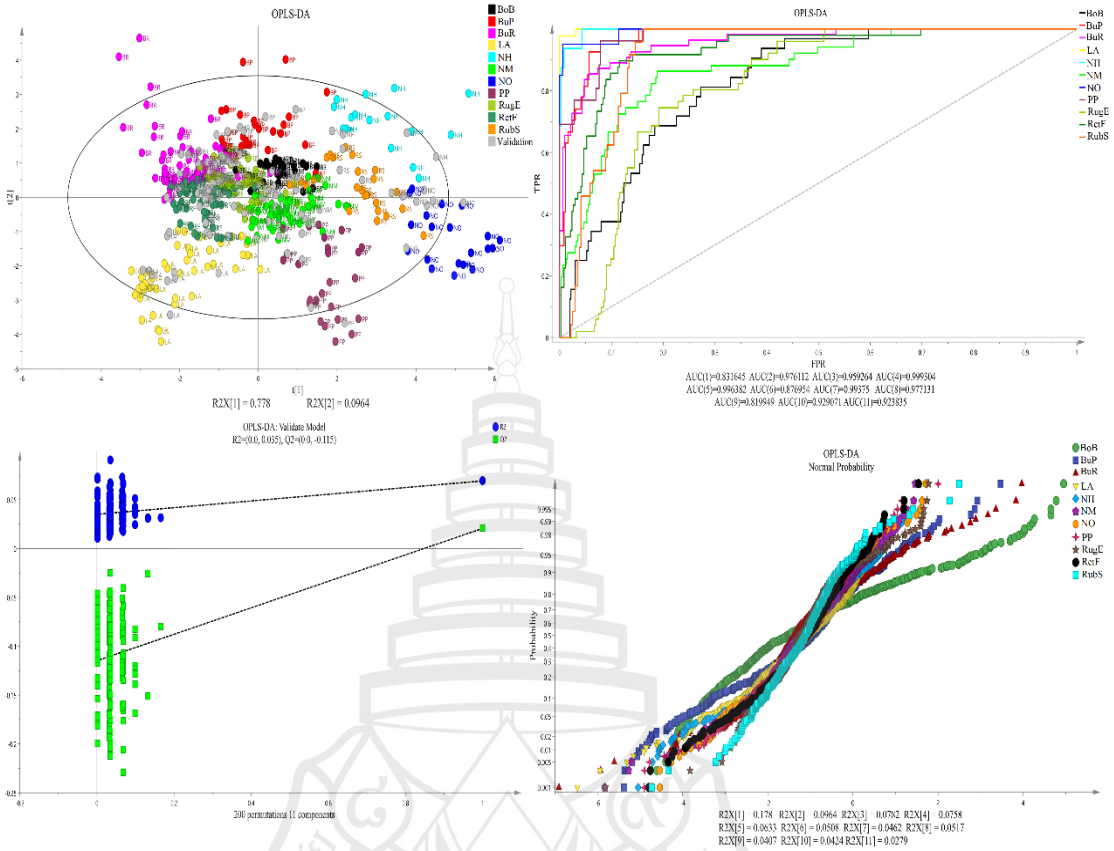
To verify the identification ability of species using characteristic chemical information, we established pattern recognition models using two methods partial least square discriminant analysis (PLS- DA) using the ropls package (appendix Figure K) and orthogonal partial least square discriminant analysis (OPLS-DA) using SIMCA-P+ version 14.1 (Figure 3.18a, 3.19a and 3.20a and Table 3.7-3.9). The PLS-DA results showed that the 11 species can be effectively identified in the two dissimilarity spaces by different chemical characteristic information (NIR spectra, HPLC fingerprint, and GC–MS volatile constituents), where the RMSEEs of the training and testing sets were 0.252 and 0.242 for NIR (appendix Figure K1), 0.22 and 0.242 for HPLC (appendix Figure K2), and 0.235 and 0.253 for GC–MS (appendix Figure K3), respectively. The OPLS-DA models showed that the 11 species could be clearly distinguished from each other in the three dissimilarity spaces by training sets of their characteristic chemistry. The cumulative contribution rates of the training sets in the first two principal components were 99.1% (NIR), 88.4% (HPLC) and 80.5% (GC–MS), respectively. The area under the curve (AUC) which represents a quantitative performance measure of the classifier, its values (Figure 3.18b, 3.19b, 3.20b) of 11 species were larger than 0.6774, and the results of 200 fold cross validation showed that the fitting effect was satisfactory with R^2 = 0.00709 and Q^2=-0.0181 for NIR; R^2 = 0.035 and Q^2=-0.115 for HPLC; R^2 = 0.044 and Q^2=-0.0615 for GC-MS (Figure 3.18c, 3.19c, 3.20c). The normal probability plots showed that the data of the training sets were approximately normally distributed (Figure 3.18d, 3.19d and 3.20d). The results of testing

sets of characteristic information of NIR, HPLC and GC–MS showed that the four evaluation indices sensitivity, specificity, efficiency and accuracy were larger than 0.60, 0.93, 0.95 and 0.93, respectively (Table 3.8-3.12). Stronger phylogenetic conservatism increases species exclusivity and identification, which provides a basis for the identification of species by chemical characteristics.



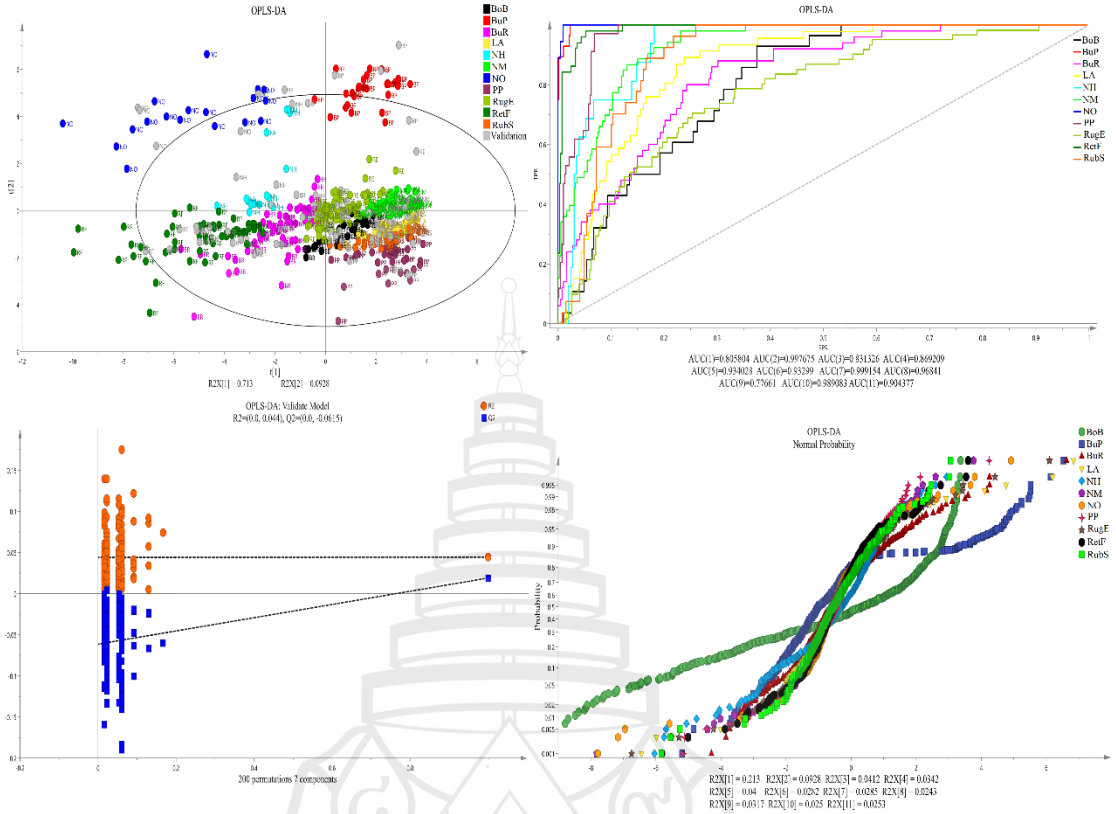
Note (a) 2D plot of the OPLS-DA model. (b) The AUC distribution of the established model. (c) 200-fold cross-validation diagram of the model. (d) The distribution of the normal probability of species in the established model

Figure 3.18 Pattern recognition model of boletes species based on characteristic spectral information



Note (a) 2D plot of the OPLS-DA model. (b) The AUC distribution of the established model. (c) 200-fold cross-validation diagram of the model. (d) The distribution of the normal probability of species in the established model

Figure 3.19 Pattern recognition model of boletes species based on characteristic chromatographical information



Note (a) 2D plot of the OPLS-DA model. (b) The AUC distribution of the established model. (c) 200-fold cross-validation diagram of the model. (d) The distribution of the normal probability of species in the established model

Figure 3.20 Pattern recognition model of boletes species based on characteristic volatile constituent information

Table 3.7 The OPLS-DA model of species established by characteristic near-infrared information

	Train calibration														
	BoB	**BuP**	**BuR**	**LA**	**NH**	**NM**	**NO**	**PP**	**RugE**	**RetF**	**RubS**	**sensitivity**	**specificity**	**efficiency**	**accuracy**
BoB	29	0	1	0	2	0	0	0	0	0	0	0.91	1.00	0.99	0.99
BuP	1	25	0	0	1	1	0	1	0	0	0	0.86	1.00	0.99	0.99
BuR	0	0	52	0	0	0	0	0	3	0	0	0.95	0.98	0.99	0.98
LA	0	0	1	40	0	2	0	0	0	1	1	0.89	1.00	0.99	0.99
NH	0	0	0	0	16	0	0	0	0	0	0	1.00	0.99	1.00	0.99
NM	0	0	1	0	0	48	0	0	1	0	0	0.96	0.99	1.00	0.99
NO	0	0	2	0	0	0	16	0	1	1	0	0.80	1.00	0.99	0.99
PP	0	0	0	0	1	0	0	24	0	0	3	0.86	1.00	0.99	0.99
RugE	0	0	0	0	0	0	0	0	53	0	0	1.00	0.98	1.00	0.98
RetF	0	0	1	0	0	1	0	0	2	44	0	0.92	0.99	0.99	0.99
RubS	0	0	0	0	0	0	0	0	0	0	26	1.00	0.99	1.00	0.99

Table 3.8 External validation of the OPLS-DA model of species established by characteristic near-infrared information

	Test validation														
	BoB	**BuP**	**BuR**	**LA**	**NH**	**NM**	**NO**	**PP**	**RugE**	**RetF**	**RubS**	**sensitivity**	**specificity**	**efficiency**	**accuracy**
BoB	5	0	0	0	1	0	0	0	0	1	0	0.71	1.00	0.98	0.98
BuP	0	7	1	0	0	0	0	0	0	1	0	0.78	1.00	0.98	0.98
BuR	0	0	9	0	0	0	0	0	2	0	0	0.82	0.94	0.98	0.93
LA	0	0	0	9	0	0	0	1	1	0	1	0.75	1.00	0.97	0.97
NH	0	0	0	0	4	0	0	0	0	0	0	1.00	0.98	1.00	0.98
NM	0	0	0	0	0	9	0	0	2	0	0	0.82	1.00	0.98	0.98
NO	0	0	1	0	1	0	5	0	0	0	0	0.71	1.00	0.98	0.98
PP	0	0	0	0	0	0	0	6	0	0	1	0.86	0.99	0.99	0.98
RugE	0	0	2	0	0	0	0	0	15	0	0	0.89	0.94	0.98	0.93
RetF	0	0	2	0	0	0	0	0	1	13	0	0.81	0.98	0.97	0.95
RubS	0	0	0	0	0	0	0	0	0	0	6	1.00	0.98	1.00	0.98

Table 3.9 The OPLS-DA model of species established by characteristic chromatographic information

	Train calibration														
	BoB	**BuP**	**BuR**	**LA**	**NH**	**NM**	**NO**	**PP**	**RugE**	**RetF**	**RubS**	**sensitivity**	**specificity**	**efficiency**	**accuracy**
BoB	26	1	0	0	1	2	0	0	2	0	0	0.81	1.00	0.98	0.98
BuP	0	25	1	0	1	0	0	0	0	0	0	0.93	1.00	0.99	0.99
BuR	0	0	50	0	0	0	0	0	2	3	0	0.91	0.99	0.99	0.98
LA	0	0	0	45	0	0	0	0	0	0	0	1.00	0.99	1.00	0.99
NH	0	0	0	1	15	0	0	0	0	0	0	0.94	0.99	1.00	0.99
NM	0	0	0	0	0	47	0	3	0	1	0	0.92	0.97	0.99	0.96
NO	0	0	0	0	0	0	19	1	0	0	0	0.95	1.00	1.00	0.99
PP	0	0	0	2	0	1	0	22	0	1	0	0.85	0.99	0.99	0.98
RugE	0	0	3	0	0	4	0	0	42	2	0	0.82	0.99	0.98	0.97
RetF	0	0	0	0	0	0	0	0	0	49	0	1.00	0.98	1.00	0.98
RubS	0	0	0	0	2	4	1	1	0	0	16	0.67	1.00	0.98	0.98

Table 3.10 External validation of the OPLS-DA model of species established by characteristic chromatographic information

	Test validation														
	BoB	**BuP**	**BuR**	**LA**	**NH**	**NM**	**NO**	**PP**	**RugE**	**RetF**	**RubS**	**sensitivity**	**specificity**	**efficiency**	**accuracy**
BoB	4	1	0	0	0	1	0	0	1	0	0	0.67	1.00	0.97	0.97
BuP	0	7	1	0	0	0	0	0	0	0	0	0.88	0.99	0.99	0.98
BuR	0	0	10	0	0	0	0	0	1	0	0	0.91	0.99	0.99	0.98
LA	0	0	0	12	0	0	0	0	0	0	0	1.00	1.00	1.00	1.00
NH	0	0	0	0	4	0	0	0	0	0	0	1.00	0.99	1.00	0.99
NM	0	0	0	0	0	9	0	0	1	0	0	0.90	0.96	0.99	0.95
NO	0	0	0	0	0	0	5	1	0	0	0	0.83	0.97	0.99	0.96
PP	0	0	0	0	0	1	1	5	0	0	0	0.71	0.99	0.98	0.97
RugE	0	0	0	0	0	0	0	0	14	4	0	0.78	0.97	0.96	0.93
RetF	0	0	0	0	0	2	0	0	0	13	0	0.87	0.96	0.98	0.94
RubS	0	0	0	0	1	0	2	0	0	0	3	0.60	1.00	0.97	0.97

Table 3.11 The OPLS-DA model of species established by characteristic volatile constituent information

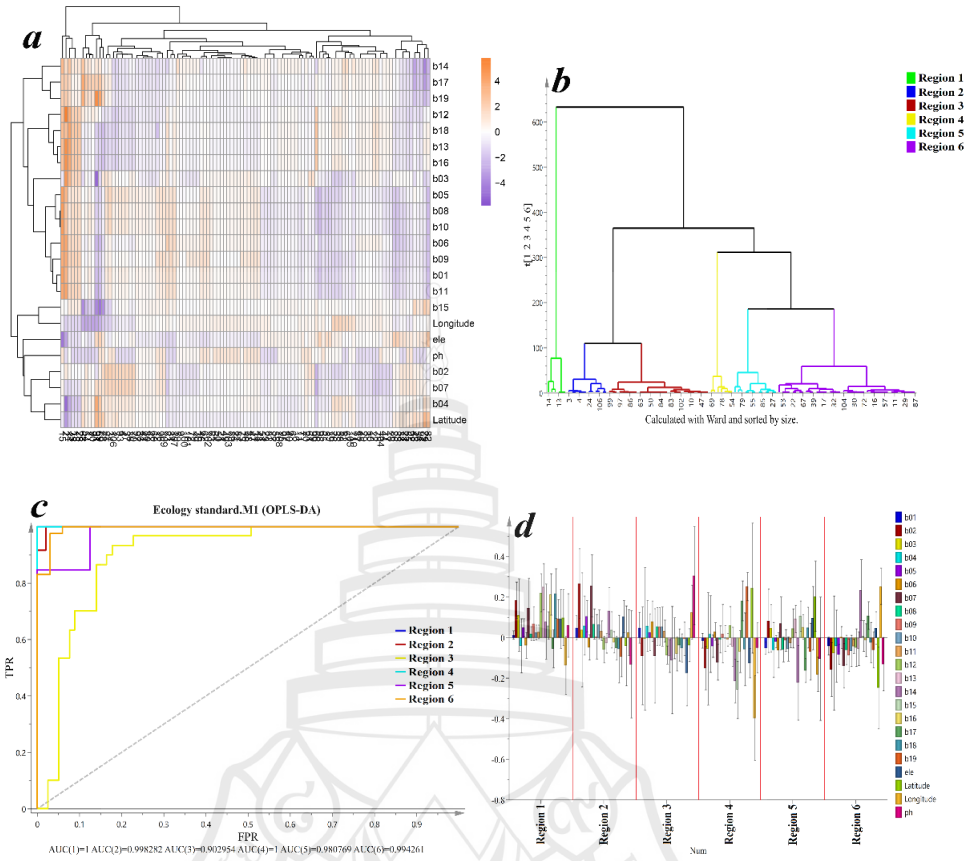
	Train calibration														
	BoB	**BuP**	**BuR**	**LA**	**NH**	**NM**	**NO**	**PP**	**RugE**	**RetF**	**RubS**	**sensitivity**	**specificity**	**efficiency**	**accuracy**
BoB	18	0	2	2	0	1	0	2	2	1	0	0.64	1.00	0.98	0.98
BuP	0	28	0	0	0	0	0	0	0	0	0	1.00	0.99	1.00	0.99
BuR	0	0	40	0	0	0	0	0	2	8	0	0.80	0.99	0.98	0.97
LA	0	0	0	38	0	6	0	2	0	0	0	0.83	0.98	0.98	0.96
NH	0	2	0	0	10	0	0	0	0	4	0	0.63	1.00	0.99	0.99
NM	0	0	0	0	0	53	0	0	0	0	0	1.00	0.97	1.00	0.97
NO	0	0	0	0	0	0	18	0	0	0	0	1.00	1.00	1.00	1.00
PP	0	0	0	0	0	0	0	34	0	0	0	1.00	0.98	1.00	0.98
RugE	0	2	2	1	0	2	0	3	50	1	0	0.82	0.99	0.97	0.96
RetF	0	0	0	0	0	0	0	0	0	51	0	1.00	0.96	1.00	0.97
RubS	0	0	0	5	0	3	0	2	0	0	17	0.63	1.00	0.98	0.98

Table 3.12 External validation of the OPLS-DA model of species established by characteristic volatile constitute information

	Test validation														
	BoB	**BuP**	**BuR**	**LA**	**NH**	**NM**	**NO**	**PP**	**RugE**	**RetF**	**RubS**	**sensitivity**	**specificity**	**efficiency**	**accuracy**
BoB	4	0	0	0	0	0	0	0	2	0	0	0.67	1.00	0.98	0.98
BuP	0	6	0	0	0	0	0	0	0	0	0	1.00	0.99	1.00	0.99
BuR	0	0	7	0	0	0	0	0	1	3	0	0.64	1.00	0.95	0.95
LA	0	0	0	7	0	2	0	1	1	0	0	0.64	0.99	0.95	0.94
NH	0	0	0	0	3	0	0	0	0	1	0	0.75	1.00	0.99	0.99
NM	0	0	0	0	0	9	0	0	0	0	0	1.00	0.96	1.00	0.96
NO	0	0	0	0	0	0	5	0	0	0	0	1.00	1.00	1.00	1.00
PP	0	0	0	0	0	0	0	4	1	0	0	0.80	0.99	0.99	0.98
RugE	0	1	0	0	0	0	0	0	6	1	0	0.75	0.94	0.98	0.92
RetF	0	0	0	0	0	0	0	0	0	12	0	1.00	0.93	1.00	0.94
RubS	0	0	0	1	0	1	0	0	0	0	3	0.60	1.00	0.98	0.98

3.4.6 Chemical Characteristic Information Effectively Distinguish the Regions of Ecology

We hypothesized that the characteristic chemical information with a lower level of phylogenetic conservatism would be better explained by contemporary ecological environmental factors, as they are less constrained by evolutionary history. To verify the hypothesis, the collection regions were divided by an unsupervised classification model of ecological environmental factors (Figure 3.21a, 3.22b, and appendix Figure N1). Next, the pattern recognition model of regions was established by chemical characteristic information obtained by the VIP method (appendix Table L). The number of clusters (K) was determined by the cluster consensus score (CCS) (CCSmean>0.85) (Jiang, Xia et al., 2022; Zhang, Lu et al., 2020), and the principal component clustering (PCAC) was obtained by cluster analysis of the score of the principal component. The cumulative distribution function (CDF) curve and PCA cluster were consistent when the number of clusters was 6. The cluster results showed that region 1 mainly belongs to the tropical and subtropical climate; region 2 and 5 mainly belong to the north temperate climate, and their obvious differences are the precipitation and temperature of the driest quarter; region 3 and 6 mainly belong to the subtropical humid monsoon climate, and there are significant differences between the mean temperature and elevation; region 4 mainly belongs to the cold and temperate climate of the plateau (Feng et al., 2017; Feng & Yang, 2018) (appendix Table B). The regions can be effectively distinguished by the value of AUC (larger than 0.9029) based on the OPLS-DA of ecological environmental factors (Figure 3.21c). The correlation coefficient between ecological environmental factors and regions showed that the main influencing factors (1) of region 1 were b01, b09, b12, b13, b16, b18 and elevation; (2) of region 2 were b02, b05 and b07; (3) of region 3 were b03, b08, and pH; (4) of region 4 were b04, b14, b17 and b19; (5) of region 5 were b15 and latitude; and (6) of region 6 were b14 and longitude (Figure 3.21a and d and appendix Table M1).



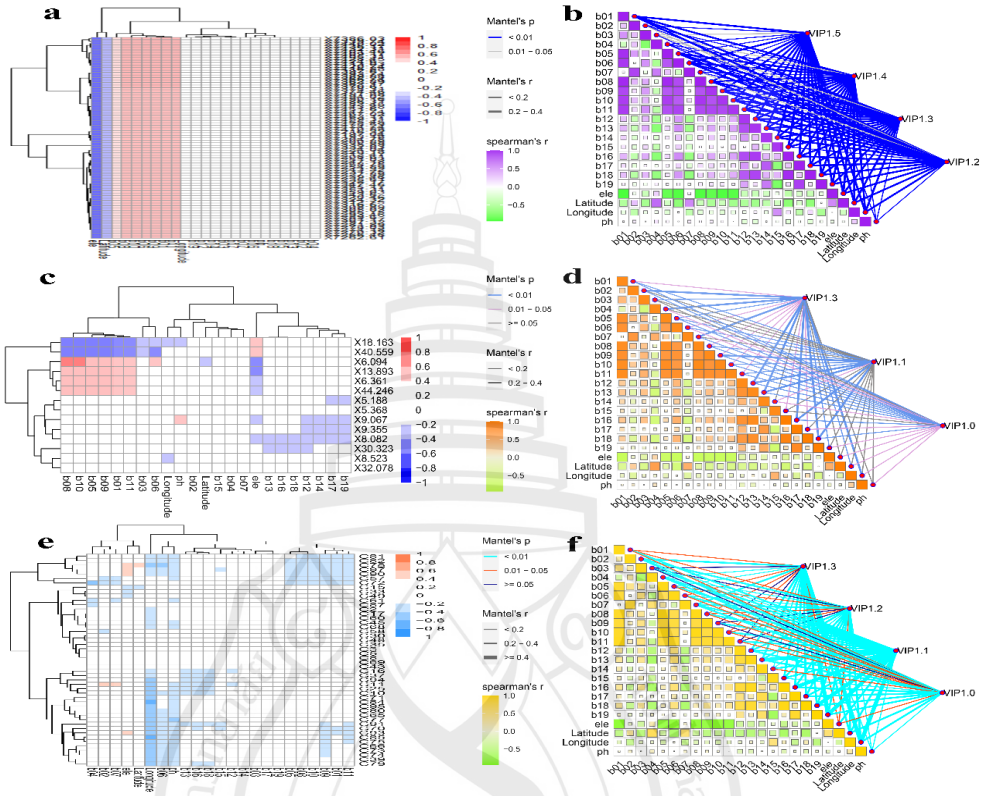
Note (a) Correlation heatmap between 110 collection sites and their corresponding ecological environmental factors. (b) The 110 collection sites were divided into six production areas through principal component cluster analysis of ecological environmental factors. (c) AUC analysis of the classification of producing areas. (d) Analysis of the contribution of different ecological environmental factors to the classification of six producing areas

Figure 3.21 The correlation between different collection sites and their ecological environmental factors and the division of producing areas of boletes

To explore whether chemical characteristic information can effectively identify regions and further analyze the influence of ecological environmental factors on chemical traits, the important chemical characteristic information was extracted by VIP (appendix

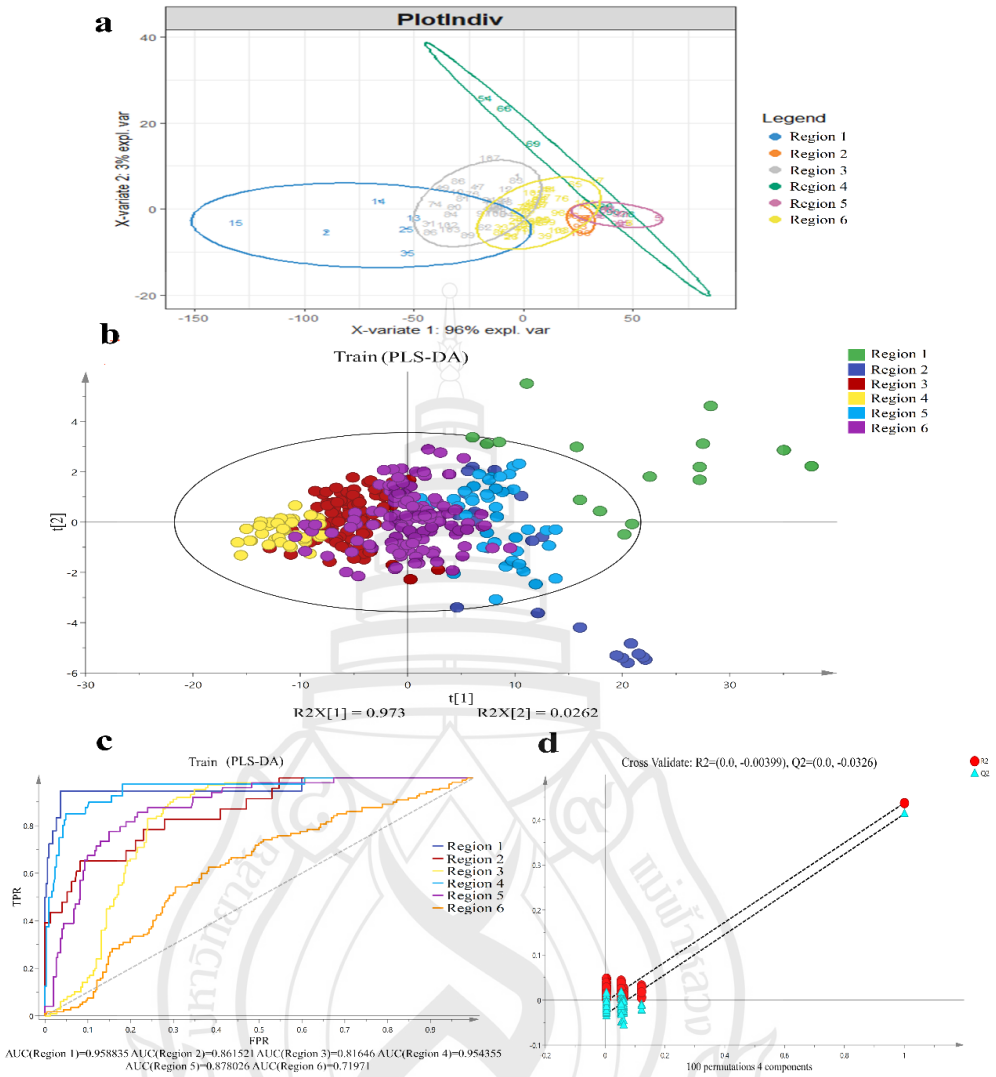
Table M), and the correlation between the important chemical characteristic information (NIR, HPLC and GC–MS) and ecological environmental factors was analyzed. The results showed that the chemical characteristic information (including NIR, HPLC and GC–MS) was mainly correlated with the ecological environmental factors including b01, b05, b06, b08, b09, b10, b11, elevation and latitude (Figure 3.22a, 3.23c, and 3.24e). The results of the Mantel test (NIR_r= 0.4848, P=1.0e^{-04}; $HPLC_r$=0.4668, P=1.0e^{-04} and $GC–MS_r$=0.5347, P=1.0e^{-04}) also showed that the extracted chemical characteristic information was significantly correlated with ecological environmental factors (Figure 3.22b, 3.23d, and 3.24f). The pattern recognition model of regions was established by PLS-DA based on the ropls package (Figure 3.23a, 3.24a and 3.25a) and SIMCA-P+ version14.1 (Figure 3.23b, 3.24b and 3.25b, and Table 3.10-3.12). The results showed that the regions were clearly distinguished in two dimensions (cumulative contribution rate NIR_R^2X>98%; HPLC $_R^2X$>66%; GC–MS $_R^2X$>60%; Figure 3.23b, 3.24b and 3.25b), the AUC values of different regions were larger than 0.71 in distinguish models of NIR, HPLC and GC–MS (Figure 3.23c, 3.24c and 3.25c), and the 100-fold cross-validation showed that the distinguished models had better classification suitability (Figure 3.23d, 3.24d and 3.25d). In addition, the results of RLQ demonstrated that the chemical characteristic information was related not only to species but also to ecological environmental factors based on the first two eigenvalues (Figure 3.26). The results of testing sets of characteristic information from NIR, HPLC and GC–MS showed that the four evaluation indices (sensitivity, specificity, efficiency and accuracy) were greater than 0.71, 0.87, 0.94 and 0.87, respectively (Table 3.10b-3.12b), which indicated that the extracted chemical characteristic information could be applied as a basis to distinguish the geographic regions. Because the geographical regions were divided by ecological environmental factors, geographical regions, as an intermediate bridge, were connected with chemical information and ecological environmental factors in this study. The results of direct and indirect relationships showed that there were universal correlations between chemical information and ecological environmental factors, which supported the hypothesis that ecological interactions might

play a more important role in driving chemical information variation in different geographical regions (Allgeier et al., 2021).



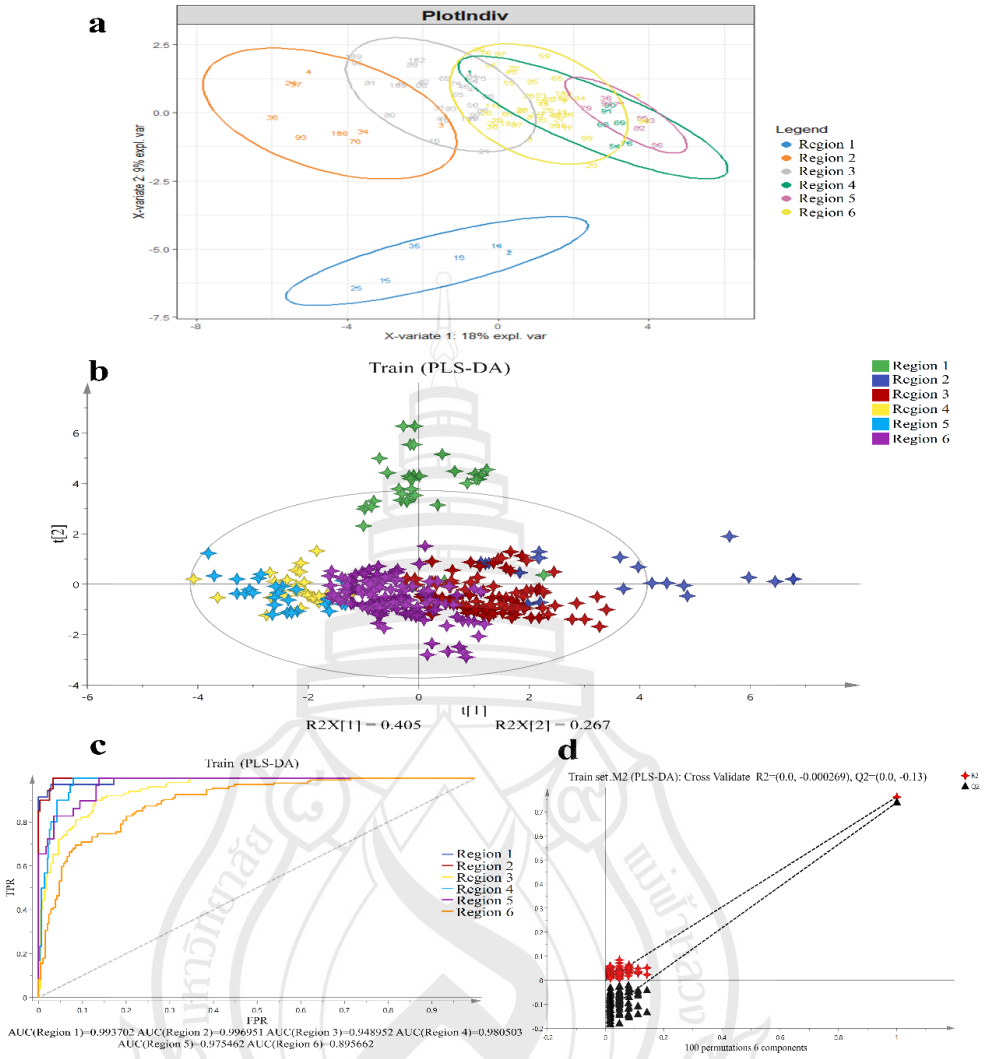
Note (a), (c) and (e) The correlation heatmap of characteristic information of spectrum, chromatography and volatile components obtained by VIP and the ecological environmental factors, respectively. (b), (d) and (f) Mantel test of the correlation between characteristic spectrum, chromatographic and volatile component information and ecological environmental factors, respectively. The triangle matrix represents the correlation between ecological environmental factors, and the lines represent the correlation between the ecological environmental factor matrix and the chemical characteristic information matrix

Figure 3.22 The correlation analysis between chemical characteristic information and ecological environmental factors of producing areas of boletes



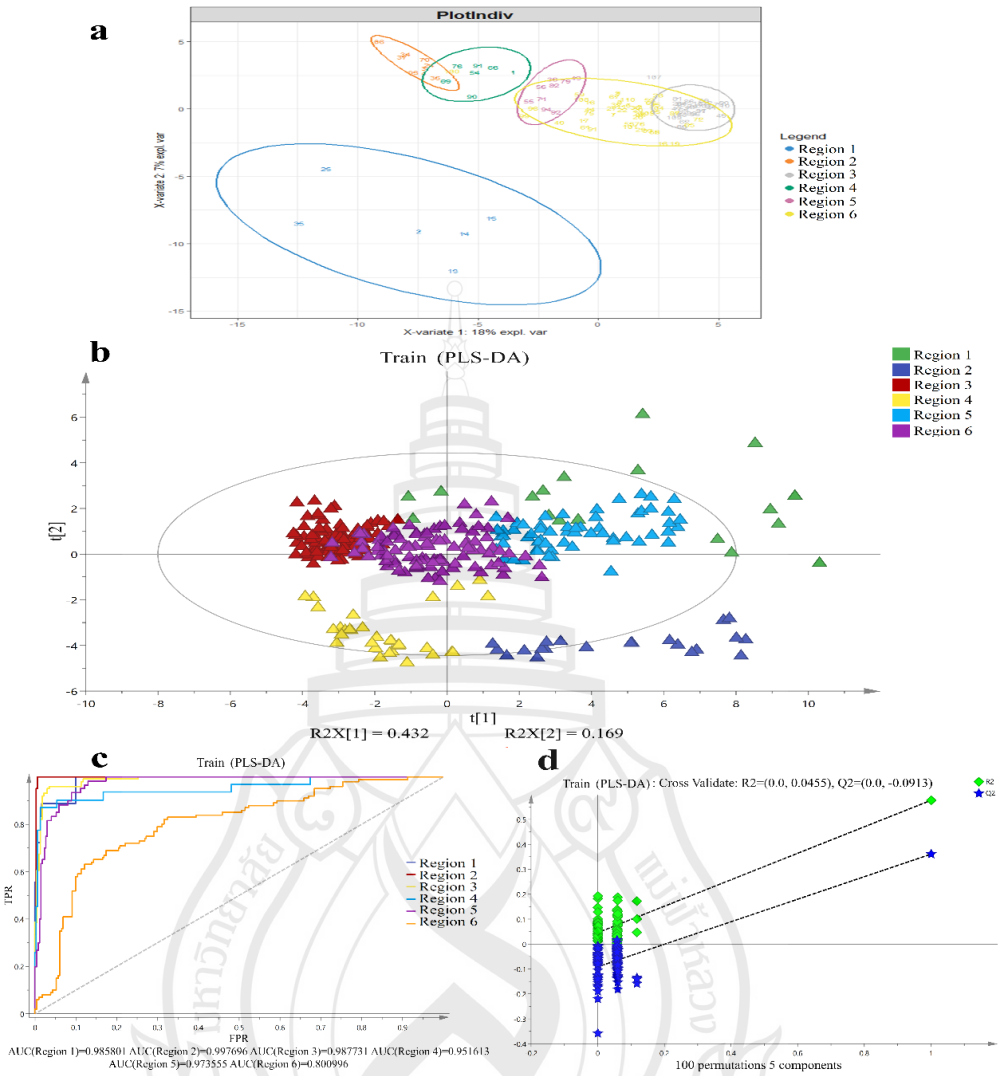
Note (a) The PLS-DA model of different regions was established by using the R language. (b) The PLS-DA model of different regions was established by using SIMICA. (c) The AUC distribution diagram of the established model. (d) 100-fold cross-validation of the established model

Figure 3.23 The PLS-DA model of characteristic spectral information of six different regions of boletes established by different methods



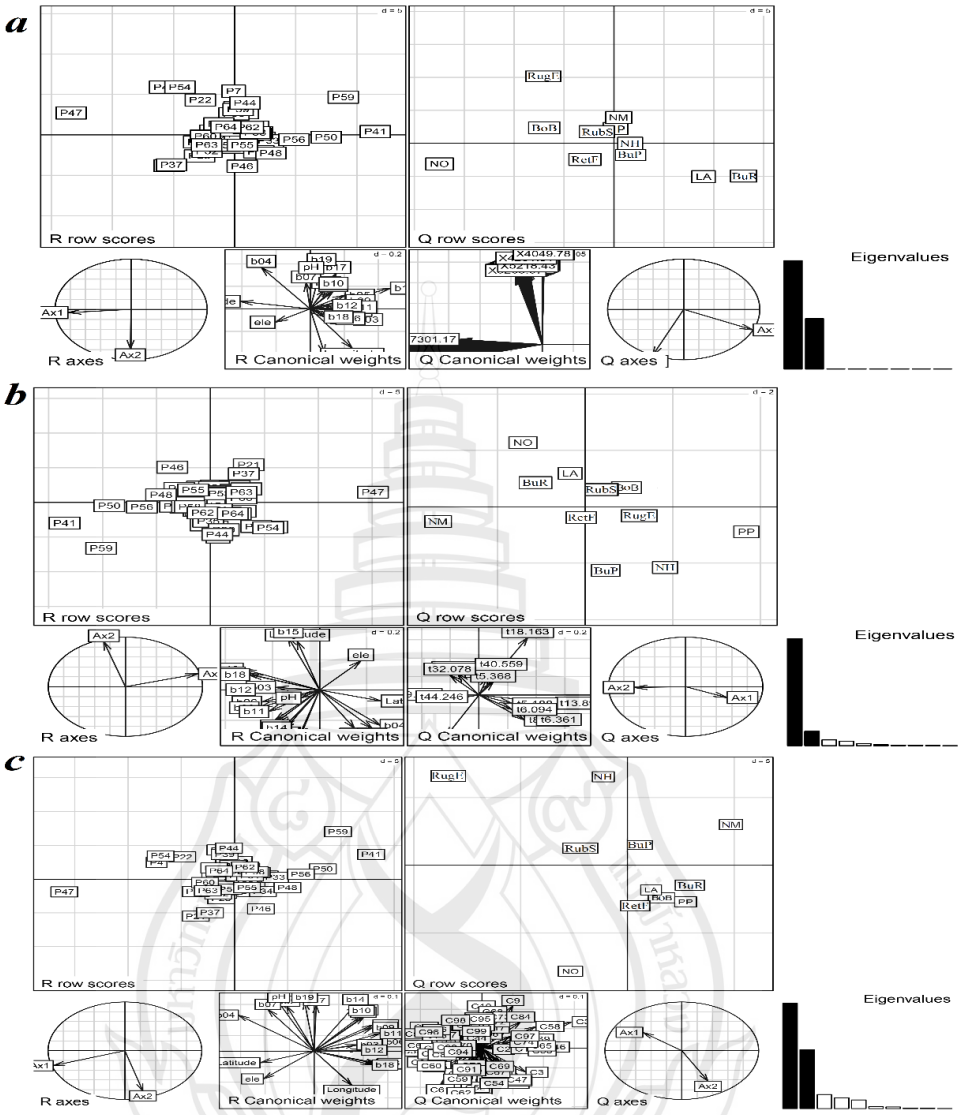
Note (a) The PLS-DA model of different regions was established by using the R language. (b) The PLS-DA model of different regions was established by using SIMICA. (c) The AUC distribution diagram of the established model. (d) 100-fold cross-validation of the established model

Figure 3.24 The PLS-DA model of characteristic chromatographic information of six different regions of boletes established by different methods



Note (a) The PLS-DA model of different regions was established by using the R language. (b) The PLS-DA model of different regions was established by using SIMICA. (c) The AUC distribution diagram of the established model. (d) 100-fold cross-validation of the established model

Figure 3.25 The PLS-DA model of characteristic volatile constituents of six different regions of boletes established by different methods



Note RLQ analysis of species, chemical characteristic information (a–c represent spectral, chromatographic and volatile components, respectively), ecological environmental factors and production areas

Figure 3.26 RLQ analysis of species, chemical characteristic information, ecological environmental factors and production areas

Table 3.13 The OPLS-DA model of regions established by characteristic near-infrared information

Train calibration of NIR										
	R 1	**R 2**	**R 3**	**R 4**	**R 5**	**R 6**	**sensitivity**	**specificity**	**efficiency**	**accuracy**
R 1	15	0	0	0	1	2	0.833	0.994	0.991	0.986
R 2	0	18	1	0	0	4	0.783	1.000	0.986	0.986
R 3	0	0	93	1	0	6	0.930	0.947	0.980	0.942
R 4	0	0	1	36	0	3	0.900	0.997	0.989	0.986
R 5	2	0	1	0	41	5	0.837	0.997	0.977	0.974
R 6	0	0	11	0	0	109	0.908	0.920	0.969	0.916

Table 3.14 External validation of the OPLS-DA model of regions established by characteristic near-infrared information

Test validation of NIR										
	R 1	**R 2**	**R 3**	**R 4**	**R 5**	**R 6**	**sensitivity**	**specificity**	**efficiency**	**accuracy**
R 1	5	0	0	0	0	1	0.833	1.000	0.992	0.992
R 2	0	5	1	0	0	1	0.714	1.000	0.983	0.983
R 3	0	0	33	0	0	4	0.892	0.943	0.967	0.928
R 4	0	0	0	11	0	2	0.846	1.000	0.983	0.983
R 5	0	0	0	0	13	3	0.813	0.990	0.975	0.967
R 6	0	0	4	0	1	36	0.878	0.878	0.958	0.878

Table 3.15 The OPLS-DA model of regions established by characteristic chromatographic information

Train calibration of HPLC-fingerprint										
	R 1	**R 2**	**R 3**	**R 4**	**R 5**	**R 6**	**sensitivity**	**specificity**	**efficiency**	**accuracy**
R 1	33	0	1	0	0	1	0.943	1.000	0.994	0.994
R 2	0	18	2	0	0	0	0.900	1.000	0.994	0.994
R 3	0	0	96	0	0	4	0.960	0.965	0.989	0.964
R 4	0	0	0	26	2	2	0.867	0.994	0.989	0.983
R 5	0	0	0	2	25	2	0.862	0.994	0.989	0.983
R 6	0	0	6	0	0	128	0.955	0.960	0.983	0.958

Table 3.16 External validation of the OPLS-DA model of regions established by characteristic chromatographic information

Test validation of HPLC-fingerprint										
	R 1	**R 2**	**R 3**	**R 4**	**R 5**	**R 6**	**sensitivity**	**specificity**	**efficiency**	**accuracy**
R 1	9	0	1	0	0	0	0.900	1.000	0.991	0.991
R 2	0	5	1	0	0	0	0.833	0.990	0.991	0.981
R 3	0	1	23	0	0	2	0.885	0.941	0.972	0.928
R 4	0	0	0	5	0	1	0.833	1.000	0.991	0.991
R 5	0	0	0	0	4	1	0.800	1.000	0.991	0.991
R 6	0	0	3	0	0	50	0.943	0.930	0.972	0.936

Table 3.17 The OPLS-DA model of regions established by characteristic volatile constituent information

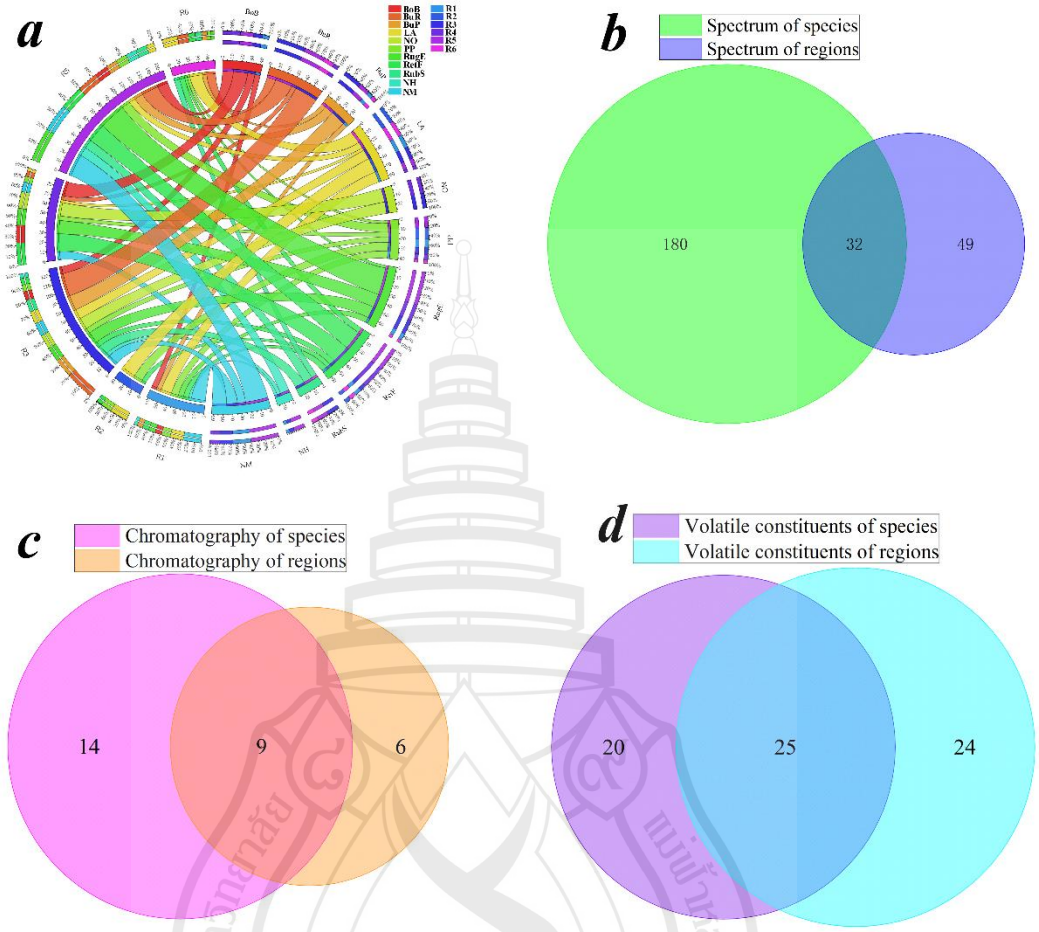
Train calibration of volatile compounds										
	R 1	**R 2**	**R 3**	**R 4**	**R 5**	**R 6**	**sensitivity**	**specificity**	**efficiency**	**accuracy**
R 1	14	0	0	0	3	1	0.778	1.000	0.988	0.988
R 2	0	21	0	0	0	0	1.000	1.000	1.000	1.000
R 3	0	0	100	0	0	1	0.990	0.979	0.997	0.982
R 4	0	0	0	28	0	3	0.903	1.000	0.991	0.991
R 5	0	0	0	0	57	3	0.950	0.971	0.991	0.968
R 6	0	0	5	0	5	90	0.900	0.967	0.970	0.947

Table 3.18 External validation of the OPLS-DA model of regions established by characteristic volatile constituent information

Test validation of volatile compounds										
	R 1	**R 2**	**R 3**	**R 4**	**R 5**	**R 6**	**sensitivity**	**specificity**	**efficiency**	**accuracy**
R 1	4	0	1	0	0	0	0.800	1.000	0.992	0.992
R 2	0	5	0	1	0	0	0.833	1.000	0.992	0.992
R 3	0	0	31	0	0	1	0.969	0.926	0.992	0.937
R 4	0	0	0	7	1	0	0.875	0.991	0.992	0.983
R 5	0	0	0	0	17	1	0.944	0.981	0.992	0.975
R 6	0	0	6	0	1	44	0.863	0.972	0.942	0.926

3.4.7 A High Degree of Overlap between the Chemical Characteristics Information for the Identification of Species and Regions

Although the relative abundances of species in different regions were different (Figure 3.27a), they were representative for analyzing the diversity of chemical information because at least 3 species were in each region. Interestingly, the chemical characteristic information selected for the identification of species (the phylogenetic signal) and regions (VIP values) partially overlapped (Figure 3.27, appendix Table H and L). The Venn diagram showed that (1) among the chemical characteristic information from NIR, 212 were related to phylogenetic signals, 81 were related to regions, and 32 were common information, accounting for 10.9% (Figure 3.27b); (2) among the chromatography characteristic information from HPLC, 23 were related to phylogenetic signals, 15 were related to regions, and 9 were common information, accounting for 23.7% (Figure 3.27c); (3) among the volatile constituents from GC–MS, 45 were related to phylogenetic signals, 49 were related to regions, and 25 were common information, accounting for 26.6% (Figure 3.27d).



Note (a) Circle map of species richness analysis in different producing areas. (b–d) Venn diagram of characteristic spectral, chromatographic and volatile component information of species and producing areas, respectively

Figure 3.27 Species richness in different producing areas and heterogeneity analysis of chemical characteristic information

Phylogenetic signal analysis showed that strong phylogenetic signals of NIR spectral information were mainly distributed at 7332.03-6144.09 cm^{-1}, 5137.44-5133.58 cm^{-1} and 4647.6-4589.75 cm^{-1}. Correlation analysis and extraction of VIP (more than 1.2) showed that significant correlations between NIR spectra information and regions were mainly distributed in the range of 7497.88-7143.04 cm^{-1} and 4026.64-4011.21 cm^{-1} (Figure

3.14a and 3.14b; Figure 3.22 and 3.27b). The common information from the NIR spectra for identification of species and regions was distributed at 7497.88-7143.04 cm^{-1}, in which approximately 7353 cm^{-1} was mainly the C-H combination (e.g., C-H_3) of hydrocarbons and aliphatic groups, 7300 cm^{-1} was mainly the C-H ($2\nu CH_3$ & δCH_3) combination of hydrocarbins and aromatic, 7194 cm^{-1} mainly showed the C-H ($2\nu_s CH_3$ & δCH_3) combination of hydrocarbons and aliphatic groups, 7168 cm^{-1} showed the C-H (e.g., C-H_2) combination of hydrocarbons and aliphatic groups, 7163 cm^{-1} mainly showed the ($2\nu CH_3$ & δCH_3) combination of hydrocarbons and aliphatic groups, and approximately 7120 cm^{-1} was mainly O-H from alcohols in CCl_4 as n-, sec-, and tert-butanol, etc. The differential spectral bands were 7143.04-6144.09 cm^{-1}, 5137.44-5133.58 cm^{-1} and 4647.6-4589.75 cm^{-1} used for identifying species, of which approximately 7140-6940 cm^{-1} was 2νO-H from phenols and aryl alcohols Ar-OH, 6995 cm^{-1} was N-H (2ν) symmetric from primary amide (R-C=O – NH2), 6940 cm^{-1} was O-H (2ν) carbohydrates (C4 hydroxyl within a crystalline matrix) Crystalline sucrose, 6916 cm^{-1} was C-H combination, ArC-H, 6897 cm^{-1} was O-H (2ν) (-CH_2-OH), Primary alcohols and H2O or C=O (4ν), 6850 cm^{-1} was cm^{-1} O-H (2ν) intra-molecularly bonded from diols, 6835 cm^{-1} was N-H (2ν),.$CONH_2$, 6812 cm^{-1} was O-H (2ν) (-C-OH), Tertiary alcohols, 6711 cm^{-1} was N-H (2ν), .CONHR, 7100-6240 cm^{-1} was 2νO-H of different aggregates, such as monomers, dimers, and polyols, 6850-6240 cm^{-1} was O-H (2ν) from hydrogen-bonded alkyl alcohols as (R-C-OH), 6540–6250 cm^{-1} was N-H (2ν) stretching from secondary amide in proteins. 5137.44-5133.58 cm^{-1} include the O-H stretching & HOH bending combination from Polysaccharides, C=O (3ν), .C=OOR of Acids and esters. 4647.6-4589.75 cm^{-1} include the C-H stretching & C=O stretching combination & C-H deformation combination from lipids. In addition, 4026.64-4011.21 cm^{-1} was used for distinguishing regions in this study, in which approximately 6320 cm^{-1} was N-H (2ν), CONHR was amide or protein, and approximately 6256 cm^{-1} was C=O/N-H [Amide I ($2\nu_s$ C=O stretching) & 3×amide II (N-H in–plane bending) combination] from polyamide and ammonia in water, approximately 6200 cm^{-1} and 6180 cm^{-1} were C-H, vinyl on O (1-ethenyloxybutane) as (CH_2=CH-C=O-) (e.g., vinyl as 1-ethenyl oxybutane

(1-ethenyl-methyl-ethyl-ketone) and polyamide). However, the band at 4026.64-4011.21 cm^{-1} mainly included the C-N-C (2v) of proteins at approximately 4049 cm^{-1}, the C-H stretching and C-C stretching combination of cellulose was at 4019 cm^{-1}, and the band at approximately 4000 cm^{-1} was the C-H stretching and C-C and C-O-C stretching combination of polysaccharides (Workman & Weyer, 2012).

For HPLC fingerprints, the peak areas and their relative retention times were satisfied via common peak identification. The results showed that 23 chromatography peaks had strong phylogenetic signals, 15 chromatography peaks had significant correlations with regions, and 9 peaks were commonly extracted by phylogenetic and VIP analysis (Figure 3.14c and 3.14d and 3.27c; appendix Table H and L). The red line in figure 3c shows that the peaks 1-5, 8-10, 12-16, 18-21, 24-25 and 27-30 were strongly correlated with phylogenetic signals, among which peaks 8, 9 and 10 were identified as uridine, guanosine and adenosine. The red line in figure 3d shows that peaks 1-2, 4-9, 12, 15, 20, 22, 27 and 29 were significantly correlated with regions, of which peaks 8 and 9 were identified as uridine and guanosine (Guo, Sun et al., 2022; Wang et al., 2021).

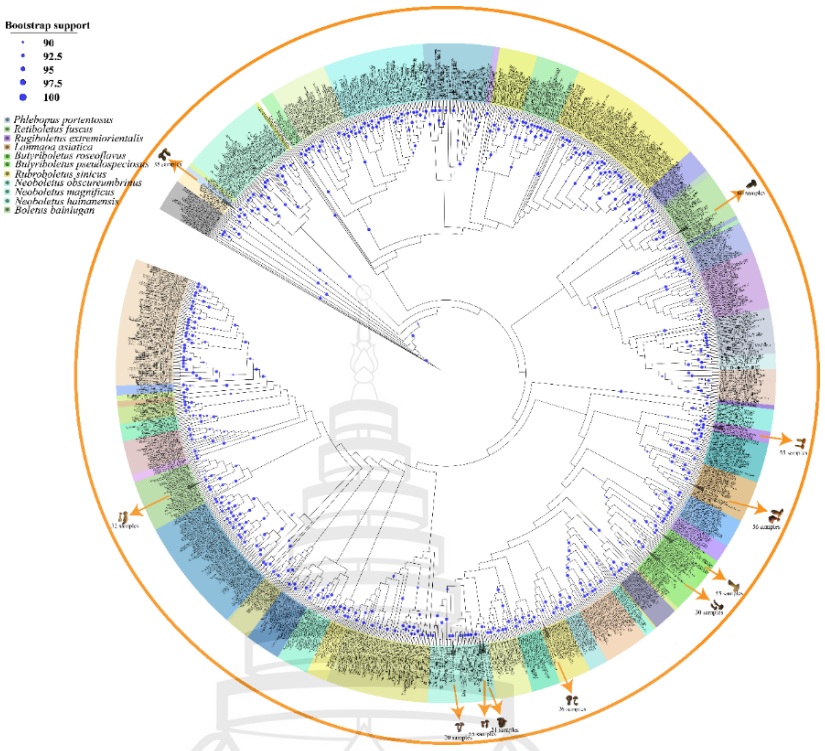
Among the 99 volatile compounds detected by GC–MS, 23 compounds had strong phylogenetic signals (such as hexadecanoic acid, tetracosane, tetradecanoic acid, phenanthrene, 2-hydroxy- propanenitrile, 1, 6-cyclodecadiene, methyl hexadecanoate, nerolidol, 2-acetyl pyrrole, 9,12-Octadecadienoicacid, methyl ester, (9E,12E)--methyl ester, Benzo[c] thiophene, diphenylamine, linoelaidic acid, (Z)-9-Hexadecenoic acid, 2-methyl-butanoic acid, tetradecanamide, dibutyl phthalate, 7,9-di-tert-butyl-1-oxaspiro(4,5)d, 1,4-xylene, gamma-Linolenic acid, Methyl 9-(Z)-octadecenoate, (Z)-9-octadecen-4-olide, 1-nonanal*etc*., K>1.0) and 21 compounds (K>0.9) were common constituents (figure 3.27d, and figure J1; tables H and L1). Some of these compounds have been found in porcini mushrooms, such as 2-methylpyrazine, 1, 4-xylene, 2, 6-dimethylpyrazine, 2-pentylfuran, phenylacetaldehyde, (E)-2-octenal, acetophenone, 1-nonanal, dodecane, tridecane, linoelaidic acid and tetradecanoic acid (Bartkiene et al., 2022; Nofer et al., 2018; Zhang, Pu et al., 2018; Aprea et al., 2015; Bozok et al., 2015). Pyrazines are typical Maillard

reaction products, e.g. 2,6-dimethylpyrazine. Phenolic components are characterized by powerful aroma characteristics with smoky, pungent, cresolic, and heavy burnt notes, which were previously detected in thermal processing vegetables and considered to stem from ferulic acid or sinapic acid, e.g. 2,4-di-tert-butylphenol (Zhang, Huang et al., 2020; Yu et al., 2008). Alkylpyrazine components have been considered to decrease the intensity of the roasted character of peanut samples, e.g. 2-methylpyrazine and 2,6-dimethylpyrazine (Lee et al., 2014; Xiao et al., 2014). 1-Octen-3-ol known as "mushroom alcohol", has been detected in large amounts in mushroom tissues and exhibits a typical mushroom-like earthy odour (Grosshauser & Schieberle, 2013). 2-Pentylfuran could lead to a beany or grassy note as the typical linoleic degradation product (Larrauri et al., 2016).

3.5 Construction of Chemical Evaluation Models of Wild Edible Boletes

3.5.1 Collection of Bolete Mushrooms

According to table O1 and Figure 3.28 and 3.29, 445 specimens including 32, 55, 30, 56, 21, 35, 55, 60, 26, 20 and 55 of the species of BoB, BuR, BuP, LA, NO, PP, RugE, RetF, RubS, NH and NM, respectively, were collected from Yunnan and Sichuan provinces in Southwest China. There were more than three specimens collected from the same sites at the same time points and the altitude ranged from 553 m to 3283 m.



Note One *Gyroporus* species of Gyroporaceae and two *Tricholomopsis* species were used as outgroups. All generic clades, including one undescribed generic clade in Boletaceae that was highly supported, also collapsed. Bootstrap support values (BS ≥ 90%) are shown above the supported branches

Figure 3.28 Phylogenetic tree of selected Boletaceae using maximum likelihood inferred from the two-gene dataset (*tef1* and *rpb2*)

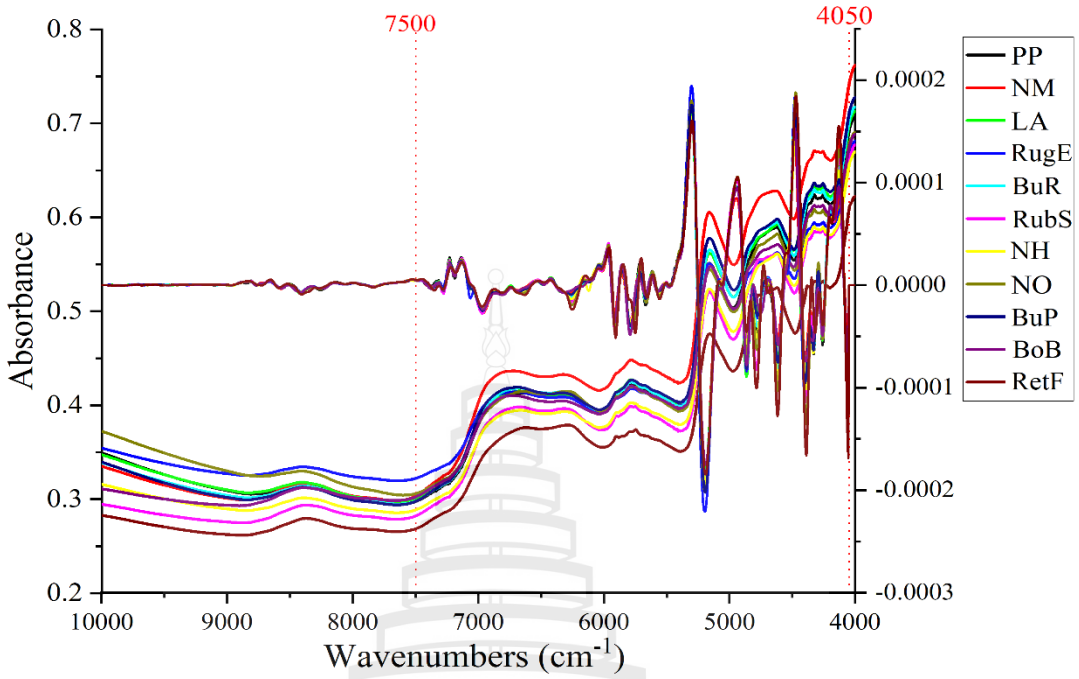


Figure 3.29 The original spectrum and second derivative spectrum of the Fourier Near Infrared spectrum of boletes

3.5.2 Volatile Compounds in Raw Bolete Mushrooms

A total of 97 VOCs were identified exactly or tentatively by SDE-GC-MS in raw boletes of 11 species, including 8 amines, 4 alcohols, 5 arenes, 10 aldehydes, 11 organic acids, 10 ketones, 18 alkanes, 13 heterocyclic compounds, and 18 esters. With only a few exceptions (such as 2-methyl-butyric acid in *Butyriboletus roseoflavus*), all 96 VOCs were detected in 11 bolete species. The results showed that the kinds of VOCs were similar, while the contents of VOCs were significantly different among different species of boletes. Among these VOCs, organic acids, such as the contents of hexadecanoic acid, linoelaidic acid and 9-octadecenoic acid, (E)- were significantly higher than others (Table 3.13).

Table 3.19 The ROAV of 44 volatile compounds in 11 species of boletes

Volatile compounds	RT (min)	CAS#	Threshold (mg/kg)	ROAV (%)										
				BoB	BuR	BuP	LA	NO	PP	RugE	RetF	RubS	NH	NM
Pyridine (Piccino et al., 2014)	3.17	110-86-1	2.0000	0.004	0.002	0.019	0.011	0.040	0.007	0.003	0.006	0.039	0.014	0.011
Pyrrole (Piccino et al., 2014)	3.23	109-97-7	20.0000	0.000	0.000	0.003	0.001	0.009	0.000	0.001	0.000	0.005	0.002	0.001
Toluene (Sinuco et al., 2021)	3.46	108-88-3	0.0730	0.251	0.266	0.692	0.290	0.550	0.456	0.047	0.230	0.726	0.667	0.371
Hexanal (Yuan et al., 2022)	3.94	66-25-1	0.5800	0.063	0.037	0.109	0.054	0.073	0.054	0.076	0.061	0.095	0.221	0.138
Furfural (Gemert, 2011)	4.51	98-01-1	2.8000	0.005	0.004	0.080	0.021	0.100	0.010	0.019	0.007	0.117	0.039	0.012
3-Methylbutanoic acid (Czerny et al., 2008)	4.61	503-74-2	0.0410	0.295	0.275	3.332	1.242	3.945	4.472	0.387	0.415	5.121	0.675	0.627
2-Methyl-butyric acid (Czerny et al., 2008; Giri et al., 2010)	4.89	116-53-0	2.2000	0.000	0.000	0.008	0.004	0.031	0.004	0.001	0.004	0.016	0.005	0.005
2-Heptanone (Yuan et al., 2022)	5.73	110-43-0	0.1400	0.029	0.015	0.134	0.048	0.014	0.190	0.008	0.033	0.086	0.207	0.076
1,2-Xylene (Giri et al., 2010)	5.84	95-47-6	0.4502	0.006	0.008	0.021	0.011	0.03	0.011	0.008	0.008	0.032	0.025	0.018
Methional (Giri et al., 2010)	6.15	3268-49-3	0.0005	83.933	66.452	77.475	85.355	26.391	68.582	9.196	40.514	48.93	86.095	71.514
(1R)-(+)-alpha-pinene (Czerny et al., 2008)	6.86	7785-70-8	0.0022	1.177	1.301	25.925	4.64	14.76	10.167	5.928	3.93	20.783	50.09	19.119
5-Methyl furfural (Boonbumrung et al., 2001)	7.55	620-02-0	1.1100	0	0	0.006	0.003	0.011	0.001	0.002	0.002	0.021	0.007	0.004
Benzaldehyde (Yuan et al., 2022)	7.61	100-52-7	0.0030	7.9	13.339	15.113	14.901	10.021	9.814	5.228	8.032	17.848	13.77	6.982
1-Decen-3-one (Yuan et al., 2022)	7.98	56606-79-2	0.0050	15.345	39.533	2.108	11.665	22.226	2.527	13.778	12.814	20.227	16.396	4.229
1-Octen-3-ol (Yuan et al., 2022)	8.08	3391-86-4	0.0010	100	100	100	100	100	100	100	100	100	100	100

Table 3.19 (continued)

Volatile compounds	RT (min)	CAS#	Threshold (mg/kg)	ROAV (%)										
				BoB	BuR	BuP	LA	NO	PP	RugE	RetF	RubS	NH	NM
2-Pentylfuran (Yuan et al., 2022)	8.34	3777-69-3	0.0060	31.399	33.867	78.103	31.303	59.868	58.835	5.297	30.199	71.836	69.467	51.006
Decane (Yuan et al., 2022)	8.63	124-18-5	0.0030	15.375	15.622	29.782	13.328	23.79	21.182	3.183	12.325	25.914	26.748	19.413
2-Acetylthiazole (Schlutt et al., 2007)	9.19	24295-03-2	0.0030	1.227	2.7	2.104	1.573	2.314	1.792	0.208	0.783	1.047	3.167	2.113
Phenylacetaldehyde (Mishra et al., 2020)	9.9	122-78-1	0.0063	1.834	1.436	17.197	5.85	14.188	3.913	3.4	5.052	12.945	20.913	11.505
(E)-2-Octenal (Yuan et al., 2022)	10.27	2548-87-0	0.0030	11.501	9.128	11.619	7.54	3.385	11.925	10.072	8.33	12.255	6.952	12.508
2-Acetyl pyrrole (Giri et al., 2010)	10.41	1072-83-9	58.5853	0	0	0	0	0.001	0	0	0	0.001	0.001	0
Acetophenone (Schirack et al., 2006)	10.53	98-86-2	0.0650	0.7	0.184	1.138	0.321	0.189	0.499	0.915	0.51	0.683	0.816	0.755
Tetramethylpyrazine (Giri et al., 2010)	11.02	1124-11-4	2.5250	0.004	0.015	0.014	0.006	0.03	0.012	0.008	0.008	0.038	0.011	0.007
1-Nonanal (Giri et al., 2010)	11.65	124-19-6	0.0011	15.846	14.727	38.269	10.422	25.244	13.93	3.859	11.08	21.451	41.294	12.19
Dodecane (Gemert, 2011)	14.42	112-40-3	10.000	0.011	0.01	0.024	0.01	0.019	0.016	0.003	0.008	0.02	0.02	0.013
Indole (Boonbumrung et al., 2001)	17.08	120-72-9	0.0110	0.191	0.13	0.842	0.746	1.434	0.18	0.457	0.346	2.412	1.396	0.403
Tetradecane (Gemert, 2011)	19.89	629-59-4	1.0000	0.03	0.029	0.083	0.031	0.055	0.041	0.012	0.029	0.061	0.065	0.042
2,4-Di-tert-butylphenol (Gemert, 2011)	22.58	96-76-4	0.5000	0.151	0.102	0.425	0.098	0.397	0.19	0.017	0.064	0.349	0.233	0.124
Nerolidol (Gemert, 2011)	23.89	7212-44-4	2.2500	0.011	0.013	0.048	0.026	0.204	0.015	0.003	0.014	0.083	0.066	0.022
Hexadecane (Gemert, 2011)	24.83	544-76-3	1.1000	0.008	0.007	0.03	0.01	0.019	0.011	0.012	0.01	0.019	0.022	0.019

Table 3.19 (continued)

Volatile compounds	RT (min)	CAS#	Threshold (mg/kg)	ROAV (%)										
				BoB	BuR	BuP	LA	NO	PP	RugE	RetF	RubS	NH	NM
Diphenylamine (Gemert, 2011)	25.35	122-39-4	1.3000	0.012	0.014	0.013	0.008	0.007	0.014	0.002	0.015	0.015	0.025	0.016
(2E,6E)-3,7,11-Trimethyl-2,6,10-dodecatrien-1-ol (Gemert, 2011)	27.52	4602-84-0	1.0000	0.096	0.075	0.703	0.268	0.656	0.136	0.075	0.149	0.655	0.564	0.33
Tetradecanoic acid (Gemert, 2011)	28.46	544-63-8	10.000	0.011	0.011	0.038	0.02	0.029	0.013	0.006	0.014	0.033	0.046	0.026
Phenanthrene (Gemert, 2011)	28.93	85-01-8	1.0000	0.009	0.01	0.042	0.02	0.048	0.007	0.019	0.012	0.056	0.051	0.026
Methyl hexadecanoate (Gemert, 2011)	31.78	112-39-0	2.0000	0.018	0.019	0.033	0.019	0.021	0.015	0.011	0.014	0.018	0.03	0.019
(Z)-9-Hexadecenoic acid (Gemert, 2011)	32.14	373-49-9	11.0000	0.018	0.02	0.145	0.036	0.083	0.026	0.017	0.028	0.086	0.085	0.051
Dibutyl phthalate (Gemert, 2011)	32.27	84-74-2	0.2600	0.483	0.585	2.49	0.802	2.413	0.508	0.236	0.392	2.164	1.591	0.777
Hexadecanoic acid (Gemert, 2011)	32.66	57-10-3	10.0000	0.545	0.671	1.308	0.808	1.005	0.569	0.334	0.62	1.102	1.409	1.037
Hexadecanoic acid-ethyl ester (Pino & Mesa, 2006)	32.92	628-97-7	2.0000	0.062	0.075	0.169	0.109	0.25	0.079	0.045	0.071	0.209	0.195	0.122
(9E,12E)-Octadeca-9,12-dienoic acid (Gemert, 2011)	33.62	60-33-3	100.00	0.001	0.001	0.003	0.002	0.002	0.004	0.001	0.001	0.003	0.004	0.003
Heptadecanoic acid (Gemert, 2011)	33.98	506-12-7	20.000	0.002	0.002	0.009	0.003	0.005	0.006	0.001	0.003	0.012	0.012	0.007
2(3H)-Furanone, 5-dodecyldihydro- (Schlutt et al., 2007)	34.46	730-46-1	89.000	0	0	0.003	0.001	0.004	0.001	0	0.001	0.004	0.003	0.002

9,12-Octadecadienoic acid (Z,Z)-, ethyl ester (Gemert, 2011)	35.16	544-35-4	0.4500	0.614	0.543	2.011	0.921	1.281	1.183	0.506	0.632	1.83	1.908	0.961
Ethyl Oleate (Gemert, 2011)	35.24	111-62-6	0.8700	0.313	0.235	0.21	0.514	1.75	0.324	0.15	0.225	1.463	0.737	0.284

3.5.3 Classification of Volatile Compounds by PCA

To more directly observe and explain the relationships of characteristic VOCs among bolete species, after homogenization, a PCA of VOCs in different species was conducted, and the results are shown in figure 3.30. The distribution map showed that the first two principal components accounted for 61.8% and 12.9% of the cumulative variance contribution rate, respectively. For the species of RugE and LA, the PCA results clearly showed that compounds such as benzaldehyde, 5-methyl-furfural, and 2, 6-dimethylpyrazine contributed to the classification of RugE, while the compounds including decane, dodecane, 9,12-Octadecadienoicacid, methyl ester, (9E,12E)-, 9,12-Octadecadienoicacid, methyl ester, (9E,12E)- methyl ester, and tetradecane played an important role in the classification of LA. Additionally, LA could be well distinguished according to the positive scores of PC1, while RugE could be well defined according to the negative scores of PC1. There was great overlap among the species, which indicated that PCA did not successfully discriminate the different bolete species based on 97 VOCs. However, there was a classification trend among species suggesting that these compounds might have different influences on the classification of different bolete species (Guo, Adelina et al., 2022; Li, Wu et al., 2021; Li, Wang et al., 2021; Jung et al., 2019). The results of PCA indicated that unsupervised analytical methods could preliminarily screen volatile components as features for the initial identification of boletus species. However, the identification efficacy was unsatisfactory and required further optimization.

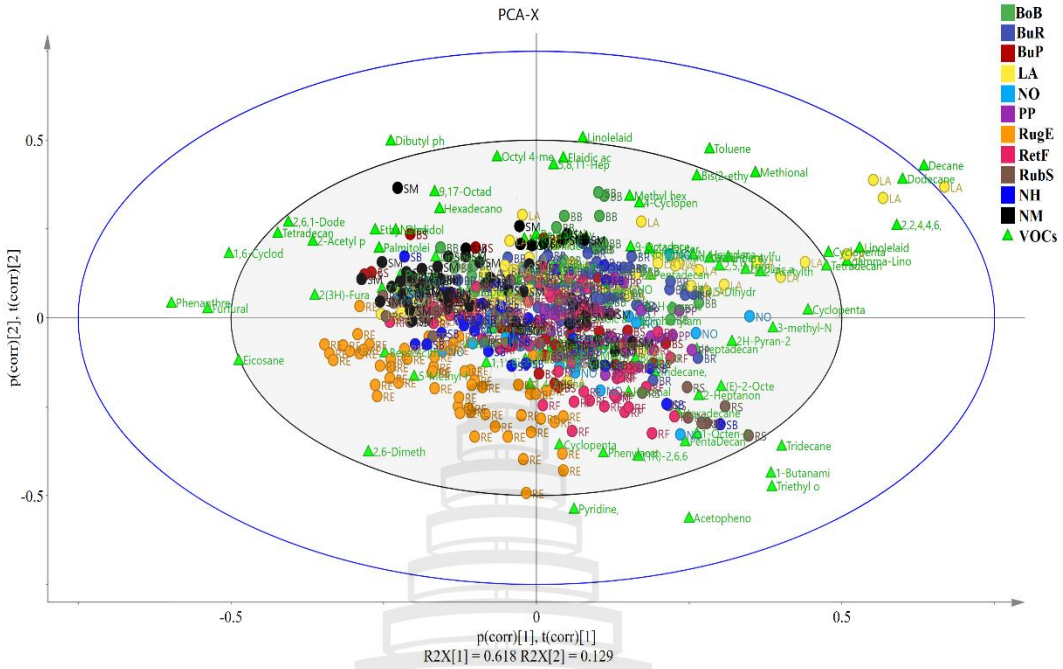


Figure 3.30 PCA loading plot of the correlation between the species of boletes and volatile compounds

3.5.4 VIP-PLS-DA Model

Further, supervised PLS-DA was performed on 97 volatiles to identify potential differences among the bolete species. The VOCs were deemed significantly different according to a variable importance in projection (VIP) value > 1 and $P < 0.05$ (Giannetti et al., 2017).

All PLS-DA models were validated based on R^2 (total variance) and Q^2 (goodness parameters) values. A total of 22 VOCs with VIP > 1 were obtained as potential markers for the classification of 11 species. These VOCs were 1-decen-3-one, methional, toluene, 2H-pyran-2-one,5,6-dihydro-, 2-pentylfuran, nerolidol, triethyl-orthoformate, hexadecanoic acid, 2,6-dimethylpyrazine, furfural, 1,6-cyclodecadiene, 1,4-xylene, methyl (9E)-9-octadecenoate, 9-octadecenoic acid,(E)-, (Z)-9-hexadecenoic acid, diisobutyl phthalate, tridecane,3-methyl-, 5,8,11-heptadecatrienoic acid methyl ester, (9E,12E)-octadeca-9,12-

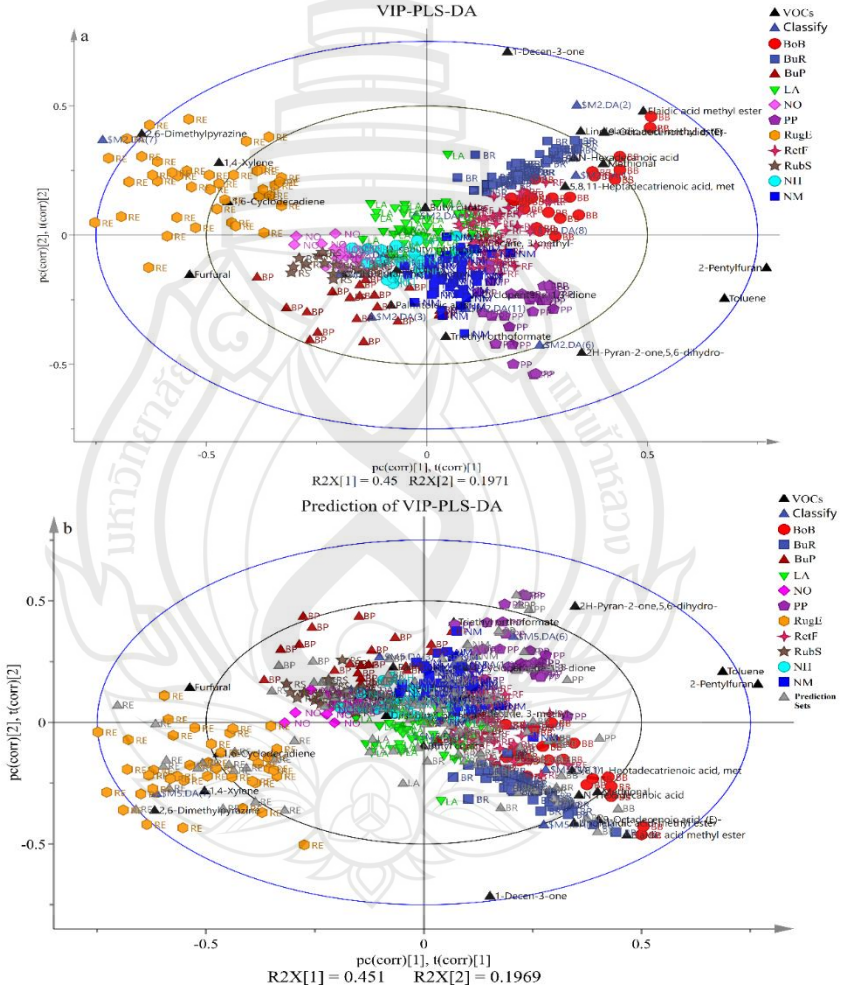
dienoic acid methyl ester, butyl-citrate, 2-cyclopentene-1,4-dione, and 2(5H)-furanone,3-methyl-. The R^2, Q^2, RMSECV and RMSEP values were 0.987, 0.901, 0.363, and 0.555, respectively (Figure 3.31a and Table 3.14). The permutation test (200 permutations) was used to confirm the validity and predictive ability of the model ($R^2 < 0.5$; $Q^2 < 0$; appendix Figure Pa). In addition, the remaining samples (130 samples) were predicted based on the identified model shown in Figure 3.31b, and the results of the prediction are shown in table 3.15. Values of *Sen*, *Spe*, *Eff* and *Acc* calculated based on the test set were 0.63-0.93, 0.95-1.00, 0.97-1.00 and 0.95-0.99, respectively. According to the above results, the 11 species of boletes could be discriminated by 22 VOCs. The accuracy of identification was 62.5 % -100 %, which suggested that the verification effect was satisfactory. Moreover, most of these compounds were consistent with previous studies reporting the characteristic VOCs in mushrooms, such as 1-decen-3-one (Ibrahimi et al., 2020), methional (Cho, Choi et al., 2006), toluene (Tagkouli et al., 2021), 2-pentylfuran (Zhang, Huang et al., 2020), and 2,6-dimethylpyrazine (Zhang, Huang et al., 2020). The results indicated that these VOCs were potential indicators for distinguishing the species of boletes, and the method of PLS-DA combined with VIP was an effective tool for the discrimination of species.

Table 3.20 The training results of the VIP-PLS-DA model

	BoB	**BuR**	**BuP**	**LA**	**NO**	**PP**	**RugE**	**RrtF**	**RubS**	**NH**	**NM**
BoB	17	3	0	0	0	0	0	2	0	0	0
BuR	0	40	0	0	0	0	0	0	0	0	0
BuP	0	1	18	1	0	1	0	0	0	0	0
LA	0	3	1	33	0	0	3	0	0	0	0
NO	0	0	1	0	12	0	2	0	0	0	0
PP	0	0	0	0	0	23	0	1	0	0	0
RugE	0	0	0	0	0	0	38	0	0	0	0
RetF	2	2	0	0	0	1	0	38	0	0	1
RubS	0	0	1	0	0	0	1	0	15	0	1
NH	0	1	0	0	0	1	0	0	0	11	0

Table 3.20 (continued)

	BoB	BuR	BuP	LA	NO	PP	RugE	RrtF	RubS	NH	NM
NM	0	1	1	1	0	1	0	0	0	0	35
Sen	0.77	1.00	0.87	0.83	0.80	0.96	1.00	0.86	0.83	0.79	0.90
Spe	0.99	0.96	0.98	0.99	1.00	0.98	0.98	0.99	1.00	1.00	0.99
Eff	8.25	8.35	8.33	8.23	8.30	8.28	8.35	8.23	8.28	8.30	8.28
Acc	0.98	0.97	0.98	0.97	0.99	0.98	0.98	0.97	0.99	0.99	0.98



Note (a) Classification model and (b) prediction model of 11 species of boletes established based on 22 volatile compounds with VIP greater than 1 by PLS-DA

Figure 3.31 Classification and prediction models of boletes established by PLS-DA

Table 3.21 The validation results of VIP-PLS-DA model

	BoB	**BuR**	**BuP**	**LA**	**NO**	**PP**	**RugE**	**RrtF**	**RubS**	**NH**	**NM**
BoB	9	1	0	0	0	0	0	0	0	0	0
BuR	1	14	0	0	0	0	0	0	0	0	0
BuP	0	0	8	0	0	1	0	0	0	0	0
LA	0	1	1	13	0	0	1	0	0	0	0
NO	0	0	1	0	4	0	1	0	0	0	0
PP	1	1	0	0	0	8	1	0	0	0	0
RugE	0	0	0	0	0	0	17	0	0	0	0
RetF	0	1	1	1	0	1	0	12	0	0	0
RubS	0	0	2	0	0	0	1	0	5	0	0
NH	0	1	1	0	0	0	0	0	0	4	0
NM	0	0	0	1	0	1	0	0	0	0	14
Sen	0.90	0.93	0.89	0.81	0.67	0.73	1.00	0.75	0.63	0.75	0.88
Spe	0.98	0.96	0.95	0.98	1.00	0.98	0.97	1.00	1.00	1.00	1.00
Eff	0.99	0.99	0.99	0.98	0.98	0.98	1.00	0.97	0.98	0.98	0.98
Acc	0.98	0.95	0.95	0.96	0.98	0.96	0.97	0.96	0.98	0.99	0.99

3.5.5 ROAV-PLS-DA Model

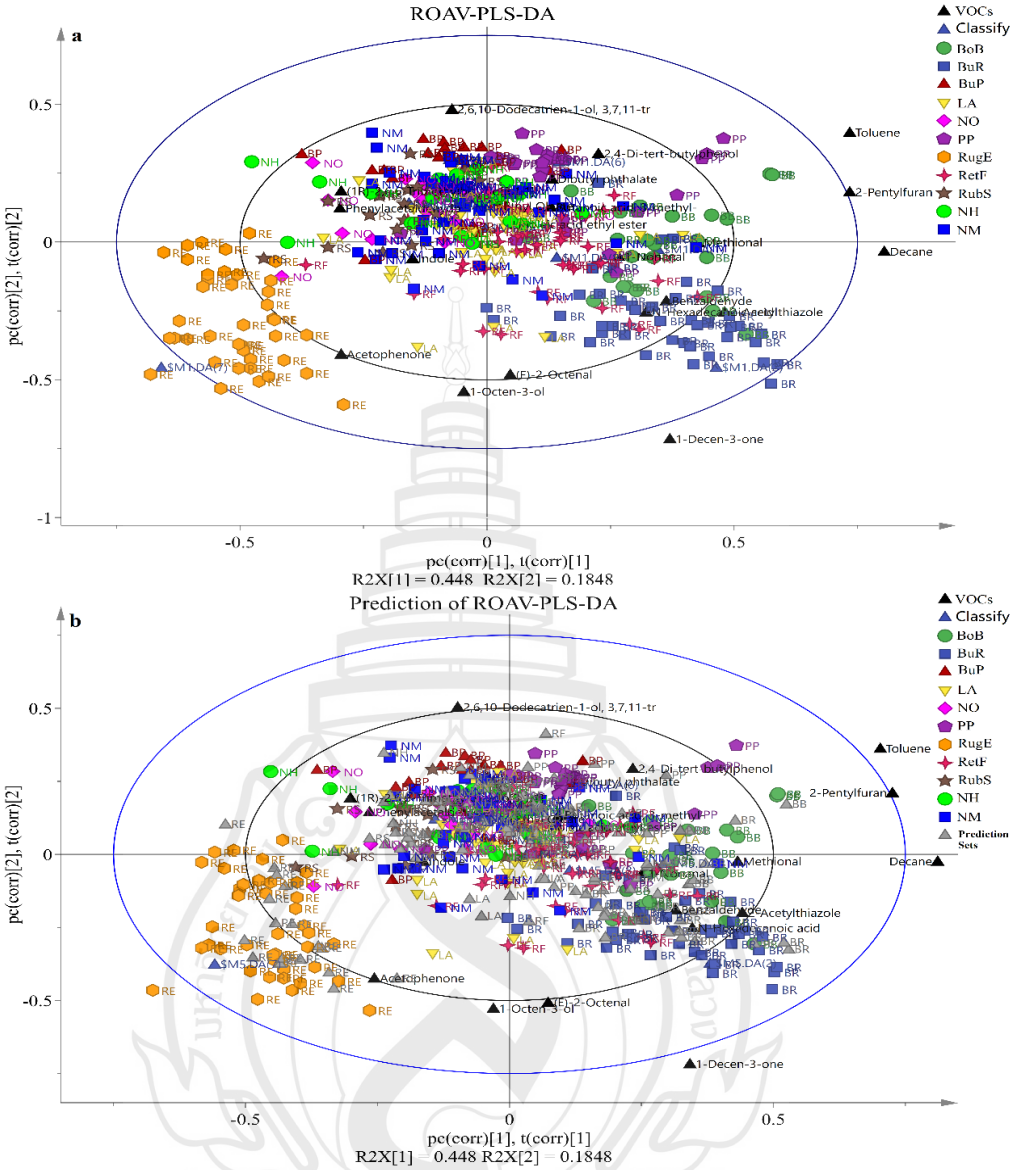
The ultimate contribution of VOCs to the overall aroma of a species depends not only on their concentrations but also on their odor threshold values. Volatile compounds with OAVs greater than 1.0 are generally considered to be likely contributors to characteristic aromas (Zhang, Huang et al., 2020). Based on the quality percentage analysis and literature reported for each volatile compound, a total of 44 VOCs were extracted, and ROAV was calculated as a new parameter for identification of boletes species. The published threshold value and the calculated ROAV for each compound are listed in Table 3.13. Normally, aroma compounds with high ROAVs (greater than 1) are treated as the major contributors to the overall aroma (Wei et al., 2019, 2020). Components with ROAVs between 0.1 and 1 could be considered to play a role in the overall aroma (Fan et al., 2019).

According to the calculated values, 11 compounds with ROAVs greater than 1 contributed significantly to the overall aroma of boletes, including 1-octen-3-ol, methional, 2-pentylfuran, 1-decen-3-one, 1-nonanal, decane, (E)-2-octenal, benzaldehyde, phenylacetaldehyde, (1R)-(+)-

alpha-pinene, and 2-acetylthiazole. Ten VOCs with ROAVs greater than 0.1 and lower than 1 also played a role in the overall aroma profiles, which included 9-octadecenenitrile,(E)-, indole, acetophenone, dibutyl-phthalate, ethyl-oleate, 3-methylbutanoic acid, hexadecanoic acid, toluene, (2E,6E)-3,7,11-Trimethyl-2,6,10-dodecatrien-1-ol and 2,4-di-tert-butylphenol. These 21 VOCs with ROVA greater than 0.1 acted as new variable datasets and were used for further analysis.

PLS-DA was carried out to gain insight into the relationship between boletes species and 21 VOCs. As shown in figure 3.32a, acetophenone had a significant influence on the classification of RE; 2,4-di-tert-butylphenol and dibutyl phthalate made an important contribution to the classification of PP; and hexadecanoic acid, benzaldehyde and 2-acetylthiazole were important factors in classifying BuR. Moreover, the compounds toluene, 2-pentylfuran, methional and decane may be key factors in the identification of BoB. These results were similar to the classification according to the PLS-DA combined with VIP. The values of R^2, Q^2, RMSECV and RMSEP were 0.974, 0.895, 0.397 and 0.608, respectively (Figure 3.32b and Table 3.16). The permutation test (200 permutations) was used to confirm the validity and predictive ability of the model ($R^2 < 0.5$; $Q^2 < 0$; appendix Figure Pb). Similarly, the remaining samples (130 samples) were predicted based on the distinguished model shown in Figure 3.32b and the results of the prediction are shown in table 5. The *Sen*, *Spe*, *Eff* and *Acc* values were 0.63-1.00, 0.95-1.00, 0.95-1.00 and 0.91-0.98 based on the test set, respectively. Based on the above results, the 11 species of boletes could be discriminated based on 21 VOCs. The accuracy of identification was 62.5 % to 100 %, which suggested that the verification effect was satisfactory. The test results indicated that the compounds with ROAVs larger than 0.1 could effectively classify the species of boletes, and might be potential markers for identifying the species of boletes.

As mentioned above, both models of VIP-PLS-DA and ROVA-PLS-DA (Figure 3.31 and 3.32, Table 3.13 and 3.17) showed good ability of classification and prediction of boletes species.



Note (a) Classification and (b) prediction models of 11 species of Boletes established based on 21 volatile compounds by ROAV-PLS-DA

Figure 3.32 Classification and prediction models of boletes established by ROAV-PLS-DA

Table 3.22 The training results of the ROAV-PLS-DA model

	BoB	**BuR**	**BuP**	**LA**	**NO**	**PP**	**RugE**	**RrtF**	**RubS**	**NH**	**NM**
BoB	17	3	0	1	0	0	0	1	0	0	0
BuR	0	40	0	0	0	0	0	0	0	0	0
BuP	0	1	15	1	0	1	0	0	0	0	3
LA	1	3	0	30	0	0	3	1	0	0	2
NO	0	1	0	1	10	0	2	0	0	0	1
PP	1	1	0	0	0	19	1	1	0	0	1
RugE	0	0	0	0	0	0	38	0	0	0	0
RetF	1	3	0	1	0	1	1	34	0	0	3
RubS	0	0	0	2	0	1	3	0	10	0	2
NH	0	1	0	1	0	0	1	0	0	11	1
NM	2	1	0	0	0	2	2	3	0	0	29
Sen	0.77	1.00	0.71	0.75	0.67	0.79	1.00	0.77	0.56	0.65	0.74
Spe	0.98	0.95	1.00	0.97	1.00	0.98	0.96	0.98	1.00	1.00	0.95
Eff	0.98	1.00	0.98	0.97	0.98	0.98	1.00	0.97	0.97	0.98	0.97
Acc	0.97	0.96	0.98	0.94	0.98	0.97	0.96	0.95	0.97	0.98	0.93

Table 3.23 The validation results of the ROAV-PLS-DA model

	BoB	**BuR**	**BuP**	**LA**	**NO**	**PP**	**RugE**	**RrtF**	**RubS**	**NH**	**NM**
BoB	7	0	0	0	0	0	0	3	0	0	0
BuR	0	15	0	0	0	0	0	0	0	0	0
BuP	0	0	7	0	0	1	0	0	0	0	1
LA	0	0	2	11	0	0	1	1	0	0	1
NO	0	0	0	1	4	0	1	0	0	0	0
PP	1	0	0	0	0	8	0	2	0	0	0
RugE	0	0	0	0	0	0	17	0	0	0	0
RetF	0	1	0	1	0	1	1	10	0	0	2
RubS	0	0	0	1	0	0	1	0	5	0	1
NH	0	1	1	0	0	0	0	0	0	4	0
NM	1	1	0	0	0	1	0	1	0	0	12
Sen	0.70	1.00	0.78	0.69	0.67	0.73	1.00	0.63	0.63	0.63	0.75
Spe	0.98	0.98	0.98	0.97	1.00	0.98	0.97	0.94	1.00	1.00	0.95
Eff	0.98	1.00	0.98	0.96	0.98	0.98	1.00	0.95	0.98	0.98	0.97
Acc	0.96	0.98	0.96	0.94	0.98	0.96	0.97	0.91	0.98	0.98	0.93

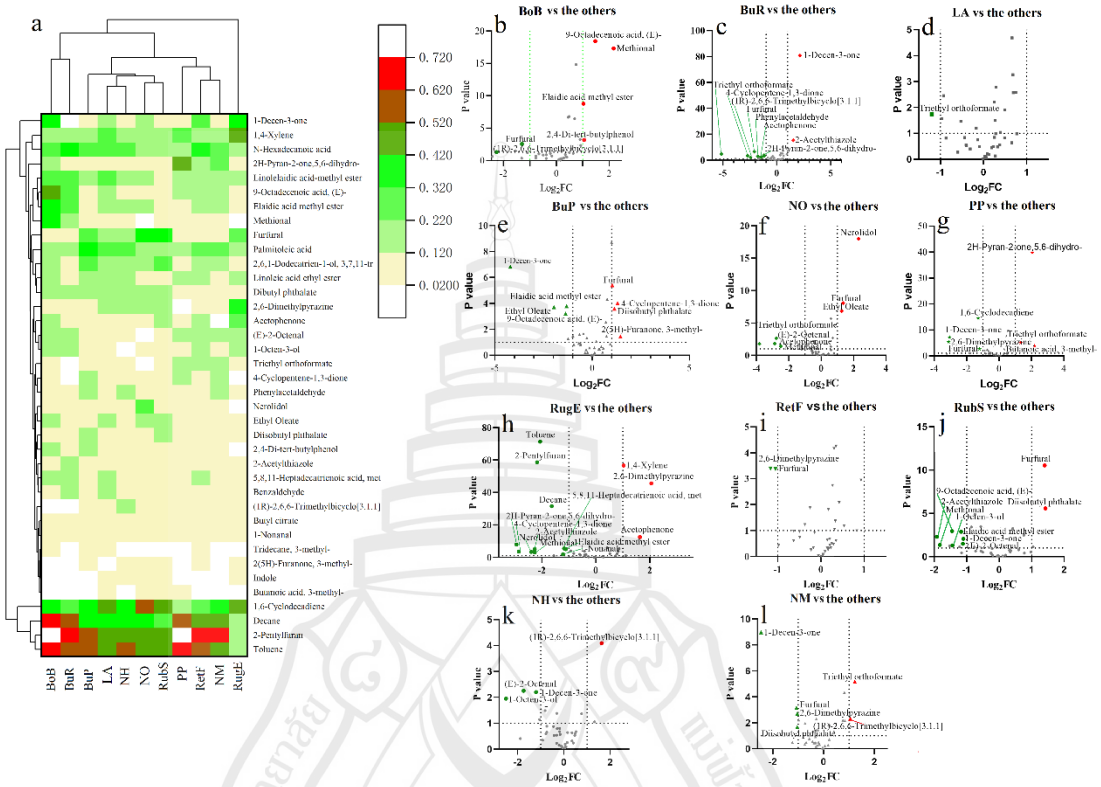
3.5.6 Selection of Markers of Interspecific Differences in Boletes

The correlated heatmap and volcano plots were carried out to explore the potential VOC markers of the species of boletes. A total of 38 compounds were selected for analyses based on the results of VIP (22 compounds) and ROAV (21 compounds) (including 5 common compounds, toluene, methional, 1-decen-3-one, 2-pentylfuran and hexadecanoic acid), as shown in Figure 3.33.

Figure 3.33 a shows the different contributions of the VOCs to the classification of the species of boletes. The compounds including toluene, 2-pentylfuram, decane, 1, 6-cyclodecadiene, 1, 4-xylene, Hexadecanoic acid, 9, 12-Octadecadienoicacid, methyl ester, (9E,12E)- methy ester, palmitoceic acid, etc. were the main factors influencing interspecific differences. To further confirm the classification effect of these VOCs for species of boletes, volcano plots were generated to analyze each independent species compared with the other 10 species (Figure 3.33 b-l). Figure 3.33 b shows that compared with the other 10 species of boletes, the percent composition of 4 VOCs (including 9-Octadecenoic acid, (E)-, methional, Methyl 9-(Z)-octadecenoate and 2,4-di-tert-butylphenol) was significantly higher than that of the other species in BoB. In contrast, 2 VOCs (furfural and (1R)-2, 6, 6-trimethylbicyclo [3.1.1]) showed significantly lower values than the other species. The results suggested that these compounds were important in distinguishing BoB from other species and could be considered characteristic markers. Figure 3.33c shows the comparison of BuR with other species. The values of 2 VOCs, 1-decen-3-one and 2-acetylthiazole were significantly higher than the others, while 7 VOCs, triethyl orthoformate, 2-Cyclopentene-1,4-dione, (1r)-(+)-alpha-pinene, furfural, phenylacetaldehyde, acetophenone and 2H-Pyran-2-one,5,6-dihydro- showed significantly lower values than the others. The results showed that these compounds could be used as markers to discriminate BuR from the other species of boletes. According to Figure 3.33 d, compared with the other species, the content of triethyl orthoformate was significantly lower in LA; hence, this compound was a key indicator for distinguishing LA from the others. In figure 3.33e, the contents of furfural, 2-Cyclopentene-1,4-dione, diisobutyl phthalate and 2(5H)-Furanone, 3-methyl- were

significantly higher in BuP than in the other species, while 4 VOCs, 1-decen-3-one, Methyl 9-(Z)-octadecenoate, ethyl-oleate and 9-Octadecenoic acid, (E)-, were significantly lower than those of the other species in BuP. In figure 3.33 f, the contents of nerolidol, furfural and ethyl-oleate were significantly higher than those of the others, and the contents of triethyl orthoformate, (E)-2-octenal, acetophenone and methonal were significantly lower than those of the other species in NO. Figure 3.33 g shows that in PP compared with the other species, the contents of 5, 6-dihydro-2H-pyran-2one, triethyl orthoformate, and 3-methylbutanoic acid were significantly higher than those of the other species. Conversely, 1, 6-cyclodecadiene, 1-decen-3-one, 2, 6-dimethylpyrazine and furfural showed significantly lower values than the others. Figure 3.33 h shows that the compounds 1,4-xylene, 2, 6-dimethylpyrazine, acetophenone (upregulated), toluence, 2-pentyfuran, decane, met-5, 8, 11-heptadecatrienoic acid, 2H-Pyran-2-one,5,6-dihydro-, 2-Cyclopentene-1,4-dione, 2-acetylthiazole, nerolidol, methional, Methyl 9-(Z)-octadecenoate, and 1-nonanal (downregulated) were key factors in the separation of LA from the other species of boletes. Figure 3.33 i shows that the compounds of 2,6-dimethylpyrazine, and furfural (downregulated) were important differentiating factors for RetF. According to Figure 3.33 j, when discriminating RubS from the other species, furfural and diisobutyl phthalate showed significantly higher values than the others, but 9-Octadecenoic acid, (E)-, 2-acetylthiazole, methional, 1-octen-3-ol, Methyl 9-(Z)-octadecenoate, 1-decen-3-one and (E)-2-octenal showed lower values than the other species, which played a significant role in distinguishing RetF from the others. As presented in figure 3.33k, the compounds (1R)-2, 6, 6-trimethylbicyclo [3.1.1] presented significantly higher values, and the values of (E)-2-octenal, 1-decen-3-one, and 1-octen-3-ol in NH were significantly lower than those of the other species; thus, these compounds were the key factors for discriminating RubS from the other species of boletes. In addition, as shown in figure 3.33l, for the discrimination of NM and other species, the percent composition of 2 VOCs, triethyl orthoformate and (1R)-2, 6, 6-trimethylbicyclo [3.1.1], was significantly higher in NM than that of the others, and 4 VOCs (1-decen-3-one, furfural, 2, 6-dimethylpyrazine and diisobutyl phthalate) showed significantly lower values in NM than the others. The results suggested that these compounds could play a

crucial role in the discrimination of bolete mushrooms.



Note (a) Correlated heatmap between boletes species and VOCs; (b-l) volcano plots of VOCs and the relationships between BoB, BuR, LA, BuP, NO, PP, RugE, RetF, RubS, NH, SM and other species

Figure 3.33 Classification effects of volatile compounds on different species of boletes

3.5.7 Fisher's Linear Discriminant Function Analysis Based on the Characteristic Markers

To determine the contribution of characteristic markers to classification, the nine characteristic markers including (1R)-(+)-alpha-pinene, 1-decen-3-one, 2,6-dimethylpyrazine, methyl (9E)-9-octadecenoate, furfural, methional, triethyl orthoformate, 1-octen-3-ol, and (E)-2-octenal, based on the significant differences in more than 4 species or with

characteristic mushroom flavor, were subjected to Fisher's linear discriminant function analysis based on the above analyses. Five characteristic markers, methyl (9E)-9-octadecenoate (X_1), 2,6-dimethylpyrazine (X_2), 1-decen-3-one (X_3), furfural (X_4) and methional (X_5) were extracted as key markers for classification, When the first two eigenvalues (the cumulative contribution rate of 91.9 %) were 3.360 and 0.977, respectively. The Fisher's linear discriminant functions of 11 species were as follows:

$$Y_{BoB} = -12.292 + 1.214X_1 + 0.816X_2 + 1.778X_3 + 0.195X_4 + 1.153X_5;$$

$$Y_{BuR} = -21.698 + 1.373X_1 - 0.171X_2 + 3.274X_3 - 0.036X_4 + 0.802X_5;$$

$$Y_{BuP} = -4.997 + 0.166X_1 + 1.649X_2 + 0.036X_3 + 1.000X_4 + 0.241X_5;$$

$$Y_{LA} = -5.88 + 0.73X_1 + 2.729X_2 + 0.791X_3 + 0.578X_4 + 0.474X_5;$$

$$Y_{NO} = -7.739 + 0.47X_1 + 2.432X_2 + 0.549X_3 + 1.247X_4 + 0.229X_5;$$

$$Y_{PP} = -3.139 + 0.375X_1 + 0.174X_2 + 0.236X_3 + 0.245X_4 + 0.261X_5;$$

$$Y_{RugE} = -10.632 + 0.41X_1 + 6.712X_2 + 1.146X_3 + 0.829X_4 + 0.336X_5;$$

$$Y_{RetF} = -5.906 + 0.891X_1 + 0.629X_2 + 1.209X_3 + 0.195X_4 + 0.365X_5;$$

$$Y_{RubS} = -7.229 + 0.233X_1 + 2.817X_2 + 0.382X_3 + 1.286X_4 + 0.265X_5;$$

$$Y_{NH} = -4.716 + 0.465X_1 + 2.384X_2 + 0.451X_3 + 0.473X_4 + 0.237X_5;$$

$$Y_{NM} = -3.11 + 0.494X_1 + 1.179X_2 + 0.832X_3 + 0.254X_4 + 0.242X_5.$$

The results of the leave-one-out method for cross-verification showed that the precision rates of 11 species were 82.86%, 94.92%, 72.73%, 74.58%, 72.73%, 75.0%, 68.97%, 79.69%, 71.43%, 66.67% and 75.86%, respectively. The results suggested that the five characteristic markers played a crucial role in establishing the linear discriminant function of bolete mushrooms. In addition, the classifications of the 11 species could be quickly recognized according to the above equations. Therefore, these equations can be used as a basis for the rapid identification of bolete species in the future.

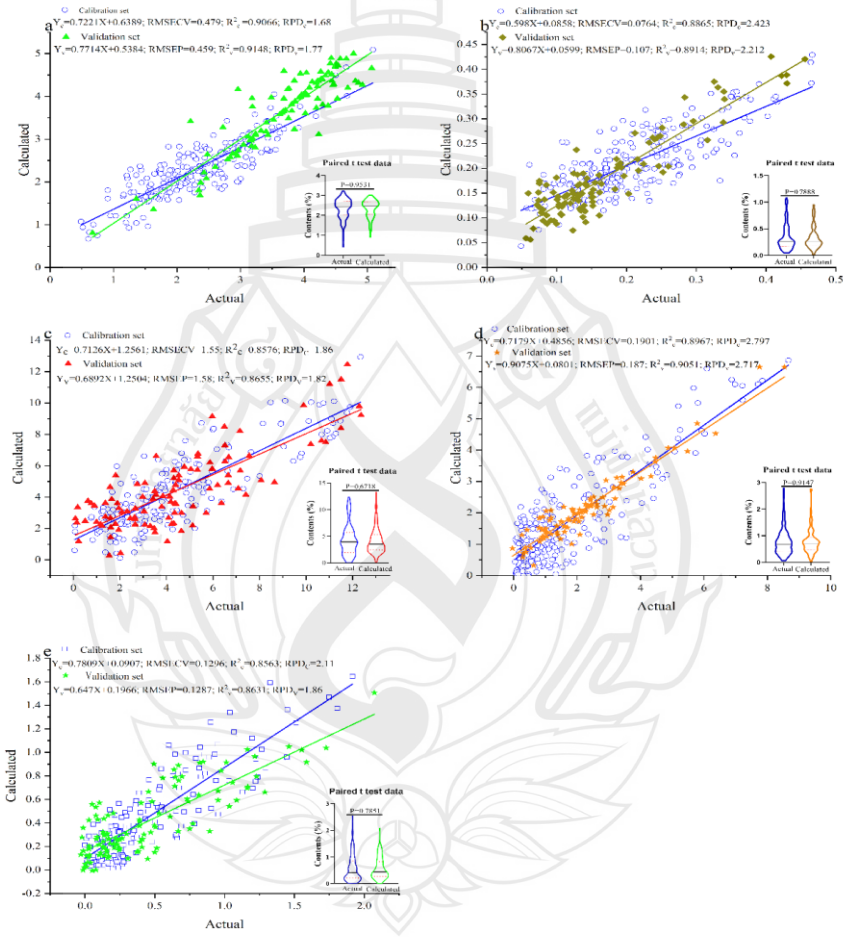
Moreover, some of those VOCs were confirmed in previous studies in which different contributions were attributed to aromas; for example, 2, 6-dimethylpyrazine, is best predicted as roasted and cacao-like (Zhang, Huang et al., 2020). 2 (5H)-furanone, furfural and phenylacetaldehyde are the major components of cooked mushrooms (Cho, Kim et al.,

2006). (1R)-2, 6, 6-trimethylbicyclo [3.1.1] is typical of woody-smelling aromas (Schreiner et al., 2018). 1-octen-3-ol (also known as “mushroom alcohol”) and methional are the key components of truffle products and are widely accepted by consumers (Phong et al., 2022). Methyl 9-(Z)-octadecenoate is a polyunsaturated fatty acid that has been found in coral fungi (Kumar et al. 2017) and *Trametes polyzona* (Pers.) Justo (Oyetayo & Akingbesote, 2022) and known to have potent antimicrobial, antioxidant, anti-inflammatory and antistaphylococcal properties (Hao et al., 2020; Salisu et al., 2019).

3.5.8 Rapid Prediction of the Contents of Characteristic Markers of Volatile Compounds

For rapid prediction, the contents of characteristic markers including Methyl 9-(Z)-octadecenoate, 2, 6-dimethylpyrazine, 1-decen-3-one, furfural, and methional were determined. The 7500–4050 cm^{-1} wavenumbers of the NIR spectrum were selected according to the variance spectrum of the second derivative (Figure 3.29), and calibration models for the total amounts were established (Figure 3.34). The sample numbers for the calibration and validation sets of each species were divided according to the 7:3 ratio by the algorithm of K–S (Kennard - stone). In multivariate regression, R^2, RMSECV and RPD values are frequently used as important indices to assess the quality of fitness (Hao et al., 2020). As shown in Figure 3.34 (up left), the relative percent contents of the five characteristic VOCs had a good linear relationship with NIR. The R^2_c, RMSECV and RPD_c of the models ranged from 0.8563 to 0.9066, 0.0764 to 1.55, and 1.68 to 2.797, respectively. According to reports (Vega-Castellote et al., 2021; Hao et al., 2020), calibration models can be used quickly to predict contents when the value of R^2 is close to 1, RMSECV is close to 0 and RPD is greater than 1.5. To verify whether the models were reliable, we carried out an evaluation based on the established validation models of the test sets (Figure 3.34, upper left) and used a paired *t*-test between the predicted values and true values (Figure 3.34, lower right). As shown in figure 3.34 (upper left), the R^2_v, RMSEP and RPD_v of the validation models were between 0.8631 and 0.9148, 0.107 and 1.58, and 1.77 and 2.717, respectively. As shown in

Figure 3.34 (lower right), the *p* values were 0.9531, 0.7888, 0.6718, 0.9147, and 0.7851, respectively. The results indicated that all of the models could accurately predict the contents of unknown samples and there was no significant difference between the predicted values and true values ($p > 0.05$). Based on the above results, it can be inferred that FT-NIR combined with PLSR provides a fast and reliable quantitative technique for predicting the contents of characteristic VOCs in bolete mushrooms.



Note (a)-(g) present the characteristic markers of Methyl 9-(Z)-octadecenoate, dimethylpyrazine, 1-decen-3-one, furfural, methional, 1-octen-3-ol, and (E)-2-octenal, respectively

Figure 3.34 Calibration and validation models of the characteristic markers of volatile compounds of boletes built by NIR combined with PLSR

CHAPTER 4

DISCUSSION

4.1 Taxonomy and Phylogeny of *Tuber* (True Truffles)

The similarities of ITS sequences of *T. maroonense* and *T. conditum* to all described *Tuber* species are lower than 95.5 % and 89.0 %, respectively. In the genus *Tuber*, species delimation based on 96 % similarity in ITS has been suggested by previous studies (Kinoshita et al., 2011). Moreover, *T. maroonense* and *T. conditum* can be distinguished from other related species by morphology alone. In addition, phylogenetically, *T. maroonense* forms a distinct branch with high support (ITS 100 % BS, and 1.0 PP) and its sister species of *T. caoi* can be distinguished by ITS1 + ITS2 and ITS-nrLSU combined ML trees. *T. conditum* can be distincted from *Tuber sp.* 10, *T. tomentosum*, *T. rapaeodorum* and *T. borchii* by ITS1 + ITS2 and ITS-nrLSU combined ML trees (Figure 3.1 and 3.2).

Morphologically, *T. maroonense* resembles *T. caoi*, *T. jinshajiangense* (Fan et al., 2016) and *T. shii* (Wang et al., 2016) of Chinese species with regards to its regularly globose ascospores with alveolar ornamentation. However, *T. caoi* and *T. jinshajiangense* have gray or pale gray and pubecens ascomata but *T. maroonense* has whitish and glabrous ascomata. There are obviously difference both *T. maroonense* and *T. shii* from their ascomata and gleba. *T. shii* has often with some superficial furrows, pale greybrown, pale brown and with distinctive silver-grey tints ascomata, its gleba with brown at maturity (Wang et al., 2016), but *T. maroonense* has whitish and brown glabrous ascomata and its gleba with brown to darck brown at maturity. Additionally, *T. maroonense* differs *T. caoi* (37.5–40 μm in one-spored asci), *T. jinshajiangense* (35–37.5 μm in one-spored asci) and *T. shii* (29–51.5 μm

in one-spored asci) by its larger ascospore (41.5–52 µm in one-spored asci). *T. conditum* differs from other species by its grey-white to grey-brown ascomata, thinner peridium (120–200 µm) and larger ascispores (49–66.5 × 34.5–60 µm in one-spored asci). The close relationship species of *T. tomentosum* has 1–6 cm diam of ascomata (Kinoshita et al., 2021), *T. pseudosphaerosporum* has 2–4.5 cm diam and white, or whitish-yellow ascomata (Fan & Yue, 2013). Furthermore, *T. maroonense* and *T. conditum* can remarkably identify other Chinese species of the Latisporum group, such as *T. alboumbilicum* (Li, Zheng et al., 2014), *T. baoshanense* (Wan et al., 2017), *T. elevatirticulatum* (Lin et al., 2018), *T. griseolivaceum* (Huang et al., 2017), *T. huiliense*, *T. luyashanense*, *T. microcarpum* (Fan et al., 2022), *T. panzhihuanense* (Deng et al., 2013), based on the color and size of ascomata. Of course, the two pairs of truffles are quite different because the phylogenetic tree places them in a different position by ITS1 + ITS2 and ITS-nrLSU combined ML trees (Figure 3.1 and 3.2).

In conclusion, we demonstrated that *T. maroonense* and *T. conditum* are new species characterized by smooth on their ascocarp surfaces. Our finding of these three species, *T. maroonense*, *T. conditum* and *T. tomentosum*, are divided within the same group by their morphologic characteristic and phylogenetic relationship. Despite, Kinoshita et al. (2021) indicated that the species of *T. tomentosum* was belong to the Macrosporum group based on its phylogenetic position. However, they were revealed that may belong to Latisporum group (Wan et al., 2016, 2017; Fan et al., 2022) by the phylogenetic relationships through adding more DNA sequences in this study.

4.2 Taxonomy and Phylogeny of *Choiromyces*

Choiromyces cerebriformis is characterized by its ascomata with larger, deeper lobes and light orange-brown gleba, and globose ascospores with short stick-like spare spines ornamentation. Both morphological data and ITS phylogeny presented herein support *C. cerebriformis* as a new species. Moreover, the ITS1+ITS2 genetic distances

between *C. cerebridormis* and *C. helanshanensis* ranged from 3.3 % to 4.4 %, with a mean of 3.7 % (Table 3.3). Most species of fungi show 1-3% intraspecific and >3% interspecific distance between ITS sequences (Nilsson et al., 2008). In *Tuber*, intraspecific ITS variation was below 3% for all species except *T. aestivum* (<3.7%), and interspecific ITS variation was at least 4% (Bonito et al., 2010). Therefore, the genetic distances we observed confirm that *C. cerebridormis* and *C. helanshanensis* can be considered as different species.

C. venosus and *C. meandriformis* have been regarded as conspecific (Wedén, 2007; Wedén et al., 2009). However, the genetic distances between *C. venosus* and *C. meandriformis* ranged from 0 % to 3.7 % (Table 3.3). So, while some specimens identified as either of those two species should indeed be considered conspecific because their ITS sequences were exactly identical, others showed genetic distances that are too large to be accommodated in a single species. Moreover, the mean intraspecific distance among ITS sequences from specimens identified as *C. meandriformis* was more than 3% (ranging from 0 to 0.073; Table 3.3), which suggests that some of those specimens belong in a different species. The specimens were either not correctly identified, or there are distinct, difficult to distinguish or cryptic species. Those species need to be carefully revised using both morphological and DNA sequence data.

4.3 Taxonomy and Phylogeny of *Melanogaster*

In this research, we introduce three novel species of hypogeous fungi belonging to *Melanogaster* (Paxillaceae, Boletales): *M. cyaneus*, *M. diqingensis*, and *M. truncatisporus*. The first two species were discovered in Yunnan Province, while the latter was collected in Sichuan Province, in southwest China. Morphologically, *M. cyaneus* stands out with its distinctive blue or bluish gleba and light brown to yellowish brown basidiomata. *M. diqingensis* can be identified by its pale yellow to brown-yellow basidiomata, featuring a scaled, lobed, or concave surface. *M. truncatisporus* is characterized by its distinct pale

yellow to deeply orange-yellow peridium and subglobose to globose or pyriform basidiospores. These characteristics differentiate them from other *Melanogaster* species found in China. Phylogenetically, our analysis based on an ITS rDNA database, including ITS1-2 and 5.8S, revealed that specimens of *M. cyaneus* and *M. truncatisporus* clustered into two independent clades with strong support (BS = 100%, PP = 1.0). *M. diqingensis* and *M. subglobisporus* formed a separate and well-supported clade (BS = 78%, PP = 1.0) (Figure 3.8). Moreover, genetic distance analysis showed that these three species share less than 93.2% ITS similarity with other *Melanogaster* species. Both the phylogenetic tree and morphological features align to support the classification of these three species as new additions to the *Melanogaster* (Figure 3.8).

Knapp (1954) and Moreau et al. (2011) proposed a division of European *Melanogaster* species into three sections based on the average length of basidiospores. These sections were defined as follows: section *Melanogaster*, with basidiospores longer than 10 μm; section *Variegati*, with basidiospores measuring 6–10 μm; and section *Rivulares*, with basidiospores ranging from 5 to 6 μm. Our multivariate statistical analysis based on wider taxon sampling and three morphological characters instead of only spore length allowed to separate species in line with Moreau et al. (2011) sections (Figure 3.10). However, in the phylogenetic tree (Figure 3.8), the three morphologically delineated sections were not monophyletic. For example, *M. panzhihuaensis* described from China was placed within the *Melanogaster* section based on morphology, but shared a sister relationship with *M. minobovatus*, also from China, which was assigned to section *Rivulares* by the multivariate morphological analysis (Figure 3.10). This placement is distinct from species classified within the *Melanogaster* section, such as *M. ambiguus* (Spain and China), *M. intermedius* (UK), *M. euryspermus* (USA), *M. tuberiformis* (Spain), *M. natsii* (China), *M. subglobisporus* (China), and *M. macrosporus* (Hungary) (Wang et al., 1995; Frank et al., 2006; Brock et al., 2009; Alvarado et al., 2021; Xu et al., 2022).

A set of 19 *Melanogaster* sequences from Germany, France, and the USA (as detailed in Table 3.4) were included in our phylogenetic analyses. The position of certain of the specimens from which these sequences were obtained was problematic, particularly concerning *M. intermedius* B-1770, and *M. variegatus* 23640 and B-1688 from Hungary, as well as *M. natsii* OSC82168 JMT7491 and OSC158336 MES297 from the USA. All those accessions belonged in species-level clades including other accessions identified as different species. The ITS rDNA sequences of *Melanogaster* sp. (Melanog002FRA, Melanog006FRA, Melanog007FRA, Melanog008FRA, Melanog011FRA, and Melanog012FRA), along with *Melanogaster* sp. (Melanog018FRA and Melanog019FRA) from France, clustered with *M. rivularis* and *M. luteus* clades, respectively. This observation is substantiated by robust support from high bootstrap values (BS = 97 and BS = 93) and posterior probability from Bayesian inference (PP = 1.0) in Figure 3.8. Consequently, we recommend classifying the first six unidentified specimens as *M. rivularis* species and the last two specimens as *M. luteus* species.

Melanogaster sp. MVC 753 FLASF 65878 (Chile) and *Melanogaster* sp. MES 1003 (Chile) exhibited less than 98.3% similarity in ITS region compared to *M. macrosporus*. Furthermore, an ITS sequence (*Melanogaster* sp. JC110118BT) from Spain, two ITS sequences (*Melanogaster* sp. OSC AHF420 from France and *Melanogaster* sp. OSC LG1042 from the USA), and two ITS sequences (*Melanogaster* sp. OK 2022a oka331 and *Melanogaster* sp. OK 2022a oka332) from Turkey exhibited less than 96.7% similarity to ITS sequences of other species of *Melanogaster*. Consequently, those accessions represent four distinct species-level lineages, designated as *M*. sp.1 to *M*. sp.4, respectively (Figure 3.8). This observation suggests the presence of four undescribed species. More research is therefore needed to validate and properly describe those putative novel species.

4.4 The Chemodiversity of Boletes Driven by Both Phylogeny and Ecological and Environmental Factors

We suggest that chemical diversity is related to phylogenetic signals and ecological environmental factors, which is the premise for the use of chemical characteristic information to identify species and geographical regions. In the present study, 509 individuals of boletes belonging to 11 species (confirmed by phylogenetic analyses) were collected and the ecological environmental factors of the sampling sites were acquired by GPS and ArcGIS. The chemical information from NIR spectra, HPLC fingerprints and volatile constituents detected by GC–MS were used to explore the correlation of chemodiversity with species and ecological environmental factors. The results verified four fundamental issues for fungal chemodiversity: (1) the chemodiversity was widespread correlated with species and ecological environmental factors; (2) phylogenetic higher conserved chemical information can be used as a basis to identify species; (3) chemical characteristic information can be used as a basis to effectively distinguish the geographical regions of species distribution; and (4) the diversity of species and the ecological environment are important to maintain the chemical diversity of wild edible fungi.

First, chemodiversity usually refers to small molecules that have a signaling (e.g., offensive or defensive) function (La Barre, 2014), which is recognized as distributed widely in animal (Smith et al., 2018), plant (Zhang et al., 2021), and microorganism (Noriega-Ortega et al., 2019; Li, Wang et al., 2021) by researchers. In this study, the STDEV of chemical information demonstrated intraspecific and interspecies differences, and chemical characteristic information was correlated with both phylogenetic signals and ecological environmental factors. The results are consistent with the hypothesis that “diversity begets diversity” (Tanentzap et al., 2019). The chemodiversity of fungi support multifunctionality in many ways, such as polysaccharides composing cell walls (Spiteller, 2015), myristate participating in the exchange of matter and energy between fungi-plants or fungi-

environments (Liebel et al., 2015; Gow et al., 2017), chokol K and (*3R*)-1-octen-3-ol attracting a pollinator (Schiest et al., 2006; Becher et al. 2018; Sugiura et al., 2020), *α*-amanitin defending animals, plants and other fungi to promote growth or generation (Chitarra et al., 2004; Rangel et al., 2021; Li, Liu et al., 2022), and volatiles taking part in their behavior management and signal transduction between fungi and their hosts (Schiest et al., 2006; Aleklett & Boddy, 2021). Overall, our study demonstrated that the chemodiversity of fungi may be driven by both the evolution of species and ecological environmental factors.

Second, the results revealed that the chemical information related to phylogenetic signals could be used to identify species of fungi. This chemical information may be related to the evolutionary history of species, e.g., chitin synthases (Torruella et al., 2015), the synthesis of genetic material (e.g., uridine, adenosine, guanosine) or the transmission of genetic signals, e.g. ergosterin as an alkaloid (Schardl et al., 2013). Although how this chemical information participates in the evolution of species of fungi is still unknown, the chemical information was verified and could be used to identify a species by establishing a pattern recognition model through chemometrics. Li, Chen et al. (2021) revealed 30 genes related to the synthesis of characteristic volatiles of mushrooms, the synthesis pathways of which were dertermined to be histidine metabolism, glutathione metabolism and biosynthesis of unsaturated fatty acids through KEGG enrichment analysis. Ditengou et al. (2015) proposed that volatile signaling by sesquiterpenes from ectomycorrhizal fungi not only reprogrammed root architecture but also improved fungal access to plant-derived carbon via root exudates, which created a win–win situation for ectomycorrhizal fungi and their hosts. These reports suggested that chemical information could be a product of the expression of specific genes in fungi during evolution or participation in the evolution of the species (Rees et al., 2018). Herein, it was verified that chemical information could be used as a potential basis for species identification due to the strong and universal relationship between chemical information and phylogenetic signals.

Third, the results revealed that there was a general relationship between chemical information and geographical regions (ecological environmental factors). However, the strength of the correlation was obviously different, such as for the volatiles pyrrole, 2-methylpyrazine, and 2-methyl-butanoci acid, which made a greater contribution to the classification of region 1 than to other regions according to the load analysis of PLS-DA. The chemical characteristic information could be used as a basis to effectively distinguish the geographical regions of species, which was consistent with the report by Ginigini et al. (2019) that the geographical environment might be one of the factors driving the chemodiversity of species (Gougeon et al., 2009). However, when chemical information is used to identify geographical regions of species, we suggest that the reliability of the identification model should be assessed through cross-validation and external validation, as in this study.

Fourth, the species diversity and geographical differences of wild edible fungi are important to maintain their chemical diversity. The shared genetics hypothesis and shared ecology provide the basis for the phenomenon of chemical diversity of species (Bailey et al., 2015; Chaturvedi et al., 2022). The origin of life is a hot topic across multiple fields, such as regarding the proteome, genome, metabolome and lipidome (Andras & Andras, 2005; Krishnamurthy & Hud, 2020). It is an indisputable fact that chemicals are involved in the production, evolution and metabolism of the whole life process. Our study shows that chemical information strongly associated with phylogenetic signals and ecological environments can identify species and geographical regions, which may be influenced by convergent species evolution. In addition, chemical information has a preferential relationship with species evolution or ecological environmental factors, such as adenine, methylated homologues, and methylated homologues, which are more strongly related to species (Roy et al., 2007; Umamaheswaran et al., 2022), while volatile organic compounds are more closely related to ecology (Guo et al., 2021).

In summary, our results support that chemical information plays an important role in both fungal evolution and species adaptation to the environment. this research provides a basis for the chemical identification of species and regions by effectively selecting chemical characteristic information and constructing scientific identification models. Additionally, this study provides a theoretical basis for environmental and species evolution to drive chemical diversity.

4.5 A Qualitative and Quantitative Analysis of Wild Boletes Based on Multivariate Statistics of Volatile Components and FT-NIR Spectra

The research of bolete flavor substances has always been the focus of flavor chemists. However, use of flavor substances to distinguish different species of boletes is still rare. In this study, the combination of PLS-DA with the VIP and ROAV analyses of VOCs was proved as an effective method for the identification of bolete mushrooms. In particular, five VOCs, including methyl (9E)-9-octadecenoate, 2,6-dimethylpyrazine, 1-decen-3-one, furfural, and methional, could be used as the key aromatic compounds for identifying and evaluating boletes. According to Fisher's linear discriminant function analysis, the discriminant equations could be used as a basis for the rapid identification of the species of boletes in the future. In addition, FT-NIR combined with PLSR provides a fast and reliable quantitative technique for predicting the contents of characteristic VOCs in boletes. According to the above strategy of qualitative and quantitative analysis, this approach could be used not only for the fast identification of species but also for the effective prediction of their contents, providing an important basis for the future exploitation of newly identified species and the quality control of bolete mushrooms.

CHAPTER 5

OVERALL CONCLUSIONS

This dissertation focused on the biodiversity of mushrooms from hypogeous fungi (*Tuber*, *Choiromyces*, and *Melanogaster*) and wild Boletales (*Boletus*, *Butyriboletus*, *Rubroboletus*, *Retiboletus*, *Lanmaoa*, *Neoboletus*, *Rugiboletus* and *Phlebopus*). The mushroom specimens of hypogeous fungi were described using morphological observation and phylogenetic analyses. The mushroom specimens of Boletales were identified using phylogenetic analyses, and their chemodiversity were analyzed by NIR, HPLC-UV and GC-MS combine with multivariate statistical analysis. The chemistry information was selected as a crucial basis for wild Boletes species identification and material quality assessment.

5.1 Taxonomy and Phylogeny of Hypogeous Fungi

Morphological and phylogenetic evidence were used for introducing and identifying hypogeous fungi taxa. A total of 6 hypogeous fungi were introducted as new species based on morphological characteristics and phylogenetic affinities, of which two, one and three species belonged to *Tuber*, *Choiromyces* and *Melanogaster* genera were proposed, respectively. As of now, China has recorded and discovered more than 60 species of *Tuber*, 7 species of *Choiromyces*, and over 11 species of *Melanogaster*. These numbers represent 20%, 30%, and 20% of the total species of *Choiromyces*, *Melanogaster*, and *Tuber*, respectively, based on the records in Index Fungorum. Despite the symbiotic relationships formed by many underground fungi with their hosts, the hosts are relatively fixed, such as Betulaceae, Cistaceae, Fagaceae, Pinaceae, and Salicaceae (Lacheva, 2015;

Türkoğlu & Castellano, 2013; Perić & Moreau, 2010; Halász, 2008; Comandini et al., 2006) plants. However, the collection and excavation of hypogeous fungi are much more challenging compared to terrestrial fungi. Although this study extensively surveyed underground fungi in the southwestern region of China, the discovery of new species was limited. Nevertheless, this provides strong evidence for further supplementing the diversity of underground fungal species in the southwestern region of China.

This study serves as a foundational basis for future research on the diversity of hypogeous fungi, the coevolution of fungi with plants, and the exploration and development of potential chemical information and functional characteristics in the southwestern region of China.

5.2 Chemodiversity and Chemotaxonomy Analyses of Wild Boletes

In this study, the wild edible Boletes (including *Boletus bainiugan* (BoB), *Butyriboletus pseudospeciosus* (BuP), *Butyriboletus roseoflavus* (BuR), *Lanmaoa asiatica* (LA), *Neoboletus obscureumbrinus* (NO), *Rugiboletus extremiorientalis* (RugE), *Rubroboletus sinicus* (RubS), *Retiboletus fuscus* (RetF), *Phlebopus portentosus* (PP), *Neoboletus hainanensis* (NH), *Neoboletus magnificus* (NM)) were investigated in southwest of China. This 11 species were identified from 509 specimens based on the multi-gene phylogeny (RPB2 and TEF1). In order to analyze the intrinsic chemodiversity of boletes and its relationship with evolution and ecological environments, their chemical information, including near infrared spectroscopy (NIR), common peaks of high–performance liquid chromatography (HPLC) and volatile constituents, were detected. Meanwhile, the relationship of evolution of 11 species were assessed using the divergence times in Basidiomycota are 53.43 to 121.2 Mya. By analyzing the correlation between molecular phylogenetic signals and chemical information, as well as the relationship between chemical information and its ecological environmental factors, we comprehensively explored the interplay of chemical heterogeneity,

evolutionary history, and ecological diversity within the boletes, a group of fungi in Southwest China. The results showed that,

5.2.1 The chemical diversity of boletes shows a broad correlation with molecular phylogenetic signals and ecological/environmental factors. This suggests that the chemical composition of boletes is jointly influenced by their evolutionary history and ecological conditions.

5.2.2 Molecular phylogenetic signals have been identified as the most reliable predictor for all analyzed chemical characteristics. This implies that the chemical makeup of boletes tends to be conserved within closely related species, making chemical information an effective tool for species identification, complementing traditional methods such as molecular and morphological identification.

5.2.3 Chemical information exhibits a strong correlation with ecological and environmental factors, making it useful for identifying bolete species and their geographical regions. This has practical significance for using chemical traits as markers for species identification and determining the geographic origin of samples.

5.2.4 The research emphasizes the dual role of evolutionary history and ecological/environmental factors in shaping the chemical diversity of boletes, deepening our understanding of the biology and ecology of these fungal populations.

In summary, this study provides a comprehensive perspective on understanding the chemical diversity of boletes and its relationship with evolution and ecological environments. These findings not only have practical implications for species identification and ecological studies but also lay a solid foundation for further exploration in this field.

5.3 Volatile Components and Key Aroma Components Predicted of Wild Boletes

In this study, our objective was to investigate the variability of VOCs in 11 boletes species using multivariate statistical analyses. VOCs were extracted through simultaneous distillation extraction and identified using gas chromatography-mass spectrometry. The findings disclosed a total of 97 VOCs in 445 samples, with alkanes and esters being the predominant compounds. PCA and ANOVA suggested potential differences among the 11 bolete species. PLS-DA in conjunction with VIP >1 and ROAV >0.1, revealed that 38 compounds (including 5 common compounds) contributed to species classification, and identity models were effectively validated.

Additionally, through the analysis of correlated heatmap and volcanic maps, 9 VOCs were identified as key compounds for the 11 species, namely (1R)-2, 6, 6-trimethylbicyclo[3.1.1], 1-decen-3-one, 2, 6-dimethylpyrazine, elaidic acid methyl ester, furfural, methional, triethyl orthoformate, 1-octen-3-ol, and (E)-2-octenal. Furthermore, Fisher's linear discriminant function analysis, combined with literature reports, indicated that 5 VOCs (elaidic acid methyl ester, 2, 6-dimethylpyrazine, 1-decen-3-one, furfural, and methional) could effectively be used for identifying the 11 bolete species.

Ultimately, Fourier Transform Near-Infrared Spectroscopy (FT-NIR) combined with PLSR emerged as a rapid and reliable quantitative technique for predicting the contents of the five characteristic VOCs in boletes. This study proposes a strategy for effective species identification and the swift prediction of characteristic aroma substances in wild edible boletes through qualitative and quantitative analyses of VOCs and FT-NIR spectra.

5.4 Research Advantages

This dissertation implemented an interdisciplinary approach for mushroom identification and quality evaluation. A combined approach was applied based on phylogenetic species concepts, fingerprint of chemical signals, and characteristic VOCs. Based on the strong correlation with phylogenetic signals, we preliminarily explored the potential of chemical information as a basis for substance identification or characterization. Utilizing chemical information, we established an effective classification model for identifying bolete species and validated the reliability of the model. Additionally, employing chemometric methods, we screened potential chemical components that could influence species classification and established content prediction models. This approach provides a method for subsequent species identification and quality assessment.

5.4.1 This research contributed six novel taxa to science with illustration and molecular data. Newly generated sequences of four loci including ITS, nrLSU, *rpb2* and *tef1*, were deposited in GenBank. Also, by combining morphological features with phylogenetic analysis, 1, 2, and 3 new species have been added to the classification of *Choriomyces*, *Tuber* and *Melanogaster* of hypogeous fungi, respectively. This will contribute valuable material for future studies on the species diversity of subterranean fungi in China.

5.4.2 For the first time, through multivariate statistical analysis, molecular phylogeny has been combined with near-infrared spectroscopy information, high-performance liquid chromatography fingerprint profiles, and volatile components. This analysis explores the extensive correlation between chemical information and the molecular phylogenetic signals of boletes species. By characterizing chemical information, a chemical classification model for 11 bolete species has been established, validating the effectiveness of the selected chemical information in identifying boletes species.

5.4.3 Furthermore, through a correlation analysis between chemical information and environmental factors in which species grow, characteristic chemical information has been identified for use in the traceability analysis of boletes species. This indicates that the intrinsic chemical heterogeneity within boletes species are generally influenced by their growth environment factors. Simultaneously, an analysis of the chemical information diversity among bolete species highlights the dual role of evolutionary history and ecological/environmental factors in shaping the chemical diversity of boletes, deepening our understanding of the biology and ecology of these fungal populations.

5.4.4 Using chemometric analysis, it is demonstrated that the intrinsic volatile components of bolete species serve as crucial criteria for species identification. Moreover, these essential volatile components, through the establishment of near-infrared spectroscopy quantitative prediction models, can effectively predict the aromatic components of boletes. This establishes a methodological foundation for the quality assessment of edible boletes based on flavor constituents.

5.5 Future Work

5.5.1 Southwestern region of China is a hotspot to explore mushroom biodiversity as many of the collections which are collected there are new to science. More collections are needed, additional collections are required to corroborate the taxonomy and phylogeny of intriguing species that have been identified as new to science solely based on individual collections. Despite the confirmation of their status as new species through distinctive morphological features and comprehensive gene phylogenies, acquiring and analyzing additional specimens is essential to enhance the understanding of their variation and establish a more dependable taxonomic system. Especially, with the continuous advancement of multi-gene concatenation or whole-genome approaches, establishing multi-gene or genomic phylogenetic analyses can provide more robust evidence for the identification of new species.

5.5.2 Additionally, southwestern region of China is one of the largest exporters and consumers of edible mushrooms. The safe consumption of wild edible mushrooms has consistently been a prominent concern in China and globally. In addition to analyzing the nutritional components and assessing the quality of edible mushrooms, it is crucial to conduct analyses of the intrinsic toxic substances present in the large fungi consumed by people. Utilizing a combination of chemical analysis methods with pharmacology and toxicology experiments, exploring the diversity and richness of the intrinsic chemical composition of large fungi holds significant importance for the development of the medicinal and pharmaceutical industry.

5.5.3 An evolutionary approach serves as valuable evidence for mushroom identification. Consequently, preserved strains can be utilized for genomics studies.

5.5.4 Chemical identification is also a method for species recognition. Through interdisciplinary analysis, a more accurate identification of species can be achieved, providing a basis for future exploration of the metabolism and synthetic pathways of chemical components.

5.5.5 OMICS techniques, bioinformatics, analytical chemistry, and biotechnology can be employed to discover new metabolites. Further development of these metabolites can lead to the identification of potential candidates for drugs, agrochemicals, and other products in the life science industry.

5.6 Publications

Yuan, T. J., Raspe, O., Li, Y. J., Wang, L., Su, K. M., Wang, Y., . . . Li, S. H. (2021). *Choiromyces cerebriformis* (Tuberaceae), a new hypogeous species from Yunnan, China. *Phytotaxa, 482*(3), 251-260. https://doi.org/10.11646/phytotaxa.482.3.3

Yuan, T. J., Luo, H. M., Su, K. M., Li, S. H., & Raspé, O. (2024). Three new *Melanogaster* species (Boletales, Paxillaceae) from southwestern China Based on morphological and molecular evidence. *MycoKeys, 107*, 141-160. https://doi.org/10.3897/mycokeys.107.123565

Yuan, T. J., Zhao, Y. L., Zhang, J., Li, S. H., Hou, Y., Yang, Y., . . . Wang, Y. Z. (inpress) Characterization of volatile profiles and markers prediction of eleven popular edible boletes using SDE-GC-MS and FT-NIR combined with chemometric analysis. (Submited to Food research international).

Yuan, T. J., Raspe, O., Luo, H. M., Su, K. M., & Li, S. H. (2023). Two novel *Tuber* species (Tuberaceae, Pezizales) from southwestern China based on morphological and molecular evidence [Manuscript in preparation].

Yuan, T. J., Zhao, Y. L., Zhang, J., Li, S. H., Hou, Y., Yang, Y., . . . Wang, Y. Z. (2023). The chemodiversity of Boletes driven by both phylogeny and ecological and environmental factors [Manuscript in preparation].

Wang, L., Tang, S. M., Zhang, X., Su, K., Li, Y., Yuan, T. J., . . . Li, S. (2020). *Tuber melanoexcavatum* sp. nov., an edible black truffle from China. *Phytotaxa, 477*(2), 269-276. https://doi.org/10.11646/phytotaxa.477.2.11

REFERENCES

REFERENCES

Ahmed, A., Kamran Taj, M., Yonglıang, Z., Taj, I., Hassani, M. T., Sajıd, M., . . . Liping, S. (2015). Chemical composition and antioxidant properties of eight wild edible boletaceae mushrooms growing in Yunnan Province of China. *Jökull Journal*, *65*(12), 146-167.

Albornoz, F. E., Dixon, K. W., & Lambers, H. (2020). Revisiting mycorrhizal dogmas, are mycorrhizas really functioning as they are widely believed to do?. *Soil Ecology Letters*, *3*(1), 73-82. https://doi.org/10.1007/s42832-020-0070-2

Aleklett, K., & Boddy, L. (2021). Fungal behavior, a new frontier in behavioural ecolgy. *Trends in Ecology & Evolution*, *36*(9), 787-796. https://doi.org/10.1016/j.tree.2021.05.006

Alfaro, M. E., Zoller, S., & Lutzoni, F. (2003). Bayes or bootstrap? A simulation study comparing the performance of Bayesian Markov Chain Monte Carlo sampling and bootstrapping in assessing phylogenetic confidence. *Molecular Biology & Evolution*, *20*(2), 225-266. https://doi.org/10.1093/molbev/msg028

Allgeier, J. E., Weeks, B. C., Munsterman, K. S., Wale, N., Wenger, S. J., Parravicini, V., . . . Burkepile, D. E. (2021). Phylogenetic conservatism drives nutrient dynamics of coral reef fishes. *Nature Communications*, *12*(1), 5432. https://doi.org/10.1038/s41467-021-25528-0

Alvarado, P., Cabero, J., Moreno-Mateos, D., Vizzini, A., Alonso, J., Lebeuf, R., . . . Vidal, J. M. (2021). Phylogenetic relationships among false truffle genera of Paxillaceae—*Alpova*, *Melanogaster*, *Neoalpova*, and *Paralpova*, gen. nov. *Mycologia*, *113*(4), 828-841. https://doi.org/10.1080/00275514.2021.1911552

Andras, P., & Andras, C. (2005). The origins of life-the ‘protein interaction world’ hypothesis, protein interactions were the first form of self-reproducing life and nucleic acids evolved later as memory molecules. *Medical Hypothesis*, *64*, 678-688. https://doi.org/10.1016/j.mehy.2004.11.029

Ankanna, S., Suhrulatha, D., & Savithramma, N. (2012). Chemotaxonomical studies of some important monocotyledons. *Botany Research International*, *5*(4), 90-96.

Anowar, F., Sadaoui, S., & Selim, B. (2021). Conceptual and empirical comparison of dimensionality reduction algorithms (pca, kpca, lda, mds, svd, lle, isomap, le, ica, t-sne). *Computer Science Review, 40*, 100378. https://doi.org/10.1016/j.cosrev.2021.100378

Aprea, E., Romano, A., Betta, E., Biasioli, F., Cappellin, L., Fanti, M., . . . Gasperi, F. (2015). Volatile compound changes during shelf life of dried Boletus edulis, comparison between SPME-GC-MS and PTR-ToF-MS analysis. *Journal of Mass Spectrometry*, *50*(1), 56-64. https://doi.org/10.1002/jms.3469

Arora, D. (2008). California porcini, Three new taxa, observations on their harvest, and the tragedy of no commons. *Economic Botany*, *62*, 356-375. https://doi.org/10.1007/s12231-008-9050-7

Arora, D., & Frank, J. L. (2014). Clarifying the butter boletes, A new genus, *butyriboletus*, is established to accommodate boletus sect. Appendiculati, and six new species are described. *Mycologia*, *106*(3), 464-480. https://doi.org/10.3852/13-052

Arraiano-Castilho, R., Bidartondo, M. I., Niskanen, T., Clarkson, J. J., Brunner, I., Zimmermann, S., . . . Suz, L. M. (2021). Habitat specialisation controls ectomycorrhizal fungi above the treeline in the European Alps. *New Phytologist*, *229*(5), 2901-2916. https://doi.org/10.1111/nph.17033

Bailey, S. F., Rodrigue, N., & Kassen, R. (2015). The effect of selection environment on the probability of parallel evolution. *Molecular Biology and Evolution*, *32*(6), 1436-1448. https://doi.org/10.1093/molbev/msv033

Barreira, J. C., Ferreira, I. C., & Oliveira, M. B. (2012). Triacylglycerol profile as a chemical fingerprint of mushroom species, Evaluation by principal component and linear discriminant analyses. *J Agric Food Chem*, *60*(42), 10592-10599. https://doi.org/10.1021/jf302442s

Bartkiene, E., Zokaityte, E., Starkute, V., Mockus, E., Klupsaite, D., Lukseviciute, J., . . . Ozogul, F. (2022). Biopreservation of wild edible mushrooms (Boletus edulis, Cantharellus, and Rozites caperata) with lactic acid bacteria possessing antimicrobial properties. *Foods*, *11*(12), 1800. https://doi.org/10.3390/foods11121800

Becher, P. G., Hagman, A., Verschut, V., Chakraborty, A., Rozpędowska, E., Lebreton, S., . . . Piškur, J. (2018). Chemical signaling and insect attraction is a conserved trait in yeasts. *Ecology and Evolution*, *8*(5), 2962-2974. https://doi.org/10.1002/ece3.3905

Bessett, A. R. (2015). *Lanmaoa roseocrispans* Bessette, A.R. Bessette, Nuhn & Halling, sp. nov. *Index Fungorum 259*, 1.

Beug, M. W. (2021). North american mushroom poisonings and adverse reactions to mushrooms 2018-2020. *Fungi*, *14*, 17-22.

Bhargava, V. V., Patel, S. C., & Desai, K. S. (2013). Importance of terpenoids and essential oils in chemotaxonomic approach. *International Journal of Herbal Medicine, 1*(2), 14-21.

Binder, M., & Bresinsky, A. (2002). *Retiboletus*, a new genus for a species-complex in the boletaceae producing retipolides producing retipolides. *Feddes Repertorium, 113*(1-2), 30-40. https://doi.org/10.1002/1522-239X(200205)113:1/2<30::AID-FEDR30>3.0.CO;2-D

Binder, M., & Hibbett, D. S. (2006). Molecular systematics and biological diversification of boletales. *Mycologia*, *98*(6), 971-981. https://doi.org/10.1080/15572536.2006.11832626

Binder, M., Larsson, K. H., Matheny, P. B., & Hibbett, D. S. (2010). Amylocorticiales ord. nov. and Jaapiales ord. nov., early diverging clades of Agaricomycetidae dominated by corticioid forms. *Mycologia*, *102*(4), 865-880. https://doi.org/10.3852/09-288

Bîrsan, C., Mardari, C., & Tanase, C. (2019). New localities and habitat conditions for Choiromyces meandriformis Vitt. (Ascomycota, Fungi) in Northern Romania. *Journal of Plant Development*, *26*, 173.

Blomberg, S., P., Garland, T. & Ives, A., R. (2003). Testing for phylogenetic signal in comparative data, behavioural traits are more labile. *Evolution*, *57*, 717-745. https://doi.org/10.1111/j.0014-3820.2003.tb00285.x

Boa, E. (2004). *Wild edible fungi a global overview of their use and importance to people* (Vol. 17). FAO non-wood forest products. Food & Agriculture Org.

Boekhout, T., Amend, A. S., El Baidouri, F., Gabaldón, T., Geml, J., Mittelbach, M., . . . Yurkov, A. (2022). Trends in yeast diversity discovery. *Fungal Diversity*, *114*(1), 491-537. https://doi.org/10.1007/s13225-021-00494-6

Bonito, G. M., Gryganskyi, A. P., Trappe, J. M., & Vilgalys, R. (2010). A global meta-analysis of *Tuber* ITS rDNA sequences, species diversity, host associations and long-distance dispersal. *Molecular Ecology*, *19*(22), 4994-5008. https://doi.org/10.1111/j.1365-294X.2010.04855.x

Bonito, G., Smith, M. E., Nowak, M., Healy, R. A., Guevara, G., Cazares, E., . . . Vilgalys, R. (2013). Historical biogeography and diversification of truffles in the Tuberaceae and their newly identified southern hemisphere sister lineage. *PLoS One*, *8*(1), E52765. https://doi.org/10.1371/journal.pone.0052765

Boonbumrung, S., Tamura, H., Mookdasanit, J., Nakamoto, H., Ishihara, M., Yoshizawa, T., . . . Varanyanond, W. (2001). Characteristic aroma components of the volatile oil of yellow keaw mango fruits determined by limited odor unit method. *Food Science and Technology Research*, *7*(3), 200-206. https://doi.org/10.3136/fstr.7.200

Bozok, N. E. S. İ. B. E., Zarifikhosroshahi, M., Kafkas, E., TAŞKIN, H., & Büyükalaca, S. (2015). Comparison of volatile compounds of fresh Boletus edulis and B. pinophilus in Marmara region of Turkey. *Notulae Botanicae Horti Agrobotanici Cluj-Napoca*, *43*(1), 192-195. https://doi.org/10.15835/nbha4319731

Bouckaert, R. R., & Drummond, A. J. (2017). bModelTest, Bayesian phylogenetic site model averaging and model comparison. *BMC Evolutionary Biology*, *17*, 1-11. https://doi.org/10.1186/s12862-017-0890-6

Brock, P. M., Döring, H., & Bidartondo, M. I. (2009). How to know unknown fungi, the role of a herbarium. *New Phytologist*, *181*(3), 719-724. https://doi.org/10.1111/j.1469-8137.2008.02703.x

Callac, P., & Chen, J. (2018). Tropical species of Agaricus. In J. E. Sánchez, G. Mata, & D. J. Royse (Eds.), *Updates on tropical mushrooms* (pp. 25-38). Basic and Applied Research.

Castellano, M. A., Trappe, J. M., Maser, Z., & Maser, S. (1986). *Key to spores of the genera of hypogeous fungi of North America, with reference to animal mycophagy*. Mad River Press.

Castresana, J. (2000). Selection of conserved blocks from multiple alignments and their use in phylogenetic analysis. *Molecular Biology and Evolution*, *17*, 540-552. https://doi.org/10.1093/oxfordjournals.molbev.a026334

Cázares, E., Guevara, G., García, J., & Trappe, J. M. (2008). *Melanogaster minisporus* sp. nov., a new sequestrate member of the Boletales from Mexico. *Revista Mexicana de Mcologia*, *28*, 67-69.

Chai, H. U. I., Liang, Z.-Q., Jiang, S., Fu, X.-L., & Zeng, N.-K. (2018). *Lanmaoa rubriceps*, a new bolete from tropical china. *Phytotaxa*, *347*(1), 71-80. https://doi.org/10.11646/phytotaxa.347.1.4

Chai, H., Liang, Z. Q., Xue, R., Jiang, S., Luo, S. H., Wang, Y., . . . Zeng, N. K. (2019). New and noteworthy boletes from subtropical and tropical china. *MycoKeys*, *46*, 55-96. https://doi.org/10.3897/mycokeys.46.31470

Chakraborty, D. (2015). A new generic record of boletaceae for indian mycobiota. *Current Research in Environmental & Applied Mycology*, *5*(2), 138-144. https://doi.org/10.5943/cream/5/2/7

Chaturvedi, S., Gompert, Z., Feder, J. L., Osborne, O. G., Muschick, M., Riesch, R., . . . Nosil, P. (2022). Climatic similarity and genomic background shape the extent of parallel adaptation in Timema stick insects. *Nature Ecology & Evolution*, *6*(12), 1952-1964. https://doi.org/10.1038/s41559-022-01909-6

Chen, J., & Liu, P.G. (2007). *Tuber latisporum* sp. nov. and related taxa, based on morphology and DNA sequence data. *Mycologia*, *99*(3), 475-481. https://doi.org/10.3852/mycologia.99.3.475

Chen, Y., Xie, M. Y., Yan, Y., Zhu, S. B., Nie, S. P., Li, C., . . . Gong, X. F. (2008). Discrimination of *Ganoderma lucidum* according to geographical origin with near infrared diffuse reflectance spectroscopy and pattern recognition techniques. *Analytica Chimica Acta*, *618*(2), 121-130. https://doi.org/10.1016/j.aca.2008.04.055

Chen, Z., Zhang, P., & Zhang, Z. (2013). Investigation and analysis of 102 mushroom poisoning cases in southern china from 1994 to 2012. *Fungal Diversity*, *64*(1), 123-131. https://doi.org/10.1007/s13225-013-0260-7

Chen, J., Sun, L. H., Su, Y., Zhao, W. Q., & Liu, P. G. (2016). *Choiromyces helanshanensis* sp. nov., a new species of subterranean truffle from China. *Mycoscience*, *57*, 279-286. https://doi.org/10.1016/j.myc.2016.04.001

Chen, Y. F., Jiang, W. W., Zhang, S. Q., Kan, J. Q., & Liang, Y. (2016). Antioxidant activity and characterization of one new polysaccharide obtained from Perigord Truffle (Tuber huidongense). *Evidence-Based Complementary and Alternative Medicine*, *2016*(1), 3537193. https://doi.org/10.1155/2016/3537193

Chen, J. B., Wang, Y., Rong, L. X., & Wang, J. J. (2018). Integrative two-dimensional correlation spectroscopy (i2DCOS) for the intuitive identification of adulterated herbal materials. *Journal of Molecular Structure*, *1163*, 327-335. https://doi.org/10.1016/j.molstruc.2018.02.061

Chen, X., Liu, H., Li, J., & Wang, Y. (2022). Rapid identification of total phenolic content levels in boletes by two-dimensional correlation spectroscopy combined with deep learning. *Vibrational Spectroscopy*, *121*, 103404. https://doi.org/10.1016/j.vibspec.2022.103404

Chen, L., Wang, Y., Liu, J., Hong, Z., Wong, K. H., Chiou, J. C., . . . Tian, L. (2023). Structural characteristics and in vitro fermentation patterns of polysaccharides from boletus mushrooms. *Food Funct*, *14*(17), 7912-7923. https://doi.org/10.1039/D3FO01085F

Chitarra, G. S., Abee, T., Rombouts, F. M., Posthumus, M. A., & Dijksterhuis, J. (2004). Germination of Penicillium paneum conidia is regulated by 1-octen-3-ol, a volatile self-inhibitor. *Applied and Environmental Microbiology*, *70*(5), 2823-2829. https://doi.org/10.1128/AEM.70.5.2823-2829.2004

Cho, I. H., Choi, H. K., & Kim, Y. S. (2006). Difference in the volatile composition of pine - mushrooms (*Tricholoma matsutake* Sing.) according to their grades. J*ournal of Agricultural and Food Chemistry*, *54*(13), 4820-4825. https://doi.org/10.1021/jf0601416

Cho, I. H., Kim, S. Y., Choi, H. K., & Kim, Y. S. (2006). Characterization of aroma - active compounds in raw and cooked pine - mushrooms (*Tricholoma matsutake* Sing.). *Journal of Agricultural and Food Chemistry*, *54*(17), 6332-6335. https://doi.org/10.1021/jf060824l

Chuankid, B., Schrey, H., Thongbai, B., Raspé, O., Arnold, N., Hyde, K. D., . . . Stadler, M. (2020). Secondary metabolites of *phlebopus* species from northern thailand. *Mycological Progress*, *19*(12), 1525-1536. https://doi.org/10.1007/s11557-020-01643-y

Cole, R. J., Schweikert, M. A., & Jarvis, B. B. (2003). *Handbook of secondary fungal metabolites* (Vol. 3). Gulf Professional Publishing.

Comandini, O., Contu, M., & Rinaldi, A. C. (2006). An overview of cistus ectomycorrhizal fungi. *Mycorrhiza*, *16*(6), 381-395. https://doi.org/10.1007/s00572-006-0047-8

Corda, A. C. J. (1831). Deutschlands Flora, Abtheilung III. *Die Pilze Deutschlands, 3*(11), 1-32.

Csorbainé, A. G., Bratek, Z., Merényi, Z., Illyès, Z., & Dimény, J. (2008). *Choiromyces meandriformis* and *mattirolomyces terfezioides*, Peculiar truffles with new perspectives. *XVII Convegno Nazionale di Micologia-Pavia*, 10-12.

Cubeta, M. A., Echandi, E., Abernethy, T., & Vilgalys, R. (1991). Characterization of anastomosis groups of binucleate Rhizoctonia species using restriction analysis of an amplified ribosomal RNA gene. *Phytopathology*, *81*(11), 1395-1400. https://doi.org/10.1094/Phyto-81-1395

Cui, Y. Y., Feng, B., Wu, G., Xu, J., & Yang, Z. L. (2016). Porcini mushrooms (Boletus sect. Boletus) from China. *Fungal Diversity*, *81*, 189-212. https://doi.org/10.1007/s13225-015-0336-7

Czerny, M., Christlbauer, M., Christlbauer, M., Fischer, A., Granvogl, M., Hammer, M., . . . Schieberle, P. (2008). Re-investigation on odour thresholds of key food aroma compounds and development of an aroma language based on odour qualities of defined aqueous odorant solutions. *European Food Research and Technology*, *228*, 265-273. https://doi.org/10.1007/s00217-008-0931-x

Daranagama, D. A., Liu, X., Chamyuang, S., Stadler, M., Bahkali, A., & Hyde, K. D. (2015). *Rhopalostroma brevistipitatum* sp. nov. from Thailand with an extended generic description for *Rhopalostroma*. *Phytotaxa*, *227*(3), 229-242. https://doi.org/10.11646/phytotaxa.227.3.2

De la Fuente, J. I., Martínez-González, C. R., Oros-Ortega, I., Guevara, G., Bandala, V. M., Córdova-Lara, I., . . . García-Jiménez, J. (2021). *Melanogaster coccolobae* sp. Nov. (paxillaceae, boletales), un hongo hipogeo tropical de las áreas urbanas de quintana roo, méxico. *Acta Botanica Mexicana,* (128). https://doi.org/10.21829/abm128.2021.1896

Deng, X. J., Liu, P. G., Liu, C. Y., & Wang, Y. (2013). A new white truffle species, *Tuber panzhihuanense* from China. *Mycological Progress*, *12*, 557-561. https://doi.org/10.1007/s11557-012-0862-6

Dentinger, B. T., Ammirati, J. F., Both, E. E., Desjardin, D. E., Halling, R. E., Henkel, T. W., . . . McLaughlin, D. J. (2010). Molecular phylogenetics of porcini mushrooms (*boletus* section *boletu*s). *Mol Phylogenet Evol*, *57*(3), 1276-1292. https://doi.org/10.1016/j.ympev.2010.10.004

Ditengou, F. A., Müller, A., Rosenkranz, M., Felten, J., Lasok, H., Van Doorn, M. M., . . . Polle, A. (2015). Volatile signalling by sesquiterpenes from ectomycorrhizal fungi reprogrammes root architecture. *Nature Communications*, *6*(1), 6279. https://doi.org/10.1038/ncomms7279

Dixon, P. (2003). VEGAN, a package of R functions for community ecology. *Journal of Vegetation Science*, *14*(6), 927-930. https://doi.org/10.1111/j.1654-1103.2003.tb02228.x

Dong, J. E., Zhang, S., Li, T., & Wang, Y. Z. (2022). 2DCOS combined with CNN and blockchain to trace the species of boletes. *Microchemical Journal*, 177, 107260. https://doi.org/10.1016/j.microc.2022.107260

Doyle, J. J., Doyle, J. L., & Brown, A. H. D. (1990). Chloroplast DNA phylogenetic affinities of newly described species in Glycine (Leguminosae, Phaseoleae). *Systematic Botany*, *1990*, 466-471. https://doi.org/10.2307/2419362

Dray, S., & Dufour, A. B. (2007). The ade4 package, implementing the duality diagram for ecologists. *J. Stat. Softw.*, *22*, 1-20. https://doi.org/10.18637/jss.v022.i04

Dray, S., Choler, P., Dolédec, S., Peres-Neto, P. R., Thuiller, W., Pavoine, S., . . . ter Braak, C. J. (2014). Combining the fourth-corner and the RLQ methods for assessing trait responses to environmental variation. *Ecology*, *95*(1), 14-21. https://doi.org/10.1890/13-0196.1

Rambaut, A., & Drummond, A. (2013) *Tracer v1. 5*. http//beast.bio.ed.ac.uk/Tracer

Drummond, A. J., Suchard, M. A., Xie, D., & Rambaut, A. (2012). Bayesian phylogenetics with BEAUti and the BEAST 1.7. *Molecular Biology and Evolution*, *29*(8), 1969-1973. https://doi.org/10.1093/molbev/mss075

Eich, E. (2008*). Solanaceae and Convolvulaceae, Secondary metabolites, Biosynthesis, chemotaxonomy, biological and economic significance (a handbook)*. Springer Science & Business Media.

Ekman, S., & Tønsberg, T. (2002). Most species of Lepraria and Leproloma form a monophyletic group closely related to Stereocaulon. *Mycological Research*, *106*(11), 1262-1276. https://doi.org/10.1017/S0953756202006718

Fan, L., & Yue, S. F. (2013). Phylogenetic divergence of three morphologically similar truffles, *Tuber sphaerosporum*, *T. sinospharosporum*, and *T. pseudoshaerosporum* sp. nov. *Mycotaxon*, *125*, 283-288. https://doi.org/10.5248/125.283

Fan, L., Feng, S., & Cao, J. Z. (2014). The phylogenetic position of *Tuber glabrum* sp. nov. and *T. sinomonosporum* nom. nov., two paradoxa-like truffle species form China. *Mycological Progress*, *13*, 241-246. https://doi.org/10.1007/s11557-013-0908-4

Fan, L., Zhang, P. R., & Yan, X. Y. (2016). Molecular analysis of Chinese truffles resembling *Tuber californicum* in morphology reveals a rich pattern of species diversity with emphasis on four new species. *Mycologia*, *108*(2), 344-353. https://doi.org/10.3852/14-343

Fan, Y., Liu, W., Xu, F., Huang, Y. J., Zhang, N. N., Li, K., . . . Zhang, H. (2019). Comparative flavor analysis of eight varieties of Xinjiang flatbreads from the Xinjiang Region of China. *Cereal Chemistry*, *96*(6), 1022 - 1035. https://doi.org/10.1002/cche.10207

Fan, L., Li, T., Xu, Y. Y., & Yan, X. Y. (2022). Species diversity, phylogeny, endemism and geography of the truffle genus Tuber in China based on morphological and molecular data. *Persoonia*, *48*, 178-202. https://doi.org/10.3767/persoonia.2022.48.05

Feng, B., Xu, J., Wu, G., Hosen, M. I., Zeng, N. K., Li, Y. C., . . . Yang, Z. L. (2012). DNA sequence analyses reveal abundant diversity, endemism and evidence for asian origin of the porcini mushrooms. *PLoS One*, *7*(5), e37567. https://doi.org/10.1371/journal.pone.0037567

Feng, B., Liu, J. W., Xu, J. P., Zhao, K., Ge, Z. W., & Yang, Z. L. (2017). Ecological and physical barriers shape genetic structure of the Alpine porcini (*Boletus reticuloceps*). *Mycorrhiza*, *27*, 261-272. https://doi.org/10.1007/s00572-016-0751-y

Feng, B., & Yang, Z. L. (2018). Studies on diversity of higher fungi in Yunnan, southwestern China, A review. *Plant Diversity*, *40*, 165-171. https://doi.org/10.1016/j.pld.2018.07.001

Ferdman, Y., Aviram, S., Rothbejerano, N., Trappe, J. M., & Kaganzur, V. (2005). Phylogenetic studies of *Terfezia pfeilii* and *Choiromyces echinulatus* (Pezizales) support new genera for southern African truffles, Kalaharituber and Eremiomyces. *Mycological Research*, *109*(2), 237-245. https://doi.org/10.1017/S0953756204001789

Frank, J. L., Barry, S., & Southworth, D. (2006). Mammal mycophagy and dispersal of mycorrhizal inoculum in Oregon white oak woodlands. *Northwest Sci.*, *80*(4), 264-273.

Friedman, M. (2016). Mushroom polysaccharides, Chemistry and antiobesity, antidiabetes, anticancer, and antibiotic properties in cells, rodents, and humans. *Foods*, *5*(4), 80. https://doi.org/10.3390/foods5040080

Frisvad, J. C., Andersen, B., & Thrane, U. (2008). The use of secondary metabolite profiling in chemotaxonomy of filamentous fungi. *Mycological Research*, *112*(2), 231-240. https://doi.org/10.1016/j.mycres.2007.08.018

Frisvad, J. C. (2015). Fungal chemotaxonomy. In S. Zeilinger, J. F. Martín, C. García-Estrada (Eds.), *Biosynthesis and molecular genetics of fungal secondary metabolites, fungal biology*. Springer.

Gámez-Virués, S., Perović, D. J., Gossner, M. M., Börschig, C., Blüthgen, N., De Jong, H., . . . Westphal, C. (2015). Landscape simplification filters species traits and drives biotic homogenization. *Nature Communications*, *6*(1), 8568. https://doi.org/10.1038/ncomms9568

Garey, J. R. (2021). Investigations in the boletes (Boletaceae) of southeastern USA, four novel species and three novel combinations. *Mycosphere*, *12*, 1038-1076. https://doi.org/10.5943/mycosphere/12/1/12

García-Palacios, P., Gross, N., Gaitán, J., & Maestre, F. T. (2018). Climate mediates the biodiversity-ecosystem stability relationship globally. *Proceedings of the National Academy of Sciences*, *115*(33), 201800425. https://doi.org/10.1073/pnas.1800425115

Ghahremani-Majd, H., & Dashti, F. (2015). Chemical composition and antioxidant properties of cultivated button mushrooms (agaricus bisporus). *Horticulture, Environment, and Biotechnology*, *56*(3), 376-382. https://doi.org/10.1007/s13580-015-0124-z

Giannetti, V., Mariani, M. B., Mannino, P., & Marini, F. (2017). Volatile fraction analysis by HS - SPME/GC - MS and chemometric modeling for traceability of apples cultivated in the Northeast Italy. *Food Control*, *78*, 215-221. https://doi.org/10.1016/j.foodcont.2017.02.036

Gilbert, E. J. (1931). *Les bolets. Librairie E*. Le François.

Gilkey, H. M. (1939). *Tuberales of North America. Oregon State Monographs, studies in botany* (vol. 1). Oregon State College.

Ginigini, J., Lecellier, G. J., Nicolas, M., Nour, M., Hnawia, E., Lebouvier, N., . . . Raharivelomanana, P. (2019). Chemodiversity of *Calophyllum inophyllum* L. oil bioactive components related to their specific geographical distribution in the South Pacific region. *PeerJ*, *7*, e6896. https://doi.org/10.7717/peerj.6896

Gioacchini, A. M., Menotta, M., Bertini, L., Rossi, I., Zeppa, S., Zambonelli, A., . . . Stocchi, V. (2005). Solid-phase microextraction gas chromatography/mass spectrometry, A new method for species identification of truffles. *Rapid Commun Mass Spectrom*, *19*(17), 2365-2370. https://doi.org/10.1002/rcm.2031

Giri, A., Osako, K., & Ohshima, T. (2010). Identification and characterisation of headspace volatiles of fish miso, a Japanese fish meat based fermented paste, with special emphasis on effect of fish species and meat washing. *Food Chemistry*, *120*(2), 621-631. https://doi.org/10.1016/j.foodchem.2009.10.036

Gong, F., Liang, Y. Z., Xie, P. S., & Chau, F. T. (2003). Information theory applied to chromatographic fingerprint of herbal medicine for quality control. *Journal of Chromatography A*, *1002*(1-2), 25-40. https://doi.org/10.1016/S0021-9673(03)00648-4

Gonmori, K., Fujita, H., Yokoyama, K., Watanabe, K., & Suzuki, O. (2011). Mushroom toxins, A forensic toxicological review. *Forensic Toxicology*, *29*(2), 85-94. https://doi.org/10.1007/s11419-011-0115-4

Gougeon, R. D., Lucio, M., Frommberger, M., Peyron, D., Chassagne, D., Alexandre, H., . . . Schmitt-Kopplin, P. (2009). The chemodiversity of wines can reveal a metabologeography expression of cooperage oak wood. *Proceedings of the National Academy of Sciences*, *106*(23), 9174-9179. https://doi.org/10.1073/pnas.0901100106

Gow, N. A. R., Latge, J-P., & Munro, C. A. (2017). The fungal cell wall, structure, biosynthesis, and function. *Microbiology Spectrum*, *5*(3), 10-1128. https://doi.org/10.1128/microbiolspec.FUNK-0035-2016

Grosshauser, S., & Schieberle, P. (2013). Characterization of the key odorants in pan-fried white mushrooms (Agaricus bisporus L.) by means of molecular sensory science, comparison with the raw mushroom tissue. *Journal of Agricultural and Food Chemistry*, *61*, 3804-3813. https://doi.org/10.1021/jf4006752

Guerin-Laguette, A. (2021). Successes and challenges in the sustainable cultivation of edible mycorrhizal fungi - furthering the dream. *Mycoscience*, *62*(1), 10-28. https://doi.org/10.47371/mycosci.2020.11.007

Guo, Y., Jud, W., Weikl, F., Ghirardo, A., Junker, R. R., Polle, A., . . . Rosenkranz, M. (2021). Volatile organic compound patterns predict fungal trophic mode and lifestyle. *Communications Biology*, *4*(1), 673. https://doi.org/10.1038/s42003-021-02198-8

Guo, Q., Adelina, N. M., Hu, J., Zhang, L., & Zhao, Y. (2022). Comparative analysis of volatile profiles in four pine - mushrooms using HS - SPME/GC - MS and E - nose. *Food Control*, *134*, 108711. https://doi.org/10.1016/j.foodcont.2021.108711

Guo, Y., Sun, K., Cheng, Y., Yu, H., Xie, Y., Zhang, H., . . . Qian, H. (2022). Authentication of shiitake powder using HPLC fingerprints combined with chemometrics. *European Food Research and Technology*, *248*(4), 1117-1123. https://doi.org/10.1007/s00217-021-03950-4

Halász, K. (2008). *Különböző stressztűrőképességű nagygombanemzetségek Kárpát-medencei leletanyagának molekuláris azonosítása és rendszerezése*. Doktori értekezés, Biológia Doktori Iskola.

Halász, K., Bratek, Z., Szegő, D., Szabolcs, R. S., Ilona, R. I., Lásztity, D., . . . Trappe, J. M. (2005). Tests of species concepts of the small, white, European group of *Tuber* spp. based on morphology and rDNA ITS sequences with special reference to *Tuber rapaeodorum*. *Mycol Progress*, *4*, 281-290. https://doi.org/10.1007/s11557-006-0132-6

Hall, T. A. (1999). BioEdit, a user-friendly biological sequence alignment editor and analysis program for Windows 95/98/NT. *Nucl. Acids. Symp. Ser.*, *41*, 95.

Halling, R., & Mueller, G. (2002). Agarics and boletes of neotropical oakwoods. *Tropical Mycology*, *1*, 1-10. https://doi.org/10.1079/9780851995427.0001

Hao, J. W., Chen, Y., & Chen, N. D. (2020). Assessment of ATR-NIR and ATR-MIR spectroscopy as an analytical tool for the quantification of the total polyphenols in *Dendrobium huoshanense*. *Phytochemical Analysis*, *31*(3), 366-374. https://doi.org/10.1002/pca.2903

Hayward, J., Tourtellot, S. G., & Horton, T. R. (2014). A revision of the *Alpova diplophloeus* complex in North America. *Mycologia*, *106*(4), 846-855. https://doi.org/10.3852/13-360

He, Y., Li, X., & Deng, X. (2007). Discrimination of varieties of tea using near infrared spectroscopy by principal component analysis and BP model. *Journal of food Engineering*, *79*(4), 1238-1242. https://doi.org/10.1016/j.jfoodeng.2006.04.042

He, M. Q., Zhao, R. L., Hyde, K. D., Begerow, D., Kemler, M., Yurkov, A., . . . Kirk, P. M. (2019). Notes, outline and divergence times of Basidiomycota. *Fungal Diversity*, *99*, 105-367. https://doi.org/10.1007/s13225-019-00435-4

Hegnauer, R. (1986). Phytochemistry and plant taxonomy—An essay on the chemotaxonomy of higher plants. *Phytochemistry*, *25*(7), 1519-1535. https://doi.org/10.1016/S0031-9422(00)81204-2

Heinemann, P. (1982). Quelques Psalliotes de Nouvelle-Guinee (Papua New Guinea). *Bulletin du Jardin botanique national de Belgique/Bulletin van de Nationale Plantentuin van Belgie*, *52*, 405-413. https://doi.org/10.2307/3667893

Hillis, D. M., & Bull, J. J. (1993). An empirical test of bootstrapping as a method for assessing confidence in phylogenetic analysis. *Systematic Biology*, *42*(2), 182-192. https://doi.org/10.2307/2992540

Hofstetter, V., Clémencon, H., Vilgalys, R., & Moncalvo, J. M. (2002). Phylogenetic analyses of the *Lyophylleae* (Agaricales, Basidiomycota) based on nuclear and mitochondrial rDNA sequences. *Mycological Research*, *106*(9), 1043-1059. https://doi.org/10.1017/S095375620200641X

Horak, E. (2005). *Röhrlinge und Blätterpilze in Europa*. Elsevier GmbH.

Horak, E. (2011). Revision of Malaysian species of Boletales s.l. (Basidiomycota) described by EJH Corner (1972, 1974). *Malay For Rec*., *51*, 1-283.

Hou, S., & Riley, C. B. (2015). Is uncorrelated linear discriminant analysis really a new method? Chemom. *Intell. Lab. Syst.*, *142*, 49-53. https://doi.org/10.1016/j.chemolab.2015.01.005

Hu, L., Liu, J. K., & Wang, F. F. (2015). Chemical consistents in the fruiting bodies of *Boletus magnificus* W. F. Chiu. *Journal of Yunnan Minzu University (Natural Sciences Edition), 24*(2), 94-97. (In China)

Hu, J. J., Zhao, G. P., Tuo, Y. L., Qi, Z. X., Yue, L., Zhang, B., . . . Li, Y. (2022). Ecological factors influencing the occurrence of macrofungi from eastern mountainous areas to the central plains of Jilin province, China. *Journal of Fungi*, *8*(8), 871. https://doi.org/10.3390/jof8080871

Huang, K. B., Chen, M., & Fan, L. (2017). *Tuber griseolivaceum* sp. nov., a new olive-gray truffle species from China based on morphological and DNA data. *Phytotaxa*, *309*(2), 166-172. https://doi.org/10.11646/phytotaxa.309.2.8

Hyde, K. D., Abdel-Wahab, M. A., Abdollahzadeh, J., Abeywickrama, P. D., Absalan, S., Afshari, N., . . . Ertz, D. (2023). Global consortium for the classification of fungi and fungus-like taxa. *Mycosphere*, *14*(1), 1960-2012. https://doi.org/10.5943/mycosphere/14/1/23

Ibrahimi, H., Gadzovska-Simic, S., Tusevski, O., & Haziri, A. (2020). Generation of flavor compounds by biotransformation of genetically modified hairy roots of *Hypericum perforatum* (L.) with basidiomycetes. *Food Science & Nutrition*, 8(6), 2809-2816. https://doi.org/10.1002/fsn3.1573

Jakobs, R., & Müller, C. (2018). Effects of intraspecific and intra-individual differences in plant quality on preferebce and performance of monophagous aphid species. *Oecologia*, *186*(1), 173-184. https://doi.org/10.1007/s00442-017-3998-x

Jargeat, P., Chaumeton, J. P., Navaud, O., Vizzini, A., & Gryta, H. (2014). The *Paxillus involutus* (Boletales, Paxillaceae) complex in Europe, genetic diversity and morphological description of the new species *Paxillus cuprinus*, typification of *P. involutus* ss, and synthesis of species boundaries. *Fungal Biology*, *118*(1), 12-31. https://doi.org/10.1016/j.funbio.2013.10.008

Jarzyna, M., A., Quintero, I., & Jetz, W. (2021). Global functional and phylogenetic structure of avian assemblages across elevation and latitude. *Ecology Letters*, *24*(2), 196-207. https://doi.org/10.1111/ele.13631

Jedidi, I. K., Ayoub, I. K., Philippe, T., & Bouzouita, N. (2017). Chemical composition and nutritional value of three tunisian wild edible mushrooms. *Journal of Food Measurement and Characterization*, *11*(4), 2069-2075. https://doi.org/10.1007/s11694-017-9590-6

Ji, K. P., Cao, Y., Zhang, C.-X., He, M.-X., Liu, J., Wang, W.-B., . . . Wang, Y. (2010). Cultivation of *phlebopus portentosus* in southern china. *Mycological Progress*, *10*(3), 293-300. https://doi.org/10.1007/s11557-010-0700-7

Jiang, S., Mi, H. X., Xie, H. J., Zhang, X., Chen, Y., Liang, Z. Q., . . . Zeng, N. K. (2021). *Neoboletus infuscatus*, a new tropical bolete from hainan, southern china. *Mycoscience*, *62*(3), 205-211. https://doi.org/10.47371/mycosci.2021.03.001

Jiang, L. Y., Pettitt, T. R., Buenfeld, N., & Smith, S. R. (2022). A critical review of the physiological, ecological, physical and chemical factors influencing the microbial degradation of concrete by fungi. *Building and Environment, 214*, 108925. https://doi.org/10.1016/j.buildenv.2022.108925

Jiang, Y., Xia, J. Y., Che, C. Y., & Wei, Y. N. (2022). Data-driven classification of prediabetes using cardiometabolic biomarkers, Data from National Health and Nutrition Examination Survey 2007-2016. *Frontiers in Endocrinology*, *13*, 937942. https://doi.org/10.3389/fendo.2022.937942

Jin, Y., Liang, T., Fu, Q., Xiao, Y. S., Feng, J. T., Ke, Y. X., . . . Liang, X. M. (2009). Fingerprint analysis of Ligusticum chuanxiong using hydrophilic interaction chromatography and reversed-phase liquid chromatography. *Journal of Chromatography A*, *1216*(11), 2136-2141. https://doi.org/10.1016/j.chroma.2008.04.010

Jung, M. Y., Lee, D. E., Cheng, H. Y., Chung, I. M., Kim, S. H., Han, J. G., . . . Kong, W. S. (2019). Characterization of volatile profiles of six popular edible mushrooms using headspace-solid-phase microextraction coupled with gas chromatography combined with chemometric analysis. *Journal of Food Science*, *84*(3), 421-429. https://doi.org/10.1111/1750-3841.14481

Justus, K., Herrmann, R., Klamann, J. D., Gruber, G., Hellwig, V., Ingerl, A., . . . Steglich, W. (2007). Retipolides - unusual spiromacrolactones from the mushrooms retiboletus retipes and r. Ornatipes. *European Journal of Organic Chemistry*, *2007*(33), 5560-5572. https://doi.org/10.1002/ejoc.200700579

Karine, P., Paul, A., Andre, G., & Russell, J. T. (2006). Fatty acid composition of lipids from mushrooms belonging to the family boletaceae. *Mycol Res*, *110*(10), 1179-1183. https://doi.org/10.1016/j.mycres.2006.05.006

Katoh, K., & Standley, D. M. (2013). MAFFT Multiple sequence alignment software version 7, Improvements in performance and usability. *Molecular Biology and Evolution*, *30*, 772-780. https://doi.org/10.1093/molbev/mst010

Keissler, K., & Lohwag, H. (1937). Fungi, in Handel-Mazzeti. *Symb Sin*., *2*, 1-83.

Kembel, S. W., Cowan, P. D., Helmus, M. R., Cornwell, W. K., Morlon, H., Ackerly, D. D., . . . Webb, C. O. (2010). Picante, R tools for integrating phylogenies and ecology. *Bioinformatics*, *26*(11), 1463-1464. https://doi.org/10.1093/bioinformatics/btq166

Kinoshita, A., Sasaki, H., & Nara, K. (2011). Phylogeny and diversity of japanese truffles (tuber spp.) inferred from sequences of four nuclear loci. *Mycologia*, *103*(4), 779-794. https://doi.org/10.3852/10-138

Kinoshita, A., Sasaki, H., Orihara, T., Nakajima, M., & Nara, K. (2021). *Tuber iryudaense* and *T. tomentosum*, two new truffles encased in tomentose mycelium from Japan. *Mycologia*, *113*(3), 653-663. https://doi.org/10.1080/00275514.2021.1875709

Kirk, P. M., Cannon, P. F., & Minter D. W. J. C., & Stalpers J. A. (2008). *Dictionary of the fungi* (10th ed.). CAB International.

Knapp, A. (1954). Die Europäischen Hypogaeen-Gattungen und ihre Gattungstypen. II. Teil (Fortsetzung). Die Gattungstypen der Melanogastraceae und weitere spezies. *Schweizerisches Zeitschrift für Pilzkunde*, *32*(8), 117-130.

Krishnamurthy, R., & Hud, N. V. (2020). Introduction, chemical evolution and the origins of Life. *Chemical Reviews*, *120*(11), 4613-4615. https://doi.org/10.1021/acs.chemrev.0c00409

Krzywinski, M., Schein, J., Birol, I., Connors, J., Gascoyne, R., Horsman, D., . . . Marra, M. A. (2009). Circos, an information aesthetic for comparative genomics. *Genome Research*, *19*(9), 1639-1645. https://doi.org/10.1101/gr.092759.109

Kuhnert, E., Surup, F., Wiebach, V., Bernecker, S., & Stadler, M. (2015). Botryane, noreudesmane and abietane terpenoids from the ascomycete Hypoxylon rickii. *Phytochemistry*, *117*, 116-122. https://doi.org/10.1016/j.phytochem.2015.06.002

Kuhnert, E., Sir, E. B., Lambert, C., Hyde, K. D., Hladki, A. I., Romero, A. I., . . . Stadler, M. (2017). Phylogenetic and chemotaxonomic resolution of the genus Annulohypoxylon (Xylariaceae) including four new species. *Fungal Diversity*, *85*, 1-43. https://doi.org/10.1007/s13225-016-0377-6

Kumar Sharma, S., & Gautam, N. (2017). Chemical and bioactive profiling, and biological activities of coral fungi from northwestern Himalayas. *Scientific Reports*, *7*(1), 1-13. https://doi.org/10.1038/srep46570

Kumar, S., Suleski, M., Craig, J. M., Kasprowicz, A. E., Sanderford, M., Li, M., . . . Hedges, S. B. (2022). TimeTree 5, an expanded resource for species divergence times. *Molecular Biology and Evolution*, *39*(8), msac174. https://doi.org/10.1093/molbev/msac174

Kumla, J., Danell, E., & Lumyong, S. (2015). Improvement of yield for a tropical black bolete, *phlebopus portentosus*, cultivation in northern thailand. *Mycoscience*, *56*(1), 114-117. https://doi.org/10.1016/j.myc.2014.04.005

La Barre, S. (2014). Marine biodiversity and chemodiversity-The treasure troves of the future. In O. Grillo (Ed.), *The dynamic balance of the planet* (pp. 69-94). BoD – Books on Demand.

Lacheva, M. (2015). New records of *Melanogaster* species (Fungi, Boletales) in Bulgaria. *Journal of Biodiversity and Environmental Sciences (JBES)*, *6*(1), 494-500.

Lambert, C., Wendt, L., Hladki, A. I., Stadler, M., & Sir, E. B. (2019). Hypomontagnella (Hypoxylaceae), a new genus segregated from Hypoxylon by a polyphasic taxonomic approach. *Mycological Progress*, *18*, 187-201. https://doi.org/10.1007/s11557-018-1452-z

Larrauri, M., Demaría, M. G., Ryan, L. C., Asensio, C. M., Grosso, N. R., & Nepote, V. (2016). Chemical and sensory quality preservation in coated almonds with the addition of antioxidants. *Journal of Food Science*, *81*(1), S208-S215. https://doi.org/10.1111/1750-3841.13164

Larsson, E., & Sundberg, H. (2011). *Lyophyllum shimeji*, A species associates with lichen pine forest in northern Fennoscandia. *Mycosience*, *52*, 289-295. https://doi.org/10.1007/S10267-010-0104-1

Lasalvia, M., Capozzi, V., & Perna, G. (2022). A comparison of PCA - LDA and PLS - DA techniques for classification of vibrational spectra. *Applied Sciences*, *12*(11), 5345. https://doi.org/10.3390/app12115345

Lauri, S. A. A. G., Andres, S. A. A. G., & Randlane, T. (2009). World survey of the genus Lepraria (Stereocaulaceae, lichenized Ascomycota). *The Lichenologist*, *41*(1), 25-60. https://doi.org/10.1017/S0024282909007993

Lee, J., Xiao, L., Zhang, G., Ebeler, S. E., & Mitchell, A. E. (2014). Influence of storage on volatile profiles in roasted almonds (Prunus dulcis). *Journal of Agricultural and Food Chemistry*, *62*, 11236-11245. https://doi.org/10.1021/jf503817g

Li, S. H., Zhao, Y. C., Yu, F. Q., Wang, X. H., Zhang, X. L., & Liu, P. G. (2011). Systematics of the easily confusing poisonous Boletes from Yunnan wild mushroom markets. *Journal of Edible Fungi*, *30*, 34-36.

Li, H. B., Wei, H. L., Peng, H. Z., Ding, H. M., Wang, L. L., He, L., . . . Fu, L. Z. (2014). *Boletus roseoflavus*, A new species of boletus in section appendiculati from china. *Mycological Progress*, *13*(1), 21-31. https://doi.org/10.1007/s11557-013-0888-4

Li, S. H., Zheng, L. Y., Liu, C. Y., Wang, Y., Li, L., Zhao, Y. C., . . . Zhou, D. Q. (2014). Two new truffles species, *Tuber alboumbilicum* and *Tuber pseudobrumale* from China. *Mycological Progress*, *13*(4), 1157-1163. https://doi.org/10.1007/s11557-014-1004-0

Li, M., Yang, R., Zhang, H., Wang, S., Chen, D., & Lin, S. (2019). Development of a flavor fingerprint by HS - GC-IMS with PCA for volatile compounds of *Tricholoma matsutake* Singer. *Food Chemistry*, *290*, 32-39. https://doi.org/10.1016/j.foodchem.2019.03.124

Li, Y. C., & Yang, Z. L. (2021). *The boletes of China: Tylopilus sl*. Springer.

Li, J., Wu, H., Wang, L., Huang, Y., & Wang, L. (2021). Key taste components in two wild edible boletus mushrooms using widely targeted metabolomics. *Biochemical Systematics and Ecology*, *96*, 104268. https://doi.org/10.1016/j.bse.2021.104268

Li, W., Chen, W. C., Wang, J. B., Feng, J., Wu, D., Zhang, Z., . . . Yang, Y. (2021). Screening candidate genes related to volatile synthesis in shiitake mushrooms and construction of regulatory networks to effectively improve mushroom aroma. *Journal of the Science of Food and Agriculture*, *101*(13), 5618-5626. https://doi.org/10.1002/jsfa.11213

Li, W., Pires, S. M., Liu, Z., Liang, J., Wang, Y., Chen, W., . . . Guo, Y. (2021). Mushroom poisoning outbreaks—china, 2010-2020. *China CDC weekly*, *3*(24), 518. https://doi.org/10.46234/ccdcw2021.134

Li, Y., Wang, S. Z., Cao, S., & Zhou, C. F. (2021). Chemodiversity of soil dissolved organic matter and its association with soil microbial communities along a chronosequence of Chinese Fir monoculture plantations. *Frontiers in Microbiology*, *12*, 729344. https://doi.org/10.3389/fmicb.2021.729344

Li, H., Zhang, H., Zhang, Y., Zhou, J., Yin, Y., He, Q., . . . Sun, C. (2022). Mushroom poisoning outbreaks—china, 2021. *China CDC weekly*, *4*(3), 35. https://doi.org/10.46234/ccdcw2021.014

Li, P., Liu, J., Saleem, M., Li, G., Luan, L., Wu, M., . . . Li, Z. (2022). Reduced chemodiversity suppresses rhizosphere microbiome functioning in the mono-cropped agroecosystems. *Microbiome*, *10*(1), 108. https://doi.org/10.1186/s40168-022-01287-y

Li, H., Zhang, Y., Zhang, H., Zhou, J., Liang, J., Yin, Y., . . . Sun, C. (2023). Mushroom poisoning outbreaks—china, 2022. *China CDC weekly*, *5*(3), 45. https://doi.org/10.46234/ccdcw2023.009

Li, X. B., Hu, C. M., Li, C. H., Ji, G. Y., Luo, S. Z., Cao, Y., . . . Yang, R. H. (2023). Lc/ms- and gc/ms-based metabolomic profiling to determine changes in flavor quality and bioactive components of *phlebopus portentosus* under low-temperature storage. *Front Nutr*, *10*, 1168025. https://doi.org/10.3389/fnut.2023.1168025

Liang, Z. Q., An, D. Y., Jiang, S., Su, M.-S., & Zeng, N. K. (2016). *Butyriboletus hainanensis* (boletaceae, boletales), A new species from tropical china. *Phytotaxa*, *267*(4), 256-262. https://doi.org/10.11646/phytotaxa.267.4.2

Liberda, E. N., Zuk, A. M., Martin, I. D., & Tsuji, L. J. (2020). Fisher's linear discriminant function analysis and its potential utility as a tool for the assessment of health - and - wellness programs in indigenous communities. *International Journal of Environmental Research and Public Health*, *17*(21), 7894. https://doi.org/10.3390/ijerph17217894

Liebel, H. T., Bidartondo, M. I., & Gebauer, G. (2015). Are carbon and nitrogen exchange between fungi and the orchid Goodyera repens affected by irradiance? *Annals of Botany*, *115*, 251-261. https://doi.org/10.1093/aob/mcu240

Lin, C. L., Tsai, M. J., Fu, C. H., Chang, T. T., Li, H. T., & Wong, K. F. (2018). *Tuber elevatireticulatum* sp. nov., A new species of whitish truffle from Taiwan. *Botanical Studies*, *59*(1), 25.

Lin, P., Yan, Z. F., Kook, M., Li, C. T., & Yi, T. H. (2022). Genetic and chemical diversity of edible mushroom pleurotus species. *Biomed Res Int*, *2022*, 6068185. https://doi.org/10.1155/2022/6068185

Lin, P., Kook, M., Yi, T. H., & Yan, Z. F. (2023). Current fungal taxonomy and developments in the identification system. *Current Microbiology*, *80*(12), 375.

Linnaeus, C. (1753). *Species plantarum* (vol. 2). Laurentius Salvius.

Liu, B., Tao, K., & Chang, M. C. (1989). Two new species of *Melanogaster* from China. *Acta Mycologica Sinica*, *8*, 210-213.

Liu, B., Tao, K., & Chang, M. C. (1990). New species and new records of hypogeous fungi from china III. *Mycosystema*, *9*(1), 25-30.

Liu, Y., Chen, D., You, Y., Zeng, S., Li, Y., Tang, Q., . . . Chen, D. (2016). Nutritional composition of boletus mushrooms from southwest china and their antihyperglycemic and antioxidant activities. *Food Chem.*, *211*, 83-91. https://doi.org/10.1016/j.foodchem.2016.05.032

Liu, H. Y., Li, Y. C., & Bau, T. (2020). New species of *retiboletus* (boletales, boletaceae) from china based on morphological and molecular data. *MycoKeys*, *67*, 33-44. https://doi.org/10.3897/mycokeys.67.51020

Liu, Q., & Wang, L. (2021). t - Test and ANOVA for data with ceiling and/or floor effects. *Behavior Research Methods*, *53*(1), 264-277. https://doi.org/10.3758/s13428-020-01407-2

Liu, S., Liu, H., Li, J., & Wang, Y. (2023). Solving the identification problems of bolete origins based on multiple data processing, Take *boletus bainiugan* as an example. *Journal of Food Composition and Analysis*, *124*, 105693. https://doi.org/10.1016/j.jfca.2023.105693

Ma, J., Xia, J., Li, H. J., Su, L. J., Xue, R., Jiang, S., . . . Tang, L. P. (2023). Four cases of reported adverse effects from black boletoi, anthracoporus nigropurpureus (boletaceae) mushroom ingestion. *Toxicon*, *230*, 107155. https://doi.org/10.1016/j.toxicon.2023.107155

Magneville, C., Loiseau, N., Albouy, C., Casajus, N., Claverie, T., Escalas, A., . . . Villéger, S. (2022). mFD, an R package to compute and illustrate the multiple facets of functional diversity. *Ecography*, *2022*(1), e05904. https://doi.org/10.1111/ecog.05904

Maire, E., Grenouillet, G., Brosse, S., & Villéger, S. (2015). How many dimensions are needed to accurately assess functional diversity? A pragmatic approach for assessing the quality of functional spaces. *Global Ecology and Biogeography*, *24*(6), 728-740. https://doi.org/10.1111/geb.12299

Malheiro, R., de Pinho, P. G., Soares, S., da Silva Ferreira, A. C., & Baptista, P. (2013). Volatile biomarkers for wild mushrooms species discrimination. *Food Research International*, *54*(1), 186-194. https://doi.org/10.1016/j.foodres.2013.06.010

Manikandan, K. (2011). Nutritional and medicinal values of mushrooms. In M. Singh, B. Vijay, S. Kamal & G. C. Wakchaure (Eds.), *Mushrooms cultivation, marketing and consumption* (pp. 11-14). Solan, Directorate of Mushroom Research.

Mao, X. L. (2000). *The macrofungi of China*. Henan sicience and technology press.

Mao, N., Zhao, T. Y., Zhang, Y. X., Li, T., Lv, H. C., & Fan, L. (2023). Boletaceae from Shanxi province of northern China with descriptions of ten new species. *Mycosphere*, *14*(1), 2013-2091. https://doi.org/10.5943/mycosphere/14/1/24

Maharachchikumbura, S. S., Chen, Y., Ariyawansa, H. A., Hyde, K. D., Haelewaters, D., Perera, R. H., . . . Stadler, M. (2021). Integrative approaches for species delimitation in Ascomycota. *Fungal Diversity*, *109*(1), 155-179. https://doi.org/10.1007/s13225-021-00486-6

Maranna, S., Nataraj, V., Kumawat, G., Chandra, S., Rajesh, V., Ramteke, R., . . . Khandekar, N. (2021). Breeding for higher yield, early maturity, wider adaptability and waterlogging tolerance in soybean (Glycine max L.), A case study. *Scientific Reports*, *11*(1), 22853. https://doi.org/10.1038/s41598-021-02064-x

Marchand, S., de Revel, G., & Bertrand, A. (2000). Approaches to wine aroma, release of aroma compounds from reactions between cysteine and carbonyl compounds in wine. *Journal of Agricultural and Food Chemistry*, *48*(10), 4890-4895. https://doi.org/10.1021/jf000149u

Matheny, P. B. (2005). Improving phylogenetic inference of mushrooms with RPB1 and RPB2 nucleotide sequences (Inocybe, Agaricales). *Molecular Phylogenetics and Evolution*, *35*(1), 1-20. https://doi.org/10.1016/j.ympev.2004.11.014

Matheny, P. B., Wang, Z., Binder, M., Curtis, J. M., Lim, Y. W., Nilsson, R. H., . . . Hibbett, D. S. (2007). Contributions of rpb2 and tef1 to the phylogeny of mushrooms and allies (Basidiomycota, Fungi). *Molecular Phylogenetics and Evolution*, *43*(2), 430-451. https://doi.org/10.1016/j.ympev.2006.08.024

Mattila, P., Könkö, K., Eurola, M., Pihlava, J. M., Astola, J., Vahteristo, L., . . . Piironen, V. (2001). Contents of vitamins, mineral elements, and some phenolic compounds in cultivated mushrooms. *J Agric Food Chem*, *49*(5), 2343-2348. https://doi.org/10.1021/jf001525d

Mei, Y., Liu, C. Y., Li, S. H., Guerin-Laguette, A., Xiao, Y. J., Tang, P., . . . Wang, Y. (2021). *Phlebopus roseus*, a new edible bolete from china, is associated with insects and plants. *Mycologia*, *113*(1), 33-42. https://doi.org/10.1080/00275514.2020.1816781

Melanogaster (fungus). (2024, April 3). In *Wikipedia*. https://upload.wikimedia.org/wikipedia/commons/5/5a/Melanogaster_tuberiformis_17757.jpg

Meng, X., Liang, H., & Luo, L. (2016). Antitumor polysaccharides from mushrooms, A review on the structural characteristics, antitumor mechanisms and immunomodulating activities. *Carbohydr Res*, *424*, 30-41. https://doi.org/10.1016/j.carres.2016.02.008

Miller, M. A., Holder, M. T., Vos, R., Midford, P. E., Liebowitz, T., Chan, L., . . . Warnow, T. (2009). *The CIPRES portal*. http://www.phylo.org/portal2/hom

Mishra, P., Biancolillo, A., Roger, J. M., Marini, F., & Rutledge, D. N. (2020). New data preprocessing trends based on ensemble of multiple preprocessing techniques. *TrAC Trends in Analytical Chemistry*, *132*, 116045. https://doi.org/10.1016/j.trac.2020.116045

Montecchi, A., & Sarasini, M. (2000). *Funghi ipogei d'Europa*. AMB Fondazione Centro Studi Micologici.

Moreau, P. A., Rochet, J., Richard, F., Chassagne, F., Manzi, S., & Gardes, M. (2011). Taxonomy of alnus-associated hypogeous species of *alpova* and *melanogaster* (basidiomycota, paxillaceae) in europe. *Cryptogamie, Mycologie*, *32*(1), 33-62. https://doi.org/10.7872/crym.v32.iss1.2012.033

Moreau, P. A., Stéphane, W., Branislav, P., Jargeat, P., Manzi, S., & Vizzini, A. (2013). *Alpova komoviana* (Boletales, Paxillaceae), a new sequestrate fungus from montenegro, with a revised phylogeny of the genus in europe. *Mycological Progress*, *12*(1), 109-119. https://doi.org/10.1007/s11557-012-0818-x

Moreno, G., Alvarado, P., & Manjon, J. L. (2012). Phylogenetic affiliation of (*Choiromyces magnusi*i and *C. venosus* Tuberaceae ascomycota) from Spain. *Mycological Progress*, *11*(2), 463-471. https://doi.org/10.1007/s11557-011-0762-1

Moreno, G., Manjón, L., Díez, J., García-Montero, L. G., & Di Massimo, G. (1997). *Tuber pseudohimalayense* sp. nov. commercialized in Spain, similar to the "Perigord" truffle. *Mycotaxon*, *63*, 217-224.

Moros, J., Garrigues, S., & de la Guardia, M. (2010). Vibrational spectroscopy provides a green tool for multi - component analysis. *TrAC Trends in Analytical Chemistry*, *29*(7), 578-591. https://doi.org/10.1016/j.trac.2009.12.012

Münkemüller, T., Lavergne, S., Bzeznik, B., Dray, S., Jombart, T., Schiffers, K., . . . Thuiller, W. (2012). How to measure and test phylogenetic signal. *Methods in Ecology and Evolution*, *3*(4), 743-756. https://doi.org/10.1111/j.2041-210X.2012.00196.x

Nakalembe, I., & Kabasa, J. D. (2013). Fatty and amino acids composition of selected wild edible mushrooms of bunyoro sub-region, uganda. *African .Journal of Food, Agriculture, Nutrition and Development*, *13*(1), 7225-7241. https://doi.org/10.18697/ajfand.56.11945

Naranjo-Ortiz, M. A., & Gabaldón, T (2019). Fungal evolution, major ecological adaptations and evolutionary transitions. *Biological Reviews*, *94*(4), 1443-1476. https://doi.org/10.1111/brv.12510

Nilsson, R. H., Kristiansson, E., Ryberg, M., Hallenberg, N., & Larsson, K. H. (2008). Intraspecific ITS variability in the kingdom fungi as expressed in the international sequence databases and its implications for molecular species identification. *Evolutionary Bioinformatics*, *4*, EBO-S653. https://doi.org/10.4137/EBO.S653

Noda, I. (1993). Generalized two-dimensional correlation method applicable to Infrared, Raman, and other types of spectroscopy. *Appied Spectroscopy*, *47*(9), 1329-1336. https://doi.org/10.1366/0003702934067694

Nöfer, J., Lech, K., Figiel, A., Szumny, A., & Carbonell-Barrachina, Á. A. (2018). The influence of drying method on volatile composition and sensory profile of Boletus edulis. *Journal of Food Quality*, *2018*(1), 2158482. https://doi.org/10.1155/2018/2158482

Noriega-Ortega, B. E., Wienhausen, G., Mentges, A., Dittmar, T., Simon, M., & Niggemann, J. (2019). Does the chemodiversity of bacterial exometabolomes sustain the chemodiversity of marine dissolved organic matter?. *Frontiers in Microbiology*, *10*, 215. https://doi.org/10.3389/fmicb.2019.00215

Nuhn, M. E., Binder, M., Taylor, A. F., Halling, R. E., & Hibbett, D. S. (2013). Phylogenetic overview of the boletineae. *Fungal Biol*, *117*(7-8), 479-511. https://doi.org/10.1016/j.funbio.2013.04.008

Nylander, J. A. A. (2004). *MrModeltest v. 2.2. Program distributed by the author*. Uppsala University, Department of systematic zoology.

Oyetayo, V. O., & Akingbesote, E. T. (2022). Assessment of the antistaphylococcal properties and bioactive compounds of raw and fermented *Trametes polyzona* (Pers.) Justo extracts. *Microbial Biosystems*, *7*(1), 1-7. https://doi.org/10.21608/mb.2022.129214.1054

Page, R. D. M. (2001). *TreeView32 v. 1.6.6.* (Distributed by the author). http,//taxonomy.zoology.gla.ac.uk/rod/rod.html

Panda, M. K., Das, S. K., Mohapatra, S., Debata, P. R., Tayung, K., & Thatoi, H. (2020). Mycochemical composition, bioactivities, and phylogenetic placement of three wild edible russula species from northern odisha, india. *Plant Biosystems - An International Journal Dealing with all Aspects of Plant Biology*, *155*(5), 1041-1055. https://doi.org/10.1080/11263504.2020.1813829

Pegler, D. N., Spooner, B. M., & Young, T. W. K. (1993). *British truffles, a revision of British hypogeous fungi*. Royal Botanic Gardens.

Pena, R., Offermann, C., Simon, J., Naumann, P. S., Geßler, A., Holst, J., . . . Polle, A. (2010). Girdling affects ectomycorrhizal fungal (EMF) diversity and reveals functional differences in EMF community composition in a beech forest. *Applied and Environmental Microbiology*, *76*(6), 1831-1841. https://doi.org/10.1128/AEM.01703-09

Pérez-Moreno, J., Guerin-Laguette, A., Rinaldi, A. C., Yu, F., Verbeken, A., Hernández-Santiago, F., . . . Martínez-Reyes, M. (2021). Edible mycorrhizal fungi of the world, What is their role in forest sustainability, food security, biocultural conservation and climate change?. *Plants, People, Planet*, *3*(5), 471-490. https://doi.org/10.1002/ppp3.10199

Perič, B., & Moreau, P. A. (2010). *Melanogaster luteus*, un hypogé rare retrouvé au Monténégro. *Mycol Montenegrina*, *12*, 77-83.

Peterson, B. G., & Carl, P. (2018). *Performance analytics, econometric tools for performance and risk analysis. R package version 1.5.2*. https//CRAN.R-project.org/package=PerformanceAnalytics

Petrini, O., Cocchi, L., Vescovi, L., & Petrini, L. (2009). Chemical elements in mushrooms, Their potential taxonomic significance. *Mycological Progress*, *8*(3), 171-180. https://doi.org/10.1007/s11557-009-0589-1

Pham, N. D. H., Suzuki, A., Pham, N. D. H., Yamada, A., Shimizu, K., Noda, K., . . . & Suzuki, A. (2012). A sheathing mycorrhiza between the tropical bolete phlebopus spongiosus and citrus maxima. *Mycoscience*, *53*(5), 347-353. https://doi.org/10.1007/S10267-011-0177-5

Philip, D. (2003). Vegan, a package of r functions for community ecology. *Journal of Vegetation Science*, *14*(6), 927-930. https://doi.org/10.1111/j.1654-1103.2003.tb02228.x

Phong, W. N., Sung, B., Cao, Z., Gibberd, M. R., Dykes, G. A., Payne, A. D., . . . Coorey, R. (2022). Impact of different processing techniques on the key volatile profile, sensory, and consumer acceptance of black truffle (*Tuber melanosporum* Vittadini). *Journal of Food Science*, *87*(9), 4174-4187. https://doi.org/10.1111/1750-3841.16275

Piattoni, F., Ori, F., Morara, M., Iotti, M., & Zambonelli, A. (2012). The role of wild boars in spore dispersal of hypogeous fungi. *Acta mycologica*, *47*(2), 145-153. https://doi.org/10.5586/am.2012.017

Piccino, S., Boulanger, R., Descroix, F., & Sing, A. S. C. (2014). Aromatic composition and potent odorants of the “specialty coffee” brew “Bourbon Pointu” correlated to its three trade classifications. *Food Research International*, *61*, 264-271. https://doi.org/10.1016/j.foodres.2013.07.034

Pino, J. A., & Mesa, J. (2006). Contribution of volatile compounds to mango (*Mangifera indica* L.) aroma. *Flavour and Fragrance Journal*, *21*(2), 207-213. https://doi.org/10.1002/ffj.1703

Qin, H. W., Yang, T. M., Yang, S. B., Yang, M. Q., Wang, Y. Z., & Zhang, J. Y. (2022). Effects of different pre - drying and drying methods on volatile compounds in the pericarp and kernel of amomum Tsao - Ko. *Frontiers in Plant Science*, *13*, 125. https://doi.org/10.3389/fpls.2022.803776

Raja, H. A., Miller, A. N., Pearce, C. J., & Oberlies, N. H. (2017). Fungal identification using molecular tools, a primer for the natural products research community. *Journal of Natural Products*, *80*(3), 756-770. https://doi.org/10.1021/acs.jnatprod.6b01085

Ramawat, K. G. (2019). An introduction to biodiversity and chemotaxonomy. In K. Ramawat (Ed.), *Biodiversity and chemotaxonomy* (pp. 1-14). Springer.

Rangel, L. I., Hamilton, O., Jonge, R. D., & Bolton, M. D. (2021). Fungal social influencers, secondary metabolites as a platform for shaping the plant-associated community. *The Plant Journal*, *108*, 632-645. https://doi.org/10.1111/tpj.15490

Rathore, H., Prasad, S., Kapri, M., Tiwari, A., & Sharma, S. (2019). Medicinal importance of mushroom mycelium, Mechanisms and applications. *Journal of Functional Foods*, *56*, 182-193. https://doi.org/10.1016/j.jff.2019.03.016

Rasool, R., Ganai, B. A., Akbar, S., Kamili, A. N., & Masood, A. (2010). Phytochemical screening of Prunella vulgaris L.-an important medicinal plant of Kashmir. n*Pak. J. Pharm. Sci*, *23*(4), 399-402.

Rees, C. A., Burklund, A., Stefanuto, P. H., Schwartzman, J. D., & Hill, J. E. (2018). Comprehensive volatile metabolic fingerprinting of bacterial and fungal pathogen group. *Journal of Breath Research*, *12*(2), 026001. https://doi.org/10.1088/1752-7163/aa8f7f

Reilly, P. O. (2011). Fascinated by Fungi: Exploring the History, Mystery, Facts, and Fiction of the Underworld Kingdom of Mushrooms. First Nature.

Rehner, S. A., & Buckley, E. (2005). A Beauveria phylogeny inferred from nuclear ITS and EF1-α sequences, evidence for cryptic diversification and links to Cordyceps teleomorphs. *Mycologia*, *97*(1), 84-98. https://doi.org/10.3852/mycologia.97.1.84

Reich, M., & Labes, A. (2017). How to boost marine fungal research, a first step towards a multidisciplinary approach by combining molecular fungal ecology and natural products chemistry. *Marine Genomics*, *36*, 57-75. https://doi.org/10.1016/j.margen.2017.09.007

Rinaldi, A. C., Comandini, O., & Kuyper, T. W. (2008). Ectomycorrhizal fungal diversity, Seperating the wheat from the chaff. *Fungal Diversity*, *33*, 1-45.

Rinkel, J., Babczyk, A., Wang, T., Stadler, M., & Dickschat, J. S. (2018). Volatiles from the hypoxylaceous fungi Hypoxylon griseobrunneum and Hypoxylon macrocarpum. *Beilstein Journal of Organic Chemistry*, *14*(1), 2974-2990. https://doi.org/10.3762/bjoc.14.277

Romero, F., Cazzato, S., Walder, F., Vogelgsang, S., Bender, S. F., & van der Heijden, M. G. (2022). Humidity and high temperature are important for predicting fungal disease outbreaks worldwide. *New Phytologist*, *234*(5), 1553-1556. https://doi.org/10.1111/nph.17340

Roncero-Ramos, I., & Delgado-Andrade, C. (2017). The beneficial role of edible mushrooms in human health. *Current Opinion in Food Science*, *14*, 122-128. https://doi.org/10.1016/j.cofs.2017.04.002

Ronquist, F., & Huelsenbeck, J. P. (2003). MrBayes 3, Bayesian phylogenetic inference under mixed models. *Bioinformatics*, *19*(12), 1572-1574. https://doi.org/10.1093/bioinformatics/btg180

Ronquist, F., Teslenko, M., van der Mark, P., Ayres, D. L., Darling, A., Höhna, S., . . . Huelsenbeck, J. P. (2012). MrBayes 3.2, efficient Bayesian phylogenetic inference and model choice across a large model space. *Systematic Biology*, *61*, 539-542. https://doi.org/10.1093/sysbio/sys029

Roy, D., Najafian, K., & Schleyer, P. V. R. (2007). Chemical evolution, The mechanism of the formation of adenine under prebiotic conditions. *Proceedings of the National Academy of Sciences*, *104*(44), 17272-17277. https://doi.org/10.1073/pnas.0708434104

Salazar, D., Lokvam, J., Mesones, I., Vásquez Pilco, M., Ayarza Zuñiga, J. M., de Valpine, P., . . . Fine, P. V. (2018). Origin and maintenance of chemical diversity in a species-rich tropical tree lineage. *Nature Ecology & Evolution*, *2*(6), 983-990. https://doi.org/10.1038/s41559-018-0552-0

Salisu, T. F., Okpuzor, J. E., & Jaja, S. I. (2019). Identification, characterization and quantification of chemical compounds in selected edible wild leafy vegetables. *Ife Journal of Science*, *21*(1), 215-227. https://doi.org/10.4314/ijs.v21i1.19

Sasaki, H., Kinoshita, A., & Nara, K. (2016). *An illustrated book of Japanese truffles*. Seibundo-shinkosha. (in Japanese).

Schardl, C. L., Young, C. A., Hesse, U., Amyotte, S. G., Andreeva, K., Calie, P. J., . . . Zeng, Z. (2013). Plant-symbiotic fungi as chemical engineers, multi-genome analysis of the Clavicipitaceae reveals dynamics of alkaloid loci. *PLoS Genetics*, *9*(2), e1003323. https://doi.org/10.1371/journal.pgen.1003323

Schiestl, F. P., Steinebrunner, F., Schulz, C., von Reuss, S., Francke, W., Weymuth, C., . . . Leuchtmann, A. (2006). Evolution of 'pollinator'- attracting signals in fungi. *Biology Letters*, *2*(3), 401-404. https://doi.org/10.1098/rsbl.2006.0479

Schirack, A. V., Drake, M. A., Sanders, T. H., & Sandeep, K. P. (2006). Characterization of aroma-active compounds in microwave blanched peanuts. *Journal of Food Science*, *71*(9), C513-C520. https://doi.org/10.1111/j.1750-3841.2006.00173.x

Schlutt, B., Moran, N., Schieberle, P., & Hofmann, T. (2007). Sensory-directed identification of creaminess-enhancing volatiles and semivolatiles in full-fat cream. *Journal of Agricultural and Food Chemistry*, *55*(23), 9634-9645. https://doi.org/10.1021/jf0721545

Schreiner, L., Bauer, P., & Buettner, A. (2018). Resolving the smell of wood - identification of odour - active compounds in Scots pine (*Pinus sylvestris* L.). *Scientific Reports*, *8*(1), 1-9. https://doi.org/10.1038/s41598-018-26626-8

Sharma, R. (2017). Ectomycorrhizal mushrooms, their diversity, ecology and practical applications. In A. Varma, R. Prasad & N. Tuteja (Eds.), *Mycorrhiza - function, diversity, state of the art* (pp. 99-131). Springer Cham.

Simmonds, M. S. J., Fang, R., Wyatt, L., Bell, E., Allkin, B., Forest, F., . . . Demissew, S. (2020). Biodiversity and patents, Overview of plants and fungi covered by patents. *Plants, People, Planet*, *2*(5), 546-556. https://doi.org/10.1002/ppp3.10144

Singdevsachan, S. K., Auroshree, P., Mishra, J., Baliyarsingh, B., Tayung, K., & Thatoi, H. (2016). Mushroom polysaccharides as potential prebiotics with their antitumor and immunomodulating properties, A review. *Bioactive Carbohydrates and Dietary Fibre*, *7*(1), 1-14. https://doi.org/10.1016/j.bcdf.2015.11.001

Singer, R. (1945). The Boletineae of Florida with notes on extralimital species. I. Strobilomycetaceae. *Farlowia*, *2*, 97-141. https://doi.org/10.5962/p.316006

Singer, R., Ivory, M., & Araujo, I. (1983). The ectotrophically mycorrhizal fungi of the Neotropical lowlands, especially central Amazonia. *Beihefte zur Nova Hedwigia*, *77*, 1-352.

Singer, R. (1986). *The Agaricales in modern taxonomy*. Sven Koeiltz Scientific Books.

Singh, R. (2016). Chemotaxonomy, A tool for plant classification. *J. Med. Plants Stud.*, *4*(2), 90-93.

Sinuco, D. C., Steinhaus, M., Schieberle, P., & Osorio, C. (2021). Changes in odour-active compounds of two varieties of Colombian guava (*Psidium guajava* L.) during ripening. *European Food Research and Technology*, *230*, 859-864. https://doi.org/10.1007/s00217-010-1232-8

Sir, E. B., Kuhnert, E., Lambert, C., Hladki, A. I., Romero, A. I., & Stadler, M. (2016). New species and reports of Hypoxylon from Argentina recognized by a polyphasic approach. *Mycological Progress*, *15*, 1-19. https://doi.org/10.1007/s11557-016-1182-z

Sitta, N., & Floriani, M. (2008). Nationalization and globalization trends in the wild mushroom commerce of italy with emphasis on porcini (*boletus edulis* and allied species). *Economic Botany*, *62*, 307-322. https://doi.org/10.1007/s12231-008-9037-4

Smith, A. H., & Thiers, H. D. (1971). *The boletes of Michigan*. University of Michigan Press.

Smith, P. M. (1976). *The chemotaxonomy of plants London*. Edward Arnold.

Smith, M. E., & Bonito, G. (2013). Systematics and ecology of edible ectomycorrhizal mushrooms. In A. Zambonelli & G. Bonito (Eds.), *Edible ectomycorrhizal mushrooms, current knowledge and future prospects* (vol. 34., pp. 17-39). Springer.

Smith, S., & Read, D. (2008). *Mycorrhizal symbiosis* (3rd ed.). Academic.

Smith, T. E., Pond, C. D., Pierce, E., Harmer, Z. P., Kwan, J., Zachariah, M. M., . . . Schmidt, E. W. (2018). Accessing chemical diversity from the uncultivated symbionts of small marine animals. *Nature Chemical Biology*, *14*(2), 179-185. https://doi.org/10.1038/nchembio.2537

Spiteller, P. (2015). Chemical ecology of fungi. *Natural Products Reports*, *32*(7), 971-993. https://doi.org/10.1039/C4NP00166D

Stadler, M., Fournier, J., Læssøe, T., Chlebicki, A., Lechat, C., Flessa, F., . . . Peršoh, D. (2010). Chemotaxonomic and phylogenetic studies of Thamnomyces (Xylariaceae). *Mycoscience*, *51*(3), 189-207. https://doi.org/10.1007/S10267-009-0028-9

Stadler, M., Hawksworth, D. L., & Fournier, J. (2014). The application of the name Xylaria hypoxylon, based on Clavaria hypoxylon of Linnaeus. *IMA Fungus*, *5*, 57-66. https://doi.org/10.5598/imafungus.2014.05.01.07

Stamatakis, A., Ludwig, T., & Meier, H. (2005). RAxML-III, a fast program for maximum likelihood-based inference of large phylogenetic trees. *Bioinformatics*, *21*, 456-463. https://doi.org/10.1093/bioinformatics/bti191

Stamatakis, A. (2006). RAxML-VI-HPC, maximum likelihood-based phylogenetic analyses with thousands of taxa and mixed models. *Bioinformatics*, *22*(21), 2688-2690. https://doi.org/10.1093/bioinformatics/btl446

Stamatakis, A. (2014). RAxML version 8, a tool for phylogenetic analysis and post-analysis of large phylogenies. *Bioinformatics, 30*(9), 1312-1313. https://doi.org/10.1093/bioinformatics/btu033

Stamatakis, A. (2015). Using RAxML to infer phylogenies. *Current Protocols in Bioinformatics*, *51*(1), 6.14.1-16.14.14. https://doi.org/10.1002/0471250953.bi0614s51

Steiner, U., & Leistner, E. (2012). Ergoline alkaloids in convolvulaceous host plants originate from epibiotic clavicipitaceous fungi of the genus Periglandula. *Fungal Ecology*, *5*(3), 316-321. https://doi.org/10.1016/j.funeco.2011.04.004

Su, L. H., Geng, C. A., Li, T. Z., Huang, X. Y., Ma, Y. B., Zhang, X. M., . . . Chen, J. J. (2020). Spiroseoflosterol, a rearranged ergostane-steroid from the fruiting bodies of *butyriboletus roseoflavus*. *J Nat Prod*, *83*(5), 1706-1710. https://doi.org/10.1021/acs.jnatprod.9b01282

Su, S., Ding, X., Hou, Y., Liu, B., Du, Z., & Liu, J. (2023). Structure elucidation, immunomodulatory activity, antitumor activity and its molecular mechanism of a novel polysaccharide from boletus reticulatus schaeff. *Food Science and Human Wellness, 12*(2), 647-661. https://doi.org/10.1016/j.fshw.2022.07.067

Sugiura, Y., Akiyama, R., Tanaka, S., Yano, K., Kameoka, H., Marui, S., . . . Saito, K. (2020). Myristate can be used as a carbon and energy source for the asymbiotic growth of arbuscular mycorrhizal fungi. *Proceedings of the National Academy of Sciences*, *117*(41), 25779-25788. https://doi.org/10.1073/pnas.2006948117

Sun, S., Coelho, M. A., Heitman, J., & Nowrousian, M. (2019). Convergent evolution of linked mating-type loci in basidiomycete fungi. *PLoS Genetics*, *15*(9), e1008365. https://doi.org/10.1371/journal.pgen.1008365

Sun, Z., Hu, M., Sun, Z., Zhu, N., Yang, J., Ma, G., . . . Xu, X. (2018). Pyrrole alkaloids from the edible mushroom *phlebopus portentosus* with their bioactive activities. *Molecules*, *23*(5), 1198. https://doi.org/10.3390/molecules23051198

Sunagawa, S., Coelho, L. P., Chaffron, S., Kultima, J. R., Labadie, K., Salazar, G., . . . Velayoudon, D. (2015). Structure and function of the global ocean microbiome. *Science*, *348*(6237), 1261359. https://doi.org/10.1126/science.1261359

Surup, F., Kuhnert, E., Lehmann, E., Heitkämper, S., Hyde, K. D., Fournier, J., . . . Stadler, M. (2014). Sporothriolide derivatives as chemotaxonomic markers for Hypoxylon monticulosum. *Mycology*, *5*(3), 110-119. https://doi.org/10.1080/21501203.2014.929600

Suwannarach, N., Kumla, J., & Lumyong, S. (2015). A new whitish truffle, *Tuber thailandicum* from northern Thailand and its ectomycorrhizal association. *Mycological Progress*, *14*, 1-12. https://doi.org/10.1007/s11557-015-1107-2

Suz, L. M., Kallow, S., Reed, K., Bidartondo, M. I., & Barsoum, N. (2017). Pine mycorrhizal communities in pure and mixed pine-oak forests, Abiotic environment trumps neighboring oak host effects. *Forest Ecology and Management*, *406*, 370-380. https://doi.org/10.1016/j.foreco.2017.09.030

Svrček, M. (1958). VIII. řad Melanogastrales-Černouškotvaré. In Č. S. R. B. Flora (Ed.), *Gasteromycetes* (pp. *527-556*, 795-802). Praha, Czechoslovakian Academy.

Tagkouli, D., Bekiaris, G., Pantazi, S., Anastasopoulou, M. E., Koutrotsios, G., Mallouchos, A., . . . Kalogeropoulos, N. (2021). Volatile profiling of *Pleurotus eryngii* and *Pleurotus ostreatus* mushrooms cultivated on agricultural and agro - industrial by - products. *Foods*, *10*(6), 1287. https://doi.org/10.3390/foods10061287

Takahashi, H., Taneyama, Y., & Degawa, Y. (2013). Notes on the boletes of Japan 1. Four new species of the genus boletus from central Honshu, Japan. *Mycoscience*, *54*(6), 458-468. https://doi.org/10.1016/j.myc.2013.02.005

Tamura, K., Dudley, J., Nei, M., & Kumar, S. (2007). MEGA4, Molecular Evolutionary Genetics Analysis (MEGA) software version 4.0. *Molecular Biology and Evolution*, *24*, 1596-1599. https://doi.org/10.1093/molbev/msm092

Tan, Y., Zeng, N. K., & Xu, B. (2022). Chemical profiles and health-promoting effects of porcini mushroom (boletus edulis), A narrative review. *Food Chem.*, *390*, 133199. https://doi.org/10.1016/j.foodchem.2022.133199

Tanentzap, A. J., Fitch, A., Orland, C., Emilson, E. J., Yakimovich, K. M., Osterholz, H., . . . Dittmar, T. (2019). Chemical and microbial diversity covary in fresh water to influence ecosystem functioning. *Proceedings of the National Academy of Sciences*, *116*(49), 24689-24695. https://doi.org/10.1073/pnas.1904896116

Tedersoo, L., May, T. W., & Smith, M. E. (2010). Ectomycorrhizal lifestyle in fungi, Global diversity, distribution, and evolution of phylogenetic lineages. *Mycorrhiza*, *20*(4), 217-263. https://doi.org/10.1007/s00572-009-0274-x

Tedersoo, L., Sánchez-Ramírez, S., Koljalg, U., Bahram, M., Döring, M., Schigel, D., . . . Abarenkov, K. (2018). High-level classification of the Fungi and a tool for evolutionary ecological analyses. *Fungal Diversity*, *90*, 135-159. https://doi.org/10.1007/s13225-018-0401-0

Thévenot, E. A., Roux, A., Xu, Y., Ezan, E., & Junot, C. (2015). Analysis of the human adult urinary metabolome variations with age, body mass index, and gender by implementing a comprehensive workflow for univariate and OPLS statistical analyses. *Journal of Proteome Research*, *14*(8), 3322-3335. https://doi.org/10.1021/acs.jproteome.5b00354

Thuiller, W., Lavergne, S., Roquet, C., Boulangeat, I., Lafourcade, B., & Araujo, M. B. (2011). Consequences of climate change on the tree of life in Europe. *Nature*, *470*(7335), 531-534. https://doi.org/10.1038/nature09705

Tian, R., Chai, H., Qiu, J. Q., Liang, Z. Q., Xie, H. J., Wang, Y., . . . Zeng, N. K. (2022). Preparation, structural characterisation, and antioxidant activities of polysaccharides from eight boletes (boletales) in tropical china. *Mycology*, *13*(3), 195-206. https://doi.org/10.1080/21501203.2022.2069172

Tian, R., Wu, L. L., Li, H. F., Liang, Z. Q., Li, P. H., Wang, Y., . . . Zeng, N. K. (2023). Purification and structure characterization of the crude polysaccharide from the fruiting bodies of *butyriboletus pseudospeciosus* and its modulation effects on gut microbiota. *Molecules, 28*(6), 2679. https://doi.org/10.3390/molecules28062679

Timling, I., Dahlberg, A., Walker, D. A., Gardes, M., Charcosset, J., Welker, J. M., . . . Taylor, D. L. (2012). Distribution and drivers of ectomycorrhizal fungal communities across the North American Arctic. *Ecosphere*, *3*(11), 1-25. https://doi.org/10.1890/ES12-00217.1

Torruella, G., De Mendoza, A., Grau-Bové, X., Antó, M., Chaplin, M. A., Del Campo, J., . . . Ruiz-Trillo, I. (2015). Phylogenomics reveals convergent evolution of lifestyles in close relatives of animals and fungi. *Current Biology*, *25*(18), 2404-2410. https://doi.org/10.1016/j.cub.2015.07.053

Trappe, J. M. (1975a). A revision of the genus *Alpova* with notes on *Rhizopogon* and the Melanogastraceae. *Beihefte zur Nova Hedwigia, 51*, 279-309.

Trappe, J. M. (1975b). Generic synonyms in the Tuberales. *Mycotaxon, 2*, 109-122.

Trappe, J. M., & Claridge, A. W. (2005). Hypogeous fungi, evolution of reproductive and dispersal strategies through interactions with anmals and mycorrhizal plants. In J. Dighton, J. F. White & P. Oudemans (Eds.), *The fungal community. Its organization and role in the ecosystem* (pp. 599-611). CRC.

Trappe, J. M., Molina, R., Luoma, D. L., Cázares, E., Pilz, D., Smith, J. E., . . . Trappe, M. J. (2009). *Diversity, ecology, and conservation of truffle fungi in forests of the Pacific Northwest*. U.S. Department of Agriculture, Forest Service, Pacific Northwest Research Station.

Trivedi D., K., & Iles, R., K. (2012). The application of SIMCA P + in shotgun metabolomics analysis of ZIC® HILIC-MS spectra of human urine-experience with the Shimadzu IT-TOF and profiling solutions data extraction software. *Journal of Chroma Tography & Separation Techniques*, *3*(6), 145. https://doi.org/10.4172/2157-7064.1000145

Trygg, J., & Wold, S. (2002). Orthogonal projections to latent structures (O-PLS). *Journal of Chemometrics, A Journal of the Chemometrics Society*, *16*(3), 119-128. https://doi.org/10.1002/cem.695

Türkoğlu, A., & Castellano, M. A. (2013). New records of truffle fungi (Basidiomycetes) from Turkey. *Turkish Journal of Botany*, *37*, 970-976. https://doi.org/10.3906/bot-1212-54

Ugbogu, E. A., Emmanuel, O., Salem, A. Z. M., & Elghandour, M. M. M. Y. (2018). Nutritional composition of *termitomyces robustus* (agaricomycetes) and *lentinus squarrosulus* (mont.) singer in south east nigeria. *Agroforestry Systems*, *94*(4), 1291-1300. https://doi.org/10.1007/s10457-018-0323-6

Umamaheswaran, R., Dutta, S., Khan, M. A., Bera, M., Bera, S., & Kumar, S. (2022). Identification of chitin in Pliocene fungi using PY-GC× GC-TOFMS, potential implications for the study of the evolution of the fungal clade in deep time. *Analytical Chemistry*, *94*(4), 1958-1964. https://doi.org/10.1021/acs.analchem.1c03143

Umoh, O. T. (2020). Chemotaxonomy, The role of phytochemicals in chemotaxonomic delineation of taxa. *Taxon*, *13*, 14. https://doi.org/10.9734/aprj/2020/v5i130100

Uzun, Y., Acar, I., & Akata, I. (2014). Notes on Turkish *Melanogaster*. *Ot Sistematik Botanik Dergisi*, *22*, 113-118.

Gemert, L. V. (2011). *Odour thresholds, compilations of odour threshold values in air, water and other media*. Oliemans Punter & Partners BV, The Netherlands.

Vega-Castellote, M., Pérez-Marín, D., Torres, I., Moreno-Rojas, J. M., & Sánchez, M. T. (2021). Exploring the potential of NIRS technology for the in situ prediction of amygdalin content and classification by bitterness of in-shell and shelled intact almonds. *Journal of Food Engineering*, *294*, 110406. https://doi.org/10.1016/j.jfoodeng.2020.110406

Vicente, M. F., Basilio, A., Cabello, A., & Peláez, F. (2003). Microbial natural products as a source of antifungals. *Clinical Microbiology and Infection*, *9*(1), 15-32. https://doi.org/10.1046/j.1469-0691.2003.00489.x

Vidal, J. M., Rocabruna, A., & Tabarés, M. (1991). Algunos hongos hipogeos (Ascomycotina y Basidiomycotina) interesantes para la micoflora española. *Butll. Soc. Catalana Micol*, *14*(15), 131-142.

Vilgalys, R., & Hester, M. (1990). Rapid genetic identification and mapping of enzymatically amplified ribosomal DNA from several Cryptococcus species. *Journal of Bacteriology*, *72*(8), 4238-4246. https://doi.org/10.1128/jb.172.8.4238-4246.1990

Villéger, S., Maire, E., & Leprieur, F. (2017). On the risks of using dendrograms to measure functional diversity and multidimensional spaces to measure phylogenetic diversity, a comment on Sobral et al. (2016). *Ecol Lett.*, *20*(4), 554-557. https://doi.org/10.1111/ele.12750

Vittadini, C. (1831). *Monographia Tuberacearum; Ex Typographia F*. Rusconi.

Vizzini, A., Zotti, M., Ryman, S., & Ghignone, S. (2010). Typification of *Octaviania rubescens* (Paxillineae, Boletales) and phylogenetic hypotheses for genus Alpova. *Mycologia*, *102*(4), 967-975. https://doi.org/10.3852/09-256

Vizzini, A. (2014). *Neoboletus Gelardi*, Simonini & Vizzini, gen. nov. *Index Fungorum*, *192*, 1.

Vizzini, A. (2015). *Lanmaoa fragrans* (Vittad.) Vizzini, Gelardi, Simonini, comb.nov. *Index Fungorum*, *235*, 1.

Wa, E., & Daba, G. M. (2022). Bioactive potential of some fascinating edible mushrooms macrolepiota, russula, amanita, vovariella and grifola as a treasure of multipurpose therapeutic natural product. *The Journal of Mycology*, *5*(1), 1-8. https://doi.org/10.23880/oajmms-16000157

Walker, G. M., & White, N. A. (2017). Introduction to fungal physiology. In K. Kavanagh (ed.), *Fungi, biology and applications* (pp. 1-35). Wiley Online Library.

Wan, S. P., Yu, F. Q., Tang, L., Wang, R., Wang, Y., Liu, P. G., . . . Zeng, Y. (2015). Ectomycorrhizae of *Tuber huidongense* and *T. Liyuanum* with castanea mollissima and pinus armandii. *Mycorrhiza*, *26*(3), 249-256. https://doi.org/10.1007/s00572-015-0663-2

Wan, S. P., Wang, X. H., Zheng, Y., & Yu, F. Q. (2016). *Tuber shidianense* and *T. calosporum*, two new truffle species from southwest China. *Mycoscience*, *57*(6), 393-399. https://doi.org/10.1016/j.myc.2016.06.007

Wan, S. P., Tang, L., Zheng, Y., & Yu, F. Q. (2017). Two novel *Tuber* species (*Tuberaceae, Pezizales*) in the *Latisporum* group from China. *Mycoscience*, *58*(5), 312-319. https://doi.org/10.1016/j.myc.2017.02.006

Wang, Y., Chang, M. C., Tao, K., & Liu, B. (1995). New species and new varieties of the genus *Melanogaster* from China. J*ournal of Shangxi University* (Nat. Sci. Ed.), *18*(4), 449-453.

Wang, Y., Moreno, G., Riousset, L. J., Manjón, J. L., Riousset, G., Fourré, G., . . . Díez, J. (1998). *Tuber pseudoexcavatum* sp. nov. A new species from China commercialized in Spain, France and Italy with additional comments on Chinese truffles. *Mycologie*, *19*(1-2), 113-120.

Wang, X. H., Liu, P. G., & Yu, F. Q. (2004). *Color atlas of wild commercial mushrooms in Yunnan*. Yunnan science and technology Press.

Wang, Y., Castellano, M. A., & Trappe, J. (2005). *Melanogaster utriculatus* sp. Nov. from Japan. *Mycotaxon*, *93*(1), 315-317.

Wang, Y., Tan, Z. M., Zhang, D. C., Murat, C., Jeandroz, S., & Le Tacon, F. (2006). Phylogenetic and populational study of the *Tuber indicum* complex. *Mycol Res*, *110*(9), 1034-1045. https://doi.org/10.1016/j.mycres.2006.06.013

Wang, Y. J., Tan, Z. M., Murat, C., Jeandroz, S., & Le Tacon, F. (2007). Molecular taxonomy of Chinese truffles belonging to the *Tuber rufum* and *Tuber puberulum* groups. *Fungal Diversity*, *24*(301), e328.

Wang, Y., & Liu, P. G. (2009). Achievements and challenges of research on truffles in China. *Acta Botanica Yunnanica Supplement*, *16*, 1-9.

Wang, Y. W., Li, X. D., & Fan, L. (2016). *Tuber shii* sp. nov., a sister species of *T. jinshajiangense* from China in Puberulum group. *Phytotaxa*, *269*(4), 279-286. https://doi.org/10.11646/phytotaxa.269.4.3

Wang, Q., Wang, F., Xu, Z., & Ding, Z. (2017). Bioactive mushroom polysaccharides, A review on monosaccharide composition, biosynthesis and regulation. *Molecules*, *22*(6), 955. https://doi.org/10.3390/molecules22060955

Wang, L., Li, J. Q., Li, T., Liu, H. G., & Wang, Y. Z. (2021). Two-dimensional correlation spectroscopy combined with deep learning method and HPLC method to identify the storage duration of porcini. *Microchemical Jounal*, *170*, 106670. https://doi.org/10.1016/j.microc.2021.106670

Wang, R., Wan, S., Yang, J., & Yu, F. (2022). *Choiromyces sichuanensis* sp. Nov., a new species from southwest china, and its mycorrhizal synthesis with three native conifers. *Diversity*, *14*(10), 837. https://doi.org/10.3390/d14100837

Wasser, S. P. (2002). Medicinal mushrooms as a source of antitumor and immunomodulating polysaccharides. *Appl Microbiol Biotechnol*, *60*(3), 258-274. https://doi.org/10.1007/s00253-002-1076-7

Wedén, C. (2007). Research on *Choiromyces venosus* - a new delicacy? *Opera Mycologica*, *1*, 42-49.

Wedén, C., Larsson, S., Burman, R., & Backlund, A. (2009).The edible truffle *Choiromyces venosus* and its use in Sweden. *Acta Botanica Yunnanica*, *31*(S16), 94-96.

Wei, J. P., Wang, S. Y., Zhang, Y. X., Yuan, Y. H., & Yue, T. L. (2019). Characterization and screening of non - Saccharomyces yeasts used to produce fragrant cider. *LWT*, *107*, 191-198. https://doi.org/10.1016/j.lwt.2019.03.028

Wei, J. P., Zhang, Y. X., Wang, Y. W., Ju, H. M; Niu, C., Song, Z. H., . . . Yue, T. L. (2020). Assessment of chemical composition and sensorial properties of ciders fermented with different non - Saccharomyces yeasts in pure and mixed fermentations. *International Journal of Food Microbiology*, *318*, 108471. https://doi.org/10.1016/j.ijfoodmicro.2019.108471

Wilkinson, R. G., Donnini, D., & Benucci, G. M. N. (2014). *Tuber melanosporum* vittad.: Truffle culture in Australia and Italy *Tuber melanosporum* vittad.: Tartuficoltura in Australia e Italia.

White, T. J., Bruns, S., Lee, S., & Taylor, J. (1990). Amplification and direct sequencing of fungal ribosomal RNA genes for phylogenetics. *PCR Protocols, A Guide to Methods and Application*, *1*, 315-322. https://doi.org/10.1016/B978-0-12-372180-8.50042-1

Wikerson, M. D., & Hayes, D. N. (2010). Consensusclusterplus, a class discovery tool with confidence assessments and item tracking. *Bioinformatics*, *26*(12), 1572-1573. https://doi.org/10.1093/bioinformatics/btq170

Workman, J. Jr., & Weyer, L. (2012). *Practical guide and spectral atlas for interpretive near-infrared spectroscopy* (2nd Ed.). CRC Press.

Wu, G., Feng, B., Xu, J. P., Zhu, X. T., Li, Y. C., Zeng, N. K., . . . Yang, Z. L. (2014). Molecular phylogenetic analyses redefine seven major clades and reveal 22 new generic clades in the fungal family Boletaceae. *Fungal Diversity*, *69*, 93-115. https://doi.org/10.1007/s13225-014-0283-8

Wu, G., Zhao, K., Li, Y. C., Zeng, N. K., Feng, B., Halling, R. E., . . . Yang, Z. L. (2016). Four new genera of the fungal family boletaceae. *Fungal Diversity*, *81*(1), 1-24. https://doi.org/10.1007/s13225-015-0322-0

Wu, G., Li, Y. C., Zhu, X. T., Zhao, K., Han, L. H., Cui, Y. Y., Li, F., . . . Yang, Z. L. (2016). One hundred noteworthy boletes from China. *Fungal Diversity*, *81*, 25-188. https://doi.org/10.1007/s13225-016-0375-8

Wu, G., Miyauchi, S., Morin, E., Kuo, A., Drula, E., Varga, T., . . . Martin, F. M. (2022). Evolutionary innovations through gain and loss of genes in the ectomycorrhizal boletales. *New Phytol*, *233*(3), 1383-1400. https://doi.org/10.1111/nph.17858

Wu, G., Li, H. L., Horak, E., Wu, K., Li, G. M., & Yang, Z. L. (2023). New taxa of Boletaceae from China. *Mycosphere*, *14*(1), 745-776. https://doi.org/10.5943/mycosphere/14/1/9

Xiao, L., Lee, J., Zhang, G., Ebeler, S. E., Wickramasinghe, N., Seiber, J., . . . Mitchell, A. E. (2014). HS-SPME GC/MS characterization of volatiles in raw and dry-roasted almonds (Prunus dulcis). *Food Chemistry*, *151*, 31-39. https://doi.org/10.1016/j.foodchem.2013.11.052

Xu, X., Yan, H., Chen, J., & Zhang, X. (2011). Bioactive proteins from mushrooms. *Biotechnol Adv*, *29*(6), 667-674. https://doi.org/10.1016/j.biotechadv.2011.05.003

Xu, J., Xu, D., Hu, Q., Ma, N., Pei, F., Su, A., . . . Ma, G. (2022). Immune regulatory functions of biologically active proteins from edible fungi. *Front Immunol*, *13*, 1034545. https://doi.org/10.3389/fimmu.2022.1034545

Xu, Y. Y., Yan, X. Y., Li, T., Zhao, T. Y., Lv, J. C., & Fan, L. (2022). The taxonomic revision of *Melanogaster* (Paxillaceae, Boletales) in China based on molecular and morphological evidence. *Mycological Progress*, *21*(12), 98. https://doi.org/10.1007/s11557-022-01842-9

Yan, X. Y., Xu, Y. Y., Li, T., Zhao, T. Y., Lv, J. C., & Fan, L. (2020). Molecular data reveals rich diversity of the sequestrate genus *Melanogaste*r (boletales, paxillaceae) with emphasis on the species from china. *Research Square*. https://doi.org/10.21203/rs.3.rs-100635/v1

Yan, Z., Liu, H., Li, T., Li, J., & Wang, Y. (2022). Two dimensional correlation spectroscopy combined with resnet, Efficient method to identify bolete species compared to traditional machine learning. *Lwt*, *162*, 113490. https://doi.org/10.1016/j.lwt.2022.113490

Yan, Z., Liu, H., Li, J., & Wang, Y. (2023). Qualitative and quantitative analysis of *lanmaoa asiatica* in different storage years based on ft-nir combined with chemometrics. *Microchemical Journal*, *189*, 108580. https://doi.org/10.1016/j.microc.2023.108580

Yang, Z. L., & Zhang, L. F. (2003). Type studies on *Clitocybe macrospora* and Xerula furfuracea var. bispora. *Mycotaxon*, *88*, 447-454.

Yang, R. J., Yang, Y. R., Dong, G. M., Zhang, W. Y., & Yu, Y. P (2014). Multivariate methods for the identification of adulterated milk based on the two-dimensional infrared correlation spectroscopy. *Analytical Methods*, *6*, 3436-3441. https://doi.org/10.1039/c4ay00442f

Yang, R. J., Dong, G. M., Sun, X. S., Yu, Y. P., Liu, H. X., Yang, Y. R., . . . Zhang, W. Y. (2015). Synchronous-asynchronous two-dimensional correlation spectroscopy for the discrimination of adulterated milk. *Analytical Methods*, *7*, 4302-4307. https://doi.org/10.1039/C5AY00134J

Yang, Y., Pan, T., & Zhang, J. (2019). Global optimization of Norris derivative filtering with application for near - infrared analysis of serum urea nitrogen. *American Journal of Analytical Chemistry*, *10*(5), 143-152. https://doi.org/10.4236/ajac.2019.105013

Yang, F., Zhao, M., Zhou, L., Zhang, M., Liu, J., & Marchioni, E. (2021). Identification and differentiation of wide edible mushrooms based on lipidomics profiling combined with principal component analysis. *J Agric Food Chem*, *69*(34), 9991-10001. https://doi.org/10.1021/acs.jafc.1c02269

Yang, M., Che, T., Li, Z., Zhang, Q., & Hu, X. (2022). Identification, taste properties and molecular docking of novel umami peptides from *Butyriboletus roseoflavus*. *European Food Research and Technology*, *248*(11), 2665-2677. https://doi.org/10.1007/s00217-022-04061-4

Yang, Y. Y., Xu, C., Wang, Y., Li, L., Yuan, L. X., Zhao, F. W., . . . Zeng, N. K. (2022). *Boletus littoreus* (Boletaceae, Boletales), a new species with a white basidioma from Hainan, China. *Phytotaxa*, *554*(2), 176-188. https://doi.org/10.11646/phytotaxa.554.2.6

Yang, Y. Q., Zhu, H. K., Chen, J. Y., Xie, J. L., Shen, S., Deng, Y. L., . . . Jiang, Y. W. (2022). Characterization of the key aroma compounds in black teas with different aroma types by using gas chromatography electronic nose, gas chromatography-ion mobility spectrometry, and odor activity value analysis. *LWT- Food Science and Technology*, *163*(1),113492. https://doi.org/10.1016/j.lwt.2022.113492

Yu, A. N., Sun, B. G., Tian, D. T., & Qu, W. Y. (2008). Analysis of volatite compounds in traditional smoke-cured bacon (CSCB) with different fiber coatings using SPME. *Food Chemistry*, *110*, 233-238. https://doi.org/10.1016/j.foodchem.2008.01.040

Yuan, H., Xu, L. J., Chang, M. C., Meng, J. L., Feng, C. P., Geng, X. R., . . . Liu, Z. Q. (2022). Effects of different cooking methods on volatile flavor compounds, nutritional constituents, and antioxidant activities of Clitocybe squamulosa. *Frontiers in Nutrition*, *9*, 1017014. https://doi.org/10.3389/fnut.2022.1017014

Zambonelli, A., Lotti, M., & Murat, C. (2016). *True true (Tuber spp.) in the world* (vol. 47, p. 401). Springer International Publishing.

Zang, M. (2006). *Flora fungorum sinicorum, Boletaceae (I)*. Science Press. (in Chinese)

Zeng, N. K., Tang, L. P., Li, Y. C., Tolgor, B., Zhu, X. T., Zhao, Q., . . . Yang, Z. L. (2012). The genus *Phylloporus* (boletaceae, boletales) from china, Morphological and multilocus DNA sequence analyses. *Fungal Diversity*, *58*(1), 73-101. https://doi.org/10.1007/s13225-012-0184-7

Zeng, N. K., Liang, Z. Q., Wu, G., Li, Y. C., Yang, Z. L., & Liang, Z. Q. (2016). The genus *Retiboletus* in china. *Mycologia*, *108*(2), 363-380. https://doi.org/10.3852/15-072

Zeng, N. K., Chai, H. U. I., Jiang, S., Xue, R. O. U., Wang, Y., Hong, D., . . . Liang, Z. Q. (2018). *Retiboletus nigrogriseus* and *Tengioboletus fujianensis*, two new boletes from the south of china. *Phytotaxa*, *367*(1), 45-54. https://doi.org/10.11646/phytotaxa.367.1.5

Zeng, X. Y., Wu, H. X., Hongsanan, S., Jeewon, R., Wen, T. C., Maharachchikumbura, S. S., . . . Hyde, K. D. (2019). Taxonomy and the evolutionary history of Micropeltidaceae. *Fungal Diversity*, *97*, 393-436. https://doi.org/10.1007/s13225-019-00431-8

Zhang, C., He, M., Liu, J., Xu, X., Cao, Y., Gao, F., . . . Wang, Y. (2017). Brief introduction to a unique edible Bolete-*Phlebopus portentosus* in Southern China. *J. Agric. Sci. Technol. B*, *7*, 386-394. https://doi.org/10.17265/2161-6264/2017.06.003

Zhang, H., Pu, D., Sun, B., Ren, F., Zhang, Y., & Chen, H. (2018). Characterization and comparison of key aroma compounds in raw and dry porcini mushroom (Boletus edulis) by aroma extract dilution analysis, quantitation and aroma recombination experiments. *Food Chemistry*, *258*, 260-268. https://doi.org/10.1016/j.foodchem.2018.03.056

Zhang, X., Hu, Q., & Weng, Q. (2018). Secondary metabolites (sms) of isaria cicadae and isaria tenuipes. *RSC Adv*, *9*(1), 172-184. https://doi.org/10.1039/C8RA09039D

Zhang, H., Huang, D., Pu, D., Zhang, Y., Chen, H., Sun, B., . . . Ren, F. (2020). Multivariate relationships among sensory attributes and volatile components in commercial dry porcini mushrooms (Boletus edulis). *Food Research International*, *133*, 109112. https://doi.org/10.1016/j.foodres.2020.109112

Zhang, S., Lu, Z., Wu, Z., Xie, J., Yang, Y., & Qiu, H. (2020). Determination of a “Specific population who could benefit from rosuvastatin”, a secondary analysis of a randomized controlled trial to uncover the novel value of rosuvastatin for the precise treatment of ARDS. *Frontiers in Medicine*, *7*, 598621. https://doi.org/10.3389/fmed.2020.598621

Zhang, Y., Deng, T., Sun, L., Landis, J. B., Moore, M. J., Wang, H., . . . Sun, H. (2021). Phylogenetic patterns suggest frequent multiple origins of secondary metabolites across the seed-plant tree of life. *National Science Review*, *8*(4), nwaa105. https://doi.org/10.1093/nsr/nwaa105

Zhang, X., Qin, W. Q., Liang, Z. Q., Tian, R., & Zeng, N. K. (2022). Rubroboletus flammeus (boletaceae, boletales), a novel species unveiled from subtropical china based on morphological and phylogenetic evidences. *Arch Microbiol*, *204*(7), 379. https://doi.org/10.1007/s00203-022-02998-4

Zhao, K., Wu, G., & Yang, Z. (2014). A new genus, *Rubroboletus*, to accommodate *Boletus sinicus* and its allies. *Phytotaxa*, *188*(2), 61-77. https://doi.org/10.11646/phytotaxa.188.2.1

Zhao, K., Wu, G., Halling, R., & Yang, Z. L. (2015). Three new combinations of *Butyriboletus* (boletaceae). *Phytotaxa*, *234*(1), 51-62. https://doi.org/10.11646/phytotaxa.234.1.3

Zhao, K., & Shao, H. M. (2017). A new edible bolete, *Rubroboletus esculentus*, from southwestern china. *Phytotaxa*, *303*(3), 243-252. https://doi.org/10.11646/phytotaxa.303.3.4

Zhao, R. L., Li, G. J., Sánchez-Ramírez, S., Stata, M., Yang, Z. L., Wu, G., . . . Hyde, K. D. (2017). A six-gene phylogenetic overview of Basidiomycota and allied phyla with estimated divergence times of higher taxa and a phyloproteomics perspective. *Fungal Diversity*, *84*, 43-74. https://doi.org/10.1007/s13225-017-0381-5

Zhao, Y. H., Dunn, R. R., Zhou, H., Si, X. F., & Ding, P. (2020). Island area, not isolation, drives taxonomic, phylogenetic and functional diversity of ants on land-bridge islands. *Journal of Biogeography*, *47*(8), 1627-1637. https://doi.org/10.1111/jbi.13860

Zhou, F., Gao, Y., Song, H. Y., Hu, H. J., Li, S. X., Liu, J. H., . . . Hu, D. M. (2022). *Retiboletus atrofuscus* (boletaceae, boletales), a new species from china. *Arch Microbiol*, *204*(7), 381. https://doi.org/10.1007/s00203-022-03006-5

Zhou, F., Gao, Y., Song, H. Y., Hu, H. J., Yang, W. J., Zhang, W., . . . Hu, D. M. (2023). Phylogenetic and morphological evidence reveal five new species of boletes from southern china. *Journal of Fungi*, *9*(8), 814. https://doi.org/10.3390/jof9080814

APPENDIX

APPENDIX A

THE DETAILED INFORMATION OF SPECIES

Table A1 Detailed information on 110 collection sites of 509 specimens and their ecological environmental factors

Sampling Namber	Region divide based on PCAC and consensus clustering	Sampling position	Latin Name	Abbreviation	Numbers
1#	Region 3	Shiping County, Honghe Prepecture	*Butyriboletus pseudospeciosus*	BuP	5
2#	Region 1	Manshenke Village, Jinghong City, Xishuangbanna Prefecture	*Phlebopus portentosus*	PP	14
3#	Region 2	Dayao County, Chuxiong Prefecture	*Phlebopus portentosus*	PP	7
4#	Region 2	Donggua Town, Chuxiong Prefecture	*Boletus bainiugan*	BoB	4
5#	Region 5	Mayou Township, Yaoan County, Chuxiong Prepecture	*Butyriboletus roseoflavus*	BuR	5
6#	Region 5	Yangmei Mountain, Yaoan County, Chuxiong Prepecture	*Rugiboletus extremiorientalis*	RugE	5
7#	Region 6	Wangjia Village, Tonghai County, Yuxi City	*Rugiboletus extremiorientalis*	RugE	5
8#	Region 6	Fengyi Village, Anning city, Kunming City	*Butyriboletus roseoflavus*	BuR	4

Table A1 (continued)

Sampling Namber	Region divide based on PCAC and consensus clustering	Sampling position	Latin Name	Abbreviation	Numbers
9#	Region 6	Tongchang, Yimen County, Yuxi City	*Boletus bainiugan*	BB	5
10#	Region 3	Jiulongchi Pond, Yuxi City	*Boletus bainiugan*	BB	5
11#	Region 6	Tongchang, Yimen County, Yuxi City	*Butyriboletus roseoflavus*	BuR	5
12#	Region 3	Tangchi Town, Yiliang County, Kunming City	*Neoboletus magnificus*	NM	6
13#	Region 1	Wenli Village, anban Town, Zhenyuan County, Pu'er City	*Lanmaoa asiatica*	LA	3
14#	Region 1	Wenli Village, anban Town, Zhenyuan County, Pu'er City	*Retiboletus fuscus*	RetF	6
15#	Region 1	Wenli Village, anban Town, Zhenyuan County, Pu'er City	*Neoboletus magnificus*	NM	5
16#	Region 6	Tongchang, Yimen County, Yuxi City	*Lanmaoa asiatica*	LA	3
17#	Region 6	Fuliangpeng Township, Eshan County, Yuxi City	*Boletus bainiugan*	BB	4
18#	Region 6	Fengyi Village, Anning city, Kunming City	*Rugiboletus extremiorientalis*	RugE	5
19#	Region 6	Fuliangpeng Township, Eshan County, Yuxi City	*Butyriboletus roseoflavus*	BuR	4
20#	Region 6	Jiuxiang Village, Yiliang County, Kunming City	*Rugiboletus extremiorientalis*	RugE	5
21#	Region 3	Jiuxi Town, Jiangchuan County, Yuxi City	*Butyriboletus roseoflavus*	BuR	4
22#	Region 6	Daweidu Village, Xiaojie Town, Eshan County, Yuxi City	*Boletus bainiugan*	BB	5
23#	Region 6	Daweidu Village, Xiaojie Town, Eshan County, Yuxi City	*Lanmaoa asiatica*	LA	3
24#	Region 2	Donggua Town, Chuxiong Prefecture	*Lanmaoa asiatica*	LA	3
25#	Region 1	Simao District, Pu'er City	*Neoboletus magnificus*	NM	5
26#	Region 6	Fuliangpeng Township, Eshan County, Yuxi City	*Lanmaoa asiatica*	LA	3
27#	Region 6	Daweidu Village, Xiaojie Town, Eshan County, Yuxi City	*Retiboletus fuscus*	RetF	6

Table A1 (continued)

Sampling Namber	Region divide based on PCAC and consensus clustering	Sampling position	Latin Name	Abbreviation	Numbers
28#	Region 6	Fuliangpeng Township, Eshan County, Yuxi City	*Rugiboletus extremiorientalis*	RugE	5
29#	Region 6	Daweidu Village, Xiaojie Town, Eshan County, Yuxi City	*Rubroboletus sinicus*	RubS	6
30#	Region 6	Fuliangpeng Township, Eshan County, Yuxi City	*Neoboletus hainanensis*	NH	5
31#	Region 3	Jiuxi Town, Jiangchuan County, Yuxi City	*Butyriboletus pseudospeciosus*	BuP	5
32#	Region 6	Daweidu Village, Xiaojie Town, Eshan County, Yuxi City	*Neoboletus magnificus*	NM	8
33#	Region 6	Fuliangpeng Township, Eshan County, Yuxi City	*Neoboletus magnificus*	NM	3
34#	Region 2	Midu County, Dali City	*Lanmaoa asiatica*	LA	3
35#	Region 1	Xinping County, Yuxi City	*Neoboletus magnificus*	NM	6
36#	Region 2	Donggua Town, Chuxiong Prefecture	*Rugiboletus extremiorientalis*	RugE	5
37#	Region 2	Mali mountain, Midu County, Dali City	*Retiboletus fuscus*	RetF	5
38#	Region 4	Longyan District, Baoshan City	*Rugiboletus extremiorientalis*	RugE	4
39#	Region 6	Luohe Township, Yuxi City	*Boletus bainiugan*	BB	5
40#	Region 6	Luohe Township, Yuxi City	*Butyriboletus pseudospeciosus*	BuP	4
41#	Region 3	Jiuxi Town, Jiangchuan County, Yuxi City	*Lanmaoa asiatica*	LA	3
42#	Region 3	Jiuxi Town, Jiangchuan County, Yuxi City	*Lanmaoa asiatica*	LA	3
43#	Region 4	Baohe Town, Weixi County, Diqing Prepecture	*Rugiboletus extremiorientalis*	RugE	3
44#	Region 6	Luohe Township, Yuxi City	*Rugiboletus extremiorientalis*	RugE	5
45#	Region 6	Longpeng Town, Shiping County, Honghe Prepecture	*Neoboletus magnificus*	NM	5
46#	Region 3	Jiuxi Town, Jiangchuan County, Yuxi City	*Neoboletus obscureumbrinus*	NO	3

Table A1 (continued)

Sampling Namber	Region divide based on PCAC and consensus clustering	Sampling position	Latin Name	Abbreviation	Numbers
47#	Region 3	Jiuxi Town, Jiangchuan County, Yuxi City	*Rugiboletus extremiorientalis*	RugE	6
48#	Region 3	Jiuxi Town, Jiangchuan County, Yuxi City	*Rubroboletus sinicus*	RubS	6
49#	Region 3	Jiuxi Town, Jiangchuan County, Yuxi City	*Neoboletus magnificus*	NM	6
50#	Region 3	Baitu Village, Daying street, Yuxi City	*Lanmaoa asiatica*	LA	3
51#	Region 6	Anhau Township, Jiangchuan County, Yuxi City	*Lanmaoa asiatica*	LA	3
52#	Region 6	Anhau Township, Jiangchuan County, Yuxi City	*Retiboletus fuscus*	RetF	7
53#	Region 6	Luohe Township, Yuxi City	*Rugiboletus extremiorientalis*	RugE	5
54#	Region 3	Shiping County, Honghe Prepecture	*Neoboletus obscureumbrinus*	NO	3
55#	Region 5	Maan Township, Dechan County, Liangshan Prepecture, Sichuan Province	*Neoboletus obscureumbrinus*	NO	4
56#	Region 5	Bicheng Town, Lufeng County, Chuxipong Prepecture	*Lanmaoa asiatica*	LA	3
57#	Region 6	Luohe Township, Yuxi City	*Retiboletus fuscus*	RetF	10
58#	Region 6	Anhau Township, Jiangchuan County, Yuxi City	*Neoboletus magnificus*	NM	5
59#	Region 6	Luohe Township, Yuxi City	*Neoboletus magnificus*	NM	3
60#	Region 3	Baitu Village, Daying street, Yuxi City	*Retiboletus fuscus*	RetF	6
61#	Region 6	Maming Township, Qujing City	*Neoboletus hainanensis*	NH	5
62#	Region 3	Liujie Town, Yimen County, Yuxi City	*Lanmaoa asiatica*	LA	3
63#	Region 3	Liujie Town, Yimen County, Yuxi City	*Neoboletus obscureumbrinus*	NO	3
64#	Region 3	Liujie Town, Yimen County, Yuxi City	*Phlebopus portentosus*	PP	7
65#	Region 6	Baoxing Village, Shangsuan Town, Jinning County, Kunming City	*Boletus bainiugan*	BoB	4

Table A1 (continued)

Sampling Namber	Region divide based on PCAC and consensus clustering	Sampling position	Latin Name	Abbreviation	Numbers
66#	Region 6	Gaoping Village, Shuangjiang Township, Eshan County, Yuxi City	*Lanmaoa asiatica*	LA	3
67#	Region 6	Meiyun Village, Yimen County, Yuxi City	*Retiboletus fuscus*	RetF	6
68#	Region 4	Datianba Township, Changning County, Baoshan City	*Phlebopus portentosus*	PP	7
69#	Region 4	Beijieshuiku Village, Longyan District, Baoshan City	*Butyriboletus roseoflavus*	BuR	5
70#	Region 2	Zixi Mountain, Nanhua County, Chuxiong Prepecture	*Lanmaoa asiatica*	LA	2
71#	Region 5	Jiyi Township, Wuding County, Chuxiong Prepecture	*Lanmaoa asiatica*	LA	3
72#	Region 6	Gaoping Village, Shuangjiang Township, Eshan County, Yuxi City	*Retiboletus fuscus*	RetF	6
73#	Region 3	Liujie Town, Yimen County, Yuxi City	*Rubroboletus sinicus*	RubS	7
74#	Region 3	Daliu Village, Liujie Town, Yimen County, Yuxi City	*Butyriboletus roseoflavus*	BuR	5
75#	Region 6	Leye Village, Sanhe Town, Honghe Prepecture	*Butyriboletus roseoflavus*	BuR	5
76#	Region 6	Gaoping Village, Shuangjiang Township, Eshan County, Yuxi City	*Neoboletus magnificus*	NM	4
77#	Region 4	Shangrila County, Diqing Prepecture	*Neoboletus obscureumbrinus*	NO	4
78#	Region 4	Beidou Township, Yunlong County, Dali City	*Butyriboletus pseudospeciosus*	BuP	3
79#	Region 5	Liangshan Township, Yuanmou County, Chuxiong Prepecture	*Butyriboletus roseoflavus*	BuR	5
80#	Region 3	Daliu Village, Liujie Town, Yimen County, Yuxi City	*Lanmaoa asiatica*	LA	3
81#	Region 3	Pubei Township, Yimen County, Yuxi City	*Rugiboletus extremiorientalis*	RugE	3
82#	Region 5	Yipinglang Town, Lufeng County, Chuxiong Prepecture	*Butyriboletus pseudospeciosus*	BuP	5
83#	Region 3	Pubei Township, Yimen County, Yuxi City	*Neoboletus magnificus*	NM	5
84#	Region 3	Xiaojie Township, Yimen County, Yuxi City	*Lanmaoa asiatica*	LA	2

Table A1 (continued)

Sampling Namber	Region divide based on PCAC and consensus clustering	Sampling position	Latin Name	Abbreviation	Numbers
85#	Region 6	Junzi Hill, Longchuan Town, Nanhua County, Chuxiong Prepecture	*Retiboletus fuscus*	RetF	6
86#	Region 3	Daying street, Yuxi City	*Lanmaoa asiatica*	LA	3
87#	Region 6	Leye Village, Sanhe Town, Honghe Prepecture	*Lanmaoa asiatica*	LA	3
88#	Region 3	Shuangjiang Town, Eshan County, Yuxi City	*Butyriboletus roseoflavus*	BuR	5
89#	Region 3	Shuangjiang Town, Eshan County, Yuxi City	*Rugiboletus extremiorientalis*	RugE	3
90#	Region 4	Tongdian Town, Lanping County, Nujiang Prepecture	*Butyriboletus pseudospeciosus*	BuP	4
91#	Region 4	Heqing County, Dali City	*Neoboletus obscureumbrinus*	NO	3
92#	Region 5	Hengshan Township, Miyi County, Pangzhihua City, Sichuan Province	*Neoboletus obscureumbrinus*	NO	4
93#	Region 2	Baizhu Mountain, Daguohe Township, Nanhua County, Chuxiong Prepecture	*Butyriboletus pseudospeciosus*	BuP	4
94#	Region 5	Liangshan Township, Yuanmou County, Chuxiong Prepecture	*Rugiboletus extremiorientalis*	RugE	3
95#	Region 6	Guihuashu Village, Yuezhou Town, Qilin District, Qujing City	*Butyriboletus pseudospeciosus*	BuP	5
96#	Region 3	Huangcaoba Village, Xishan District, Kunming City	*Butyriboletus roseoflavus*	BuR	5
97#	Region 3	Hongta District, Yuxi City	*Butyriboletus pseudospeciosus*	BuP	3
98#	Region 6	Guihuashu Village, Yuezhou Town, Qilin District, Qujing City	*Lanmaoa asiatica*	LA	2
99#	Region 6	Maan Village, Tianzhong Township, Yimen County, Yuxi City	*Boletus bainiugan*	BoB	7
100#	Region 6	Guihuashu Village, Yuezhou Town, Qilin District, Qujing City	*Retiboletus fuscus*	RetF	6
101#	Region 6	Tadian Town, Eshan County, Yuxi City	*Butyriboletus roseoflavus*	BuR	4
102#	Region 3	Beicheng District, Yuxi City	*Rubroboletus sinicus*	RubS	7
103#	Region 3	Yimen County, Yuxi City	*Rugiboletus extremiorientalis*	RugE	3

Table A1 (continued)

Sampling Namber	Region divide based on PCAC and consensus clustering	Sampling position	Latin Name	Abbreviation	Numbers
104#	Region 6	Kunyan street, Jinning County, Kunming City	*Butyriboletus roseoflavus*	BuR	5
105#	Region 6	Puxiong Township, Jianshui County, Honghe Prepecture	*Butyriboletus roseoflavus*	BuR	5
106#	Region 2	Yaoan County, Chuxiong Prepecture	*Neoboletus hainanensis*	NH	5
107#	Region 3	Chahe Township, Eshan County, Yuxi City	*Neoboletus obscureumbrinus*	NO	3
108#	Region 6	Wujie Township, Nanhua County, Chuxiong Prepecture	*Rubroboletus sinicus*	RubS	6
109#	Region 3	Yimen County, Yuxi City	*Neoboletus hainanensis*	NH	5
110#	Region 6	Shidong Village, Longquan Town, Yimen County, Yuxi City	*Rugiboletus extremiorientalis*	RugE	5

Table A2 Detailed ecological factors for samples collection

Sampling Number	Longitude	Latitude	Elevation	b01	b02	b03	b04	b05	b06	b07	b08	b09	b10	b11	b12	b13	b14	b15	b16	b17	b18	b19	pH
1#	102.65	23.8	1898	15.58	10.27	48.43	414.69	24.3	3.1	21.2	19.85	9.90	19.85	9.90	1037	210	14	85.02	585	47	585	47	5.1
2#	100.66	21.98	984	21.18	11.43	52.41	330.43	30.5	8.7	21.8	23.88	18.10	24.28	16.55	1613	313	15	82.37	850	59	693	69	5.2
3#	101.26	25.79	1921	16.36	11.95	47.99	460.62	26.7	1.8	24.9	21.20	10.18	21.20	10.18	752	148	10	81.82	406	34	406	34	5.1
4#	101.51	25.07	1797	16.90	11.95	47.80	463.82	27	2	25	21.67	10.57	21.67	10.57	817	163	11	83.73	450	37	450	37	5.1
5#	101.37	25.53	2155	14.77	11.55	47.93	445.51	24.8	0.7	24.1	19.42	8.77	19.42	8.77	794	157	10	82.76	433	35	433	35	7.8
6#	101.37	25.53	2155	14.77	11.55	47.93	445.51	24.8	0.7	24.1	19.42	8.77	19.42	8.77	794	157	10	82.76	433	35	433	35	7.8
7#	102.76	24.12	1806	15.65	10.24	47.64	432.21	24.4	2.9	21.5	20.13	9.70	20.13	9.70	960	192	12	84.75	540	43	540	43	7.8
8#	102.32	24.68	1980	15.20	11.64	49.12	437.56	24.8	1.1	23.7	19.70	9.23	19.70	9.23	897	178	12	83.56	496	40	496	40	7.8
9#	102.03	24.71	2309	13.75	10.60	47.11	428.23	22.9	0.4	22.5	18.17	7.90	18.17	7.90	923	183	12	83.38	508	42	508	42	6.6
10#	102.52	24.43	1689	16.58	11.22	48.35	447.76	26	2.8	23.2	21.13	12.17	21.13	10.40	888	171	14	81.37	484	46	484	46	7.8
11#	102.09	24.69	1993	15.08	10.95	47.20	437.67	24.5	1.3	23.2	19.55	9.08	19.55	9.08	898	179	12	83.73	497	40	497	40	4.8
12#	102.1	25.03	1648	17.21	11.36	47.13	454.11	27.1	3	24.1	21.78	13.00	21.82	11.02	821	166	10	85.37	460	35	373	36	7.8
13#	100.74	23.79	1590	18.29	11.00	49.55	400.79	27	4.8	22.2	22.43	14.35	22.43	12.75	1190	245	14	86.46	672	46	672	50	4.9
14#	100.74	23.79	1590	18.29	11.00	49.55	400.79	27	4.8	22.2	22.43	14.35	22.43	12.75	1190	245	14	86.46	672	46	672	50	4.9
15#	100.74	23.79	1590	18.29	11.00	49.55	400.79	27	4.8	22.2	22.43	14.35	22.43	12.75	1190	245	14	86.46	672	46	672	50	4.9
16#	102.04	24.71	2307	13.74	10.62	47.19	428.53	22.9	0.4	22.5	18.17	7.88	18.17	7.88	924	184	12	83.61	509	41	509	41	6.6
17#	102.09	24.31	1973	15.47	10.88	47.94	426.80	24.7	2	22.7	19.82	9.60	19.82	9.60	949	190	13	84.16	528	43	528	43	6.8

Table A2 (continued)

Sampling Namber	Longitude	Latitude	Elevation	b01	b02	b03	b04	b05	b06	b07	b08	b09	b10	b11	b12	b13	b14	b15	b16	b17	b18	b19	pH
18#	102.33	24.69	1976	15.21	11.69	49.12	439.58	24.9	1.1	23.8	19.73	9.23	19.73	9.23	894	177	12	83.49	494	40	494	40	6.6
19#	102.09	24.31	1973	15.47	10.88	47.94	426.80	24.7	2	22.7	19.82	9.60	19.82	9.60	949	190	13	84.16	528	43	528	43	6.8
20#	103.39	25.11	1847	15.15	10.91	47.22	463.52	24.7	1.6	23.1	20.02	8.87	20.02	8.87	923	176	13	82.66	508	44	508	44	6.6
21#	102.63	24.3	1740	16.13	11.03	48.18	441.72	25.5	2.6	22.9	20.67	10.08	20.67	10.08	900	177	12	83.00	497	42	497	42	7.8
22#	102.38	24.09	1873	15.79	10.60	48.18	423.59	24.8	2.8	22	20.15	10.00	20.15	10.00	962	194	13	83.61	534	45	534	45	5
23#	102.38	24.09	1873	15.79	10.60	48.18	423.59	24.8	2.8	22	20.15	10.00	20.15	10.00	962	194	13	83.61	534	45	534	45	5
24#	101.51	25.07	1797	16.90	11.95	47.80	463.82	27	2	25	21.67	10.57	21.67	10.57	817	163	11	83.73	450	37	450	37	5.1
25#	101.03	23.07	1620	17.98	11.15	50.91	375.77	26.9	5	21.9	21.75	14.32	21.75	12.75	1375	289	17	86.85	777	56	777	61	6.5
26#	102.09	24.31	1973	15.47	10.88	47.94	426.80	24.7	2	22.7	19.82	9.60	19.82	9.60	949	190	13	84.16	528	43	528	43	6.8
27#	102.38	24.09	1873	15.79	10.60	48.18	423.59	24.8	2.8	22	20.15	10.00	20.15	10.00	962	194	13	83.61	534	45	534	45	5
28#	102.09	24.31	1973	15.47	10.88	47.94	426.80	24.7	2	22.7	19.82	9.60	19.82	9.60	949	190	13	84.16	528	43	528	43	6.8
29#	102.38	24.09	1873	15.79	10.60	48.18	423.59	24.8	2.8	22	20.15	10.00	20.15	10.00	962	194	13	83.61	534	45	534	45	5
30#	102.09	24.31	1973	15.47	10.88	47.94	426.80	24.7	2	22.7	19.82	9.60	19.82	9.60	949	190	13	84.16	528	43	528	43	6.8
31#	102.64	24.3	1714	16.25	11.09	48.22	443.42	25.7	2.7	23	20.78	10.17	20.78	10.17	898	176	12	83.03	496	42	496	42	7.8
32#	102.38	24.09	1873	15.79	10.60	48.18	423.59	24.8	2.8	22	20.15	10.00	20.15	10.00	962	194	13	83.61	534	45	534	45	5
33#	102.09	24.31	1973	15.47	10.88	47.94	426.80	24.7	2	22.7	19.82	9.60	19.82	9.60	949	190	13	84.16	528	43	528	43	6.8
34#	100.49	25.34	1674	17.79	12.18	48.70	468.84	28.1	3.1	25	22.73	11.45	22.73	11.45	841	152	13	74.22	432	49	432	49	7.8

Table A2 (continued)

Sampling Namber	Longitude	Latitude	Elevation	b01	b02	b03	b04	b05	b06	b07	b08	b09	b10	b11	b12	b13	b14	b15	b16	b17	b18	b19	pH
35#	101.57	24.06	553	22.48	11.03	47.15	446.52	32.3	8.9	23.4	26.90	18.27	26.90	16.32	1258	261	18	83.54	704	60	704	69	7.8
36#	101.51	25.07	1797	16.90	11.95	47.80	463.82	27	2	25	21.67	10.57	21.67	10.57	817	163	11	83.73	450	37	450	37	5.1
37#	100.51	25.34	1781	17.26	12.20	49.00	462.02	27.6	2.7	24.9	22.17	11.03	22.17	11.03	828	149	12	73.87	423	48	423	48	6.6
38#	99.16	25.12	1685	16.29	11.01	47.66	456.64	25.1	2	23.1	21.10	10.03	21.10	10.03	1021	181	13	73.39	511	59	511	59	4.8
39#	102.38	24.31	1772	15.97	10.50	47.30	434.83	25	2.8	22.2	20.42	10.00	20.42	10.00	909	180	13	82.34	499	45	499	45	6.8
40#	102.39	24.33	1726	16.14	10.52	47.16	438.31	25.2	2.9	22.3	20.63	11.95	20.63	10.13	900	177	13	82.41	494	44	494	44	6.8
41#	102.63	24.3	1740	16.13	11.03	48.18	441.72	25.5	2.6	22.9	20.67	10.08	20.67	10.08	900	177	12	83.00	497	42	497	42	7.8
42#	102.63	24.3	1740	16.13	11.03	48.18	441.72	25.5	2.6	22.9	20.67	10.08	20.67	10.08	900	177	12	83.00	497	42	497	42	7.8
43#	99.28	27.18	2323	12.56	10.53	42.99	529.15	22.9	1.6	24.5	18.17	6.65	18.65	5.70	974	155	14	61.00	406	59	403	100	5
44#	102.38	24.31	1772	15.97	10.50	47.30	434.83	25	2.8	22.2	20.42	10.00	20.42	10.00	909	180	13	82.34	499	45	499	45	6.8
45#	102.65	23.8	1898	15.58	10.27	48.43	414.69	24.3	3.1	21.2	19.85	9.90	19.85	9.90	1037	210	14	85.02	585	47	585	47	5.1
46#	102.64	24.3	1714	16.25	11.09	48.22	443.42	25.7	2.7	23	20.78	10.17	20.78	10.17	898	176	12	83.03	496	42	496	42	7.8
47#	102.64	24.3	1714	16.25	11.09	48.22	443.42	25.7	2.7	23	20.78	10.17	20.78	10.17	898	176	12	83.03	496	42	496	42	7.8
48#	102.64	24.3	1714	16.25	11.09	48.22	443.42	25.7	2.7	23	20.78	10.17	20.78	10.17	898	176	12	83.03	496	42	496	42	7.8
49#	102.63	24.3	1740	16.13	11.03	48.18	441.72	25.5	2.6	22.9	20.67	10.08	20.67	10.08	900	177	12	83.00	497	42	497	42	7.8
50#	102.49	24.34	1622	16.95	11.18	48.20	450.09	26.4	3.2	23.2	21.53	12.58	21.53	10.75	886	173	13	82.38	486	43	486	44	7.8
51#	102.66	24.41	2005	14.66	10.74	47.95	431.45	23.8	1.4	22.4	19.10	8.77	19.10	8.77	939	185	13	82.92	518	45	518	45	5.1

Table A2 (continued)

Sampling Number	Longitude	Latitude	Elevation	b01	b02	b03	b04	b05	b06	b07	b08	b09	b10	b11	b12	b13	b14	b15	b16	b17	b18	b19	pH
52#	102.66	24.41	2005	14.66	10.74	47.95	431.45	23.8	1.4	22.4	19.10	8.77	19.10	8.77	939	185	13	82.92	518	45	518	45	5.1
53#	102.39	24.33	1726	16.14	10.52	47.16	438.31	25.2	2.9	22.3	20.63	11.95	20.63	10.13	900	177	13	82.41	494	44	494	44	6.8
54#	102.49	23.7	1442	18.00	10.29	48.78	416.19	26.7	5.6	21.1	22.25	12.28	22.25	12.28	1027	211	10	87.90	595	40	595	40	4.9
55#	102.01	27.43	2263	14.17	10.92	46.45	475.11	24.1	0.6	23.5	19.47	7.93	19.47	7.93	894	200	5	96.01	526	19	526	19	5.1
56#	101.84	25.34	2245	14.12	11.53	47.86	446.96	24	0.1	24.1	18.75	8.05	18.75	8.05	838	168	11	84.29	463	37	463	37	5.1
57#	102.39	24.33	1726	16.14	10.52	47.16	438.31	25.2	2.9	22.3	20.63	11.95	20.63	10.13	900	177	13	82.41	494	44	494	44	6.8
58#	102.66	24.41	2005	14.66	10.74	47.95	431.45	23.8	1.4	22.4	19.10	8.77	19.10	8.77	939	185	13	82.92	518	45	518	45	5.1
59#	102.39	24.33	1726	16.14	10.52	47.16	438.31	25.2	2.9	22.3	20.63	11.95	20.63	10.13	900	177	13	82.41	494	44	494	44	6.8
60#	102.5	24.34	1621	16.98	11.22	48.14	450.79	26.5	3.2	23.3	21.57	12.60	21.57	10.78	882	173	13	82.61	485	43	485	44	7.8
61#	103.3	25.25	1962	14.37	10.56	46.72	457.04	23.6	1	22.6	19.17	8.17	19.17	8.17	922	175	14	81.82	503	46	503	46	6.8
62#	102.23	24.82	1692	16.53	11.12	47.30	450.65	26.1	2.6	23.5	21.12	10.37	21.12	10.37	853	172	11	84.25	474	38	474	38	6.8
63#	102.23	24.82	1692	16.53	11.12	47.30	450.65	26.1	2.6	23.5	21.12	10.37	21.12	10.37	853	172	11	84.25	474	38	474	38	6.8
64#	102.02	24.07	1496	18.05	10.88	48.33	428.56	27.3	4.8	22.5	22.40	12.17	22.40	12.17	986	200	12	85.69	558	42	558	42	4.8
65#	102.54	24.59	1958	14.91	11.10	48.26	434.86	24.3	1.3	23	19.38	8.95	19.38	8.95	917	180	13	82.56	504	43	504	43	6.8
66#	102.3	24.21	2069	14.75	10.28	47.39	420.70	23.6	1.9	21.7	19.10	8.98	19.10	8.98	964	193	13	83.39	533	45	533	45	6.8
67#	102.09	24.69	1993	15.08	10.95	47.20	437.67	24.5	1.3	23.2	19.55	9.08	19.55	9.08	898	179	12	83.73	497	40	497	40	4.8
68#	99.51	25.04	1620	16.93	11.08	47.57	447.68	26.1	2.8	23.3	21.58	10.75	21.58	10.75	964	173	14	73.72	488	58	488	58	4.8

Table A2 (continued)

Sampling Namber	Longitude	Latitude	Elevation	b01	b02	b03	b04	b05	b06	b07	b08	b09	b10	b11	b12	b13	b14	b15	b16	b17	b18	b19	pH
69#	99.27	25.18	1754	16.20	11.47	48.01	458.71	25.5	1.6	23.9	21.03	9.92	21.03	9.92	982	173	14	71.05	481	61	481	61	4.9
70#	101.12	25.22	1984	16.13	12.03	48.33	460.71	26.3	1.4	24.9	20.98	9.90	20.98	9.90	814	157	12	80.42	436	40	436	40	5.1
71#	102.26	26.09	2025	15.39	11.34	46.87	455.00	25.7	1.5	24.2	20.12	9.28	20.12	9.28	831	180	7	93.12	487	24	487	24	5.1
72#	102.3	24.21	2069	14.75	10.28	47.39	420.70	23.6	1.9	21.7	19.10	8.98	19.10	8.98	964	193	13	83.39	533	45	533	45	6.8
73#	102.23	24.82	1692	16.53	11.12	47.30	450.65	26.1	2.6	23.5	21.12	10.37	21.12	10.37	853	172	11	84.25	474	38	474	38	6.8
74#	102.23	24.84	1732	16.29	11.06	47.06	448.90	25.9	2.4	23.5	20.87	10.15	20.87	10.15	858	173	11	84.45	477	38	477	38	6.8
75#	103.62	24.47	1832	15.05	10.58	47.00	462.25	24.4	1.9	22.5	19.88	8.72	19.88	8.72	975	185	15	81.91	538	49	538	49	5
76#	102.3	24.21	2069	14.75	10.28	47.39	420.70	23.6	1.9	21.7	19.10	8.98	19.10	8.98	964	193	13	83.39	533	45	533	45	6.8
77#	99.7	27.83	3283	6.83	12.68	44.98	594.03	18.7	9.5	28.2	13.18	0.15	13.67	0.77	707	133	8	67.60	333	35	332	45	6.5
78#	99.36	25.88	1850	15.68	10.97	46.70	463.62	25.2	1.7	23.5	20.63	10.10	20.63	9.40	1040	164	17	61.14	478	71	478	83	5.1
79#	101.96	25.73	2138	15.15	11.33	47.78	439.48	25.1	1.4	23.7	19.73	9.25	19.73	9.25	799	167	9	87.89	451	30	451	30	5.1
80#	102.23	24.84	1732	16.29	11.06	47.06	448.90	25.9	2.4	23.5	20.87	10.15	20.87	10.15	858	173	11	84.45	477	38	477	38	6.8
81#	102.18	24.61	1695	16.74	11.33	47.78	445.74	26.5	2.8	23.7	21.23	10.62	21.23	10.62	872	172	11	83.69	483	39	483	39	6.6
82#	101.84	25.34	2245	14.12	11.53	47.86	446.96	24	0.1	24.1	18.75	8.05	18.75	8.05	838	168	11	84.29	463	37	463	37	5.1
83#	102.49	24.93	1847	15.84	11.43	47.80	455.68	25.5	1.6	23.9	20.55	9.62	20.55	9.62	900	180	13	83.08	498	44	498	44	7.8
84#	102.46	24.15	1535	17.28	11.08	48.15	445.60	26.7	3.7	23	21.78	13.03	21.78	11.15	923	184	11	84.37	517	42	517	42	7.8
85#	101.33	25.37	2516	13.00	11.20	48.07	437.98	22.5	0.8	23.3	17.68	7.12	17.68	7.12	848	165	12	80.20	453	42	453	42	6.5

Table A2 (continued)

Sampling Number	Longitude	Latitude	Elevation	b01	b02	b03	b04	b05	b06	b07	b08	b09	b10	b11	b12	b13	b14	b15	b16	b17	b18	b19	pH
86#	102.5	24.34	1621	16.98	11.22	48.14	450.79	26.5	3.2	23.3	21.57	12.60	21.57	10.78	882	173	13	82.61	485	43	485	44	7.8
87#	103.62	24.47	1832	15.05	10.58	47.00	462.25	24.4	1.9	22.5	19.88	8.72	19.88	8.72	975	185	15	81.91	538	49	538	49	5
88#	102.41	24.17	1540	17.21	10.90	48.02	443.12	26.5	3.8	22.7	21.73	12.98	21.73	11.13	931	185	12	84.36	521	43	521	43	7.8
89#	102.41	24.17	1540	17.21	10.90	48.02	443.12	26.5	3.8	22.7	21.73	12.98	21.73	11.13	931	185	12	84.36	521	43	521	43	7.8
90#	99.52	26.69	2444	12.74	11.33	46.60	499.48	22.7	1.6	24.3	18.45	6.98	18.45	6.22	928	146	14	57.30	391	61	391	88	7.8
91#	100.17	26.56	2203	14.48	11.91	48.80	465.27	24.6	0.2	24.4	19.68	8.93	19.68	8.35	829	134	12	60.46	372	52	372	65	7.8
92#	102.3	26.97	2558	12.12	10.71	46.76	459.94	21.6	1.3	22.9	17.27	6.07	17.27	6.07	930	199	8	93.06	539	26	539	26	6.5
93#	101.12	25.22	1984	16.13	12.03	48.33	460.71	26.3	1.4	24.9	20.98	9.90	20.98	9.90	814	157	12	80.42	436	40	436	40	5.1
94#	101.96	25.73	2138	15.15	11.33	47.78	439.48	25.1	1.4	23.7	19.73	9.25	19.73	9.25	799	167	9	87.89	451	30	451	30	5.1
95#	103.96	25.27	2035	13.92	10.38	46.32	475.51	23.2	0.8	22.4	19.00	7.45	19.00	7.45	1029	194	13	83.17	562	45	562	45	6.6
96#	102.56	24.34	1714	16.53	10.97	48.10	443.18	25.9	3.1	22.8	21.10	10.47	21.10	10.47	894	177	12	83.37	495	42	495	42	6.8
97#	102.54	24.34	1670	16.78	11.12	48.33	447.90	26.2	3.2	23	21.37	12.43	21.37	10.62	897	177	13	83.49	497	43	497	43	6.8
98#	103.96	25.27	2035	13.92	10.38	46.32	475.51	23.2	0.8	22.4	19.00	7.45	19.00	7.45	1029	194	13	83.17	562	45	562	45	6.6
99#	102.29	24.58	2061	14.73	11.12	48.12	433.31	24.2	1.1	23.1	19.17	8.80	19.17	8.80	909	180	12	83.81	503	40	503	40	7.8
100#	103.96	25.27	2035	13.92	10.38	46.32	475.51	23.2	0.8	22.4	19.00	7.45	19.00	7.45	1029	194	13	83.17	562	45	562	45	6.6
101#	102.16	24.25	1835	16.10	10.71	47.81	427.87	25.2	2.8	22.4	20.47	12.03	20.47	10.22	953	187	15	82.00	523	48	523	49	6.8
102#	102.55	24.43	1659	16.76	11.27	48.56	449.80	26.2	3	23.2	21.33	12.33	21.33	10.55	882	171	13	81.99	482	44	482	44	7.8

Table A2 (continued)

Sampling Namber	Longitude	Latitude	Elevation	b01	b02	b03	b04	b05	b06	b07	b08	b09	b10	b11	b12	b13	b14	b15	b16	b17	b18	b19	pH
103#	102.16	24.67	1587	17.41	11.65	48.14	454.12	27.3	3.1	24.2	22.02	13.15	22.02	11.18	871	175	11	84.59	486	39	486	39	7.8
104#	102.65	24.52	2061	14.15	10.63	47.43	427.26	23.3	0.9	22.4	18.52	8.30	18.52	8.30	936	184	13	83.06	516	44	516	44	7.8
105#	103	23.5	2125	14.03	9.71	48.06	403.98	22.4	2.2	20.2	18.18	8.47	18.18	8.47	1192	246	10	86.63	675	46	675	46	6.5
106#	101.24	25.51	1880	16.50	12.01	48.03	462.19	26.8	1.8	25	21.33	10.25	21.33	10.25	766	151	10	81.76	414	36	414	36	7.8
107#	102.24	24.28	1474	17.70	10.78	47.71	433.52	27	4.4	22.6	22.07	13.58	22.07	11.73	921	182	12	84.30	515	42	515	43	5.1
108#	101.33	25.37	2516	13.00	11.20	48.07	437.98	22.5	0.8	23.3	17.68	7.12	17.68	7.12	848	165	12	80.20	453	42	453	42	6.5
109#	102.16	24.67	1587	17.41	11.65	48.14	454.12	27.3	3.1	24.2	22.02	13.15	22.02	11.18	871	175	11	84.59	486	39	486	39	7.8
110#	102.29	24.76	2463	12.74	10.40	47.49	423.22	21.6	0.3	21.9	17.18	6.98	17.18	6.98	947	188	13	82.99	520	44	520	44	6.8

Table A3 The detailed description of ecological environmental factors

Factors of ecology and environment	Explanation of factors	Unite
b01	Mean annual temperature	℃
b02	Mean of monthly (max temperature min temperature)	℃
b03	Isothermality (Bio2/Bio7) (×100)	1
b04	SD of temperature seasonality	1
b05	Max temperature of warmest month	℃
b06	Min temperature of coldest month	℃
b07	Temperature annual range (Bio5Bio6)	℃
b08	Mean temperature of wettest quarter	℃
b09	Mean temperature of driest quarter	℃
b10	Mean temperature of warmest quarter	℃
b11	Mean temperature of coldest quarter	℃
b12	Annual precipitation	mm
b13	Precipitation of wettest month	mm
b14	Precipitation of driest month	mm
b15	Coefficient of variation of precipitation seasonality	1
b16	Precipitation of wettest quarter	mm
b17	Precipitation of driest quarter	mm
b18	Precipitation of warmest quarter	mm
b19	Precipitation of coldest quarter	mm

Table A3 (continued)

Factors of ecology and environment	Explanation of factors	Unite
pH	Potential of hydrogen of soil	1
Latitude	The latitude of collection sites recorded by GPS	º
Longitude	The longitude of collection sites recorded by GPS	º
Elevation	The elevation of collection sites recorded by GPS	m

APPENDIX B

THE DETAILED INFORMATION OF PHYLOGENETIC ANALYSES

Table B Bayesian phylogenetic trees of 11 species of Boletes

Species	Bank note	RPB2	TEF1	Species	Bank note	RPB2	TEF1
Buchwaldoboletus xylophilus	X.H. Deng1 (FHMU5848)	MW820947	MW897338	*Leccinellum alborufescens*	FHMU1908	MK816333	MK816330
Strobilomyces hongoi	SH1-5	AB589439		*Crocinoboletus rufoaureus*	FHMU:1975	MK850942	MK850947
Strobilomyces hongoi	SH1-6	AB589441		*Crocinoboletus pinetorum*	FHMU:1146	MK850943	MK850945
Boletus reticulatus	BR1-1	AB589453		*Crocinoboletus laetissimus*	FHMU:2030	MK850944	MK850948
Boletellus areolatus	BLT-12	AB999755		*Sutorius maculatoides*	OR0758	MN067498	MN067481
Boletellus areolatus	BLT-124	AB999780		*Sutorius mucosus*	OR0851	MN067499	MN067483
Boletellus aurocontextus	BLT-126	AB999781		*Sutorius pachypus*	OR0411	MN067500	MN067484
Boletellus emodensis	BLT-128	AB999782		*Sutorius pachypus*	SV0098	MN067501	MN067485
Boletellus aurocontextus	BLT-130	AB999783		*Sutorius pseudotylopilus*	SV0401	MN067502	MN067486
Strobilomyces floccopus	AFTOL-ID 716	AY786065	AY883428	*Sutorius pseudotylopilus*	SV0415	MN067503	MN067487

Table B (continued)

Species	Bank note	RPB2	TEF1	Species	Bank note	RPB2	TEF1
Boletellus projectellus	AFTOL-ID 713	AY787218	AY879116	*Sutorius rubinus*	OR0409	MN067505	MN067489
Chamonixia sp.	Muroi361	DQ219046	DQ219224	*Sutorius rubinus*	OR1255	MN067506	MN067490
Tricholomopsis decora	AFTOL-ID 537	DQ408112	DQ029195	*Sutorius ubonensis*	SV0032	MN067507	MN067491
Phlebopus marginatus	REH8883	FJ536645	FJ536678	*Sutorius ubonensis*	SV0203	MN067508	MN067492
Phlebopus portentosus	REH8795	FJ536647	FJ536680	*Sutorius obscuripellis*	OR0949	MN067510	MN067494
Gyrodon lividus	REG Gl1	GU187786	GU187701	*Tylopilus leucomycelinus*	JBSD127419	MN095209	
Porphyrellus porphyrosporus	MB97-023	GU187800	GU187734	*Tylopilus leucomycelinus*	JBSD127420	MN095210	
Boletus umbilicatus	HKAS:63126	JN205455		*Tylopilus sp.*	HKAS105251	MN304792	MN304798
Phylloporus maculatus	HKAS:59730	JQ678700	JQ967194	*Tylopilus sp.*	HKAS105252	MN304793	MN304799
Xerocomus magniporus	HKAS:59820	JQ678701	JQ967195	*Aureoboletus rubellus*	HKAS105266	MN304795	
Borofutus dhakanus	HKAS73789	JQ928597	JQ928576	*Aureoboletus rubellus*	HKAS105267	MN304796	
Borofutus dhakanus	HKAS73792	JQ928598	JQ928575	*Imleria floridana*	Franck_4234	MN584682	MN584685
Zangia roseola	HKAS52661	JQ928604	JQ928584	*Imleria floridana*	Franck_4235	MN584683	MN584686
Imleria obscurebrunnea	HKAS52557	KC215234	KC215243	*Exsudoporus ruber*	KUN-HKAS 106891	MT063120	MT063123
Imleria parva	HKAS59437	KC215237	KC215250	*Exsudoporus ruber*	KUN-HKAS 103513	MT063121	MT063124
Imleria parva	HKAS55341	KC215238	KC215251	*Retiboletus sp.*	OR0570	MT085479	MT085476
Imleria subalpina	HKAS74712	KC215239	KC215246	*Indoporus sp. YL-2020a*	HKAS107153	MT110409	MT110335
Imleria subalpina	HKAS56375	KC215240	KC215244	*Anthracoporus cystidiatus*	HKAS55375	MT110410	KT990816
Imleria obscurebrunnea	HKAS50477	KC215241	KC215245	*Tylopilus sp. YL-2020g*	HKAS106331	MT110413	MT110337
Porphyrellus holophaeus	HKAS:50508	KF112553	KF112244	*Porphyrellus griseus*	HKAS 82849	MT110414	
Neoboletus brunneissimus	HKAS:52660	KF112650	KF112143	*Porphyrellus orientifumosipes*	HKAS84710	MT110415	MT110339
Boletus sinensis	HKAS:76851	KF112651	KF112144	*Tylopilus otsuensis*	HKAS50240	MT110417	KT990753

Table B (continued)

Species	Bank note	RPB2	TEF1	Species	Bank note	RPB2	TEF1
Boletus magnificus	HKAS:74939	KF112653	KF112148	*Tylopilus argillaceus*	HKAS90201	MT110419	KT990783
Neoboletus magnificus	HKAS:74939	KF112653	KF112148	*Tylopilus sp. YL-2020e*	HKAS80605	MT110420	MT110344
Boletus magnificus	HKAS:54096	KF112654	KF112149	*Tylopilus atroviolaceobrunneus*	HKAS84351	MT110421	KT990819
Neoboletus magnificus	HKAS:54096	KF112654	KF112149	*Tylopilus sp.*	HKAS84693	MT110425	MT110352
Rubroboletus sinicus	HKAS:68620	KF112661	KF112146	*Tylopilus albopurpureus*	HKAS 88998	MT110426	MT110353
Lanmaoa flavorubra	NY775777	KF112681	KF112160	*Tylopilus himalayanus*	HKAS91278	MT110427	MT110354
Xerocomellus chrysenteron	HKAS:56494	KF112685	KF112172	*Boletus sinoaurantiacus*	HKAS89413	MT110428	MT110356
Xerocomellus cisalpinus	PDD94421	KF112686	KF112171	*Leccinellum griseum*	HKAS77060	MT110429	MT110358
Tylopilus alpinus	HKAS:55438	KF112687	KF112191	*Pseudoaustroboletus valens*	HKAS52602	MT110430	
Tylopilus brunneirubens	HKAS:53388	KF112688	KF112192	*Pseudoaustroboletus valens*	HKAS 82644	MT110431	MT110359
Retiboletus griseus	HKAS:63590	KF112691	KF112178	*Retiboletus pseudogriseus*	HKAS106467	MT110432	MT110361
Boletus edulis	HMJAU4637	KF112704	KF112202	*Austroboletus olivaceobrunneus*	HKAS 92428	MT110434	MT110363
Boletus rufoaureus	HKAS:59820	KF112709		*Mucilopilus cinnamomeus*	HKAS 59572	MT110435	
Boletus rufoaureus	HKAS:53424	KF112710	KF112206	*Mucilopilus ruber*	HKAS 84555	MT110436	MT110364
Crocinoboletus rufoaureus	HKAS53424	KF112710	KF112206	*Mucilopilus ruber*	HKAS84632	MT110437	MT110365
Pulveroboletus aff. ravenelii	HKAS 53351	KF112712	KF112261	*Veloporphyrellus alpinus*	KUN:HKAS68301	MT110438	JX984550
Pulveroboletus sp.	HKAS 74933	KF112713	KF112262	*Veloporphyrellus pseudovelatus*	KUN:HKAS52258	MT110439	JX984551
Leccinum extremiorientale	HKAS:63635	KF112720	KF112198	*Veloporphyrellus pseudovelatus*	KUN:HKAS59444	MT110440	JX984553
Leccinum monticola	HKAS:76669	KF112723	KF112249	*Veloporphyrellus castaneus*	HKAS 107147	MT110441	MT110366
Leccinum quercinum	HKAS:63502	KF112724	KF112250	*Veloporphyrellus castaneus*	Chen30640	MT110442	MT110367
Leccinum variicolor	HKAS:57758	KF112725	KF112251	*Fistulinella olivaceoalba*	HKAS59845	MT110443	MT110369
Leccinellum citrinum	HKAS:53427	KF112727	KF112253	*Hymenoboletus filiformis*	HKAS 82811	MT110446	MT110371

Table B (continued)

Species	Bank note	RPB2	TEF1	Species	Bank note	RPB2	TEF1
Leccinellum sp.	HKAS 53427	KF112727	KF112253	*Hymenoboletus sp. YL-2022c*	HKAS76988	MT110447	MT110372
Leccinellum aff. Crocipodium	HKAS 76658	KF112728	KF112252	*Hymenoboletus sp. YL-2020c*	HKAS77009	MT110448	MT110373
Rossbeevera yunnanensis	HKAS:70601	KF112729		*Hymenoboletus griseoviridis*	MHHNU_Chen30371	MT110449	MT110374
Tylocinum griseolum	HKAS:50281	KF112730	KF112284	*Harrya subalpina*	HKAS50546	MT110450	KT990879
Veloporphyrellus gracilioides	HKAS:53590	KF112734	KF112210	*Harrya chromapes*	HKAS59217	MT110451	HQ326864
Tylopilus plumbeoviolaceoides	HKAS50210	KF112738	KF112221	*Chiua virens*	HKAS50543	MT110452	KT990751
Tylopilus phaeoruber	HKAS 74925	KF112739	KF112222	*Heimioporus japonicus*	SV0016	MT136766	MT136771
Tylopilus aurantiacus	HKAS:59700	KF112740	KF112223	*Heimioporus japonicus*	SV0050	MT136767	MT136772
Aureoboletus gentilis	MG372a	KF112741	KF134014	*Tylopilus hayatae*	FCME 2013	MT164324	MT164321
Aureoboletus mirabilis	HKAS:57776	KF112743	KF112229	*Tylopilus hayatae*	UAEH 180	MT164325	MT164322
Aureoboletus moravicus	MG374a	KF112745	KF112232	*Retiboletus ornatipes*	MBsn	MT219515	MT219516
Boletellus aff. Shichianus	HKAS 56317	KF112753	KF112239	*Butyriboletus regius*	KUN-HKAS 84878	MT269661	MT269659
Aureoboletus longicollis	HKAS:53398	KF112755	KF112238	*Pulveroboletus fragrans*	SV455	MT468188	MT468187
Boletellus shichianus	HKAS:76852	KF112756	KF112237	*Fistulinella gloeocarpa*	BSD130769	MT590756	
Boletellus aff. emodensis	HKAS 52678	KF112757	KF112305	*Aureoboletus erythraeus*	FHMU1053	MT650124	MT650112
Boletellus ananas	NY796159	KF112760	KF112308	*Veloboletus limbatus*	REH9228	MT747397	MN413636
Boletus violaceofuscus	HKAS62900	KF112762	KF112219	*Phylloporus gajari*	OR1108	MT861162	MT861169
Austroboletus albovirescens	HKAS:59624	KF112765	KF112217	*Phylloporus gajari*	OR1184	MT861163	MT861171
Xerocomus punctilifer	HKAS:74744	KF112772	KF112285	*Austroboletus asper*	BRI:AQ0796265	MT928122	
Xerocomus punctilifer	HKAS:52269	KF112773	KF112286	*Tylopilus rubrotinctus*	KK259	MW165282	MW165264
Phylloporus rubrosquamosus	HKAS:52552	KF112780	KF112289	*Tylopilus griseolus*	Wu1847	MW165284	MW165266

Table B (continued)

Species	Bank note	RPB2	TEF1	Species	Bank note	RPB2	TEF1
Xerocomus magniporus	HKAS:58000	KF112781	KF112293	*Austroboletus subvirens*	Wu2027	MW165285	MW165262
Phylloporus luxiensis	HKAS:75077	KF112785	KF112298	*Tylopilus violaceorubrus*	Wu1956	MW165286	
Phylloporus imbricatus	HKAS:68642	KF112786	KF112299	*Royoungia coccineinana*	JLK645	MW165287	MW165271
Fistulinella olivaceoalba	HKAS:53367	KF112790	KF112304	*Hymenoboletus griseoviridis*	Zhao1557	MW165288	MW165270
Zangia erythrocephala	HKAS:75046	KF112791	KF112269	*Tylopilus rubrotinctus*	LF1101	MW165291	
Harrya chromapes	HKAS:50527	KF112792	KF112270	*Leccinum holopus*	Yang5972	MW439258	MW439266
Tylopilus virens	HKAS:76678	KF112793	KF112272	*Leccinum album*	Li1072	MW439260	MW439267
Chiua viridula	HKAS 74928	KF112794	KF112273	*Leccinum parascabrum*	Wu1784	MW439264	MW439271
Hymenoboletus luteopurpureus	HKAS:46334	KF112795	KF112271	*Leccinum parascabrum*	Li1700	MW439265	MW439272
Royoungia rubina	HKAS:53379	KF112796	KF112274	*Amoenoboletus granulopunctatus*	KUN-HKAS 86007	MW560079	MZ741478
Tylopilus otsuensis	HKAS:53401	KF112797	KF112224	*Amoenoboletus granulopunctatus*	HKAS80250	MW560080	MW566746
Tylopilus microsporus	HKAS:59661	KF112798	KF112225	*Amoenoboletus granulopunctatus*	MHHNU9490	MW560081	MW566747
Tylopilus violatinctus	HKAS:50208	KF112799	KF112283	*Imperator torosus*	MB000258	MW560082	MW566748
Buchwaldoboletus lignicola	HKAS:76674	KF112819	KF112277	*Cyanoboletus bessettei*	ARB1393A	MW737457	MW737482
Gyroporus castaneus	HKAS:63505	KF112826	KY419086	*Cyanoboletus bessettei*	ARB1393B	MW737458	MW737483
Gyroporus castaneus	HKAS:76672	KF112827	KF112311	*Cyanoboletus cyaneitinctus*	Farid_340	MW737461	
Boletus brunneissimus	HKAS:54618	KF739696	KF739772	*Lanmaoa sublurida*	Farid_343	MW737462	MW737486
Boletus brunneissimus	HKAS:57451	KF739702	KF739778	*Lanmaoa sublurida*	Farid_631	MW737464	MW737487
Boletus roseoflavus	HKAS:53405	KF739704	KF739780	*Cyanoboletus cyaneitinctus*	Farid_920	MW737465	
Boletus roseoflavus	HKAS:63593	KF739706	KF739782	*Pulchroboletus rubricitrinus*	Farid_335	MW737466	
Butyriboletus roseoflavus	HKAS63593	KF739706	KJ184571	*Aureoboletus pseudoauriporus*	JAB_320	MW737468	MW737489
Boletus roseoflavus	HKAS:63609	KF739707	KF739783	*Aureoboletus pseudoauriporus*	JAB_80	MW737471	MW737490

Table B (continued)

Species	Bank note	RPB2	TEF1	Species	Bank note	RPB2	TEF1
Rugiboletus brunneiporus	HKAS 83209	KM605168	KM605144	*Xerocomellus bolinii*	AB_95	MW737472	MW737491
Rugiboletus extremiorientalis	HKAS 76663	KM605170	KM605147	*Hortiboletus coccyginus*	JLF3093	MW737473	
Rugiboletus brunneiporus	HKAS 83210	KM605171	KM605145	*Xerocomellus atropurpureus*	JLF3620	MW737477	MW737495
Neoboletus brunneissimus	HKAS 57451	KM605172	KM605149	*Buchwaldoboletus xylophilus*	X.H. Deng2(FHMU5849)	MW820948	MW897339
Neoboletus brunneissimus	HKAS 50538	KM605173	KM605150	*Chalciporus vulparius*	N.K. Zeng4978(FHMU5554)	MW925936	MW925930
Lanmaoa asiatica	HKAS 54095	KM605174	KM605151	*Chalciporus vulparius*	N.K. Zeng4979(FHMU5560)	MW925937	MW925931
Lanmaoa asiatica	HKAS 63592	KM605175	KM605152	*Chalciporus hainanensis*	GDGM44464	MZ165604	MZ165612
Lanmaoa asiatica	HKAS:63603	KM605176	KM605153	*Chalciporus citrinoaurantius*	GDGM44717	MZ165607	MZ165616
Lanmaoa angustispora	HKAS 74752	KM605177	KM605154	*Chalciporus citrinoaurantius*	GDGM44776	MZ165608	MZ165617
Lanmaoa angustispora	HKAS 74759	KM605178	KM605155	*Chalciporus hainanensis*	GDGM46161	MZ165609	MZ165613
Baorangia pseudocalopus	HKAS5739	KM605179	KJ184570	*Cupreoboletus poikilochromus*	TUR-A 208926	MZ277222	MZ277233
Rubroboletus latisporus	HKAS:63517	KP055028	KP055019	*Cupreoboletus poikilochromus*	TUR-A 208927	MZ277223	
Rubroboletus latisporus	HKAS:80358	KP055029	KP055020	*Boletus flavosanguineus*	TUR-A 208905	MZ277231	MZ277239
Caloboletus calopus	BR5020159063805	KP055030	KJ184566	*Leccinum pseudoborneense*	Zhao776	MZ543308	MZ543306
Hourangia cheoi	Wu203	KP136981	KP136939	*Leccinum pseudoborneense*	Zhao773	MZ543309	MZ543307
Hourangia cheoi	Tang572	KP136985	KP136943	*Austroboletus yourkae*	NY02072669	MZ647701	
Austroboletus rarus	BRI:AQ0794045	KP242086		*Austroboletus yourkae*	BRI:AQ1024215	MZ647702	
Austroboletus rostrupii	BRI:AQ0795785	KP242089		*Austroboletus occidentalis*	Syme2082	MZ647703	

Table B (continued)

Species	Bank note	RPB2	TEF1	Species	Bank note	RPB2	TEF1
Austroboletus lacunosus	BRI:AQ0795787	KP242090		*Leccinum duriusculum*	Yang5971	MZ707779	MZ707785
Austroboletus rostrupii	BRI:AQ0807887	KP242092		*Leccinum melaneum*	FB491	MZ707780	MZ707786
Austroboletus lacunosus	BRI:AQ0795784	KP242095		*Leccinum versipelle*	LJW418	MZ707781	MZ707789
Austroboletus mutabilis	BRI:AQ0875885	KP242118		*Leccinum versipelle*	FB27	MZ707782	MZ707790
Austroboletus mutabilis	BRI:AQ0794618	KP242119		*Paxilloboletus latisporus*	ADK5072	MZ707870	MZ707866
Austroboletus asper	PERTH6658407	KP242126		*Paxilloboletus latisporus*	ADK5117	MZ707871	
Austroboletus austrovirens	BRI:AQ0794622	KP242132		*Paxilloboletus africanus*	ADK3703	MZ707874	
Austroboletus austrovirens	BRI:AQ0795791	KP242133		*Paxilloboletus africanus*	ADK5006	MZ707875	
Parvixerocomus pseudoaokii	HKAS 80480	KP658470		*Spongispora temasekensis*	CMF5	MZ824748	MZ803023
Retiboletus kauffmanii	G.Wu352	KP739299	KP739301	*Pseudoaustroboletus cf. valens*	OR0477	MZ824750	MZ803025
Phylloporus attenuatus	HKAS:76167	KR094786	KR094790	*Buchwaldoboletus hemichrysus*	FLAS-F-68320	MZ869818	MZ869813
Phylloporus attenuatus	HKAS:76168	KR094787	KR094791	*Buchwaldoboletus lignicola*	FLAS-F-58917	MZ869820	MZ869815
Nigroboletus roseonigrescens	ZT 13553	KT220594	KT220596	*Chalciporus piperatus*	MO334053	MZ869821	MZ869816
Aureoboletus formosus	GDGM44441	KT291751	KT291744	*Pseudoboletus parasiticus*	MES3141	MZ869822	MZ869817
Aureoboletus formosus	GDGM44444	KT291752	MK165833	*Hemileccinum albidum*	feng1359	MZ936322	MZ936360
Aureoboletus marroninus	GDGM43288	KT291753	KT291746	*Hemileccinum albidum*	Qin916	MZ936326	MZ936361
Aureoboletus tenuis	GDGM42601	KT291754	KT291745	*Hemileccinum brevisporum*	kuanzhao487	MZ936328	MZ936362
Afroboletus costatisporus	ADK4644	KT823991	KT824024	*Hemileccinum brevisporum*	cai334	MZ936329	MZ936363
Xerocomus cisalpinus	ADK4864	KT823993	KT824026	*Hemileccinum ferrugineipes*	LJW584	MZ936330	MZ973011
Aureoboletus gentilis	ADK4865	KT823994	KT824027	*Hemileccinum ferrugineipes*	WPM350	MZ936331	MZ973012
Rubinoboletus rubinus	AF2835	KT823995	KT824028	*Hemileccinum parvum*	wu1645	MZ936332	MZ973009
Chalciporus africanus	JD0517	KT823996	KT824029	*Hemileccinum parvum*	wu2299	MZ936333	MZ973010

Table B (continued)

Species	Bank note	RPB2	TEF1	Species	Bank note	RPB2	TEF1
Retiboletus griseus	MB03-079	KT823997	KT824030	*Boletellus cubensis*		MZ962254	
Retiboletus nigerrimus	OR049	KT824000	KT824033	*Boletus durhamensis*	1676394	MZ962255	
Phylloporus castanopsidis	OR052	KT824002	KT824035	*Neoboletus antillanus*	1	MZ962260	MZ962269
Boletus albobrunnescens	OR131	KT824006	KT824039	*Neoboletus antillanus*	2	MZ962261	MZ962270
Pulveroboletus fragrans	OR673	KT824010	KT824043	*Butyriboletus pseudoroseoflavus*	T274	OL739126	OL739124
Cyanoboletus pulverulentus	RW109	KT824013	KT824046	*Butyriboletus brunneoides*	BJTC FM688	OL771222	OL799251
Suillellus luridus	VDKO0241b	KT824014	KT824047	*Butyriboletus brunneoides*	BJTC FM1816	OL771223	OL799255
Rubroboletus satanas	VDKO0968	KT824019	KT824052	*Butyriboletus sinoregius*	BJTC FM755	OL771224	OL799252
Leccinellum crocipodium	VDKO1006	KT824021	KT824054	*Butyriboletus sinoregius*	BJTC FM1103	OL771225	OL799253
Leccinum schistophilum	VDKO1128	KT824022	KT824055	*Butyriboletus sinoregius*	BJTC FM1240	OL771226	OL799254
Royoungia coccineinana	HKAS68927	KT990347		*Exsudoporus floridanus*	FLAS-F-59069	OL960503	OL960496
Aureoboletus catenarius	HKAS54463	KT990348	KT990710	*Exsudoporus floridanus*	FLAS-F-61008	OL960504	OL960497
Aureoboletus catenarius	HKAS54467	KT990349	KT990711	*Exsudoporus frostii*	FLAS-F-60742	OL960506	OL960499
Aureoboletus duplicatoporus	HKAS63009	KT990350	KT990712	*Exsudoporus frostii*	iNat35326745	OL960507	OL960500
Aureoboletus duplicatoporus	HKAS83115	KT990351	KT990713	*Exsudoporus permagnificus*	AB B15-271	OL960509	
Aureoboletus tomentosus	HKAS59694	KT990352	KT990714	*Exsudoporus permagnificus*	MG829	OL960510	OL960502
Aureoboletus tomentosus	HKAS80485	KT990353	KT990715	*Brasilioporus olivaceoflavidus*	VIES 9901322	OM160576	OM160555
Aureoboletus nephrosporus	HKAS67931	KT990357	KT990720	*Brasilioporus simoniarum*	VIES 9901327	OM160577	OM160557
Aureoboletus nephrosporus	HKAS74929	KT990358	KT990721	*Butyriboletus subregius*	T95	OM285109	OM285111
Aureoboletus tenuis	HKAS75104	KT990359	KT990722	*Butyriboletus subregius*	T198	OM285110	OM285112
Aureoboletus viscidipes	HKAS77103	KT990360	KT990723	*Suillellus lacrymibasidiatus*	w3229	OM285114	OM285116
Aureoboletus yunnanensis	HKAS75050	KT990361	KT990724	*Suillellus lacrymibasidiatus*	w3194	OM285115	OM285117

Table B (continued)

Species	Bank note	RPB2	TEF1	Species	Bank note	RPB2	TEF1
Aureoboletus zangii	HKAS74751	KT990362	KT990725	*Retiboletus ater*	li1215	ON004079	MT010621
Aureoboletus zangii	HKAS74766	KT990363	KT990726	*Retiboletus ornatipes*	Halling10163	ON004084	MT010626
Aureoboletus thibetanus	HKAS57692	KT990365	KT990728	*Retiboletus sinogriseus*	qin449	ON004089	ON055263
Aureoboletus thibetanus	HKAS89494	KT990366	KT990729	*Retiboletus zhangfeii*	Wu1651	ON004094	ON055266
Boletellus indistinctus	HKAS80681	KT990368	KT990734	*Retiboletus pseudogriseus*	Zeng647	ON004096	MT010623
Boletellus indistinctus	HKAS90215	KT990369	KT990735	*Boletellus wenshanensis*	532624MF_103_Wu2281	ON007375	ON007378
Boletellus obscurococcineus	HKAS77662	KT990372		*Boletellus putuoensis*	FHMU6907	ON155834	ON155822
Boletus botryoides	HKAS53403	KT990375	KT990738	*Boletellus putuoensis*	FHMU6959	ON155835	
Boletus reticuloceps	HKAS51232	KT990376	KT990739	*Boletellus brunoflavus*	GDGM87994	ON390838	ON390826
Butyriboletus subsplendidus	HKAS50444	KT990379	KT990742	*Boletellus brunoflavus*	B21061253	ON390839	ON390828
Butyriboletus pseudospeciosus	HKAS63513	KT990380	KT990743	*Boletus littoreus*	FHMU5921	ON494595	ON505822
Butyriboletus pseudospeciosus	HKAS63596	KT990381	KT990744	*Boletus littoreus*	FHMU5919	ON494596	ON505823
Tylopilus porphyrosporus	HKAS48585	KT990382	KT990745	*Harrya moniliformis*	KD 22-034	OP688418	
Tylopilus porphyrosporus	HKAS49182	KT990383	KT990746	*Villoboletus persicinus*	BJTC FM1904	OP792033	OP792036
Tylopilus felleus	HKAS90203	KT990384	KT990747	*Villoboletus persicinus*	BJTC FM1906	OP792034	OP792037
Mucilopilus castaneiceps	HKAS71039	KT990385	KT990748	*Tropicoboletus ruborculus*	JBSD133074 (ANGE1406)	OQ117431	OQ110624
Porphyrellus castaneus	HKAS63076	KT990386	KT990749	*Tropicoboletus ruborculus*	MO439745-komille277	OQ117432	OQ110625
Tylocinum griseolum	HKAS50209	KT990388		*Xerocomus coccolobae*	JBSD133068	OQ117435	OQ110627
Abtylopilus scabrosus	HKAS50211	KT990389	KT990752	*Xerocomus coccolobae*	JBSD133069	OQ117436	OQ110628
Chiua angusticystidiata	HKAS50282	KT990390	KT990754	*Acyanoboletus controversus*	HKAS126560	OQ873490	OQ873451
Mucilopilus castaneiceps	HKAS50338	KT990391	KT990755	*Acyanoboletus controversus*	HKAS101248		OQ873452

Table B (continued)

Species	Bank note	RPB2	TEF1	Species	Bank note	RPB2	TEF1
Chiua virens	HKAS49445	KT990393	KT990757	*Acyanoboletus dissimilis*	ZT14030	OQ873492	OQ873453
Chiua viridula	MHHNU7346	KT990394		*Cyanoboletus fagaceophilus*	HKAS126556	OQ873494	OQ873455
Caloboletus yunnanensis	HKAS63040	KT990395	KJ619471	*Cyanoboletus fagaceophilus*	HKAS80691	OQ873495	OQ873456
Caloboletus yunnanensis	HKAS69214	KT990396	KJ184568	*Neoboletus brunneorubrocarpus*	HKAS126559	OQ873496	OQ873457
Chalciporus piperatus	HKAS84882	KT990397	KT990758	*Rubroboletus flavus*	HKAS90906	OQ873497	OQ873459
Chalciporus rubinelloides	HKAS57362	KT990398	KT990759	*Rubroboletus serpentiformis*	HKAS126557	OQ873498	OQ873460
Chalciporus rubinelloides	HKAS58728	KT990399	KT990760	*Rubroboletus serpentiformis*	HKAS126547	OQ873499	OQ873461
Chalciporus rubinelloides	HKAS74952	KT990400	KT990761	*Suillellus flaviporus*	HKAS126554	OQ873502	OQ873464
Cyanoboletus brunneoruber	HKAS80579-1	KT990401	KT990763	*Suillellus flaviporus*	HKAS126555	OQ873503	OQ873465
Cyanoboletus brunneoruber	HKAS80579-2	KT990402	KT990764	*Suillellus pinophilus*	HKAS126550	OQ873504	OQ873466
Gymnogaster boletoides	NY01194009	KT990406	KT990768	*Suillellus yunnanensis*	HKAS126548	OQ873505	OQ873467
Heimioporus subretisporus	HKAS80581	KT990407	KT990769	*Suillellus yunnanensis*	HKAS126549	OQ873506	OQ873468
Heimioporus subretisporus	HKAS80582	KT990409	KT990770	*Hongoboletus ventricosus*	TNS-F-44611	OQ873507	
Xerocomus impolitus	HKAS84869	KT990410	KT990771	*Hongoboletus ventricosus*	TNS-F-44612	OQ873508	
Hemileccinum rugosum	HKAS84970	KT990412	KT990773	*Paxillus vernalis*	AFTOL-ID 715		DQ457629
Hemileccinum rugosum	HKAS84355	KT990413	KT990774	*Paxillus filamentosus*	REG Pf1		GU187736
Hortiboletus amygdalinus	HKAS54242	KT990415	KT990776	*Leccinum album*	HKAS53417		HQ326861
Hortiboletus amygdalinus	HKAS54166	KT990416	KT990777	*Leccinum manzanitae*	HKAS51277		HQ326862
Hortiboletus subpaludosus	HKAS52659	KT990417	KT990778	*Tylopilus felleus*	HKAS54926		HQ326866
Hortiboletus subpaludosus	HKAS68158	KT990418	KT990779	*Tylopilus violatinctus*	HKAS50279		HQ326868
Leccinellum cremeum	HKAS90639	KT990420	KT990781	*Tylopilus neofelleus*	HKAS50319		HQ326869
Leccinellum sp.	HKAS 53410	KT990421		*Zangia citrina*	HKAS52677		HQ326871

Table B (continued)

Species	Bank note	RPB2	TEF1	Species	Bank note	RPB2	TEF1
Leccinum scabrum	HKAS53604	KT990422		*Zangia citrina*	HKAS52684		HQ326872
Leccinum scabrum	HKAS56371	KT990423	KT990782	*Zangia olivacea*	HKAS45445		HQ326873
Tylopilus argillaceus	HKAS90186	KT990424	KT990784	*Zangia olivacea*	HKAS55830		HQ326874
Tylopilus balloui	HKAS51151	KT990425		*Zangia olivaceobrunnea*	HKAS52275		HQ326875
Harrya sp.	HKAS 51181	KT990426	KT990785	*Zangia olivaceobrunnea*	HKAS52272		HQ326876
Royoungia reticulata	HKAS52253	KT990427	KT990786	*Zangia roseola*	HKAS52649		HQ326878
Chiua olivaceoreticulata	HKAS59706	KT990428	KT990787	*Octaviania japonimontana*	KPM-NC-0017810		JN378427
Royoungia reticulata	HKAS59704	KT990429		*Octaviania japonimontana*	KPM-NC-0017812		JN378428
Neoboletus ferrugineus	HKAS77617	KT990430	KT990788	*Rossbeevera vittatispora*	OSC61484 (Trappe 16856)		JN378446
Neoboletus ferrugineus	HKAS77718	KT990431	KT990789	*Leccinum vulpinum*	KPM-NC-0017834		JN378456
Neoboletus hainanensis	HKAS74880	KT990432	KT990790	*Austroboletus subvirens*	KPM-NC-0017836		JN378458
Neoboletus obscureumbrinus	HKAS63498	KT990433	KT990791	*Solioccasus polychromus*	R.E. Halling 9417		JQ287644
Neoboletus obscureumbrinus	HKAS77774	KT990434	KT990792	*Tylopilus ferrugineus*	MB06-053		JQ327016
Neoboletus obscureumbrinus	HKAS89014	KT990435	KT990793	*Boletus inedulis*	MB06-044		JQ327020
Neoboletus rubriporus	HKAS83026	KT990437	KT990795	*Boletus bicolor*	2858		JQ327021
Neoboletus rubriporus	HKAS89174	KT990438	KT990796	*Boletus bicolor var. borealis*	2858		JQ327021
Neoboletus sanguineoides	HKAS57766	KT990440	KT990799	*Neoboletus luridiformis*	AT2001087		JQ327023
Neoboletus sanguineoides	HKAS74733	KT990441	KT990800	*Boletus amygdalinus*	112605ba		JQ327024
Neoboletus sanguineus	HKAS80823	KT990442	KT990802	*Boletus peckii*	3959		JQ327026
Neoboletus sanguineus	HKAS80849	KT990443	KT990803	*Phylloporus pelletieri*	Pp1		JQ327036
Neoboletus tomentulosus	HKAS77614	KT990445	KT990805	*Leccinum sp.*	MB06-040		JQ327038

Table B (continued)

Species	Bank note	RPB2	TEF1	Species	Bank note	RPB2	TEF1
Neoboletus tomentulosus	HKAS77656	KT990446	KT990806	*Phylloporus brunneiceps*	HKAS 59551		JQ967156
Neoboletus venenatus	HKAS63535	KT990448	KT990807	*Phylloporus brunneiceps*	HKAS 59726		JQ967157
Neoboletus hainanensis	HKAS63515	KT990449	KT990808	*Phylloporus imbricatus*	HKAS 54861		JQ967162
Neoboletus hainanensis	HKAS90209	KT990450	KT990809	*Phylloporus luxiensis*	HKAS 57036		JQ967164
Pulveroboletus aff. ravenelii	HKAS50203	KT990451	KT990810	*Phylloporus maculatus*	HKAS 56683		JQ967167
Pulveroboletus macrosporus	HKAS59530	KT990452	KT990811	*Phylloporus pachycystidiatus*	HKAS 54540		JQ967168
Pulveroboletus macrosporus	HKAS57628	KT990453	KT990812	*Phylloporus pachycystidiatus*	HKAS 54541		JQ967169
Pulveroboletus sp.	HKAS52615	KT990454	KT990813	*Phylloporus parvisporus*	HKAS 59725		JQ967170
Pulveroboletus sp.	HKAS55369	KT990455	KT990814	*Phylloporus parvisporus*	HKAS 54768		JQ967171
Pulveroboletus sp.	HKAS74926	KT990456	KT990815	*Phylloporus rubeolus*	HKAS 52573		JQ967172
Tylopilus obscureviolaceus	HKAS90202	KT990457	KT990817	*Phylloporus rubeolus*	HKAS 54543		JQ967174
Tylopilus griseipurpureus	HKAS90200	KT990458	KT990818	*Phylloporus rubrosquamosus*	HKAS 54559		JQ967175
Anthracoporus nigropurpureus	HKAS52685	KT990459	KT990821	*Phylloporus rufescens*	HKAS 59722		JQ967176
Anthracoporus nigropurpureus	HKAS53370	KT990460	KT990822	*Phylloporus rufescens*	HKAS 59723		JQ967177
Porphyrellus orientifumosipes	HKAS53372	KT990461	KT990823	*Phylloporus yunnanensis*	HKAS 56999		JQ967180
Retiboletus nigerrimus	HKAS53418	KT990462	KT990824	*Phylloporus yunnanensis*	HKAS 58673		JQ967181
Harrya alpina	HKAS 52820	KT990463	KT990826	*Gymnogaster boletoides*	REH9455		JX889683
Retiboletus sinensis	HKAS59832	KT990464	KT990827	*Tylopilus balloui*	REH9467		JX889686
Retiboletus kauffmanii	HKAS63584	KT990465	KT990828	*Tylopilus cyanogranulifer*	REH9508		JX889688
Retiboletus fuscus	HKAS63624	KT990466	KT990829	*Tylopilus cyanogranulifer*	REH9527		JX889689
Retiboletus fuscus	HKAS74756	KT990467	KT990830	*Tylopilus propriorichromapes*	REH9445		JX889693
Rubroboletus rhodoxanthus	HKAS84879	KT990468	KT990831	*Royoungia boletoides*	Trappe 27456		JX889696

Table B (continued)

Species	Bank note	RPB2	TEF1	Species	Bank note	RPB2	TEF1
Rugiboletus extremiorientalis	HKAS74754	KT990469	KT990832	*Harrya atriceps*	REH7403		JX889702
Strobilomyces atrosquamosus	HKAS78563	KT990470	KT990833	*Austroboletus lacunosus*	REH9146		JX889709
Strobilomyces seminudus	HKAS80400	KT990471	KT990834	*Royoungia boletoides*	REH8851		JX889710
Strobilomyces seminudus	HKAS82848	KT990472	KT990835	*Tylopilus queenslandianus*	TWO1096		JX889711
Strobilomyces strobilaceus	WU0016537	KT990474	KT990837	*Austroboletus fusisporus*	HKAS75207		JX889718
Strobilomyces verruculosus	HKAS59637	KT990475	KT990838	*Veloporphyrellus alpinus*	KUN:HKAS57490		JX984549
Suillellus amygdalinus	NY00035656	KT990477	KT990840	*Veloporphyrellus velatus*	KUN:HKAS63668		JX984554
Suillellus subamygdalinus	HKAS53641	KT990478	KT990841	*Veloporphyrellus conicus*	CFMR:BZ1670		JX984555
Suillellus subamygdalinus	HKAS74745	KT990479	KT990843	*Xerocomus badius*	HKAS74714		KC215242
Tengioboletus glutinosus	HKAS53452	KT990480	KT990844	*Xerocomus subtomentosus*	KM168813		KC215249
Tengioboletus reticulatus	HKAS52241	KT990481	KT990845	*Rossbeevera westraliensis*	MEL2219011		KC552066
Tengioboletus reticulatus	HKAS53453	KT990482	KT990846	*Rossbeevera westraliensis*	MEL2322708		KC552067
Xanthoconium affine var. maculosum	NY01193907	KT990485	KT990849	*Rossbeevera eucyanea*	KPM-NC-0018043		KC552071
Xanthoconium affine	NY00815399	KT990486	KT990850	*Rossbeevera griseovelutina*	TNS-F-36992		KC552075
Xanthoconium porophyllum	HKAS90217	KT990487	KT990851	*Rossbeevera griseovelutina*	TNS-F-36991		KC552077
Xanthoconium sinense	HKAS77651	KT990488	KT990853	*Rossbeevera paracyanea*	KPM-NC-0017847		KC552078
Xanthoconium sinense	HKAS77758	KT990489	KT990854	*Rossbeevera paracyanea*	KPM-NC-0017848		KC552079
Xanthoconium sinense	HKAS80118	KT990490	KT990855	*Rossbeevera yunnanensis*	KPM-NC-0017850		KC552080
Xerocomus subparvus	HKAS50295	KT990491		*Turmalinea persicina*	KPM-NC-0018007		KC552087
Xerocomellus corneri	HKAS52503	KT990492	KT990856	*Turmalinea persicina*	KPM-NC-0018008		KC552088
Xerocomellus corneri	HKAS90206	KT990493	KT990857	*Turmalinea yuwanensis*	KPM-NC-0018011		KC552089
Xerocomellus communis	HKAS50467	KT990494	KT990858	*Turmalinea mesomorpha*	KPM-NC-0018014		KC552091

Table B (continued)

Species	Bank note	RPB2	TEF1	Species	Bank note	RPB2	TEF1
Xerocomellus communis	HKAS68204	KT990495	KT990859	*Turmalinea mesomorpha*	KPM-NC-0018015		KC552092
Xerocomus subparvus	HKAS82184	KT990496	KT990866	*Austroboletus niveus*	MEL2053830		KC552099
Xerocomus fraternus	HKAS55328	KT990497	KT990869	*Austroboletus occidentalis*	MEL2300518		KC552100
Harrya atrogrisea	HKAS50542	KT990499	KT990880	*Aureoboletus innixus*	MB03-104		KF030400
Harrya moniliformis	HKAS49627	KT990500	KT990881	*Boletus abruptibulbus*	4588		KF030401
Harrya subalpina	HKAS52809	KT990501	KT990882	*Aureoboletus roxanae*	DS626-07		KF030402
Porphyrellus castaneus	HKAS52554	KT990502	KT990883	*Boletus bicolor*	MB07-001		KF030405
Tylopilus violaceobrunneus	HKAS89443	KT990504	KT990886	*Boletus rufomaculatus*	4414		KF030406
Sutorius eximius	HKAS59657	KT990505	KT990887	*Lanmaoa pseudosensibilis*	DS615-07		KF030407
Anthracoporus holophaeus	HKAS59407	KT990506	KT990888	*Boletus pulchriceps*	DS 4514		KF030409
Porphyrellus holophaeus	HKAS59407	KT990506	KT990888	*Rubroboletus rhodosanguineus*	4252		KF030412
Tylopilus brunneirubens	HKAS59664	KT990507	MT110349	*Rubroboletus dupainii*	JAM0607		KF030413
Pulveroboletus ravenelii	REH2565	KU665637	KU665636	*Xerocomellus atropurpureus*	NY1193858		KF030416
Butyriboletus hainanensis	S.D.Yang112	KU961657	KU961655	*Xerocomellus cisalpinus*	AT2005034		KF030417
Butyriboletus hainanensis	N.K.Zeng1197	KU961658		*Boletus pulverulentus*	9606		KF030418
Xerocomus puniceiporus	HKAS 80683	KU974146	KU974138	*Bothia castanella*	MB03-053		KF030421
Pulveroboletus icterinus	N.K.Zeng1561	KX453838	KX453846	*Xerocomus badius*	MB03-098a		KF030423
Pulveroboletus subrufus	N.K.Zeng1857	KX453841	KX453855	*Imleria pallida*	179/97		KF030424
Butyriboletus hainanensis	N.K.Zeng2418	KX453856	KU961656	*Boletus mottiae*	NY:00705247		KF030426
Strobilomyces alpinus	HKAS77969	KX869380	KX869254	*Boletus subalpinus*	27882		KF030427
Strobilomyces alpinus	HKAS94051	KX869381	KX869255	*Xanthoconium stramineum*	3518		KF030428
Strobilomyces atrosquamosus	HKAS84682	KX869387	KX869261	*Tylopilus badiceps*	78206		KF030429

Table B (continued)

Species	Bank note	RPB2	TEF1	Species	Bank note	RPB2	TEF1
Strobilomyces brunneolepidotus	HKAS84683	KX869390	KX869264	*Boletus semigastroideus*	PBM3076		KF030430
Strobilomyces brunneolepidotus	HKAS81935	KX869391	KX869265	*Boletus separans*	DPL2704		KF030431
Strobilomyces confusus	WU17132	KX869393	KX869267	*Boletellus chrysenteroides*	3838		KF030432
Strobilomyces confusus	WU17130	KX869394	KX869268	*Boletus morrisii*	8206		KF030433
Strobilomyces echinatus	PC0723576	KX869396	KX869270	*Xerocomus tenax*	REH6871		KF030437
Strobilomyces echinatus	Sydney778	KX869397	KX869271	*Xerocomus perplexus*	MB00-005		KF030438
Strobilomyces echinocephalus	HKAS59420	KX869400	KX869274	*Tylopilus plumbeoviolaceus*	MB06-056		KF030439
Strobilomyces foveatus	FRI69468	KX869402	KX869276	*Chalciporus amarellus*	DS4640-3		KF030440
Strobilomyces foveatus	FRI62957	KX869403	KX869277	*Chalciporus pseudorubinellus*	4302		KF030441
Strobilomyces glabellus	HKAS74887	KX869404	KX869278	*Paxillus obscurosporus*	Po1		KF030442
Strobilomyces glabriceps	HKAS74755	KX869408	KX869282	*Pseudoboletus parasiticus*	Xpa1		KF030443
Strobilomyces glabriceps	HKAS67811	KX869409	KX869283	*Anthracoporus holophaeus*	HKAS:74894		KF112245
Strobilomyces latirimosus	HKAS74865	KX869410	KX869284	*Parvixerocomus aokii*	HKAS:59812		KF112266
Strobilomyces latirimosus	HKAS53348	KX869415	KX869289	*Octaviania durianelloides*	KPM-NC0017829		KJ001079
Strobilomyces mirandus	HKAS59408	KX869419	KX869293	*Turmalinea yuwanensis*	KPM-NC0023377		KJ001083
Strobilomyces mollis	HKAS59833	KX869422	KX869295	*Boletus pseudocalopus*	HKAS75739		KJ184570
Strobilomyces montosus	HKAS74809	KX869423	KX869296	*Caloboletus firmus*	NY00796115		KJ619464
Strobilomyces montosus	HKAS74910	KX869424	KX869297	*Caloboletus panniformis*	HKAS77530		KJ619469
Strobilomyces parvirimosus	HKAS74911	KX869428	KX869301	*Boletus sinicus*	HKAS56304		KJ619483
Strobilomyces parvirimosus	HKAS74547	KX869429	KX869302	*Pulchroboletus roseoalbidus*	AMB 12757		KJ729512
Strobilomyces pteroreticulosporus	HKAS91274	KX869433	KX869306	*Alessioporus ichnusanus*	AMB 12756		KJ729513
Strobilomyces strobilaceus	HKAS95079	KX869444	KX869317	*Bothia fujianensis*	HKAS82694		KM272860

Table B (continued)

Species	Bank note	RPB2	TEF1	Species	Bank note	RPB2	TEF1
Strobilomyces subnudus	HKAS59435	KX869445	KX869318	*Boletus durhamensis*	CFMR:Both 4561		KM668212
Strobilomyces subnudus	HKAS82418	KX869448	KX869321	*Rossbeevera cryptocyanea*	KPM-NC0023928		KP222914
Strobilomyces velutinus	HKAS84755	KX869449	KX869322	*Lanmaoa roseocrispans*	ARB92-10		KP327616
Strobilomyces velutinus	HKAS84776	KX869450	KX869323	*Boletellus deceptivus*	REH9634		KP327672
Strobilomyces velutipes	NY1034411	KX869452	KX869325	*Boletellus elatus*	TMI22101		KP327673
Strobilomyces velutipes	NY1034409	KX869453	KX869326	*Boletellus elatus*	06-204NR		KP327674
Strobilomyces verruculosus	HMAS261688	KX869457		*Aureoboletus projectellus*	NYBG13392		KP327675
Strobilomyces anthracinus	HKAS74532	KX869459	KX869330	*Heimioporus mandarinus*	FRIM4636		KP327677
Strobilomyces anthracinus	HKAS52570	KX869460	KX869331	*Boletellus russellii*	MEN11-031		KP327678
Strobilomyces cingulatus	HKAS73175	KX869461	KX869332	*Heimioporus ivoryi*	REH8620		KP327683
Strobilomyces cingulatus	HKAS75582	KX869463	KX869334	*Boletellus emodensis*	REH8742		KP327686
Strobilomyces microreticulatus	HKAS74963	KX869465	KX869336	*Heimioporus mandarinus*	REH8785		KP327688
Strobilomyces microreticulatus	HKAS74863	KX869466	KX869337	*Boletellus areolatus*	NY817443		KP327689
Strobilomyces albidus	HKAS89104	KX869469	KX869340	*Boletellus squamosus*	NY817440		KP327690
Strobilomyces albidus	HKAS74924	KX869470	KX869341	*Boletellus emodensis*	REH8904		KP327691
Strobilomyces douformis	HKAS87097	KX869474	KX869345	*Boletellus badiovinosus*	REH8923		KP327693
Strobilomyces douformis	HKAS87134	KX869475	KX869346	*Heimioporus fruticicola*	REH8958		KP327695
Strobilomyces pinophilus	HKAS80300	KX869479	KX869350	*Heimioporus fruticicola*	REH8962		KP327696
Strobilomyces pinophilus	HKAS94132	KX869480	KX869351	*Boletellus deceptivus*	REH9017		KP327697
Strobilomyces densisquamosus	HKAS82354	KX869481	KX869352	*Boletellus sinapipes*	REH9018		KP327698
Strobilomyces densisquamosus	HKAS84945	KX869482	KX869353	*Boletellus obscurococcineus*	REH9038		KP327700
Strobilomyces calidus	HKAS87084	KX869487	KX869358	*Boletellus obscurococcineus*	REH9061		KP327701

Table B (continued)

Species	Bank note	RPB2	TEF1	Species	Bank note	RPB2	TEF1
Strobilomyces calidus	HKAS84700	KX869488	KX869359	*Boletellus reminiscens*	REH9284		KP327702
Boletus reticuloceps	HKAS55431	KX869508	KX869379	*Heimioporus australis*	REH9288		KP327703
Aureoboletus quercus-spinosae	GDGM43758	KY039959	MK165837	*Boletellus sinapipes*	REH9408		KP327704
Aureoboletus quercus-spinosae	GDGM43786	KY039960	MK165838	*Boletellus ananiceps*	REH9484		KP327705
Rubroboletus legaliae	MB-000295	KY272134	KY272137	*Boletellus dissiliens*	REH9624		KP327706
Rubroboletus esculentus	K.Zhao893	KY272135	KY272138	*Boletellus dissiliens*	REH9688		KP327707
Rubroboletus esculentus	Hui M.Shao-F1	KY272136	KY272139	*Aureoboletus mirabilis*	REH9765		KP327709
Butyriboletus roseoflavus	HKAS:54099	KY419036	KF739779	*Heimioporus cooloolae*	REH9817		KP327710
Caloboletus panniformis	HKAS57410	KY419037	KJ184567	*Heimioporus cooloolae*	REH9852		KP327711
Afroboletus luteolus	Yorou 3071	KY553123	KY553133	*Boletellus ananiceps*	3794		KP327712
Afroboletus luteolus	Yorou 4599	KY553125	KY553135	*Retiboletus sinensis*	HKAS83955		KP739302
Afroboletus multijugus	PC 0723578	KY553127	KY553137	*Retiboletus zhangfeii*	HKAS83962		KP739306
Afroboletus multijugus	PC 0723572	KY553128	KY553138	*Aureoboletus clavatus*	HKAS59802		KR052053
Strobilomyces echinocephalus	HKAS 78560	KY553129	KY553140	*Aureoboletus clavatus*	GDGM42984		KR052055
Strobilomyces mirandus	HKAS 84701	KY553130	KY553142	*Phylloporus catenulatus*	HKAS:76156		KR094788
Strobilomyces pteroreticulosporus	HKAS 81881	KY553131	KY553143	*Phylloporus catenulatus*	HKAS:76157		KR094789
Guyanaporus albipodus	Henkel 8848	LC043083		*Butyriboletus appendiculatus*	MB000286		KT002634
Singerocomus inundabilis	Henkel 9199	LC043089		*Butyriboletus brunneus*	NY00013631		KT002635
Singerocomus inundabilis	Aime 4004	LC043092		*Butyriboletus pseudoregius*	BR50201533559-51		KT002638
Costatisporus cyanescens	Henkel 9061	LC053664		*Boletus pulchriceps*	R. Chapman 0945		KT002639
Boletus edulis	TZ12	LN714632		*Butyriboletus regius*	MB000287		KT002640
Pulchroboletus sclerotiorum	FLAS-F-60334	MF614164	MF614165	*Boletus roseopurpureus*	E.E. Both 3765		KT002641

Table B (continued)

Species	Bank note	RPB2	TEF1	Species	Bank note	RPB2	TEF1
Pulchroboletus sclerotiorum	FLAS-F-60333	MF614169	MF614167	*Butyriboletus subappendiculatus*	MB000260		KT002642
Heimioporus gaojiaocong	N.K. Zeng2138	MF962423		*Butyriboletus yicibus*	HKAS68010		KT002643
Aureoboletus moravicus	VDKO1120	MG212615	MG212573	*Butyriboletus yicibus*	HKAS 57503		KT002644
Boletus aereus	VDKO1055	MG212617	MG212575	*Nigroboletus roseonigrescens*	GDGM 43238		KT220595
Butyriboletus appendiculatus	VDKO0193b	MG212624	MG212582	*Boletellus aff. emodensis*	HKAS50223		KT990731
Butyriboletus pseudoregius	VDKO0925	MG212625	MG212583	*Tylocinum griseolum*	HKAS52612		KT990825
Fistulinella prunicolor	REH9502	MG212630	MG212588	*Xanthoconium purpureum*	NY00720964		KT990852
Hemileccinum depilatum	AF2845	MG212633	MG212591	*Xerocomus fulvipes*	HKAS52556		KT990860
Xerocomus depilatus	AF2845	MG212633	MG212591	*Xerocomus velutinus*	HKAS68135		KT990861
Xerocomus impolitus	ADK4078	MG212634	MG212592	*Xerocomus sp*	HKAS57339		KT990862
Leccinum roseofractum	VDKO0938	MG212635	MG212593	*Xerocomus sp*	HKAS57765		KT990863
Leccinum variicolor	VDKO0844	MG212636	MG212594	*Xerocomus microcapoides*	HKAS53374		KT990867
Sutorius junquilleus	AF2922	MG212638	MG212596	*Xerocomus microcapoides*	HKAS54753		KT990868
Parvixerocomus pseudoaokii	OR0155	MG212639	MG212597	*Xerocomus fraternus*	HKAS52526		KT990870
Boletus kauffmanii	OR0278	MG212643	MG212601	*Xerocomus piceicola*	HKAS76492		KT990872
Rhodactina rostratispora	SV170	MG212645	MG212605	*Xerocomus rugosellus*	HKAS68292		KT990873
Rhodactina rostratispora	SV208	MG212646	MG212606	*Xerocomus subparvus*	HKAS55384		KT990874
Spongiforma thailandica	DED 7873	MG212648	KF030436	*Xerocomus yunnanensis*	HKAS68420		KT990877
Sutorius eximius	REH9400	MG212653	JQ327029	*Xerocomus yunnanensis*	HKAS68282		KT990878
Tylopilus vinaceipallidus	OR0137	MG212656	MG212613	*Chiua olivaceoreticulata*	HKAS59676		KT990884
Xerocomus subtomentosus	VDKO0987	MG212657	MG212614	*Boletus sinoedulis*	BTH1_H1		KU518947

Table B (continued)

Species	Bank note	RPB2	TEF1	Species	Bank note	RPB2	TEF1
Caloboletus inedulis	BOTH3963	MG897434	MG897424	*Boletus sinoedulis*	BTH1_H2		KU518948
Baorangia rufomaculata	BOTH4144	MG897435	MG897425	*Boletus viscidiceps*	HKAS57435		KU518950
Rubroboletus rhodosanguineus	BOTH4263	MG897436	MG897426	*Pulveroboletus flaviscabrosus*	HKAS82616		KX453842
Lanmaoa pallidorosea	BOTH4432	MG897437	MG897427	*Pulveroboletus flaviscabrosus*	HKAS 83190		KX453843
Boletus roseopurpureus	BOTH4497	MG897438	MG897428	*Pulveroboletus icterinus*	N.K.Zeng2573		KX453849
Lanmaoa carminipes	BOTH4591	MG897439	MG897429	*Pulveroboletus ridleyi*	N.K.Zeng555		KX453850
Pulveroboletus brunneopunctatus	OR0147	MG897440	MG897430	*Pulveroboletus ridleyi*	N.K.Zeng852		KX453851
Baorangia major	OR0404	MG897442	MG897432	*Pulveroboletus subrufus*	HKAS84926		KX453854
Baorangia major	OR0486	MG897443	MG897433	*Afrocastellanoa ivoryana*	Arora 126		KX685715
Spongispora temasekensis	SING 0206334	MG979394	MG979392	*Heliogaster columellifer*	KPM-NC 23012		KX685718
Erythrophylloporus cinnabarinus	GDGM44440	MH374033	MH378801	*Xanthoconium fusciceps*	N.K.Zeng2483		KY271046
Erythrophylloporus cinnabarinus	GDGM70536	MH374035	MH378802	*Baorangia pseudocalopus*	HKAS:63607		KY419085
Strobilomyces rubrobrunneus	HKAS:101906	MH485369	MH485372	*Caloboletus xiangtoushanensis*	GDGM44833		KY800418
Strobilomyces rubrobrunneus	HKAS:101905	MH485370		*Caloboletus xiangtoushanensis*	GDGM45160		KY800419
Phylloporus bellus	OR0473	MH580818	MH580798	*Rubroboletus legaliae*	PRM 921886		LT797168
Phylloporus castanopsidis	BC074	MH580819	MH580799	*Heimioporus gaojiaocong*	N.K. Zeng2864		MF962414
Phylloporus pelletieri	WU18746	MH580821	MH580801	*Cyanoboletus instabilis*	N.K.Zeng2862		MG030478
Phylloporus rhodoxanthus	WU17978	MH580824	MH580805	*Lanmaoa rubriceps*	N.K.Zeng2773		MG030479
Phylloporus rubiginosus	BC063	MH580826	MH580807	*Rhodactina himalayensis*	CMU25117		MG212603
Phylloporus rubiginosus	OR0169	MH580827	MH580808	*Tylopilus callainus*	N.K.Zeng1460		MG365904
Phylloporus subbacillisporus	OR0436	MH580831	MH580812	*Tylopilus callainus*	N.K.Zeng1464		MG365904
Phylloporus subrubeolus	BC022	MH580832	MH580813	*Boletellus russellii*	JLF5411		MH193374

Table B (continued)

Species	Bank note	RPB2	TEF1	Species	Bank note	RPB2	TEF1
Phylloporus subrubeolus	BC0612	MH580833	MH580814	*Heimioporus conicus*	N.K.Zeng3109		MH241053
Aureoboletus viscosus	OR0361	MH614751	MH614703	*Heimioporus conicus*	N.K.Zeng3114		MH241054
Boletellus ananas	KM123769	MH614754	MH614707	*Lanmaoa pallidorosea*	Mushroom Observer #210760		MH318610
Rubinoboletus aff. Rubinus	OR0139	MH614758	MH614712	*Boletus peckii*	Observer #246697		MH318614
Erythrophylloporus aurantiacus	REH7271	MH614761	MH614715	*Boletus subvelutipes*	Mushroom_Observer#248499		MH337276
Erythrophylloporus fagicola	Garay215	MH614762	MH614716	*Boletus subvelutipes*	Mushroom_Observer #242312		MH337277
Erythrophylloporus paucicarpus	OR1135	MH614764	MH614718	*Lanmaoa flavorubra*	NY817328		MH337278
Erythrophylloporus paucicarpus	OR1151	MH614765	MH614719	*Boletus carminiporus*	Observer #246870		MH337279
Erythrophylloporus suthepensis	OR0402	MH614766	MH614720	*Boletus fagicola*	Observer #245071		MH337283
Erythrophylloporus suthepensis	SV0236	MH614767	MH614721	*Boletus nobilis*	Observer #255270		MH337285
Fistulinella prunicolor	REH9880	MH614771	MH614725	*Boletus aff. Gertrudiae*	Observer #255268		MH337287
Corneroboletus indecorus	OR0863	MH614772	MH614726	*Boletus sensibilis*	Observer #280056		MH337290
Xerocomellus porosporus	VDKO0311	MH614773	MH614727	*Boletellus pseudochrysenteroides*	Observer #288188		MH337293
Hortiboletus rubellus	VDKO0403	MH614774		*Boletus sensibilis*	Observer #288555		MH337295
Hourangia cf. pumila	OR0762	MH614775	MH614728	*Caloboletus peckii*	Observer #283600		MH337297
Tylopilus ferrugineus	BOTH3639	MH614789	MH614742	*Boletus aff. Edulis*	Observer #278521B		MH337303
Veloporphyrellus conicus	REH8510	MH614792	MH614745	*Caloboletus peckii*	Observer #286124		MH347321
Xerocomellus rippariellus	VDKO0404	MH614793	MH614746	*Baorangia bicolor*	Observer #282994		MH347322
Suillellus queletii	VDKO1185	MH645604	MH645598	*Retiboletus nigrogriseus*	FHMU2045		MH367487

Table B (continued)

Species	Bank note	RPB2	TEF1	Species	Bank note	RPB2	TEF1
Aureoboletus velutipes	GDGM44713	MH700226	MH700191	*Retiboletus nigrogriseus*	FHMU2205		MH367490
Aureoboletus velutipes	GDGM42608	MH700227	MH700190	*Phylloporopsis boletinoides*	CORT 014483		MH588316
Aureoboletus glutinosus	GDGM44477	MH700229	MH700205	*Phylloporopsis boletinoides*	CORT 010991		MH588317
Aureoboletus glutinosus	GDGM44479	MH700230	MH700204	*Austroboletus niveus*	PDD:105246		MH594049
Aureoboletus miniatoaurantiacus	GDGM42855	MH700233	MH700202	*Austroboletus novae-zelandiae*	PDD:105097		MH594051
Aureoboletus miniatoaurantiacus	GDGM53274	MH700234	MH700201	*Imleria pallida*	BOTH4356		MH614708
Aureoboletus raphanaceus	GDGM44832	MH700236	MH700194	*Singerocomus inundabilis*	TWH9199		MH645596
Aureoboletus raphanaceus	GDGM52590	MH700238	MH700193	*Singerocomus rubriflavus*	TWH9585		MH645597
Aureoboletus griseorufescens	GDGM28490	MH700241		*Lanmaoa rubriceps*	N.K.Zeng3006		MH879712
Aureoboletus griseorufescens	ZM131	MH700242		*Lanmaoa macrocarpa*	N.K.Zeng3021		MH879713
Phylloporus pusillus	OR1310	MH706703	MH580804	*Lanmaoa macrocarpa*	N.K.Zeng3251		MH879714
Ionosporus longipes	LEE1180	MH712031	MT085471	*Neoboletus multipunctatus*	N.K.Zeng2498		MH879722
Ionosporus australis	REH10131	MH712034		*Chalciporus radiatus*	N.K.Zeng1379 (FHMU930)		MH879738
Ionosporus australis	REH9814	MH712035		*Chalciporus radiatus*	N.K.Zeng1414 (FHMU959)		MH879739
Butyriboletus huangnianlaii	N.K.Zeng3245 (FHMU2206)	MH879740	MH879717	*Neoboletus multipunctatus*	N.K.Zeng3324		MK061358
Butyriboletus huangnianlaii	N.K.Zeng3246 (FHMU2207)	MH879741	MH879718	*Aureoboletus longicollis*	GDGM44739		MK165845
Sutorius subrufus	N.K.Zeng3043	MH879745	MH879728	*Aureoboletus clavatus*	GDGM42992		MK165847
Sutorius subrufus	N.K.Zeng3045	MH879746	MH879729	*Heimioporus sinensis*	GDGM44783		MK165976

Table B (continued)

Species	Bank note	RPB2	TEF1	Species	Bank note	RPB2	TEF1
Caloboletus guanyui	N.K.Zeng3058 (FHMU2019)	MH879751	MH879734	*Heimioporus sinensis*	GDGM44447		MK165977
Caloboletus guanyui	N.K.Zeng3079 (FHMU2040)	MH879752	MH879736	*Phylloporus rimosus*	Montoya_4834		MK314102
Pulveroboletus sokponianus	SAB0629	MH983003	MH983002	*Phylloporus rimosus*	Cesar_61		MK314103
Pulveroboletus sp. 3 OR-2019	OR0644	MK058522	MK058519	*Phylloporus quercophilus*	Garay_373		MK314105
Pulveroboletus sp. 3 OR-2019	OR0686	MK058523	MK058520	*Phylloporus quercophilus*	Montoya_5239		MK314106
Strobilomyces minor	HKAS:101909	MK183827	MK183829	*Austroboletus gracilis*	CFMR:BOS-562		MK721068
Strobilomyces minor	HKAS:101910	MK183828	MK183830	*Crocinoboletus pinetorum*	FHMU:3123		MK850946
Strobilomyces sculptus	HKAS:101911	MK241487	MK241490	*Crocinoboletus laetissimus*	FHMU:3124		MK850949
Strobilomyces sculptus	HKAS:102606	MK241488	MK241491	*Sutorius maculatoides*	WAT25793		MN067482
Indoporus shoreae	AP 6693	MK243367		*Boletus miniato-olivaceus*	Observer #320058		MN124179
Indoporus shoreae	AP 6697	MK243368		*Tylopilus variobrunneus*	Observer #287518		MN124182
Strobilomyces huangshanensis	HKAS:102612	MK329216	MK329218	*Amoenoboletus weberi*	Observer #288704		MN124186
Strobilomyces huangshanensis	HKAS:102613	MK329217	MK329219	*Tylopilus variobrunneus*	Observer #281620		MN124189
Rossbeevera bispora	GDGM 45612	MK350308		*Boletus billieae*	Observer #333089		MN124190
Rossbeevera bispora	GDGM 45639	MK350309		*Amylotrama clelandii*	TL2898		MN413633
Rossbeevera griseobrunnea	GDGM 45913	MK350311	MK350307	*Amylotrama clelandii*	AD58886		MN413634
Cacaoporus pallidicarneus	SV0221	MK372286	MK372273	*Amylotrama banrockensis*	AD58672		MN413637
Cacaoporus pallidicarneus	SV0451	MK372287	MK372274	*Veloporphyrellus vulpinus*	LE315547		MN597965
Cacaoporus tenebrosus	SV0224	MK372291	MK372278	*Veloporphyrellus vulpinus*	LE315544		MN597966
Cacaoporus tenebrosus	SV0452	MK372292	MK372280	*Boletus candidissimus*	LE315542		MN597967

Table B (continued)

Species	Bank note	RPB2	TEF1	Species	Bank note	RPB2	TEF1
Neoboletus antillanus	JBSD127417	MK488082		*Retiboletus sinogriseus*	LJ260		MT010619
Phlebopus roseus	MY2017275	MK747252	MK736295	*Retiboletus ater*	li1214		MT010622
Phlebopus roseus	MY2017277	MK747253	MK736296	*Retiboletus brunneolus*	LC_LJW23		MT010625
Aureoboletus auriflammeus	CFMR:BOS-699	MK766269	MK721060	*Phlebopus portentosus*	FG-DZ5		MT024825
Aureoboletus innixus	CFMR:BOS-544	MK766270	MK721061	*Phlebopus portentosus*	FG-MH2		MT024836
Aureoboletus projectellus	MICH:KUO-09111014	MK766271	MK721062	*Tylopilus sp. YL-2021g*	HKAS106466		MT110338
Aureoboletus roxanae	CFMR:BOS-698	MK766272	MK721063	*Porphyrellus cyaneotinctus*	HKAS80183		MT110340
Aureoboletus russellii	CFMR BOS-716	MK766273	MK721064	*Tylopilus rigens*	HKAS106432		MT110347
Aureoboletus singeri	CFMR:BZ-2395	MK766274	MK721065	*Tylopilus rigens*	HKAS106429		MT110348
Australopilus palumanus	NY:1193890	MK766275	MK721066	*Tylopilus himalayanus*	HKAS93425		MT110355
Australopilus palumanus	NY:1193865	MK766276	MK721067	*Fistulinella salmonea*	HKAS106323		MT110368
Austroboletus gracilis	CFMR:BOS-547	MK766277	MK721069	*Erythrophylloporus flammans*	LE312491		MT293596
Austroboletus subflavidus	CFMR BZ-3178	MK766278	MK721070	*Hortiboletus arduinus*	FHMU3323		MT646447
Boletus harrisonii	MICH:KUO-09071204	MK766280	MK721072	*Hortiboletus arduinus*	FHMU3324		MT646448

Table B (continued)

Species	Bank note	RPB2	TEF1	Species	Bank note	RPB2	TEF1
Boletus harrisonii	MICH:KUO-09071204	MK766280	MK721072	*Hortiboletus arduinus*	FHMU3324		MT646448
Leccinum longicurvipes	MICH:KUO-09241111	MK766282	MK721074	*Hortiboletus napaeus*	FHMU3328		MT646451
Leccinum longicurvipes	MICH:KUO-10200708	MK766283	MK721075	*Hortiboletus napaeus*	FHMU3329		MT646452
Boletus rubriceps	MICH:KUO-08150719	MK766284	MK721076	*Aureoboletus erythraeus*	FHMU3144		MT650114
Boletus separans	MICH KUO-06201002	MK766285	MK721077	*Aureoboletus venustus*	FHMU3146		MT650115
Boletus subfraternus	MICH:KUO-08101302	MK766286	MK721078	*Hourangia dilatata*	FHMU3143		MT650117
Caloboletus firmus	CFMR:BZ-1721	MK766288	MK721080	*Hourangia dilatata*	FHMU2954		MT650118
Caloboletus inedulis	MICH KUO-07031403	MK766289	MK721081	*Hourangia nigropunctata*	FHMU3084		MT650122
Chamonixia brevicolumna	DBG:F023359	MK766290	MK721082	*Hourangia nigropunctata*	FHMU3108		MT650123
Chamonixia brevicolumna	DBG:F28707	MK766291	MK721083	*Phlebopus spongiosus*	BC0166		MT769252
Chamonixia caespitosa	OSC:47025	MK766292	MK721084	*Rossbeevera eucyanea*	KPM-NC 28182		MT874786
Chamonixia caespitosa	OSC-117571	MK766293	MK721085	*Rossbeevera cryptocyanea*	KPM-NC 26877		MT874787
Cyanoboletus pulverulentus	MICH:KUO-09220408	MK766294	MK721086	*Rossbeevera bispora*	KPM-NC 28186		MT874788
Harrya atriceps	NY:1193851	MK766295	MK721087	*Octaviania tomentosa*	KPM-NC 27955		MT874799

Table B (continued)

Species	Bank note	RPB2	TEF1	Species	Bank note	RPB2	TEF1
Heimioporus betula	MICH:KUO-10030904	MK766298	MK721090	*Octaviania tomentosa*	KPM NC 27954		MT874802
Hemileccinum subglabripes	MICH:KUO-07070702	MK766299	MK721091	*Octaviania tenuipes*	KPM-NC 25370		MT874808
Hemileccinum subglabripes	MICH:KUO-07230802	MK766300	MK721092	*Octaviania tenuipes*	KPM-NC 27965		MT874811
Hortiboletus campestris	MICH:KUO-08240502	MK766302	MK721094	*Leccinum subradicatum*	KPM-NC 24518		MT874822
Hortiboletus rubellus	MICH:KUO-06081002	MK766303	MK721095	*Tylopilus subotsuensis*	LE312526		MW014271
Imleria badia	CFMR:BOS-564	MK766304	MK721096	*Tylopilus subotsuensis*	LE312527		MW014272
Imleria badia	MICH:KUO-09110404	MK766305	MK721097	*Austroboletus olivaceoglutinosus*	Xu132		MW165263
Leccinellum albellum	MICH:KUO-07241101	MK766308	MK721100	*Tylopilus castanoides*	Liu780		MW165267
Leccinellum albellum	MICH:KUO-09200807	MK766309	MK721101	*Tylopilus pseudoalpinus*	Hlh306		MW165268
Leccinellum corsicum	K(M)-142735	MK766310	MK721102	*Neoboletus infuscatus*	N.K.Zeng4030		MW307256
Leccinellum crocipodium	MICH:KUO-07050707	MK766311	MK721103	*Neoboletus infuscatus*	N.K.Zeng4031		MW307257
Leccinellum lepidum	K(M):142974	MK766312	MK721105	*Baorangia duplicatopora*	FHMU5879		MW485969

Table B (continued)

Species	Bank note	RPB2	TEF1	Species	Bank note	RPB2	TEF1
Leccinellum pseudoscabrum	CFMR:DPL-11432	MK766313	MK721106	*Baorangia duplicatopora*	FHMU5880		MW485970
Leccinellum pseudoscabrum	MICH:KUO-10200710	MK766314	MK721107	*Austroboletus brunneisquamus*	FHMU5874		MW512636
Leccinellum viscosum	NY:01194025	MK766315	MK721110	*Austroboletus brunneisquamus*	FHMU5876		MW512637
Leccinum andinum	NY:181460	MK766316	MK721111	*Amoenoboletus mcrobbii*	PDD97418		MW566744
Leccinum andinum	NY:00796145	MK766317	MK721112	*Amoenoboletus miraculosus*	ZT14046		MW566745
Leccinum aurantiacum	L:0342207	MK766318	MK721113	*Phylloporus tenuissimus*	N.K. Zeng3514		MW574452
Leccinum cf. duriusculum	CFMR:DLC2002-252	MK766319	MK721114	*Phylloporus grossus*	N.K. Zeng3309		MW574462
Leccinum cf. duriusculum	MICH:KUO-09120708	MK766320	MK721115	*Phylloporus grossus*	N.K. Zeng3335		MW574464
Leccinum holopus	MICH:KUO-09150707	MK766322	MK721117	*Phylloporus microsquamus*	N.K. Zeng3549		MW574473
Leccinum manzanitae	NY:14041	MK766324	MK721119	*Phylloporus microsquamus*	N.K. Zeng3560		MW574474
Leccinum monticola	NY-760388	MK766325	MK721120	*Tylopilus phaseolisporus*	NY:REH 8827		MW620810
Hemileccinum rubropunctum	NY:792788	MK766327	MK721122	*Hemileccinum floridanum*	AB16		MW737481
Hemileccinum rubropunctum	NY:01193924	MK766328	MK721123	*Hemileccinum floridanum*	JAB_142		MW737488
Leccinum rugosiceps	CFMR:BOS-866	MK766329	MK721124	*Xerocomellus amylosporus*	JLF3498		MW737492
Leccinum rugosiceps	MICH WS-06291501	MK766330	MK721126	*Xerocomellus dryophilus*	LF4134		MW737493

Table B (continued)

Species	Bank note	RPB2	TEF1	Species	Bank note	RPB2	TEF1
Leccinum snellii	CFMR BOS-579	MK766331	MK721127	*Xerocomellus dryophilus*	JLF4791		MW737494
Leccinum tablense	NY:760387	MK766332	MK721128	*Tylopilus oradivensis*	NY:REH 8187		MW815572
Leccinum tablense	NY:00796175	MK766333	MK721129	*Tylopilus neofelleus*	N.K. Zeng2851		MW925754
Leccinum talamancae	NY:00815455	MK766334	MK721130	*Tylopilus atroviolaceobrunneus*	N.K. Zeng1328		MW925777
Leccinum talamancae	NY:00815453	MK766335	MK721131	*Tylopilus pseudoballoui*	N.K. Zeng4500		MW925788
Leccinum violaceotinctum	CFMR:BZ-1676	MK766337	MK721133	*Tylopilus yangzhuliangii*	N.K. Zeng3358		MW925820
Leccinum violaceotinctum	CFMR:BZ-3169	MK766338	MK721134	*Tylopilus yangzhuliangii*	N.K. Zeng3359		MW925821
Octaviania tasmanica	NY:2072530	MK766354	MK721151	*Tylopilus pseudoballoui*	N.K. Zeng4791		MW925864
Octaviania tasmanica	NY:02449788	MK766355	MK721152	*Boletellus squamosus*	N.K. Zeng4051		MW925898
Phylloporus centroamericanus	NY:577537	MK766357	MK721154	*Ionosporus longipes*	LE315589		MZ424890
Phylloporus leucomycelinus	NY:1193895	MK766358	MK721155	*Hortiboletus rupicapreus*	LE312678		MZ424893
Phylloporus scabripes	CFMR:BZ-3174	MK766359	MK721156	*Hortiboletus rupicapreus*	LE312677		MZ424894
Retiboletus griseus	MICH:KUO-07041401	MK766360	MK721157	*Leccinum schistophilum*	LJW445		MZ707788
Rossbeevera pachydermis	NY:1491237	MK766361	MK721159	*Boletus kundabungkid*	MEL2417154		OK323368
Rossbeevera pachydermis	NY:02449764	MK766362	MK721160	*Sutorius obscuripellis*	HKAS107150		OK557209
Rossbeevera vittatispora	NY-1034425	MK766363	MK721161	*Tricholomopsis yunnanensis*	Liang271		OL632198
Sutorius australiensis	NY:1194055	MK766367	MK721165	*Tricholomopsis yunnanensis*	Rui390		OL632199
Sutorius australiensis	NY-02072542	MK766368	MK721166	*Brasilioporus olivaceoflavidus*	VIES 9901323		OM160556

Table B (continued)

Species	Bank note	RPB2	TEF1	Species	Bank note	RPB2	TEF1
Porphyrellus sordidus	MICH:KUO-06240801	MK766371	MK721169	*Fistulinella ruschii*	ICN 192818		OM160558
Xerocomellus chrysenteron	MICH:KUO-09260903	MK766374	MK721172	*Nevesoporus nigrostipitatus*	VIES 9901383		OM160562
Xerocomus ferrugineus	CFMR:BOS-545	MK766375	MK721173	*Singerocomus rubriflavus*	GAS900		OM160564
Xerocomus ferrugineus	MICH:KUO-08100701	MK766376	MK721174	*Aureoboletus guangdongensis*	FHMU3797		OM321040
Xerocomus hortonii	MICH:KUO-07050706	MK766377	MK721175	*Boletellus wenshanensis*	532624MF_205_Wu2042		ON007377
Xerocomus spadiceus	MICH:KUO-07080702	MK766378	MK721176	*Phylloporus alboinfuscatus*	N.K. Zeng4784		ON868513
Xerocomus tenax	MICH KUO-08241404	MK766379	MK721177	*Phylloporus alboinfuscatus*	N.K. Zeng4787		ON868514
Leccinellum quercophilum	NY:01293386	MK766380	MK721178	*Rubroboletus flavus*	HKAS126558		OQ873458
Phylloporus bellus	NY:1393461	MK766382	MK721179	*Buchwaldoboletus hemichrysus*	FLAS-F-60314		MZ869814
Leccinellum alborufescens	FHMU1758	MK816332	MK816329				

APPENDIX C

THE DETAILED INFORMATION OF AGARICOMYCOTINA

Table C Maximum clade credibility tree of Agaricomycotina

Oder	Family	Genus	Species	strain/voucher	ITS	LSU	RPB1	RPB2	TEF1
Agaricales	Agaricaceae	Agaricus	Agaricus campestris	AFTOL-ID 1492	DQ486682	DQ110871	DQ516068		
Agaricales	Agaricaceae	Cercopemyces	Cercopemyces crocodilinus	UTC 258260	NR_175602	NG_071239	JX409898		
Agaricales	Agaricaceae	Chlorophyllum	Chlorophyllum africanum	PREM 62141	MG741963	MG742042		MG742071	MG742099
Agaricales	Agaricaceae	Clarkeinda	Clarkeinda trachodes	KUBOT-KRMK-2020-26	MW425600	MW425592			
Agaricales	Agaricaceae	Coniolepiota	Coniolepiota spongodes	HKAS:77574	KC625531	KC625530			
Agaricales	Agaricaceae	Coprinus	Coprinus comatus	AFTOL-ID 626	AY854066	AY635772	AY857983	AY780934	AY881026

Table C (continued)

Oder	Family	Genus	Species	strain/voucher	ITS	LSU	RPB1	RPB2	TEF1
Agaricales	Agaricaceae	Eriocybe	Eriocybe chionea	E.C. Vellinga ecv3616	HM488753	HM488772		HM488801	
Agaricales	Agaricaceae	Lacrymaria	Lacrymaria glareosa	WU16293	HQ872015	HQ847134			HQ847208
Agaricales	Agaricaceae	Lepiota	Lepiota cristata	ZRL20151133	LT716026	KY418841	KY418963	KY418992	KY419048
Agaricales	Agaricaceae	Leucocoprinus	Leucocoprinus fragilissimus	ZRL20151466	LT716029	KY418844	KY418965	KY418994	KY419049
Agaricales	Agaricaceae	Leucoagaricus	Leucoagaricus badius	SH148	KU647736	NG_064403		KU900506	KU900510
Agaricales	Agaricaceae	Macrolepiota	Macrolepiota dolichaula	xml2013058	LT716021	KY418836		KY418988	KY419044
Agaricales	Agaricaceae	Micropsalliota	Micropsalliota globocystis	ZRL2013465	LT716024	KY418839		KY418991	KY419046
Agaricales	Agaricaceae	Verrucospora	Verrucospora flavofusca	AFTOL-ID 655	DQ241779	DQ470825			
Agaricales	Agaricaceae	Lycoperdon	Lycoperdon ericaeum	ZRL20151498	LT716030	KY418845	KY418966	KY418995	
Agaricales	Amanitaceae	Amanita	Amanita fulvisquamea	CMUB-39993	OQ780689	OQ780671		OQ740051	OQ740069
Agaricales	Amanitaceae	Catatrama	Catatrama costaricensis	DAOM:211663		KT833804		KT833819	KT833834
Agaricales	Amanitaceae	Limacella	Limacella glioderma	MB 000750		KT833809		KT833824	KT833837
Agaricales	Amanitaceae	Limacellopsis	Limacellopsis asiatica	HKAS:76497		KT833811		KT833826	KT833839
Agaricales	Clavariaceae	Clavulinopsis	Clavulinopsis corallinorosacea	PBM3380	KP257144	HQ877707		KP257265	

Table C (continued)

Oder	Family	Genus	Species	strain/voucher	ITS	LSU	RPB1	RPB2	TEF1
Agaricales	Clavariaceae	Hodophilus	Hodophilus paupertinus	Ceska110301	KP257157	KP257228		KP257272	
Agaricales	Clavariaceae	Lamelloclavaria	Lamelloclavaria petersenii	SAV F-3493	KP257171	NG_060318		KP257285	
Agaricales	Clavariaceae	Ramariopsis	Ramariopsis avellaneo-inversa	AMB 18574	MT055954	MT053233			
Agaricales	Cortinariaceae	Cortinarius	Cortinarius iodes	AFTOL-ID 285		AY702013	AY857984	AY536285	AY881027
Agaricales	Cortinariaceae	Phlegmacium	Phlegmacium georgiolens	GS03-1	MK358093	MK358068	MK340961		
Agaricales	Cortinariaceae	Quadrispora	Quadrispora oblongispora	Trappe 18111	AF325566	AF388746			
Agaricales	Entolomataceae	Clitocella	Clitocella orientalis	KUN-HKAS 78763 (Zhao1504)		MN065728		MN148165	MN166276
Agaricales	Entolomataceae	Clitopilus	Clitopilus amygdaliformis	KUN-HKAS 87950 (Zhao2184)	MN061290	MN065680		MN148118	MN166230
Agaricales	Entolomataceae	Entocybe	Entocybe nitida	TENN:067505	KU058498	KU058535	KU139031	KU138998	
Agaricales	Entolomataceae	Entoloma	Entoloma prunuloides	AFTOL-ID 523	DQ206983	AY700180	DQ447898	DQ385883	DQ457633
Agaricales	Entolomataceae	Nolanea	Nolanea caribaea	SP:FK1790		MH190214		MH190114	MH190146
Agaricales	Hygrophoraceae	Cora	Cora arachnoidea	DIC279	KF443232	KF443256		KF443266	

Table C (continued)

Oder	Family	Genus	Species	strain/voucher	ITS	LSU	RPB1	RPB2	TEF1
Agaricales	Hygrophoraceae	Gliophorus	Gliophorus psittacinus	CFMR DEN-25	KF291075	KF291076		KF291078	
Agaricales	Hygrophoraceae	Humidicutis	Humidicutis sp.	CFMR BZ-3923	KF291110	KF291111			
Agaricales	Hygrophoraceae	Hygrocybe	Hygrocybe coccinea	AFTOL-ID 1715	DQ490629	DQ457676	DQ447910	DQ472723	GU187705
Agaricales	Hygrophoraceae	Neohygrocybe	Neohygrocybe ovina	GWG H. ovina Rhosisaf (ABS)	KF291233	KF291234		KF291236	
Agaricales	Hygrophoraceae	Porpolomopsis	Porpolomopsis calyptriformis	CFMR ENG-3	KF291242	KF291243		KF291245	
Agaricales	Hymenogastraceae	Gymnopilus	Gymnopilus picreus	ZRL2015011	LT716066	KY418882	KY418980	KY419027	KY419077
Agaricales	Hymenogastraceae	Psathyloma	Psathyloma catervatim	PBM3420	HQ840663	HQ840664		HQ840666	
Agaricales	Lyophyllaceae	Asterophora	Asterophora agaricoides	CBS170.86			EF421021	DQ367431	DQ367424
Agaricales	Lyophyllaceae	Blastosporella	Blastosporella zonata	TJB8371	EU708340	EU708337			MZ574160
Agaricales	Lyophyllaceae	Gerhardtia	Gerhardtia sp.	HC01/025	EF421103	EF421091	EF421028	EF420994	EF421060
Agaricales	Lyophyllaceae	Hypsizygus	Hypsizygus tessulatus	AFTOL-ID 1898	DQ917653	DQ917664	DQ917665		
Agaricales	Lyophyllaceae	Lyophyllum	Lyophyllum sp. PBM 2688	AFTOL-ID 1487	DQ182502	DQ094785	DQ516075		
Agaricales	Lyophyllaceae	Myochromella	Myochromella boudieri	TB01	OM867845	OM906012			OM974138

Table C (continued)

Oder	Family	Genus	Species	strain/voucher	ITS	LSU	RPB1	RPB2	TEF1
Agaricales	Lyophyllaceae	Ossicaulis	Ossicaulis yunnanensis	EJ152	KY411962	KY411960			KY411964
Agaricales	Lyophyllaceae	Tephrocybe	Tephrocybe gibberosa	CBS328.50	AF357041		EF421039	EF421005	EF421073
Agaricales	Lyophyllaceae	Tricholomella	Tricholomella constricta	HC84/75	DQ825429		DQ825422	DQ825412	
Agaricales	Marasmiaceae	Campanella	Campanella tristis	JAC9038	OQ282776	OQ282738			
Agaricales	Marasmiaceae	Chaetocalathus	Chaetocalathus cocciformis	JAC12666	OQ282795	OQ282751			
Agaricales	Marasmiaceae	Crinipellis	Crinipellis sp.	ZRL20151264	LT716051	KY418867		KY419013	KY419069
Agaricales	Marasmiaceae	Marasmius	Marasmius alliaceus	AFTOL-ID 556	AY854076	AY635776	AY860526	AY786060	AY883431
Agaricales	Mycenaceae	Favolaschia	Favolaschia brevistipitata	Dai 19780	MZ661772	MZ661742			MZ959383
Agaricales	Mycenaceae	Mycena	Mycena aurantiidisca	AFTOL-ID 1685	DQ490646	DQ470811	DQ447927	DQ474122	GU187728
Agaricales	Mycenaceae	Panellus	Panellus stypticus	DSH 93-213		AF518634			
Agaricales	Omphalotaceae	Anthracophyllum	Anthracophyllum archeri	AFTOL-ID 973	DQ404387	AY745709	DQ435799	DQ385877	DQ028586
Agaricales	Omphalotaceae	Gymnopus	Gymnopus confluens	ZRL20151148	LT716054	KY418870	KY418976	KY419016	KY419070
Agaricales	Omphalotaceae	Lentinula	Lentinula edodes	DMRO327	MK603500		OQ975905		
Agaricales	Omphalotaceae	Marasmius	Marasmius alliaceus	AFTOL-ID 556	AY854076	AY635776	AY860525	AY786060	AY883430

Table C (continued)

Oder	Family	Genus	Species	strain/voucher	ITS	LSU	RPB1	RPB2	TEF1
Agaricales	Omphalotaceae	Mycetinis	Mycetinis scorodonius	TFB4749	DQ450006	KY019626			
Agaricales	Omphalotaceae	Omphalotus	Omphalotus olearius	AFTOL-ID 1718	DQ494681	DQ470816			
Agaricales	Omphalotaceae	Rhodocollybia	Rhodocollybia maculata	AFTOL-ID 540	DQ404383	AY639880	DQ447936	AY787220	DQ061279
Agaricales	Physalacriaceae	Armillaria	Armillaria mellea	AFTOL-ID 449	AY789081	AY700194	AY788849	AY780938	AY881023
Agaricales	Physalacriaceae	Cibaomyces	Cibaomyces glutinis	HKAS 71038	KJ024100	KJ024105		MH014058	MH014054
Agaricales	Physalacriaceae	Cryptomarasmius	Cryptomarasmius crescentiae	BRNM 714678	FJ936147	FJ936141			
Agaricales	Physalacriaceae	Cylindrobasidium	Cylindrobasidium laeve	AFTOL-ID 453	DQ205682	DQ234541	DQ447896	AY536283	DQ408151
Agaricales	Physalacriaceae	Cyptotrama	Cyptotrama asprata	Yang5676	KR607193	KR607153		KT201659	
Agaricales	Physalacriaceae	Dactylosporina	Dactylosporina glutinosa	MCA 1775	HM005074	HM005137		KY359142	KU170936
Agaricales	Physalacriaceae	Flammulina	Flammulina velutipes	AFTOL-ID 558	AY854073	AY639883	AY858966	AY786055	AY883423
Agaricales	Physalacriaceae	Oudemansiella	Oudemansiella radicata	AFTOL-ID 561	DQ241780	AY645051	DQ447946	AY786067	DQ029194
Agaricales	Physalacriaceae	Rhodotus	Rhodotus asperior	HKAS 56754	KC179737	NG_059484		KC179755	KC179730
Agaricales	Physalacriaceae	Strobilurus	Strobilurus stephanocystis	MCVE26717	MF063183	MF063118		MF063227	MF063264
Agaricales	Physalacriaceae	Xerula	Xerula furfuracea	AFTOL-ID 538	DQ494703	AY691890			

Table C (continued)

Oder	Family	Genus	Species	strain/voucher	ITS	LSU	RPB1	RPB2	TEF1
Agaricales	Pleurotaceae	Hohenbuehelia	Hohenbuehelia mastrucata	TRTC 152314	NR_154082	NG_060671			KU355451
Agaricales	Pleurotaceae	Pleurotus	Pleurotus ostreatus	JZB2101002	JN126327			JN126367	JN126347
Agaricales	Pluteaceae	Melanoleuca	Melanoleuca albomarginata	BRNM 817818	MT270938			MT268627	MT268554
Agaricales	Pluteaceae	Pluteus	Pluteus romellii	AFTOL-ID 625	AY854065	AY634279	AY862187	AY786063	AY883433
Agaricales	Pluteaceae	Volvariella	Volvariella ptilotricha	LE 313324	NR_164612				MK940805
Agaricales	Psathyrellaceae	Coprinellus	Coprinellus micaceus	SFSU DEH351	AY461832				GQ257815
Agaricales	Psathyrellaceae	Coprinopsis	Coprinopsis atramentaria	SZMC-NL-4245	FN396123	FN396172			FN396225
Agaricales	Psathyrellaceae	Parasola	Parasola conopilea	ZRL20151990	LT716064	KY418880		KY419025	
Agaricales	Psathyrellaceae	Psathyrella	Psathyrella candolleana	ZRL20151400	LT716063	KY418879	KY418978	KY419024	KY419075
Agaricales	Psathyrellaceae	Tulosesus	Tulosesus callinus	DJS20130129003	MG857120	MG857117			OL630938
Agaricales	Pterulaceae	Myrmecopterula	Myrmecopterula nudihortorum	K(M) 190547	MK953241	MK953394		MK944365	
Agaricales	Pterulaceae	Pterula	Pterula multifida	KM195746	MK953335	MK953399	MK944372		
Agaricales	Stephanosporaceae	Cristinia	Cristinia sp.	FP-100305	GU187526	GU187585	GU187470	GU187793	GU187718
Agaricales	Stephanosporaceae	Stephanospora	Stephanospora hystrispora	Tle1202	KM086901	KM086995			KM087082
Agaricales	Tricholomataceae	Corneriella	Porpoloma portentosum	REH5788	KJ417299	KJ417211		KJ424387	

Table C (continued)

Oder	Family	Genus	Species	strain/voucher	ITS	LSU	RPB1	RPB2	TEF1
Agaricales	Tricholomataceae	Dennisiomyces	Dennisiomyces fibrillosus	GC18110903	MK569405	MK569399		MK577920	
Agaricales	Tricholomataceae	Hemimycena	Hemimycena gracilis	AFTOL-ID 1732	DQ490623	DQ457671	DQ447905	DQ472719	GU187709
Agaricales	Tricholomataceae	Leucopaxillus	Leucopaxillus giganteus	AMB 18858	OQ657181	OQ651259		OQ672605	OQ672609
Agaricales	Tricholomataceae	Omphalina	Omphalina mutila	CCBAS343	LN714577			LN714684	
Agaricales	Tricholomataceae	Porpoloma	Porpoloma terreum	REH5830	KJ417305	KJ417215		KJ424391	
Agaricales	Tricholomataceae	Pseudobaeospora	Pseudobaeospora cellulodermа	TENN:067659	KU058501	KU058538	KU139042	KU139001	
Agaricales	Tricholomataceae	Resupinatus	Resupinatus striatulus	JA Cussta 8634	MH137829	MH430597			MH449591
Agaricales	Tricholomataceae	Tricholoma	Tricholoma megalophaeum	NS4666	MW597305			MZ514888	MZ970675
Agaricales	Tubariaceae	Flammulaster	Flammulaster sp.	PBM3449	HQ827176	HQ827177			
Agaricales	Tubariaceae	Pachylepyrium	Pachylepyrium fulvidula	MICH 11636	NR_170724	NG_073595			
Agaricales	Tubariaceae	Tubaria	Tubaria confragosa	AFTOL-ID 498	DQ267126	AY700190	DQ447944	DQ408113	
Amylocorticiales	Amylocorticiaceae	Podoserpula	Podoserpula pusio	PERTH E6761	NR_119594	NG_060070		GU187804	
Amylocorticiales	Amylocorticiaceae	Serpulomyces	Ceraceomyces borealis	CFMR:L-8014	GU187512	GU187570		GU187782	GU187686
Atheliales	Aporpiaceae	Aporpium	Aporpium hexagonoides	TFM:F-27498	AB871755	AB871736			

Table C (continued)

Oder	Family	Genus	Species	strain/voucher	ITS	LSU	RPB1	RPB2	TEF1
Atheliales	Atheliaceae	Amphinema	Amphinema byssoides	CBS 397.50	MH856679	MH868196			
Atheliales	Atheliaceae	Piloderma	Piloderma fallax	CFMR:S-12	GU187535	GU187591		GU187797	GU187738
Auriculariales	Auriculariaceae	Auricularia	Auricularia sp. PBM2295	AFTOL-ID 1681	DQ200918	AY634277		DQ366278	DQ408143
Auriculariales	Auriculariaceae	Tremellochaete	Tremellochaete japonica	Wu 251				MN819823	MN819845
Auriculariales	Exidiaceae	Adustochaete	Adustochaete yunnanensis	CLZhao 4401	MZ911966	MZ950630			
Auriculariales	Exidiaceae	Eichleriella	Eichleriella xinpingensis	SWFC 812	NR_164605	NG_068882			
Auriculariales	Exidiaceae	Exidia	Exidia uvapsassa	AFTOL-ID 461	DQ241776	AY645056			
Auriculariales	Exidiaceae	Exidiopsis	Exidiopsis calcea	MW 331	AF291280	AF291326			
Bartheletiales	Bartheletiaceae	Bartheletia	Bartheletia paradoxa	NN46: 196-1		MW404634			
Boletales	Astraeaceae	Astraeus	Astraeus hygrometricus	MB 05-029			FJ536586	FJ536623	FJ536663
Boletales	Boletaceae	Austroboletus	Austroboletus albovirescens	HKAS 59624		KF112485	KF112570	KF112765	KF112217
Boletales	Boletaceae	Afroboletus	Afroboletus luteolus	Yorou 3141			KY553114	KY553124	KY553134
Boletales	Boletaceae	Boletus	Boletus aereus	VDKO1055				MG212617	MG212575
Boletales	Boletaceae	Boletus	Boletus bainiugan	HKAS55285	JN563911	KM820801	KM820812		

Table C (continued)

Oder	Family	Genus	Species	strain/voucher	ITS	LSU	RPB1	RPB2	TEF1
Boletales	Boletaceae	Butyriboletus	Butyriboletus pseudospeciosus	HKAS63513		KT990541	KT990909	KT990380	KT990743
Boletales	Boletaceae	Butyriboletus	Butyriboletus pseudospeciosus	N.K.Zeng2127	MH885349	MH879687			MH879716
Boletales	Boletaceae	Butyriboletus	Butyriboletus roseoflavus	N.K.Zeng2123	MH885348	MH879686			MH879715
Boletales	Boletaceae	Butyriboletus	Butyriboletus roseoflavus	HKAS:54099		KF739665	KF739741	KF739703	KF739779
Boletales	Boletaceae	Rubroboletus	Rubroboletus sinicus	HKAS68620	MW520195	KY418896	KF112504	KF112661	KF112146
Boletales	Boletaceae	Rubroboletus	Rubroboletus sinicus	HKAS56304	KJ605666	KJ605673	KJ619482	KP055031	KJ619483
Boletales	Boletaceae	Strobilomyces	Strobilomyces floccopus	AFTOL-ID 716	AY854068	AY645053	AY858964	AY786065	AY883428
Boletales	Boletaceae	Tylopilus	Tylopilus porphyrosporus	HKAS:76671		KF112482	KF112611	KF112718	KF112243
Boletales	Boletaceae	Xerocomellus	Xerocomellus communis	HKAS50467		KT990670	KT991008	KT990494	KT990858
Boletales	Boletaceae	Buchwaldoboletus	Buchwaldoboletus lignicola	FLAS-F-58917	MZ855279		MZ868933	MZ869820	MZ869815
Boletales	Boletaceae	Chalciporus	Chalciporus citrinoaurantius	GDGM44776	OM877502	MZ157131		MZ165608	MZ165617
Boletales	Boletaceae	Leccinellum	Leccinellum alborufescens	FHMU1758	MK816326	MK816321		MK816332	MK816329

Table C (continued)

Oder	Family	Genus	Species	strain/voucher	ITS	LSU	RPB1	RPB2	TEF1
Boletales	Boletaceae	Leccinum	Leccinum album	Li1072	MZ392873	MW413907		MW439260	MW439267
Boletales	Boletaceae	Retiboletus	Retiboletus fuscus	HKAS74756		KT990636	KT990980	KT990467	KT990830
Boletales	Boletaceae	Retiboletus	Retiboletus fuscus	HKAS83946	KP739264	KP739280			KP739300
Boletales	Boletaceae	Spongiforma	Spongiforma thailandica	DED 7873	NR_119699	NG_042464	KF030387		KF030436
Boletales	Boletaceae	Aureoboletus	Aureoboletus erythraeus	FHMU1053	MT650099	MT650074		MT650124	MT650112
Boletales	Boletaceae	Boletellus	Boletellus shichianus	AFTOL-ID 532	DQ200921	AY647211		DQ366280	DQ408145
Boletales	Boletaceae	Boletellus	Boletellus projectellus	AFTOL-ID 713	AY789082	DQ534582	AY788850	AY787218	AY879116
Boletales	Boletaceae	Corneroboletus	Corneroboletus indecorus	HKAS:63126	JN205456	JN205457		JN205455	
Boletales	Boletaceae	Phylloporus	Phylloporus subbacillisporus	OR0436	MH686274			MH580831	MH580812
Boletales	Boletaceae	Pulchroboletus	Pulchroboletus sclerotiorum	FLAS-F-60334	MF098660			MF614164	MF614165
Boletales	Boletaceae	Veloboletus	Veloboletus limbatus	REH9228				MT747397	MN413636
Boletales	Boletaceae	Xerocomus	Xerocomus fraternus	HKAS55328		KT990681		KT990497	KT990869
Boletales	Boletaceae	Harrya	Harrya atrogrisea	HKAS50542		KT990694	KT991024	KT990499	KT990880
Boletales	Boletaceae	Zangia	Zangia erythrocephala	HKAS:75046		KF112414	KF112579	KF112791	KF112269
Boletales	Boletaceae	Bothia	Bothia fujianensis	HKAS82694	KM269195	KM269193			KM272860

Table C (continued)

Oder	Family	Genus	Species	strain/voucher	ITS	LSU	RPB1	RPB2	TEF1
Boletales	Boletaceae	Hongoboletus	Hongoboletus ventricosus	TNS-F-44611	OQ888710	OQ888732	OQ873487	OQ873507	
Boletales	Boletaceae	Lanmaoa	Lanmaoa asiatica	HKAS 63603		KM605143	KM605165	KM605176	KM605153
Boletales	Boletaceae	Lanmaoa	Lanmaoa asiatica	N.K.Zeng2125	MG030477	MG030470			MG030481
Boletales	Boletaceae	Neoboletus	Neoboletus hainanensis	HKAS90209		KT990615	KT990965	KT990450	KT990809
Boletales	Boletaceae	Neoboletus	Neoboletus hainanensis	HKAS63515		KT990614	KT990964	KT990449	KT990808
Boletales	Boletaceae	Neoboletus	Neoboletus obscureumbrinus	N.K.Zeng3091	MH885355	MH879694		MH879742	MH879723
Boletales	Boletaceae	Neoboletus	Neoboletus obscureumbrinus	N.K.Zeng3098	MH885357	MH879696		MH879744	MH879725
Boletales	Boletaceae	Neoboletus	Neoboletus magnificus	HKAS:54096		KF112324	KF112495	KF112654	KF112149
Boletales	Boletaceae	Neoboletus	Neoboletus magnificus	HKAS:74939		KF112320	KF112494	KF112653	KF112148
Boletales	Boletaceae	Rugiboletus	Rugiboletus extremiorientalis	HKAS 76663		KM605135	KM605159	KM605170	KM605147
Boletales	Boletaceae	Rugiboletus	Rugiboletus extremiorientalis	HKAS 63591		KM605136	KM605160		KM605148
Boletales	Boletinellaceae	Boletinellus	Boletinellus sp.	ZGCSN163	OP542551	OP526842			
Boletales	Boletinellaceae	Phlebopus	Phlebopus_portentosus	FHMU5935	MW783452	MW783432			MW897345

Table C (continued)

Oder	Family	Genus	Species	strain/voucher	ITS	LSU	RPB1	RPB2	TEF1
Boletales	Calostomataceae	Calostoma	Calostoma cinnabarinum	AFTOL-ID 439	AY854064	AY645054	AY857979	AY780939	AY879117
Boletales	Coniophoraceae	Coniophora	Coniophora arida	AFTOL-ID 698	DQ202271	DQ366282	GU187492		DQ408146
Boletales	Coniophoraceae	Gyrodontium	Gyrodontium sacchari	MUCL:40589		GU187579	GU187460	GU187764	GU187703
Boletales	Coniophoraceae	Penttilamyces	Penttilamyces romellii	Yuan 8676	MT705723	MT704603		MT764193	MT755579
Boletales	Diplocystaceae	Diplocystis	Diplocystis wrightii	Ang-1	DQ644139	DQ644134			
Boletales	Gomphidiaceae	Chroogomphus	Chroogomphus roseolus	HKAS102283	MH827599	MH827604		MH827612	MH827594
Boletales	Gomphidiaceae	Gomphidius	Gomphidius roseus	MB95-038			GU187459	GU187818	GU187702
Boletales	Gyroporaceae	Gyroporus	Gyroporus mcnabbii	E8155		EF561627		MN119500	GU187704
Boletales	Hygrophoropsidaceae	Hygrophoropsis	Hygrophoropsis aurantiaca	AFTOL-ID 714	AY854067	AY684156	AY858961	AY786059	AY883427
Boletales	Melanogastraceae	Alpova	Alpova concolor	S053	KF835994				
Boletales	Melanogastraceae	Corditubera	Corditubera bovonei	Verbeken 99-189	OQ566921	GU144405			
Boletales	Melanogastraceae	Melanogaster	Melanogaster sp.	WXH_9068	ON427482			ON533874	
Boletales	Paxillaceae	Gyrodon	Gyrodon lividus	REG Gl1	DQ534568		GU187461	GU187786	GU187701
Boletales	Paxillaceae	Paragyrodon	Paragyrodon sphaerosporus	MB06-066	GU187540	GU187593		GU187803	GU187737
Boletales	Paxillaceae	Paxillus	Paxillus vernalis	AFTOL-ID 715	DQ647827	AY645059			DQ457629

Table C (continued)

Oder	Family	Genus	Species	strain/voucher	ITS	LSU	RPB1	RPB2	TEF1
Boletales	Pisolithaceae	Pisolithus	Pisolithus aurantioscabrosus	AWW297	EU718112	EU718146	FJ536608	FJ536648	FJ536681
Boletales	Sclerodermataceae	Scleroderma	Scleroderma sp.	PDD:103563	KP191816	KP191692			MH594113
Boletales	Sclerodermataceae	Tremellogaster	Tremellogaster surinamensis	MCA 1985			FJ536622	FJ536662	FJ536693
Boletales	Serpulaceae	Austropaxillus	Austropaxillus sp.	HN3458	DQ534572	DQ534671			
Boletales	Serpulaceae	Serpula	Serpula himantioides	AFTOL-ID 1387				DQ366283	DQ059046
Boletales	Suillaceae	Psiloboletinus	Psiloboletinus lariceti	LE 325744	MK940820	MK940818			MK940817
Boletales	Suillaceae	Suillus	Suillus quiescens	TDB3048	KU721185	KU721355	KU852199	KU852289	KU721757
Boletales	Tapinellineae	Bondarcevomyces	Bondarcevomyces taxi	Dai2524	DQ534575	DQ534672			GU187683
Boletales	Tapinellineae	Pseudomerulius	Pseudomerulius aureus	CFMR:FP-103859	GU187534	GU187590	GU187474	GU187799	GU187731
Boletales	Tapinellineae	Tapinella	Tapinella atrotomentosa	Ta86	DQ534573	AF352048			
Boletales	Truncocolumellaceae	Truncocolumella	Truncocolumella sp.	OSC 67369	KT968570	KT968624			
Cantharellales	Botryobasidiaceae	Botryobasidium	Botryobasidium subcoronatum	AFTOL-ID 614	DQ200924	AY647212		DQ366284	
Cantharellales	Cantharellaceae	Cantharellus	Cantharellus subincarnatus	BB 06.096	KF981372	KF294602		KF294676	JX192963
Cantharellales	Cantharellaceae	Craterellus	Craterellus yunnanensis	N.K. Zeng2778 (FHMU1767)	OM835791	OK570080			OK562592

Table C (continued)

Oder	Family	Genus	Species	strain/voucher	ITS	LSU	RPB1	RPB2	TEF1
Cantharellales	Cantharellaceae	Neoburgoa	Neoburgoa freyi	JL596-16	KX423754	KX423755			
Cantharellales	Ceratobasidiaceae	Ceratobasidium	Ceratobasidium ramicola	CBS 133.82	DQ278931			DQ301708	DQ301646
Cantharellales	Ceratobasidiaceae	Rhizoctonia	Rhizoctonia solani	CFC-0947	MT216900			MZ701836	
Cantharellales	Ceratobasidiaceae	Thanatephorus	Thanatephorus cucumeris	RhDAG18	MF804911			MF804914	
Cantharellales	Hydnaceae	Clavulina	Clavulina tuxtlasana	UNAM:FCME 27279	MK547196	MT903238		MK519633	
Cantharellales	Hydnaceae	Hydnum	Hydnum subberkeleyanum	TUMH 64075	NR_176700				LC622506
Cantharellales	Hydnaceae	Minimedusa	Minimedusa obcoronata	CBS:120605	GQ303278	GQ303309			
Cantharellales	Tulasnellaceae	Tulasnella	Tulasnella pruinosa	AFTOL-ID 610	DQ457642			DQ381839	DQ061274
Corticiales	Corticiaceae	Acanthophysellum	Acanthophysellum cerussatum	He6725	MW533100	MW528954			
Corticiales	Corticiaceae	Laetisaria	Laetisaria lichenicola	CBS:128705	MH864964				
Corticiales	Corticiaceae	Marchandiomyces	Marchandiomyces marsonii	ATCC MYA-4210	NR_164214	NG_059434			
Corticiales	Dendrominiaceae	Dendrominia	Dendrominia dryina	MG159	JX892936	JX892937			
Corticiales	Punctulariaceae	Dendrocorticiopsis	Dendrocorticiopsis orientalis	WEI 20-173	MW580925	MW580927			

Table C (continued)

Oder	Family	Genus	Species	strain/voucher	ITS	LSU	RPB1	RPB2	TEF1
Corticiales	Punctulariaceae	Punctularia	Punctularia strigosozonata	He 4980	MW507073	MW507013			
Corticiales	Punctulariaceae	Punctulariopsis	Punctulariopsis sp. YX-2020a	He 4513	MW507082	MW507024			
Corticiales	Vuilleminiaceae	Cytidia	Cytidia salicina	He 4908	MW507083	MW507025			
Corticiales	Vuilleminiaceae	Vuilleminia	Vuilleminia comedens	AFTOL-ID 1247	DQ398959			DQ381844	
Cystofilobasidiales	Mrakiaceae	Itersonilia	Itersonilia perplexans	CBS:363.85	MH861890	MH873579			
Cystofilobasidiales	Mrakiaceae	Mrakia	Mrakia blollopis	CBS 8921	AY038826	NG_057710	KF036509		KF037184
Cystofilobasidiales	Mrakiaceae	Tausonia	Tausonia pullulans	CBS 2532	AF444417	NG_042352			
Cystofilobasidiales	Mrakiaceae	Udeniomyces	Udeniomyces puniceus	AFTOL-ID 1822	DQ836007	DQ836005	DQ838575	DQ836008	
Cystofilobasidiales	Cystofilobasidiaceae	Cystofilobasidium	Cystofilobasidium aff. Macerans	EPV598K4	OR123529	OR123655			OR139193
Dacrymycetales	Cerinomycetaceae	Cerinomyces	Cerinomyces inermis	PDD87816	MW191887				MW130324
Dacrymycetales	Cerinomycetaceae	Cerinomyces	Cerinomyces neuhoffii	CWU6281	MW191925	MW159031	MW130366		MW130335
Dacrymycetales	Dacrymycetaceae	Calocera	Calocera cornea	AFTOL-ID 438	AY789083	AY701526	AY857980	AY536286	AY881019
Dacrymycetales	Dacrymycetaceae	Dacrymyces	Dacrymyces sp. FPL8953	AFTOL-ID 528	DQ205684	AY691892	DQ785785	DQ381845	DQ028587
Dacrymycetales	Dacrymycetaceae	Dacryopinax	Dacryopinax spathularia	AFTOL-ID 454	AY854070	AY701525	AY857981	AY786054	AY881020

Table C (continued)

Oder	Family	Genus	Species	strain/voucher	ITS	LSU	RPB1	RPB2	TEF1
Dacrymycetales	Dacrymycetaceae	Dendrodacrys	Dendrodacrys laetum	H7008757	OP529841				OP477360
Dacrymycetales	Dacrymycetaceae	Ditiola	Ditiola peziziformis	H:Haikonen 24269	MW191972	MW159070	MW130377	MW130420	MW130316
Dacrymycetales	Dacrymycetaceae	Guepiniopsis	Guepiniopsis buccina	AFTOL-ID 888	DQ206986	AY745711		DQ385875	DQ028588
Dacrymycetales	Dacrymycetaceae	Calocera	Calocera glossoides	CWU6247	MW191968	MW159084	MW130388	MW130428	MW130307
Dacrymycetales	Dacrymycetaceae	Dacrymyces	Dacrymyces invisibilis	14597MD	MH230100	MH230102			
Dacrymycetales	Dacrymycetaceae	Dacryonaema	Dacryonaema macrosporum	UPS F-941000	NR_172167		MN580217	MN580306	
Dacrymycetales	Dacrymycetaceae	Dacryonaema	Dacryonaema rufum	UPS F-730180	MN595678	MN593496			
Dacrymycetales	Dacrymycetaceae	Dendrodacrys	Dendrodacrys brasiliense	URM 94628	OP529840		OP477354		OP477367
Dacrymycetales	Dacrymycetaceae	Ditiola	Ditiola peziziformis	H:Haikonen 24269	MW191972	MW159070	MW130377	MW130420	MW130316
Dacrymycetales	Dacrymycetaceae	Femsjonia	Femsjonia uniseptata	TNS F-54019	NR_164095	NG_060435			
Dacrymycetales	Dacrymycetaceae	Unilacryma	Unilacryma bispora	UPS F-941257	NR_172168		MN580256	MN580315	MN580370
Filobasidiales	Piskurozymaceae	Piskurozyma	Piskurozyma sp.	XZY30M1	OP470277	OP470181	OP784856	OP771462	
Filobasidiales	Piskurozymaceae	Solicoccozyma	Solicoccozyma sp.	ATC4C	MG909555		MH187158	MH187161	MH187167
Filobasidiales	Filobasidiaceae	Filobasidium	Filobasidium wieringae	PB782	KX078414			KX078448	KX078437
Filobasidiales	Filobasidiaceae	Goffeauzyma	Goffeauzyma siamensis	DMKU-PAL39	MW669577	LC604627		LC656481	LC656484
Filobasidiales	Filobasidiaceae	Heterocephalacria	Heterocephalacria sp.	TFL1-L	MG909556		MH187159	MH187162	MH187168

Table C (continued)

Oder	Family	Genus	Species	strain/voucher	ITS	LSU	RPB1	RPB2	TEF1
Filobasidiales	Filobasidiaceae	Naganishia	Cryptococcus liquefaciens	CBS968			KF036381	KF036794	KF037066
Filobasidiales	Filobasidiaceae	Zyzygomyces	Zyzygomyces bachmannii	RP415	MG553538	MG553350			
Geastrales	Sphaerobolaceae	Sphaerobolus	Sphaerobolus stellatus	SS12	AY487959			DQ219062	DQ219237
Geastrales	Geastraceae	Geastrum	Geastrum recolligens	OSC41996		DQ218486		DQ219052	DQ219230
Geastrales	Geastraceae	Myriostoma	Myriostoma coliforme	OSC40741		DQ218606		DQ219055	DQ219231
Geastrales	Geastraceae	Radiigera	Radiigera bushnellii	T26259		DQ218608		DQ219058	DQ219233
Geastrales	Geastraceae	Schenella	Schenella pityophila	Herb. Zamora 530	KF988346	KF988464	KF988599		
Gloeophyllales	Gloeophyllaceae	Gloeophyllum	Gloeophyllum sepiarium	Wilcox-3BB	HM536091	NG_060630		HM536109	HM536110
Gloeophyllales	Gloeophyllaceae	Neolentinus	Neolentinus lepideus	DAOM:208724	HM536098	HM536075		HM536119	HM536120
Gomphales	Gomphaceae	Austrogautieria	Austrogautieria chlorospora	OSC46596		DQ218477		DQ218948	DQ219125
Gomphales	Gomphaceae	Clavariadelphus	Clavariadelphus alpinus	HKAS 57396	MK705888	MK704464		MK736708	MK736689
Gomphales	Gomphaceae	Gloeocantharellus	Gloeocantharellus sp.	OSC122875		DQ218617		DQ219072	DQ219249
Gomphales	Gomphaceae	Phaeoclavulina	Phaeoclavulina carovinacea	TUR-A 209584	ON561378	ON530902		ON550479	ON550480
Gomphales	Gomphaceae	Ramaria	Ramaria rubella	AFTOL-ID 724	AY854078	AY645057	AY864866	AY786064	AY883435

Table C (continued)

Oder	Family	Genus	Species	strain/voucher	ITS	LSU	RPB1	RPB2	TEF1
Holtermanniales	Holtermanniales	Holtermannia	Holtermannia corniformis	CBS6979	AF410472		KF036485	KF036899	KF037162
Holtermanniales	Holtermanniales	Holtermanniella	Holtermanniella festucosa	EPV165K3	OR123537	OR123662			OR139196
Hymenochaetales	Hirschioporaceae	Hirschioporus	Hirschioporus fuscoviolaceus	TF152	MW160686	MW162622			
Hymenochaetales	Hirschioporaceae	Pallidohirschioporus	Pallidohirschioporus versicolor	Dai 19331	OQ453386	OQ474951			OQ874762
Hymenochaetales	Hirschioporaceae	Perennihirschioporus	Perennihirschioporus perennis	Dai 19295	OL470315	OQ474956			OQ874779
Hymenochaetales	Hymenochaetaceae	Arambarria	Arambarria destruens	CGP474	KY907682	KY907692			KY907676
Hymenochaetales	Hymenochaetaceae	Cyclomyces	Cyclomyces setiporus	Cui8349	JQ279516	JQ279638			
Hymenochaetales	Hymenochaetaceae	Fomitiporella	Fomitiporella chinensis	Cui11230	KX181309	KY693759	KY693894	KY693910	KY693958
Hymenochaetales	Hymenochaetaceae	Fomitiporia	Fomitiporia cupressicola	MUCL 52486	JQ087877	JQ087904		JQ087965	JQ087931
Hymenochaetales	Hymenochaetaceae	Fulvifomes	Fulvifomes elaeodendri	CMW47825	MH599094	MH599134			MT108964
Hymenochaetales	Hymenochaetaceae	Fuscoporia	Fuscoporia gilva	CMW47749	MH599106	MH599129			MT108963
Hymenochaetales	Hymenochaetaceae	Hydnochaete	Hydnochaete duportii	AFTOL-ID 666	DQ404386	AY635770			DQ435793
Hymenochaetales	Hymenochaetaceae	Inocutis	Inocutis dryophila	DLL2012-001	KU139186	KU139255		KU139317	
Hymenochaetales	Hymenochaetaceae	Inonotus	Inonotus linteus	MUCL 47139	GU461973	GU462002			GU461936

Table C (continued)

Oder	Family	Genus	Species	strain/voucher	ITS	LSU	RPB1	RPB2	TEF1
Hymenochaetales	Hymenochaetaceae	Neomensularia	Neomensularia rectiseta	Dai 15136	KX676497	KX676499			
Hymenochaetales	Hymenochaetaceae	Nothophellinus	Nothophellinus andinopatagonicus	JV 1911/20	MZ484532	MZ437391			
Hymenochaetales	Hymenochaetaceae	Onnia	Onnia leporina	Dai 20866	OM677245	OM677252			OM800829
Hymenochaetales	Hymenochaetaceae	Phellinopsis	Phellinopsis conchata	L-7601	KU139188	KU139257		KU139315	KU139377
Hymenochaetales	Hymenochaetaceae	Phellinotus	Phellinotus piptadeniae	FLOR 63101	MZ954846	MZ964970			OK000619
Hymenochaetales	Hymenochaetaceae	Phellinus	Phellinus castanopsidis	CUI:10157	JQ837945	JQ837957			KU936784
Hymenochaetales	Hymenochaetaceae	Phylloporia	Phylloporia lespedezae	Dai17067	MH151180			MH161212	MH167420
Hymenochaetales	Hymenochaetaceae	Porodaedalea	Porodaedalea microsperma	Cui 12047	ON358117	ON529260	ON604660	ON604672	MG585299
Hymenochaetales	Hymenochaetaceae	Pseudoinonotus	Pseudoinonotus tibeticus	Dai 22974	OL473606	OL473619			
Hymenochaetales	Hymenochaetaceae	Sanghuangporus	Sanghuangporus vaninii	DMR-95-1-T	KU139198	KU139258		KU139318	KU139380
Hymenochaetales	Hymenochaetaceae	Tropicoporus	Tropicoporus drechsleri	CTES 570140	MG242439	MG242444			OK000620
Hymenochaetales	Rickenellaceae	Cantharellopsis	Cantharellopsis prescotii	HRL2135	MF319049	MF318900			

Table C (continued)

Oder	Family	Genus	Species	strain/voucher	ITS	LSU	RPB1	RPB2	TEF1
Hymenochaetales	Rickenellaceae	Rickenella	Rickenella fibula	AFTOL-ID 486	DQ241782	AY700195	DQ832204	DQ408115	DQ435794
Hymenochaetales	Rickenellaceae	Tsugacorticium	Tsugacorticium kenaicum	CFMR:HHB 17347		JN368211			
Hymenochaetales	Schizoporaceae	Hyphodontia	Hyphodontia setulosa	HHB-6891-Sp	KP135382	KP135267	KP134864	KP134901	MZ913650
Hymenochaetales	Schizoporaceae	Kneiffiella	Kneiffiella subalutacea	GEL2196	DQ340341	DQ340362			
Hymenochaetales	Schizoporaceae	Oxyporus	Oxyporus corticola	HMAS:254729		LC164936		KX506082	KX506087
Hymenochaetales	Schizoporaceae	Schizopora	Schizopora radula	MA:Fungi:90707	KY962837	KY962855		KY967061	
Hymenochaetales	Schizoporaceae	Xylodon	Xylodon serpentiformis	LWZ20170818-4	MT319476	MT319213	MT326339		MT326365
Hymenochaetales	Trichaptaceae	Trichaptum	Trichaptum perrottetii	B2626	OQ449093	OQ449032			OQ874777
Hysterangiales	Hysterangiaceae	Aroramyces	Aroramyces gelatinosporus	H4010		DQ218524		DQ218941	DQ219118
Hysterangiales	Hysterangiaceae	Gallacea	Gallacea scleroderma	OSC59621		AY574645		DQ218961	DQ219139
Hysterangiales	Hysterangiaceae	Hysterangium	Hysterangium setchellii	OSC58071		DQ218552		DQ218991	DQ219167
Hysterangiales	Mesophelliaceae	Andebbia	Andebbia pachythrix	OSC58809		DQ218523		DQ218940	DQ219117
Hysterangiales	Mesophelliaceae	Castoreum	Castoreum sp.	OSC122814		DQ218536		DQ218956	DQ219134
Hysterangiales	Mesophelliaceae	Gummiglobus	Gummiglobus agglutinosporus	OSC58784		DQ218544		DQ218967	

Table C (continued)

Oder	Family	Genus	Species	strain/voucher	ITS	LSU	RPB1	RPB2	TEF1
Hysterangiales	Mesophelliaceae	Malajczukia	Malajczukia ingratissima	OSC59296		DQ218509		DQ219031	DQ219209
Hysterangiales	Mesophelliaceae	Mesophellia	Mesophellia trabalis	OSC59282		DQ218592		DQ219036	DQ219214
Hysterangiales	Mesophelliaceae	Nothocastoreum	Nothocastoreum cretaceum	OSC79925		DQ218594		DQ219037	DQ219216
Jaapiales	Jaapiaceae	Jaapia	Jaapia argillacea	CBS:252.74	NR_119766	NG_042523	GU187463	GU187788	GU187711
Phallales	Clathraceae	Abrachium	Abrachium floriforme	UFRN Fungos 1481		NG_058558		JF968442	
Phallales	Clathraceae	Anthurus	Anthurus archeri	REB2182				DQ219081	DQ219260
Phallales	Clathraceae	Aseroe	Aseroe rubra	OSC122632		DQ218625		DQ219082	DQ219261
Phallales	Phallaceae	Dictyophora	Dictyophora duplicata	OSC38819		DQ218481		DQ219087	DQ219265
Phallales	Phallaceae	Ileodictyon	Ileodictyon gracile	MEL2054561		DQ218636		DQ219096	DQ219273
Phallales	Phallaceae	Mutinus	Mutinus verrucosus	UFRN-Fungos 2026	MF447811	MF447809			
Phallales	Phallaceae	Phallus	Phallus dongsun	L 7012	ON566135	ON566153			
Phallales	Phallaceae	Protubera	Protubera nothofagi	OSC59699		AY574644		DQ219040	DQ219219
Phallales	Phallaceae	Staheliomyces	Staheliomyces sp.	UFRN-Fungos 2177	MW546292	MW546307			
Polyporales	Adustoporiaceae	Adustoporia	Adustoporia sinuosa	Cui 16252	OM039269	OM039169	OM037741	OM037767	OM037791
Polyporales	Adustoporiaceae	Austroporia	Austroporia stratosa	Cui 16619	MW377266	MW377346	MW337163	MW337032	MW337095
Polyporales	Adustoporiaceae	Lentoporia	Lentoporia carbonica	Cui 12212	KR605816	KR605755			KR610745
Polyporales	Adustoporiaceae	Resinoporia	Resinoporia cincta	Dai 12739	MG787603	MG787651			MG787870

Table C (continued)

Oder	Family	Genus	Species	strain/voucher	ITS	LSU	RPB1	RPB2	TEF1
Polyporales	Adustoporiaceae	Rhodonia	Rhodonia tianshanensis	Dai 15934	MF462024	MG210494		MG199962	
Polyporales	Auriporiaceae	Auriporia	Auriporia aurea	Cui 10665	KX966182	KX966183			KX966184
Polyporales	Auriporiaceae	Auriporia	Auriporia aurulenta	Cui 2545	MW377262	ON417202			
Polyporales	Cerrenaceae	Cerrena	Cerrena zonata	Cui 18502	ON417154	ON417204	ON424674	ON424758	ON424827
Polyporales	Cerrenaceae	Pseudolagarobasidium	Pseudolagarobasidium baiyunshanensis	Han 405	MT428549	MT428547			
Polyporales	Cerrenaceae	Pseudospongipellis	Pseudospongipellis unicolor	RLG7638sp	KY948751		KY948942		
Polyporales	Cerrenaceae	Radulodon	Radulodon casearius	Cui 17979	ON417185	ON417236	ON424727		ON424868
Polyporales	Dacryobolaceae	Dacryobolus	Dacryobolus montanus	He 6314	ON417157	ON417207		ON424761	ON424832
Polyporales	Dacryobolaceae	Gloeocystidium	Cylindrobasidium ipidophilum	B1472	MN475150	MZ268147			
Polyporales	Epitheliaceae	Epithele	Epithele efibulata	CBS:406.83	MH861622	MH873338			
Polyporales	Fibroporiaceae	Fibroporia	Fibroporia ceracea	Dai 13013	KU550476	KU550490		KU550547	KU550563
Polyporales	Fibroporiaceae	Pseudofibroporia	Pseudofibroporia citrinella	He 20120721	KU550477	KU550500		KU550555	KU550574
Polyporales	Fomitopsidaceae	Antrodia	Antrodia aridula	Dai 24525	OP854667	OP856750		OP851381	OP851386
Polyporales	Fomitopsidaceae	Brunneoporus	Brunneoporus malicola	Cui 7258	MG787586	MG787631	ON424670	MG787806	MG787853

Table C (continued)

Oder	Family	Genus	Species	strain/voucher	ITS	LSU	RPB1	RPB2	TEF1
Polyporales	Fomitopsidaceae	Buglossoporus	Buglossoporus eucalypticola	Dai 13660	KR605808	KR605747		KR610825	KR610736
Polyporales	Fomitopsidaceae	Daedalea	Daedalea radiata	Cui 8624	KR605793	KR605732		ON424762	KR610721
Polyporales	Fomitopsidaceae	Fomitopsis	Fomitopsis abieticola	Cui 10532	MN148230	OL621246		MN158174	MN161745
Polyporales	Fomitopsidaceae	Fuscopostia	Fuscopostia duplicata	Dai 13411	KF699125		KX901174	KR610845	KR610756
Polyporales	Fomitopsidaceae	Neoantrodia	Neoantrodia serialiformis	Dai 19181	ON417169	ON417219	ON424706	ON424783	ON424845
Polyporales	Fomitopsidaceae	Neolentiporus	Neolentiporus sp. SL-2020a	Cui 13923	MW377309	MW377387	ON424708	ON424785	ON424847
Polyporales	Fomitopsidaceae	Rhodofomes	Rhodofomes subfeei	Dai 10430	KR605788	KR605727		KR610792	KR610702
Polyporales	Fomitopsidaceae	Rhodofomitopsis	Rhodofomitopsis africana	Cui 16362	ON417189	ON417240	ON424733	ON424809	ON424873
Polyporales	Fragiliporiaceae	Fragiliporia	Fragiliporia fragilis	Dai 13561	KJ734262	KJ734266		KJ790250	KJ790247
Polyporales	Gelatoporiaceae	Cinereomyces	Cinereomyces fimbriatus	CLZhao 10461	MT809039	NG_154043			
Polyporales	Gelatoporiaceae	Gelatoporia	Gelatoporia subvermispora	Dai 22847	ON417160	ON417210		ON424773	ON424836
Polyporales	Gelatoporiaceae	Obba	Obba rivulosa	Cui 16482	ON417172	ON417222		ON424788	ON424850
Polyporales	Gelatoporiaceae	Sebipora	Sebipora aquosa	Dai 13268	KX161648	KX161661			
Polyporales	Grifolaceae	Grifola	Grifola sordulenta	AFTOL-ID 562	AY854085		AY864879	AY786058	AY885154

Table C (continued)

Oder	Family	Genus	Species	strain/voucher	ITS	LSU	RPB1	RPB2	TEF1
Polyporales	Incrustoporiaceae	Gloeoporellus	Gloeoporellus merulinus	Cui 16650	ON682365	ON680817	ON688472	ON688493	ON688513
Polyporales	Incrustoporiaceae	Skeletocutis	Skeletocutis subalbomarginata	Dai 19599	MN908954	MN905045			
Polyporales	Incrustoporiaceae	Tyromyces	Tyromyces chioneus	Cui 7191	KF698744	KF698755			
Polyporales	Irpicaceae	Ceriporia	Ceriporia aurantiocarnescens	HHB-12714-Sp	KP135046		KP134790		
Polyporales	Irpicaceae	Crystallicutis	Crystallicutis serpens	Wu 1608-81		MZ637109	MZ748435	OK136094	MZ913699
Polyporales	Irpicaceae	Efibula	Efibula gracilis	FD-455	KP135027	MZ637116	KP134804	OK136077	MZ913679
Polyporales	Irpicaceae	Flavodon	Flavodon flavus	Wu 0705-1		MZ637149	MZ748432	OK136087	MZ913683
Polyporales	Irpicaceae	Gloeoporus	Gloeoporus dichrous	Cui 16931	ON682366	ON680818	ON688473	ON688494	ON688514
Polyporales	Irpicaceae	Irpex	Irpex sp.	Wu 910807-35			MZ748433	OK136088	MZ913684
Polyporales	Irpicaceae	Meruliopsis	Meruliopsis albostramineus	HHB-10729	KP135051	KP135229	KP134787	KP134926	
Polyporales	Irpicaceae	Phanerochaetella	Phanerochaetella exilis	HHB-6988-Sp	KP135001	KP135236	KP134799	KP134918	
Polyporales	Ischnodermataceae	Ischnoderma	Ischnoderma benzoinum	Cui 17058	ON417164	ON417214	ON424699	ON424777	ON424839
Polyporales	Laetiporaceae	Laetiporus	Laetiporus sulphureus	AFTOL-ID 769	DQ221108	AY684162	KP134881	DQ408118	
Polyporales	Laetiporaceae	Wolfiporiopsis	Wolfiporiopsis castanopsidis	Cui 16296		MW377409	MW337210	MW337081	MW337152

Table C (continued)

Oder	Family	Genus	Species	strain/voucher	ITS	LSU	RPB1	RPB2	TEF1
Polyporales	Laricifomitaceae	Gilbertsonia	Gilbertsonia angulopora	FP-133019	KC585354	KC585182			
Polyporales	Laricifomitaceae	Laricifomes	Laricifomes officinalis	Kotiranta 27358	ON994757	ON924689	OP022460		
Polyporales	Laricifomitaceae	Ryvardenia	Ryvardenia cretacea	Cui 16731	MW377324	MW337204		MW337077	MW337144
Polyporales	Meripilaceae	Physisporinus	Physisporinus vitreus	Cui 16859	ON417180	ON417230	ON424720	ON424798	ON424859
Polyporales	Meruliaceae	Aurantiporus	Aurantiporus albidus	Cui 16665	ON682354	ON680806	ON688459	ON688480	ON688501
Polyporales	Meruliaceae	Ceriporiopsis	Ceriporiopsis semisupina	Chen 3327	MZ636937	MZ637100	MZ748451	OK136061	MZ913700
Polyporales	Meruliaceae	Climacodon	Climacodon septentrionalis	AFTOL-ID 767	AY854082	AY684165	AY864873	AY780941	AY885151
Polyporales	Meruliaceae	Crustodontia	Crustodontia tongxiniana	CLZhao 5217	MT020778	MT020756	ON892526	ON918558	ON892521
Polyporales	Meruliaceae	Hydnophlebia	Hydnophlebia fissurata	CLZhao 2900			ON892527	ON892536	ON968926
Polyporales	Meruliaceae	Phlebia	Phlebia fuscotuberculata	CLZhao 10239	MT020760	MT020738	ON892525	ON892538	ON936910
Polyporales	Meruliaceae	Sarcodontia	Sarcodontia crocea	BRNM:761841	KX831471	KX831473			
Polyporales	Meruliaceae	Scopuloides	Scopuloides rimosa	Wu 1507-117		MZ637284	MZ748464	OK136048	MZ913666
Polyporales	Panaceae	Cymatoderma	Cymatoderma sp.	OMC1427	KY948826	KY948872	KY948971		
Polyporales	Panaceae	Panus	Panus conchatus	Dai 23421	ON417176	ON417226	ON424716	ON424794	ON424855
Polyporales	Phaeolaceae	Wolfiporia	Wolfiporia hoelen	Dai 20041	MW251878	MW251867		MW250273	MW250262

Table C (continued)

Oder	Family	Genus	Species	strain/voucher	ITS	LSU	RPB1	RPB2	TEF1
Polyporales	Phanerochaetaceae	Bjerkandera	Bjerkandera adusta	Cui 16682	ON682356	ON680808	ON688461	ON688482	ON688503
Polyporales	Phanerochaetaceae	Crepatura	Crepatura ellipsospora	CLZhao 1260	MK343693	MK343697			
Polyporales	Phanerochaetaceae	Donkia	Donkia pulcherrima	TNM:GC 1707-11	LC378994	LC379152	LC379157	LC387351	LC387371
Polyporales	Phanerochaetaceae	Hapalopilus	Hapalopilus rutilans	FP-102473-Sp	MZ636981	MZ637142	MZ748407	OK136004	MZ913723
Polyporales	Phanerochaetaceae	Hyphodermella	Hyphodermella rosae	GC 1608-2		MZ637148	MZ748411	OK135983	MZ913592
Polyporales	Phanerochaetaceae	Phanerochaete	Phanerochaete ginnsii	Wu 9210-22	MZ422807	MZ637193	MZ748402		MZ913614
Polyporales	Phanerochaetaceae	Phanerodontia	Phanerodontia chrysosporium	PC139	MZ422797	MZ637186	MZ748405	OK136036	MZ913606
Polyporales	Phanerochaetaceae	Rhizochaete	Rhizochaete fouquieriae	KKN-121	AY219390		MZ748362	OK135988	MZ913708
Polyporales	Phanerochaetaceae	Roseograndinia	Roseograndinia jilinensis	Wu 1307-132		MZ637274	MZ748412	OK135984	MZ913631
Polyporales	Piptoporellaceae	Piptoporellus	Piptoporellus triqueter	Dai 13121	KR605807	KR605746		KR610827	KR610738
Polyporales	Podoscyphaceae	Abortiporus	Abortiporus biennis	Cui 17845	ON417149	ON417197	ON424663	ON424750	ON424821
Polyporales	Podoscyphaceae	Podoscypha	Podoscypha venustula	Cui 16923	ON417181	ON417231	ON424722	ON424799	ON424860
Polyporales	Polyporaceae	Abundisporus	Abundisporus mollissimus	Cui 6257	NR_154677	NG_057015			KF181156
Polyporales	Polyporaceae	Amauroderma	Amauroderma subresinosum	Dai 18634	MK119825	MK119904		MK121508	MK121573
Polyporales	Polyporaceae	Cerioporus	Cerioporus mollis	Cui 16224	OK642176	OK642227		OK665311	OK665191

Table C (continued)

Oder	Family	Genus	Species	strain/voucher	ITS	LSU	RPB1	RPB2	TEF1
Polyporales	Polyporaceae	Coriolopsis	Coriolopsis dendriformis	Cui 6719	KC867408	NG_075183			OK665193
Polyporales	Polyporaceae	Crassisporus	Crassisporus leucoporus	Cui 16801	MK116488	MK116497		MK122993	MK122986
Polyporales	Polyporaceae	Cryptoporus	Cryptoporus sinensis	Cui 17418	OK642180	OK642231			OK665196
Polyporales	Polyporaceae	Daedaleopsis	Daedaleopsis septentrionalis	Dai2802a	KU892443	KU892473			
Polyporales	Polyporaceae	Datroniella	Datroniella sp.	Cui 10646			KX885084		KX838425
Polyporales	Polyporaceae	Dentocorticium	Dentocorticium sulphurellum	FP11801	JN165018			JN164876	JN164903
Polyporales	Polyporaceae	Earliella	Earliella scabrosa	Cui 16857	OK642184	OK642237	OK665277	OK665315	OK665201
Polyporales	Polyporaceae	Favolus	Favolus pseudogrammocephalus	MP218	MN648689	MN648717			
Polyporales	Polyporaceae	Fomes	Fomes fomentarius	Cui 14094	OK642186	OK642239			OK665203
Polyporales	Polyporaceae	Fomitella	Fomitella supina	17695 (H)	KY948711	KY948841	KY948910		
Polyporales	Polyporaceae	Funalia	Funalia cystidiata	Cui 14378	OK642187	OK642240		OK665316	OK665205
Polyporales	Polyporaceae	Ganoderma	Ganoderma hoehnelianum	Cui 13982	MG279178	MZ355071		MG367515	MG367570
Polyporales	Polyporaceae	Grammothele	Grammothele hainanensis	Cui 14514	OK642191	OK642246	OK665282		OK665209

Table C (continued)

Oder	Family	Genus	Species	strain/voucher	ITS	LSU	RPB1	RPB2	TEF1
Polyporales	Polyporaceae	Grammothelopsis	Grammothelopsis subtropica	Cui 9035	NR_158463	NG_060642			KF181124
Polyporales	Polyporaceae	Haploporus	Haploporus nepalensis	Cui 10729	KU941856	KU941880		KU941927	KU941943
Polyporales	Polyporaceae	Hexagonia	Hexagonia cucullata	Cui 8707	KX880623	KX880662			KX880881
Polyporales	Polyporaceae	Jorgewrightia	Jorgewrightia tropica	Cui 13660	KY449437	KY449448			MZ618630
Polyporales	Polyporaceae	Lenzites	Lenzites betulinus	Cui 16971	OK642201	OK642256	OK665292		OK665222
Polyporales	Polyporaceae	Lignosus	Lignosus rhinocerotis	Benjamin143		KX900694		KX900803	KX900833
Polyporales	Polyporaceae	Lopharia	Lopharia cinerascens	FP105043sp	JN165019	JN164813	JN164840	JN164874	JN164900
Polyporales	Polyporaceae	Mariorajchenbergia	Mariorajchenbergia subcavernulosa	Cui 10050		OK642253	OK665288	OK665327	OK665220
Polyporales	Polyporaceae	Megasporoporia	Megasporoporia minuta	Cui 13945	OK642178	OK642229		OK665312	OK665194
Polyporales	Polyporaceae	Megasporoporiella	Megasporoporiella lacerata	Yuan 3874	OK642199	MW694926	MZ029049		OL687159
Polyporales	Polyporaceae	Melanoderma	Melanoderma microcarpum	Cui 10970	KX900662	KX900712	KX900791	KX900814	KX900845
Polyporales	Polyporaceae	Microporus	Microporus affinis	Cui 8818	KX880614	KX880654			KX880874
Polyporales	Polyporaceae	Neodatronia	Neodatronia sinensis	Cui 14457	OK642177	OK642228	OK665274		OK665192
Polyporales	Polyporaceae	Neofavolus	Neofavolus squamatus	Cui 12175	KX900070	NG_075213		KX900317	KX900370

Table C (continued)

Oder	Family	Genus	Species	strain/voucher	ITS	LSU	RPB1	RPB2	TEF1
Polyporales	Polyporaceae	Neofomitella	Neofomitella australiensis	Cui 16642	MK192444	MK192464	MK192517		MK192534
Polyporales	Polyporaceae	Perenniporia	Perenniporia hainaniana	Cui 6364	JQ861743	NG_060100			KF181138
Polyporales	Polyporaceae	Perenniporiella	Perenniporiella chaquenia	MUCL 49758	FJ411085	NG_042478			HM467602
Polyporales	Polyporaceae	Picipes	Picipes ailaoshanensis	Cui 12578	KX900067			KX900315	KX900368
Polyporales	Polyporaceae	Polyporus	Polyporus squamosus	AFTOL-ID 704	DQ267123	AY629320	DQ831023	DQ408120	DQ028601
Polyporales	Polyporaceae	Porogramme	Porogramme cylindrica	Dai 22348		ON261644	OP556544	OP556576	OP556564
Polyporales	Polyporaceae	Pseudofavolus	Pseudofavolus cucullatus	Dai 13584	KX900071	KX900185			KX900371
Polyporales	Polyporaceae	Pycnoporus	Pycnoporus sp. ZW02.30	AFTOL-ID 772	DQ411525	AY684160		DQ408121	DQ028600
Polyporales	Polyporaceae	Sanguinoderma	Sanguinoderma sp. YFS-2022b	Dai 20438	OP700314	OP700347		OP696848	OP696869
Polyporales	Polyporaceae	Sparsitubus	Sparsitubus nelumbiformis	Cui 6590	KX880632	MG847268	KX880819		KX880888
Polyporales	Polyporaceae	Tomophagus	Tomophagus cattienensis	Dai 18487	MZ354988			MZ358845	MZ221747

Table C (continued)

Oder	Family	Genus	Species	strain/voucher	ITS	LSU	RPB1	RPB2	TEF1
Polyporales	Polyporaceae	Trametes	Trametes cystidiolophora	Cui 8087	KX880635	KX880677		KX880858	KX880894
Polyporales	Polyporaceae	Vanderbylia	Vanderbylia cinnamomea	CLZhao 8961	MT372780	MT372790			
Polyporales	Postiaceae	Amaropostia	Amaropostia hainanensis	Cui 5367	KX900910	KX900980	KX901172	KX901224	
Polyporales	Postiaceae	Aurantipostia	Aurantipostia macrospora	Cui 16604	MW377258		MW337157	MW337026	MW337089
Polyporales	Postiaceae	Austropostia	Austropostia plumbea	Cui 16550	MW377270		MW337167	MW337036	MW337099
Polyporales	Postiaceae	Cyanosporus	Cyanosporus magnus	Cui 16983	MW182180	MW182234	MW191555	MW191569	MW191539
Polyporales	Postiaceae	Oligoporus	Oligoporus romellii	Dai 21034	MW377312	MW377390	MW337198	ON424790	MW337135
Polyporales	Postiaceae	Osteina	Osteina undosa	Cui 16651	MW377313	MW377391	MW337199	MW337069	MW337136
Polyporales	Postiaceae	Postia	Postia sublowei	Cui 9597	KX900900	KX900970			KX901265
Polyporales	Sparassidaceae	Sparassis	Sparassis crispa	AFTOL-ID 703	DQ250597	AY629321		DQ408122	DQ056289
Polyporales	Steccherinaceae	Antrodiella	Antrodiella micra	CLZhao 10185	MZ713651	MZ713834	OK000925	OK000937	OK000964
Polyporales	Steccherinaceae	Cabalodontia	Cabalodontia albofibrillosa	CLZhao 8722	MZ713669	MZ713811			
Polyporales	Steccherinaceae	Loweomyces	Loweomyces fractipes	RP 197	KP859304	KP859309			
Polyporales	Steccherinaceae	Steccherinum	Steccherinum xanthum	CLZhao 5044	MW204590	MW204579	OK000936		OK000983

Table C (continued)

Oder	Family	Genus	Species	strain/voucher	ITS	LSU	RPB1	RPB2	TEF1
Polyporales	Taiwanofungaceae	Taiwanofungus	Taiwanofungus camphoratus	Cui 17235	MW377328	MW377405	ON424748		MW337148
Polyporales	Taiwanofungaceae	Taiwanofungus	Taiwanofungus salmoneus	B147	EU232202	EU232278			
Russulales	Albatrellaceae	Albatrellopsis	Albatrellopsis flettii	Dai 12873	MW807370	MW811451			
Russulales	Auriscalpiaceae	Artomyces	Artomyces microsporus	ZRL2015014	LT716081	KY418906	KY418986	KY419042	
Russulales	Auriscalpiaceae	Auriscalpium	Auriscalpium microsporum	HKAS:87012	KY485963	KY485991		KY495316	
Russulales	Bondarzewiaceae	Bondarzewia	Bondarzewia occidentalis	HHB 14803	KM243329	KM243332	KX066163		KX066142
Russulales	Bondarzewiaceae	Heterobasidion	Heterobasidion annosum	AFTOL-ID 470	DQ206988		DQ667160	AH013701	DQ028583
Russulales	Bondarzewiaceae	Lauriliella	Lauriliella taiwanensis	Yao7025	KY434105	KY425690			
Russulales	Bondarzewiaceae	Lauriliella	Lauriliella taxodii	FP-106256-Sp	KY172898	KY172913			
Russulales	Echinodontiaceae	Echinodontiellum	Echinodontiellum japonicum	Dai7378	KY172887	KY172902			
Russulales	Echinodontiaceae	Echinodontium	Echinodontium tinctorium	AFTOL-ID 455	AY854088		AY864882	AY218482	AY885157
Russulales	Hericiaceae	Hericium	Hericium americanum	AFTOL-ID 469	DQ206987	DQ411538		DQ408127	DQ028585

Table C (continued)

Oder	Family	Genus	Species	strain/voucher	ITS	LSU	RPB1	RPB2	TEF1
Russulales	Hericiaceae	Pseudowrightoporia	Pseudowrightoporia crassihypha	Yuan 6247	KM107873	KM107892			
Russulales	Hericiaceae	Wrightoporiopsis	Wrightoporiopsis amylohypha	Yuan 3579	KM107877	KM107896			
Russulales	Lachnocladiaceae	Lachnocladium	Lachnocladium sp.	AFTOL-ID 1556	DQ192176	DQ154110			
Russulales	Russulaceae	Lactarius	Lactarius lignyotus	AFTOL-ID 681	DQ221107	AY631898		DQ408128	DQ435787
Russulales	Russulaceae	Lactifluus	Lactifluus sp. VH-2016	253/BB 98.029		KU237489	KU237638	KU237775	KU237918
Russulales	Russulaceae	Multifurca	Multifurca ochricompacta	580/BB 07.010		KU237565	KU237709	KU237851	KU237994
Russulales	Russulaceae	Russula	Russula nigrocarpa	K19071603	MN688794	NG_153890	MT085531	MT085662	MT085630
Russulales	Stereaceae	Acanthobasidium	Acanthobasidium delicatum	CBS:233.86	MH861948	MH873638			
Russulales	Stereaceae	Acanthophysium	Acanthophysium bisporum	CBS 239.86	NR_159629	NG_067431			
Russulales	Stereaceae	Conferticium	Conferticium ochraceum	He6072	OM100742	OM083974			
Russulales	Stereaceae	Neoaleurodiscus	Neoaleurodiscus fujii	Wu0807-41	FJ799922	FJ799924			
Russulales	Stereaceae	Stereodiscus	Stereodiscus trivialis	FQ1611	OP964613	OP558006			
Russulales	Terrestriporiaceae	Terrestriporia	Terrestriporia alba	Dai18556			MW290317	MW290308	MW290325
Russulales	Wrightoporiaceae	Amylosporus	Amylosporus annosus	BJFC:Dai 18638	MH647058	MH647054			

Table C (continued)

Oder	Family	Genus	Species	strain/voucher	ITS	LSU	RPB1	RPB2	TEF1
Sebacinales	Sebacinaceae	Ditangium	Ditangium altaicum	LE 231836	MH836338				MH910034
Sebacinales	Sebacinaceae	Ditangium	Ditangium cerasi	LE 254072	MH836335				MH910028
Sebacinales	Sebacinaceae	Ditangium	Ditangium incarnatum	LE 303419	MH836337				MH910032
Sebacinales	Sebacinaceae	Paulisebacina	Paulisebacina allantoidea	RoKi 179	KF061266	AF291367		KF061301	
Sebacinales	Sebacinaceae	Tremelloscypha	Tremelloscypha dichroa	Ryvarden 45376	KF061283			KF061308	
Sebacinales	Sebacinaceae	Tremelloscypha	Tremelloscypha gelatinosa	GG 23605	AF490394	AF291376			
Sebacinales	Serendipitaceae	Serendipita	Piriformospora indica		DQ411527			DQ408131	
Thelephorales	Bankeraceae	Bankera	Bankera fuligineoalba	REB-285	JN135196			KF007978	
Thelephorales	Bankeraceae	Bankera	Bankera violascens	RGC14-033	MH310793			OK632674	
Thelephorales	Bankeraceae	Boletopsis	Boletopsis tibetana	Dai 20896	OL673013	OL673000			
Thelephorales	Bankeraceae	Phellodon	Phellodon cinereofuscus	Cui 16962	MZ225583	MZ225605	MZ352084	MZ343200	
Thelephorales	Thelephoraceae	Amaurodon	Amaurodon caeruleocaseus	MEL 2231735	NR_182441	NG_153840			
Thelephorales	Thelephoraceae	Hydnellum	Hydnellum fibulatum	Yuan14656	MW579958				
Thelephorales	Thelephoraceae	Lenzitopsis	Lenzitopsis daii	TU115383		MT732078		MT724774	
Thelephorales	Thelephoraceae	Lenzitopsis	Lenzitopsis oxycedri	TU115268		MT732079		MT724775	

Table C (continued)

Oder	Family	Genus	Species	strain/voucher	ITS	LSU	RPB1	RPB2	TEF1
Thelephorales	Thelephoraceae	Polyozellus	Polyozellus marymargaretae	TU117347	MF100841	MT732082		MT724778	
Thelephorales	Thelephoraceae	Thelephora	Thelephora ganbajun	ZRL20151295	LT716082	KY418908	KY418987	KY419043	KY419093
Thelephorales	Thelephoraceae	Tomentella	Tomentella sp.	AFTOL-ID 1016	DQ835998	DQ835997		DQ835999	
Trechisporales	Hydnodontaceae	Dextrinocystis	Dextrinocystis calamicola	He5700	MK204534	MK204547			
Trechisporales	Hydnodontaceae	Litschauerella	Litschauerella gladiola	He3171	MK204555	MK204556			
Trechisporales	Hydnodontaceae	Porpomyces	Porpomyces submucidus	Dai 13708	KT152144	KT152146			MW478702
Trechisporales	Hydnodontaceae	Scytinopogon	Scytinopogon havencampii	SFSU:DED8300	KT253946	KT253947			
Tremellales	Bulleraceae	Bullera	Bullera dendrophila	CBS 6074	FJ534871	FJ534901	FJ534917	FJ534933	FJ534856
Tremellales	Bulleraceae	Fonsecazyma	Fonsecazyma sp.	YN107M4	OP470252	OP470156	OP784833	OP771439	
Tremellales	Bulleraceae	Genolevuria	Genolevuria paynescottiae	BRIP 45079a	OK626335	OK626336			
Tremellales	Bulleraceae	Pseudotremella	Pseudotremella nivalis	Dai20670				OL880274	OL880349
Tremellales	Bulleribasidiaceae	Bulleribasidium	Bulleribasidium sp.	ZJ1541			OL952764	OL952775	OM103764
Tremellales	Bulleribasidiaceae	Derxomyces	Derxomyces sp.	MT-4A-7	OP470245	OP470149	OP784827	OP771432	
Tremellales	Bulleribasidiaceae	Dioszegia	Dioszegia aff. Patagonica	EPV358K3	OR123531				OR139194
Tremellales	Bulleribasidiaceae	Hannaella	Hannaella sp.	YN14M1	OP470256	OP470160	OP784837	OP771443	

Table C (continued)

Oder	Family	Genus	Species	strain/voucher	ITS	LSU	RPB1	RPB2	TEF1
Tremellales	Bulleribasidiaceae	Vishniacozyma	Vishniacozyma foliicola	EPV158K7	OR123553	OR123679			OR139201
Tremellales	Carcinomycetaceae	Carcinomyces	Bullera arundinariae	CBS9931			KF036319	KF036732	KF037004
Tremellales	Cryptococcaceae	Cryptococcus	Cryptococcus humicola	AFTOL-ID 1552	DQ645516	DQ645514	DQ645518	DQ645517	DQ645519
Tremellales	Cryptococcaceae	Kwoniella	Kwoniella mangroviensis	CBS 10435	EF174040		HE997000	HE996974	HE997047
Tremellales	Cryptococcaceae	Teunia	Teunia rudbeckiae	CGMCC2.5840			MT268698		MT268695
Tremellales	Naemateliaceae	Dimennazyma	Dimennazyma cisti-albidi	CBS:10049	KY103339				
Tremellales	Naemateliaceae	Naematelia	Naematelia encephala	CBS6968	AF410474		KF036525	KF036941	KF037203
Tremellales	Phaeotremellaceae	Gelidatrema	Gelidatrema spencermartinsiae	CBS 10760	NR_137691				
Tremellales	Phaeotremellaceae	Phaeotremella	Phaeotremella eugeniae	LE 303429	NR_158846	NG_060192			MF095825
Tremellales	Rhynchogastremaceae	Bandoniozyma	Bandoniozyma complexa	CBS11570			KF036317	KF036730	KF037002
Tremellales	Rhynchogastremaceae	Papiliotrema	Papiliotrema bandonii	CBS9107	GU327539		KF036518	KF036932	KF037194
Tremellales	Rhynchogastremaceae	Rhynchogastrema	Rhynchogastrema tunnelae	CBS:8024	NR_111074	NG_042390			

Table C (continued)

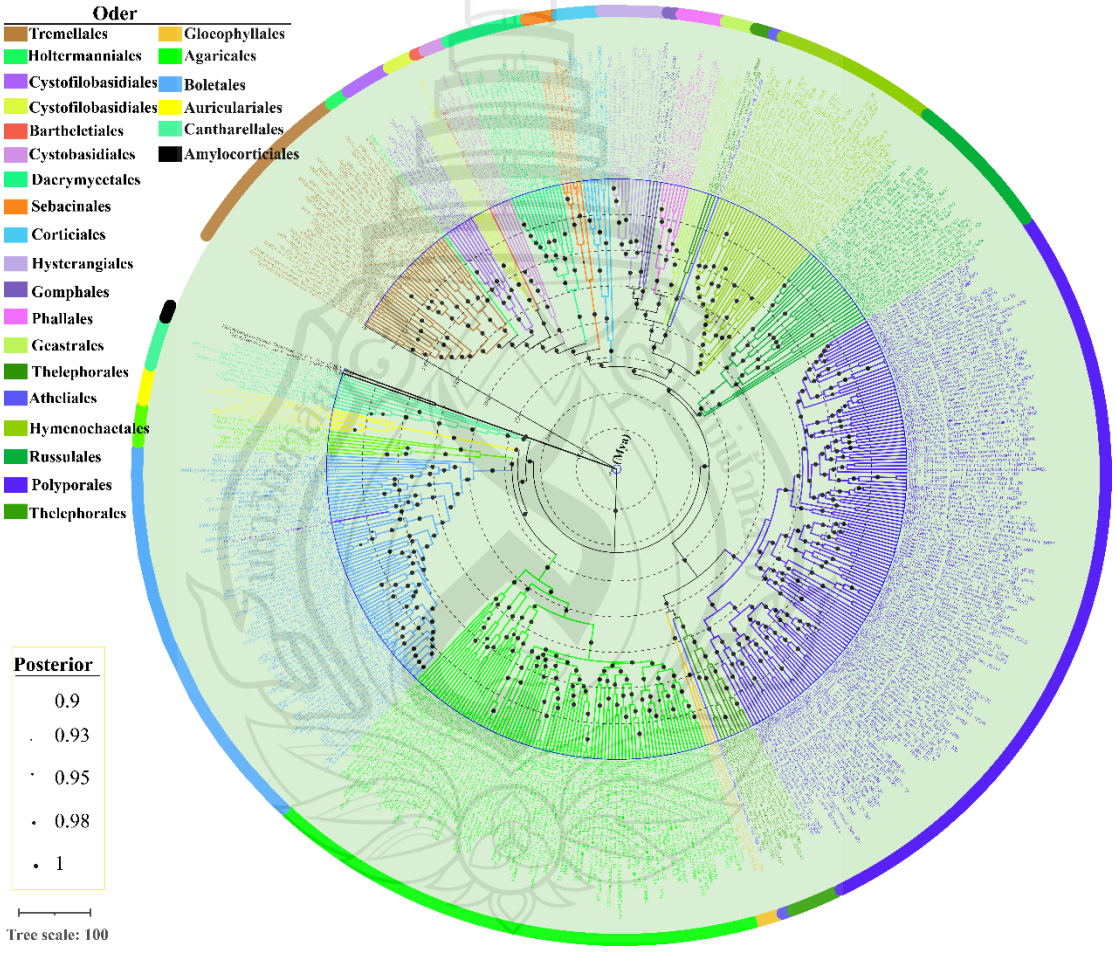
Oder	Family	Genus	Species	strain/voucher	ITS	LSU	RPB1	RPB2	TEF1
Tremellales	Sirobasidiaceae	Fibulobasidium	Fibulobasidium murrhardtense	CBS:9109	NR_121466	NG_058289			
Tremellales	Sirobasidiaceae	Sirobasidium	Sirobasidium magnum	CBS 6803	AF444314		KF036520	KF036935	KF037197
Tremellales	Syzygosporaceae	Syzygospora	Syzygospora alba	AM147	JN053509	JN043616			
Tremellales	Tetragoniomycetaceae	Bandonia	Bandonia marina	CBS 5235	NR_144778	NG_058617			
Tremellales	Tetragoniomycetaceae	Cryptotrichosporon	Cryptotrichosporon anacardii	CBS 9551	AY549985	AY550002	KF036417	KF036830	KF037101
Tremellales	Tetragoniomycetaceae	Takashimella	Takashimella lagerstroemiae	CBS 10483	NR_154532	NG_067313			
Tremellales	Tetragoniomycetaceae	Tetragoniomyces	Tetragoniomyces uliginosus	AM186	JN053514	JN043621			
Tremellales	Tremellaceae	Biatoropsis	Biatoropsis usnearum	AM144	KJ404858	KJ437203			
Tremellales	Tremellaceae	Tremella	Tremella mesenterica	Dai18046			OL880438	OL880303	OL880371
Trichosporonales	Trichosporonaceae	Aegeritella	Aegeritella tuberculata	WA51216	KT259307	KT380846			
Trichosporonales	Trichosporonaceae	Apiotrichum	Apiotrichum porosum	CBS:2040	KY101689	KY106143			
Trichosporonales	Trichosporonaceae	Cutaneotrichosporon	Cutaneotrichosporon suis	NCAIM Y.02224	MH886393	MH886396			
Trichosporonales	Trichosporonaceae	Haglerozyma	Haglerozyma chiarellii	CBS 11177	KY103494	KY107775			

Table C (continued)

Oder	Family	Genus	Species	strain/voucher	ITS	LSU	RPB1	RPB2	TEF1
Trichosporonales	Trichosporonaceae	Pascua	Pascua guehoae	CBS8521	AF410476				
Trichosporonales	Trichosporonaceae	Prillingera	Prillingera fragicola	WSWS01	MW450478	MW466578			
Naohideales	Naohideaceae	Naohidea	Naohidea sebcea	CBS 8477	DQ911616	NG_042442	KF706508	KF706535	KF706487
Erythrobasidiales	Erythrobasidiaceae	Cyrenella	Cyrenella elegans	CBS:274.82	MH861497	NG_058875	KJ708080	KJ708168	
Cystobasidiales	Microsporomycetaceae	Microsporomyces	Microsporomyces magnisporus	JCM 11898			KJ708013	KJ708317	KJ707780
Sakaguchia	Sakaguchiaceae	Sakaguchia	Sakaguchia lamellibrachiae	CBS:9598	KY105306	KY109533	KJ708098	KJ708314	KJ707876
Erythrobasidiales	Erythrobasidiaceae	Bannoa	Bannoa bischofiae	JCM 10338	B035721	NG_058609	KJ708018	KJ708292	KJ707777
Erythrobasidiales	Erythrobasidiaceae	Erythrobasidium	Erythrobasidium hasegawianum	AS2.1923			KF706506	KF706534	KJ707776

APPENDIX D

THE DETAILED INFORMATION OF AGARICOMYCOTINA



Note Posterior probabilities that are equal to or greater than 0.9 are annotated order.

Figure D Maximum clade credibility tree of Agaricomycotina based on ITS, LSU, RPB1, RPB2 and TEF1 genes

APPENDIX E

THE AVERAGE COMPONENTS OF 11 SPECIES OF BOLETES

Table E1 Near infrared spectroscopy of 11 species of Boletes

Wavenumbers (cm-1)	BoB	NH	NM	BuR	LA	NO	PP	RetF	RubS	RugE	BuP
7497.88	0.0927	0.0893	0.0893	0.0800	0.0838	0.1064	0.0928	0.0941	0.0912	0.0939	0.0900
7494.02	0.0929	0.0895	0.0894	0.0802	0.0839	0.1065	0.0929	0.0942	0.0914	0.0941	0.0901
7490.16	0.0930	0.0896	0.0896	0.0803	0.0840	0.1066	0.0930	0.0943	0.0915	0.0943	0.0902
7486.31	0.0932	0.0897	0.0897	0.0804	0.0841	0.1067	0.0932	0.0944	0.0917	0.0945	0.0904
7482.45	0.0933	0.0899	0.0899	0.0805	0.0842	0.1068	0.0933	0.0945	0.0918	0.0947	0.0905
7478.59	0.0934	0.0900	0.0900	0.0807	0.0843	0.1069	0.0935	0.0946	0.0919	0.0949	0.0907
7474.74	0.0936	0.0901	0.0902	0.0808	0.0844	0.1070	0.0936	0.0947	0.0921	0.0951	0.0908
7470.88	0.0937	0.0903	0.0903	0.0810	0.0846	0.1071	0.0938	0.0948	0.0922	0.0953	0.0909
7467.02	0.0939	0.0904	0.0905	0.0811	0.0847	0.1072	0.0939	0.0949	0.0924	0.0955	0.0911
7463.17	0.0940	0.0905	0.0907	0.0813	0.0848	0.1074	0.0941	0.0950	0.0926	0.0957	0.0912

Table E1 (continued)

Wavenumbers (cm-1)	BoB	NH	NM	BuR	LA	NO	PP	RetF	RubS	RugE	BuP
7459.31	0.0942	0.0907	0.0908	0.0814	0.0850	0.1075	0.0942	0.0952	0.0927	0.0959	0.0914
7455.45	0.0943	0.0908	0.0910	0.0816	0.0851	0.1076	0.0944	0.0953	0.0929	0.0961	0.0916
7451.6	0.0945	0.0910	0.0912	0.0817	0.0853	0.1078	0.0945	0.0954	0.0931	0.0964	0.0917
7447.74	0.0947	0.0912	0.0914	0.0819	0.0854	0.1079	0.0947	0.0956	0.0932	0.0966	0.0919
7443.88	0.0949	0.0914	0.0916	0.0821	0.0856	0.1080	0.0949	0.0957	0.0934	0.0968	0.0921
7440.02	0.0951	0.0915	0.0918	0.0822	0.0857	0.1082	0.0951	0.0959	0.0936	0.0971	0.0923
7436.17	0.0953	0.0917	0.0920	0.0824	0.0859	0.1083	0.0953	0.0960	0.0938	0.0973	0.0925
7432.31	0.0955	0.0919	0.0922	0.0826	0.0861	0.1085	0.0955	0.0962	0.0940	0.0976	0.0927
7428.45	0.0957	0.0921	0.0925	0.0828	0.0862	0.1086	0.0957	0.0963	0.0942	0.0979	0.0929
7424.6	0.0959	0.0923	0.0927	0.0830	0.0864	0.1088	0.0959	0.0965	0.0944	0.0981	0.0931
7420.74	0.0961	0.0925	0.0929	0.0832	0.0866	0.1089	0.0961	0.0967	0.0947	0.0984	0.0933
7416.88	0.0963	0.0926	0.0931	0.0834	0.0868	0.1091	0.0963	0.0969	0.0949	0.0987	0.0936
7413.03	0.0965	0.0928	0.0934	0.0836	0.0870	0.1093	0.0965	0.0970	0.0951	0.0990	0.0938
7409.17	0.0967	0.0930	0.0936	0.0838	0.0872	0.1094	0.0967	0.0972	0.0953	0.0992	0.0940
7405.31	0.0969	0.0933	0.0939	0.0840	0.0873	0.1096	0.0970	0.0974	0.0955	0.0995	0.0943
7401.46	0.0972	0.0935	0.0941	0.0842	0.0875	0.1098	0.0972	0.0976	0.0958	0.0998	0.0945
7397.6	0.0974	0.0937	0.0944	0.0844	0.0877	0.1100	0.0974	0.0978	0.0960	0.1001	0.0947
7393.74	0.0976	0.0939	0.0946	0.0847	0.0880	0.1101	0.0977	0.0980	0.0963	0.1004	0.0950
7389.88	0.0978	0.0941	0.0948	0.0848	0.0881	0.1103	0.0978	0.0982	0.0964	0.1006	0.0952
7386.03	0.0980	0.0942	0.0950	0.0850	0.0883	0.1104	0.0980	0.0983	0.0966	0.1008	0.0954
7382.17	0.0982	0.0943	0.0952	0.0851	0.0884	0.1106	0.0982	0.0985	0.0968	0.1011	0.0956

Table E1 (continued)

Wavenumbers (cm-1)	BoB	NH	NM	BuR	LA	NO	PP	RetF	RubS	RugE	BuP
7378.31	0.0983	0.0944	0.0954	0.0853	0.0886	0.1107	0.0983	0.0987	0.0969	0.1013	0.0958
7374.46	0.0985	0.0947	0.0957	0.0855	0.0888	0.1109	0.0986	0.0989	0.0972	0.1016	0.0960
7370.6	0.0988	0.0949	0.0959	0.0858	0.0890	0.1110	0.0988	0.0991	0.0974	0.1019	0.0963
7366.74	0.0990	0.0951	0.0962	0.0860	0.0892	0.1112	0.0990	0.0993	0.0977	0.1022	0.0965
7362.89	0.0992	0.0954	0.0964	0.0863	0.0895	0.1114	0.0993	0.0995	0.0979	0.1025	0.0967
7359.03	0.0994	0.0956	0.0966	0.0865	0.0896	0.1115	0.0994	0.0997	0.0981	0.1027	0.0969
7355.17	0.0996	0.0957	0.0968	0.0866	0.0898	0.1117	0.0996	0.0998	0.0983	0.1029	0.0971
7351.31	0.0997	0.0959	0.0970	0.0868	0.0900	0.1118	0.0997	0.1000	0.0984	0.1031	0.0973
7347.46	0.0999	0.0961	0.0972	0.0870	0.0901	0.1119	0.0999	0.1002	0.0986	0.1033	0.0975
7343.6	0.1000	0.0961	0.0974	0.0871	0.0902	0.1120	0.1000	0.1003	0.0987	0.1035	0.0977
7339.74	0.1002	0.0961	0.0976	0.0872	0.0904	0.1121	0.1002	0.1005	0.0988	0.1037	0.0978
7335.89	0.1003	0.0964	0.0977	0.0874	0.0905	0.1123	0.1004	0.1006	0.0990	0.1040	0.0980
7332.03	0.1005	0.0968	0.0979	0.0877	0.0907	0.1124	0.1005	0.1007	0.0993	0.1042	0.0981
7328.17	0.1007	0.0969	0.0981	0.0878	0.0908	0.1125	0.1007	0.1009	0.0995	0.1044	0.0983
7324.32	0.1009	0.0971	0.0983	0.0880	0.0910	0.1127	0.1009	0.1011	0.0996	0.1047	0.0985
7320.46	0.1011	0.0973	0.0986	0.0882	0.0912	0.1129	0.1011	0.1013	0.0999	0.1050	0.0987
7316.6	0.1013	0.0976	0.0988	0.0885	0.0914	0.1130	0.1014	0.1015	0.1001	0.1053	0.0989
7312.75	0.1015	0.0978	0.0990	0.0886	0.0916	0.1132	0.1015	0.1017	0.1003	0.1055	0.0991
7308.89	0.1017	0.0979	0.0992	0.0888	0.0917	0.1133	0.1017	0.1018	0.1005	0.1057	0.0993
7305.03	0.1019	0.0981	0.0994	0.0890	0.0919	0.1135	0.1019	0.1020	0.1007	0.1059	0.0995
7301.17	0.1020	0.0983	0.0996	0.0892	0.0921	0.1136	0.1020	0.1022	0.1009	0.1062	0.0997

Table E1 (continued)

Wavenumbers (cm-1)	BoB	NH	NM	BuR	LA	NO	PP	RetF	RubS	RugE	BuP
7297.32	0.1022	0.0985	0.0998	0.0893	0.0922	0.1138	0.1022	0.1023	0.1011	0.1064	0.0999
7293.46	0.1024	0.0987	0.1000	0.0896	0.0924	0.1139	0.1024	0.1025	0.1013	0.1067	0.1001
7289.6	0.1026	0.0990	0.1002	0.0898	0.0926	0.1141	0.1026	0.1027	0.1015	0.1069	0.1003
7285.75	0.1028	0.0992	0.1005	0.0900	0.0928	0.1143	0.1028	0.1029	0.1017	0.1072	0.1005
7281.89	0.1030	0.0994	0.1007	0.0902	0.0930	0.1144	0.1030	0.1031	0.1020	0.1075	0.1008
7278.03	0.1032	0.0997	0.1009	0.0904	0.0932	0.1146	0.1032	0.1033	0.1022	0.1077	0.1010
7274.18	0.1034	0.0999	0.1011	0.0906	0.0934	0.1148	0.1035	0.1036	0.1025	0.1080	0.1012
7270.32	0.1037	0.1002	0.1014	0.0908	0.0936	0.1150	0.1037	0.1038	0.1027	0.1083	0.1014
7266.46	0.1038	0.1004	0.1016	0.0910	0.0937	0.1152	0.1038	0.1039	0.1029	0.1085	0.1016
7262.61	0.1040	0.1006	0.1017	0.0911	0.0939	0.1153	0.1040	0.1041	0.1031	0.1087	0.1018
7258.75	0.1041	0.1007	0.1019	0.0913	0.0940	0.1155	0.1041	0.1042	0.1032	0.1089	0.1019
7254.89	0.1043	0.1009	0.1021	0.0914	0.0942	0.1156	0.1043	0.1043	0.1034	0.1092	0.1021
7251.03	0.1044	0.1010	0.1023	0.0915	0.0943	0.1157	0.1044	0.1045	0.1035	0.1093	0.1022
7247.18	0.1044	0.1010	0.1024	0.0915	0.0944	0.1159	0.1045	0.1046	0.1036	0.1095	0.1024
7243.32	0.1045	0.1011	0.1025	0.0916	0.0945	0.1160	0.1045	0.1046	0.1037	0.1096	0.1025
7239.46	0.1046	0.1011	0.1027	0.0916	0.0945	0.1161	0.1046	0.1047	0.1037	0.1098	0.1026
7235.61	0.1047	0.1013	0.1029	0.0918	0.0947	0.1163	0.1047	0.1049	0.1039	0.1100	0.1028
7231.75	0.1049	0.1015	0.1031	0.0920	0.0949	0.1165	0.1050	0.1051	0.1042	0.1103	0.1031
7227.89	0.1051	0.1017	0.1034	0.0921	0.0951	0.1167	0.1052	0.1053	0.1044	0.1106	0.1033
7224.04	0.1054	0.1019	0.1036	0.0923	0.0953	0.1169	0.1054	0.1055	0.1046	0.1109	0.1035
7220.18	0.1057	0.1023	0.1040	0.0926	0.0955	0.1172	0.1057	0.1058	0.1050	0.1113	0.1039

Table E1 (continued)

Wavenumbers (cm-1)	BoB	NH	NM	BuR	LA	NO	PP	RetF	RubS	RugE	BuP
7216.32	0.1060	0.1027	0.1044	0.0929	0.0959	0.1176	0.1060	0.1061	0.1054	0.1118	0.1042
7212.47	0.1064	0.1032	0.1048	0.0933	0.0962	0.1180	0.1064	0.1064	0.1059	0.1123	0.1046
7208.61	0.1068	0.1037	0.1053	0.0938	0.0966	0.1184	0.1068	0.1068	0.1064	0.1129	0.1051
7204.75	0.1072	0.1041	0.1057	0.0941	0.0969	0.1187	0.1072	0.1072	0.1068	0.1134	0.1055
7200.89	0.1075	0.1045	0.1061	0.0944	0.0972	0.1191	0.1075	0.1075	0.1072	0.1139	0.1059
7197.04	0.1079	0.1049	0.1066	0.0948	0.0976	0.1195	0.1079	0.1079	0.1077	0.1145	0.1064
7193.18	0.1083	0.1054	0.1071	0.0952	0.0980	0.1199	0.1083	0.1083	0.1082	0.1150	0.1069
7189.32	0.1087	0.1059	0.1076	0.0956	0.0984	0.1203	0.1087	0.1087	0.1086	0.1156	0.1073
7185.47	0.1091	0.1063	0.1081	0.0960	0.0987	0.1207	0.1091	0.1091	0.1091	0.1162	0.1078
7181.61	0.1095	0.1067	0.1086	0.0964	0.0991	0.1212	0.1095	0.1096	0.1096	0.1168	0.1083
7177.75	0.1099	0.1071	0.1091	0.0967	0.0995	0.1216	0.1099	0.1100	0.1100	0.1174	0.1088
7173.9	0.1103	0.1076	0.1096	0.0971	0.0999	0.1220	0.1103	0.1104	0.1105	0.1180	0.1093
7170.04	0.1106	0.1080	0.1101	0.0975	0.1003	0.1224	0.1107	0.1108	0.1109	0.1185	0.1097
7166.18	0.1110	0.1083	0.1106	0.0978	0.1006	0.1227	0.1110	0.1112	0.1113	0.1191	0.1102
7162.33	0.1114	0.1086	0.1111	0.0981	0.1010	0.1231	0.1114	0.1116	0.1117	0.1197	0.1107
7158.47	0.1119	0.1092	0.1117	0.0986	0.1015	0.1236	0.1119	0.1121	0.1123	0.1204	0.1112
7154.61	0.1124	0.1099	0.1124	0.0992	0.1020	0.1242	0.1125	0.1126	0.1130	0.1212	0.1119
7150.75	0.1130	0.1105	0.1130	0.0998	0.1025	0.1247	0.1130	0.1131	0.1137	0.1220	0.1125
7146.9	0.1136	0.1112	0.1137	0.1004	0.1030	0.1253	0.1136	0.1137	0.1143	0.1228	0.1131
7143.04	0.1141	0.1117	0.1144	0.1008	0.1035	0.1258	0.1141	0.1142	0.1149	0.1236	0.1137
7139.18	0.1146	0.1122	0.1150	0.1012	0.1040	0.1263	0.1146	0.1147	0.1155	0.1244	0.1144

Table E1 (continued)

Wavenumbers (cm-1)	BoB	NH	NM	BuR	LA	NO	PP	RetF	RubS	RugE	BuP
7135.33	0.1151	0.1127	0.1157	0.1018	0.1045	0.1269	0.1152	0.1153	0.1161	0.1252	0.1150
7131.47	0.1157	0.1133	0.1165	0.1023	0.1050	0.1274	0.1157	0.1158	0.1167	0.1260	0.1157
7127.61	0.1164	0.1142	0.1173	0.1030	0.1057	0.1281	0.1164	0.1165	0.1176	0.1270	0.1165
7123.76	0.1171	0.1152	0.1181	0.1039	0.1064	0.1288	0.1171	0.1172	0.1185	0.1281	0.1173
7119.9	0.1178	0.1159	0.1190	0.1045	0.1070	0.1295	0.1178	0.1179	0.1193	0.1291	0.1181
7116.04	0.1185	0.1165	0.1199	0.1051	0.1077	0.1302	0.1185	0.1186	0.1200	0.1301	0.1190
7112.19	0.1192	0.1173	0.1208	0.1059	0.1084	0.1309	0.1193	0.1194	0.1209	0.1312	0.1198
7108.33	0.1200	0.1182	0.1217	0.1066	0.1091	0.1316	0.1200	0.1201	0.1218	0.1322	0.1207
7104.47	0.1208	0.1191	0.1227	0.1074	0.1098	0.1324	0.1208	0.1209	0.1227	0.1333	0.1216
7100.61	0.1216	0.1199	0.1237	0.1082	0.1106	0.1332	0.1216	0.1217	0.1236	0.1345	0.1225
7096.76	0.1224	0.1209	0.1247	0.1090	0.1114	0.1340	0.1224	0.1225	0.1245	0.1357	0.1235
7092.9	0.1233	0.1219	0.1257	0.1099	0.1122	0.1348	0.1233	0.1234	0.1255	0.1369	0.1245
7089.04	0.1242	0.1229	0.1268	0.1109	0.1131	0.1357	0.1242	0.1243	0.1266	0.1382	0.1255
7085.19	0.1252	0.1240	0.1279	0.1118	0.1139	0.1366	0.1252	0.1252	0.1276	0.1395	0.1265
7081.33	0.1261	0.1250	0.1290	0.1127	0.1148	0.1375	0.1261	0.1261	0.1286	0.1407	0.1275
7077.47	0.1269	0.1259	0.1300	0.1136	0.1156	0.1384	0.1270	0.1269	0.1296	0.1419	0.1285
7073.62	0.1279	0.1269	0.1311	0.1145	0.1165	0.1394	0.1279	0.1278	0.1306	0.1432	0.1296
7069.76	0.1288	0.1279	0.1322	0.1154	0.1173	0.1403	0.1288	0.1287	0.1316	0.1445	0.1306
7065.9	0.1297	0.1289	0.1333	0.1164	0.1182	0.1412	0.1297	0.1296	0.1326	0.1458	0.1317
7062.04	0.1307	0.1299	0.1344	0.1173	0.1191	0.1421	0.1307	0.1305	0.1337	0.1471	0.1327
7058.19	0.1316	0.1310	0.1355	0.1183	0.1199	0.1429	0.1316	0.1314	0.1347	0.1484	0.1337

Table E1 (continued)

Wavenumbers (cm-1)	BoB	NH	NM	BuR	LA	NO	PP	RetF	RubS	RugE	BuP
7054.33	0.1325	0.1320	0.1366	0.1193	0.1208	0.1437	0.1326	0.1323	0.1357	0.1497	0.1348
7050.47	0.1335	0.1329	0.1377	0.1202	0.1216	0.1445	0.1335	0.1331	0.1367	0.1509	0.1357
7046.62	0.1343	0.1339	0.1387	0.1211	0.1224	0.1451	0.1344	0.1340	0.1377	0.1522	0.1367
7042.76	0.1352	0.1348	0.1397	0.1221	0.1233	0.1458	0.1353	0.1349	0.1386	0.1534	0.1377
7038.9	0.1361	0.1357	0.1408	0.1230	0.1241	0.1464	0.1362	0.1357	0.1396	0.1546	0.1387
7035.05	0.1371	0.1367	0.1419	0.1239	0.1249	0.1472	0.1371	0.1366	0.1406	0.1559	0.1397
7031.19	0.1381	0.1378	0.1430	0.1250	0.1258	0.1481	0.1381	0.1375	0.1416	0.1573	0.1408
7027.33	0.1391	0.1388	0.1441	0.1260	0.1267	0.1489	0.1391	0.1384	0.1427	0.1586	0.1418
7023.48	0.1401	0.1398	0.1452	0.1270	0.1276	0.1497	0.1401	0.1394	0.1437	0.1599	0.1429
7019.62	0.1410	0.1408	0.1463	0.1280	0.1285	0.1505	0.1410	0.1402	0.1447	0.1612	0.1439
7015.76	0.1420	0.1418	0.1473	0.1290	0.1293	0.1513	0.1420	0.1411	0.1457	0.1624	0.1449
7011.9	0.1429	0.1428	0.1484	0.1299	0.1302	0.1521	0.1429	0.1420	0.1467	0.1637	0.1460
7008.05	0.1439	0.1438	0.1495	0.1309	0.1311	0.1529	0.1439	0.1429	0.1477	0.1650	0.1470
7004.19	0.1448	0.1447	0.1505	0.1319	0.1319	0.1537	0.1448	0.1437	0.1486	0.1662	0.1480
7000.33	0.1457	0.1457	0.1515	0.1328	0.1328	0.1544	0.1457	0.1446	0.1496	0.1674	0.1489
6996.48	0.1466	0.1466	0.1525	0.1337	0.1336	0.1551	0.1466	0.1454	0.1505	0.1686	0.1499
6992.62	0.1475	0.1475	0.1536	0.1347	0.1344	0.1558	0.1475	0.1463	0.1514	0.1698	0.1509
6988.76	0.1484	0.1484	0.1545	0.1355	0.1352	0.1565	0.1484	0.1471	0.1523	0.1710	0.1518
6984.91	0.1492	0.1492	0.1555	0.1364	0.1360	0.1572	0.1492	0.1478	0.1532	0.1721	0.1527
6981.05	0.1501	0.1501	0.1564	0.1372	0.1367	0.1579	0.1501	0.1486	0.1540	0.1732	0.1536
6977.19	0.1509	0.1509	0.1573	0.1381	0.1375	0.1586		0.1494	0.1549	0.1743	0.1545

Table E1 (continued)

Wavenumbers (cm-1)	BoB	NH	NM	BuR	LA	NO	PP	RetF	RubS	RugE	BuP
6973.34	0.1517	0.1517	0.1582	0.1389	0.1382	0.1592	0.1517	0.1501	0.1557	0.1753	0.1553
6969.48	0.1525	0.1525	0.1590	0.1396	0.1389	0.1599	0.1525	0.1508	0.1565	0.1764	0.1561
6965.62	0.1533	0.1533	0.1598	0.1404	0.1395	0.1605	0.1533	0.1515	0.1572	0.1774	0.1569
6961.76	0.1540	0.1540	0.1606	0.1411	0.1402	0.1611	0.1540	0.1522	0.1580	0.1784	0.1577
6957.91	0.1547	0.1547	0.1614	0.1418	0.1408	0.1616	0.1547	0.1528	0.1586	0.1793	0.1584
6954.05	0.1554	0.1553	0.1621	0.1424	0.1414	0.1621	0.1554	0.1534	0.1593	0.1801	0.1591
6950.19	0.1560	0.1559	0.1628	0.1430	0.1419	0.1626	0.1560	0.1540	0.1599	0.1809	0.1598
6946.34	0.1566	0.1564	0.1634	0.1436	0.1425	0.1631	0.1566	0.1545	0.1604	0.1817	0.1604
6942.48	0.1572	0.1570	0.1641	0.1442	0.1430	0.1635	0.1572	0.1550	0.1610	0.1824	0.1610
6938.62	0.1578	0.1576	0.1647	0.1447	0.1435	0.1640	0.1578	0.1556	0.1615	0.1831	0.1616
6934.77	0.1583	0.1581	0.1652	0.1452	0.1439	0.1644	0.1583	0.1561	0.1620	0.1838	0.1622
6930.91	0.1588	0.1585	0.1658	0.1457	0.1444	0.1648	0.1588	0.1565	0.1625	0.1844	0.1627
6927.05	0.1593	0.1590	0.1663	0.1462	0.1448	0.1651	0.1593	0.1570	0.1630	0.1850	0.1632
6923.2	0.1598	0.1594	0.1668	0.1466	0.1452	0.1655	0.1598	0.1574	0.1634	0.1855	0.1637
6919.34	0.1602	0.1598	0.1672	0.1470	0.1455	0.1658	0.1602	0.1578	0.1638	0.1861	0.1642
6915.48	0.1606	0.1601	0.1677	0.1474	0.1459	0.1661	0.1606	0.1582	0.1641	0.1865	0.1647
6911.62	0.1611	0.1605	0.1681	0.1478	0.1463	0.1664	0.1611	0.1586	0.1646	0.1871	0.1651
6907.77	0.1615	0.1610	0.1686	0.1483	0.1467	0.1668	0.1615	0.1590	0.1650	0.1876	0.1656
6903.91	0.1619	0.1614	0.1690	0.1487	0.1470	0.1671	0.1619	0.1594	0.1654	0.1880	0.1661
6900.05	0.1623	0.1617	0.1694	0.1491	0.1474	0.1674	0.1623	0.1598	0.1657	0.1885	0.1665
6896.2	0.1627	0.1621	0.1698	0.1494	0.1477	0.1676	0.1627	0.1602	0.1661	0.1889	0.1669

Table E1 (continued)

Wavenumbers (cm-1)	BoB	NH	NM	BuR	LA	NO	PP	RetF	RubS	RugE	BuP
6892.34	0.1630	0.1624	0.1702	0.1498	0.1480	0.1679	0.1630	0.1605	0.1664	0.1893	0.1673
6888.48	0.1634	0.1627	0.1706	0.1501	0.1483	0.1682	0.1634	0.1609	0.1667	0.1897	0.1677
6884.63	0.1637	0.1630	0.1709	0.1504	0.1486	0.1684	0.1637	0.1612	0.1670	0.1900	0.1681
6880.77	0.1640	0.1633	0.1713	0.1507	0.1489	0.1687	0.1640	0.1616	0.1673	0.1904	0.1685
6876.91	0.1644	0.1637	0.1716	0.1511	0.1492	0.1689	0.1644	0.1619	0.1676	0.1908	0.1689
6873.06	0.1647	0.1640	0.1720	0.1514	0.1495	0.1692	0.1647	0.1623	0.1679	0.1912	0.1692
6869.2	0.1650	0.1644	0.1723	0.1518	0.1498	0.1694	0.1650	0.1626	0.1683	0.1915	0.1696
6865.34	0.1653	0.1647	0.1727	0.1521	0.1501	0.1697	0.1653	0.1630	0.1686	0.1918	0.1700
6861.48	0.1656	0.1649	0.1730	0.1524	0.1504	0.1699	0.1656	0.1633	0.1688	0.1922	0.1704
6857.63	0.1659	0.1652	0.1733	0.1527	0.1507	0.1701	0.1659	0.1636	0.1691	0.1925	0.1707
6853.77	0.1662	0.1655	0.1736	0.1530	0.1510	0.1704	0.1662	0.1640	0.1694	0.1928	0.1711
6849.91	0.1665	0.1658	0.1739	0.1533	0.1512	0.1706	0.1665	0.1643	0.1697	0.1931	0.1714
6846.06	0.1667	0.1661	0.1742	0.1536	0.1515	0.1708	0.1667	0.1646	0.1699	0.1934	0.1718
6842.2	0.1670	0.1664	0.1745	0.1539	0.1517	0.1710	0.1670	0.1649	0.1702	0.1936	0.1721
6838.34	0.1672	0.1666	0.1747	0.1542	0.1520	0.1712	0.1672	0.1653	0.1704	0.1939	0.1724
6834.49	0.1675	0.1669	0.1750	0.1544	0.1522	0.1714	0.1675	0.1656	0.1707	0.1942	0.1727
6830.63	0.1677	0.1671	0.1752	0.1547	0.1525	0.1716	0.1677	0.1659	0.1709	0.1944	0.1730
6826.77	0.1679	0.1674	0.1755	0.1550	0.1527	0.1718	0.1679	0.1662	0.1711	0.1946	0.1733
6822.92	0.1681	0.1676	0.1757	0.1552	0.1529	0.1720	0.1681	0.1665	0.1714	0.1949	0.1736
6819.06	0.1683	0.1678	0.1760	0.1555	0.1531	0.1721	0.1683	0.1668	0.1716	0.1951	0.1739
6815.2	0.1685	0.1681	0.1762	0.1557	0.1534	0.1723	0.1685	0.1670	0.1718	0.1953	0.1741

Table E1 (continued)

Wavenumbers (cm-1)	BoB	NH	NM	BuR	LA	NO	PP	RetF	RubS	RugE	BuP
6811.34	0.1687	0.1683	0.1764	0.1559	0.1536	0.1724	0.1687	0.1673	0.1719	0.1954	0.1744
6807.49	0.1689	0.1685	0.1766	0.1561	0.1537	0.1726	0.1688	0.1676	0.1721	0.1956	0.1746
6803.63	0.1690	0.1687	0.1767	0.1563	0.1539	0.1727	0.1690	0.1678	0.1723	0.1958	0.1748
6799.77	0.1691	0.1688	0.1769	0.1565	0.1541	0.1728	0.1691	0.1680	0.1724	0.1959	0.1751
6795.92	0.1693	0.1690	0.1770	0.1567	0.1542	0.1729	0.1693	0.1683	0.1725	0.1960	0.1753
6792.06	0.1694	0.1691	0.1772	0.1569	0.1544	0.1730	0.1694	0.1685	0.1727	0.1961	0.1754
6788.2	0.1695	0.1693	0.1773	0.1570	0.1546	0.1731	0.1695	0.1687	0.1728	0.1962	0.1756
6784.35	0.1696	0.1695	0.1774	0.1572	0.1547	0.1732	0.1696	0.1689	0.1729	0.1964	0.1758
6780.49	0.1697	0.1697	0.1776	0.1574	0.1549	0.1733	0.1697	0.1691	0.1731	0.1965	0.1760
6776.63	0.1698	0.1698	0.1777	0.1576	0.1550	0.1734	0.1698	0.1694	0.1732	0.1966	0.1761
6772.77	0.1699	0.1699	0.1778	0.1577	0.1551	0.1735	0.1699	0.1695	0.1733	0.1966	0.1762
6768.92	0.1699	0.1700	0.1778	0.1578	0.1552	0.1735	0.1699	0.1697	0.1733	0.1966	0.1763
6765.06	0.1699	0.1701	0.1779	0.1579	0.1553	0.1735	0.1699	0.1699	0.1734	0.1966	0.1764
6761.2	0.1700	0.1702	0.1779	0.1580	0.1554	0.1736	0.1699	0.1700	0.1735	0.1966	0.1765
6757.35	0.1700	0.1703	0.1780	0.1581	0.1555	0.1736	0.1700	0.1702	0.1735	0.1967	0.1766
6753.49	0.1700	0.1704	0.1781	0.1582	0.1556	0.1736	0.1700	0.1703	0.1736	0.1967	0.1767
6749.63	0.1701	0.1705	0.1781	0.1583	0.1557	0.1737	0.1700	0.1705	0.1737	0.1967	0.1768
6745.78	0.1701	0.1706	0.1782	0.1584	0.1558	0.1737	0.1701	0.1706	0.1738	0.1967	0.1769
6741.92	0.1701	0.1707	0.1782	0.1585	0.1558	0.1737	0.1701	0.1708	0.1738	0.1967	0.1770
6738.06	0.1701	0.1708	0.1783	0.1586	0.1559	0.1738	0.1701	0.1710	0.1739	0.1967	0.1771
6734.21	0.1701	0.1709	0.1784	0.1587	0.1560	0.1738	0.1701	0.1711	0.1740	0.1968	0.1772

Table E1 (continued)

Wavenumbers (cm-1)	BoB	NH	NM	BuR	LA	NO	PP	RetF	RubS	RugE	BuP
6730.35	0.1702	0.1711	0.1784	0.1588	0.1561	0.1739	0.1702	0.1713	0.1741	0.1968	0.1773
6726.49	0.1702	0.1712	0.1785	0.1589	0.1562	0.1739	0.1702	0.1715	0.1742	0.1968	0.1774
6722.63	0.1702	0.1713	0.1785	0.1590	0.1563	0.1739	0.1702	0.1716	0.1743	0.1968	0.1775
6718.78	0.1702	0.1714	0.1786	0.1591	0.1564	0.1740	0.1702	0.1718	0.1744	0.1967	0.1775
6714.92	0.1702	0.1715	0.1787	0.1592	0.1565	0.1740	0.1702	0.1719	0.1745	0.1967	0.1776
6711.06	0.1702	0.1716	0.1787	0.1592	0.1565	0.1740	0.1702	0.1721	0.1745	0.1967	0.1777
6707.21	0.1702	0.1717	0.1787	0.1593	0.1566	0.1740	0.1702	0.1722	0.1746	0.1967	0.1778
6703.35	0.1702	0.1718	0.1788	0.1594	0.1567	0.1741	0.1702	0.1724	0.1747	0.1967	0.1778
6699.49	0.1702	0.1719	0.1788	0.1594	0.1568	0.1741	0.1702	0.1725	0.1748	0.1967	0.1779
6695.64	0.1702	0.1720	0.1789	0.1595	0.1568	0.1741	0.1702	0.1726	0.1748	0.1966	0.1780
6691.78	0.1702	0.1720	0.1789	0.1595	0.1569	0.1741	0.1701	0.1728	0.1749	0.1966	0.1780
6687.92	0.1701	0.1721	0.1789	0.1596	0.1569	0.1741	0.1701	0.1729	0.1749	0.1966	0.1780
6684.07	0.1701	0.1722	0.1789	0.1596	0.1570	0.1741	0.1701	0.1730	0.1750	0.1965	0.1780
6680.21	0.1700	0.1722	0.1788	0.1596	0.1570	0.1741	0.1700	0.1731	0.1750	0.1964	0.1781
6676.35	0.1700	0.1723	0.1788	0.1597	0.1570	0.1740	0.1700	0.1731	0.1750	0.1964	0.1781
6672.49	0.1699	0.1723	0.1788	0.1597	0.1570	0.1740	0.1699	0.1732	0.1750	0.1963	0.1780
6668.64	0.1699	0.1723	0.1787	0.1597	0.1570	0.1739	0.1698	0.1733	0.1750	0.1962	0.1780
6664.78	0.1698	0.1723	0.1787	0.1596	0.1570	0.1739	0.1698	0.1733	0.1750	0.1961	0.1780
6660.92	0.1697	0.1724	0.1786	0.1596	0.1570	0.1738	0.1697	0.1734	0.1749	0.1960	0.1780
6657.07	0.1696	0.1724	0.1785	0.1596	0.1570	0.1738	0.1696	0.1734	0.1749	0.1959	0.1779
6653.21	0.1695	0.1724	0.1785	0.1596	0.1570	0.1737	0.1695	0.1734	0.1749	0.1957	0.1779

Table E1 (continued)

Wavenumbers (cm-1)	BoB	NH	NM	BuR	LA	NO	PP	RetF	RubS	RugE	BuP
6649.35	0.1694	0.1723	0.1784	0.1595	0.1570	0.1736	0.1694	0.1735	0.1748	0.1956	0.1778
6645.5	0.1693	0.1723	0.1783	0.1595	0.1569	0.1735	0.1693	0.1735	0.1748	0.1955	0.1778
6641.64	0.1692	0.1723	0.1782	0.1594	0.1569	0.1734	0.1692	0.1735	0.1747	0.1954	0.1777
6637.78	0.1691	0.1723	0.1781	0.1594	0.1568	0.1734	0.1691	0.1735	0.1746	0.1952	0.1776
6633.93	0.1690	0.1722	0.1780	0.1593	0.1568	0.1733	0.1690	0.1735	0.1745	0.1951	0.1775
6630.07	0.1689	0.1722	0.1779	0.1593	0.1567	0.1732	0.1689	0.1735	0.1745	0.1950	0.1774
6626.21	0.1688	0.1722	0.1778	0.1592	0.1567	0.1731	0.1688	0.1735	0.1744	0.1948	0.1774
6622.35	0.1687	0.1721	0.1776	0.1591	0.1566	0.1730	0.1687	0.1735	0.1743	0.1947	0.1773
6618.5	0.1686	0.1721	0.1775	0.1590	0.1565	0.1729	0.1686	0.1734	0.1742	0.1945	0.1771
6614.64	0.1684	0.1720	0.1774	0.1589	0.1565	0.1727	0.1684	0.1734	0.1741	0.1944	0.1770
6610.78	0.1683	0.1719	0.1772	0.1588	0.1564	0.1726	0.1683	0.1733	0.1740	0.1942	0.1769
6606.93	0.1682	0.1719	0.1771	0.1587	0.1563	0.1725	0.1682	0.1733	0.1739	0.1941	0.1768
6603.07	0.1681	0.1718	0.1770	0.1586	0.1562	0.1724	0.1681	0.1732	0.1738	0.1939	0.1767
6599.21	0.1679	0.1717	0.1768	0.1584	0.1561	0.1723	0.1679	0.1731	0.1736	0.1938	0.1765
6595.36	0.1678	0.1716	0.1767	0.1583	0.1560	0.1721	0.1678	0.1730	0.1735	0.1936	0.1764
6591.5	0.1677	0.1715	0.1765	0.1582	0.1559	0.1720	0.1677	0.1729	0.1734	0.1935	0.1763
6587.64	0.1676	0.1714	0.1764	0.1581	0.1558	0.1719	0.1675	0.1728	0.1733	0.1933	0.1761
6583.79	0.1674	0.1713	0.1762	0.1579	0.1557	0.1718	0.1674	0.1728	0.1731	0.1931	0.1760
6579.93	0.1673	0.1712	0.1760	0.1578	0.1556	0.1716	0.1673	0.1727	0.1730	0.1930	0.1758
6576.07	0.1671	0.1711	0.1759	0.1577	0.1554	0.1715	0.1671	0.1726	0.1729	0.1928	0.1757
6572.21	0.1670	0.1710	0.1757	0.1576	0.1553	0.1714	0.1670	0.1725	0.1727	0.1927	0.1756

Table E1 (continued)

Wavenumbers (cm-1)	BoB	NH	NM	BuR	LA	NO	PP	RetF	RubS	RugE	BuP
6568.36	0.1669	0.1709	0.1756	0.1574	0.1552	0.1712	0.1669	0.1724	0.1726	0.1926	0.1754
6564.5	0.1668	0.1708	0.1754	0.1573	0.1551	0.1711	0.1668	0.1723	0.1725	0.1924	0.1753
6560.64	0.1666	0.1707	0.1753	0.1572	0.1551	0.1710	0.1666	0.1722	0.1724	0.1923	0.1751
6556.79	0.1665	0.1707	0.1751	0.1571	0.1550	0.1709	0.1665	0.1722	0.1723	0.1922	0.1750
6552.93	0.1664	0.1706	0.1750	0.1570	0.1549	0.1708	0.1664	0.1721	0.1721	0.1921	0.1749
6549.07	0.1663	0.1705	0.1749	0.1569	0.1548	0.1707	0.1663	0.1720	0.1720	0.1920	0.1748
6545.22	0.1662	0.1704	0.1747	0.1568	0.1547	0.1706	0.1662	0.1719	0.1719	0.1919	0.1747
6541.36	0.1661	0.1704	0.1746	0.1567	0.1546	0.1705	0.1661	0.1719	0.1718	0.1918	0.1746
6537.5	0.1660	0.1703	0.1745	0.1567	0.1546	0.1704	0.1660	0.1718	0.1717	0.1917	0.1744
6533.65	0.1659	0.1703	0.1744	0.1566	0.1545	0.1703	0.1659	0.1717	0.1716	0.1916	0.1743
6529.79	0.1658	0.1702	0.1743	0.1565	0.1544	0.1702	0.1658	0.1717	0.1715	0.1915	0.1742
6525.93	0.1657	0.1701	0.1742	0.1564	0.1544	0.1701	0.1657	0.1716	0.1715	0.1914	0.1742
6522.07	0.1656	0.1701	0.1741	0.1564	0.1543	0.1700	0.1656	0.1716	0.1714	0.1914	0.1741
6518.22	0.1656	0.1700	0.1740	0.1563	0.1543	0.1699	0.1655	0.1715	0.1713	0.1913	0.1740
6514.36	0.1655	0.1700	0.1739	0.1563	0.1542	0.1699	0.1655	0.1715	0.1713	0.1913	0.1739
6510.5	0.1654	0.1700	0.1738	0.1562	0.1542	0.1698	0.1654	0.1715	0.1712	0.1912	0.1739
6506.65	0.1654	0.1700	0.1738	0.1562	0.1542	0.1698	0.1654	0.1714	0.1712	0.1912	0.1738
6502.79	0.1653	0.1699	0.1737	0.1562	0.1541	0.1697	0.1653	0.1714	0.1711	0.1912	0.1738
6498.93	0.1653	0.1699	0.1736	0.1562	0.1541	0.1696	0.1653	0.1714	0.1711	0.1912	0.1737
6495.08	0.1652	0.1699	0.1736	0.1562	0.1541	0.1696	0.1652	0.1714	0.1710	0.1912	0.1737
6491.22	0.1652	0.1699	0.1735	0.1562	0.1541	0.1695	0.1652	0.1714	0.1710	0.1912	0.1737

Table E1 (continued)

Wavenumbers (cm-1)	BoB	NH	NM	BuR	LA	NO	PP	RetF	RubS	RugE	BuP
6487.36	0.1651	0.1699	0.1735	0.1562	0.1541	0.1695	0.1651	0.1714	0.1709	0.1912	0.1736
6483.5	0.1651	0.1699	0.1734	0.1562	0.1541	0.1695	0.1651	0.1714	0.1709	0.1912	0.1736
6479.65	0.1651	0.1699	0.1733	0.1561	0.1541	0.1694	0.1651	0.1714	0.1708	0.1911	0.1736
6475.79	0.1650	0.1699	0.1733	0.1561	0.1540	0.1693	0.1650	0.1713	0.1708	0.1911	0.1735
6471.93	0.1650	0.1699	0.1732	0.1562	0.1540	0.1693	0.1650	0.1713	0.1707	0.1911	0.1735
6468.08	0.1650	0.1699	0.1732	0.1562	0.1540	0.1692	0.1650	0.1713	0.1707	0.1911	0.1735
6464.22	0.1649	0.1699	0.1731	0.1562	0.1540	0.1692	0.1649	0.1713	0.1706	0.1911	0.1735
6460.36	0.1649	0.1698	0.1730	0.1562	0.1540	0.1691	0.1649	0.1713	0.1705	0.1911	0.1734
6456.51	0.1648	0.1698	0.1730	0.1562	0.1540	0.1691	0.1648	0.1713	0.1705	0.1911	0.1734
6452.65	0.1648	0.1698	0.1729	0.1562	0.1540	0.1690	0.1648	0.1713	0.1704	0.1911	0.1734
6448.79	0.1647	0.1698	0.1728	0.1562	0.1540	0.1689	0.1647	0.1713	0.1704	0.1911	0.1733
6444.94	0.1647	0.1698	0.1728	0.1562	0.1540	0.1689	0.1647	0.1713	0.1703	0.1911	0.1733
6441.08	0.1646	0.1698	0.1727	0.1562	0.1540	0.1688	0.1646	0.1713	0.1702	0.1911	0.1732
6437.22	0.1646	0.1698	0.1727	0.1563	0.1540	0.1688	0.1646	0.1713	0.1702	0.1911	0.1732
6433.36	0.1645	0.1698	0.1726	0.1563	0.1540	0.1687	0.1645	0.1713	0.1702	0.1911	0.1732
6429.51	0.1645	0.1698	0.1726	0.1563	0.1540	0.1687	0.1645	0.1713	0.1701	0.1911	0.1732
6425.65	0.1645	0.1699	0.1726	0.1564	0.1540	0.1687	0.1645	0.1714	0.1701	0.1912	0.1732
6421.79	0.1645	0.1699	0.1725	0.1564	0.1541	0.1686	0.1645	0.1714	0.1701	0.1912	0.1732
6417.94	0.1645	0.1700	0.1725	0.1565	0.1541	0.1686	0.1645	0.1714	0.1701	0.1912	0.1732
6414.08	0.1646	0.1700	0.1725	0.1566	0.1542	0.1686	0.1645	0.1715	0.1701	0.1913	0.1733
6410.22	0.1646	0.1701	0.1726	0.1566	0.1542	0.1686	0.1646	0.1716	0.1702	0.1914	0.1733

Table E1 (continued)

Wavenumbers (cm-1)	BoB	NH	NM	BuR	LA	NO	PP	RetF	RubS	RugE	BuP
6406.37	0.1646	0.1702	0.1726	0.1567	0.1543	0.1687	0.1646	0.1716	0.1702	0.1914	0.1734
6402.51	0.1647	0.1702	0.1726	0.1568	0.1543	0.1687	0.1647	0.1717	0.1703	0.1915	0.1734
6398.65	0.1647	0.1703	0.1727	0.1568	0.1544	0.1687	0.1647	0.1718	0.1703	0.1916	0.1735
6394.8	0.1648	0.1704	0.1727	0.1569	0.1545	0.1687	0.1648	0.1719	0.1704	0.1917	0.1736
6390.94	0.1649	0.1705	0.1728	0.1570	0.1546	0.1688	0.1649	0.1720	0.1705	0.1918	0.1737
6387.08	0.1649	0.1706	0.1729	0.1571	0.1546	0.1688	0.1649	0.1721	0.1706	0.1919	0.1738
6383.22	0.1650	0.1707	0.1729	0.1572	0.1547	0.1689	0.1650	0.1722	0.1707	0.1920	0.1738
6379.37	0.1651	0.1709	0.1730	0.1573	0.1548	0.1689	0.1651	0.1723	0.1708	0.1921	0.1739
6375.51	0.1651	0.1710	0.1731	0.1574	0.1549	0.1690	0.1651	0.1725	0.1709	0.1922	0.1740
6371.65	0.1652	0.1711	0.1732	0.1575	0.1550	0.1691	0.1652	0.1726	0.1710	0.1923	0.1741
6367.8	0.1653	0.1712	0.1732	0.1576	0.1551	0.1691	0.1652	0.1727	0.1711	0.1924	0.1741
6363.94	0.1653	0.1713	0.1733	0.1577	0.1552	0.1692	0.1653	0.1728	0.1712	0.1925	0.1742
6360.08	0.1654	0.1715	0.1734	0.1578	0.1553	0.1692	0.1654	0.1730	0.1712	0.1926	0.1743
6356.23	0.1654	0.1715	0.1734	0.1578	0.1553	0.1692	0.1654	0.1730	0.1713	0.1926	0.1743
6352.37	0.1654	0.1716	0.1735	0.1578	0.1554	0.1692	0.1654	0.1731	0.1713	0.1927	0.1744
6348.51	0.1655	0.1717	0.1735	0.1579	0.1554	0.1693	0.1655	0.1732	0.1714	0.1928	0.1744
6344.66	0.1655	0.1717	0.1735	0.1579	0.1554	0.1693	0.1655	0.1732	0.1714	0.1928	0.1744
6340.8	0.1655	0.1718	0.1735	0.1579	0.1555	0.1693	0.1655	0.1733	0.1715	0.1929	0.1744
6336.94	0.1655	0.1719	0.1735	0.1580	0.1556	0.1693	0.1655	0.1734	0.1715	0.1929	0.1745
6333.08	0.1655	0.1720	0.1735	0.1581	0.1556	0.1693	0.1655	0.1735	0.1715	0.1929	0.1745
6329.23	0.1655	0.1720	0.1736	0.1581	0.1557	0.1693	0.1655	0.1736	0.1716	0.1930	0.1745

Table E1 (continued)

Wavenumbers (cm-1)	BoB	NH	NM	BuR	LA	NO	PP	RetF	RubS	RugE	BuP
6325.37	0.1655	0.1721	0.1735	0.1581	0.1557	0.1693	0.1655	0.1737	0.1716	0.1930	0.1745
6321.51	0.1655	0.1721	0.1735	0.1581	0.1557	0.1693	0.1655	0.1737	0.1716	0.1930	0.1745
6317.66	0.1654	0.1722	0.1735	0.1582	0.1557	0.1693	0.1654	0.1738	0.1715	0.1930	0.1745
6313.8	0.1654	0.1722	0.1735	0.1582	0.1558	0.1692	0.1654	0.1738	0.1715	0.1930	0.1745
6309.94	0.1653	0.1722	0.1734	0.1582	0.1557	0.1692	0.1653	0.1738	0.1715	0.1929	0.1745
6306.09	0.1653	0.1722	0.1733	0.1581	0.1557	0.1692	0.1653	0.1739	0.1714	0.1929	0.1744
6302.23	0.1652	0.1722	0.1733	0.1581	0.1557	0.1691	0.1652	0.1739	0.1714	0.1928	0.1743
6298.37	0.1651	0.1722	0.1732	0.1580	0.1557	0.1690	0.1651	0.1738	0.1713	0.1928	0.1742
6294.52	0.1651	0.1722	0.1731	0.1580	0.1556	0.1690	0.1650	0.1738	0.1713	0.1927	0.1742
6290.66	0.1650	0.1722	0.1730	0.1579	0.1556	0.1689	0.1650	0.1739	0.1712	0.1926	0.1741
6286.8	0.1649	0.1722	0.1729	0.1578	0.1556	0.1688	0.1649	0.1738	0.1711	0.1925	0.1740
6282.94	0.1648	0.1721	0.1728	0.1578	0.1555	0.1688	0.1647	0.1738	0.1711	0.1924	0.1739
6279.09	0.1646	0.1721	0.1727	0.1577	0.1555	0.1687	0.1646	0.1738	0.1710	0.1923	0.1738
6275.23	0.1645	0.1721	0.1726	0.1576	0.1554	0.1686	0.1645	0.1738	0.1709	0.1922	0.1737
6271.37	0.1644	0.1720	0.1725	0.1576	0.1554	0.1685	0.1644	0.1738	0.1708	0.1921	0.1736
6267.52	0.1643	0.1720	0.1723	0.1575	0.1553	0.1684	0.1643	0.1738	0.1707	0.1919	0.1735
6263.66	0.1642	0.1719	0.1722	0.1573	0.1552	0.1683	0.1641	0.1737	0.1705	0.1918	0.1733
6259.8	0.1640	0.1717	0.1720	0.1572	0.1551	0.1681	0.1640	0.1735	0.1704	0.1916	0.1731
6255.95	0.1639	0.1716	0.1718	0.1570	0.1549	0.1680	0.1639	0.1734	0.1702	0.1915	0.1729
6252.09	0.1637	0.1714	0.1716	0.1568	0.1548	0.1678	0.1637	0.1732	0.1701	0.1913	0.1727
6248.23	0.1636	0.1712	0.1714	0.1565	0.1546	0.1677	0.1636	0.1731	0.1699	0.1911	0.1725

Table E1 (continued)

Wavenumbers (cm-1)	BoB	NH	NM	BuR	LA	NO	PP	RetF	RubS	RugE	BuP
6244.38	0.1634	0.1710	0.1712	0.1563	0.1544	0.1675	0.1634	0.1728	0.1697	0.1909	0.1723
6240.52	0.1632	0.1708	0.1710	0.1560	0.1542	0.1673	0.1632	0.1726	0.1695	0.1907	0.1720
6236.66	0.1630	0.1705	0.1707	0.1557	0.1540	0.1671	0.1630	0.1724	0.1692	0.1904	0.1717
6232.8	0.1629	0.1703	0.1705	0.1555	0.1538	0.1669	0.1629	0.1721	0.1690	0.1902	0.1715
6228.95	0.1627	0.1700	0.1702	0.1552	0.1535	0.1667	0.1627	0.1718	0.1688	0.1900	0.1712
6225.09	0.1625	0.1697	0.1699	0.1549	0.1533	0.1664	0.1625	0.1715	0.1685	0.1897	0.1709
6221.23	0.1623	0.1694	0.1697	0.1545	0.1530	0.1662	0.1623	0.1712	0.1682	0.1894	0.1706
6217.38	0.1621	0.1691	0.1694	0.1542	0.1528	0.1660	0.1621	0.1709	0.1680	0.1892	0.1702
6213.52	0.1619	0.1687	0.1691	0.1538	0.1525	0.1657	0.1619	0.1705	0.1677	0.1889	0.1699
6209.66	0.1617	0.1684	0.1688	0.1535	0.1522	0.1654	0.1617	0.1701	0.1674	0.1887	0.1696
6205.81	0.1615	0.1680	0.1685	0.1531	0.1519	0.1652	0.1615	0.1697	0.1671	0.1884	0.1692
6201.95	0.1613	0.1677	0.1682	0.1527	0.1516	0.1649	0.1613	0.1693	0.1669	0.1881	0.1689
6198.09	0.1611	0.1673	0.1679	0.1523	0.1513	0.1647	0.1611	0.1689	0.1666	0.1878	0.1685
6194.23	0.1609	0.1669	0.1676	0.1520	0.1510	0.1644	0.1609	0.1685	0.1663	0.1876	0.1682
6190.38	0.1607	0.1665	0.1673	0.1516	0.1507	0.1641	0.1607	0.1681	0.1660	0.1873	0.1679
6186.52	0.1605	0.1662	0.1670	0.1512	0.1504	0.1639	0.1605	0.1677	0.1657	0.1870	0.1675
6182.66	0.1603	0.1658	0.1667	0.1508	0.1501	0.1636	0.1603	0.1674	0.1654	0.1867	0.1672
6178.81	0.1601	0.1654	0.1664	0.1504	0.1498	0.1634	0.1601	0.1670	0.1651	0.1864	0.1668
6174.95	0.1599	0.1650	0.1661	0.1501	0.1495	0.1631	0.1599	0.1666	0.1648	0.1861	0.1665
6171.09	0.1597	0.1646	0.1658	0.1497	0.1492	0.1629	0.1597	0.1662	0.1646	0.1858	0.1661
6167.24	0.1595	0.1643	0.1656	0.1493	0.1490	0.1626	0.1595	0.1658	0.1643	0.1855	0.1658

Table E1 (continued)

Wavenumbers (cm-1)	BoB	NH	NM	BuR	LA	NO	PP	RetF	RubS	RugE	BuP
6163.38	0.1593	0.1639	0.1653	0.1489	0.1487	0.1624	0.1593	0.1655	0.1640	0.1852	0.1655
6159.52	0.1591	0.1635	0.1650	0.1486	0.1484	0.1621	0.1591	0.1651	0.1637	0.1849	0.1651
6155.67	0.1589	0.1632	0.1647	0.1482	0.1482	0.1619	0.1589	0.1647	0.1634	0.1846	0.1648
6151.81	0.1587	0.1628	0.1644	0.1478	0.1480	0.1616	0.1587	0.1644	0.1631	0.1844	0.1645
6147.95	0.1584	0.1624	0.1641	0.1475	0.1477	0.1614	0.1584	0.1640	0.1629	0.1841	0.1642
6144.09	0.1582	0.1621	0.1639	0.1471	0.1475	0.1612	0.1582	0.1637	0.1626	0.1838	0.1638
6140.24	0.1580	0.1618	0.1636	0.1468	0.1473	0.1609	0.1580	0.1633	0.1623	0.1835	0.1635
6136.38	0.1578	0.1615	0.1634	0.1465	0.1472	0.1607	0.1578	0.1630	0.1621	0.1832	0.1632
6132.52	0.1576	0.1611	0.1631	0.1462	0.1471	0.1605	0.1576	0.1627	0.1618	0.1829	0.1629
6128.67	0.1574	0.1608	0.1629	0.1459	0.1469	0.1603	0.1574	0.1624	0.1615	0.1826	0.1626
6124.81	0.1572	0.1606	0.1627	0.1456	0.1468	0.1601	0.1572	0.1621	0.1613	0.1824	0.1623
6120.95	0.1570	0.1603	0.1624	0.1453	0.1465	0.1599	0.1570	0.1618	0.1611	0.1821	0.1620
6117.1	0.1568	0.1600	0.1622	0.1450	0.1464	0.1597	0.1568	0.1615	0.1608	0.1819	0.1618
6113.24	0.1566	0.1597	0.1620	0.1448	0.1462	0.1595	0.1566	0.1612	0.1606	0.1816	0.1615
6109.38	0.1564	0.1595	0.1618	0.1445	0.1459	0.1593	0.1564	0.1609	0.1604	0.1814	0.1612
6105.53	0.1562	0.1592	0.1615	0.1442	0.1456	0.1591	0.1562	0.1606	0.1602	0.1811	0.1610
6101.67	0.1561	0.1589	0.1613	0.1439	0.1453	0.1589	0.1561	0.1603	0.1600	0.1809	0.1607
6097.81	0.1559	0.1587	0.1610	0.1437	0.1449	0.1588	0.1559	0.1600	0.1597	0.1806	0.1605
6093.95	0.1558	0.1584	0.1608	0.1434	0.1447	0.1586	0.1558	0.1598	0.1595	0.1804	0.1602
6090.1	0.1556	0.1582	0.1606	0.1432	0.1445	0.1584	0.1556	0.1595	0.1594	0.1802	0.1600
6086.24	0.1555	0.1579	0.1604	0.1429	0.1442	0.1582	0.1555	0.1592	0.1592	0.1800	0.1598

Table E1 (continued)

Wavenumbers (cm-1)	BoB	NH	NM	BuR	LA	NO	PP	RetF	RubS	RugE	BuP
6082.38	0.1553	0.1577	0.1602	0.1427	0.1439	0.1581	0.1553	0.1589	0.1590	0.1798	0.1596
6078.53	0.1552	0.1575	0.1600	0.1425	0.1437	0.1579	0.1552	0.1587	0.1588	0.1796	0.1594
6074.67	0.1550	0.1573	0.1598	0.1422	0.1436	0.1578	0.1550	0.1584	0.1587	0.1794	0.1592
6070.81	0.1549	0.1571	0.1597	0.1420	0.1434	0.1576	0.1549	0.1582	0.1585	0.1793	0.1590
6066.96	0.1548	0.1569	0.1595	0.1418	0.1433	0.1575	0.1548	0.1579	0.1584	0.1791	0.1588
6063.1	0.1547	0.1568	0.1593	0.1416	0.1431	0.1573	0.1547	0.1577	0.1582	0.1789	0.1586
6059.24	0.1545	0.1566	0.1592	0.1415	0.1430	0.1572	0.1545	0.1575	0.1581	0.1788	0.1585
6055.39	0.1544	0.1564	0.1590	0.1413	0.1429	0.1571	0.1544	0.1572	0.1580	0.1786	0.1583
6051.53	0.1543	0.1563	0.1589	0.1411	0.1427	0.1570	0.1543	0.1570	0.1578	0.1785	0.1581
6047.67	0.1542	0.1562	0.1588	0.1410	0.1426	0.1569	0.1542	0.1569	0.1578	0.1784	0.1580
6043.81	0.1541	0.1561	0.1587	0.1408	0.1426	0.1568	0.1542	0.1567	0.1577	0.1783	0.1579
6039.96	0.1541	0.1560	0.1587	0.1407	0.1425	0.1568	0.1541	0.1566	0.1576	0.1782	0.1578
6036.1	0.1540	0.1559	0.1586	0.1406	0.1424	0.1567	0.1541	0.1564	0.1576	0.1782	0.1578
6032.24	0.1541	0.1559	0.1587	0.1406	0.1424	0.1567	0.1541	0.1564	0.1577	0.1783	0.1578
6028.39	0.1542	0.1560	0.1588	0.1406	0.1425	0.1568	0.1542	0.1564	0.1578	0.1784	0.1579
6024.53	0.1543	0.1561	0.1589	0.1406	0.1425	0.1569	0.1543	0.1564	0.1580	0.1786	0.1580
6020.67	0.1545	0.1562	0.1590	0.1406	0.1426	0.1570	0.1545	0.1564	0.1581	0.1788	0.1581
6016.82	0.1546	0.1563	0.1592	0.1406	0.1427	0.1571	0.1546	0.1564	0.1583	0.1789	0.1582
6012.96	0.1547	0.1564	0.1593	0.1406	0.1428	0.1572	0.1547	0.1564	0.1585	0.1791	0.1583
6009.1	0.1549	0.1565	0.1595	0.1407	0.1429	0.1573	0.1549	0.1565	0.1587	0.1793	0.1585
6005.25	0.1551	0.1566	0.1597	0.1407	0.1430	0.1575	0.1551	0.1566	0.1589	0.1795	0.1587

Table E1 (continued)

Wavenumbers (cm-1)	BoB	NH	NM	BuR	LA	NO	PP	RetF	RubS	RugE	BuP
6001.39	0.1552	0.1567	0.1599	0.1407	0.1431	0.1576	0.1552	0.1567	0.1591	0.1797	0.1588
5997.53	0.1553	0.1568	0.1600	0.1407	0.1431	0.1577	0.1553	0.1567	0.1592	0.1798	0.1589
5993.67	0.1554	0.1569	0.1602	0.1408	0.1432	0.1578	0.1554	0.1568	0.1594	0.1800	0.1590
5989.82	0.1555	0.1570	0.1604	0.1408	0.1433	0.1580	0.1555	0.1569	0.1595	0.1801	0.1591
5985.96	0.1557	0.1572	0.1607	0.1409	0.1435	0.1582	0.1557	0.1570	0.1598	0.1804	0.1593
5982.1	0.1560	0.1574	0.1610	0.1410	0.1437	0.1584	0.1560	0.1573	0.1601	0.1807	0.1596
5978.25	0.1563	0.1577	0.1613	0.1412	0.1439	0.1587	0.1563	0.1575	0.1604	0.1810	0.1599
5974.39	0.1566	0.1579	0.1617	0.1414	0.1442	0.1590	0.1566	0.1578	0.1608	0.1814	0.1602
5970.53	0.1569	0.1583	0.1621	0.1416	0.1445	0.1593	0.1569	0.1581	0.1612	0.1818	0.1606
5966.68	0.1574	0.1586	0.1626	0.1419	0.1449	0.1597	0.1574	0.1584	0.1617	0.1823	0.1610
5962.82	0.1578	0.1590	0.1631	0.1422	0.1453	0.1601	0.1578	0.1588	0.1623	0.1827	0.1615
5958.96	0.1583	0.1595	0.1636	0.1426	0.1457	0.1605	0.1583	0.1592	0.1628	0.1833	0.1620
5955.1	0.1589	0.1600	0.1642	0.1430	0.1461	0.1610	0.1589	0.1596	0.1635	0.1839	0.1626
5951.25	0.1594	0.1605	0.1649	0.1434	0.1466	0.1615	0.1595	0.1601	0.1642	0.1845	0.1632
5947.39	0.1601	0.1611	0.1656	0.1439	0.1472	0.1621	0.1601	0.1607	0.1649	0.1852	0.1638
5943.53	0.1608	0.1617	0.1663	0.1444	0.1477	0.1626	0.1608	0.1612	0.1657	0.1859	0.1646
5939.68	0.1615	0.1624	0.1671	0.1451	0.1484	0.1632	0.1615	0.1618	0.1665	0.1868	0.1653
5935.82	0.1624	0.1631	0.1679	0.1458	0.1491	0.1639	0.1624	0.1625	0.1673	0.1876	0.1662
5931.96	0.1632	0.1639	0.1688	0.1465	0.1498	0.1645	0.1632	0.1632	0.1682	0.1886	0.1670
5928.11	0.1642	0.1647	0.1697	0.1473	0.1506	0.1652	0.1642	0.1639	0.1691	0.1896	0.1680
5924.25	0.1649	0.1656	0.1706	0.1481	0.1513	0.1659	0.1649	0.1648	0.1700	0.1904	0.1690

Table E1 (continued)

Wavenumbers (cm-1)	BoB	NH	NM	BuR	LA	NO	PP	RetF	RubS	RugE	BuP
5920.39	0.1656	0.1665	0.1714	0.1490	0.1521	0.1666	0.1656	0.1658	0.1708	0.1913	0.1700
5916.54	0.1662	0.1675	0.1723	0.1500	0.1530	0.1673	0.1662	0.1669	0.1717	0.1922	0.1709
5912.68	0.1669	0.1685	0.1733	0.1510	0.1538	0.1680	0.1669	0.1680	0.1726	0.1931	0.1719
5908.82	0.1673	0.1690	0.1737	0.1514	0.1542	0.1683	0.1673	0.1685	0.1731	0.1936	0.1723
5904.96	0.1676	0.1694	0.1740	0.1517	0.1545	0.1685	0.1676	0.1688	0.1735	0.1940	0.1726
5901.11	0.1678	0.1698	0.1743	0.1518	0.1548	0.1687	0.1678	0.1691	0.1738	0.1943	0.1728
5897.25	0.1680	0.1701	0.1745	0.1518	0.1550	0.1688	0.1680	0.1692	0.1741	0.1946	0.1729
5893.39	0.1682	0.1703	0.1747	0.1519	0.1551	0.1690	0.1682	0.1693	0.1743	0.1949	0.1731
5889.54	0.1684	0.1704	0.1749	0.1519	0.1552	0.1691	0.1684	0.1694	0.1745	0.1952	0.1733
5885.68	0.1685	0.1704	0.1750	0.1517	0.1551	0.1691	0.1685	0.1692	0.1746	0.1953	0.1733
5881.82	0.1685	0.1703	0.1750	0.1514	0.1549	0.1690	0.1685	0.1689	0.1747	0.1955	0.1732
5877.97	0.1688	0.1707	0.1754	0.1517	0.1552	0.1693	0.1688	0.1693	0.1751	0.1960	0.1736
5874.11	0.1692	0.1713	0.1759	0.1522	0.1556	0.1696	0.1692	0.1697	0.1755	0.1965	0.1741
5870.25	0.1695	0.1718	0.1763	0.1525	0.1559	0.1699	0.1695	0.1701	0.1760	0.1971	0.1745
5866.4	0.1698	0.1724	0.1767	0.1528	0.1562	0.1703	0.1698	0.1705	0.1764	0.1976	0.1750
5862.54	0.1701	0.1727	0.1770	0.1531	0.1564	0.1704	0.1701	0.1707	0.1767	0.1980	0.1753
5858.68	0.1703	0.1729	0.1772	0.1532	0.1566	0.1706	0.1703	0.1709	0.1769	0.1983	0.1755
5854.82	0.1706	0.1732	0.1775	0.1535	0.1569	0.1708	0.1706	0.1711	0.1772	0.1987	0.1758
5850.97	0.1709	0.1736	0.1778	0.1538	0.1571	0.1710	0.1709	0.1713	0.1774	0.1991	0.1761
5847.11	0.1713	0.1739	0.1782	0.1540	0.1574	0.1713	0.1713	0.1716	0.1778	0.1995	0.1764
5843.25	0.1717	0.1743	0.1786	0.1543	0.1578	0.1716	0.1717	0.1719	0.1783	0.2001	0.1768

Table E1 (continued)

Wavenumbers (cm-1)	BoB	NH	NM	BuR	LA	NO	PP	RetF	RubS	RugE	BuP
5839.4	0.1722	0.1747	0.1790	0.1546	0.1581	0.1719	0.1722	0.1721	0.1787	0.2005	0.1772
5835.54	0.1726	0.1750	0.1794	0.1549	0.1585	0.1722	0.1727	0.1724	0.1791	0.2011	0.1775
5831.68	0.1732	0.1755	0.1800	0.1553	0.1589	0.1727	0.1732	0.1728	0.1796	0.2016	0.1780
5827.83	0.1737	0.1760	0.1805	0.1557	0.1593	0.1731	0.1738	0.1732	0.1802	0.2022	0.1786
5823.97	0.1744	0.1765	0.1811	0.1562	0.1598	0.1736	0.1744	0.1736	0.1807	0.2029	0.1792
5820.11	0.1750	0.1771	0.1817	0.1567	0.1603	0.1741	0.1750	0.1741	0.1813	0.2035	0.1798
5816.26	0.1756	0.1776	0.1823	0.1573	0.1608	0.1746	0.1756	0.1747	0.1819	0.2042	0.1804
5812.4	0.1762	0.1783	0.1829	0.1579	0.1613	0.1751	0.1762	0.1753	0.1825	0.2048	0.1811
5808.54	0.1768	0.1789	0.1836	0.1585	0.1618	0.1757	0.1768	0.1760	0.1832	0.2054	0.1818
5804.68	0.1775	0.1796	0.1843	0.1592	0.1624	0.1762	0.1775	0.1767	0.1839	0.2061	0.1826
5800.83	0.1779	0.1800	0.1847	0.1595	0.1626	0.1766	0.1779	0.1770	0.1843	0.2065	0.1830
5796.97	0.1781	0.1802	0.1849	0.1596	0.1628	0.1768	0.1781	0.1771	0.1845	0.2068	0.1831
5793.11	0.1784	0.1805	0.1852	0.1598	0.1629	0.1770	0.1784	0.1774	0.1849	0.2071	0.1834
5789.26	0.1786	0.1808	0.1854	0.1599	0.1631	0.1772	0.1787	0.1775	0.1851	0.2074	0.1835
5785.4	0.1788	0.1809	0.1856	0.1600	0.1632	0.1774	0.1788	0.1777	0.1853	0.2075	0.1836
5781.54	0.1789	0.1809	0.1857	0.1600	0.1632	0.1774	0.1789	0.1777	0.1853	0.2076	0.1837
5777.69	0.1789	0.1808	0.1857	0.1599	0.1632	0.1775	0.1789	0.1777	0.1853	0.2076	0.1836
5773.83	0.1788	0.1807	0.1857	0.1598	0.1632	0.1774	0.1788	0.1776	0.1852	0.2075	0.1835
5769.97	0.1787	0.1806	0.1856	0.1598	0.1631	0.1774	0.1787	0.1777	0.1851	0.2073	0.1834
5766.12	0.1784	0.1804	0.1855	0.1599	0.1631	0.1774	0.1784	0.1777	0.1849	0.2071	0.1833
5762.26	0.1781	0.1801	0.1853	0.1598	0.1630	0.1772	0.1781	0.1777	0.1847	0.2068	0.1831

Table E1 (continued)

Wavenumbers (cm-1)	BoB	NH	NM	BuR	LA	NO	PP	RetF	RubS	RugE	BuP
5758.4	0.1777	0.1798	0.1851	0.1598	0.1629	0.1771	0.1778	0.1776	0.1844	0.2064	0.1829
5754.54	0.1775	0.1796	0.1849	0.1598	0.1628	0.1770	0.1775	0.1776	0.1842	0.2061	0.1827
5750.69	0.1773	0.1795	0.1848	0.1599	0.1628	0.1769	0.1773	0.1776	0.1840	0.2059	0.1826
5746.83	0.1770	0.1793	0.1846	0.1599	0.1627	0.1767	0.1770	0.1776	0.1837	0.2056	0.1825
5742.97	0.1767	0.1791	0.1843	0.1600	0.1626	0.1766	0.1767	0.1776	0.1835	0.2053	0.1823
5739.12	0.1765	0.1786	0.1840	0.1596	0.1623	0.1763	0.1765	0.1771	0.1831	0.2050	0.1820
5735.26	0.1762	0.1781	0.1836	0.1590	0.1618	0.1759	0.1762	0.1765	0.1826	0.2046	0.1815
5731.4	0.1760	0.1775	0.1831	0.1584	0.1614	0.1756	0.1760	0.1758	0.1822	0.2043	0.1810
5727.55	0.1757	0.1769	0.1826	0.1577	0.1608	0.1751	0.1757	0.1751	0.1817	0.2039	0.1805
5723.69	0.1755	0.1766	0.1824	0.1574	0.1606	0.1749	0.1755	0.1747	0.1814	0.2037	0.1802
5719.83	0.1754	0.1763	0.1822	0.1572	0.1604	0.1747	0.1754	0.1744	0.1812	0.2035	0.1800
5715.98	0.1752	0.1760	0.1819	0.1569	0.1602	0.1745	0.1752	0.1740	0.1809	0.2033	0.1797
5712.12	0.1751	0.1757	0.1817	0.1566	0.1599	0.1743	0.1751	0.1736	0.1806	0.2032	0.1794
5708.26	0.1749	0.1755	0.1815	0.1564	0.1597	0.1741	0.1749	0.1734	0.1804	0.2030	0.1792
5704.4	0.1747	0.1754	0.1814	0.1561	0.1595	0.1740	0.1747	0.1732	0.1803	0.2030	0.1791
5700.55	0.1745	0.1753	0.1812	0.1560	0.1594	0.1739	0.1746	0.1730	0.1801	0.2029	0.1790
5696.69	0.1744	0.1752	0.1811	0.1558	0.1592	0.1739	0.1744	0.1729	0.1800	0.2029	0.1789
5692.83	0.1743	0.1752	0.1811	0.1557	0.1591	0.1738	0.1743	0.1728	0.1800	0.2028	0.1788
5688.98	0.1742	0.1751	0.1810	0.1556	0.1590	0.1738	0.1742	0.1728	0.1799	0.2028	0.1788
5685.12	0.1741	0.1752	0.1810	0.1556	0.1590	0.1738	0.1741	0.1728	0.1799	0.2028	0.1788
5681.26	0.1740	0.1752	0.1810	0.1556	0.1589	0.1738	0.1740	0.1728	0.1799	0.2028	0.1789

Table E1 (continued)

Wavenumbers (cm-1)	BoB	NH	NM	BuR	LA	NO	PP	RetF	RubS	RugE	BuP
5677.41	0.1738	0.1752	0.1809	0.1555	0.1588	0.1737	0.1738	0.1727	0.1798	0.2028	0.1788
5673.55	0.1737	0.1751	0.1808	0.1553	0.1587	0.1736	0.1737	0.1726	0.1796	0.2027	0.1787
5669.69	0.1736	0.1750	0.1807	0.1553	0.1586	0.1736	0.1736	0.1725	0.1796	0.2026	0.1786
5665.83	0.1735	0.1750	0.1806	0.1552	0.1585	0.1735	0.1735	0.1724	0.1794	0.2026	0.1785
5661.98	0.1732	0.1747	0.1804	0.1550	0.1583	0.1734	0.1732	0.1722	0.1792	0.2023	0.1783
5658.12	0.1729	0.1744	0.1801	0.1548	0.1581	0.1732	0.1729	0.1720	0.1788	0.2020	0.1780
5654.26	0.1726	0.1741	0.1798	0.1547	0.1579	0.1729	0.1727	0.1718	0.1785	0.2017	0.1777
5650.41	0.1723	0.1737	0.1795	0.1545	0.1577	0.1727	0.1723	0.1715	0.1781	0.2014	0.1774
5646.55	0.1720	0.1734	0.1792	0.1543	0.1575	0.1725	0.1721	0.1712	0.1778	0.2011	0.1771
5642.69	0.1718	0.1730	0.1789	0.1540	0.1572	0.1722	0.1718	0.1709	0.1775	0.2007	0.1768
5638.84	0.1715	0.1726	0.1785	0.1538	0.1569	0.1720	0.1715	0.1706	0.1771	0.2004	0.1764
5634.98	0.1711	0.1722	0.1781	0.1535	0.1567	0.1717	0.1712	0.1702	0.1767	0.2000	0.1760
5631.12	0.1709	0.1719	0.1778	0.1532	0.1564	0.1714	0.1709	0.1699	0.1763	0.1997	0.1757
5627.27	0.1707	0.1716	0.1776	0.1529	0.1561	0.1712	0.1707	0.1695	0.1760	0.1994	0.1753
5623.41	0.1705	0.1712	0.1772	0.1526	0.1558	0.1710	0.1705	0.1692	0.1757	0.1991	0.1750
5619.55	0.1702	0.1708	0.1769	0.1522	0.1555	0.1707	0.1703	0.1688	0.1754	0.1988	0.1746
5615.69	0.1701	0.1706	0.1767	0.1520	0.1553	0.1705	0.1701	0.1686	0.1751	0.1985	0.1744
5611.84	0.1699	0.1703	0.1765	0.1519	0.1552	0.1704	0.1699	0.1684	0.1749	0.1983	0.1741
5607.98	0.1697	0.1701	0.1763	0.1517	0.1550	0.1702	0.1697	0.1682	0.1747	0.1981	0.1739
5604.12	0.1696	0.1699	0.1762	0.1515	0.1548	0.1701	0.1696	0.1680	0.1745	0.1979	0.1737
5600.27	0.1695	0.1698	0.1760	0.1514	0.1547	0.1700	0.1695	0.1678	0.1744	0.1977	0.1736

Table E1 (continued)

Wavenumbers (cm-1)	BoB	NH	NM	BuR	LA	NO	PP	RetF	RubS	RugE	BuP
5596.41	0.1693	0.1696	0.1759	0.1512	0.1545	0.1698	0.1693	0.1676	0.1742	0.1975	0.1734
5592.55	0.1692	0.1695	0.1757	0.1511	0.1544	0.1697	0.1692	0.1675	0.1741	0.1974	0.1733
5588.7	0.1691	0.1694	0.1756	0.1510	0.1543	0.1697	0.1691	0.1674	0.1740	0.1972	0.1731
5584.84	0.1690	0.1692	0.1755	0.1509	0.1542	0.1695	0.1690	0.1672	0.1738	0.1970	0.1730
5580.98	0.1688	0.1691	0.1753	0.1507	0.1541	0.1694	0.1688	0.1671	0.1737	0.1969	0.1728
5577.13	0.1687	0.1689	0.1752	0.1506	0.1539	0.1693	0.1687	0.1670	0.1736	0.1967	0.1726
5573.27	0.1685	0.1688	0.1751	0.1505	0.1538	0.1692	0.1686	0.1669	0.1735	0.1965	0.1725
5569.41	0.1684	0.1687	0.1749	0.1503	0.1537	0.1691	0.1684	0.1668	0.1733	0.1963	0.1723
5565.55	0.1682	0.1686	0.1748	0.1502	0.1535	0.1690	0.1682	0.1666	0.1732	0.1961	0.1721
5561.7	0.1680	0.1684	0.1746	0.1500	0.1534	0.1688	0.1680	0.1665	0.1730	0.1958	0.1719
5557.84	0.1678	0.1683	0.1744	0.1499	0.1532	0.1687	0.1678	0.1664	0.1729	0.1956	0.1717
5553.98	0.1675	0.1680	0.1742	0.1497	0.1530	0.1685	0.1675	0.1661	0.1726	0.1953	0.1714
5550.13	0.1673	0.1678	0.1740	0.1494	0.1528	0.1683	0.1673	0.1659	0.1724	0.1950	0.1712
5546.27	0.1670	0.1675	0.1737	0.1492	0.1526	0.1681	0.1670	0.1656	0.1721	0.1947	0.1709
5542.41	0.1668	0.1672	0.1735	0.1489	0.1523	0.1679	0.1668	0.1654	0.1719	0.1944	0.1706
5538.56	0.1665	0.1670	0.1732	0.1486	0.1521	0.1677	0.1666	0.1651	0.1717	0.1941	0.1704
5534.7	0.1663	0.1667	0.1730	0.1484	0.1519	0.1676	0.1664	0.1649	0.1715	0.1939	0.1701
5530.84	0.1661	0.1665	0.1728	0.1481	0.1517	0.1674	0.1661	0.1646	0.1712	0.1936	0.1699
5526.99	0.1659	0.1662	0.1725	0.1478	0.1514	0.1672	0.1659	0.1643	0.1710	0.1933	0.1696
5523.13	0.1657	0.1659	0.1723	0.1476	0.1512	0.1670	0.1657	0.1640	0.1708	0.1930	0.1693
5519.27	0.1655	0.1656	0.1720	0.1473	0.1509	0.1668	0.1655	0.1637	0.1705	0.1927	0.1691

Table E1 (continued)

Wavenumbers (cm-1)	BoB	NH	NM	BuR	LA	NO	PP	RetF	RubS	RugE	BuP
5515.41	0.1652	0.1653	0.1718	0.1470	0.1507	0.1666	0.1653	0.1634	0.1702	0.1925	0.1688
5511.56	0.1650	0.1650	0.1716	0.1466	0.1504	0.1663	0.1650	0.1631	0.1700	0.1922	0.1686
5507.7	0.1648	0.1647	0.1713	0.1464	0.1502	0.1661	0.1648	0.1629	0.1697	0.1919	0.1683
5503.84	0.1646	0.1645	0.1711	0.1462	0.1500	0.1660	0.1646	0.1626	0.1695	0.1916	0.1681
5499.99	0.1643	0.1642	0.1708	0.1459	0.1498	0.1658	0.1644	0.1623	0.1692	0.1914	0.1678
5496.13	0.1641	0.1639	0.1706	0.1456	0.1495	0.1656	0.1641	0.1620	0.1690	0.1911	0.1675
5492.27	0.1639	0.1635	0.1704	0.1453	0.1493	0.1654	0.1639	0.1618	0.1687	0.1909	0.1673
5488.42	0.1637	0.1631	0.1702	0.1450	0.1492	0.1653	0.1637	0.1616	0.1684	0.1906	0.1670
5484.56	0.1635	0.1630	0.1700	0.1449	0.1490	0.1651	0.1635	0.1614	0.1683	0.1905	0.1668
5480.7	0.1634	0.1631	0.1698	0.1449	0.1488	0.1650	0.1634	0.1611	0.1683	0.1903	0.1665
5476.85	0.1631	0.1628	0.1696	0.1446	0.1486	0.1648	0.1631	0.1609	0.1680	0.1900	0.1663
5472.99	0.1629	0.1623	0.1693	0.1442	0.1484	0.1646	0.1629	0.1606	0.1676	0.1897	0.1660
5469.13	0.1626	0.1620	0.1691	0.1440	0.1482	0.1644	0.1626	0.1603	0.1674	0.1895	0.1657
5465.27	0.1623	0.1617	0.1688	0.1437	0.1479	0.1642	0.1624	0.1600	0.1671	0.1892	0.1654
5461.42	0.1621	0.1615	0.1686	0.1435	0.1477	0.1640	0.1621	0.1598	0.1669	0.1889	0.1651
5457.56	0.1619	0.1613	0.1684	0.1433	0.1476	0.1639	0.1619	0.1596	0.1667	0.1888	0.1649
5453.7	0.1617	0.1611	0.1682	0.1431	0.1474	0.1637	0.1617	0.1593	0.1665	0.1885	0.1647
5449.85	0.1615	0.1609	0.1680	0.1429	0.1472	0.1636	0.1615	0.1591	0.1663	0.1883	0.1644
5445.99	0.1612	0.1605	0.1677	0.1425	0.1469	0.1633	0.1612	0.1588	0.1659	0.1880	0.1641
5442.13	0.1609	0.1599	0.1674	0.1420	0.1466	0.1630	0.1609	0.1584	0.1655	0.1876	0.1637
5438.28	0.1605	0.1596	0.1670	0.1417	0.1464	0.1628	0.1605	0.1581	0.1652	0.1873	0.1634

Table E1 (continued)

Wavenumbers (cm-1)	BoB	NH	NM	BuR	LA	NO	PP	RetF	RubS	RugE	BuP
5434.42	0.1602	0.1593	0.1667	0.1414	0.1460	0.1625	0.1602	0.1577	0.1649	0.1869	0.1630
5430.56	0.1600	0.1591	0.1665	0.1412	0.1459	0.1624	0.1600	0.1576	0.1647	0.1868	0.1628
5426.71	0.1600	0.1590	0.1665	0.1411	0.1459	0.1624	0.1600	0.1575	0.1647	0.1867	0.1627
5422.85	0.1599	0.1591	0.1664	0.1410	0.1458	0.1623	0.1599	0.1573	0.1646	0.1867	0.1626
5418.99	0.1599	0.1593	0.1663	0.1411	0.1457	0.1623	0.1599	0.1572	0.1647	0.1867	0.1625
5415.13	0.1597	0.1590	0.1661	0.1408	0.1455	0.1622	0.1597	0.1570	0.1645	0.1864	0.1623
5411.28	0.1594	0.1586	0.1659	0.1404	0.1453	0.1620	0.1594	0.1567	0.1642	0.1861	0.1620
5407.42	0.1592	0.1580	0.1657	0.1400	0.1451	0.1618	0.1592	0.1565	0.1639	0.1859	0.1618
5403.56	0.1590	0.1580	0.1655	0.1398	0.1449	0.1617	0.1590	0.1563	0.1637	0.1857	0.1616
5399.71	0.1590	0.1581	0.1655	0.1398	0.1449	0.1617	0.1590	0.1562	0.1638	0.1857	0.1616
5395.85	0.1591	0.1584	0.1656	0.1400	0.1450	0.1619	0.1591	0.1563	0.1640	0.1859	0.1617
5391.99	0.1592	0.1585	0.1657	0.1400	0.1450	0.1620	0.1592	0.1564	0.1641	0.1860	0.1618
5388.14	0.1593	0.1585	0.1658	0.1400	0.1451	0.1622	0.1593	0.1565	0.1643	0.1862	0.1619
5384.28	0.1594	0.1586	0.1659	0.1400	0.1452	0.1623	0.1594	0.1565	0.1644	0.1863	0.1620
5380.42	0.1594	0.1587	0.1660	0.1400	0.1453	0.1624	0.1594	0.1566	0.1645	0.1865	0.1621
5376.56	0.1595	0.1588	0.1662	0.1400	0.1454	0.1626	0.1596	0.1567	0.1646	0.1867	0.1623
5372.71	0.1597	0.1589	0.1664	0.1401	0.1455	0.1628	0.1597	0.1568	0.1648	0.1869	0.1625
5368.85	0.1600	0.1592	0.1668	0.1403	0.1458	0.1631	0.1600	0.1571	0.1652	0.1873	0.1628
5364.99	0.1603	0.1596	0.1672	0.1406	0.1461	0.1635	0.1603	0.1574	0.1656	0.1878	0.1632
5361.14	0.1607	0.1601	0.1677	0.1410	0.1464	0.1640	0.1607	0.1578	0.1661	0.1883	0.1637
5357.28	0.1611	0.1606	0.1682	0.1414	0.1468	0.1645	0.1611	0.1582	0.1666	0.1890	0.1642

Table E1 (continued)

Wavenumbers (cm-1)	BoB	NH	NM	BuR	LA	NO	PP	RetF	RubS	RugE	BuP
5353.42	0.1613	0.1608	0.1686	0.1415	0.1471	0.1648	0.1614	0.1585	0.1669	0.1894	0.1646
5349.57	0.1615	0.1609	0.1690	0.1416	0.1473	0.1651	0.1615	0.1588	0.1672	0.1897	0.1650
5345.71	0.1617	0.1610	0.1694	0.1418	0.1476	0.1655	0.1618	0.1591	0.1675	0.1902	0.1654
5341.85	0.1619	0.1612	0.1699	0.1419	0.1479	0.1659	0.1620	0.1595	0.1678	0.1907	0.1659
5338	0.1627	0.1621	0.1709	0.1426	0.1486	0.1668	0.1627	0.1603	0.1687	0.1918	0.1669
5334.14	0.1637	0.1633	0.1721	0.1436	0.1495	0.1679	0.1637	0.1613	0.1700	0.1932	0.1680
5330.28	0.1647	0.1645	0.1733	0.1445	0.1504	0.1690	0.1647	0.1623	0.1712	0.1946	0.1692
5326.42	0.1658	0.1658	0.1746	0.1455	0.1515	0.1702	0.1658	0.1634	0.1725	0.1962	0.1705
5322.57	0.1670	0.1672	0.1762	0.1467	0.1526	0.1716	0.1670	0.1647	0.1740	0.1979	0.1720
5318.71	0.1683	0.1688	0.1779	0.1479	0.1539	0.1731	0.1683	0.1661	0.1756	0.1998	0.1736
5314.85	0.1698	0.1705	0.1797	0.1493	0.1553	0.1747	0.1698	0.1677	0.1775	0.2019	0.1754
5311	0.1714	0.1724	0.1817	0.1509	0.1568	0.1765	0.1714	0.1694	0.1794	0.2042	0.1774
5307.14	0.1732	0.1744	0.1840	0.1525	0.1585	0.1786	0.1732	0.1713	0.1816	0.2068	0.1797
5303.28	0.1751	0.1765	0.1865	0.1543	0.1604	0.1808	0.1751	0.1734	0.1839	0.2096	0.1821
5299.43	0.1772	0.1789	0.1892	0.1563	0.1624	0.1832	0.1772	0.1757	0.1865	0.2126	0.1848
5295.57	0.1794	0.1814	0.1921	0.1584	0.1646	0.1858	0.1795	0.1781	0.1892	0.2158	0.1876
5291.71	0.1821	0.1844	0.1956	0.1609	0.1672	0.1889	0.1821	0.1810	0.1925	0.2197	0.1910
5287.86	0.1851	0.1877	0.1994	0.1637	0.1701	0.1922	0.1851	0.1841	0.1960	0.2239	0.1947
5284	0.1882	0.1912	0.2034	0.1667	0.1731	0.1958	0.1882	0.1875	0.1998	0.2283	0.1986
5280.14	0.1916	0.1949	0.2078	0.1698	0.1764	0.1997	0.1916	0.1911	0.2039	0.2331	0.2028
5276.28	0.1953	0.1992	0.2124	0.1733	0.1799	0.2038	0.1953	0.1949	0.2083	0.2384	0.2074

Table E1 (continued)

Wavenumbers (cm-1)	BoB	NH	NM	BuR	LA	NO	PP	RetF	RubS	RugE	BuP
5272.43	0.1992	0.2038	0.2174	0.1771	0.1836	0.2082	0.1992	0.1990	0.2130	0.2440	0.2122
5268.57	0.2033	0.2083	0.2227	0.1810	0.1877	0.2129	0.2033	0.2034	0.2179	0.2499	0.2173
5264.71	0.2077	0.2130	0.2284	0.1851	0.1919	0.2178	0.2077	0.2080	0.2230	0.2561	0.2227
5260.86	0.2122	0.2180	0.2340	0.1894	0.1962	0.2227	0.2122	0.2126	0.2282	0.2624	0.2281
5257	0.2168	0.2231	0.2398	0.1938	0.2006	0.2278	0.2168	0.2174	0.2336	0.2690	0.2336
5253.14	0.2217	0.2285	0.2460	0.1984	0.2052	0.2331	0.2217	0.2224	0.2392	0.2759	0.2394
5249.29	0.2268	0.2340	0.2524	0.2033	0.2101	0.2387	0.2268	0.2276	0.2451	0.2830	0.2455
5245.43	0.2317	0.2393	0.2585	0.2079	0.2147	0.2438	0.2317	0.2325	0.2506	0.2898	0.2512
5241.57	0.2366	0.2445	0.2645	0.2126	0.2193	0.2490	0.2366	0.2374	0.2561	0.2966	0.2568
5237.72	0.2418	0.2501	0.2708	0.2176	0.2241	0.2543	0.2418	0.2426	0.2619	0.3038	0.2627
5233.86	0.2470	0.2559	0.2772	0.2227	0.2290	0.2597	0.2470	0.2477	0.2676	0.3110	0.2686
5230	0.2517	0.2607	0.2829	0.2272	0.2333	0.2645	0.2517	0.2524	0.2727	0.3174	0.2739
5226.14	0.2562	0.2651	0.2884	0.2314	0.2375	0.2690	0.2562	0.2568	0.2774	0.3235	0.2789
5222.29	0.2608	0.2698	0.2939	0.2358	0.2417	0.2736	0.2608	0.2612	0.2822	0.3297	0.2839
5218.43	0.2653	0.2742	0.2993	0.2400	0.2458	0.2780	0.2652	0.2656	0.2868	0.3358	0.2888
5214.57	0.2695	0.2786	0.3043	0.2441	0.2497	0.2821	0.2695	0.2696	0.2913	0.3416	0.2933
5210.72	0.2736	0.2829	0.3090	0.2482	0.2534	0.2860	0.2736	0.2734	0.2956	0.3471	0.2977
5206.86	0.2774	0.2862	0.3136	0.2516	0.2568	0.2896	0.2773	0.2770	0.2993	0.3521	0.3017
5203	0.2809	0.2891	0.3178	0.2548	0.2601	0.2929	0.2809	0.2804	0.3026	0.3567	0.3055
5199.15	0.2844	0.2924	0.3218	0.2580	0.2630	0.2960	0.2843	0.2835	0.3061	0.3612	0.3090
5195.29	0.2876	0.2956	0.3254	0.2610	0.2658	0.2988	0.2876	0.2864	0.3093	0.3652	0.3123

Table E1 (continued)

Wavenumbers (cm-1)	BoB	NH	NM	BuR	LA	NO	PP	RetF	RubS	RugE	BuP
5191.43	0.2906	0.2983	0.3287	0.2637	0.2684	0.3014	0.2906	0.2891	0.3121	0.3689	0.3153
5187.58	0.2934	0.3007	0.3317	0.2661	0.2707	0.3037	0.2934	0.2915	0.3146	0.3722	0.3179
5183.72	0.2958	0.3026	0.3342	0.2681	0.2725	0.3056	0.2957	0.2934	0.3167	0.3748	0.3202
5179.86	0.2978	0.3041	0.3362	0.2697	0.2740	0.3071	0.2977	0.2951	0.3185	0.3769	0.3221
5176	0.2995	0.3054	0.3379	0.2710	0.2753	0.3083	0.2995	0.2965	0.3199	0.3787	0.3237
5172.15	0.3010	0.3064	0.3392	0.2720	0.2763	0.3092	0.3010	0.2976	0.3211	0.3799	0.3250
5168.29	0.3023	0.3071	0.3403	0.2728	0.2771	0.3099	0.3022	0.2984	0.3220	0.3809	0.3260
5164.43	0.3032	0.3075	0.3410	0.2732	0.2776	0.3103	0.3032	0.2990	0.3226	0.3815	0.3267
5160.58	0.3039	0.3076	0.3413	0.2734	0.2777	0.3104	0.3038	0.2993	0.3228	0.3817	0.3271
5156.72	0.3042	0.3074	0.3412	0.2732	0.2776	0.3101	0.3042	0.2993	0.3228	0.3814	0.3272
5152.86	0.3046	0.3072	0.3412	0.2730	0.2776	0.3099	0.3045	0.2993	0.3227	0.3812	0.3272
5149.01	0.3047	0.3069	0.3409	0.2727	0.2773	0.3095	0.3047	0.2992	0.3225	0.3807	0.3271
5145.15	0.3045	0.3063	0.3402	0.2721	0.2768	0.3089	0.3045	0.2987	0.3220	0.3799	0.3266
5141.29	0.3042	0.3054	0.3393	0.2712	0.2761	0.3080	0.3042	0.2980	0.3212	0.3788	0.3259
5137.44	0.3038	0.3046	0.3384	0.2704	0.2754	0.3071	0.3037	0.2974	0.3204	0.3777	0.3252
5133.58	0.3032	0.3036	0.3374	0.2695	0.2746	0.3061	0.3032	0.2966	0.3195	0.3765	0.3243
5129.72	0.3024	0.3025	0.3360	0.2683	0.2735	0.3049	0.3024	0.2956	0.3184	0.3750	0.3232
5125.86	0.3014	0.3011	0.3345	0.2670	0.2723	0.3035	0.3014	0.2944	0.3171	0.3734	0.3219
5122.01	0.3005	0.2999	0.3331	0.2658	0.2713	0.3023	0.3005	0.2934	0.3159	0.3718	0.3207
5118.15	0.2995	0.2986	0.3316	0.2646	0.2702	0.3010	0.2995	0.2922	0.3146	0.3702	0.3194
5114.29	0.2983	0.2971	0.3300	0.2631	0.2689	0.2995	0.2983	0.2910	0.3132	0.3684	0.3180

Table E1 (continued)

Wavenumbers (cm-1)	BoB	NH	NM	BuR	LA	NO	PP	RetF	RubS	RugE	BuP
5110.44	0.2970	0.2956	0.3282	0.2616	0.2675	0.2980	0.2970	0.2896	0.3116	0.3665	0.3164
5106.58	0.2958	0.2942	0.3266	0.2603	0.2663	0.2966	0.2958	0.2884	0.3102	0.3647	0.3150
5102.72	0.2946	0.2929	0.3250	0.2589	0.2650	0.2952	0.2946	0.2871	0.3089	0.3630	0.3134
5098.87	0.2932	0.2915	0.3233	0.2575	0.2637	0.2937	0.2932	0.2858	0.3074	0.3611	0.3118
5095.01	0.2918	0.2900	0.3215	0.2560	0.2623	0.2922	0.2918	0.2845	0.3059	0.3592	0.3101
5091.15	0.2905	0.2887	0.3199	0.2546	0.2611	0.2908	0.2905	0.2832	0.3045	0.3575	0.3087
5087.29	0.2893	0.2874	0.3183	0.2533	0.2599	0.2894	0.2893	0.2820	0.3032	0.3557	0.3072
5083.44	0.2880	0.2860	0.3167	0.2519	0.2586	0.2881	0.2880	0.2808	0.3018	0.3540	0.3057
5079.58	0.2867	0.2847	0.3151	0.2506	0.2574	0.2867	0.2867	0.2796	0.3005	0.3523	0.3042
5075.72	0.2854	0.2834	0.3136	0.2493	0.2562	0.2854	0.2854	0.2784	0.2993	0.3506	0.3028
5071.87	0.2842	0.2822	0.3121	0.2480	0.2550	0.2841	0.2842	0.2773	0.2980	0.3490	0.3014
5068.01	0.2830	0.2810	0.3107	0.2467	0.2538	0.2828	0.2830	0.2761	0.2968	0.3473	0.3000
5064.15	0.2818	0.2798	0.3092	0.2455	0.2527	0.2816	0.2818	0.2750	0.2956	0.3458	0.2986
5060.3	0.2805	0.2785	0.3077	0.2442	0.2515	0.2803	0.2805	0.2738	0.2943	0.3441	0.2972
5056.44	0.2793	0.2773	0.3062	0.2429	0.2503	0.2790	0.2793	0.2726	0.2930	0.3425	0.2958
5052.58	0.2780	0.2761	0.3047	0.2416	0.2492	0.2777	0.2780	0.2715	0.2918	0.3408	0.2944
5048.73	0.2768	0.2748	0.3032	0.2404	0.2480	0.2764	0.2768	0.2703	0.2906	0.3392	0.2930
5044.87	0.2755	0.2735	0.3017	0.2391	0.2469	0.2751	0.2755	0.2691	0.2893	0.3376	0.2915
5041.01	0.2741	0.2723	0.3001	0.2378	0.2457	0.2738	0.2742	0.2679	0.2879	0.3359	0.2900
5037.15	0.2728	0.2710	0.2985	0.2366	0.2445	0.2725	0.2728	0.2666	0.2866	0.3342	0.2885
5033.3	0.2715	0.2697	0.2969	0.2353	0.2433	0.2712	0.2715	0.2654	0.2853	0.3326	0.2870

Table E1 (continued)

Wavenumbers (cm-1)	BoB	NH	NM	BuR	LA	NO	PP	RetF	RubS	RugE	BuP
5029.44	0.2701	0.2685	0.2954	0.2341	0.2422	0.2699	0.2702	0.2642	0.2840	0.3310	0.2856
5025.58	0.2689	0.2673	0.2939	0.2329	0.2411	0.2687	0.2689	0.2630	0.2827	0.3294	0.2842
5021.73	0.2675	0.2660	0.2924	0.2317	0.2399	0.2675	0.2676	0.2618	0.2814	0.3278	0.2828
5017.87	0.2662	0.2648	0.2908	0.2306	0.2388	0.2662	0.2663	0.2606	0.2801	0.3262	0.2814
5014.01	0.2650	0.2637	0.2895	0.2295	0.2378	0.2651	0.2651	0.2595	0.2790	0.3248	0.2801
5010.16	0.2639	0.2627	0.2881	0.2285	0.2369	0.2641	0.2639	0.2585	0.2778	0.3234	0.2789
5006.3	0.2628	0.2617	0.2868	0.2276	0.2360	0.2630	0.2628	0.2574	0.2767	0.3221	0.2777
5002.44	0.2617	0.2607	0.2855	0.2266	0.2351	0.2620	0.2617	0.2564	0.2757	0.3207	0.2766
4998.59	0.2607	0.2598	0.2844	0.2259	0.2344	0.2611	0.2607	0.2555	0.2748	0.3196	0.2756
4994.73	0.2598	0.2590	0.2834	0.2252	0.2337	0.2603	0.2598	0.2547	0.2740	0.3186	0.2748
4990.87	0.2589	0.2583	0.2824	0.2245	0.2331	0.2596	0.2590	0.2540	0.2732	0.3176	0.2739
4987.01	0.2581	0.2576	0.2815	0.2239	0.2326	0.2589	0.2582	0.2532	0.2725	0.3167	0.2732
4983.16	0.2576	0.2572	0.2808	0.2235	0.2322	0.2584	0.2576	0.2527	0.2720	0.3160	0.2727
4979.3	0.2571	0.2570	0.2803	0.2232	0.2319	0.2579	0.2571	0.2524	0.2716	0.3155	0.2722
4975.44	0.2567	0.2568	0.2798	0.2230	0.2316	0.2575	0.2567	0.2520	0.2713	0.3151	0.2719
4971.59	0.2563	0.2567	0.2795	0.2229	0.2314	0.2572	0.2564	0.2518	0.2711	0.3147	0.2716
4967.73	0.2562	0.2567	0.2793	0.2230	0.2314	0.2571	0.2562	0.2517	0.2711	0.3146	0.2716
4963.87	0.2561	0.2568	0.2792	0.2231	0.2315	0.2570	0.2561	0.2517	0.2711	0.3146	0.2716
4960.02	0.2561	0.2571	0.2792	0.2234	0.2317	0.2571	0.2562	0.2518	0.2713	0.3147	0.2718
4956.16	0.2563	0.2574	0.2794	0.2237	0.2320	0.2572	0.2563	0.2520	0.2716	0.3150	0.2721
4952.3	0.2566	0.2580	0.2797	0.2242	0.2324	0.2575	0.2566	0.2523	0.2721	0.3155	0.2726

Table E1 (continued)

Wavenumbers (cm-1)	BoB	NH	NM	BuR	LA	NO	PP	RetF	RubS	RugE	BuP
4948.45	0.2570	0.2587	0.2802	0.2249	0.2329	0.2579	0.2570	0.2528	0.2727	0.3161	0.2732
4944.59	0.2575	0.2595	0.2808	0.2257	0.2335	0.2583	0.2576	0.2535	0.2734	0.3168	0.2739
4940.73	0.2582	0.2605	0.2816	0.2266	0.2342	0.2589	0.2582	0.2542	0.2743	0.3177	0.2748
4936.87	0.2590	0.2616	0.2825	0.2277	0.2351	0.2597	0.2590	0.2551	0.2753	0.3188	0.2758
4933.02	0.2600	0.2628	0.2836	0.2289	0.2362	0.2605	0.2600	0.2561	0.2765	0.3200	0.2770
4929.16	0.2610	0.2642	0.2848	0.2302	0.2373	0.2614	0.2611	0.2573	0.2778	0.3214	0.2783
4925.3	0.2622	0.2657	0.2862	0.2317	0.2386	0.2625	0.2623	0.2585	0.2793	0.3230	0.2797
4921.45	0.2637	0.2674	0.2878	0.2333	0.2400	0.2637	0.2637	0.2600	0.2809	0.3247	0.2814
4917.59	0.2652	0.2692	0.2895	0.2351	0.2415	0.2651	0.2653	0.2616	0.2826	0.3266	0.2833
4913.73	0.2670	0.2711	0.2914	0.2370	0.2432	0.2665	0.2670	0.2633	0.2846	0.3286	0.2853
4909.88	0.2688	0.2732	0.2935	0.2391	0.2450	0.2681	0.2688	0.2652	0.2867	0.3308	0.2875
4906.02	0.2708	0.2754	0.2957	0.2413	0.2470	0.2698	0.2708	0.2673	0.2889	0.3332	0.2898
4902.16	0.2729	0.2778	0.2981	0.2437	0.2491	0.2717	0.2729	0.2695	0.2913	0.3357	0.2922
4898.31	0.2751	0.2803	0.3006	0.2462	0.2513	0.2737	0.2751	0.2719	0.2938	0.3383	0.2947
4894.45	0.2775	0.2830	0.3034	0.2489	0.2537	0.2758	0.2775	0.2744	0.2966	0.3411	0.2974
4890.59	0.2798	0.2856	0.3061	0.2515	0.2560	0.2779	0.2798	0.2769	0.2992	0.3439	0.3000
4886.73	0.2821	0.2883	0.3089	0.2542	0.2584	0.2800	0.2821	0.2795	0.3020	0.3468	0.3027
4882.88	0.2846	0.2911	0.3118	0.2571	0.2610	0.2823	0.2846	0.2823	0.3049	0.3498	0.3056
4879.02	0.2872	0.2941	0.3149	0.2600	0.2636	0.2847	0.2872	0.2852	0.3080	0.3529	0.3085
4875.16	0.2893	0.2966	0.3174	0.2626	0.2659	0.2867	0.2893	0.2876	0.3104	0.3556	0.3111
4871.31	0.2913	0.2989	0.3198	0.2651	0.2680	0.2885	0.2913	0.2899	0.3126	0.3582	0.3135

Table E1 (continued)

Wavenumbers (cm-1)	BoB	NH	NM	BuR	LA	NO	PP	RetF	RubS	RugE	BuP
4867.45	0.2935	0.3014	0.3224	0.2677	0.2702	0.2904	0.2935	0.2924	0.3150	0.3609	0.3161
4863.59	0.2955	0.3038	0.3248	0.2703	0.2724	0.2923	0.2955	0.2948	0.3172	0.3635	0.3186
4859.74	0.2970	0.3056	0.3266	0.2724	0.2742	0.2936	0.2970	0.2966	0.3188	0.3656	0.3204
4855.88	0.2982	0.3072	0.3280	0.2744	0.2757	0.2946	0.2982	0.2983	0.3201	0.3674	0.3220
4852.02	0.2994	0.3088	0.3294	0.2763	0.2772	0.2956	0.2994	0.2999	0.3213	0.3692	0.3235
4848.17	0.3004	0.3102	0.3305	0.2781	0.2785	0.2964	0.3004	0.3013	0.3223	0.3707	0.3249
4844.31	0.3013	0.3115	0.3315	0.2799	0.2798	0.2972	0.3013	0.3027	0.3232	0.3722	0.3262
4840.45	0.3022	0.3128	0.3324	0.2816	0.2810	0.2978	0.3021	0.3040	0.3240	0.3736	0.3273
4836.59	0.3028	0.3138	0.3331	0.2832	0.2821	0.2983	0.3028	0.3051	0.3245	0.3747	0.3283
4832.74	0.3032	0.3147	0.3335	0.2846	0.2831	0.2986	0.3032	0.3061	0.3248	0.3757	0.3291
4828.88	0.3040	0.3161	0.3344	0.2865	0.2844	0.2993	0.3040	0.3076	0.3256	0.3771	0.3303
4825.02	0.3049	0.3176	0.3355	0.2885	0.2859	0.3000	0.3048	0.3092	0.3265	0.3785	0.3317
4821.17	0.3055	0.3189	0.3363	0.2904	0.2872	0.3006	0.3055	0.3106	0.3272	0.3798	0.3329
4817.31	0.3062	0.3203	0.3371	0.2924	0.2885	0.3012	0.3062	0.3121	0.3279	0.3810	0.3341
4813.45	0.3070	0.3217	0.3381	0.2943	0.2900	0.3020	0.3070	0.3137	0.3288	0.3824	0.3354
4809.6	0.3080	0.3232	0.3392	0.2963	0.2914	0.3029	0.3079	0.3153	0.3298	0.3838	0.3369
4805.74	0.3089	0.3247	0.3403	0.2983	0.2929	0.3038	0.3088	0.3169	0.3308	0.3853	0.3383
4801.88	0.3098	0.3263	0.3415	0.3003	0.2945	0.3047	0.3098	0.3186	0.3318	0.3867	0.3398
4798.02	0.3106	0.3276	0.3425	0.3019	0.2957	0.3054	0.3106	0.3200	0.3328	0.3880	0.3409
4794.17	0.3114	0.3289	0.3434	0.3032	0.2968	0.3061	0.3114	0.3212	0.3337	0.3893	0.3419
4790.31	0.3123	0.3302	0.3444	0.3047	0.2980	0.3069	0.3122	0.3225	0.3346	0.3906	0.3430

Table E1 (continued)

Wavenumbers (cm-1)	BoB	NH	NM	BuR	LA	NO	PP	RetF	RubS	RugE	BuP
4786.45	0.3131	0.3315	0.3453	0.3060	0.2992	0.3077	0.3131	0.3237	0.3356	0.3918	0.3440
4782.6	0.3140	0.3326	0.3462	0.3071	0.3002	0.3084	0.3139	0.3247	0.3365	0.3930	0.3450
4778.74	0.3149	0.3336	0.3470	0.3081	0.3011	0.3090	0.3148	0.3257	0.3373	0.3942	0.3460
4774.88	0.3157	0.3347	0.3478	0.3090	0.3020	0.3097	0.3157	0.3266	0.3382	0.3953	0.3469
4771.03	0.3166	0.3356	0.3486	0.3098	0.3028	0.3103	0.3166	0.3275	0.3390	0.3964	0.3478
4767.17	0.3174	0.3363	0.3492	0.3102	0.3034	0.3107	0.3173	0.3280	0.3396	0.3972	0.3484
4763.31	0.3180	0.3369	0.3496	0.3105	0.3038	0.3111	0.3180	0.3284	0.3401	0.3980	0.3489
4759.46	0.3187	0.3374	0.3501	0.3106	0.3042	0.3114	0.3187	0.3287	0.3407	0.3988	0.3493
4755.6	0.3193	0.3378	0.3504	0.3106	0.3044	0.3116	0.3193	0.3288	0.3411	0.3995	0.3497
4751.74	0.3199	0.3382	0.3508	0.3107	0.3048	0.3119	0.3199	0.3291	0.3415	0.4001	0.3501
4747.88	0.3205	0.3386	0.3511	0.3108	0.3051	0.3121	0.3205	0.3293	0.3419	0.4007	0.3505
4744.03	0.3210	0.3388	0.3514	0.3106	0.3053	0.3123	0.3210	0.3293	0.3423	0.4012	0.3507
4740.17	0.3215	0.3390	0.3516	0.3104	0.3054	0.3124	0.3215	0.3293	0.3426	0.4016	0.3509
4736.31	0.3219	0.3395	0.3519	0.3105	0.3059	0.3127	0.3219	0.3296	0.3430	0.4021	0.3513
4732.46	0.3224	0.3399	0.3523	0.3107	0.3064	0.3129	0.3223	0.3299	0.3434	0.4025	0.3517
4728.6	0.3226	0.3403	0.3526	0.3109	0.3068	0.3131	0.3226	0.3302	0.3438	0.4029	0.3518
4724.74	0.3227	0.3407	0.3529	0.3110	0.3073	0.3133	0.3227	0.3305	0.3442	0.4032	0.3518
4720.89	0.3229	0.3412	0.3533	0.3113	0.3077	0.3136	0.3229	0.3310	0.3446	0.4035	0.3519
4717.03	0.3230	0.3418	0.3536	0.3117	0.3081	0.3140	0.3230	0.3315	0.3451	0.4039	0.3521
4713.17	0.3232	0.3423	0.3540	0.3121	0.3085	0.3143	0.3232	0.3321	0.3456	0.4042	0.3523
4709.32	0.3233	0.3429	0.3544	0.3126	0.3090	0.3146	0.3233	0.3327	0.3461	0.4045	0.3526

Table E1 (continued)

Wavenumbers (cm-1)	BoB	NH	NM	BuR	LA	NO	PP	RetF	RubS	RugE	BuP
4705.46	0.3235	0.3433	0.3548	0.3128	0.3093	0.3149	0.3235	0.3331	0.3465	0.4047	0.3528
4701.6	0.3237	0.3437	0.3551	0.3129	0.3096	0.3152	0.3237	0.3335	0.3469	0.4050	0.3530
4697.74	0.3239	0.3441	0.3554	0.3132	0.3098	0.3154	0.3239	0.3339	0.3473	0.4052	0.3533
4693.89	0.3241	0.3445	0.3558	0.3134	0.3101	0.3157	0.3241	0.3343	0.3477	0.4054	0.3536
4690.03	0.3243	0.3449	0.3562	0.3136	0.3104	0.3161	0.3243	0.3347	0.3482	0.4056	0.3539
4686.17	0.3246	0.3453	0.3566	0.3137	0.3108	0.3165	0.3246	0.3351	0.3487	0.4059	0.3542
4682.32	0.3249	0.3457	0.3571	0.3139	0.3111	0.3168	0.3248	0.3355	0.3492	0.4062	0.3545
4678.46	0.3252	0.3461	0.3575	0.3140	0.3114	0.3172	0.3251	0.3359	0.3497	0.4064	0.3548
4674.6	0.3255	0.3465	0.3580	0.3142	0.3118	0.3177	0.3255	0.3363	0.3503	0.4067	0.3552
4670.75	0.3259	0.3469	0.3586	0.3144	0.3122	0.3181	0.3258	0.3368	0.3508	0.4070	0.3556
4666.89	0.3262	0.3473	0.3592	0.3146	0.3126	0.3186	0.3262	0.3372	0.3514	0.4073	0.3560
4663.03	0.3266	0.3477	0.3597	0.3148	0.3131	0.3191	0.3266	0.3376	0.3521	0.4076	0.3565
4659.18	0.3269	0.3480	0.3602	0.3150	0.3134	0.3195	0.3269	0.3380	0.3525	0.4077	0.3568
4655.32	0.3271	0.3482	0.3605	0.3152	0.3138	0.3198	0.3270	0.3384	0.3529	0.4077	0.3570
4651.46	0.3273	0.3484	0.3609	0.3154	0.3141	0.3202	0.3273	0.3388	0.3534	0.4078	0.3573
4647.6	0.3275	0.3486	0.3613	0.3156	0.3145	0.3206	0.3275	0.3391	0.3538	0.4077	0.3576
4643.75	0.3278	0.3489	0.3618	0.3159	0.3150	0.3211	0.3278	0.3396	0.3543	0.4079	0.3580
4639.89	0.3282	0.3492	0.3624	0.3163	0.3155	0.3216	0.3282	0.3402	0.3549	0.4081	0.3585
4636.03	0.3286	0.3495	0.3629	0.3167	0.3160	0.3221	0.3286	0.3408	0.3554	0.4082	0.3589
4632.18	0.3290	0.3499	0.3634	0.3171	0.3165	0.3226	0.3290	0.3413	0.3559	0.4083	0.3594
4628.32	0.3292	0.3500	0.3638	0.3172	0.3168	0.3228	0.3292	0.3417	0.3563	0.4083	0.3596

Table E1 (continued)

Wavenumbers (cm-1)	BoB	NH	NM	BuR	LA	NO	PP	RetF	RubS	RugE	BuP
4624.46	0.3294	0.3500	0.3640	0.3174	0.3171	0.3230	0.3293	0.3419	0.3565	0.4082	0.3598
4620.61	0.3295	0.3500	0.3643	0.3175	0.3173	0.3232	0.3295	0.3422	0.3568	0.4081	0.3599
4616.75	0.3297	0.3500	0.3645	0.3177	0.3176	0.3234	0.3297	0.3425	0.3570	0.4079	0.3601
4612.89	0.3295	0.3493	0.3640	0.3169	0.3171	0.3230	0.3295	0.3418	0.3566	0.4073	0.3595
4609.04	0.3292	0.3483	0.3633	0.3157	0.3164	0.3224	0.3292	0.3408	0.3560	0.4064	0.3586
4605.18	0.3288	0.3473	0.3626	0.3145	0.3156	0.3217	0.3288	0.3398	0.3554	0.4055	0.3576
4601.32	0.3283	0.3460	0.3616	0.3131	0.3146	0.3209	0.3283	0.3384	0.3546	0.4045	0.3565
4597.46	0.3277	0.3448	0.3606	0.3117	0.3135	0.3200	0.3277	0.3372	0.3537	0.4033	0.3553
4593.61	0.3269	0.3435	0.3594	0.3102	0.3123	0.3191	0.3269	0.3359	0.3527	0.4021	0.3540
4589.75	0.3260	0.3420	0.3581	0.3085	0.3109	0.3180	0.3260	0.3343	0.3515	0.4008	0.3524
4585.89	0.3250	0.3403	0.3566	0.3065	0.3093	0.3167	0.3250	0.3325	0.3501	0.3993	0.3507
4582.04	0.3240	0.3389	0.3552	0.3048	0.3079	0.3157	0.3240	0.3309	0.3489	0.3979	0.3492
4578.18	0.3230	0.3374	0.3539	0.3031	0.3065	0.3146	0.3230	0.3294	0.3477	0.3966	0.3477
4574.32	0.3218	0.3357	0.3524	0.3012	0.3049	0.3134	0.3218	0.3276	0.3464	0.3951	0.3459
4570.47	0.3206	0.3340	0.3508	0.2992	0.3032	0.3121	0.3206	0.3258	0.3450	0.3935	0.3441
4566.61	0.3195	0.3325	0.3494	0.2975	0.3017	0.3110	0.3195	0.3242	0.3437	0.3921	0.3426
4562.75	0.3185	0.3310	0.3480	0.2958	0.3003	0.3098	0.3185	0.3227	0.3424	0.3906	0.3411
4558.9	0.3173	0.3294	0.3465	0.2940	0.2988	0.3087	0.3173	0.3210	0.3411	0.3891	0.3395
4555.04	0.3161	0.3279	0.3451	0.2923	0.2973	0.3075	0.3161	0.3194	0.3398	0.3875	0.3379
4551.18	0.3151	0.3265	0.3438	0.2908	0.2960	0.3065	0.3151	0.3180	0.3386	0.3862	0.3364
4547.32	0.3140	0.3252	0.3425	0.2893	0.2947	0.3055	0.3140	0.3167	0.3375	0.3849	0.3351

Table E1 (continued)

Wavenumbers (cm-1)	BoB	NH	NM	BuR	LA	NO	PP	RetF	RubS	RugE	BuP
4543.47	0.3130	0.3240	0.3413	0.2879	0.2935	0.3046	0.3130	0.3154	0.3364	0.3836	0.3338
4539.61	0.3120	0.3227	0.3401	0.2866	0.2923	0.3036	0.3120	0.3141	0.3353	0.3823	0.3325
4535.75	0.3111	0.3215	0.3389	0.2852	0.2911	0.3028	0.3111	0.3128	0.3343	0.3812	0.3312
4531.9	0.3103	0.3204	0.3378	0.2839	0.2900	0.3020	0.3103	0.3115	0.3333	0.3800	0.3301
4528.04	0.3095	0.3193	0.3367	0.2827	0.2889	0.3013	0.3095	0.3103	0.3324	0.3790	0.3289
4524.18	0.3088	0.3182	0.3356	0.2815	0.2878	0.3006	0.3088	0.3091	0.3315	0.3779	0.3279
4520.33	0.3079	0.3171	0.3344	0.2802	0.2867	0.2996	0.3079	0.3078	0.3305	0.3769	0.3267
4516.47	0.3071	0.3160	0.3332	0.2791	0.2857	0.2984	0.3071	0.3066	0.3295	0.3758	0.3255
4512.61	0.3063	0.3149	0.3321	0.2779	0.2846	0.2973	0.3063	0.3054	0.3285	0.3748	0.3244
4508.75	0.3055	0.3138	0.3309	0.2768	0.2836	0.2962	0.3055	0.3042	0.3276	0.3737	0.3233
4504.9	0.3048	0.3129	0.3299	0.2758	0.2828	0.2952	0.3048	0.3031	0.3267	0.3729	0.3222
4501.04	0.3042	0.3120	0.3290	0.2747	0.2821	0.2944	0.3042	0.3019	0.3260	0.3722	0.3212
4497.18	0.3035	0.3111	0.3280	0.2737	0.2815	0.2935	0.3035	0.3008	0.3252	0.3714	0.3202
4493.33	0.3029	0.3102	0.3271	0.2728	0.2809	0.2926	0.3029	0.2997	0.3244	0.3708	0.3193
4489.47	0.3029	0.3100	0.3269	0.2723	0.2807	0.2923	0.3029	0.2991	0.3244	0.3708	0.3190
4485.61	0.3032	0.3101	0.3270	0.2721	0.2806	0.2923	0.3032	0.2987	0.3246	0.3712	0.3190
4481.76	0.3035	0.3101	0.3271	0.2719	0.2807	0.2922	0.3035	0.2983	0.3249	0.3717	0.3191
4477.9	0.3040	0.3104	0.3274	0.2719	0.2809	0.2924	0.3040	0.2981	0.3254	0.3723	0.3193
4474.04	0.3052	0.3113	0.3284	0.2725	0.2813	0.2932	0.3052	0.2985	0.3266	0.3738	0.3203
4470.19	0.3066	0.3127	0.3297	0.2734	0.2819	0.2943	0.3066	0.2993	0.3282	0.3758	0.3217
4466.33	0.3083	0.3142	0.3313	0.2745	0.2827	0.2956	0.3083	0.3002	0.3299	0.3780	0.3233

Table E1 (continued)

Wavenumbers (cm-1)	BoB	NH	NM	BuR	LA	NO	PP	RetF	RubS	RugE	BuP
4462.47	0.3103	0.3161	0.3333	0.2759	0.2835	0.2972	0.3103	0.3014	0.3321	0.3806	0.3253
4458.61	0.3126	0.3184	0.3358	0.2777	0.2852	0.2992	0.3126	0.3031	0.3346	0.3836	0.3277
4454.76	0.3152	0.3210	0.3387	0.2798	0.2873	0.3015	0.3152	0.3052	0.3375	0.3871	0.3305
4450.9	0.3182	0.3240	0.3420	0.2822	0.2895	0.3041	0.3182	0.3075	0.3407	0.3910	0.3336
4447.04	0.3215	0.3273	0.3456	0.2850	0.2921	0.3071	0.3215	0.3102	0.3443	0.3953	0.3371
4443.19	0.3243	0.3303	0.3491	0.2876	0.2946	0.3098	0.3243	0.3130	0.3475	0.3989	0.3403
4439.33	0.3272	0.3333	0.3526	0.2904	0.2972	0.3127	0.3272	0.3159	0.3508	0.4025	0.3437
4435.47	0.3304	0.3368	0.3565	0.2935	0.3002	0.3160	0.3303	0.3192	0.3545	0.4065	0.3474
4431.62	0.3337	0.3404	0.3607	0.2968	0.3035	0.3194	0.3336	0.3228	0.3583	0.4106	0.3513
4427.76	0.3363	0.3435	0.3641	0.2996	0.3062	0.3223	0.3363	0.3258	0.3614	0.4137	0.3545
4423.9	0.3388	0.3464	0.3673	0.3023	0.3089	0.3250	0.3388	0.3289	0.3643	0.4166	0.3576
4420.05	0.3415	0.3496	0.3708	0.3053	0.3118	0.3280	0.3414	0.3322	0.3673	0.4196	0.3609
4416.19	0.3440	0.3528	0.3742	0.3083	0.3148	0.3309	0.3440	0.3355	0.3703	0.4225	0.3642
4412.33	0.3467	0.3557	0.3772	0.3110	0.3174	0.3334	0.3467	0.3385	0.3732	0.4255	0.3673
4408.47	0.3495	0.3587	0.3801	0.3137	0.3200	0.3358	0.3495	0.3412	0.3759	0.4285	0.3703
4404.62	0.3522	0.3616	0.3830	0.3163	0.3226	0.3382	0.3521	0.3441	0.3786	0.4313	0.3732
4400.76	0.3548	0.3645	0.3857	0.3189	0.3251	0.3405	0.3548	0.3468	0.3811	0.4341	0.3760
4396.9	0.3571	0.3675	0.3885	0.3221	0.3280	0.3428	0.3571	0.3502	0.3837	0.4368	0.3789
4393.05	0.3593	0.3707	0.3912	0.3256	0.3310	0.3451	0.3593	0.3539	0.3863	0.4394	0.3818
4389.19	0.3614	0.3737	0.3938	0.3289	0.3340	0.3472	0.3614	0.3574	0.3888	0.4419	0.3845
4385.33	0.3634	0.3768	0.3964	0.3324	0.3370	0.3493	0.3634	0.3611	0.3912	0.4443	0.3872

Table E1 (continued)

Wavenumbers (cm-1)	BoB	NH	NM	BuR	LA	NO	PP	RetF	RubS	RugE	BuP
4381.48	0.3652	0.3783	0.3979	0.3336	0.3385	0.3505	0.3651	0.3626	0.3928	0.4461	0.3886
4377.62	0.3667	0.3791	0.3990	0.3339	0.3394	0.3513	0.3667	0.3633	0.3940	0.4475	0.3894
4373.76	0.3681	0.3800	0.4000	0.3345	0.3405	0.3521	0.3681	0.3641	0.3951	0.4488	0.3903
4369.91	0.3694	0.3805	0.4007	0.3344	0.3410	0.3526	0.3693	0.3645	0.3959	0.4499	0.3907
4366.05	0.3704	0.3810	0.4016	0.3351	0.3418	0.3531	0.3704	0.3650	0.3967	0.4509	0.3916
4362.19	0.3713	0.3814	0.4024	0.3359	0.3424	0.3536	0.3712	0.3654	0.3975	0.4516	0.3924
4358.33	0.3719	0.3813	0.4028	0.3360	0.3426	0.3537	0.3719	0.3652	0.3979	0.4521	0.3927
4354.48	0.3725	0.3810	0.4031	0.3360	0.3426	0.3537	0.3724	0.3647	0.3982	0.4524	0.3929
4350.62	0.3737	0.3824	0.4045	0.3373	0.3440	0.3547	0.3736	0.3658	0.3995	0.4539	0.3944
4346.76	0.3750	0.3843	0.4063	0.3390	0.3458	0.3560	0.3750	0.3673	0.4012	0.4558	0.3963
4342.91	0.3762	0.3859	0.4079	0.3405	0.3474	0.3571	0.3762	0.3685	0.4027	0.4575	0.3980
4339.05	0.3775	0.3878	0.4097	0.3422	0.3492	0.3583	0.3775	0.3699	0.4043	0.4594	0.3999
4335.19	0.3782	0.3895	0.4110	0.3431	0.3499	0.3593	0.3782	0.3710	0.4055	0.4610	0.4012
4331.34	0.3788	0.3911	0.4120	0.3438	0.3503	0.3603	0.3788	0.3720	0.4065	0.4626	0.4025
4327.48	0.3794	0.3922	0.4130	0.3446	0.3508	0.3612	0.3794	0.3730	0.4074	0.4640	0.4034
4323.62	0.3799	0.3931	0.4138	0.3454	0.3510	0.3620	0.3799	0.3740	0.4080	0.4653	0.4041
4319.77	0.3797	0.3925	0.4133	0.3454	0.3507	0.3616	0.3797	0.3735	0.4074	0.4652	0.4037
4315.91	0.3791	0.3910	0.4122	0.3451	0.3499	0.3606	0.3791	0.3724	0.4061	0.4644	0.4026
4312.05	0.3785	0.3897	0.4109	0.3448	0.3491	0.3598	0.3785	0.3713	0.4049	0.4637	0.4017
4308.19	0.3776	0.3878	0.4093	0.3442	0.3480	0.3586	0.3776	0.3697	0.4032	0.4625	0.4004
4304.34	0.3777	0.3877	0.4092	0.3444	0.3479	0.3585	0.3777	0.3695	0.4031	0.4627	0.4003

Table E1 (continued)

Wavenumbers (cm-1)	BoB	NH	NM	BuR	LA	NO	PP	RetF	RubS	RugE	BuP
4300.48	0.3782	0.3882	0.4096	0.3448	0.3481	0.3588	0.3782	0.3698	0.4036	0.4632	0.4005
4296.62	0.3783	0.3880	0.4094	0.3449	0.3480	0.3588	0.3783	0.3695	0.4035	0.4633	0.4003
4292.77	0.3786	0.3881	0.4094	0.3451	0.3480	0.3588	0.3786	0.3694	0.4036	0.4635	0.4002
4288.91	0.3784	0.3879	0.4092	0.3448	0.3478	0.3587	0.3784	0.3692	0.4035	0.4631	0.3999
4285.05	0.3781	0.3878	0.4090	0.3444	0.3474	0.3587	0.3781	0.3689	0.4033	0.4626	0.3995
4281.2	0.3780	0.3878	0.4089	0.3440	0.3471	0.3587	0.3780	0.3688	0.4033	0.4621	0.3993
4277.34	0.3778	0.3878	0.4089	0.3436	0.3468	0.3588	0.3777	0.3687	0.4033	0.4616	0.3990
4273.48	0.3781	0.3884	0.4094	0.3440	0.3473	0.3593	0.3781	0.3692	0.4038	0.4618	0.3995
4269.63	0.3787	0.3893	0.4103	0.3449	0.3481	0.3599	0.3786	0.3700	0.4045	0.4624	0.4003
4265.77	0.3791	0.3903	0.4111	0.3455	0.3488	0.3606	0.3791	0.3708	0.4053	0.4629	0.4011
4261.91	0.3797	0.3914	0.4122	0.3464	0.3497	0.3614	0.3797	0.3717	0.4062	0.4635	0.4021
4258.05	0.3798	0.3921	0.4125	0.3468	0.3501	0.3617	0.3798	0.3724	0.4064	0.4635	0.4025
4254.2	0.3796	0.3927	0.4126	0.3472	0.3503	0.3619	0.3796	0.3729	0.4065	0.4635	0.4027
4250.34	0.3789	0.3918	0.4120	0.3466	0.3498	0.3615	0.3789	0.3725	0.4056	0.4626	0.4018
4246.48	0.3777	0.3902	0.4108	0.3456	0.3488	0.3607	0.3777	0.3716	0.4042	0.4612	0.4002
4242.63	0.3764	0.3885	0.4093	0.3444	0.3476	0.3597	0.3764	0.3702	0.4026	0.4596	0.3985
4238.77	0.3747	0.3862	0.4075	0.3428	0.3460	0.3583	0.3747	0.3684	0.4007	0.4578	0.3963
4234.91	0.3735	0.3850	0.4063	0.3418	0.3450	0.3574	0.3735	0.3673	0.3994	0.4565	0.3950
4231.06	0.3724	0.3840	0.4051	0.3409	0.3440	0.3565	0.3724	0.3663	0.3982	0.4553	0.3939
4227.2	0.3716	0.3834	0.4045	0.3403	0.3434	0.3561	0.3716	0.3657	0.3975	0.4546	0.3931
4223.34	0.3712	0.3831	0.4041	0.3399	0.3432	0.3559	0.3711	0.3655	0.3970	0.4542	0.3927

Table E1 (continued)

Wavenumbers (cm-1)	BoB	NH	NM	BuR	LA	NO	PP	RetF	RubS	RugE	BuP
4219.48	0.3706	0.3828	0.4038	0.3395	0.3428	0.3558	0.3706	0.3653	0.3966	0.4538	0.3923
4215.63	0.3702	0.3827	0.4036	0.3393	0.3427	0.3557	0.3702	0.3653	0.3963	0.4536	0.3921
4211.77	0.3694	0.3821	0.4030	0.3387	0.3421	0.3553	0.3694	0.3647	0.3956	0.4529	0.3915
4207.91	0.3686	0.3813	0.4024	0.3380	0.3415	0.3549	0.3686	0.3640	0.3948	0.4521	0.3908
4204.06	0.3680	0.3808	0.4019	0.3375	0.3410	0.3546	0.3680	0.3634	0.3942	0.4515	0.3903
4200.2	0.3673	0.3803	0.4015	0.3369	0.3405	0.3543	0.3673	0.3629	0.3936	0.4509	0.3898
4196.34	0.3673	0.3803	0.4015	0.3371	0.3406	0.3544	0.3672	0.3630	0.3935	0.4508	0.3899
4192.49	0.3674	0.3807	0.4019	0.3376	0.3409	0.3547	0.3674	0.3634	0.3938	0.4510	0.3903
4188.63	0.3676	0.3810	0.4022	0.3381	0.3412	0.3551	0.3675	0.3637	0.3941	0.4511	0.3906
4184.77	0.3679	0.3816	0.4027	0.3388	0.3417	0.3555	0.3679	0.3642	0.3945	0.4514	0.3912
4180.92	0.3685	0.3821	0.4034	0.3393	0.3422	0.3561	0.3685	0.3646	0.3951	0.4521	0.3918
4177.06	0.3693	0.3827	0.4041	0.3399	0.3428	0.3568	0.3693	0.3650	0.3958	0.4531	0.3926
4173.2	0.3702	0.3835	0.4051	0.3407	0.3435	0.3576	0.3702	0.3656	0.3967	0.4542	0.3936
4169.34	0.3714	0.3844	0.4062	0.3417	0.3443	0.3586	0.3714	0.3663	0.3978	0.4555	0.3947
4165.49	0.3725	0.3853	0.4074	0.3425	0.3452	0.3595	0.3724	0.3671	0.3988	0.4569	0.3958
4161.63	0.3736	0.3862	0.4086	0.3434	0.3461	0.3606	0.3736	0.3679	0.3998	0.4583	0.3970
4157.77	0.3749	0.3872	0.4100	0.3444	0.3472	0.3618	0.3749	0.3687	0.4011	0.4600	0.3983
4153.92	0.3764	0.3883	0.4116	0.3455	0.3483	0.3631	0.3763	0.3697	0.4024	0.4619	0.3997
4150.06	0.3775	0.3894	0.4131	0.3466	0.3494	0.3644	0.3775	0.3708	0.4036	0.4634	0.4011
4146.2	0.3786	0.3906	0.4146	0.3477	0.3505	0.3658	0.3785	0.3720	0.4048	0.4650	0.4025
4142.35	0.3797	0.3918	0.4163	0.3489	0.3517	0.3672	0.3797	0.3733	0.4061	0.4667	0.4039

Table E1 (continued)

Wavenumbers (cm-1)	BoB	NH	NM	BuR	LA	NO	PP	RetF	RubS	RugE	BuP
4138.49	0.3809	0.3931	0.4180	0.3501	0.3529	0.3688	0.3809	0.3747	0.4074	0.4684	0.4055
4134.63	0.3828	0.3950	0.4203	0.3520	0.3546	0.3707	0.3827	0.3765	0.4093	0.4706	0.4076
4130.78	0.3849	0.3971	0.4227	0.3542	0.3567	0.3728	0.3849	0.3785	0.4115	0.4732	0.4100
4126.92	0.3870	0.3993	0.4252	0.3564	0.3587	0.3749	0.3870	0.3805	0.4137	0.4757	0.4124
4123.06	0.3894	0.4017	0.4279	0.3588	0.3610	0.3773	0.3893	0.3828	0.4161	0.4784	0.4151
4119.2	0.3920	0.4045	0.4310	0.3617	0.3635	0.3800	0.3920	0.3855	0.4190	0.4816	0.4182
4115.35	0.3949	0.4077	0.4344	0.3648	0.3663	0.3829	0.3949	0.3885	0.4221	0.4851	0.4217
4111.49	0.3981	0.4110	0.4379	0.3681	0.3692	0.3860	0.3980	0.3916	0.4254	0.4888	0.4254
4107.63	0.4014	0.4146	0.4417	0.3717	0.3724	0.3893	0.4014	0.3950	0.4290	0.4927	0.4294
4103.78	0.4049	0.4186	0.4460	0.3757	0.3760	0.3929	0.4049	0.3990	0.4329	0.4970	0.4337
4099.92	0.4086	0.4229	0.4505	0.3801	0.3799	0.3969	0.4085	0.4033	0.4370	0.5016	0.4383
4096.06	0.4125	0.4276	0.4553	0.3847	0.3840	0.4010	0.4125	0.4079	0.4414	0.5064	0.4433
4092.21	0.4167	0.4325	0.4605	0.3897	0.3884	0.4054	0.4166	0.4128	0.4461	0.5116	0.4485
4088.35	0.4204	0.4367	0.4651	0.3938	0.3921	0.4094	0.4204	0.4169	0.4504	0.5163	0.4531
4084.49	0.4241	0.4409	0.4696	0.3978	0.3957	0.4133	0.4241	0.4209	0.4545	0.5209	0.4575
4080.64	0.4281	0.4453	0.4745	0.4022	0.3996	0.4175	0.4280	0.4252	0.4590	0.5259	0.4623
4076.78	0.4321	0.4498	0.4794	0.4065	0.4036	0.4217	0.4320	0.4296	0.4635	0.5310	0.4671
4072.92	0.4358	0.4544	0.4843	0.4110	0.4076	0.4259	0.4358	0.4341	0.4680	0.5360	0.4719
4069.06	0.4396	0.4590	0.4892	0.4156	0.4116	0.4301	0.4395	0.4386	0.4725	0.5411	0.4767
4065.21	0.4433	0.4636	0.4942	0.4201	0.4157	0.4344	0.4433	0.4432	0.4771	0.5462	0.4816
4061.35	0.4471	0.4683	0.4992	0.4247	0.4197	0.4388	0.4470	0.4478	0.4817	0.5514	0.4865

Table E1 (continued)

Wavenumbers (cm-1)	BoB	NH	NM	BuR	LA	NO	PP	RetF	RubS	RugE	BuP
4057.49	0.4506	0.4726	0.5037	0.4291	0.4236	0.4427	0.4505	0.4522	0.4858	0.5561	0.4909
4053.64	0.4539	0.4767	0.5079	0.4334	0.4273	0.4464	0.4538	0.4565	0.4897	0.5606	0.4952
4049.78	0.4572	0.4810	0.5123	0.4378	0.4311	0.4501	0.4571	0.4607	0.4937	0.5651	0.4995
4045.92	0.4604	0.4851	0.5165	0.4422	0.4348	0.4538	0.4603	0.4649	0.4975	0.5696	0.5037
4042.07	0.4632	0.4879	0.5197	0.4449	0.4373	0.4566	0.4631	0.4674	0.5004	0.5733	0.5067
4038.21	0.4659	0.4901	0.5224	0.4469	0.4391	0.4590	0.4658	0.4692	0.5028	0.5767	0.5091
4034.35	0.4684	0.4923	0.5249	0.4489	0.4410	0.4613	0.4683	0.4709	0.5052	0.5801	0.5114
4030.5	0.4708	0.4941	0.5271	0.4503	0.4424	0.4633	0.4707	0.4721	0.5072	0.5831	0.5133
4026.64	0.4728	0.4962	0.5296	0.4527	0.4444	0.4654	0.4727	0.4740	0.5093	0.5860	0.5154
4022.78	0.4745	0.4983	0.5319	0.4552	0.4464	0.4674	0.4744	0.4760	0.5112	0.5888	0.5175
4018.92	0.4760	0.4998	0.5338	0.4571	0.4480	0.4690	0.4759	0.4774	0.5127	0.5912	0.5191
4015.07	0.4774	0.5012	0.5356	0.4589	0.4495	0.4705	0.4772	0.4787	0.5140	0.5934	0.5205
4011.21	0.4782	0.5024	0.5369	0.4601	0.4504	0.4716	0.4781	0.4796	0.5151	0.5951	0.5214
4007.35	0.4788	0.5033	0.5379	0.4610	0.4512	0.4726	0.4787	0.4804	0.5159	0.5963	0.5220
4003.5	0.4791	0.5041	0.5387	0.4619	0.4518	0.4733	0.4790	0.4810	0.5165	0.5974	0.5224
3999.64	0.4792	0.5046	0.5393	0.4624	0.4522	0.4738	0.4791	0.4814	0.5169	0.5981	0.5225

Table E2 Common chromatographic peaks of 11 species of Boletes

Common peaks (mAU)	Time (min)	PP	BoB	NM	RetF	LA	BuR	BuP	NO	RubS	RugE	NH
P1	**5.1858**	56.0694	15.6353	5.5781	5.2025	41.8802	1.7144	10.7216	17.5849	9.7828	14.5925	3.6471
P2	**5.3658**	48.8126	30.5517	21.7271	29.7815	13.2645	11.3365	19.7639	23.9494	22.9156	18.4762	4.5661
P3	**5.3925**	25.9822	34.1177	1117.4357	16.7517	296.8958	3.7661	662.1275	30.7410	52.6911	482.0913	12.1687
P4	**6.0925**	1029.5106	360.9750	392.1972	115.8285	77.9824	220.3369	517.8356	1076.8488	209.7480	341.3268	341.6634
P5	**6.3658**	45.0600	24.6520	153.8195	29.8653	41.6734	15.3006	103.7740	95.1714	55.3077	50.2669	70.0452
P6	**8.0858**	77.8017	732.7089	1107.5497	730.3958	1005.3526	600.9725	822.3418	709.5006	852.3515	834.1022	757.2090
P7	**8.5259**	401.5015	54.0640	47.7736	133.3640	47.6288	68.4868	89.7486	84.6895	87.8426	29.0080	42.8448
P8	**9.0659**	30.4074	14.0059	34.9264	28.1144	35.5503	15.0579	57.0647	36.2902	42.1528	43.2542	12.1031
P9	**9.3526**	9.1693	561.3955	905.4030	523.3586	615.5092	353.9942	738.5450	555.8562	529.2868	769.6210	91.6381
P10	**10.1526**	19.4968	87.4914	174.3753	141.9298	110.5233	125.5393	197.9026	112.5573	192.8014	189.2125	302.0192
P11	**12.1328**	22.6835	13.2942	14.6771	7.0865	10.6594	6.5936	7.9003	39.9572	20.8142	16.6693	10.4456
P12	**13.8929**	35.7454	10.4942	33.6444	29.5680	5.2534	6.3646	8.8191	46.1869	10.8376	11.3840	8.4312
P13	**16.6597**	12.5807	139.9073	27.6633	55.2166	47.2211	82.8742	43.3236	6.3163	50.5960	71.2439	9.2282
P14	**16.8463**	45.5737	13.9915	39.2173	29.5908	13.2880	9.5574	6.7729	28.9634	35.6905	13.4440	35.6008
P15	**18.1662**	77.0730	130.2632	53.5483	18.9182	230.3762	68.3620	39.4334	17.1295	40.8223	51.8475	58.5768
P16	**20.9860**	13.7125	14.0465	18.3950	7.0609	9.7561	15.3499	35.9925	56.9290	9.6413	125.9293	55.9180
P17	**21.4727**	12.5612	44.7742	31.6199	41.1736	10.3826	0.3257	25.5180	17.8284	34.0402	48.7549	23.4905
P18	**23.6658**	6.8964	22.9344	27.5468	52.1984	13.6955	12.0116	35.9967	71.2028	18.2393	28.0465	5.9201
P19	**29.8254**	19.5994	4.0363	31.2800	16.8293	28.1315	9.7872	17.2111	17.0220	16.1247	23.8233	15.0660
P20	**30.3254**	3.1831	20.6537	19.2995	33.1760	19.6469	70.6831	13.8879	18.6559	21.0346	15.9653	9.0784

Table E2 (continued)

Common peaks (mAU)	Time (min)	PP	BoB	NM	RetF	LA	BuR	BuP	NO	RubS	RugE	NH
P21	**31.2386**	17.3249	4.1744	32.2232	50.8588	12.5939	18.3632	4.3934	12.3685	11.3027	13.7909	6.4545
P22	**32.0786**	2.1846	11.1879	8.0625	7.1633	2.4518	19.7165	7.2424	19.9546	11.9818	0.9400	1.9096
P23	**34.5858**	5.0167	25.2675	60.0974	45.8560	48.0745	2.3316	37.9998	37.9237	22.8581	16.9665	28.3351
P24	**35.7660**	0.3139	8.0102	11.1551	37.4832	3.8722	38.7899	8.3753	12.1632	7.5621	7.0800	1.4253
P25	**36.3862**	1.3414	3.7834	9.8747	13.8993	6.3809	1.8317	6.9998	7.8302	10.4586	18.9047	7.8434
P26	**39.0267**	27.7514	33.5765	29.6608	29.7613	4.8804	31.2190	35.9061	28.8710	33.8867	32.5661	34.8198
P27	**40.5537**	17.3272	32.5380	9.3800	18.0462	32.8101	20.5958	15.6465	1.2577	14.2645	7.2019	1.6062
P28	**42.7209**	14.8021	15.5379	15.3963	8.3079	8.0977	18.0185	16.5444	17.5933	18.7311	21.4896	26.4855
P29	**44.2478**	37.3908	13.4765	14.3848	9.9729	3.8428	5.8462	10.3801	32.1971	7.4622	8.5475	5.6904
P30	**44.6346**	9.9791	10.3759	12.1314	6.7984	2.5469	4.0210	7.0924	23.6956	4.7156	10.1071	5.2930

Table E3 Percentages of volatile components of 11 species of Boletes

NO	Compounds (%)	CAS#	RT (min)	BoB	BuR	BuP	LA	NO	PP	RugE	RetF	RubS	NH	NM
C1	Pyridine	110-86-1	3.17	0.294	0.261	0.391	2.973	1.741	0.098	0.198	0.274	1.543	0.585	1.336
C2	Pyrrole	109-97-7	3.23	0.31	0.219	2.978	3.812	1.923	0.184	1.059	0.392	3.64	1.127	2.254
C3	Toluene	108-88-3	3.46	0.925	0.929	0.806	1.091	0.9	0.819	0.182	0.675	0.796	0.857	0.833
C4	2-Hydroxy-Propanenitrile	78-97-7	3.76	0.633	3.971	4.072	5.515	1.461	0.279	4.133	1.185	0.835	1.077	2.251
C5	Hexanal	66-25-1	3.94	1.664	0.7	3.972	2.104	2.241	2.658	5.841	6.232	21.863	0.73	0.523
C6	Triethyl orthoformate	122-51-0	3.96	1.518	46.15	10.069	2.75	11.667	7.394	8.328	36.059	21.544	3.498	12.621
C7	2(5H)-Furanone, 3-methyl-	22122-36-7	4.31	0.109	0.24	3.017	0.361	0.963	0.092	1.258	0.183	0.283	0.315	0.295
C8	2-Methylpyrazine	109-08-0	4.38	0.177	0.34	0.804	0.288	0.66	0.141	0.304	0.23	0.323	0.854	0.319
C9	Furfural	98-01-1	4.51	0.931	0.318	3.443	1.268	1.767	0.454	6.798	0.518	3.832	3.483	7.65
C10	3-methylbutanoic acid	503-74-2	4.61	1.04	0.197	3.19	1.346	1.277	0.154	5.635	0.303	3.443	2.827	4.164
C11	2-methyl-butyric acid	116-53-0	4.89	0.424	0	1.688	3.508	2.466	0.123	0.912	0.383	1.314	1.97	2.468
C12	Ethylbenzene	100-41-4	5.13	0.125	0.138	0.146	0.279	0.279	0.076	0.34	0.122	0.185	0.488	0.167
C13	1,4-Xylene	106-42-3	5.32	0.235	0.303	0.296	0.491	0.296	0.214	0.535	0.237	0.303	0.3	0.237
C14	2-Cyclopentene-1,4-dione	930-60-9	5.55	0.924	1.591	0.398	7.569	0.674	0.235	0.323	0.516	0.763	0.827	0.483
C15	2-Heptanone	110-43-0	5.73	0.225	0.209	0.145	0.383	0.881	0.218	0.162	0.194	0.2	0.29	0.19
C16	1,2-xylene	95-47-6	5.84	0.15	0.21	0.147	0.307	0.358	0.122	0.208	0.391	0.131	1.229	0.253

Table E3 (continued)

NO	Compounds (%)	CAS#	RT (min)	BoB	BuR	BuP	LA	NO	PP	RugE	RetF	RubS	NH	NM
C17	1,2,3,4,5-Pentamethylcyclopentadiene	4045-44-7	5.88	0.977	0.484	2.833	0.514	1.352	0.175	0.923	0.702	0.625	0.748	1.369
C18	Methional	3268-49-3	6.15	3.452	1.279	1.215	1.868	4.997	1.983	0.272	0.461	0.262	0.352	0.376
C19	2,6-Dimethylpyrazine	108-50-9	6.27	0.262	0.221	0.347	0.41	0.503	0.389	0.566	0.209	0.705	0.572	0.313
C20	1-Methyl-1H-pyrrole-2-carbalde	1192-58-1	6.49	0.696	0.643	0.705	0.268	1.205	0.193	0.233	0.627	0.506	0.514	0.291
C21	(1r)-(+)-alpha-pinene	7785-70-8	6.86	0.134	0.166	1.644	0.7	0.118	0.538	1.423	1.248	8.136	0.339	0.273
C22	1-(Pyridin-1(4H)-yl)ethanone	67402-83-9	7.15	0.16	0.146	0.246	1.366	0.21	0.118	0.245	0.338	0.235	0.321	0.351
C23	4,5-Dihydro-5-methyl-2(3H)-fur	108-29-2	7.24	0.264	0.173	0.36	0.218	1.056	0.252	0.386	0.237	0.383	0.412	0.264
C24	Tetrahydrothiophen-3-one	1003-04-9	7.39	0.211	0.224	0.405	0.463	0.139	0.162	1.347	0.418	2.966	1.255	0.27
C25	5-Methyl furfural	620-02-0	7.55	0.186	0.099	0.263	0.211	0.221	0.13	0.37	0.177	0.273	0.449	0.207
C26	Benzaldehyde	100-52-7	7.61	0.817	1.344	0.648	0.398	0.916	0.434	1.836	0.6	0.762	0.692	0.67
C27	1-Decen-3-one	56606-79-2	7.98	4.456	13.619	2.277	3.308	2.228	3.159	9.141	4.556	1.838	2.247	2.529
C28	Tetraethyl orthosilicate	78-10-4	8.01	3.417	2.741	1.009	1.42	7.764	1.272	21.033	1.447	14.183	1.106	1.122
C29	1-Octen-3-ol	3391-86-4	8.08	10.329	15.448	18.604	24.058	64.467	4.938	45.045	8.058	1.806	0.285	2.565
C30	2-Pentylfuran	3777-69-3	8.34	8.907	9.079	7.996	8.895	7.92	8.576	0.748	10.119	7.965	6.915	7.152
C31	Decane	124-18-5	8.63	1.63	1.811	1.41	1.681	1.257	1.323	0.478	1.809	1.479	1.344	1.336

Table E3 (continued)

NO	Compounds (%)	CAS#	RT (min)	BoB	BuR	BuP	LA	NO	PP	RugE	RetF	RubS	NH	NM
C32	2-Acetylthiazole	24295-03-2	9.19	0.123	0.297	0.232	0.283	0.168	0.174	0.186	0.281	0.253	0.185	0.377
C33	2,2,4,4,6,8,8-heptamethyl-Nonane	4390-04-9	9.4	1.122	1.186	0.987	1.21	1.834	1.085	2.146	1.296	1.061	1.008	0.981
C34	2H-Pyran-2-one,5,6-dihydro-	3393-45-1	9.63	1.471	1.055	1.197	1.377	2.917	1.401	0.326	2.124	1.289	0.842	1.024
C35	1-Butanamine,3-methyl-N-(3-methylbutylidene)-	35448-31-8	9.85	0.238	0.606	6.327	1.352	13.706	1.785	1.8	7.919	21.11	4.066	2.984
C36	Phenylacetaldehyde	122-78-1	9.9	0.733	0.444	6.427	0.89	4.375	1.143	2.383	2.844	23.206	1.396	1.744
C37	2,5,9-Trimethyldecane	62108-22-9	10	0.593	0.506	0.924	0.642	1.584	0.839	0.496	0.762	0.606	0.483	0.818
C38	(E)-2-Octenal	2548-87-0	10.27	1.49	0.966	0.532	0.284	1.202	0.778	4.648	0.792	0.594	0.733	0.342
C39	2-Acetyl pyrrole	1072-83-9	10.41	0.731	0.502	0.359	0.643	0.553	0.211	0.588	0.357	0.593	0.93	0.799
C40	Acetophenone	98-86-2	10.53	3.049	1.246	1.317	2.041	0.688	1.242	11.922	1.817	1.938	0.525	0.274
C41	Tetramethylpyrazine	1124-11-4	11.02	0.576	2.872	0.585	0.444	5.862	1.744	0.872	0.679	0.785	1.055	0.892
C42	1-Nonanal	124-19-6	11.65	0.645	0.557	0.463	0.359	0.768	0.273	0.394	0.452	0.894	0.51	0.46
C43	1-Propanamine,N-(2-furanylmethylene)-2-methyl-	85098-92-6	12	0.12	0.183	0.383	0.377	0.166	0.219	0.7	0.229	0.642	101.009	0.343
C44	N-(3-Methylbutyl) acetamide	13434-12-3	12.46	0.432	0.412	1.782	0.627	1.027	0.251	0.323	0.398	0.918	1.25	0.544
C45	Undecane, 3-methyl-	1002-43-3	13.6	0.382	0.144	0.129	0.203	0.353	0.126	0.365	0.199	0.224	0.205	0.236
C46	Benzo[c] thiophene	270-82-6	14.24	2.365	2.456	2.424	2.291	2.565	2.596	1.972	2.183	2.371	2.515	2.52

Table E3 (continued)

NO	Compounds (%)	CAS#	RT (min)	BoB	BuR	BuP	LA	NO	PP	RugE	RetF	RubS	NH	NM
C47	Dodecane	112-40-3	14.42	3.625	3.87	3.527	3.686	3.558	3.685	1.402	3.763	3.552	3.478	3.218
C48	Cyclopentane, pentyl-	3741-00-2	15.63	0.397	0.365	0.377	0.476	2.178	0.429	3.605	0.366	0.345	0.305	0.325
C49	N-Propylbenzylideneamine	6852-55-7	16.28	0.206	0.173	0.343	0.614	5.29	0.256	0.287	0.369	0.802	0.277	0.857
C50	Indole	120-72-9	17.08	0.368	0.211	0.355	0.39	0.767	0.254	1.046	0.199	0.462	0.869	0.32
C51	Tridecane	629-50-5	17.22	0.426	0.546	0.835	0.768	1.126	0.459	0.607	2.504	1.051	1.367	0.348
C52	Tridecane, 3-methyl-	6418-41-3	19.11	0.228	0.202	0.24	0.348	2.116	0.179	0.173	0.354	0.27	0.287	0.181
C53	3-methyl-N-propyl-1-Butanamine	78579-58-5	19.49	0.175	0.624	0.831	1.796	1.11	0.374	0.589	0.915	1.088	0.402	1.413
C54	Tetradecane	629-59-4	19.89	1.106	1.236	1.05	1.271	0.978	0.879	0.598	1.749	1.097	0.996	0.928
C55	Cyclopentane, nonyl-	2882-98-6	21.16	0.4	0.391	0.375	0.664	0.368	0.335	1.975	0.711	0.381	0.368	0.388
C56	3-Phenylpyridine	1008-88-4	21.53	0.155	0.234	0.452	0.405	0.209	0.213	0.604	1.183	0.631	0.412	0.28
C57	2,4-Di-tert-butylphenol	96-76-4	22.58	0.558	0.401	1.023	0.687	0.416	0.461	0.515	0.589	0.958	0.997	0.554
C58	Nerolidol	7212-44-4	23.89	0.648	0.277	0.983	0.689	0.961	0.23	0.775	0.79	0.978	1.249	1.517
C59	PentaDecane, 3-methyl-	2882-96-4	24.13	0.243	0.224	0.338	0.317	0.776	0.229	0.367	0.539	0.348	0.439	0.275
C60	Hexadecane	544-76-3	24.83	0.291	0.363	0.424	0.447	0.921	0.232	0.65	0.629	0.42	0.425	0.339
C61	Diphenylamine	122-39-4	25.35	0.682	0.341	0.167	0.68	0.124	0.505	0.387	0.744	0.25	0.189	0.178
C62	Undecylcyclopentane	6785-23-5	26.12	0.41	0.453	0.501	0.654	0.803	0.335	0.413	0.539	0.524	0.5	0.372
C63	2,2',5,5'-tetramethylbiphenyl	3075-84-1	26.55	0.115	0.231	0.242	0.288	0.192	0.146	0.254	0.36	0.395	0.156	0.221

Table E3 (continued)

NO	Compounds (%)	CAS#	RT (min)	BoB	BuR	BuP	LA	NO	PP	RugE	RetF	RubS	NH	NM
C64	(2E,6E)-3,7,11-Trimethyl-2,6,10-dodecatrien-1-ol	106-28-5	27.52	4.268	4.97	5.884	5.088	9.08	1.898	9.359	5.574	8.772	11.391	3.632
C65	Tetradecanoic acid	544-63-8	28.46	10.269	3.6	4.116	5.571	7.719	0.663	7.287	9.688	6.624	11.429	12.559
C66	Phenanthrene	85-01-8	28.93	0.622	0.54	0.711	0.735	1.03	0.21	0.811	0.713	0.943	1.131	0.73
C67	Methyl pentadecanoate	7132-64-1	29.91	1.578	1.378	1.106	0.389	1.886	0.121	0.409	0.271	0.438	1.014	0.61
C68	Diisobutyl phthalate	84-69-5	30.47	3.128	3.066	9.021	2.879	3.172	0.946	11.024	2.813	27.571	39.021	14.237
C69	Pentadecanoic acid	1002-84-2	30.57	8.466	5.465	9.987	11.303	126.573	0.465	24.427	12.067	17.827	29.874	37.484
C70	7,9-Di-tert-butyl-1-oxaspiro(4,5)deca-6,9-diene-2,8-dione	82304-66-3	31.36	0.819	0.644	1.201	0.876	3.153	0.378	1.944	0.919	1.167	1.915	1.468
C71	Methyl hexadecanoate	112-39-0	31.78	0.998	1.069	1.421	1.1	1.621	0.374	1.846	0.814	1.241	1.354	1.192
C72	(Z)-9-Hexadecenoic acid	373-49-9	32.14	21.429	8.748	27.023	17.275	27.689	1.144	45.5	33.391	28.679	29.533	43.811
C73	Dibutyl phthalate	84-74-2	32.27	3.979	4.06	13.96	6.208	10.148	1.257	8.375	5.881	8.367	13.351	10.245
C74	Hexadecanoic acid	57-10-3	32.66	227.906	143.101	207.601	244.33	326.144	57.438	297.943	291.528	309.681	351.744	360.899
C75	Ethyl hexadecanoate	628-97-7	32.92	5.301	4.758	6.552	7.37	9.584	2.061	10.577	11.115	8.681	20.762	6.862
C76	Eicosane	112-95-8	33.04	3.229	4.124	6.34	4.75	24.371	1.489	9.326	6.151	7.8	11.429	6.291
C77	Linoleic acid	60-33-3	33.62	2.228	3.139	6.115	5.629	4.561	1.28	8.461	3.271	14.807	6.152	5.468
C78	Heptadecanoic acid	506-12-7	33.98	1.951	1.23	2.175	2.019	8.967	0.311	12.57	2.616	4.787	4.151	4.429
C79	5,8,11-Heptadecatrienoic acid methyl ester	22117-08-4	34.06	3.188	3.168	4.635	4.227	15.22	1.723	5.54	3.776	5.476	7.103	4.263

Table E3 (continued)

NO	Compounds (%)	CAS#	RT (min)	BoB	BuR	BuP	LA	NO	PP	RugE	RetF	RubS	NH	NM
C80	9-Octadecenenitrile, (E)-	112-91-4	34.16	2.344	2.474	4.46	3.2	5.661	1.632	5.161	5.718	4.64	6.238	3.192
C81	9,12-Octadecadienoicacid, methyl ester, (9E,12E)-	2566-97-4	34.32	3.726	3.768	5.317	5.394	5.374	1.827	7.193	4.177	6.308	6.27	5.301
C82	Methyl 9-(Z)-octadecenoate	1937-62-8	34.41	3.113	2.213	2.454	3.055	5.562	0.646	4.935	2.703	3.699	5.658	2.538
C83	2(3H)-Furanone, 5-dodecyldihydro-	730-46-1	34.46	2.741	2.478	2.858	3.281	10.331	0.967	6.401	2.867	5.639	7.075	3.354
C84	Linoelaidic acid	506-21-8	35.04	285.797	112.665	310.368	282.29	397.989	54.519	358.054	175.941	443.668	975.282	618.683
C85	9-Octadecenoic acid, (E)-	112-79-8	35.1	108.355	59.966	60.899	90.674	121.919	35.569	141.454	78.035	293.258	455.163	126.224
C86	ETHYL LINOLEATE	7619-08-1	35.15	18.596	14.2	19.802	21.577	6.406	10.358	35.949	27.141	20.194	20.282	21.099
C87	9,12-Octadecadienoic acid (Z,Z)-, ethyl ester	544-35-4	35.16	17.867	16.07	23.984	17.712	41.905	12.174	37.026	22.968	32.488	104.963	24.787
C88	Ethyl Oleate	111-62-6	35.24	19.309	8.397	11.272	21.492	22.259	4.503	35.206	13.986	33.791	85.239	29.15
C89	Tetradecanamide	638-58-4	35.45	8.552	6.602	14.968	11.592	17.054	3.726	18.532	7.825	16.758	18.978	13.809
C90	Cis-trans-Nepetalactone	21651-62-7	35.57	16.25	12.657	18.114	16.463	13.525	6.045	24.981	14.105	28.206	30.574	21.561
C91	Butyl citrate	77-94-1	36.12	3.477	2.918	4.573	4.923	17.274	1.282	8.966	4.456	4.097	1.459	5.239
C92	1,6-Cyclodecadiene	7049-13-0	36.45	5.438	5.194	7.657	7.162	8.967	2.385	9.37	6.031	8.645	11.607	8.091
C93	(Z)-9-octadecen-4-olide	59303-50-3	36.53	4.278	3.765	4.481	4.737	10.683	1.467	8.208	4.218	9.961	10.804	5.398
C94	gamma-Linolenic acid	506-26-3	36.73	5.359	5.28	5.677	5.186	15.936	1.445	8.745	4.344	9.471	13.446	6.383

Table E3 (continued)

NO	Compounds (%)	CAS#	RT (min)	BoB	BuR	BuP	LA	NO	PP	RugE	RetF	RubS	NH	NM
C95	Octyl 4-methoxycinnamate	5466-77-3	36.87	3.592	3.693	4.229	6.261	2.558	1.73	7.278	4.764	8.556	43.329	6.564
C96	Oleamide	301-02-0	37.29	7.007	6.011	10.895	9.834	12.536	3.996	18.215	7.945	12.622	13.469	9.52
C97	9,17-Octadecadienal, (Z)-	56554-35-9	37.75	4.253	5.681	2.874	3.271	2.899	1.268	3.914	3.133	5.709	5.753	4.092
C98	Bis(2-ethylhexyl) phthalate	117-81-7	39.22	2.532	3.233	5.329	4.115	3.04	1.311	4.854	3.071	4.868	6.046	3.251
C99	Tetracosane	646-31-1	40.89	0.029	22.221	2.492	12.246	0.697	30.789	9.134	2.697	1.276	0.326	2.837

APPENDIX F

DISTANCE MATRIX BETWEEN PHYLOGENETIC SIGNALS AND CHEMICAL CHARACTERISTIC INFORMATION OF SPECIES

Table F1 Distance matrix between phylogenetic signals information of species

	BoB	**RubS**	**RetF**	**NH**	**NM**	**NO**	**BuP**	**BuR**	**RugE**	**LA**	**PP**
BoB	1.0000	0.2572	0.1771	0.2572	0.2572	0.3545	0.2572	0.1771	0.6737	0.0991	0.0000
RubS		1.0000	0.2572	0.0533	0.0979	0.3545	0.0979	0.2572	0.6737	0.2572	0.2572
RetF			1.0000	0.2572	0.2572	0.3545	0.2572	0.0692	0.6737	0.1771	0.1771
NH				1.0000	0.0979	0.3545	0.0979	0.2572	0.6737	0.2572	0.2572
NM					1.0000	0.3545	0.0735	0.2572	0.6737	0.2572	0.2572
NO						1.0000	0.3545	0.3545	0.6737	0.3545	0.3545
BuP							1.0000	0.2572	0.6737	0.2572	0.2572
BuR								1.0000	0.6737	0.1771	0.1771
RugE									1.0000	0.6737	0.6737
LA										1.0000	0.0991
PP											1.0000

Table F2 Distance matrix between NIR characteristic information of species

	BoB	**RubS**	**RetF**	**NH**	**NM**	**NO**	**BuP**	**BuR**	**RugE**	**LA**	**PP**
BoB	1.0000										
RubS	0.1492	1.0000									
RetF	0.1797	0.3262	1.0000								
NH	0.1006	0.0533	0.2775	1.0000							
NM	0.2104	0.0937	0.3136	0.1377	1.0000						
NO	0.2759	0.4013	0.3450	0.3512	0.4861	1.0000					
BuP	0.2049	0.0557	0.3819	0.1044	0.0735	0.4362	1.0000				
BuR	0.2379	0.3871	0.0692	0.3384	0.3746	0.2764	0.4428	1.0000			
RugE	0.6677	0.5185	0.8446	0.5671	0.5310	0.8098	0.4628	0.9056	1.0000		

Table F2 (continued)

	BoB	RubS	RetF	NH	NM	NO	BuP	BuR	RugE	LA	PP
LA	0.0991	0.2438	0.0841	0.1966	0.2313	0.3421	0.2995	0.1433	0.7623	1.0000	
PP	0.0000	0.1492	0.1797	0.1006	0.2104	0.2759	0.2049	0.2379	0.6677	0.0991	1.0000

Table F3 Distance matrix between HPLC-fingerprint characteristic information of species

	BoB	**RubS**	**RetF**	**NH**	**NM**	**NO**	**BuP**	**BuR**	**RugE**	**LA**	**PP**
BoB	1.0000										
RubS	0.2284	1.0000									
RetF	0.2459	0.2994	1.0000								
NH	0.2549	0.2578	0.2758	1.0000							
NM	0.3020	0.3492	0.3520	0.3410	1.0000						
NO	0.4178	0.4653	0.4909	0.3712	0.2358	1.0000					
BuP	0.1819	0.2479	0.2802	0.2204	0.3975	0.4592	1.0000				
BuR	0.3070	0.3908	0.2496	0.3596	0.4288	0.5971	0.2886	1.0000			
RugE	0.1900	0.2557	0.2898	0.2297	0.3705	0.4535	0.2114	0.2780	1.0000		
LA	0.3271	0.3748	0.3292	0.4216	0.4209	0.5700	0.3436	0.3259	0.3292	1.0000	
PP	0.3969	0.5245	0.3860	0.4422	0.4875	0.4666	0.4236	0.4581	0.4235	0.5585	1.0000

Table F4 Distance matrix between GC-MS characteristic information of species

	BoB	**RubS**	**RetF**	**NH**	**NM**	**NO**	**BuP**	**BuR**	**RugE**	**LA**	**PP**
BoB	1.0000										
RubS	0.2465	1.0000									
RetF	0.1572	0.2636	1.0000								
NH	0.3743	0.1932	0.3745	1.0000							
NM	0.2407	0.1871	0.2495	0.2263	1.0000						
NO	0.3310	0.1859	0.3529	0.2069	0.2522	1.0000					
BuP	0.2428	0.1971	0.2167	0.2622	0.1797	0.2495	1.0000				
BuR	0.1825	0.3002	0.2282	0.4307	0.3081	0.4045	0.2306	1.0000			
RugE	0.4617	0.3647	0.4545	0.4279	0.4132	0.3861	0.4209	0.5097	1.0000		
LA	0.2582	0.3048	0.2563	0.4310	0.2823	0.3839	0.2613	0.2826	0.4754	1.0000	
PP	0.3017	0.4548	0.3176	0.5713	0.4222	0.5283	0.3552	0.2383	0.6600	0.4254	1.0000

APPENDIX G

DISTANCE MATRIX OF ECOLOGICAL ENVIRONMENTAL FACTORS AND CHARACTERISTIC CHEMICAL INFORMATION OF DIFFERENT PRODUCING AREAS

Table G1 Distance matrix of ecological environmental factors of different producing areas

	Region1	**Region2**	**Region3**	**Region4**	**Region5**	**Region6**
Region1	0.0000	0.2566	0.3128	0.3654	0.3812	0.2791
Region2		0.0000	0.2195	0.2592	0.2472	0.1722
Region3			0.0000	0.1145	0.1654	0.0958
Region4				0.0000	0.1268	0.1515
Region5					0.0000	0.1713
Region6						0.0000

Table G2 Distance matrix of NIR characteristic information of different producing areas

	Region1	**Region2**	**Region3**	**Region4**	**Region5**	**Region6**
Region1	0.0000					
Region2	0.1331	0.0000				
Region3	0.0589	0.0898	0.0000			
Region4	0.1132	0.0558	0.0567	0.0000		
Region5	0.0781	0.0641	0.0290	0.0581	0.0000	
Region6	0.1141	0.0357	0.0582	0.0364	0.0381	0.0000

Table G3 Distance matrix of HPLC-fingerprint characteristic information of different producing areas

	Region1	**Region2**	**Region3**	**Region4**	**Region5**	**Region6**
Region1	0.0000					
Region2	0.2635	0.0000				
Region3	0.2450	0.2283	0.0000			
Region4	0.1903	0.2682	0.3034	0.0000		
Region5	0.2510	0.3453	0.1920	0.3006	0.0000	
Region6	0.2331	0.2486	0.0716	0.2834	0.1771	0.0000

Table G4 Distance matrix of GC-MS characteristic information of different producing areas

	Region1	**Region2**	**Region3**	**Region4**	**Region5**	**Region6**
Region1	0.0000					
Region2	0.1987	0.0000				
Region3	0.2554	0.2066	0.0000			
Region4	0.1973	0.2105	0.3428	0.0000		
Region5	0.2937	0.2543	0.2474	0.3871	0.0000	
Region6	0.3001	0.3016	0.4196	0.2045	0.4343	0.0000

APPENDIX H

DETECTION RESULTS OF DIFFERENT CHEMICAL INFORMATION PHYLOGENETIC SIGNALS

Table H1 Detection results of different spectral information phylogenetic signals

Wavenumbers (cm-1)	K	PIC.variance.obs	PIC.variance.rnd.mean	PIC.variance.P	PIC.variance.Z
7497.88	0.685	1.22E-06	9.99E-07	0.92	1.501
7494.02	0.686	1.21E-06	9.83E-07	0.942	1.623
7490.16	0.687	1.20E-06	9.90E-07	0.913	1.443
7486.31	0.689	1.20E-06	9.86E-07	0.921	1.462
7482.45	0.690	1.19E-06	9.77E-07	0.914	1.496
7478.59	0.692	1.18E-06	9.78E-07	0.921	1.464
7474.74	0.693	1.18E-06	9.77E-07	0.927	1.449
7470.88	0.694	1.17E-06	9.69E-07	0.899	1.413
7467.02	0.696	1.16E-06	9.70E-07	0.884	1.321
7463.17	0.697	1.15E-06	9.68E-07	0.902	1.361
7459.31	0.699	1.15E-06	9.55E-07	0.911	1.395
7455.45	0.700	1.14E-06	9.60E-07	0.887	1.275
7451.6	0.702	1.13E-06	9.54E-07	0.886	1.280
7447.74	0.704	1.12E-06	9.44E-07	0.912	1.364
7443.88	0.706	1.11E-06	9.39E-07	0.886	1.290
7440.02	0.708	1.11E-06	9.42E-07	0.869	1.163
7436.17	0.709	1.10E-06	9.28E-07	0.901	1.320
7432.31	0.711	1.09E-06	9.25E-07	0.888	1.248
7428.45	0.713	1.08E-06	9.15E-07	0.896	1.279
7424.6	0.715	1.07E-06	9.21E-07	0.854	1.123
7420.74	0.717	1.06E-06	9.13E-07	0.864	1.148
7416.88	0.719	1.05E-06	9.08E-07	0.869	1.142
7413.03	0.721	1.05E-06	9.03E-07	0.854	1.108
7409.17	0.723	1.04E-06	8.98E-07	0.849	1.097

Table H1 (continued)

Wavenumbers (cm-1)	K	PIC.variance.obs	PIC.variance.rnd.mean	PIC.variance.P	PIC.variance.Z
7405.31	0.725	1.03E-06	8.94E-07	0.854	1.079
7401.46	0.727	1.02E-06	8.88E-07	0.85	1.075
7397.6	0.729	1.02E-06	8.83E-07	0.846	1.044
7393.74	0.731	1.01E-06	8.86E-07	0.812	0.927
7389.88	0.733	1.00E-06	8.80E-07	0.823	0.963
7386.03	0.735	9.92E-07	8.67E-07	0.834	1.022
7382.17	0.738	9.81E-07	8.68E-07	0.807	0.917
7378.31	0.740	9.72E-07	8.62E-07	0.803	0.880
7374.46	0.741	9.68E-07	8.63E-07	0.808	0.882
7370.6	0.743	9.65E-07	8.54E-07	0.795	0.907
7366.74	0.745	9.57E-07	8.52E-07	0.775	0.849
7362.89	0.747	9.53E-07	8.45E-07	0.795	0.894
7359.03	0.749	9.47E-07	8.49E-07	0.768	0.790
7355.17	0.751	9.39E-07	8.45E-07	0.768	0.771
7351.31	0.753	9.34E-07	8.36E-07	0.787	0.831
7347.46	0.755	9.26E-07	8.34E-07	0.765	0.752
7343.6	0.757	9.15E-07	8.30E-07	0.76	0.729
7339.74	0.759	9.09E-07	8.24E-07	0.762	0.726
7335.89	0.759	9.18E-07	8.35E-07	0.731	0.705
7332.03	0.761	9.15E-07	8.34E-07	0.736	0.684
7328.17	0.763	9.01E-07	8.21E-07	0.724	0.669
7324.32	0.765	8.98E-07	8.23E-07	0.736	0.647
7320.46	0.766	9.02E-07	8.24E-07	0.741	0.677
7316.6	0.767	9.00E-07	8.34E-07	0.702	0.541
7312.75	0.769	8.91E-07	8.21E-07	0.727	0.608
7308.89	0.771	8.85E-07	8.18E-07	0.705	0.550
7305.03	0.772	8.87E-07	8.22E-07	0.694	0.562
7301.17	0.774	8.87E-07	8.15E-07	0.728	0.617
7297.32	0.775	8.81E-07	8.17E-07	0.691	0.551
7293.46	0.777	8.77E-07	8.17E-07	0.686	0.530
7289.6	0.778	8.76E-07	8.17E-07	0.698	0.514
7285.75	0.779	8.76E-07	8.14E-07	0.688	0.514
7281.89	0.780	8.76E-07	8.16E-07	0.68	0.507
7278.03	0.782	8.75E-07	8.20E-07	0.668	0.444
7274.18	0.783	8.72E-07	8.22E-07	0.659	0.408
7270.32	0.784	8.72E-07	8.20E-07	0.682	0.438

Table H1 (continued)

Wavenumbers (cm-1)	K	PIC.variance.obs	PIC.variance.rnd.mean	PIC.variance.P	PIC.variance.Z
7266.46	0.785	8.72E-07	8.20E-07	0.644	0.416
7262.61	0.787	8.69E-07	8.19E-07	0.669	0.422
7258.75	0.788	8.71E-07	8.21E-07	0.675	0.411
7254.89	0.789	8.69E-07	8.20E-07	0.659	0.408
7251.03	0.791	8.67E-07	8.18E-07	0.663	0.406
7247.18	0.792	8.69E-07	8.24E-07	0.661	0.381
7243.32	0.794	8.57E-07	8.16E-07	0.644	0.349
7239.46	0.795	8.63E-07	8.24E-07	0.642	0.318
7235.61	0.797	8.63E-07	8.28E-07	0.619	0.287
7231.75	0.800	8.53E-07	8.19E-07	0.629	0.280
7227.89	0.801	8.62E-07	8.25E-07	0.648	0.305
7224.04	0.802	8.69E-07	8.36E-07	0.64	0.278
7220.18	0.804	8.68E-07	8.36E-07	0.639	0.262
7216.32	0.806	8.70E-07	8.44E-07	0.62	0.206
7212.47	0.807	8.75E-07	8.47E-07	0.647	0.231
7208.61	0.809	8.77E-07	8.42E-07	0.657	0.284
7204.75	0.812	8.72E-07	8.49E-07	0.614	0.182
7200.89	0.814	8.77E-07	8.52E-07	0.629	0.189
7197.04	0.816	8.84E-07	8.60E-07	0.611	0.190
7193.18	0.818	8.87E-07	8.71E-07	0.587	0.123
7189.32	0.820	8.92E-07	8.77E-07	0.597	0.107
7185.47	0.822	8.93E-07	8.79E-07	0.606	0.102
7181.61	0.825	8.91E-07	8.83E-07	0.605	0.061
7177.75	0.827	9.01E-07	8.92E-07	0.607	0.074
7173.9	0.828	9.10E-07	8.93E-07	0.637	0.125
7170.04	0.831	9.10E-07	9.01E-07	0.604	0.069
7166.18	0.833	9.13E-07	9.09E-07	0.585	0.026
7162.33	0.834	9.19E-07	9.16E-07	0.581	0.022
7158.47	0.836	9.31E-07	9.26E-07	0.61	0.034
7154.61	0.836	9.46E-07	9.43E-07	0.593	0.026
7150.75	0.837	9.56E-07	9.59E-07	0.592	-0.019
7146.9	0.839	9.64E-07	9.70E-07	0.575	-0.038
7143.04	0.841	9.69E-07	9.76E-07	0.578	-0.045
7139.18	0.842	9.80E-07	9.84E-07	0.583	-0.025

Table H1 (continued)

Wavenumbers (cm-1)	K	PIC.variance.obs	PIC.variance.rnd.mean	PIC.variance.P	PIC.variance.Z
7135.33	0.842	9.99E-07	1.00E-06	0.562	-0.018
7131.47	0.842	1.02E-06	1.03E-06	0.563	-0.038
7127.61	0.842	1.04E-06	1.06E-06	0.549	-0.105
7123.76	0.841	1.06E-06	1.06E-06	0.578	-0.014
7119.9	0.842	1.07E-06	1.07E-06	0.591	-0.001
7116.04	0.841	1.09E-06	1.09E-06	0.588	0.028
7112.19	0.840	1.12E-06	1.12E-06	0.574	0.006
7108.33	0.839	1.14E-06	1.14E-06	0.574	-0.020
7104.47	0.838	1.16E-06	1.16E-06	0.564	-0.004
7100.61	0.836	1.19E-06	1.19E-06	0.587	0.015
7096.76	0.835	1.22E-06	1.23E-06	0.564	-0.051
7092.9	0.834	1.25E-06	1.24E-06	0.553	0.018
7089.04	0.832	1.28E-06	1.28E-06	0.57	0.012
7085.19	0.830	1.31E-06	1.30E-06	0.591	0.056
7081.33	0.828	1.34E-06	1.32E-06	0.606	0.101
7077.47	0.827	1.37E-06	1.35E-06	0.589	0.071
7073.62	0.825	1.40E-06	1.38E-06	0.588	0.098
7069.76	0.823	1.42E-06	1.39E-06	0.63	0.139
7065.9	0.822	1.46E-06	1.43E-06	0.609	0.131
7062.04	0.819	1.50E-06	1.46E-06	0.62	0.151
7058.19	0.817	1.53E-06	1.48E-06	0.631	0.199
7054.33	0.814	1.57E-06	1.53E-06	0.633	0.169
7050.47	0.811	1.61E-06	1.57E-06	0.605	0.149
7046.62	0.808	1.65E-06	1.59E-06	0.639	0.209
7042.76	0.805	1.69E-06	1.61E-06	0.671	0.315
7038.9	0.803	1.73E-06	1.66E-06	0.658	0.267
7035.05	0.800	1.77E-06	1.68E-06	0.66	0.314
7031.19	0.798	1.80E-06	1.71E-06	0.674	0.351
7027.33	0.796	1.84E-06	1.76E-06	0.669	0.314
7023.48	0.794	1.88E-06	1.79E-06	0.652	0.301
7019.62	0.792	1.91E-06	1.82E-06	0.657	0.356
7015.76	0.790	1.95E-06	1.84E-06	0.673	0.381
7011.9	0.788	1.99E-06	1.88E-06	0.659	0.377
7008.05	0.786	2.03E-06	1.90E-06	0.707	0.436

Table H1 (continued)

Wavenumbers (cm-1)	K	PIC.variance.obs	PIC.variance.rnd.mean	PIC.variance.P	PIC.variance.Z
7004.19	0.784	2.06E-06	1.95E-06	0.669	0.390
7000.33	0.782	2.10E-06	1.97E-06	0.699	0.445
6996.48	0.781	2.13E-06	1.97E-06	0.734	0.546
6992.62	0.779	2.17E-06	2.04E-06	0.684	0.413
6988.76	0.778	2.20E-06	2.02E-06	0.753	0.589
6984.91	0.777	2.23E-06	2.08E-06	0.696	0.465
6981.05	0.776	2.26E-06	2.09E-06	0.714	0.528
6977.19	0.774	2.29E-06	2.12E-06	0.705	0.514
6973.34	0.773	2.32E-06	2.15E-06	0.74	0.535
6969.48	0.772	2.35E-06	2.18E-06	0.7	0.508
6965.62	0.771	2.38E-06	2.19E-06	0.727	0.552
6961.76	0.771	2.40E-06	2.22E-06	0.72	0.507
6957.91	0.770	2.43E-06	2.22E-06	0.736	0.598
6954.05	0.769	2.45E-06	2.24E-06	0.75	0.610
6950.19	0.768	2.47E-06	2.27E-06	0.732	0.571
6946.34	0.768	2.49E-06	2.28E-06	0.742	0.596
6942.48	0.767	2.51E-06	2.31E-06	0.735	0.550
6938.62	0.767	2.53E-06	2.32E-06	0.752	0.606
6934.77	0.766	2.54E-06	2.34E-06	0.732	0.564
6930.91	0.766	2.56E-06	2.34E-06	0.756	0.601
6927.05	0.765	2.57E-06	2.35E-06	0.741	0.623
6923.2	0.765	2.59E-06	2.36E-06	0.758	0.638
6919.34	0.765	2.60E-06	2.39E-06	0.722	0.564
6915.48	0.764	2.61E-06	2.39E-06	0.736	0.579
6911.62	0.764	2.62E-06	2.41E-06	0.734	0.564
6907.77	0.763	2.63E-06	2.41E-06	0.732	0.599
6903.91	0.763	2.64E-06	2.45E-06	0.711	0.502
6900.05	0.763	2.65E-06	2.41E-06	0.769	0.651
6896.2	0.763	2.66E-06	2.42E-06	0.752	0.639
6892.34	0.763	2.67E-06	2.43E-06	0.752	0.657
6888.48	0.762	2.68E-06	2.43E-06	0.762	0.659
6884.63	0.762	2.69E-06	2.45E-06	0.747	0.626
6880.77	0.762	2.69E-06	2.44E-06	0.766	0.644
6876.91	0.762	2.70E-06	2.48E-06	0.743	0.568

Table H1 (continued)

Wavenumbers (cm-1)	K	PIC.variance.obs	PIC.variance.rnd.mean	PIC.variance.P	PIC.variance.Z
6873.06	0.761	2.71E-06	2.45E-06	0.756	0.651
6869.2	0.761	2.71E-06	2.46E-06	0.762	0.660
6865.34	0.761	2.72E-06	2.48E-06	0.757	0.617
6861.48	0.761	2.72E-06	2.49E-06	0.739	0.591
6857.63	0.761	2.73E-06	2.48E-06	0.768	0.645
6853.77	0.761	2.73E-06	2.47E-06	0.786	0.712
6849.91	0.761	2.74E-06	2.49E-06	0.765	0.633
6846.06	0.761	2.74E-06	2.51E-06	0.751	0.610
6842.2	0.761	2.75E-06	2.49E-06	0.76	0.671
6838.34	0.761	2.75E-06	2.49E-06	0.756	0.664
6834.49	0.761	2.75E-06	2.51E-06	0.749	0.619
6830.63	0.761	2.75E-06	2.53E-06	0.734	0.548
6826.77	0.760	2.76E-06	2.51E-06	0.746	0.608
6822.92	0.760	2.76E-06	2.53E-06	0.739	0.577
6819.06	0.760	2.76E-06	2.51E-06	0.76	0.638
6815.2	0.760	2.76E-06	2.49E-06	0.781	0.731
6811.34	0.760	2.76E-06	2.51E-06	0.759	0.649
6807.49	0.760	2.76E-06	2.50E-06	0.765	0.649
6803.63	0.760	2.76E-06	2.51E-06	0.767	0.658
6799.77	0.761	2.76E-06	2.52E-06	0.753	0.621
6795.92	0.761	2.76E-06	2.51E-06	0.761	0.649
6792.06	0.761	2.76E-06	2.50E-06	0.767	0.668
6788.2	0.761	2.75E-06	2.52E-06	0.743	0.610
6784.35	0.761	2.75E-06	2.48E-06	0.778	0.736
6780.49	0.761	2.75E-06	2.52E-06	0.739	0.592
6776.63	0.761	2.75E-06	2.51E-06	0.758	0.606
6772.77	0.761	2.74E-06	2.48E-06	0.766	0.681
6768.92	0.761	2.74E-06	2.49E-06	0.74	0.627
6765.06	0.761	2.73E-06	2.47E-06	0.767	0.689
6761.2	0.761	2.73E-06	2.48E-06	0.775	0.661
6757.35	0.761	2.73E-06	2.46E-06	0.771	0.698
6753.49	0.761	2.72E-06	2.48E-06	0.748	0.619
6749.63	0.761	2.72E-06	2.49E-06	0.74	0.566
6745.78	0.761	2.71E-06	2.46E-06	0.747	0.650

Table H1 (continued)

Wavenumbers (cm-1)	K	PIC.variance.obs	PIC.variance.rnd.mean	PIC.variance.P	PIC.variance.Z
6741.92	0.761	2.71E-06	2.47E-06	0.758	0.587
6738.06	0.761	2.70E-06	2.45E-06	0.759	0.658
6734.21	0.761	2.70E-06	2.47E-06	0.744	0.590
6730.35	0.761	2.70E-06	2.44E-06	0.781	0.718
6726.49	0.761	2.69E-06	2.45E-06	0.755	0.645
6722.63	0.760	2.69E-06	2.44E-06	0.769	0.656
6718.78	0.760	2.68E-06	2.44E-06	0.751	0.650
6714.92	0.760	2.68E-06	2.45E-06	0.745	0.596
6711.06	0.760	2.68E-06	2.45E-06	0.76	0.592
6707.21	0.760	2.67E-06	2.42E-06	0.77	0.686
6703.35	0.760	2.67E-06	2.44E-06	0.738	0.608
6699.49	0.760	2.66E-06	2.42E-06	0.758	0.665
6695.64	0.760	2.66E-06	2.44E-06	0.748	0.582
6691.78	0.760	2.65E-06	2.40E-06	0.759	0.652
6687.92	0.760	2.65E-06	2.42E-06	0.736	0.591
6684.07	0.760	2.64E-06	2.39E-06	0.746	0.615
6680.21	0.760	2.63E-06	2.39E-06	0.76	0.634
6676.35	0.759	2.63E-06	2.38E-06	0.77	0.667
6672.49	0.759	2.62E-06	2.36E-06	0.79	0.722
6668.64	0.759	2.61E-06	2.38E-06	0.755	0.618
6664.78	0.759	2.61E-06	2.39E-06	0.742	0.570
6660.92	0.759	2.60E-06	2.36E-06	0.755	0.624
6657.07	0.759	2.59E-06	2.36E-06	0.755	0.617
6653.21	0.759	2.59E-06	2.37E-06	0.751	0.580
6649.35	0.759	2.58E-06	2.36E-06	0.748	0.603
6645.5	0.759	2.57E-06	2.35E-06	0.756	0.594
6641.64	0.759	2.57E-06	2.31E-06	0.784	0.719
6637.78	0.759	2.56E-06	2.34E-06	0.741	0.584
6633.93	0.759	2.55E-06	2.31E-06	0.768	0.670
6630.07	0.759	2.54E-06	2.34E-06	0.747	0.577
6626.21	0.759	2.54E-06	2.32E-06	0.735	0.593
6622.35	0.759	2.53E-06	2.29E-06	0.755	0.653
6618.5	0.759	2.52E-06	2.30E-06	0.75	0.617
6614.64	0.758	2.52E-06	2.30E-06	0.745	0.582

Table H1 (continued)

Wavenumbers (cm-1)	K	PIC.variance.obs	PIC.variance.rnd.mean	PIC.variance.P	PIC.variance.Z
6610.78	0.758	2.51E-06	2.25E-06	0.793	0.770
6606.93	0.758	2.51E-06	2.27E-06	0.774	0.659
6603.07	0.758	2.50E-06	2.28E-06	0.754	0.621
6599.21	0.758	2.49E-06	2.25E-06	0.778	0.694
6595.36	0.758	2.49E-06	2.26E-06	0.767	0.637
6591.5	0.758	2.48E-06	2.25E-06	0.769	0.617
6587.64	0.758	2.48E-06	2.26E-06	0.774	0.647
6583.79	0.758	2.47E-06	2.23E-06	0.773	0.690
6579.93	0.758	2.47E-06	2.24E-06	0.766	0.639
6576.07	0.758	2.46E-06	2.24E-06	0.753	0.649
6572.21	0.758	2.46E-06	2.23E-06	0.753	0.648
6568.36	0.758	2.45E-06	2.22E-06	0.769	0.672
6564.5	0.758	2.45E-06	2.21E-06	0.778	0.681
6560.64	0.758	2.44E-06	2.22E-06	0.768	0.643
6556.79	0.758	2.44E-06	2.23E-06	0.756	0.612
6552.93	0.758	2.43E-06	2.21E-06	0.771	0.648
6549.07	0.758	2.43E-06	2.23E-06	0.752	0.589
6545.22	0.758	2.43E-06	2.20E-06	0.777	0.679
6541.36	0.758	2.42E-06	2.19E-06	0.761	0.679
6537.5	0.758	2.42E-06	2.22E-06	0.741	0.561
6533.65	0.758	2.42E-06	2.20E-06	0.752	0.623
6529.79	0.758	2.41E-06	2.18E-06	0.771	0.676
6525.93	0.758	2.41E-06	2.18E-06	0.767	0.668
6522.07	0.758	2.41E-06	2.17E-06	0.787	0.711
6518.22	0.758	2.41E-06	2.19E-06	0.758	0.620
6514.36	0.758	2.41E-06	2.18E-06	0.771	0.664
6510.5	0.759	2.40E-06	2.18E-06	0.753	0.646
6506.65	0.759	2.40E-06	2.18E-06	0.759	0.668
6502.79	0.759	2.40E-06	2.18E-06	0.753	0.627
6498.93	0.759	2.40E-06	2.18E-06	0.767	0.653
6495.08	0.759	2.40E-06	2.20E-06	0.752	0.587
6491.22	0.759	2.40E-06	2.19E-06	0.765	0.612
6487.36	0.759	2.40E-06	2.18E-06	0.756	0.607
6483.5	0.759	2.40E-06	2.16E-06	0.788	0.691

Table H1 (continued)

Wavenumbers (cm-1)	K	PIC.variance.obs	PIC.variance.rnd.mean	PIC.variance.P	PIC.variance.Z
6479.65	0.759	2.39E-06	2.17E-06	0.765	0.661
6475.79	0.760	2.39E-06	2.17E-06	0.771	0.688
6471.93	0.760	2.39E-06	2.19E-06	0.748	0.598
6468.08	0.760	2.39E-06	2.17E-06	0.739	0.620
6464.22	0.760	2.39E-06	2.19E-06	0.747	0.577
6460.36	0.760	2.39E-06	2.17E-06	0.764	0.656
6456.51	0.761	2.39E-06	2.17E-06	0.751	0.617
6452.65	0.761	2.38E-06	2.17E-06	0.762	0.622
6448.79	0.761	2.38E-06	2.17E-06	0.751	0.607
6444.94	0.761	2.38E-06	2.18E-06	0.762	0.605
6441.08	0.762	2.38E-06	2.17E-06	0.752	0.621
6437.22	0.762	2.38E-06	2.15E-06	0.762	0.666
6433.36	0.762	2.37E-06	2.15E-06	0.766	0.666
6429.51	0.762	2.37E-06	2.16E-06	0.738	0.605
6425.65	0.762	2.37E-06	2.16E-06	0.742	0.615
6421.79	0.762	2.37E-06	2.16E-06	0.768	0.612
6417.94	0.763	2.37E-06	2.15E-06	0.748	0.636
6414.08	0.763	2.37E-06	2.16E-06	0.77	0.627
6410.22	0.763	2.37E-06	2.16E-06	0.754	0.588
6406.37	0.763	2.37E-06	2.17E-06	0.738	0.594
6402.51	0.763	2.37E-06	2.15E-06	0.771	0.659
6398.65	0.763	2.37E-06	2.16E-06	0.76	0.585
6394.8	0.763	2.37E-06	2.17E-06	0.756	0.593
6390.94	0.763	2.37E-06	2.13E-06	0.781	0.714
6387.08	0.763	2.37E-06	2.16E-06	0.768	0.647
6383.22	0.763	2.37E-06	2.18E-06	0.738	0.563
6379.37	0.762	2.37E-06	2.16E-06	0.773	0.621
6375.51	0.762	2.38E-06	2.16E-06	0.761	0.634
6371.65	0.762	2.38E-06	2.15E-06	0.783	0.663
6367.8	0.762	2.38E-06	2.17E-06	0.758	0.622
6363.94	0.762	2.38E-06	2.17E-06	0.768	0.625
6360.08	0.762	2.38E-06	2.16E-06	0.774	0.655
6356.23	0.762	2.38E-06	2.17E-06	0.756	0.613
6352.37	0.762	2.38E-06	2.16E-06	0.761	0.649

Table H1 (continued)

Wavenumbers (cm-1)	K	PIC.variance.obs	PIC.variance.rnd.mean	PIC.variance.P	PIC.variance.Z
6348.51	0.761	2.38E-06	2.18E-06	0.747	0.565
6344.66	0.761	2.38E-06	2.19E-06	0.743	0.563
6340.8	0.761	2.38E-06	2.19E-06	0.741	0.564
6336.94	0.761	2.38E-06	2.16E-06	0.774	0.637
6333.08	0.761	2.38E-06	2.16E-06	0.761	0.628
6329.23	0.761	2.38E-06	2.15E-06	0.774	0.682
6325.37	0.761	2.37E-06	2.15E-06	0.778	0.638
6321.51	0.761	2.37E-06	2.17E-06	0.741	0.569
6317.66	0.761	2.37E-06	2.16E-06	0.753	0.616
6313.8	0.761	2.37E-06	2.17E-06	0.745	0.596
6309.94	0.760	2.37E-06	2.14E-06	0.776	0.659
6306.09	0.760	2.37E-06	2.16E-06	0.752	0.590
6302.23	0.760	2.36E-06	2.15E-06	0.765	0.640
6298.37	0.760	2.36E-06	2.16E-06	0.75	0.580
6294.52	0.760	2.36E-06	2.12E-06	0.778	0.723
6290.66	0.760	2.35E-06	2.14E-06	0.748	0.643
6286.8	0.760	2.35E-06	2.12E-06	0.78	0.679
6282.94	0.760	2.34E-06	2.14E-06	0.741	0.589
6279.09	0.760	2.34E-06	2.12E-06	0.777	0.674
6275.23	0.760	2.33E-06	2.14E-06	0.756	0.601
6271.37	0.760	2.33E-06	2.11E-06	0.781	0.682
6267.52	0.760	2.33E-06	2.10E-06	0.78	0.657
6263.66	0.760	2.32E-06	2.09E-06	0.792	0.715
6259.8	0.760	2.32E-06	2.11E-06	0.759	0.633
6255.95	0.760	2.31E-06	2.11E-06	0.755	0.587
6252.09	0.760	2.31E-06	2.09E-06	0.774	0.690
6248.23	0.760	2.30E-06	2.08E-06	0.778	0.697
6244.38	0.760	2.30E-06	2.10E-06	0.757	0.581
6240.52	0.760	2.29E-06	2.08E-06	0.767	0.671
6236.66	0.760	2.29E-06	2.09E-06	0.754	0.596
6232.8	0.761	2.29E-06	2.07E-06	0.787	0.663
6228.95	0.761	2.28E-06	2.08E-06	0.778	0.648
6225.09	0.761	2.28E-06	2.06E-06	0.766	0.674
6221.23	0.761	2.27E-06	2.07E-06	0.768	0.610

Table H1 (continued)

Wavenumbers (cm-1)	K	PIC.variance.obs	PIC.variance.rnd.mean	PIC.variance.P	PIC.variance.Z
6217.38	0.762	2.27E-06	2.07E-06	0.757	0.582
6213.52	0.762	2.26E-06	2.06E-06	0.744	0.637
6209.66	0.763	2.26E-06	2.08E-06	0.735	0.552
6205.81	0.763	2.26E-06	2.06E-06	0.739	0.574
6201.95	0.764	2.25E-06	2.06E-06	0.754	0.586
6198.09	0.764	2.25E-06	2.05E-06	0.752	0.616
6194.23	0.765	2.24E-06	2.06E-06	0.746	0.590
6190.38	0.765	2.24E-06	2.06E-06	0.738	0.563
6186.52	0.766	2.24E-06	2.05E-06	0.747	0.562
6182.66	0.766	2.23E-06	2.04E-06	0.759	0.585
6178.81	0.767	2.23E-06	2.03E-06	0.756	0.601
6174.95	0.767	2.22E-06	2.04E-06	0.735	0.563
6171.09	0.768	2.22E-06	2.05E-06	0.712	0.508
6167.24	0.769	2.21E-06	2.04E-06	0.726	0.522
6163.38	0.769	2.21E-06	2.02E-06	0.746	0.585
6159.52	0.770	2.20E-06	2.03E-06	0.743	0.556
6155.67	0.770	2.20E-06	2.03E-06	0.72	0.517
6151.81	0.771	2.19E-06	2.00E-06	0.755	0.583
6147.95	0.771	2.19E-06	2.00E-06	0.731	0.549
6144.09	0.772	2.18E-06	2.01E-06	0.723	0.531
6140.24	0.772	2.18E-06	2.01E-06	0.735	0.524
6136.38	0.772	2.17E-06	2.00E-06	0.73	0.522
6132.52	0.773	2.17E-06	2.00E-06	0.736	0.535
6128.67	0.773	2.16E-06	2.00E-06	0.726	0.529
6124.81	0.774	2.16E-06	2.01E-06	0.713	0.463
6120.95	0.774	2.15E-06	1.98E-06	0.726	0.564
6117.1	0.774	2.15E-06	2.00E-06	0.715	0.486
6113.24	0.775	2.15E-06	1.99E-06	0.718	0.489
6109.38	0.775	2.14E-06	2.00E-06	0.708	0.460
6105.53	0.775	2.14E-06	1.99E-06	0.712	0.462
6101.67	0.775	2.14E-06	1.99E-06	0.717	0.490
6097.81	0.775	2.14E-06	1.98E-06	0.73	0.501
6093.95	0.775	2.14E-06	1.98E-06	0.728	0.510
6090.1	0.776	2.13E-06	1.98E-06	0.723	0.496

Table H1 (continued)

Wavenumbers (cm-1)	K	PIC.variance.obs	PIC.variance.rnd.mean	PIC.variance.P	PIC.variance.Z
6086.24	0.776	2.13E-06	1.96E-06	0.731	0.556
6082.38	0.776	2.13E-06	1.98E-06	0.708	0.463
6078.53	0.777	2.13E-06	1.98E-06	0.713	0.485
6074.67	0.777	2.13E-06	1.99E-06	0.693	0.423
6070.81	0.777	2.12E-06	1.99E-06	0.695	0.429
6066.96	0.778	2.12E-06	1.96E-06	0.722	0.538
6063.1	0.778	2.12E-06	1.97E-06	0.718	0.484
6059.24	0.778	2.12E-06	1.96E-06	0.723	0.504
6055.39	0.778	2.12E-06	1.97E-06	0.715	0.478
6051.53	0.779	2.12E-06	1.98E-06	0.695	0.438
6047.67	0.779	2.12E-06	1.98E-06	0.695	0.424
6043.81	0.779	2.12E-06	1.97E-06	0.696	0.464
6039.96	0.779	2.12E-06	1.98E-06	0.708	0.479
6036.1	0.779	2.13E-06	2.00E-06	0.704	0.394
6032.24	0.779	2.13E-06	1.99E-06	0.697	0.457
6028.39	0.779	2.14E-06	2.00E-06	0.695	0.452
6024.53	0.779	2.15E-06	2.01E-06	0.702	0.445
6020.67	0.779	2.16E-06	2.02E-06	0.683	0.418
6016.82	0.779	2.17E-06	2.02E-06	0.705	0.455
6012.96	0.778	2.18E-06	2.03E-06	0.699	0.482
6009.1	0.778	2.19E-06	2.05E-06	0.708	0.444
6005.25	0.778	2.20E-06	2.04E-06	0.712	0.475
6001.39	0.778	2.20E-06	2.08E-06	0.681	0.374
5997.53	0.778	2.21E-06	2.04E-06	0.734	0.522
5993.67	0.778	2.22E-06	2.07E-06	0.698	0.449
5989.82	0.778	2.23E-06	2.08E-06	0.695	0.440
5985.96	0.778	2.24E-06	2.08E-06	0.715	0.488
5982.1	0.777	2.25E-06	2.10E-06	0.695	0.451
5978.25	0.777	2.26E-06	2.10E-06	0.708	0.511
5974.39	0.776	2.27E-06	2.13E-06	0.697	0.419
5970.53	0.776	2.29E-06	2.14E-06	0.706	0.425
5966.68	0.775	2.30E-06	2.14E-06	0.724	0.471
5962.82	0.775	2.32E-06	2.17E-06	0.7	0.453
5958.96	0.774	2.34E-06	2.16E-06	0.722	0.520

Table H1 (continued)

Wavenumbers (cm-1)	K	PIC.variance.obs	PIC.variance.rnd.mean	PIC.variance.P	PIC.variance.Z
5955.1	0.773	2.36E-06	2.20E-06	0.71	0.472
5951.25	0.772	2.38E-06	2.20E-06	0.72	0.512
5947.39	0.771	2.40E-06	2.23E-06	0.712	0.502
5943.53	0.770	2.43E-06	2.22E-06	0.742	0.578
5939.68	0.770	2.45E-06	2.26E-06	0.732	0.530
5935.82	0.769	2.47E-06	2.26E-06	0.748	0.602
5931.96	0.768	2.49E-06	2.30E-06	0.731	0.522
5928.11	0.768	2.52E-06	2.32E-06	0.724	0.564
5924.25	0.767	2.55E-06	2.36E-06	0.707	0.488
5920.39	0.766	2.56E-06	2.36E-06	0.712	0.542
5916.54	0.766	2.58E-06	2.35E-06	0.744	0.594
5912.68	0.765	2.59E-06	2.35E-06	0.763	0.665
5908.82	0.764	2.60E-06	2.38E-06	0.746	0.587
5904.96	0.763	2.61E-06	2.40E-06	0.732	0.537
5901.11	0.761	2.62E-06	2.40E-06	0.754	0.563
5897.25	0.760	2.63E-06	2.41E-06	0.743	0.589
5893.39	0.759	2.65E-06	2.41E-06	0.754	0.642
5889.54	0.759	2.67E-06	2.43E-06	0.75	0.634
5885.68	0.759	2.70E-06	2.44E-06	0.759	0.661
5881.82	0.758	2.72E-06	2.48E-06	0.751	0.642
5877.97	0.757	2.74E-06	2.50E-06	0.757	0.631
5874.11	0.757	2.77E-06	2.51E-06	0.761	0.639
5870.25	0.756	2.79E-06	2.52E-06	0.766	0.686
5866.4	0.755	2.80E-06	2.54E-06	0.766	0.673
5862.54	0.755	2.82E-06	2.54E-06	0.778	0.729
5858.68	0.754	2.83E-06	2.55E-06	0.772	0.719
5854.82	0.754	2.85E-06	2.60E-06	0.744	0.596
5850.97	0.754	2.87E-06	2.58E-06	0.8	0.726
5847.11	0.753	2.88E-06	2.61E-06	0.769	0.674
5843.25	0.753	2.90E-06	2.61E-06	0.792	0.746
5839.4	0.752	2.92E-06	2.61E-06	0.796	0.802
5835.54	0.752	2.94E-06	2.64E-06	0.782	0.733
5831.68	0.752	2.96E-06	2.65E-06	0.794	0.764
5827.83	0.751	2.98E-06	2.66E-06	0.789	0.781

Table H1 (continued)

Wavenumbers (cm-1)	K	PIC.variance.obs	PIC.variance.rnd.mean	PIC.variance.P	PIC.variance.Z
5823.97	0.751	3.00E-06	2.71E-06	0.777	0.685
5820.11	0.751	3.02E-06	2.70E-06	0.794	0.754
5816.26	0.751	3.04E-06	2.72E-06	0.793	0.744
5812.4	0.750	3.05E-06	2.74E-06	0.787	0.724
5808.54	0.750	3.07E-06	2.78E-06	0.766	0.657
5804.68	0.750	3.08E-06	2.76E-06	0.798	0.761
5800.83	0.749	3.09E-06	2.78E-06	0.786	0.758
5796.97	0.749	3.10E-06	2.79E-06	0.797	0.749
5793.11	0.749	3.12E-06	2.80E-06	0.793	0.739
5789.26	0.748	3.12E-06	2.79E-06	0.799	0.799
5785.4	0.748	3.13E-06	2.80E-06	0.781	0.755
5781.54	0.749	3.13E-06	2.80E-06	0.802	0.754
5777.69	0.749	3.12E-06	2.79E-06	0.793	0.769
5773.83	0.750	3.11E-06	2.79E-06	0.81	0.795
5769.97	0.750	3.10E-06	2.79E-06	0.759	0.689
5766.12	0.751	3.08E-06	2.77E-06	0.769	0.717
5762.26	0.752	3.06E-06	2.76E-06	0.775	0.703
5758.4	0.752	3.05E-06	2.73E-06	0.803	0.743
5754.54	0.753	3.03E-06	2.70E-06	0.796	0.792
5750.69	0.754	3.02E-06	2.74E-06	0.771	0.670
5746.83	0.754	3.01E-06	2.72E-06	0.757	0.679
5742.97	0.755	3.00E-06	2.73E-06	0.751	0.644
5739.12	0.755	3.00E-06	2.72E-06	0.773	0.684
5735.26	0.755	3.00E-06	2.70E-06	0.773	0.703
5731.4	0.755	3.01E-06	2.71E-06	0.78	0.732
5727.55	0.755	3.01E-06	2.72E-06	0.777	0.673
5723.69	0.755	3.01E-06	2.72E-06	0.76	0.667
5719.83	0.755	3.01E-06	2.73E-06	0.759	0.683
5715.98	0.756	3.02E-06	2.75E-06	0.745	0.598
5712.12	0.756	3.02E-06	2.73E-06	0.776	0.675
5708.26	0.756	3.03E-06	2.73E-06	0.77	0.711
5704.4	0.756	3.03E-06	2.74E-06	0.771	0.691
5700.55	0.756	3.04E-06	2.76E-06	0.752	0.624
5696.69	0.756	3.05E-06	2.75E-06	0.771	0.677

Table H1 (continued)

Wavenumbers (cm-1)	K	PIC.variance.obs	PIC.variance.rnd.mean	PIC.variance.P	PIC.variance.Z
5692.83	0.755	3.05E-06	2.76E-06	0.766	0.681
5688.98	0.755	3.06E-06	2.76E-06	0.766	0.713
5685.12	0.755	3.06E-06	2.77E-06	0.77	0.654
5681.26	0.755	3.06E-06	2.76E-06	0.773	0.713
5677.41	0.755	3.07E-06	2.79E-06	0.751	0.630
5673.55	0.755	3.07E-06	2.78E-06	0.758	0.655
5669.69	0.755	3.07E-06	2.79E-06	0.754	0.633
5665.83	0.756	3.06E-06	2.76E-06	0.761	0.682
5661.98	0.756	3.05E-06	2.74E-06	0.791	0.730
5658.12	0.757	3.04E-06	2.75E-06	0.765	0.693
5654.26	0.757	3.03E-06	2.74E-06	0.764	0.683
5650.41	0.757	3.02E-06	2.75E-06	0.756	0.626
5646.55	0.758	3.01E-06	2.74E-06	0.771	0.637
5642.69	0.758	3.00E-06	2.73E-06	0.758	0.614
5638.84	0.758	2.99E-06	2.71E-06	0.764	0.665
5634.98	0.759	2.98E-06	2.70E-06	0.778	0.695
5631.12	0.759	2.98E-06	2.73E-06	0.727	0.550
5627.27	0.759	2.97E-06	2.69E-06	0.775	0.703
5623.41	0.759	2.97E-06	2.70E-06	0.749	0.619
5619.55	0.759	2.96E-06	2.68E-06	0.774	0.686
5615.69	0.759	2.96E-06	2.70E-06	0.741	0.603
5611.84	0.759	2.95E-06	2.69E-06	0.757	0.629
5607.98	0.760	2.95E-06	2.68E-06	0.742	0.610
5604.12	0.760	2.94E-06	2.69E-06	0.74	0.591
5600.27	0.760	2.94E-06	2.69E-06	0.73	0.592
5596.41	0.760	2.94E-06	2.66E-06	0.768	0.677
5592.55	0.760	2.93E-06	2.67E-06	0.752	0.630
5588.7	0.760	2.93E-06	2.66E-06	0.759	0.639
5584.84	0.760	2.93E-06	2.65E-06	0.775	0.698
5580.98	0.760	2.92E-06	2.65E-06	0.762	0.663
5577.13	0.760	2.92E-06	2.64E-06	0.767	0.679
5573.27	0.760	2.91E-06	2.65E-06	0.745	0.623
5569.41	0.760	2.91E-06	2.64E-06	0.741	0.639
5565.55	0.760	2.90E-06	2.64E-06	0.748	0.619

Table H1 (continued)

Wavenumbers (cm-1)	K	PIC.variance.obs	PIC.variance.rnd.mean	PIC.variance.P	PIC.variance.Z
5561.7	0.760	2.90E-06	2.63E-06	0.761	0.632
5557.84	0.761	2.89E-06	2.64E-06	0.759	0.612
5553.98	0.761	2.88E-06	2.64E-06	0.753	0.611
5550.13	0.761	2.88E-06	2.63E-06	0.736	0.590
5546.27	0.761	2.87E-06	2.61E-06	0.75	0.669
5542.41	0.762	2.87E-06	2.62E-06	0.752	0.599
5538.56	0.762	2.86E-06	2.61E-06	0.752	0.636
5534.7	0.762	2.86E-06	2.59E-06	0.774	0.666
5530.84	0.762	2.86E-06	2.61E-06	0.74	0.609
5526.99	0.762	2.86E-06	2.60E-06	0.761	0.638
5523.13	0.763	2.85E-06	2.60E-06	0.754	0.623
5519.27	0.763	2.85E-06	2.59E-06	0.759	0.648
5515.41	0.763	2.85E-06	2.60E-06	0.752	0.621
5511.56	0.763	2.85E-06	2.63E-06	0.729	0.519
5507.7	0.764	2.84E-06	2.60E-06	0.736	0.580
5503.84	0.764	2.84E-06	2.57E-06	0.774	0.686
5499.99	0.764	2.84E-06	2.60E-06	0.747	0.598
5496.13	0.765	2.83E-06	2.60E-06	0.72	0.539
5492.27	0.765	2.82E-06	2.57E-06	0.745	0.633
5488.42	0.765	2.82E-06	2.59E-06	0.735	0.584
5484.56	0.766	2.82E-06	2.60E-06	0.719	0.557
5480.7	0.766	2.82E-06	2.57E-06	0.747	0.601
5476.85	0.766	2.81E-06	2.57E-06	0.745	0.608
5472.99	0.767	2.81E-06	2.57E-06	0.731	0.587
5469.13	0.767	2.80E-06	2.58E-06	0.725	0.547
5465.27	0.767	2.80E-06	2.59E-06	0.716	0.512
5461.42	0.768	2.80E-06	2.57E-06	0.735	0.556
5457.56	0.768	2.79E-06	2.58E-06	0.711	0.525
5453.7	0.769	2.80E-06	2.58E-06	0.721	0.547
5449.85	0.769	2.79E-06	2.57E-06	0.725	0.548
5445.99	0.769	2.78E-06	2.57E-06	0.718	0.531
5442.13	0.769	2.78E-06	2.53E-06	0.748	0.611
5438.28	0.770	2.78E-06	2.56E-06	0.733	0.535
5434.42	0.770	2.78E-06	2.56E-06	0.732	0.539

Table H1 (continued)

Wavenumbers (cm-1)	K	PIC.variance.obs	PIC.variance.rnd.mean	PIC.variance.P	PIC.variance.Z
5430.56	0.770	2.77E-06	2.57E-06	0.723	0.507
5426.71	0.771	2.77E-06	2.56E-06	0.696	0.490
5422.85	0.771	2.78E-06	2.58E-06	0.704	0.486
5418.99	0.772	2.78E-06	2.57E-06	0.724	0.552
5415.13	0.771	2.78E-06	2.57E-06	0.711	0.505
5411.28	0.772	2.77E-06	2.55E-06	0.718	0.542
5407.42	0.772	2.78E-06	2.57E-06	0.678	0.477
5403.56	0.772	2.79E-06	2.58E-06	0.703	0.522
5399.71	0.773	2.80E-06	2.57E-06	0.732	0.554
5395.85	0.772	2.80E-06	2.58E-06	0.725	0.543
5391.99	0.773	2.81E-06	2.60E-06	0.712	0.499
5388.14	0.773	2.82E-06	2.60E-06	0.717	0.526
5384.28	0.773	2.83E-06	2.60E-06	0.734	0.582
5380.42	0.773	2.84E-06	2.63E-06	0.714	0.528
5376.56	0.772	2.85E-06	2.65E-06	0.713	0.494
5372.71	0.773	2.88E-06	2.65E-06	0.73	0.569
5368.85	0.773	2.90E-06	2.69E-06	0.701	0.487
5364.99	0.772	2.92E-06	2.72E-06	0.711	0.487
5361.14	0.772	2.95E-06	2.73E-06	0.728	0.533
5357.28	0.772	2.97E-06	2.75E-06	0.712	0.488
5353.42	0.771	2.99E-06	2.75E-06	0.725	0.575
5349.57	0.771	3.03E-06	2.77E-06	0.753	0.650
5345.71	0.770	3.07E-06	2.82E-06	0.725	0.551
5341.85	0.770	3.11E-06	2.85E-06	0.738	0.579
5338	0.769	3.16E-06	2.90E-06	0.722	0.574
5334.14	0.769	3.22E-06	2.96E-06	0.731	0.570
5330.28	0.768	3.28E-06	3.02E-06	0.74	0.557
5326.42	0.768	3.34E-06	3.04E-06	0.756	0.638
5322.57	0.767	3.42E-06	3.15E-06	0.71	0.553
5318.71	0.767	3.50E-06	3.19E-06	0.744	0.603
5314.85	0.766	3.59E-06	3.29E-06	0.74	0.565
5311	0.765	3.68E-06	3.37E-06	0.729	0.580
5307.14	0.764	3.78E-06	3.44E-06	0.755	0.640
5303.28	0.763	3.90E-06	3.54E-06	0.745	0.658

Table H1 (continued)

Wavenumbers (cm-1)	K	PIC.variance.obs	PIC.variance.rnd.mean	PIC.variance.P	PIC.variance.Z
5299.43	0.762	4.02E-06	3.63E-06	0.779	0.704
5295.57	0.761	4.16E-06	3.80E-06	0.746	0.605
5291.71	0.760	4.30E-06	3.89E-06	0.769	0.680
5287.86	0.759	4.46E-06	4.09E-06	0.725	0.589
5284	0.758	4.62E-06	4.18E-06	0.767	0.672
5280.14	0.757	4.80E-06	4.36E-06	0.759	0.657
5276.28	0.756	4.99E-06	4.48E-06	0.793	0.735
5272.43	0.755	5.17E-06	4.71E-06	0.744	0.618
5268.57	0.754	5.35E-06	4.84E-06	0.768	0.693
5264.71	0.753	5.54E-06	4.92E-06	0.828	0.848
5260.86	0.752	5.75E-06	5.19E-06	0.786	0.727
5257	0.752	5.93E-06	5.34E-06	0.782	0.726
5253.14	0.751	6.11E-06	5.49E-06	0.788	0.746
5249.29	0.751	6.28E-06	5.65E-06	0.777	0.719
5245.43	0.750	6.44E-06	5.81E-06	0.773	0.703
5241.57	0.751	6.61E-06	5.94E-06	0.784	0.740
5237.72	0.751	6.74E-06	6.09E-06	0.773	0.693
5233.86	0.751	6.87E-06	6.15E-06	0.794	0.741
5230	0.751	6.98E-06	6.25E-06	0.799	0.773
5226.14	0.751	7.09E-06	6.32E-06	0.804	0.792
5222.29	0.751	7.19E-06	6.44E-06	0.796	0.753
5218.43	0.752	7.27E-06	6.57E-06	0.773	0.724
5214.57	0.752	7.35E-06	6.65E-06	0.791	0.694
5210.72	0.753	7.41E-06	6.66E-06	0.801	0.739
5206.86	0.753	7.46E-06	6.65E-06	0.807	0.777
5203	0.754	7.52E-06	6.81E-06	0.783	0.682
5199.15	0.754	7.55E-06	6.81E-06	0.782	0.701
5195.29	0.755	7.58E-06	6.86E-06	0.773	0.707
5191.43	0.755	7.59E-06	6.87E-06	0.768	0.654
5187.58	0.756	7.60E-06	6.87E-06	0.779	0.661
5183.72	0.756	7.61E-06	6.87E-06	0.785	0.699
5179.86	0.756	7.61E-06	6.81E-06	0.809	0.760
5176	0.757	7.60E-06	6.90E-06	0.778	0.655
5172.15	0.757	7.59E-06	6.86E-06	0.792	0.690

Table H1 (continued)

Wavenumbers (cm-1)	K	PIC.variance.obs	PIC.variance.rnd.mean	PIC.variance.P	PIC.variance.Z
5168.29	0.758	7.58E-06	6.87E-06	0.763	0.644
5164.43	0.758	7.56E-06	6.82E-06	0.794	0.732
5160.58	0.758	7.53E-06	6.81E-06	0.784	0.704
5156.72	0.759	7.51E-06	6.84E-06	0.781	0.645
5152.86	0.759	7.49E-06	6.77E-06	0.777	0.675
5149.01	0.759	7.47E-06	6.79E-06	0.771	0.637
5145.15	0.760	7.44E-06	6.73E-06	0.766	0.685
5141.29	0.760	7.42E-06	6.76E-06	0.77	0.635
5137.44	0.760	7.39E-06	6.70E-06	0.778	0.692
5133.58	0.761	7.36E-06	6.75E-06	0.733	0.554
5129.72	0.761	7.33E-06	6.64E-06	0.79	0.697
5125.86	0.761	7.31E-06	6.63E-06	0.769	0.668
5122.01	0.761	7.28E-06	6.64E-06	0.771	0.616
5118.15	0.762	7.25E-06	6.62E-06	0.755	0.605
5114.29	0.762	7.22E-06	6.60E-06	0.747	0.589
5110.44	0.762	7.19E-06	6.57E-06	0.75	0.605
5106.58	0.762	7.16E-06	6.59E-06	0.737	0.556
5102.72	0.762	7.13E-06	6.53E-06	0.749	0.597
5098.87	0.762	7.10E-06	6.47E-06	0.761	0.633
5095.01	0.762	7.07E-06	6.41E-06	0.781	0.673
5091.15	0.762	7.04E-06	6.41E-06	0.776	0.647
5087.29	0.762	7.01E-06	6.40E-06	0.746	0.623
5083.44	0.762	6.98E-06	6.38E-06	0.76	0.601
5079.58	0.762	6.96E-06	6.34E-06	0.766	0.640
5075.72	0.762	6.92E-06	6.32E-06	0.77	0.617
5071.87	0.762	6.90E-06	6.22E-06	0.778	0.691
5068.01	0.762	6.87E-06	6.27E-06	0.764	0.615
5064.15	0.762	6.85E-06	6.18E-06	0.774	0.697
5060.3	0.762	6.82E-06	6.18E-06	0.768	0.670
5056.44	0.762	6.79E-06	6.14E-06	0.785	0.708
5052.58	0.762	6.77E-06	6.17E-06	0.758	0.616
5048.73	0.762	6.74E-06	6.16E-06	0.758	0.625
5044.87	0.762	6.71E-06	6.15E-06	0.738	0.596
5041.01	0.763	6.69E-06	6.05E-06	0.77	0.687

Table H1 (continued)

Wavenumbers (cm-1)	K	PIC.variance.obs	PIC.variance.rnd.mean	PIC.variance.P	PIC.variance.Z
5037.15	0.763	6.66E-06	6.07E-06	0.76	0.643
5033.3	0.763	6.64E-06	6.02E-06	0.777	0.677
5029.44	0.763	6.61E-06	6.04E-06	0.768	0.636
5025.58	0.764	6.58E-06	6.01E-06	0.761	0.616
5021.73	0.764	6.56E-06	5.99E-06	0.759	0.599
5017.87	0.764	6.54E-06	6.01E-06	0.721	0.556
5014.01	0.765	6.51E-06	5.97E-06	0.745	0.590
5010.16	0.765	6.50E-06	5.96E-06	0.746	0.587
5006.3	0.765	6.47E-06	5.95E-06	0.75	0.571
5002.44	0.766	6.46E-06	5.91E-06	0.738	0.604
4998.59	0.766	6.44E-06	5.87E-06	0.766	0.638
4994.73	0.767	6.43E-06	5.91E-06	0.756	0.565
4990.87	0.767	6.41E-06	5.86E-06	0.726	0.596
4987.01	0.767	6.40E-06	5.91E-06	0.74	0.530
4983.16	0.767	6.39E-06	5.87E-06	0.741	0.571
4979.3	0.767	6.39E-06	5.84E-06	0.746	0.620
4975.44	0.767	6.38E-06	5.88E-06	0.733	0.539
4971.59	0.767	6.38E-06	5.85E-06	0.728	0.572
4967.73	0.768	6.38E-06	5.89E-06	0.737	0.530
4963.87	0.768	6.38E-06	5.86E-06	0.752	0.557
4960.02	0.768	6.38E-06	5.85E-06	0.752	0.575
4956.16	0.767	6.38E-06	5.83E-06	0.752	0.622
4952.3	0.767	6.38E-06	5.87E-06	0.732	0.552
4948.45	0.767	6.39E-06	5.84E-06	0.753	0.594
4944.59	0.767	6.39E-06	5.90E-06	0.728	0.569
4940.73	0.766	6.40E-06	5.87E-06	0.747	0.592
4936.87	0.766	6.41E-06	5.89E-06	0.746	0.570
4933.02	0.765	6.42E-06	5.84E-06	0.777	0.648
4929.16	0.765	6.43E-06	5.87E-06	0.753	0.609
4925.3	0.764	6.44E-06	5.89E-06	0.753	0.594
4921.45	0.764	6.45E-06	5.92E-06	0.731	0.571
4917.59	0.763	6.46E-06	5.91E-06	0.756	0.605
4913.73	0.762	6.47E-06	5.93E-06	0.742	0.590
4909.88	0.761	6.48E-06	5.89E-06	0.759	0.662

Table H1 (continued)

Wavenumbers (cm-1)	K	PIC.variance.obs	PIC.variance.rnd.mean	PIC.variance.P	PIC.variance.Z
4906.02	0.760	6.49E-06	5.95E-06	0.735	0.571
4902.16	0.759	6.50E-06	5.89E-06	0.784	0.676
4898.31	0.758	6.50E-06	5.92E-06	0.762	0.620
4894.45	0.757	6.50E-06	5.88E-06	0.778	0.693
4890.59	0.756	6.50E-06	5.89E-06	0.774	0.661
4886.73	0.755	6.51E-06	5.90E-06	0.781	0.668
4882.88	0.754	6.51E-06	5.90E-06	0.748	0.679
4879.02	0.754	6.52E-06	5.86E-06	0.788	0.744
4875.16	0.753	6.53E-06	5.85E-06	0.797	0.769
4871.31	0.752	6.53E-06	5.84E-06	0.797	0.760
4867.45	0.752	6.53E-06	5.86E-06	0.796	0.747
4863.59	0.752	6.53E-06	5.83E-06	0.792	0.761
4859.74	0.752	6.53E-06	5.85E-06	0.781	0.704
4855.88	0.752	6.52E-06	5.85E-06	0.794	0.740
4852.02	0.752	6.50E-06	5.87E-06	0.777	0.686
4848.17	0.753	6.48E-06	5.85E-06	0.784	0.698
4844.31	0.754	6.46E-06	5.78E-06	0.792	0.775
4840.45	0.755	6.44E-06	5.80E-06	0.775	0.701
4836.59	0.756	6.41E-06	5.77E-06	0.776	0.678
4832.74	0.757	6.38E-06	5.80E-06	0.776	0.653
4828.88	0.758	6.34E-06	5.72E-06	0.783	0.708
4825.02	0.760	6.31E-06	5.73E-06	0.757	0.650
4821.17	0.761	6.28E-06	5.70E-06	0.772	0.620
4817.31	0.762	6.25E-06	5.71E-06	0.746	0.584
4813.45	0.764	6.22E-06	5.66E-06	0.756	0.611
4809.6	0.765	6.19E-06	5.61E-06	0.789	0.699
4805.74	0.766	6.17E-06	5.69E-06	0.738	0.529
4801.88	0.767	6.15E-06	5.60E-06	0.763	0.617
4798.02	0.768	6.13E-06	5.63E-06	0.756	0.566
4794.17	0.769	6.12E-06	5.65E-06	0.738	0.517
4790.31	0.770	6.10E-06	5.62E-06	0.734	0.558
4786.45	0.770	6.10E-06	5.67E-06	0.715	0.481
4782.6	0.771	6.10E-06	5.58E-06	0.749	0.603
4778.74	0.771	6.10E-06	5.64E-06	0.728	0.523

Table H1 (continued)

Wavenumbers (cm-1)	K	PIC.variance.obs	PIC.variance.rnd.mean	PIC.variance.P	PIC.variance.Z
4774.88	0.772	6.11E-06	5.66E-06	0.728	0.506
4771.03	0.772	6.12E-06	5.67E-06	0.724	0.495
4767.17	0.772	6.14E-06	5.67E-06	0.731	0.521
4763.31	0.772	6.16E-06	5.66E-06	0.756	0.556
4759.46	0.771	6.18E-06	5.67E-06	0.749	0.552
4755.6	0.771	6.20E-06	5.71E-06	0.739	0.537
4751.74	0.771	6.22E-06	5.75E-06	0.736	0.532
4747.88	0.771	6.25E-06	5.77E-06	0.749	0.523
4744.03	0.771	6.27E-06	5.78E-06	0.707	0.524
4740.17	0.771	6.29E-06	5.77E-06	0.737	0.563
4736.31	0.771	6.31E-06	5.79E-06	0.748	0.566
4732.46	0.771	6.32E-06	5.84E-06	0.712	0.499
4728.6	0.771	6.32E-06	5.83E-06	0.731	0.537
4724.74	0.772	6.32E-06	5.82E-06	0.727	0.544
4720.89	0.772	6.32E-06	5.85E-06	0.728	0.518
4717.03	0.772	6.33E-06	5.83E-06	0.736	0.548
4713.17	0.772	6.33E-06	5.84E-06	0.747	0.557
4709.32	0.773	6.34E-06	5.84E-06	0.743	0.535
4705.46	0.773	6.35E-06	5.85E-06	0.741	0.549
4701.6	0.773	6.36E-06	5.88E-06	0.726	0.508
4697.74	0.773	6.37E-06	5.89E-06	0.715	0.504
4693.89	0.773	6.38E-06	5.95E-06	0.707	0.447
4690.03	0.773	6.39E-06	5.91E-06	0.727	0.510
4686.17	0.774	6.40E-06	5.91E-06	0.741	0.528
4682.32	0.774	6.41E-06	5.88E-06	0.736	0.574
4678.46	0.774	6.43E-06	5.93E-06	0.725	0.529
4674.6	0.774	6.44E-06	5.98E-06	0.706	0.475
4670.75	0.774	6.45E-06	6.01E-06	0.724	0.454
4666.89	0.774	6.45E-06	5.94E-06	0.742	0.559
4663.03	0.774	6.46E-06	6.02E-06	0.703	0.461
4659.18	0.775	6.46E-06	5.95E-06	0.737	0.544
4655.32	0.775	6.46E-06	6.00E-06	0.713	0.481
4651.46	0.775	6.45E-06	5.99E-06	0.726	0.485
4647.6	0.776	6.45E-06	6.00E-06	0.731	0.481

Table H1 (continued)

Wavenumbers (cm-1)	K	PIC.variance.obs	PIC.variance.rnd.mean	PIC.variance.P	PIC.variance.Z
4643.75	0.776	6.44E-06	5.97E-06	0.735	0.515
4639.89	0.776	6.44E-06	5.98E-06	0.723	0.477
4636.03	0.777	6.43E-06	5.99E-06	0.713	0.492
4632.18	0.777	6.42E-06	5.99E-06	0.719	0.461
4628.32	0.778	6.41E-06	5.98E-06	0.721	0.463
4624.46	0.778	6.40E-06	5.98E-06	0.715	0.418
4620.61	0.778	6.39E-06	5.97E-06	0.694	0.455
4616.75	0.778	6.39E-06	5.98E-06	0.706	0.442
4612.89	0.778	6.39E-06	6.00E-06	0.694	0.413
4609.04	0.777	6.40E-06	5.90E-06	0.739	0.542
4605.18	0.776	6.40E-06	5.95E-06	0.718	0.498
4601.32	0.776	6.41E-06	5.94E-06	0.73	0.515
4597.46	0.775	6.42E-06	5.95E-06	0.721	0.496
4593.61	0.774	6.43E-06	5.92E-06	0.752	0.563
4589.75	0.773	6.43E-06	5.97E-06	0.723	0.482
4585.89	0.772	6.44E-06	5.94E-06	0.74	0.521
4582.04	0.771	6.45E-06	5.92E-06	0.735	0.575
4578.18	0.770	6.47E-06	5.95E-06	0.731	0.556
4574.32	0.768	6.48E-06	5.97E-06	0.75	0.568
4570.47	0.767	6.49E-06	5.94E-06	0.754	0.607
4566.61	0.766	6.50E-06	5.94E-06	0.747	0.599
4562.75	0.765	6.51E-06	5.91E-06	0.76	0.633
4558.9	0.765	6.51E-06	5.95E-06	0.764	0.613
4555.04	0.764	6.52E-06	6.00E-06	0.727	0.540
4551.18	0.763	6.53E-06	5.97E-06	0.753	0.596
4547.32	0.762	6.54E-06	5.97E-06	0.747	0.604
4543.47	0.761	6.54E-06	5.96E-06	0.76	0.635
4539.61	0.760	6.55E-06	5.94E-06	0.768	0.657
4535.75	0.759	6.55E-06	5.91E-06	0.78	0.716
4531.9	0.758	6.56E-06	5.95E-06	0.765	0.671
4528.04	0.758	6.56E-06	5.91E-06	0.776	0.686
4524.18	0.757	6.56E-06	5.95E-06	0.756	0.632
4520.33	0.757	6.55E-06	5.94E-06	0.783	0.686
4516.47	0.757	6.55E-06	5.94E-06	0.778	0.665

Table H1 (continued)

Wavenumbers (cm-1)	K	PIC.variance.obs	PIC.variance.rnd.mean	PIC.variance.P	PIC.variance.Z
4512.61	0.756	6.54E-06	5.90E-06	0.783	0.700
4508.75	0.756	6.54E-06	5.89E-06	0.787	0.722
4504.9	0.756	6.53E-06	5.92E-06	0.781	0.675
4501.04	0.756	6.53E-06	5.94E-06	0.752	0.633
4497.18	0.756	6.53E-06	5.91E-06	0.78	0.687
4493.33	0.755	6.53E-06	5.90E-06	0.768	0.685
4489.47	0.755	6.54E-06	5.88E-06	0.784	0.728
4485.61	0.755	6.56E-06	5.93E-06	0.773	0.701
4481.76	0.754	6.59E-06	5.91E-06	0.79	0.739
4477.9	0.753	6.63E-06	6.00E-06	0.765	0.657
4474.04	0.752	6.67E-06	6.03E-06	0.769	0.690
4470.19	0.751	6.71E-06	5.97E-06	0.801	0.806
4466.33	0.750	6.76E-06	6.08E-06	0.793	0.736
4462.47	0.749	6.81E-06	6.07E-06	0.796	0.779
4458.61	0.748	6.86E-06	6.13E-06	0.798	0.782
4454.76	0.747	6.91E-06	6.19E-06	0.781	0.738
4450.9	0.746	6.95E-06	6.24E-06	0.785	0.746
4447.04	0.746	7.00E-06	6.21E-06	0.815	0.808
4443.19	0.745	7.03E-06	6.26E-06	0.809	0.799
4439.33	0.744	7.07E-06	6.32E-06	0.784	0.755
4435.47	0.743	7.09E-06	6.30E-06	0.807	0.811
4431.62	0.743	7.10E-06	6.29E-06	0.826	0.834
4427.76	0.743	7.11E-06	6.27E-06	0.818	0.869
4423.9	0.742	7.12E-06	6.33E-06	0.8	0.822
4420.05	0.742	7.14E-06	6.31E-06	0.81	0.825
4416.19	0.742	7.16E-06	6.32E-06	0.812	0.861
4412.33	0.742	7.18E-06	6.34E-06	0.822	0.839
4408.47	0.742	7.20E-06	6.38E-06	0.81	0.852
4404.62	0.742	7.19E-06	6.38E-06	0.801	0.823
4400.76	0.742	7.18E-06	6.39E-06	0.808	0.833
4396.9	0.743	7.14E-06	6.35E-06	0.782	0.778
4393.05	0.744	7.09E-06	6.30E-06	0.815	0.808
4389.19	0.744	7.05E-06	6.27E-06	0.812	0.818
4385.33	0.743	7.05E-06	6.31E-06	0.794	0.766

Table H1 (continued)

Wavenumbers (cm-1)	K	PIC.variance.obs	PIC.variance.rnd.mean	PIC.variance.P	PIC.variance.Z
4381.48	0.742	7.07E-06	6.32E-06	0.798	0.773
4377.62	0.741	7.09E-06	6.29E-06	0.823	0.840
4373.76	0.740	7.09E-06	6.27E-06	0.804	0.836
4369.91	0.741	7.08E-06	6.32E-06	0.811	0.786
4366.05	0.741	7.08E-06	6.29E-06	0.811	0.795
4362.19	0.741	7.09E-06	6.25E-06	0.812	0.869
4358.33	0.742	7.09E-06	6.32E-06	0.802	0.754
4354.48	0.742	7.09E-06	6.24E-06	0.831	0.910
4350.62	0.743	7.08E-06	6.29E-06	0.8	0.811
4346.76	0.744	7.06E-06	6.26E-06	0.823	0.843
4342.91	0.744	7.07E-06	6.29E-06	0.809	0.792
4339.05	0.744	7.09E-06	6.27E-06	0.811	0.830
4335.19	0.743	7.10E-06	6.32E-06	0.807	0.816
4331.34	0.743	7.10E-06	6.28E-06	0.826	0.883
4327.48	0.742	7.09E-06	6.33E-06	0.803	0.782
4323.62	0.742	7.06E-06	6.27E-06	0.816	0.832
4319.77	0.743	7.02E-06	6.20E-06	0.834	0.899
4315.91	0.743	6.99E-06	6.16E-06	0.826	0.873
4312.05	0.743	6.95E-06	6.22E-06	0.803	0.751
4308.19	0.743	6.93E-06	6.12E-06	0.806	0.844
4304.34	0.743	6.92E-06	6.15E-06	0.812	0.825
4300.48	0.742	6.93E-06	6.18E-06	0.805	0.786
4296.62	0.741	6.92E-06	6.19E-06	0.778	0.743
4292.77	0.740	6.93E-06	6.16E-06	0.813	0.825
4288.91	0.739	6.94E-06	6.14E-06	0.811	0.848
4285.05	0.738	6.96E-06	6.20E-06	0.792	0.794
4281.2	0.737	6.99E-06	6.14E-06	0.835	0.939
4277.34	0.737	7.01E-06	6.17E-06	0.835	0.884
4273.48	0.737	7.03E-06	6.17E-06	0.831	0.917
4269.63	0.737	7.05E-06	6.17E-06	0.832	0.948
4265.77	0.737	7.06E-06	6.21E-06	0.818	0.864
4261.91	0.737	7.07E-06	6.25E-06	0.816	0.863
4258.05	0.737	7.07E-06	6.26E-06	0.808	0.833
4254.2	0.737	7.06E-06	6.18E-06	0.826	0.898

Table H1 (continued)

Wavenumbers (cm-1)	K	PIC.variance.obs	PIC.variance.rnd.mean	PIC.variance.P	PIC.variance.Z
4250.34	0.737	7.05E-06	6.20E-06	0.835	0.918
4246.48	0.737	7.05E-06	6.21E-06	0.825	0.885
4242.63	0.737	7.05E-06	6.23E-06	0.819	0.860
4238.77	0.737	7.07E-06	6.26E-06	0.81	0.828
4234.91	0.737	7.08E-06	6.24E-06	0.825	0.853
4231.06	0.737	7.10E-06	6.25E-06	0.823	0.898
4227.2	0.737	7.11E-06	6.26E-06	0.821	0.847
4223.34	0.737	7.13E-06	6.27E-06	0.816	0.871
4219.48	0.737	7.15E-06	6.29E-06	0.834	0.871
4215.63	0.737	7.18E-06	6.28E-06	0.839	0.947
4211.77	0.737	7.20E-06	6.38E-06	0.802	0.821
4207.91	0.737	7.22E-06	6.39E-06	0.815	0.853
4204.06	0.738	7.23E-06	6.44E-06	0.805	0.779
4200.2	0.738	7.25E-06	6.40E-06	0.825	0.862
4196.34	0.738	7.25E-06	6.41E-06	0.815	0.837
4192.49	0.739	7.25E-06	6.41E-06	0.817	0.822
4188.63	0.739	7.26E-06	6.39E-06	0.825	0.898
4184.77	0.739	7.28E-06	6.42E-06	0.822	0.874
4180.92	0.739	7.29E-06	6.39E-06	0.835	0.964
4177.06	0.739	7.31E-06	6.42E-06	0.832	0.899
4173.2	0.739	7.33E-06	6.48E-06	0.822	0.881
4169.34	0.739	7.35E-06	6.50E-06	0.821	0.853
4165.49	0.740	7.36E-06	6.50E-06	0.807	0.819
4161.63	0.740	7.39E-06	6.53E-06	0.834	0.849
4157.77	0.739	7.42E-06	6.58E-06	0.793	0.815
4153.92	0.739	7.44E-06	6.62E-06	0.791	0.793
4150.06	0.739	7.47E-06	6.56E-06	0.831	0.894
4146.2	0.739	7.49E-06	6.69E-06	0.8	0.795
4142.35	0.739	7.52E-06	6.66E-06	0.814	0.795
4138.49	0.739	7.54E-06	6.65E-06	0.843	0.926
4134.63	0.739	7.55E-06	6.68E-06	0.817	0.852
4130.78	0.739	7.57E-06	6.68E-06	0.83	0.861
4126.92	0.739	7.58E-06	6.71E-06	0.812	0.832
4123.06	0.739	7.59E-06	6.73E-06	0.821	0.818

Table H1 (continued)

Wavenumbers (cm-1)	K	PIC.variance.obs	PIC.variance.rnd.mean	PIC.variance.P	PIC.variance.Z
4119.2	0.739	7.60E-06	6.71E-06	0.817	0.847
4115.35	0.740	7.61E-06	6.71E-06	0.827	0.899
4111.49	0.740	7.61E-06	6.73E-06	0.827	0.877
4107.63	0.740	7.62E-06	6.76E-06	0.808	0.798
4103.78	0.741	7.63E-06	6.78E-06	0.809	0.826
4099.92	0.741	7.65E-06	6.78E-06	0.808	0.827
4096.06	0.741	7.66E-06	6.81E-06	0.815	0.817
4092.21	0.741	7.68E-06	6.85E-06	0.806	0.759
4088.35	0.741	7.70E-06	6.83E-06	0.812	0.820
4084.49	0.741	7.73E-06	6.84E-06	0.821	0.838
4080.64	0.741	7.76E-06	6.86E-06	0.82	0.842
4076.78	0.742	7.79E-06	6.84E-06	0.837	0.919
4072.92	0.742	7.83E-06	6.89E-06	0.84	0.885
4069.06	0.743	7.85E-06	7.00E-06	0.817	0.782
4065.21	0.743	7.86E-06	6.99E-06	0.809	0.827
4061.35	0.744	7.87E-06	7.05E-06	0.797	0.738
4057.49	0.745	7.88E-06	7.07E-06	0.787	0.715
4053.64	0.745	7.89E-06	7.00E-06	0.804	0.801
4049.78	0.746	7.89E-06	7.04E-06	0.805	0.754
4045.92	0.746	7.92E-06	7.03E-06	0.813	0.816
4042.07	0.745	7.97E-06	7.15E-06	0.787	0.745
4038.21	0.745	8.03E-06	7.07E-06	0.825	0.887
4034.35	0.744	8.07E-06	7.16E-06	0.812	0.794
4030.5	0.744	8.11E-06	7.22E-06	0.814	0.797
4026.64	0.744	8.14E-06	7.24E-06	0.811	0.809
4022.78	0.744	8.17E-06	7.28E-06	0.814	0.796
4018.92	0.745	8.19E-06	7.23E-06	0.827	0.843
4015.07	0.745	8.21E-06	7.32E-06	0.825	0.783
4011.21	0.745	8.24E-06	7.30E-06	0.814	0.818
4007.35	0.745	8.27E-06	7.42E-06	0.793	0.714
4003.5	0.744	8.30E-06	7.38E-06	0.822	0.805
3999.64	0.744	8.33E-06	7.44E-06	0.804	0.746

Table H2 Detection results of different chromatographic information phylogenetic signals

Time (min)	K	PIC.variance.obs	PIC.variance.rnd.mean	PIC.variance.P	PIC.variance.Z
5.186	0.82610	0.00016	0.00015	0.68800	0.52630
5.366	0.68540	0.00030	0.00024	0.96500	1.70211
5.392	0.98709	0.00018	0.00021	0.20200	-0.90992
6.092	0.94278	0.00016	0.00017	0.36600	-0.35730
6.366	0.83533	0.00024	0.00022	0.64400	0.44314
8.086	0.70935	0.00006	0.00005	0.90500	1.27265
8.526	0.66312	0.00013	0.00010	0.97600	1.89857
9.066	0.83425	0.00023	0.00023	0.55600	0.05349
9.353	0.74026	0.00015	0.00013	0.89800	1.33797
10.153	1.13739	0.00005	0.00006	0.03500	-1.42920
12.133	0.97126	0.00018	0.00021	0.19600	-0.90834
13.893	0.90763	0.00014	0.00014	0.35200	-0.27672
16.660	0.77498	0.00010	0.00009	0.75800	0.79731
16.846	1.03548	0.00011	0.00012	0.17100	-0.94568
18.166	0.79726	0.00012	0.00011	0.75800	0.73625
20.986	1.01858	0.00018	0.00020	0.29300	-0.59416
21.473	0.92264	0.00015	0.00016	0.32300	-0.52387
23.666	1.13652	0.00005	0.00006	0.03700	-1.67061
29.825	1.10005	0.00006	0.00008	0.06700	-1.45162
30.325	0.91591	0.00055	0.00058	0.38300	-0.33055
31.239	0.75845	0.00037	0.00033	0.76500	0.80144
32.079	1.10947	0.00015	0.00018	0.13300	-1.26428
34.586	0.79786	0.00014	0.00013	0.72300	0.65640
35.766	0.90450	0.00027	0.00026	0.62600	0.17150
36.386	1.08121	0.00009	0.00011	0.10700	-1.38921
39.027	1.03845	0.00022	0.00027	0.13400	-1.07986
40.554	1.26448	0.00010	0.00014	0.00700	-1.90807
42.721	0.81411	0.00048	0.00046	0.59500	0.22599
44.248	1.03342	0.00013	0.00016	0.17100	-1.01140
44.635	0.97367	0.00014	0.00016	0.17600	-0.98523

Table H3 Detection results of different volatile components information phylogenetic signals

NO	Compounds (%)	K	PIC.variance .obs	PIC.variance. rnd.mean	PIC. variance.P	PIC. variance.Z
C1	Pyridine	0.947	0.010	0.011	0.263	-0.671
C10	3-methylbutanoic acid	0.837	0.044	0.043	0.585	0.201
C11	2-methyl-Butanoic acid	1.075	0.013	0.017	0.102	-1.360
C12	Ethylbenzene	0.903	0.000	0.000	0.408	-0.247
C13	1,4-Xylene	1.031	0.000	0.000	0.124	-1.242
C14	2-Cyclopentene-1,4-dione	0.996	0.049	0.058	0.127	-0.916
C15	2-Heptanone	0.698	0.001	0.001	0.836	1.154
C16	1,2-xylene	0.803	0.001	0.001	0.669	0.387
C17	1,2,3,4,5-Pentamethylcyclopentadiene	0.819	0.007	0.007	0.675	0.414
C18	Methional	0.617	0.041	0.030	0.996	2.231
C19	2,6-Dimethylpyrazine	0.756	0.000	0.000	0.759	0.731
C2	Pyrrole	0.800	0.026	0.025	0.646	0.463
C20	1H-Pyrrole-2-carboxaldehyde, 1-met	0.763	0.001	0.001	0.875	1.233
C21	(1r)-(+)-alpha-pinene	0.825	0.071	0.070	0.524	0.101
C22	1-(Pyridin-1(4H)-yl)ethanone	0.995	0.001	0.002	0.158	-0.804
C23	4,5-Dihydro-5-methyl-2(3H)-fur	0.713	0.001	0.001	0.849	1.115
C24	Tetrahydrothiophen-3-one	0.789	0.010	0.009	0.679	0.452
C25	5-Methyl furfural	0.795	0.000	0.000	0.701	0.510
C26	Benzaldehyde	0.943	0.002	0.002	0.287	-0.621
C27	1-Decen-3-one	0.845	0.172	0.175	0.449	-0.090
C28	Tetraethyl orthosilicate	0.867	0.554	0.569	0.442	-0.163
C29	1-Octen-3-ol	0.661	6.727	5.286	0.956	1.700
C3	Toluene	0.929	0.001	0.001	0.285	-0.592
C30	2-Pentylfuran	0.947	0.070	0.079	0.253	-0.664
C31	Decane	0.934	0.002	0.002	0.262	-0.585
C32	2-Acetylthiazole	0.668	0.000	0.000	0.953	1.784
C33	2,2,4,4,6,8,8-heptamethyl-Nonane	0.757	0.002	0.002	0.715	0.665
C34	2H-Pyran-2-one,5,6-dihydro-	0.687	0.007	0.006	0.902	1.420
C35	1-Butanamine,3-methyl-N-(3-methylbutylidene)-	0.762	0.613	0.542	0.785	0.843
C36	Phenylacetaldehyde	0.801	0.589	0.556	0.639	0.319

Table H3 (continued)

NO	Compounds (%)	K	PIC.variance .obs	PIC.variance. rnd.mean	PIC. variance.P	PIC. variance.Z
C37	2,5,9-Trimethyldecane	0.677	0.002	0.001	0.922	1.535
C38	(E)-2-Octenal	0.925	0.017	0.019	0.323	-0.532
C39	2-Acetyl pyrrole	1.133	0.000	0.001	0.094	-1.301
C4	2-hydroxy-Propanenitrile	1.231	0.028	0.041	0.016	-2.237
C40	Acetophenone	0.997	0.116	0.139	0.139	-0.908
C41	Tetramethylpyrazine	0.666	0.042	0.034	0.903	1.471
C42	1-Nonanal	1.007	0.000	0.000	0.304	-0.622
C43	1-Propanamine,N-(2-furanylmethylene)-2-methyl-	0.713	14.151	12.075	0.773	0.923
C44	N-(3-Methylbutyl) acetamide	0.798	0.003	0.003	0.748	0.651
C45	Undecane, 3-methyl-	0.930	0.000	0.000	0.341	-0.464
C46	Benzo[c]thiophene	1.099	0.000	0.000	0.064	-1.494
C47	Dodecane	0.936	0.005	0.006	0.283	-0.567
C48	Cyclopentane, pentyl-	0.831	0.015	0.015	0.524	-0.016
C49	N-Propylbenzylideneamine	0.708	0.035	0.028	0.821	1.112
C5	Hexanal	0.858	0.472	0.479	0.481	-0.088
C50	Indole	0.881	0.001	0.001	0.381	-0.291
C51	Tridecane	0.840	0.005	0.005	0.570	0.071
C52	Tridecane, 3-methyl-	0.665	0.005	0.004	0.932	1.486
C53	3-methyl-N-propyl-1-Butanamine	0.833	0.003	0.003	0.576	0.161
C54	Tetradecane	0.967	0.001	0.001	0.221	-0.775
C55	Cyclopentane, nonyl-	0.985	0.003	0.003	0.164	-0.793
C56	3-Phenylpyridine	0.896	0.001	0.001	0.383	-0.368
C57	2,4-Di-tert-butylphenol	0.679	0.001	0.001	0.988	1.829
C58	Nerolidol	1.143	0.002	0.002	0.106	-1.226
C59	PentaDecane, 3-methyl-	0.755	0.000	0.000	0.795	0.863
C6	Triethyl orthoformate	0.811	2.778	2.648	0.600	0.320
C60	Hexadecane	0.733	0.001	0.001	0.862	1.145
C61	Diphenylamine	1.088	0.001	0.001	0.088	-1.450
C62	undecyl-Cyclopentane	0.715	0.000	0.000	0.905	1.420
C63	2,2’,5,5’-tetramethylbiphenyl	0.843	0.000	0.000	0.490	-0.040
C64	(2E,6E)-3,7,11-Trimethyl-2,6,10-dodecatrien-1-ol	0.847	0.115	0.108	0.648	0.419
C65	Tetradecanoic acid	1.346	0.119	0.168	0.014	-2.033

Table H3 (continued)

NO	Compounds (%)	K	PIC.variance .obs	PIC.variance.rnd. mean	PIC. variance.P	PIC. variance.Z
C66	Phenanthrene	1.242	0.001	0.001	0.047	-1.446
C67	Methyl pentadecanoate	0.874	0.005	0.005	0.563	0.221
C68	Diisobutyl phthalate	0.767	2.184	1.947	0.768	0.803
C69	Pentadecanoic acid	0.878	15.902	15.914	0.484	-0.004
C7	2(5H)-Furanone, 3-methyl-	0.816	0.010	0.010	0.576	0.192
C70	7,9-Di-tert-butyl-1-oxaspiro(4,5)d	1.034	0.007	0.008	0.216	-0.845
C71	Methyl hexadecanoate	1.183	0.002	0.002	0.053	-1.382
C72	(Z)-9-Hexadecenoic acid	1.082	1.970	2.310	0.166	-0.991
C73	Dibutyl phthalate	1.041	0.183	0.205	0.229	-0.763
C74	Hexadecanoic acid	1.535	70.408	112.603	0.001	-2.524
C75	Hexadecanoic acid, ethyl ester	0.877	0.309	0.307	0.553	0.038
C76	Eicosane	0.847	0.514	0.491	0.639	0.282
C77	Linoleic acid	0.812	0.187	0.176	0.683	0.422
C78	Heptadecanoic acid	0.942	0.158	0.172	0.310	-0.541
C79	5,8,11-Heptadecatrienoic acid, met	0.816	0.180	0.167	0.683	0.434
C8	2-Methylpyrazine	0.923	0.001	0.001	0.401	-0.270
C80	oleonitrile	0.908	0.032	0.032	0.463	-0.029
C81	9,12-Octadecadienoicacid, methyl ester, (9E,12E)--methyl ester	1.114	0.024	0.029	0.140	-1.141
C82	Methyl 9-(Z)-octadecenoate	1.026	0.027	0.031	0.241	-0.760
C83	2(3H)-Furanone, 5-dodecyldihydro-	0.912	0.093	0.095	0.446	-0.174
C84	Linoelaidic acid	1.086	704.401	851.682	0.138	-1.074
C85	9-Octadecenoic acid, (E)-	0.816	212.459	201.243	0.622	0.332
C86	Ethyl linoleate	0.862	0.787	0.805	0.483	-0.151
C87	9-Octadecenenitrile, (E)-	0.833	9.010	8.595	0.608	0.265
C88	Ethyl Oleate	0.855	6.430	6.298	0.567	0.128
C89	Tetradecanamide	1.050	0.310	0.358	0.197	-0.965
C9	Furfural	0.803	0.091	0.085	0.653	0.484
C90	Nepetalacton	0.914	0.686	0.695	0.481	-0.091
C91	Butyl citrate	0.698	0.319	0.258	0.897	1.349
C92	1,6-Cyclodecadiene	1.197	0.063	0.081	0.061	-1.434

Table H3 (continued)

NO	Compounds (%)	K	PIC.variance .obs	PIC.variance.rnd. mean	PIC. variance.P	PIC. variance.Z
C93	(Z)-9-octadecen-4-olide	1.009	0.118	0.132	0.219	-0.752
C94	gamma-Linolenic acid	1.027	0.205	0.229	0.235	-0.709
C95	Octyl 4-methoxycinnamate	0.717	2.130	1.797	0.798	1.022
C96	Oleamide	0.976	0.186	0.206	0.270	-0.635
C97	(Z)-9,17-Octadecadienal	0.935	0.026	0.026	0.524	-0.034
C98	Bis(2-ethylhexyl) phthalate	0.873	0.026	0.025	0.578	0.186
C99	Tetracosane	1.359	0.981	1.351	0.042	-1.769

APPENDIX I

THE TWO-DIMENSIONAL CORRELATION SPECTRA AND HPLC-FINGERPRINT

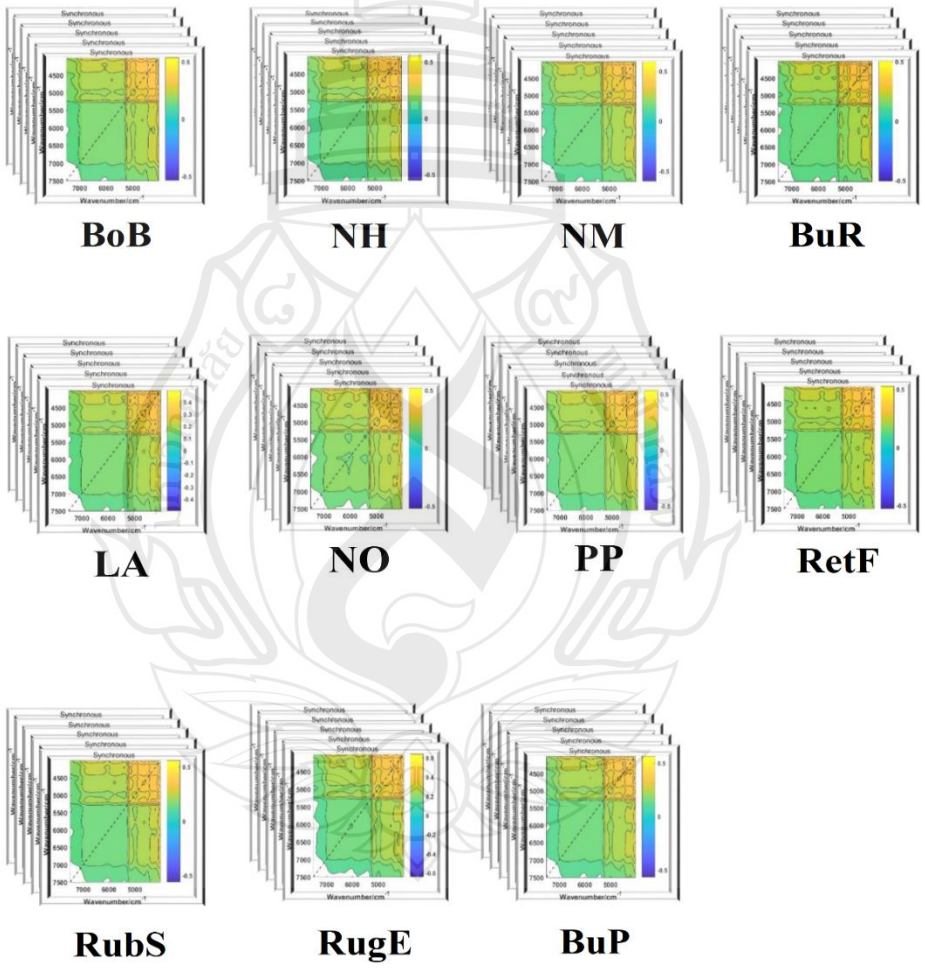


Figure I1 Two-dimensional correlation spectra matrix of 11 species of boletes

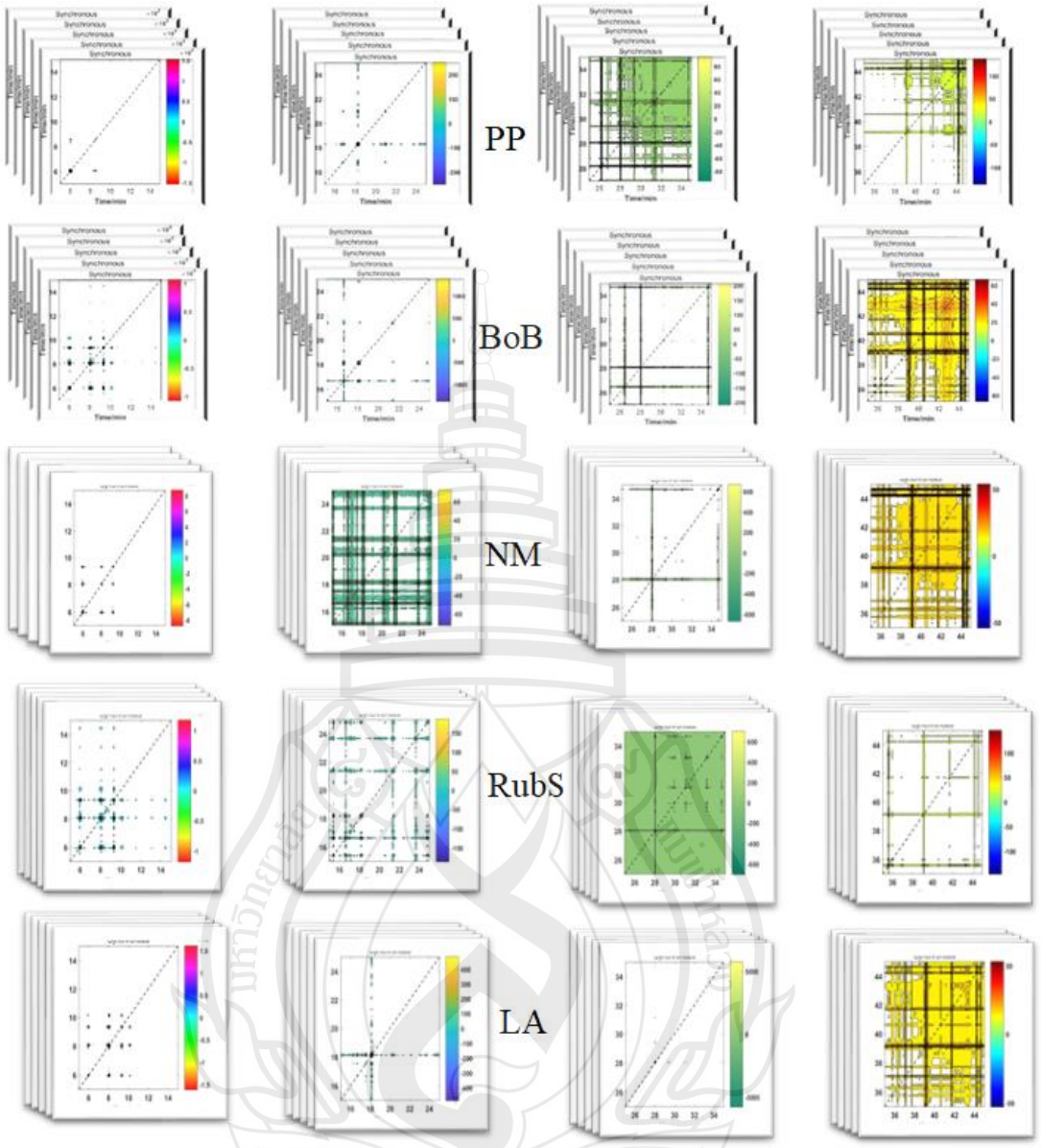


Figure I2 Two-dimensional correlation chromatogram matrix of 11 species of boletes

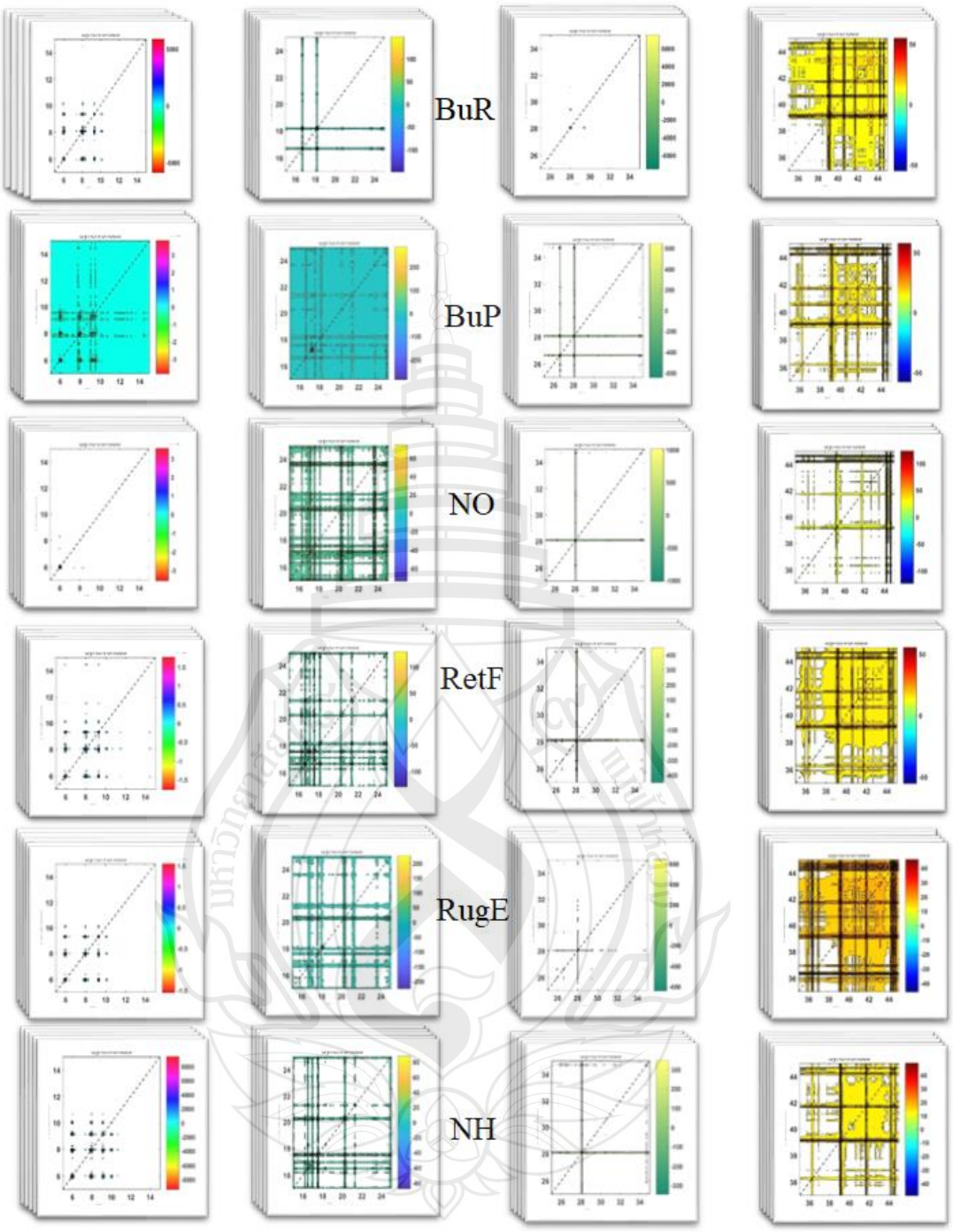


Figure I2 (continued)

APPENDIX J

THE CHEMICAL STRUCTURAL FORMULA OF VOCs BY GC-MS

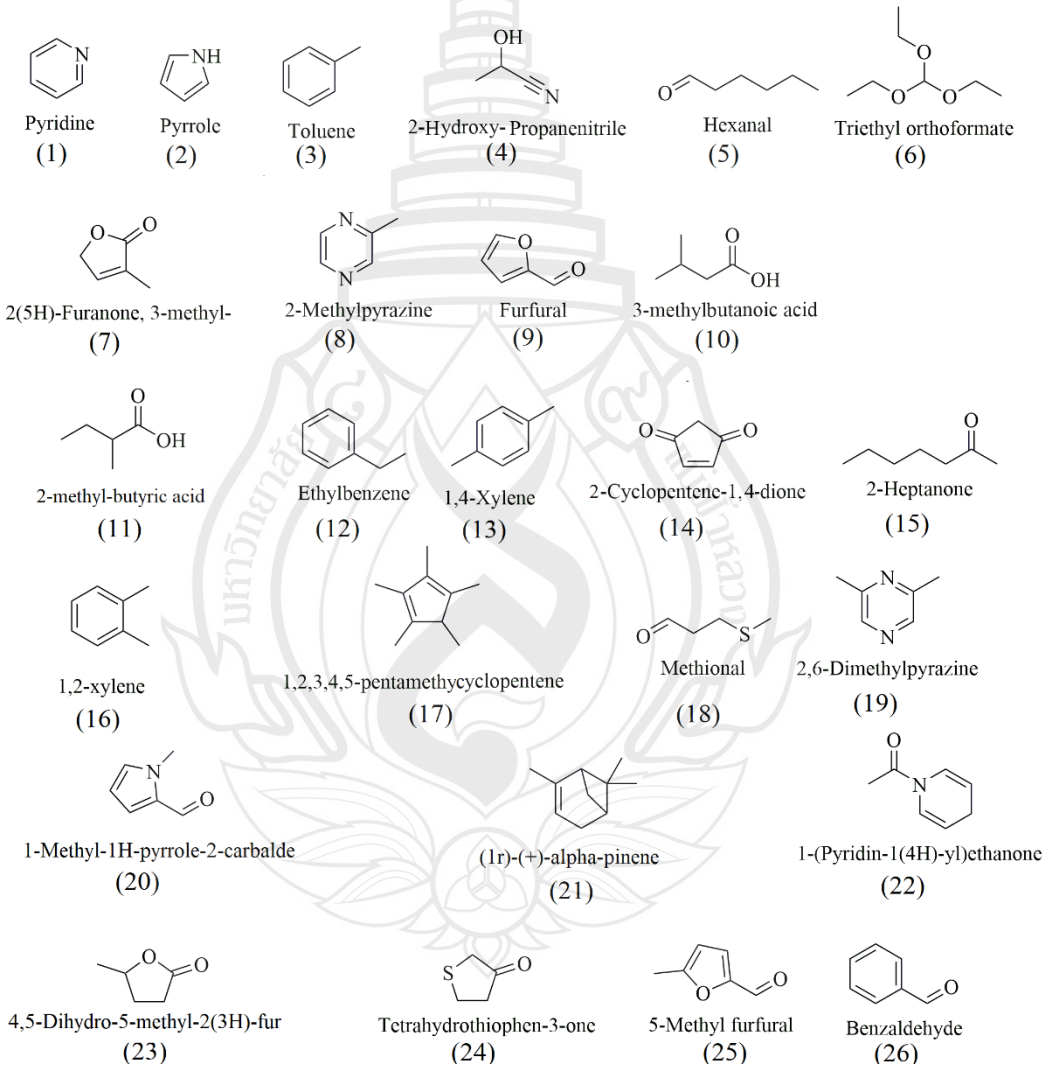


Figure J1 The structural formulas of 99 volatile component

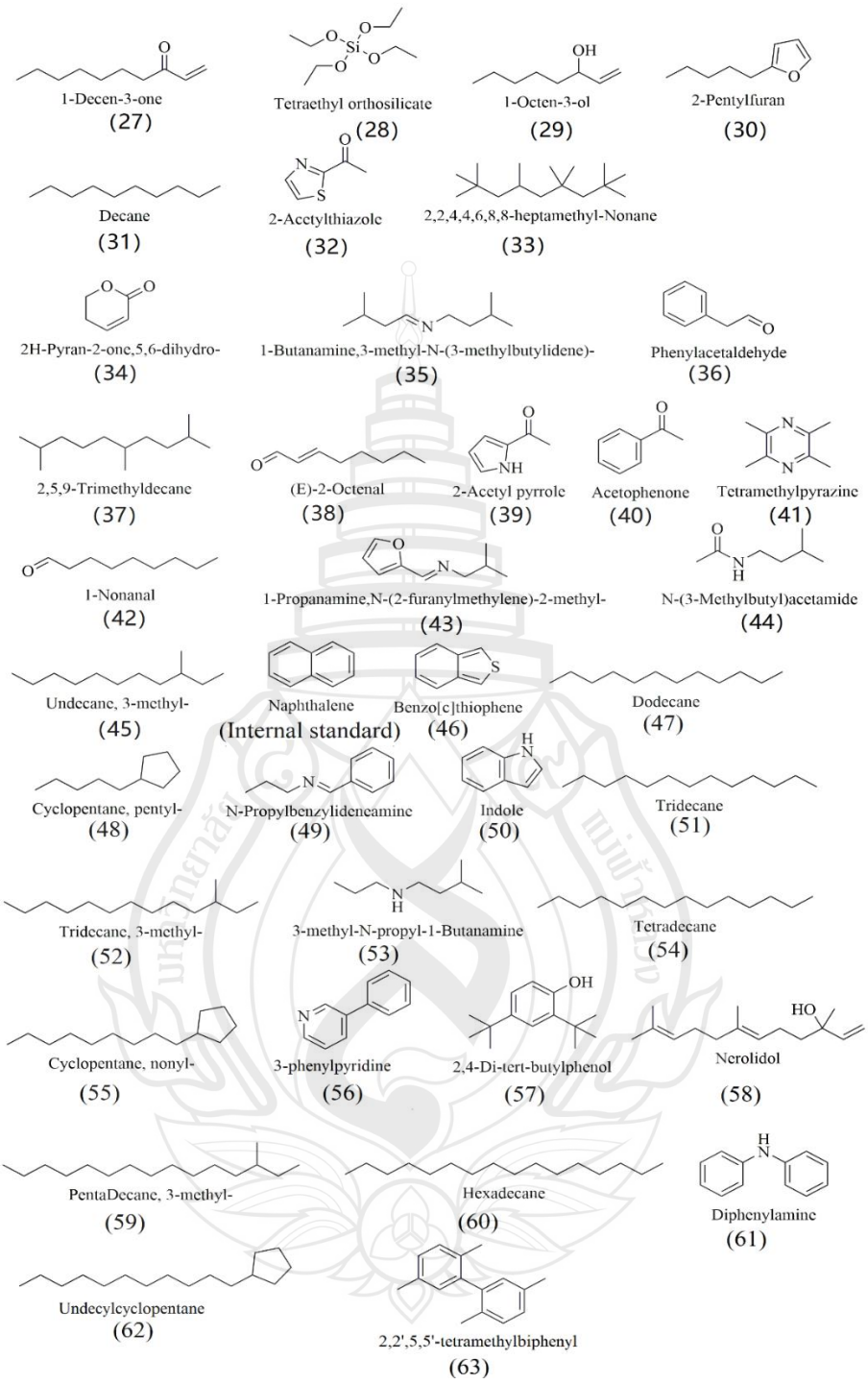


Figure J1 (continued)

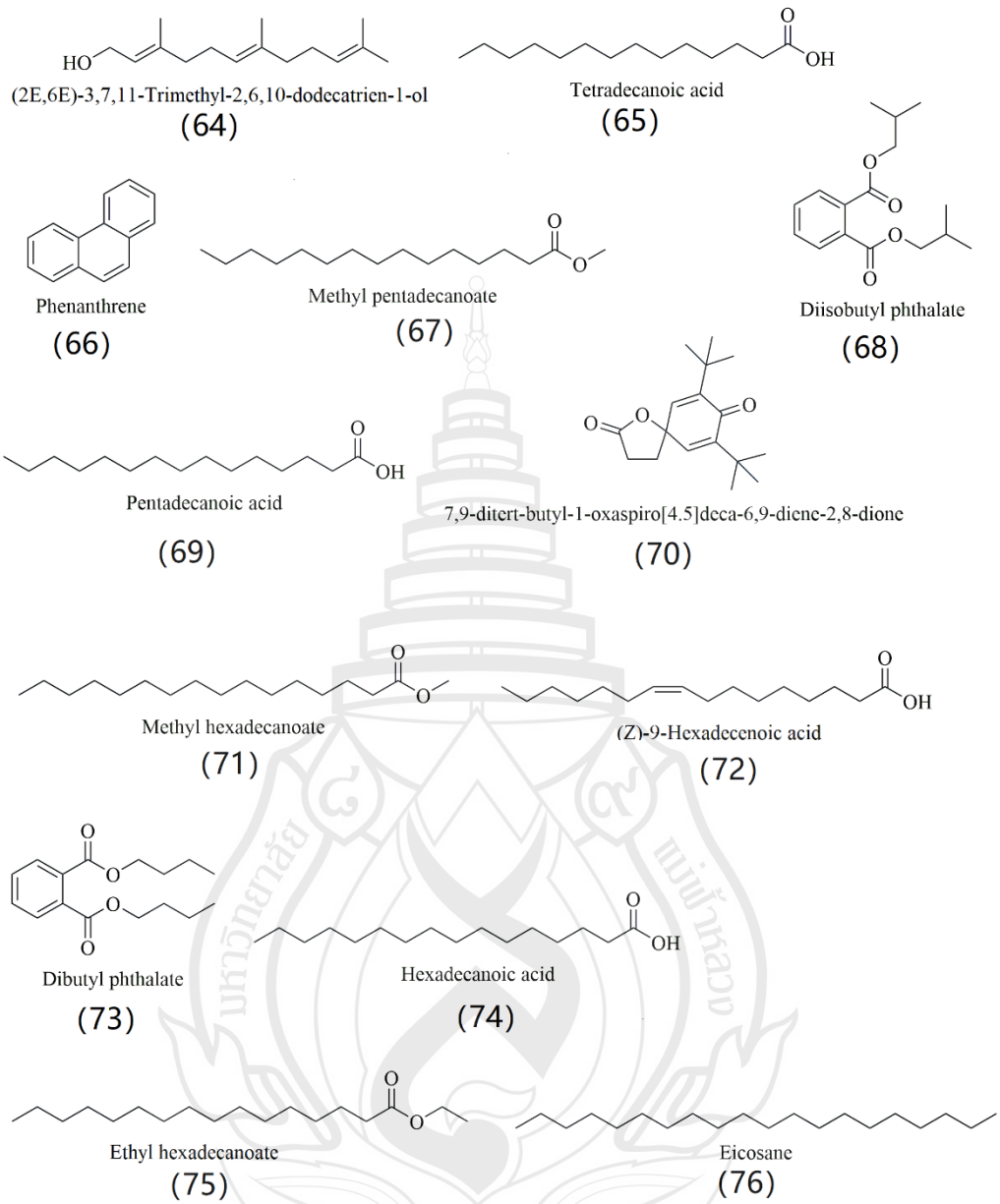


Figure J1 (continued)

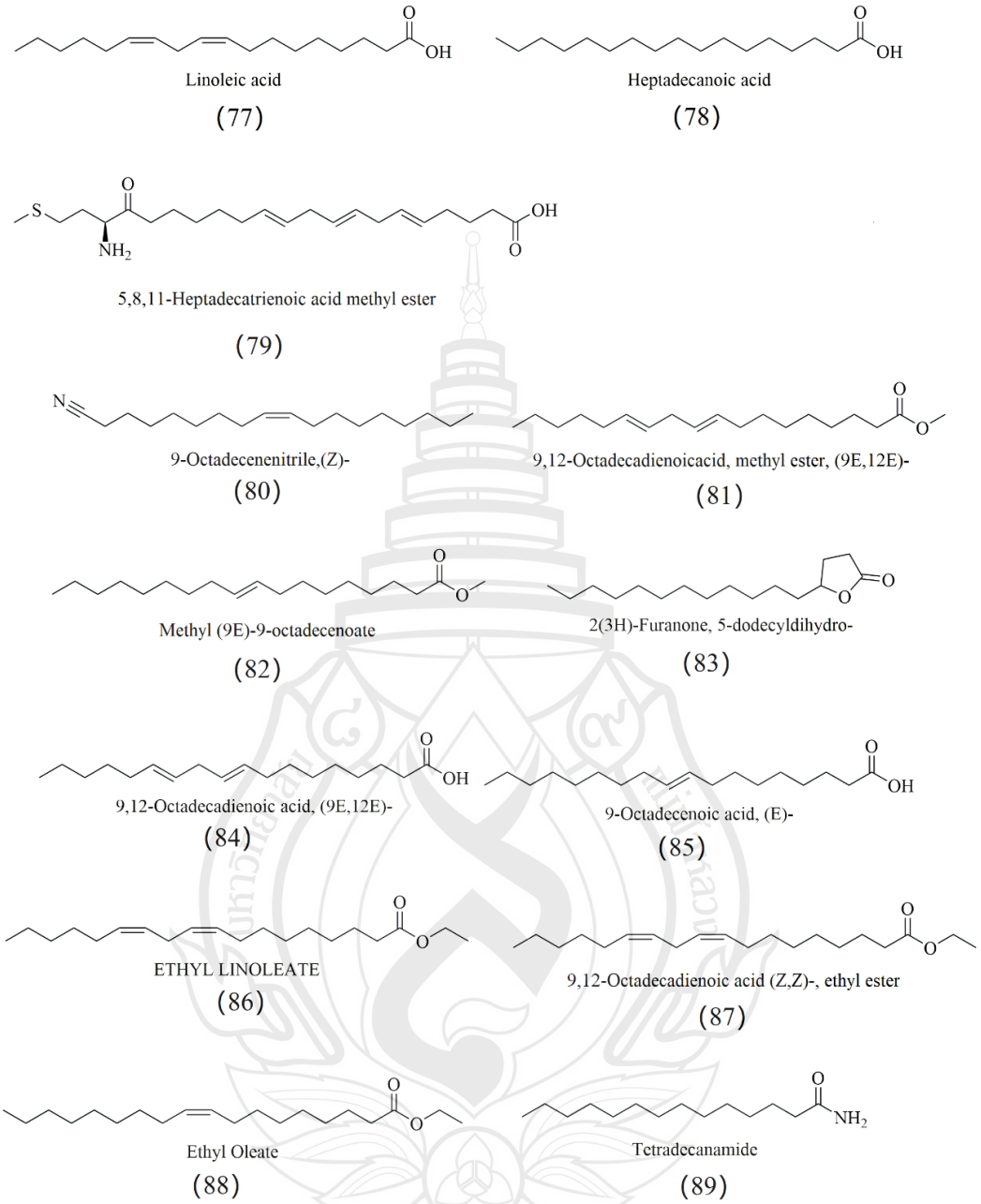
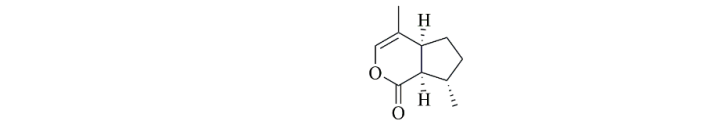
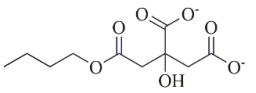


Figure J1 (continued)



(4aS,7S,7aR)-4,7-Dimethyl-5,6,7,7a-tetrahydro-4aH-cyclopenta[c]pyran-1-one

(90)

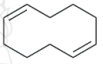


Butyl citrate

Caution: A net charge appears to be present

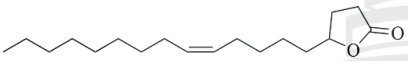
This name appears to be ambiguous

(91)



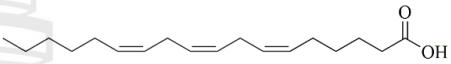
1,6-Cyclodecadiene

(92)



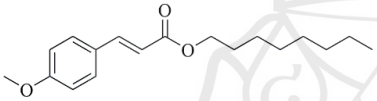
(Z)-9-octadecen-4-olide

(93)



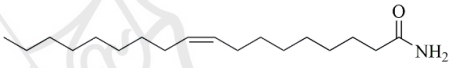
gamma-Linolenic acid

(94)



Octyl 4-methoxycinnamate

(95)



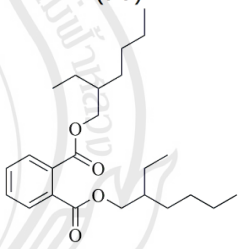
Oleamide

(96)



9,17-Octadecadienal, (Z)-

(97)



Bis(2-ethylhexyl) phthalate

(98)

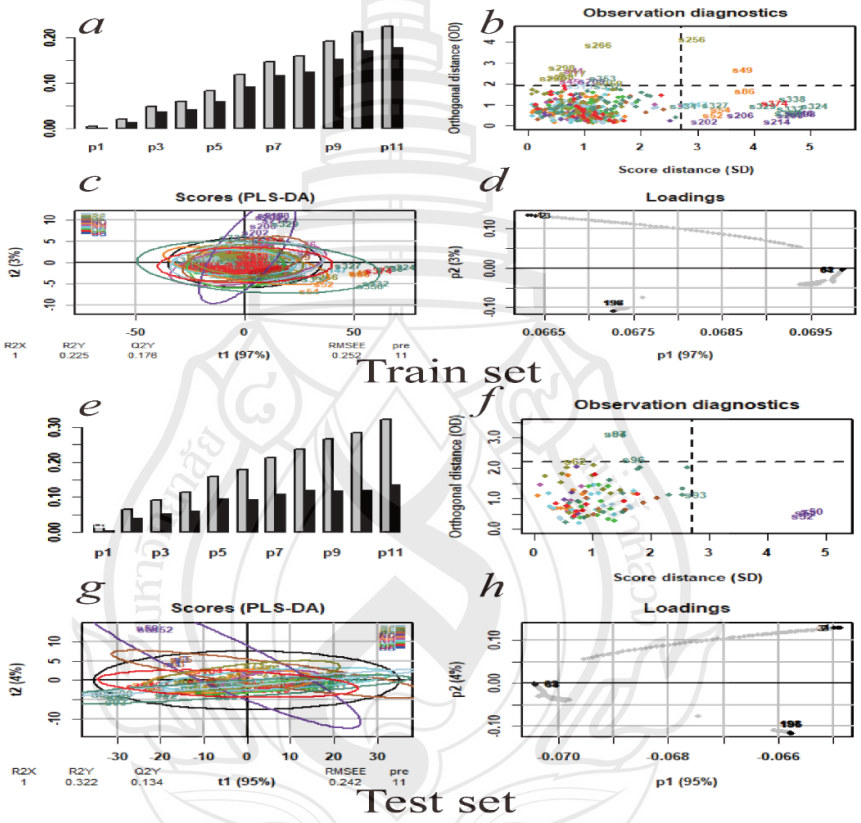


Tetracosane (99)

Figure J1 (continued)

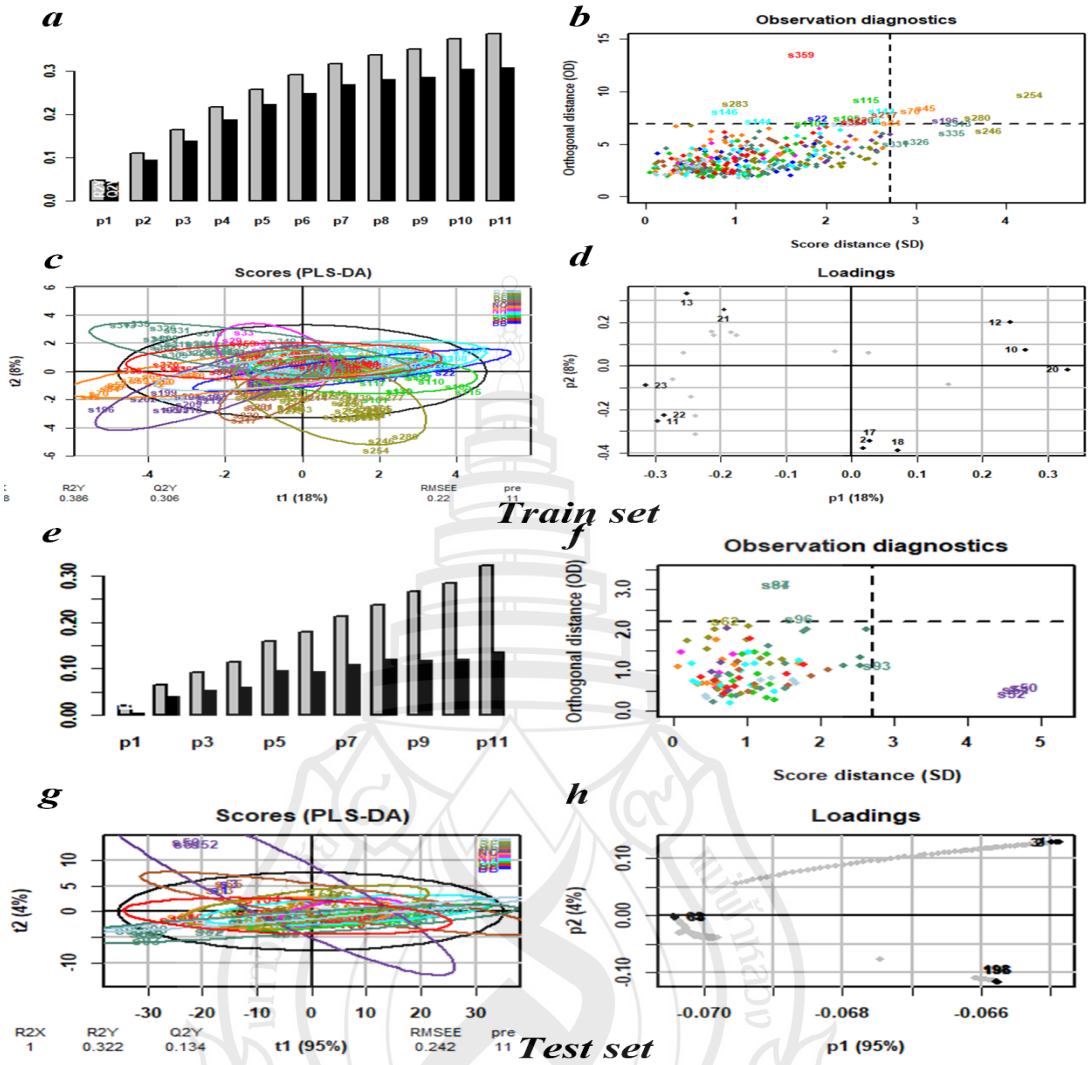
APPENDIX K

THE CHEMICAL STRUCTURAL FORMULA OF VOCs BY GC-MS



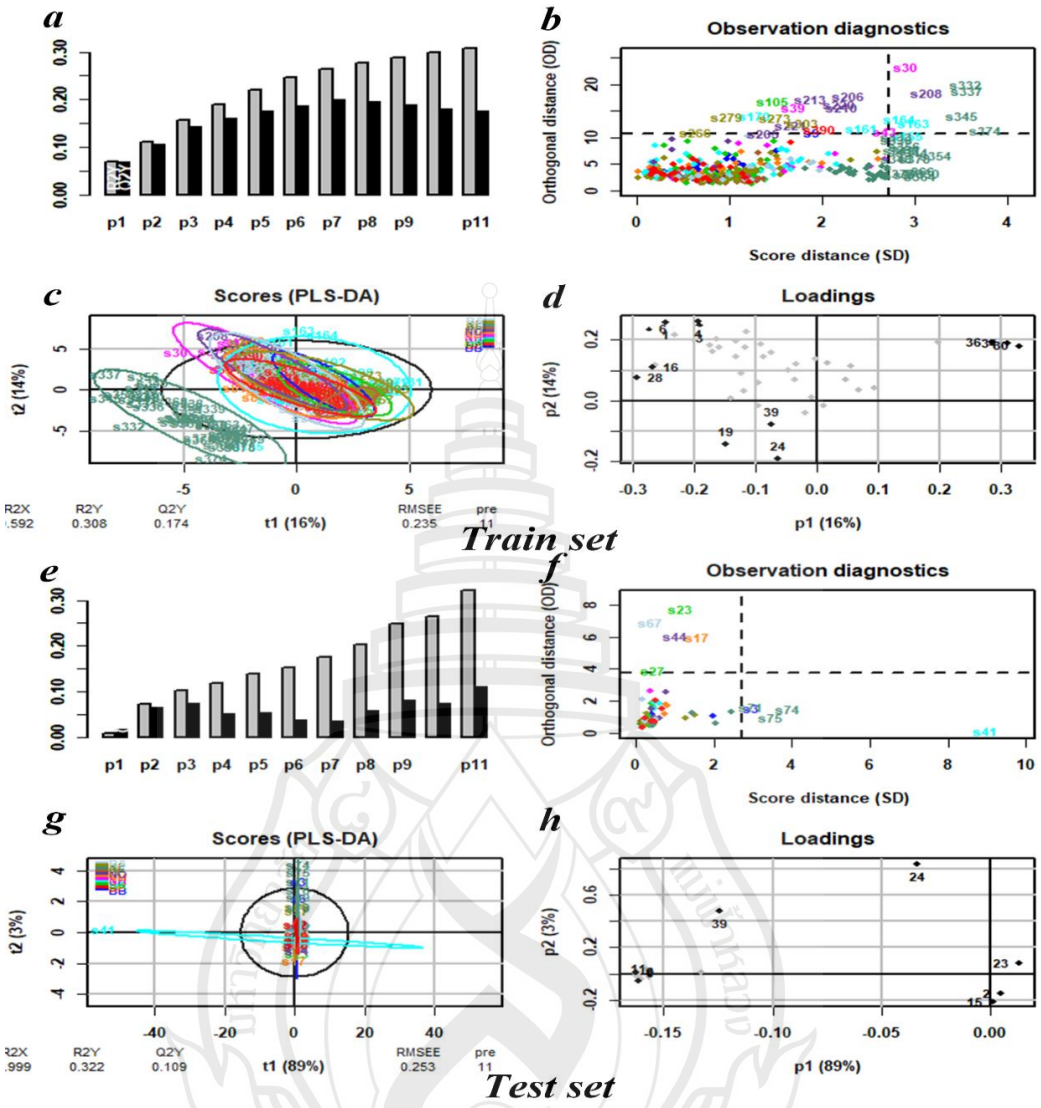
Note a, e Cumulative contribution rate of the principal component variance of the training set and test set, respectively. b, f Projection orthogonal-score distance distribution of the training set and test set. c, g PLS-DA score distribution map of training set and test set, respectively. d, h PLS-DA load diagram of the training set and test set.

Figure K1 The PLS-DA classification and verification model diagram of 11 species of boletes established by using R language based on the characteristic spectral information



Note a, e Cumulative contribution rate of the principal component variance of the training set and test set, respectively. b, f Projection orthogonal-score distance distribution of the training set and test set. c, g PLS-DA score distribution map of the training set and test set. d, h PLS-DA load diagram of the training set and test set.

Figure K2 The PLS-DA classification and verification model diagram of 11 species of boletes established by using R language based on the characteristic chromatographic information



Note a, e Cumulative contribution rate of the principal component variance of the training set and test set, respectively. b, f Projection orthogonal-score distance distribution of training set and test set, respectively. c, g PLS-DA score distribution map of the training set and test set. d, h PLS-DA load diagram of the training set and test set

Figure K3 PLS-DA classification and verification model diagram of 11 species of boletes established by using R language based on volatile constituent information

APPENDIX L

THE VIP SCREEN OF THE CHEMICAL INFORMATION SIGNIFICANTLY CORRELATED WITH REFION CLASSIFICATION

Table L1 VIP screen of the spectral, chromatographic and volatile component information significantly correlated with region classification

Spectroscopy		HPLC-fingerprint		Volatile compounds	
Wavenumbers (cm^{-1})	VIP	Time (min)	VIP	Compounds (%)	VIP
7497.88	1.550	5.188	1.237	Diisobutyl phthalate	1.7215
7494.02	1.543	5.368	1.046	1,2-xylene	1.54
7490.16	1.536	6.094	1.189	2-methyl-1-Propanamine,N-(2-furanylmethylene)	1.4936
7486.31	1.529	6.361	1.347	Linoelaidic acid	1.4335
7482.45	1.520	8.082	1.047	Linoleic acid	1.3476
7478.59	1.512	8.523	1.458	3-Phenylpyridine	1.3161
7474.74	1.504	9.067	1.247	1,6-Cyclodecadiene	1.2965
7470.88	1.496	9.355	1.087	2,2,4,4,6,8,8-heptamethyl-Nonane	1.2916

Table L1 (continued)

Spectroscopy		HPLC-fingerprint		Volatile compounds	
Wavenumbers (cm^{-1})	**VIP**	**Time (min)**	**VIP**	**Compounds (%)**	**VIP**
7467.02	1.489	13.893	1.311	(Z)-9-Hexadecenoic acid	1.283
7463.17	1.480	18.163	1.094	Methyl hexadecanoate	1.2631
7459.31	1.471	30.323	1.373	oleonitrile	1.2589
7455.45	1.463	32.078	1.011	Nepetalacton	1.2431
7451.6	1.455	40.559	1.057	Hexadecanoic acid	1.2409
7447.74	1.448	44.246	1.028	Dibutyl phthalate	1.2345
7443.88	1.439			2,5,9-Trimethyldecane	1.2291
7440.02	1.430			Pentadecanoic acid	1.2212
7436.17	1.421			9,12-Octadecadienoicacid, methyl ester, (9E,12E)--methyl ester	1.2118
7432.31	1.413			5,8,11-Heptadecatrienoic acid, met	1.2059
7428.45	1.405			Undecane, 3-methyl-	1.1961
7424.6	1.397			7,9-Di-tert-butyl-1-oxaspiro(4,5)d	1.1873
7420.74	1.388			2-Heptanone	1.1863
7416.88	1.379			5-Methyl furfural	1.1859
7413.03	1.372			Cyclopentane, pentyl-	1.1819
7409.17	1.365			(2E,6E)-3,7,11-Trimethyl-2,6,10-dodecatrien-1-ol	1.1778
7405.31	1.357			gamma-Linolenic acid	1.1653
7401.46	1.349			2-Acetyl pyrrole	1.161
7397.6	1.342			1,2,3,4,5-Pentamethylcyclopentadiene	1.1532
7393.74	1.334			3-methylbutanoic acid	1.1276

Table L1 (continued)

Spectroscopy		HPLC-fingerprint		Volatile compounds	
Wavenumbers (cm^{-1})	**VIP**	**Time (min)**	**VIP**	**Compounds (%)**	**VIP**
7389.88	1.327			Oleamide	1.1271
7386.03	1.320			Hexadecane	1.1253
7382.17	1.311			Pyrrole	1.1176
7378.31	1.302			Toluene	1.1106
7374.46	1.298			2(3H)-Furanone, 5-dodecyldihydro-	1.1076
7370.6	1.293			Tetradecanamide	1.0925
7366.74	1.286			2-methyl-butanoic acid	1.0826
7362.89	1.281			Tetradecanoic acid	1.0669
7359.03	1.275			2-Methylpyrazine	1.0612
7355.17	1.267			PentaDecane, 3-methyl-	1.0592
7351.31	1.263			(Z)-9-octadecen-4-olide	1.0568
7347.46	1.256			Hexanal	1.0484
7343.6	1.247			2,4-Di-tert-butylphenol	1.0341
7339.74	1.240			ETHYL LINOLEATE	1.0333
7335.89	1.243			1-Butanamine,3-methyl-N-(3-methylbutylidene)-	1.0297
7332.03	1.240			2-Pentylfuran	1.0288
7328.17	1.229			Dodecane	1.027
7324.32	1.225			Eicosane	1.0209
7320.46	1.225			Heptadecanoic acid	1.0065
7316.6	1.221			Methyl pentadecanoate	1.0051

Table L1 (continued)

Spectroscopy		HPLC-fingerprint		Volatile compounds	
Wavenumbers (cm^{-1})	**VIP**	**Time (min)**	**VIP**	**Compounds (%)**	**VIP**
7312.75	1.213				
7308.89	1.206				
7305.03	1.204				
7301.17	1.202				
5268.57	1.206				
5264.71	1.217				
5260.86	1.219				
5257	1.219				
5253.14	1.221				
5249.29	1.224				
5245.43	1.228				
5241.57	1.220				
5237.72	1.214				
5233.86	1.215				
5230	1.215				
5226.14	1.214				
5222.29	1.209				
5218.43	1.204				
5206.86	1.204				
4261.91	1.203				

Table L1 (continued)

Spectroscopy		HPLC-fingerprint		Volatile compounds	
Wavenumbers (cm^{-1})	**VIP**	**Time (min)**	**VIP**	**Compounds (%)**	**VIP**
4258.05	1.206				
4049.78	1.200				
4045.92	1.202				
4042.07	1.204				
4038.21	1.206				
4034.35	1.207				
4030.5	1.207				
4026.64	1.207				
4022.78	1.205				
4018.92	1.204				
4015.07	1.203				
4011.21	1.200				

APPENDIX M

CORRELATION COEFFICIENT BETWEEN ECOLOGICAL ENVIROMENTAL FACTORS AND PRODUCING AREAS

Table M1 Correlation coefficient between ecological environmental factors and producing areas

Factors	CoeffCS of Region1	CoeffCS of Region 2	CoeffCS of Region 3	CoeffCS of Region 4	CoeffCS of Region 5	CoeffCS of Region 6
b01	0.1157	0.0840	0.0170	-0.1045	-0.0410	-0.0441
b02	0.1662	0.2663	-0.0684	-0.1456	0.0726	-0.1622
b03	-0.0474	0.0301	0.1567	0.0318	-0.0415	-0.1299
b04	-0.0883	0.0395	0.0625	0.0627	-0.0580	-0.0345
b05	0.0780	0.1092	0.0026	-0.0603	-0.0064	-0.0749
b06	-0.0609	-0.0535	0.0927	0.0507	-0.0678	-0.0026
b07	0.1904	0.2555	-0.1396	-0.1475	0.0997	-0.1181
b08	-0.0277	0.0440	0.0520	0.0413	-0.0512	-0.0500
b09	0.1608	0.0189	-0.0159	-0.0412	0.0228	-0.0677
b10	0.0903	0.0844	0.0262	-0.0570	-0.0445	-0.0626
b11	0.1125	0.0624	0.0047	-0.0819	-0.0186	-0.0437
b12	0.2511	-0.0429	-0.0840	0.0268	0.0417	-0.0545
b13	0.3096	-0.0184	-0.1366	-0.0865	0.1159	-0.0417
b14	0.2229	0.1388	-0.2620	-0.2968	-0.1381	0.2896
b15	0.1212	0.0398	-0.0724	-0.2897	0.1454	0.0333
b16	0.2178	-0.0275	-0.0978	-0.0676	0.0636	-0.0030
b17	-0.1242	-0.0548	0.0354	0.2208	-0.2016	0.0843
b18	0.2865	-0.0441	-0.1021	-0.1067	0.0761	-0.0092
b19	0.1319	-0.0756	-0.0024	0.2122	-0.0742	-0.0688
ele	0.1304	0.1063	-0.2116	-0.1499	0.1179	0.0620
Latitude	0.1529	-0.0518	-0.1300	0.2329	0.2584	-0.2094
Longitude	-0.1172	0.0311	0.1159	-0.4153	-0.1765	0.2565
pH	0.0557	-0.1284	0.3207	-0.0554	-0.1127	-0.1355

APPENDIX N

THE CONTRIBUTION DIAGRAM OF ECOLOGICAL ENVIRONMENTAL FACTORS TO DIFFERENT REGIONS ANALYZED BY CONSENSUS CLUSTER PLUS

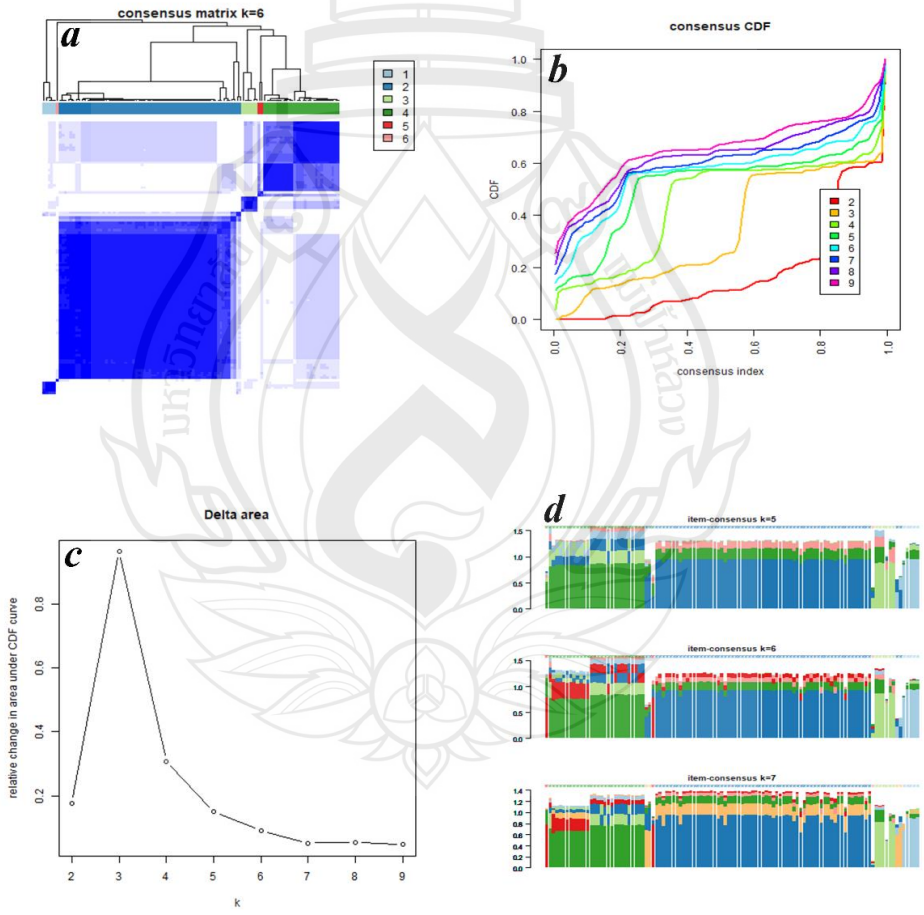


Figure N1 The contribution diagram of ecological environmental factors to different regions analyzed by Consensus Cluster Plus

APPENDIX O

THE SPECIMENS AND RESULTS OF VOLATILE COMPONENTS

Table O1 The detailed information of specimens

Sampling position	Latin Name	Abbreviation	Numbers	Longitude	Latitude	Elevation (M)
Shiping County, Honghe Prepecture	*Boletus bainiugan*	BoB	4	101.51	25.07	1797
Manshenke Village, Jinghong City, Xishuangbanna Prefecture	*Boletus bainiugan*	BoB	4	102.03	24.71	2309
Dayao County, Chuxiong Prefecture	*Boletus bainiugan*	BoB	4	102.52	24.43	1689
Donggua Town, Chuxiong Prefecture	*Boletus bainiugan*	BoB	4	102.09	24.31	1973
Mayou Township, Yaoan County, Chuxiong Prepecture	*Boletus bainiugan*	BoB	4	102.38	24.09	1873
Yangmei Mountain, Yaoan County, Chuxiong Prepecture	*Boletus bainiugan*	BoB	4	102.38	24.31	1772
Wangjia Village, Tonghai County, Yuxi City	*Boletus bainiugan*	BoB	4	102.54	24.59	1958
Fengyi Village, Anning city, Kunming City	*Boletus bainiugan*	BoB	4	102.29	24.58	2061
Tongchang, Yimen County, Yuxi City	*Butyriboletus roseoflavus*	BuR	4	101.37	25.53	2155
Jiulongchi Pond, Yuxi City	*Butyriboletus roseoflavus*	BuR	3	102.32	24.68	1980
Tongchang, Yimen County, Yuxi City	*Butyriboletus roseoflavus*	BuR	5	102.09	24.69	1993

Table O1 (continued)

Sampling position	Latin Name	Abbreviation	Numbers	Longitude	Latitude	Elevation (M)
Tangchi Town, Yiliang County, Kunming City	*Butyriboletus roseoflavus*	BuR	3	102.09	24.31	1973
Wenli Village, anban Town, Zhenyuan County, Pu'er City	*Butyriboletus roseoflavus*	BuR	4	102.63	24.3	1740
Wenli Village, anban Town, Zhenyuan County, Pu'er City	*Butyriboletus roseoflavus*	BuR	4	99.27	25.18	1754
Wenli Village, anban Town, Zhenyuan County, Pu'er City	*Butyriboletus roseoflavus*	BuR	4	102.23	24.84	1732
Tongchang, Yimen County, Yuxi City	*Butyriboletus roseoflavus*	BuR	4	103.62	24.47	1832
Fuliangpeng Township, Eshan County, Yuxi City	*Butyriboletus roseoflavus*	BuR	4	101.96	25.73	2138
Fengyi Village, Anning city, Kunming City	*Butyriboletus roseoflavus*	BuR	3	102.41	24.17	1540
Fuliangpeng Township, Eshan County, Yuxi City	*Butyriboletus roseoflavus*	BuR	5	102.56	24.34	1714
Jiuxiang Village, Yiliang County, Kunming City	*Butyriboletus roseoflavus*	BuR	3	102.16	24.25	1835
Jiuxi Town, Jiangchuan County, Yuxi City	*Butyriboletus roseoflavus*	BuR	4	102.65	24.52	2061
Daweidu Village, Xiaojie Town, Eshan County, Yuxi City	*Butyriboletus roseoflavus*	BuR	5	103	23.5	2125
Daweidu Village, Xiaojie Town, Eshan County, Yuxi City	*Butyriboletus pseudospeciosus*	BuP	4	102.65	23.8	1898
Donggua Town, Chuxiong Prefecture	*Butyriboletus pseudospeciosus*	BuP	3	102.64	24.3	1714
Simao District, Pu'er City	*Butyriboletus pseudospeciosus*	BuP	3	102.39	24.33	1726
Fuliangpeng Township, Eshan County, Yuxi City	*Butyriboletus pseudospeciosus*	BuP	3	99.36	25.88	1850
Daweidu Village, Xiaojie Town, Eshan County, Yuxi City	*Butyriboletus pseudospeciosus*	BuP	4	101.84	25.34	2245
Fuliangpeng Township, Eshan County, Yuxi City	*Butyriboletus pseudospeciosus*	BuP	3	99.52	26.69	2444
Daweidu Village, Xiaojie Town, Eshan County, Yuxi City	*Butyriboletus pseudospeciosus*	BuP	3	101.12	25.22	1984
Fuliangpeng Township, Eshan County, Yuxi City	*Butyriboletus pseudospeciosus*	BuP	4	103.96	25.27	2035
Jiuxi Town, Jiangchuan County, Yuxi City	*Butyriboletus pseudospeciosus*	BuP	3	102.54	24.34	1670

Table O1 (continued)

Sampling position	Latin Name	Abbreviation	Numbers	Longitude	Latitude	Elevation (M)
Daweidu Village, Xiaojie Town, Eshan County, Yuxi City	*Lanmaoa asiatica*	LA	3	100.74	23.79	1590
Fuliangpeng Township, Eshan County, Yuxi City	*Lanmaoa asiatica*	LA	3	102.04	24.71	2307
Midu County, Dali City	*Lanmaoa asiatica*	LA	3	102.38	24.09	1873
Xinping County, Yuxi City	*Lanmaoa asiatica*	LA	3	101.51	25.07	1797
Donggua Town, Chuxiong Prefecture	*Lanmaoa asiatica*	LA	3	102.09	24.31	1973
Mali mountain, Midu County, Dali City	*Lanmaoa asiatica*	LA	5	100.49	25.34	1674
Luohe Township, Yuxi City	*Lanmaoa asiatica*	LA	3	102.63	24.3	1740
Luohe Township, Yuxi City	*Lanmaoa asiatica*	LA	3	102.49	24.34	1622
Jiuxi Town, Jiangchuan County, Yuxi City	*Lanmaoa asiatica*	LA	3	102.66	24.41	2005
Jiuxi Town, Jiangchuan County, Yuxi City	*Lanmaoa asiatica*	LA	3	101.84	25.34	2245
Baohe Town, Weixi County, Diqing Prepecture	*Lanmaoa asiatica*	LA	3	102.23	24.82	1692
Luohe Township, Yuxi City	*Lanmaoa asiatica*	LA	3	102.3	24.21	2069
Longpeng Town, Shiping County, Honghe Prepecture	*Lanmaoa asiatica*	LA	3	101.12	25.22	1984
Jiuxi Town, Jiangchuan County, Yuxi City	*Lanmaoa asiatica*	LA	3	102.26	26.09	2025
Jiuxi Town, Jiangchuan County, Yuxi City	*Lanmaoa asiatica*	LA	3	102.23	24.84	1732
Jiuxi Town, Jiangchuan County, Yuxi City	*Lanmaoa asiatica*	LA	3	102.46	24.15	1535
Baitu Village, Daying street, Yuxi City	*Lanmaoa asiatica*	LA	3	103.62	24.47	1832
Anhau Township, Jiangchuan County, Yuxi City	*Lanmaoa asiatica*	LA	3	103.96	25.27	2035
Anhau Township, Jiangchuan County, Yuxi City	*Neoboletus obscureumbrinus*	NO	3	102.64	24.3	1714

Table O1 (continued)

Sampling position	Latin Name	Abbreviation	Numbers	Longitude	Latitude	Elevation (M)
Luohe Township, Yuxi City	*Neoboletus obscureumbrinus*	NO	3	102.49	23.7	1442
Shiping County, Honghe Prepecture	*Neoboletus obscureumbrinus*	NO	3	102.01	27.43	2263
Maan Township, Dechan County, Liangshan Prepecture, Sichuan Province	*Neoboletus obscureumbrinus*	NO	3	102.23	24.82	1692
Bicheng Town, Lufeng County, Chuxipong Prepecture	*Neoboletus obscureumbrinus*	NO	3	99.7	27.83	3283
Luohe Township, Yuxi City	*Neoboletus obscureumbrinus*	NO	3	100.17	26.56	2203
Anhau Township, Jiangchuan County, Yuxi City	*Neoboletus obscureumbrinus*	NO	3	102.3	26.97	2558
Baitu Village, Daying street, Yuxi City	*Phlebopus portentosus*	PP	9	100.66	21.98	984
Maming Township, Qujing City	*Phlebopus portentosus*	PP	9	101.26	25.79	1921
Liujie Town, Yimen County, Yuxi City	*Phlebopus portentosus*	PP	8	102.02	24.07	1496
Liujie Town, Yimen County, Yuxi City	*Phlebopus portentosus*	PP	9	99.51	25.04	1620
Liujie Town, Yimen County, Yuxi City	*Rugiboletus extremiorientalis*	RugE	3	101.37	25.53	2155
Baoxing Village, Shangsuan Town, Jinning County, Kunming City	*Rugiboletus extremiorientalis*	RugE	3	102.76	24.12	1806
Gaoping Village, Shuangjiang Township, Eshan County, Yuxi City	*Rugiboletus extremiorientalis*	RugE	3	102.33	24.69	1976
Meiyun Village, Yimen County, Yuxi City	*Rugiboletus extremiorientalis*	RugE	3	103.39	25.11	1847
Datianba Township, Changning County, Baoshan City	*Rugiboletus extremiorientalis*	RugE	5	102.09	24.31	1973
Beijieshuiku Village, Longyan District, Baoshan City	*Rugiboletus extremiorientalis*	RugE	3	101.51	25.07	1797
Zixi Mountain, Nanhua County, Chuxiong Prepecture	*Rugiboletus extremiorientalis*	RugE	3	99.16	25.12	1685
Jiyi Township, Wuding County, Chuxiong Prepecture	*Rugiboletus extremiorientalis*	RugE	3	99.28	27.18	2323
Gaoping Village, Shuangjiang Township, Eshan County, Yuxi City	*Rugiboletus extremiorientalis*	RugE	4	102.38	24.31	1772

Table O1 (continued)

Sampling position	Latin Name	Abbreviation	Numbers	Longitude	Latitude	Elevation (M)
Liujie Town, Yimen County, Yuxi City	*Rugiboletus extremiorientalis*	RugE	3	102.64	24.3	1714
Daliu Village, Liujie Town, Yimen County, Yuxi City	*Rugiboletus extremiorientalis*	RugE	5	102.39	24.33	1726
Leye Village, Sanhe Town, Honghe Prepecture	*Rugiboletus extremiorientalis*	RugE	3	102.18	24.61	1695
Gaoping Village, Shuangjiang Township, Eshan County, Yuxi City	*Rugiboletus extremiorientalis*	RugE	3	102.41	24.17	1540
Shangri-la County, Diqing Prepecture	*Rugiboletus extremiorientalis*	RugE	3	101.96	25.73	2138
Beidou Township, Yunlong County, Dali City	*Rugiboletus extremiorientalis*	RugE	3	102.16	24.67	1587
Liangshan Township, Yuanmou County, Chuxiong Prepecture	*Rugiboletus extremiorientalis*	RugE	5	102.29	24.76	2463
Daliu Village, Liujie Town, Yimen County, Yuxi City	*Retiboletus fuscus*	RetF	6	100.74	23.79	1590
Pubei Township, Yimen County, Yuxi City	*Retiboletus fuscus*	RetF	6	102.38	24.09	1873
Yipinglang Town, Lufeng County, Chuxiong Prepecture	*Retiboletus fuscus*	RetF	5	100.51	25.34	1781
Pubei Township, Yimen County, Yuxi City	*Retiboletus fuscus*	RetF	7	102.66	24.41	2005
Xiaojie Township, Yimen County, Yuxi City	*Retiboletus fuscus*	RetF	6	102.39	24.33	1726
Junzi Hill, Longchuan Town, Nanhua County, Chuxiong Prepecture	*Retiboletus fuscus*	RetF	6	102.5	24.34	1621
Daying street, Yuxi City	*Retiboletus fuscus*	RetF	6	102.09	24.69	1993
Leye Village, Sanhe Town, Honghe Prepecture	*Retiboletus fuscus*	RetF	6	102.3	24.21	2069
Shuangjiang Town, Eshan County, Yuxi City	*Retiboletus fuscus*	RetF	6	101.33	25.37	2516
Shuangjiang Town, Eshan County, Yuxi City	*Retiboletus fuscus*	RetF	6	103.96	25.27	2035
Tongdian Town, Lanping County, Nujiang Prepecture	*Rubroboletus sinicus*	RubS	6	102.38	24.09	1873
Heqing County, Dali City	*Rubroboletus sinicus*	RubS	5	102.64	24.3	1714

Table O1 (continued)

Sampling position	Latin Name	Abbreviation	Numbers	Longitude	Latitude	Elevation (M)
Hengshan Township, Miyi County, Pangzhihua City, Sichuan Province	*Rubroboletus sinicus*	RubS	5	102.23	24.82	1692
Baizhu Mountain, Daguohe Township, Nanhua County, Chuxiong Prepecture	*Rubroboletus sinicus*	RubS	5	102.55	24.43	1659
Liangshan Township, Yuanmou County, Chuxiong Prepecture	*Rubroboletus sinicus*	RubS	5	101.33	25.37	2516
Guihuashu Village, Yuezhou Town, Qilin District, Qujing City	*Neoboletus hainanensis*	NH	5	102.09	24.31	1973
Huangcaoba Village, Xishan District, Kunming City	*Neoboletus hainanensis*	NH	7	103.3	25.25	1962
Hongta District, Yuxi City	*Neoboletus hainanensis*	NH	8	101.24	25.51	1880
Guihuashu Village, Yuezhou Town, Qilin District, Qujing City	*Neoboletus hainanensis*	NH	5	102.16	24.67	1587
Maan Village, Tianzhong Township, Yimen County, Yuxi City	*Neoboletus magnificus*	NM	5	102.1	25.03	1648
Guihuashu Village, Yuezhou Town, Qilin District, Qujing City	*Neoboletus magnificus*	NM	5	100.74	23.79	1590
Tadian Town, Eshan County, Yuxi City	*Neoboletus magnificus*	NM	5	101.03	23.07	1620
Beicheng District, Yuxi City	*Neoboletus magnificus*	NM	5	102.38	24.09	1873
Yimen County, Yuxi City	*Neoboletus magnificus*	NM	3	102.09	24.31	1973
Kunyan street, Jinning County, Kunming City	*Neoboletus magnificus*	NM	5	101.57	24.06	553
Puxiong Township, Jianshui County, Honghe Prepecture	*Neoboletus magnificus*	NM	5	102.65	23.8	1898
Yaoan County, Chuxiong Prepecture	*Neoboletus magnificus*	NM	5	102.63	24.3	1740
Chahe Township, Eshan County, Yuxi City	*Neoboletus magnificus*	NM	5	102.66	24.41	2005
Wujie Township, Nanhua County, Chuxiong Prepecture	*Neoboletus magnificus*	NM	3	102.39	24.33	1726
Yimen County, Yuxi City	*Neoboletus magnificus*	NM	4	102.3	24.21	2069
Shidong Village, Longquan Town, Yimen County, Yuxi City	*Neoboletus magnificus*	NM	5	102.49	24.93	1847

Table O2 The contents of VOCs of 11 boletes species based on ANOVA

	English name	Relative percentage (%)										
		BoB (32)	**BuR (55)**	**BuP (30)**	**LA (56)**	**NO (21)**	**PP (35)**	**RugE (55)**	**RetF (60)**	**RubS (26)**	**NH (25)**	**NM (55)**
Amine	1-Butanamine,3-methyl-N-(3-methylbutylidene)-	0.7±0.36^{a}	1.7±2.15^{a}	8.87±7.01^{d}	2.69±2.92^{ab}	7.71±7.08^{cd}	2.88±2.51^{ab}	2.02±1.79^{a}	7.94±6.03^{cd}	6.18±8.88^{bcd}	3.56±5.39^{ab}	4.57±3.31^{abc}
	1-Propanamine,N-(2-furanylmethylene)-2-methyl-	0.54±0.82^{a}	0.5±0.5^{a}	1.15±2.1^{a}	0.8±1.04^{a}	0.45±0.81^{a}	0.41±0.24^{a}	0.79±0.52^{a}	0.38±0.2^{a}	0.46±0.5^{a}	3.16±6.67^{b}	0.76±0.58^{a}
	N-(3-Methylbutyl) acetamide	1.04±0.69^{ab}	0.92±0.06^{ab}	1.6±1.4^{b}	0.92±0.65^{ab}	1.06±1.48^{ab}	0.6±0.47^{a}	0.46±0.21^{a}	0.5±0.37^{a}	0.37±0.35^{a}	0.52±0.34^{a}	0.81±0.77^{a}
	N-Propylbenzylideneamine	0.6±0.37^{a}	1.11±0.95^{a}	1.06±1.79^{a}	0.69±0.49^{a}	3.88±7.32^{b}	0.51±0.33^{a}	0.38±0.24^{a}	0.52±0.43^{a}	0.5±0.46^{a}	0.92±1.43^{a}	1.28±0.84^{a}
	3-methyl-N-propyl-1-Butanamine	0.54±0.31^{a}	0.63±0.54^{ab}	1.06±0.61^{abc}	3.04±2.95^{d}	0.84±0.96^{abc}	0.59±0.4^{a}	0.58±0.3^{a}	1.12±0.69	1.38±1.53^{abc}	1.93±2.32^{bcd}	2.05±1.58^{cd}
	Diphenylamine	1.32±2.14^{ab}	1.92±0.72^{b}	0.53±0.46^{a}	0.85±0.79^{a}	0.51±0.85^{a}	1.73±2.41^{ab}	0.39±0.22^{a}	0.9±0.89^{a}	0.58±0.4^{a}	0.85±1.44^{a}	0.38±0.32^{a}
	Tetradecanamide	14.11±7.21^{e}	10.73±6.42^{ab}	8.9±5.59^{ab}	10.61±5.92^{bcd}	7.62±5.56^{ab}	6.32±3.29^{a}	9.69±4.4^{bc}	8.15±4.9^{ab}	10.64±6.89^{bcd}	12.55±7.11^{cde}	13.66±7.1^{de}
	Oleamide	14.77±6.44^{e}	13.06±8.85^{de}	10.1±6.3^{bcd}	10.43±6.87^{cd}	6.81±7.11^{ab}	6.51±5.21^{a}	11.2±5.74^{cd}	8.6±4.37^{abc}	8.4±8.14^{abc}	8.69±7.07^{abc}	10.13±6.9^{bcd}
Alcohol	1-Octen-3-ol	7.58±5.08^{ab}	9.2±8.59^{ab}	5.07±5.66^{a}	7.6±4.77^{ab}	7.72±9.06^{ab}	6.32±6.6^{a}	8.45±6.55^{ab}	9.9±8.17^{ab}	6.29±8.25^{a}	13.68±16.13^{b}	5.87±7.42^{a}
	2,4-Di-tert-butylphenol	4.55±8.9^{d}	1.79±2.56^{abc}	3.59±4.62^{cd}	2.41±2.74^{abc}	0.8±1.75^{a}	2.6±3.22^{bc}	0.65±1.03^{a}	1.17±0.92^{ab}	3.7±4.22^{cd}	2.43±3.25^{abc}	2.68±2.2^{bc}
	Nerolidol	2.92±2.51^{b}	1.52±2.4^{ab}	2.29±2.16^{ab}	1.26±0.88^{ab}	0.61±0.41^{a}	1.71±2.67^{ab}	0.98±1.15^{a}	1.54±1.16^{ab}	2.21±1.73^{ab}	1.28±0.76^{ab}	7.52±7.33^{c}
	(2E,6E)-3,7,11-Trimethyl-2,6,10-dodecatrien-1-ol	12.19±10.7^{bc}	7.88±7.81^{a}	14.57±11.16^{c}	7.82±7.03^{ab}	6.58±7.36^{a}	5.98±4.78^{a}	5.91±5.21^{a}	9.11±9.62^{ab}	16.34±14.24^{c}	8.45±5.31^{ab}	7.93±6.71^{ab}

Table O2 (continued)

English name		Relative percentage (%)										
		BoB (32)	**BuR (55)**	**BuP (30)**	**LA (56)**	**NO (21)**	**PP (35)**	**RugE (55)**	**RetF (60)**	**RubS (26)**	**NH (25)**	**NM (55)**
Arene	Toluene	1.17±0.32^{de}	1.14±0.37^{de}	0.92±0.31^{c}	0.92±0.35^{c}	0.76±0.23^{b}	1.29±0.3^{e}	0.23±0.11^{a}	0.76±0.3^{b}	0.88±0.23^{bc}	0.76±0.24^{b}	1.06±0.37^{d}
	Ethylbenzene	0.51±0.32^{bc}	0.25±0.24^{a}	0.33±0.29^{a}	0.26±0.16^{a}	0.49±0.35^{b}	0.62±0.35^{c}	0.38±0.12^{ab}	0.31±0.26^{a}	0.34±0.26^{a}	0.27±0.24^{a}	0.35±0.29^{a}
	1,4-Xylene	0.27±0.04^{a}	0.31±0.09^{abc}	0.34±0.12^{bc}	0.42±0.29^{d}	0.26±0.07^{a}	0.3±0.04^{abc}	0.62±0.11^{e}	0.29±0.12^{abc}	0.28±0.06^{ab}	0.35±0.11^{c}	0.31±0.12^{abc}
	1,2-xylene	0.22±0.18^{a}	0.3±0.21^{abc}	0.29±0.2^{ab}	0.35±0.23^{abc}	0.3±0.28^{ab}	0.26±0.23^{a}	0.32±0.19^{abc}	0.43±0.28^{c}	0.34±0.24^{abc}	0.39±0.31^{bc}	0.27±0.18^{ab}
	2,2',5,5'-tetramethylbiphenyl	0.48±0.31^{a}	0.34±0.29^{a}	0.4±0.28^{a}	0.52±0.26^{a}	0.37±0.29^{a}	0.36±0.1^{a}	0.41±0.24^{a}	0.54±0.29^{a}	0.49±0.29^{a}	0.33±0.21^{a}	0.48±0.26^{a}
Aldehyde	Hexanal	2.3±1.68^{abc}	1.02±0.68^{a}	3.44±4.23^{c}	2.36±2.45^{abc}	1.7±1.52^{ab}	3.56±1.51^{c}	3.01±3.6^{bc}	3.68±3.48^{c}	2.6±3.45^{abc}	1.33±1.42^{ab}	1.05±2.73^{a}
	Furfural	1.14±0.77^{abc}	0.6±0.57^{a}	2.81±3.04^{de}	2.07±1.82^{cd}	1.89±1.92^{bcd}	0.98±0.66^{ab}	3.39±2.36^{e}	0.75±0.72^{a}	3.17±2.26^{e}	3.19±2.85^{e}	4.81±3.02^{f}
	Methional	2.46±2.82^{cd}	1.43±0.93^{ab}	1.51±2.21^{abc}	3.19±3.56^{d}	1.82±2.97^{abc}	2.7±2.85^{cd}	0.57±0.79^{a}	0.71±0.59^{a}	0.56±0.38^{a}	2.53±4.19^{bc}	1.1±1.12^{a}
	1-Methyl-1H-pyrrole-2-carbalde	0.99±1.01^{bc}	1.2±0.87^{cd}	0.96±1.03^{bc}	0.91±1.22^{abc}	1.6±2.26^{d}	0.49±0.42^{ab}	0.38±0.26^{a}	1.09±0.88^{cd}	0.39±0.32^{a}	1.03±1.39^{bc}	0.41±0.32^{a}
	5-Methyl furfural	0.39±0.34^{a}	0.48±0.14^{a}	0.24±0.1^{a}	0.24±0.09^{a}	0.52±0.79^{a}	0.38±0.22^{a}	0.32±0.26^{a}	0.44±0.39^{a}	0.37±0.31^{a}	0.37±0.16^{a}	0.28±0.18^{a}
	Benzaldehyde	1.39±1.18^{ab}	1.83±1.41^{b}	1.17±1.43^{ab}	1.92±2.73^{b}	1.47±1.37^{ab}	0.94±0.95^{a}	1.05±1.36^{ab}	1.09±1^{ab}	1.3±1.91^{ab}	1.08±1.01^{ab}	1.19±1.91^{ab}
	Phenylacetaldehyde	0.82±0.53^{a}	0.56±0.42^{a}	4.33±3.86^{e}	1.29±1.7^{ab}	2.72±4.17^{cd}	1.55±1.11^{abc}	1.75±1.95^{abc}	2.58±2.16^{bcd}	1.75±2.08^{abc}	3.2±3.57^{de}	2.02±2.2^{abcd}
	(E)-2-Octenal	1.94±1.96^{e}	1.41±1.04^{cde}	0.89±1.28^{abc}	0.99±1.33^{abcd}	0.65±0.68^{ab}	1.4±1.08^{abcde}	2.94±2.32^{f}	1.44±1.48^{bcde}	0.59±1^{a}	1.78±2.36^{de}	0.81±1.04^{abc}
	1-Nonanal	0.98±0.55^{ab}	0.85±0.64^{ab}	0.72±0.49^{a}	1.43±2.71^{b}	0.58±0.43^{a}	0.6±0.47^{a}	0.41±0.28^{a}	0.62±0.4^{a}	0.92±2.1^{ab}	0.69±0.43^{a}	0.56±0.4^{a}
	9,17-Octadecadienal, (Z)-	4.67±3.29^{cde}	5.86±3.79^{cde}	2.38±2.04^{a}	5.82±3.27^{e}	2.93±3.29^{ab}	2.41±1.8^{a}	3.07±2.14^{ab}	3.51±2.04^{abc}	4.14±2.46^{bcd}	5.29±3.52^{de}	4.75±2.62^{cde}

Table O2 (continued)

	English name	Relative percentage (%)										
		BoB (32)	**BuR (55)**	**BuP (30)**	**LA (56)**	**NO (21)**	**PP (35)**	**RugE (55)**	**RetF (60)**	**RubS (26)**	**NH (25)**	**NM (55)**
Acids	3-methylbutanoic acid	0.93±0.8^{a}	1.45±3.64^{ab}	5.06±8.06^{ab}	6.98±5.92^{b}	0.8±1^{a}	1.96±2.34^{ab}	2.8±7.8^{ab}	0.67±0.62^{a}	1.26±0.56^{ab}	4.27±1.76^{ab}	1.58±0.87^{ab}
	2-methyl-butyric acid	0.37±0.17^{a}	0.00±0.00	3.41±4^{c}	0.98±0.87^{b}	4.27±6.17^{c}	2.77±4.38^{c}	0.56±0.26^{a}	0.52±0.34^{a}	0.57±0.2^{a}	0.92±1.03^{b}	0.84±0.5^{b}
	Tetradecanoic acid	8.1±6.11^{bc}	7.89±5.76^{abc}	3.79±3.12^{a}	9.86±3.86^{c}	5±3.6^{ab}	5±4.75^{ab}	3.97±2.33^{a}	5.8±4.01^{ab}	8.38±9.53^{bc}	5.37±2.75^{ab}	6.44±3.26^{ab}
	Pentadecanoic acid	7.02±5.15^{a}	10.41±8^{a}	6.83±8.06^{a}	29.96±60.97^{b}	27.26±48.1^{b}	11.45±31.8^{a}	13.83±9.13^{a}	7.85±5.33^{a}	13.88±7.57^{a}	13.53±8.39^{a}	18.14±9.1^{ab}
	(Z)-9-Hexadecenoic acid	18±11.37^{bcd}	13.82±9.92^{b}	17.55±11.75^{bcd}	15.82±12.77^{bcd}	13.11±6.58^{b}	3.97±4.6^{a}	15.58±9.65^{ab}	22.08±17.21^{cd}	11.58±5.04^{b}	13.57±10.57^{b}	22.26±13.5^{d}
	Hexadecanoic acid	196.44±123.59^{a}	302.69±165.08^{c}	219.6±96.14^{ab}	279.89±203.21^{bc}	211.58±176.82^{ab}	167.76±91.08^{a}	179.28±97.31^{a}	219.5±120.82^{ab}	146.52±83.51^{a}	189.79±168.27^{a}	206.47±162.62^{a}
	Linoleic acid	3.53±2.6^{a}	6.67±5.01^{ab}	5.33±3.53^{a}	20.69±37.08^{c}	2.49±3^{a}	3.82±2.22^{a}	4.38±3.04^{a}	5.64±5.9^{a}	13.99±19.09^{bc}	7.13±11.84^{ab}	3.87±3.3^{a}
	Heptadecanoic acid	3.69±5.98^{ab}	2.83±1.42^{ab}	3.32±2.26^{ab}	6.73±10.9^{ab}	4.83±13.44^{ab}	2.41±3.62^{ab}	2.44±1.1ab	3.98±4.53^{ab}	7.15±16.56^{b}	7.2±15.34^{b}	2.35±1.2^{a}
	Linoelaidic acid	273.44±141.46^{d}	213.76±126.23^{bc}	185.36±113.77^{ab}	244.76±138.28^{bcd}	216.98±72.55^{bcd}	134.59±130.1^{a}	205.63±129.21^{bc}	133.58±82.21^{a}	245.83±95.55^{bcd}	253.89±146.54^{cd}	261.99±151.36^{cd}
Ketones	9-Octadecenoic acid, (E)-	175.83±110.13^{c}	108.55±55.07^{ab}	96.51±36.02^{ab}	84.44±61.58^{ab}	78.49±49.44^{ab}	86.28±69^{ab}	88.44±70.8^{ab}	63.05±38.81^{a}	104.46±90.99^{ab}	108.65±74.44^{b}	91.49±74.44^{ab}
	gamma-Linolenic acid	8.37±5.84^{a}	17.14±17.1^{ab}	6.42±4.68^{a}	38.62±79.95^{c}	27±46.3^{bc}	15.33±25.7^{ab}	9.38±8.14^{ab}	7.42±6.94^{a}	13.48±24.67^{ab}	11.65±16.29^{ab}	4.06±2.33^{a}
	2(5H)-Furanone, 3-methyl-	0.34±0.26^{a}	0.43±0.25^{a}	2.37±3.35^{b}	0.41±0.24^{a}	0.8±0.42^{a}	0.37±0.21^{a}	0.67±0.83^{a}	0.5±0.31^{a}	0.52±0.61^{a}	0.42±0.32^{a}	0.41±0.22^{a}
	2-Cyclopentene-1,4-dione	0.92±1.03^{a}	0.79±1.5^{a}	1.53±2.89^{ab}	4.9±4.64^{c}	0.65±0.55^{a}	1.24±0.97^{ab}	0.5±0.41^{a}	0.83±0.78^{a}	1.28±1.52^{ab}	2.25±2.71^{b}	1.72±3.07^{ab}
	2-Heptanone	0.31±0.18^{a}	0.56±0.47^{ab}	0.3±0.31^{a}	0.59±0.84^{ab}	0.52±0.4^{ab}	0.92±0.52^{c}	0.47±0.25^{ab}	0.4±0.24^{ab}	0.93±1.59^{c}	0.71±0.67^{bc}	0.41±0.19^{ab}
	Tetrahydrothiophen-3-one	0.31±0.17^{a}	0.42±0.34^{a}	0.98±1.37^{a}	1.36±2.26^{ab}	0.34±0.2^{a}	0.57±0.38^{a}	2.22±4.13^{bc}	0.62±0.48^{a}	3.14±2.69^{c}	1.34±2.39^{ab}	0.77±1.24^{a}
	1-Decen-3-one	4.5±1.31^{c}	6.96±4.26^{d}	3.55±2.81^{bc}	2.74±1.62^{ab}	1.71±2.47^{a}	4.78±2.21^{c}	4.84±2.03^{c}	4.52±3.07^{c}	2.79±2.03^{ab}	1.76±1.17^{a}	3.41±1.34^{bc}
	2H-Pyran-2-one,5,6-dihydro-	1.82±1.19^{bcd}	0.98±0.87^{ab}	2.58±1.92^{de}	2.07±1.98^{cde}	1.4±2.03^{bc}	5.18±3.05^{f}	0.41±0.33^{a}	2.9±1.73^{e}	1.71±1.03^{bcd}	2.1±2.33^{cde}	1.69±1.28^{bcd}

Table O2 (continued)

English name		Relative percentage (%)										
		BoB (32)	**BuR (55)**	**BuP (30)**	**LA (56)**	**NO (21)**	**PP (35)**	**RugE (55)**	**RetF (60)**	**RubS (26)**	**NH (25)**	**NM (55)**
Alkanes	2-Acetyl pyrrole	0.91 ± 0.82^{bc}	0.5 ± 0.22^{abc}	0.96 ± 1.06^{c}	0.73 ± 0.84^{abc}	0.62 ± 0.33^{abc}	0.36 ± 0.18^{a}	0.77 ± 0.72^{abc}	0.45 ± 0.21^{ab}	0.69 ± 0.45^{abc}	0.81 ± 0.75^{abc}	0.89 ± 0.6^{bc}
	Acetophenone	2.03 ± 2.64^{bcd}	0.57 ± 0.56^{abc}	2.04 ± 2.65^{bcd}	0.94 ± 1.85^{abc}	0.65 ± 0.81^{ab}	2.14 ± 1.94^{cd}	4.84 ± 3.44^{e}	2.06 ± 1.96^{bcd}	3.36 ± 5.12^{d}	1.75 ± 2.34^{abc}	0.42 ± 0.54^{a}
	7,9-Di-tert-butyl-1-oxaspiro(4,5)deca-6,9-diene-2,8-dione	1.05 ± 0.51^{ab}	0.73 ± 0.69^{a}	1.8 ± 2.4^{bcd}	1.59 ± 1.72^{bcd}	2.75 ± 2.13^{ef}	1.62 ± 0.76^{bcd}	1.99 ± 1.9^{cde}	1.38 ± 1.16^{abc}	2.32 ± 1.66^{def}	2.82 ± 2.76^{f}	2.13 ± 1.2^{cdef}
	2(3H)-Furanone, 5-dodecyldihydro-	3.01 ± 1.62^{ab}	2.36 ± 1.79^{a}	5.29 ± 3.14^{def}	3.84 ± 2.33^{bc}	5.58 ± 2.79^{ef}	3.95 ± 2.41^{bc}	4.05 ± 2.63^{bcd}	4.13 ± 2.38^{bcd}	6.24 ± 1.96^{f}	5.05 ± 2.3^{cdef}	4.54 ± 1.98^{cde}
	1,2,3,4,5-Pentamethylcyclopentadiene	1.24 ± 1.14^{bcde}	0.6 ± 0.52^{abc}	1.33 ± 1.94^{cde}	0.7 ± 0.53^{abcd}	0.47 ± 0.36^{a}	0.38 ± 0.27^{a}	0.66 ± 0.52^{abc}	0.72 ± 0.64^{abcd}	0.54 ± 0.36^{ab}	1.4 ± 2.97^{de}	1.53 ± 1.31^{e}
	Decane	2.56 ± 0.57^{g}	2.25 ± 0.69^{f}	1.58 ± 0.6^{cd}	1.97 ± 0.83^{ef}	1.18 ± 0.45^{b}	1.9 ± 0.59^{de}	0.7 ± 0.48^{a}	1.88 ± 0.7^{de}	1.77 ± 0.6^{cde}	1.5 ± 0.58^{c}	1.78 ± 0.66^{cde}
	2-Acetylthiazole	0.27 ± 0.17^{a}	0.4 ± 0.26^{ab}	0.36 ± 0.22^{ab}	0.36 ± 0.15^{ab}	0.49 ± 0.39^{bc}	0.36 ± 0.34^{ab}	0.35 ± 0.19^{ab}	0.44 ± 0.32^{ab}	0.25 ± 0.15^{a}	0.29 ± 0.14^{ab}	0.64 ± 0.52^{c}
	2,2,4,4,6,8,8-heptamethyl-Nonane	1.8 ± 0.49^{b}	1.48 ± 0.53^{ab}	1.18 ± 0.44^{ab}	1.47 ± 0.62^{ab}	1.69 ± 2.37^{ab}	1.59 ± 0.46^{ab}	1.01 ± 0.66^{a}	1.39 ± 0.45^{ab}	1.3 ± 0.61^{ab}	1.36 ± 1.34^{ab}	1.28 ± 0.46^{ab}
Heterocyclic compounds	2,5,9-Trimethyldecane	0.96 ± 0.43^{bcde}	0.66 ± 0.43^{abc}	1.32 ± 1.11^{e}	0.76 ± 0.43^{abcd}	1.24 ± 1.98^{de}	1.17 ± 0.69^{de}	0.4 ± 0.46^{a}	0.83 ± 0.38^{abcde}	0.57 ± 0.34^{ab}	0.64 ± 0.34^{abc}	1.11 ± 1.16^{cde}
	Undecane, 3-methyl-	0.51 ± 0.7^{cde}	0.18 ± 0.06^{a}	0.29 ± 0.26^{ab}	0.39 ± 0.27^{bc}	0.57 ± 0.37^{de}	0.28 ± 0.23^{ab}	0.6 ± 0.46^{e}	0.3 ± 0.24^{ab}	0.54 ± 0.44^{cde}	0.41 ± 0.29^{bcd}	0.27 ± 0.18^{ab}
	Dodecane	5.76 ± 1.58^{f}	4.68 ± 1.62^{de}	4 ± 1.37^{bc}	4.27 ± 1.72^{cd}	3.26 ± 1.51^{b}	5.33 ± 1.44^{ef}	1.92 ± 1.06^{a}	3.89 ± 1.47^{bc}	4.07 ± 1.73^{c}	3.77 ± 1.62^{bc}	4.38 ± 1.76^{cd}
	Cyclopentane, pentyl-	0.67 ± 0.32^{bc}	0.47 ± 0.31^{ab}	0.46 ± 0.3^{ab}	0.52 ± 0.26^{abc}	0.99 ± 1.16^{d}	0.62 ± 0.21^{abc}	0.75 ± 1.02^{c}	0.39 ± 0.16^{a}	0.42 ± 0.21^{ab}	0.51 ± 0.39^{abc}	0.42 ± 0.18^{ab}
	Tridecane	0.68 ± 0.3^{ab}	0.68 ± 0.27^{ab}	1.17 ± 0.5^{cd}	0.89 ± 0.42^{bc}	1.02 ± 1.07^{bcd}	0.7 ± 0.38^{ab}	0.88 ± 0.72^{bc}	0.89 ± 0.89^{bc}	1.35 ± 1.14^{d}	1.18 ± 1.19^{cd}	0.42 ± 0.18^{a}
	Tridecane, 3-methyl-	0.36 ± 0.11^{a}	0.24 ± 0.08^{a}	0.35 ± 0.17^{a}	0.43 ± 0.33^{a}	1.34 ± 3.69^{b}	0.3 ± 0.19^{a}	0.37 ± 0.29^{a}	0.35 ± 0.23^{a}	0.25 ± 0.26^{a}	1.05 ± 2.69^{b}	0.24 ± 0.13^{a}
	Tetradecane	1.77 ± 0.42^{e}	1.59 ± 1.01^{cde}	1.28 ± 0.43^{bcd}	1.61 ± 0.66^{de}	0.89 ± 0.3^{ab}	1.34 ± 0.45^{cd}	0.81 ± 0.43^{a}	1.6 ± 1.7^{de}	1.35 ± 0.83^{cd}	1.12 ± 0.43^{abc}	1.26 ± 0.41^{bcd}

Table O2 (continued)

	English name	Relative percentage (%)										
		BoB (32)	**BuR (55)**	**BuP (30)**	**LA (56)**	**NO (21)**	**PP (35)**	**RugE (55)**	**RetF (60)**	**RubS (26)**	**NH (25)**	**NM (55)**
	Cyclopentane, nonyl-	0.63±0.54^{a}	0.45±0.23^{a}	0.46±0.35^{a}	0.66±1.01^{a}	0.35±0.19^{a}	0.48±0.2^{a}	1.87±2.32^{b}	0.68±0.57^{a}	0.46±0.33^{a}	0.48±0.49^{a}	0.47±0.6^{a}
	PentaDecane, 3-methyl-	0.37±0.1^{a}	0.28±0.13^{a}	0.41±0.23^{a}	0.35±0.16^{a}	0.67±0.7^{b}	0.33±0.13^{a}	0.47±0.5^{a}	0.44±0.4^{a}	0.43±0.3^{a}	0.68±0.85^{b}	0.33±0.14^{a}
	Hexadecane	0.45±0.14^{a}	0.44±0.15^{a}	0.48±0.32^{a}	0.51±0.23^{a}	1.08±1.7^{b}	0.34±0.15^{a}	0.88±0.48^{b}	0.58±0.67^{a}	0.5±0.32^{a}	0.5±0.45^{a}	0.43±0.16^{a}
Heterocyclic	Undecylcyclopentane	0.63±0.21^{a}	0.49±0.16^{a}	0.62±0.41^{a}	0.83±0.56^{b}	0.67±1.07^{ab}	0.49±0.16^{a}	0.57±0.28^{a}	0.52±0.39^{a}	0.66±0.45^{ab}	0.53±0.36^{a}	0.46±0.14^{a}
compounds	Eicosane	4.38±2.06^{b}	4.75±2.21^{b}	5.61±2.28^{b}	4.84±3.23^{b}	5.4±6.82^{b}	2.04±1.39^{a}	7.65±4.54^{c}	4.89±2.74^{b}	4.72±3.25^{b}	5.1±2.55^{b}	5.91±1.97^{b}
	1,6-Cyclodecadiene	7.73±2.83^{de}	5.72±2.33^{b}	7.17±2.9^{de}	6.63±3.77^{bcd}	6.8±3.57^{cd}	3.25±1.47^{a}	8.46±4.06^{e}	5.39±2.52^{bc}	6.98±3.41^{de}	7.7±3.89^{de}	8.53±3.59^{e}
	Tetracosane	8.14±10.7^{b}	3.7±3.41^{a}	1.59±1.51^{a}	9.34±7.74^{b}	0.71±0.86^{a}	8.78±10.97^{b}	3.12±2.95^{a}	1.81±1.83^{a}	1.61±2.25^{a}	1.25±2.33^{a}	1.65±2.14^{a}
	Pyridine	0.43±0.58^{a}	0.4±0.58^{a}	0.54±0.39^{a}	1.68±1.91^{b}	1.67±2.68^{b}	0.26±0.25^{a}	0.52±0.63^{a}	0.34±0.34^{a}	0.82±1.04^{a}	0.93±1.5^{a}	1.59±1.4^{b}
	Pyrrole	0.39±0.17^{ab}	0.28±0.16^{a}	1.37±1.61^{bc}	2.41±3.47^{d}	1.18±2.03^{ab}	0.26±0.19^{a}	1.29±2.15^{abc}	0.41±0.29^{ab}	2.35±3.96^{d}	1.02±1.46^{ab}	2.23±2.23^{cd}
	2-hydroxy-Propanenitrile	0.81±0.4^{ab}	1.19±0.73^{abc}	2.69±2.92^{d}	2.33±3.28^{cd}	0.99±0.63^{abc}	0.45±0.3^{a}	4.06±4.39^{e}	1.25±1.52^{abc}	0.97±1.15^{abc}	2.92±4.99^{de}	2.2±2^{bcd}
	2-Methylpyrazine	0.41±0.29^{ab}	0.39±0.26^{ab}	0.69±0.96^{ab}	0.32±0.21^{ab}	0.72±1.39^{b}	0.35±0.23^{ab}	0.71±1.21^{ab}	0.3±0.2^{a}	0.39±0.24^{ab}	0.35±0.31^{ab}	0.54±0.3^{ab}
	2,6-Dimethylpyrazine	0.34±0.17^{a}	0.27±0.13^{a}	0.31±0.15^{a}	0.54±0.43^{a}	0.48±0.39^{a}	0.49±0.8^{a}	1.37±0.95^{c}	0.42±0.32^{a}	0.92±0.53^{b}	0.48±0.28^{a}	0.34±0.23^{a}
Esters	(1r)-(+)-alpha-pinene	0.23±0.2^{a}	0.25±0.27^{a}	2.45±3.59^{c}	0.5±0.4^{ab}	0.46±0.28^{ab}	0.74±0.64^{ab}	2.17±1.97^{c}	1.19±1.12^{b}	2.01±3.98^{c}	0.56±0.55^{ab}	0.38±0.48^{ab}
	1-(Pyridin-1(4H)-yl)ethanone	0.27±0.15^{a}	0.43±0.3^{ab}	0.39±0.28^{ab}	0.67±0.63^{b}	0.56±0.39^{ab}	0.32±0.32^{ab}	0.4±0.26^{ab}	0.46±0.53^{ab}	0.37±0.38^{ab}	0.57±1.02^{ab}	0.46±0.62^{ab}
	2-Pentylfuran	8.04±4.59^{cd}	8.26±3.99^{d}	6.8±3.08^{bcd}	6.59±3.35^{bcd}	6.19±2.82^{b}	10.72±3.69^{e}	2.03±1.85^{a}	7.46±4.25^{bcd}	6.87±2.88^{bcd}	6.43±3.37^{bc}	7.7±2.03^{bcd}
	Tetramethylpyrazine	0.8±0.35^{ab}	1.93±1.72^{c}	0.5±0.36^{a}	0.44±0.37^{a}	2.79±3.72^{c}	1.49±2.01^{b}	1.51±1.39^{b}	0.64±0.68^{a}	0.77±0.79^{ab}	0.81±0.97^{ab}	1.02±0.72^{ab}
	Benzo[c]thiophene	2.92±0.68^{c}	2.83±0.8^{bc}	2.45±1.13^{abc}	2.18±0.84^{a}	2.37±0.96^{ab}	3.76±1.09^{d}	4.34±1.92^{e}	2.32±0.73^{ab}	2.29±0.94^{ab}	2.46±1.16^{abc}	2.95±0.86^{c}
	Indole	0.51±0.26^{a}	0.33±0.2^{a}	0.42±0.18^{a}	0.34±0.22^{a}	0.83±0.82^{ab}	0.4±0.27^{a}	1.05±2.57^{b}	0.33±0.25^{a}	0.48±0.49^{a}	0.46±0.47^{a}	0.4±0.24^{a}
	3-Phenylpyridine	0.27±0.22^{a}	0.29±0.15^{a}	0.54±0.42^{a}	0.43±0.38^{a}	0.52±0.28^{a}	0.34±0.24^{a}	1.35±1.25^{b}	1.07±0.77^{b}	0.37±0.24^{a}	0.49±0.31^{a}	0.33±0.25^{a}

Table O2 (continued)

	English name	Relative percentage (%)										
		BoB (32)	**BuR (55)**	**BuP (30)**	**LA (56)**	**NO (21)**	**PP (35)**	**RugE (55)**	**RetF (60)**	**RubS (26)**	**NH (25)**	**NM (55)**
	Phenanthrene	0.83±0.58^{bcd}	0.68±0.5^{b}	0.73±0.72^{bc}	0.71±0.41^{bc}	0.96±0.45^{cd}	0.3±0.14^{a}	1.56±0.77^{e}	0.77±0.63^{bcd}	1.02±0.38^{d}	0.93±0.47^{cd}	0.9±0.43^{cd}
	Triethyl orthoformate	3.28±4.21^{a}	7.33±1.91^{abc}	10.36±10.02^{abcd}	6.89±9.67^{ab}	7.72±10.9^{abc}	17.81±15.5^{cd}	8.75±13.44^{abc}	19.2±20.96^{d}	14.26±21.8^{bcd}	9.03±14.16^{abcd}	14.2±15.5^{bcd}
Esters	4,5-Dihydro-5-methyl-2(3H)-fur	0.57±0.4^{a}	0.37±0.23^{a}	0.54±0.55^{a}	1.52±3.84^{b}	0.87±1.03a	0.74±0.59^{a}	0.4±0.34^{a}	0.41±0.28^{a}	0.33±0.22^{a}	0.49±0.65^{a}	0.35±0.18^{a}
	Tetraethyl orthosilicate	4.74±0.1^{c}	0.96±0.47^{a}	1.23±1.21^{ab}	2.56±2.4^{b}	5.51±8.78^{c}	4.25±2.65^{c}	4.68±5.17^{c}	0.99±0.79^{a}	4.79±5.76^{c}	1.85±3.02^{ab}	1.91±1.09^{ab}
	Methyl pentadecanoate	2.62±4.19^{d}	2.53±3.01^{cd}	1.06±1.09^{abc}	0.62±0.59^{ab}	1.67±1.36^{bcd}	0.41±0.19^{a}	0.37±0.22^{a}	0.34±0.23^{a}	0.48±0.33^{a}	1.24±1.2^{abc}	0.76±0.89^{ab}
	Diisobutyl phthalate	6.68±4.76^{ab}	6.07±4.13^{ab}	6.28±9.01^{ab}	6.44±3.81^{ab}	2.31±3.21^{a}	2.97±1.91^{a}	5.25±6.47^{ab}	3.94±3.37^{a}	9.67±15.4^{b}	16.42±19.98^{c}	16.04±12.4^{c}
	Methyl hexadecanoate	1.93±1.88^{c}	2.01±1.51^{c}	1.73±1.25^{c}	1.87±1.74^{c}	1.5±1.5^{bc}	0.98±0.64^{ab}	1.38±0.85^{bc}	0.93±0.7^{ab}	0.58±0.5^{a}	1.39±1.38^{bc}	1.76±1.5^{c}
	Dibutyl phthalate	7.65±5.33^{b}	6.71±4.97^{ab}	13.79±13.71^{c}	7.44±4.02^{b}	6.68±3.92^{ab}	3.71±1.76a	4.16±3.52^{a}	4.87±3.16^{ab}	4.33±3.59^{a}	6.15±5.9^{ab}	11.23±7.62^{c}
	Ethyl hexadecanoate	8.09±4.56^{de}	7.57±4.02^{bcd}	7.43±3.41^{cde}	7.4±3.08^{cde}	6.41±4.67^{bcd}	5.32±2.51^{ab}	5.57±2.82^{abc}	8.53±4.53^{e}	4.01±2.9^{a}	6.15±4.55^{bc}	6.67±3.22^{bcd}
	5,8,11-Heptadecatrienoic acid methyl ester	5.53±2.69^{b}	4.94±2.48^{ab}	4.77±3.32^{ab}	5.59±2.22^{b}	9.69±11.23^{c}	4.99±2.1^{ab}	3.14±1.38^{a}	3.49±1.7^{a}	3.21±2.15^{a}	4.23±2.85^{ab}	5.51±3.36^{b}
Esters	9,12-Octadecadienoicacid, methyl ester, (9E,12E)-methyl ester	7.14±5.21^{c}	5.85±3.08^{bc}	5.91±3.16^{bc}	6.99±4.43^{c}	4.45±2.31^{ab}	4.85±2.1^{b}	4.51±1.97^{ab}	4.32±2.66^{ab}	3.11±1.72^{a}	4.39±3.71^{ab}	6.82±4.19^{c}
	9,12-Octadecadienoicacid, methyl ester, (Z,Z)-	8.32±7.76^{a}	16.44±31.78^{a}	8.38±7.34^{a}	50.07±91.02^{b}	9.22±15.72^{a}	12.35±17.3^{a}	4.99±5.28^{a}	6.03±5.46^{a}	18.81±32.34^{a}	12.84±15.61^{a}	4.08±2.29^{a}
	Methyl 9-(Z)-octadecenoate	4.88±2.99^{d}	3.51±1.58^{bc}	3.15±1.85^{abc}	3.59±2.74^{c}	2.77±2.5^{abc}	1.94±1.13^{a}	2.9±1.96^{abc}	2.66±2.14^{abc}	2.18±2.03^{ab}	2.62±2.28^{abc}	3.2±1.53^{bc}
	Ethy linoleate	29.04±19.82^{d}	24.98±14.23^{cd}	22.86±21.57^{cd}	23.42±12.5^{cd}	5.34±9.34^{a}	25.75±13.5^{cd}	16.82±12.64^{bc}	20±11.21^{cd}	9.17±8.5^{ab}	7.73±9.3^{a}	28.54±17.6^{d}
	9-Octadecenenitrile, (E)-	32.73±28^{d}	18.06±9.73^{a}	20.75±12.48^{ab}	23.06±12.42^{abc}	18.74±12.1^{ab}	30.02±16.3^{cd}	16.42±9.25^{a}	19.12±9.56^{ab}	15.17±9.43^{a}	14.81±12.8^{a}	25.54±13^{bcd}

Table O2 (continued)

English name	Relative percentage (%)										
	BoB (32)	**BuR (55)**	**BuP (30)**	**LA (56)**	**NO (21)**	**PP (35)**	**RugE (55)**	**RetF (60)**	**RubS (26)**	**NH (25)**	**NM (55)**
Ethyl Oleate	22.65±14.85^{c}	10.54±6.25^{a}	10.55±4.96^{ab}	18.08±12.11^{bc}	13.01±13.3^{ab}	11.13±9.5^{ab}	12.65±7.74^{ab}	9.09±6.25^{a}	12.32±12.31^{ab}	21.13±23.27^{c}	29.75±22^{d}
Butyl citrate	5.5±2.39^{b}	4.12±1.77^{ab}	5.02±1.97^{ab}	5.4±2.5^{b}	10.27±10.1^{c}	3.82±2.89^{ab}	5.78±2.89^{b}	3.86±2.18^{ab}	2.19±2.71^{a}	9.29±15.25^{c}	5.56±1.97^{b}
Octyl 4-methoxycinnamate	6.32±4.03^{cd}	5.67±2.85^{bc}	4.04±1.91^{abc}	6.3±3.27^{cd}	1.88±2.93^{a}	5.56±4.14^{cd}	3.82±2.34^{abc}	4.06±2.6^{abc}	5.64±2.8^{cd}	2.75±3.3^{ab}	7.59±4.32^{d}
Bis(2-ethylhexyl) phthalate	4.96±4^{bc}	4.25±2.76^{bc}	5.5±5.01^{c}	7.61±7.81^{d}	2.31±1.33^{a}	4.34±4.2^{abc}	3.26±3.6^{ab}	3.13±2.22^{ab}	2.61±2.1^{a}	2.94±2.67^{ab}	3.81±1.89^{abc}

APPENDIX P

THE RESULTS OF CROSS VALIDATION

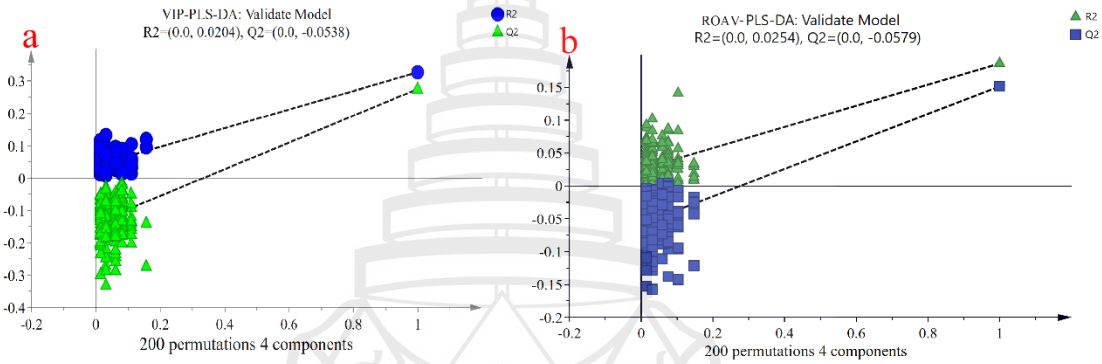


Figure P The results of cross validation of 200 permutations of VIP-PLS-DA (a) and ROAV-PLS-DA (b).

APPENDIX Q

THE PUBLISHED PARPERS

MycoKeys

MycoKeys 107: 141–160 (2024)
DOI: 10.3897/mycokeys.107.123565

Research Article

Three new *Melanogaster* species (Boletales, Paxillaceae) from southwestern China based on morphological and molecular evidence

Tian-Jun Yuan[1,2], Hong-Mei Luo[2], Kai-Mei Su[2], Shu-Hong Li[2], Olivier Raspé[1]

1 School of Science, Mae Fah Luang University, Chiang Rai 57100, Thailand
2 Institute of Biotechnology and Germplasm Resources, Yunnan Academy of Agricultural Sciences, Kunming 650223, Yunnan, China
Corresponding authors: Shu-Hong Li (shuhongfungi@126.com); Olivier Raspé (Olivier.Ras@mfu.ac.th)

Abstract

Three newly discovered *Melanogaster* species, namely *M. cyaneus*, *M. diqingensis*, and *M. truncatisporus*, are introduced and illustrated based on both morphological and molecular data from Sichuan and Yunnan provinces in China. A multigene phylogenetic analysis (nrITS, nrLSU, and *rpb2*) was performed mainly to verify the placement of the new species in *Melanogaster*. A second, nrITS-only phylogenetic analysis comprising more *Melanogaster* species for which only ITS sequences were available, was used to infer the relationship between the new species and as many known *Melanogaster* species as possible. Specimens of *M. cyaneus*, *M. diqingensis*, and *M. truncatisporus* formed three independent clades in a phylogenetic tree inferred from the ITS data set. The robust support from ITS for these clades and genetic similarity with other species being lower than 93.2% suggest that these three species are indeed distinct from the other *Melanogaster* species in the phylogeny. Morphologically, *M. cyaneus* is characterized by its blue or bluish gleba, light brown to yellowish brown peridium, and subglobose to globose basidiospores, 6.2–15 × 4.6–9.0 µm. *Melanogaster diqingensis* is distinguished from other *Melanogaster* species by its pale yellow to brown-yellow peridium and obovate to subglobose basidiospores, 3.0–5.1 × 2.0–4.0 µm. *Melanogaster truncatisporus* is diagnosed by its subglobose to globose or irregularly elongate-pyriform basidiomata, pale yellow to deeply orange-yellow peridium, and subglobose to globose or pyriform, truncate basidiospores. Additionally, infrageneric classification based on the number of peridium layers, the average thickness of the peridium, and the average length and width of basidiospores was tested with *M. cyaneus*, *M. diqingensis*, and *M. truncatisporus*. Orthogonal partial least squares discriminant (OPLS-DA) analysis placed the three new species within the *Melanogaster*, *Rivulares*, and *Variegati* sections, respectively. However, the morphologically circumscribed sections were not monophyletic in the phylogenetic tree. Therefore, the current infrageneric classification should be abandoned.

Key words: False truffles, gasteroid Boletales, phylogeny, taxonomy, three new species

OPEN ACCESS

This article is part of:
Diversity, taxonomy, and systematics of macrofungi from tropical Asia
Edited by Olivier Raspé, Rui-Lin Zhao, Jennifer Luangsa-ard

Academic editor: Jennifer Luangsa-ard
Received: 20 March 2024
Accepted: 19 June 2024
Published: 26 July 2024

Citation: Yuan T-J, Luo H-M, Su K-M, Li S-H, Raspé O (2024) Three new *Melanogaster* species (Boletales, Paxillaceae) from southwestern China based on morphological and molecular evidence. MycoKeys 107: 141–160. https://doi.org/10.3897/mycokeys.107.123565

Copyright: © Tian-Jun Yuan et al.
This is an open access article distributed under terms of the Creative Commons Attribution License (Attribution 4.0 International – CC BY 4.0).

Phytotaxa 482 (3): 251–260
https://www.mapress.com/j/pt/
Copyright © 2021 Magnolia Press

Article

ISSN 1179-3155 (print edition)
PHYTOTAXA
ISSN 1179-3163 (online edition)

https://doi.org/10.11646/phytotaxa.482.3.3

Choiromyces cerebriformis (Tuberaceae), a new hypogeous species from Yunnan, China

TIAN-JUN YUAN[1,2,6], OLIVIER RASPÉ[2,3,7*], YONG-JUN LI[1,8], LI WANG[1,2,9], KAI-MEI SU[1,10], YUN WANG[1,11], HONG-YAN SU[4,12], HAI-KUANG XIONG[5,13] & SHU-HONG LI[1,14*]

[1] *Biotechnology and Germplasm Resources Institute, Yunnan Academy of Agricultural Sciences, Kunming 650223 Yunnan, China.*
[2] *Center of Excellence in Fungal Research, Mae Fah Luang University, Chiang Rai 57100 Thailand.*
[3] *School of Science, Mae Fah Luang University, Chiang Rai 57100 Thailand.*
[4] *College of Agriculture & Biological Sciences, Dali University, Dali 671003, Yunnan, China.*
[5] *Yongren Yesenda Fungus Industry Co.LTD, Chuxiong 651499, Yunnan, China.*
[6] yuantianj@126.com; https://orcid.org/0000-0002-1254-7287
[7] olivier.ras@mfu.ac.th; http://orcid.org/0000-0002-8426-2133
[8] Tch_510@126.com; https://orcid.org/0000-0003-2407-9334
[9] lwang20@126.com; https://orcid.org/0000-0002-1889-591X
[10] kaimei@xina.com; https://orcid.org/0000-0001-5964-8897
[11] wangy10melrose@hotmail.com; https://orcid.org/0000-0003-1102-6540
[12] suhongyan16@163.com; https://orcid.org/0000-0002-2655-6491
[13] 265695418@qq.com; https://orcid.org/0000-0001-8507-863X
[14] shuhongfungi@126.com; https://orcid.org/0000-0001-5806-9148
*Correspondence: Olivier Raspé olivier.ras@mfu.ac.th; Shu-Hong Li shuhongfungi@126.com

Abstract

A new hypogeous species, *Choiromyces cerebriformis sp. nov.* is described and illustrated from Yunnan province, China. Both morphological evidence and sequence analyses of the internal transcribed spacer region (ITS1-5.8S-ITS2) support the species as new to science. *C. cerebriformis* differs from other *Choiromyces* species in having ascomata with larger lobes and light orange-brown gleba, and globose ascospores with short stick-like sparse spines ornamentation. Morphological differences and genetic distances with the similar species *C. helanshanensis* and *C. alveolatus* are discussed. A phenotypic key including related species is provided.

Keywords: ITS, False Truffle, One new species, Phylogeny, Taxonomy

Introduction

Choiromyces Vittad., commonly known as pig truffles, is a small but common genus in Pezizales, Ascomycotina. It was described by Vittadini with the type species *Choiromyces meandriformis* Vittad. (Vittadini 1831). Since then, new species have only sporadically been discovered in Asia, Europe and North America (Pegler *et al.* 1993; Chen *at al.* 2016). The classification of the genus within Pezizales has long been controversial. It was placed in Helvellaceae by Pegler *et al.* (1993), but has gradually been accepted within Tuberaceae (Hansen & Pfister 2006; Bonito *et al.* 2013; Wijayawardene *et al.* 2017). There are 30 *Choiromyces* records in Index Fungorum (http://www.indexfungorum.org/Names/Names.asp), but only seven species have been accepted, namely *C. alveolatus* (Harkn.) Trappe, *C. cookei* Gilkey, *C. ellipsosporus* Gilkey, *C. helanshanensis* (Chen *at al.* 2016; Rashmi *et al.* 2019), C. magnusii (Mattir.) Paol., *C. meandriformis*, *C. tetrasporus* Velen., and *C. venosus* (Fr.) Th. Fr.. *C. venosus*, however, has commonly been considered conspecific with *C. meandriformis* (Wedén *et al.* 2009). Three *Choiromyces* species have been reported from China, *C. alevolatus*, *C. venosus*, and *C. helanshanensis* (Tao 1988; Zhang 1990; Chen *at al.* 2016). *Choiromyces*, like other genera of Pezizales, are known to occur as endophytes, pathogens and saprobes (Rashmi *et al.* 2019; Phookamsak *et al.* 2019).

In 2019 and 2020, abundant *Tuber*-like ascomata were found in Yongren county, Chuxiong state, and Shangri-La County, Diqing Autonomous Prefecture, Yunnan, China. Based on morphological and molecular evidence, those

Accepted by Ruvishika Jayawardena: 30 Dec. 2020; published: 3 Feb. 2021



CURRICULUM VITAE

CURRICULUM VITAE

NAME Tianjun Yuan

EDUCATIONAL BACKGROUND

2011 Master of Organic Chemistry
Yunnan Nationalities University

2008 Bachelor of Biotechnology
Yunnan Nationalities University